UNIVERSITAT POLITÈCNICA DE CATALUNYA BARCELONATECH

Morpho-functionality of the toothed whale external ear canal

by
Steffen De Vreese

Joint PhD programme in Veterinary and Marine Sciences

MORPHO-FUNCTIONALITY of the TOOTHED WHALE EXTERNAL EAR CANAL

Thesis submitted to obtain the title of Doctor in Veterinary Sciences by the Università degli Studi di Padova and Doctor in Marine Sciences by the Universitat Politècnica de Catalunya

Doctoral dissertation by
Steffen De Vreese

Supervisors
Prof. Dr. Sandro Mazzariol
Prof. Dr. Michel André

Coordinators
Prof. Dr. Valentina Zappulli
Prof. Dr. Agustín Sanchez-Arcilla

Department of Comparative Biomedicine and Food Science (BCA), Università degli Studi di Padova (UniPd), Italy
Laboratory of Applied Bioacoustics (LAB), Universitat Politècnica de Catalunya (UPC), Spain

University with Administrative Responsibility: Università degli Studi di Padova
Hosting University: Universitat Politècnica de Catalunya
Performed with the financial contribution of the Cariparo Foundation

GENERAL TABLE OF CONTENTS

Detailed tables of contents are provided at the beginning of each chapter

ANNEXES

ANNEXES

3 Annexed figures

3.1 Macroscopic anatomy

Figure 458. Left lateral macroscopic view of a striped dolphin head (ID 12691-Sc1).

Figure 459. Macroscopic of images of the left and right side of a striped dolphin head cut into transverse slabs. The arrows show the position of the external ear opening, which is easy to find in this specimen as it is situated at the caudal end of the linear pigmentation ventrocaudal to the eye.

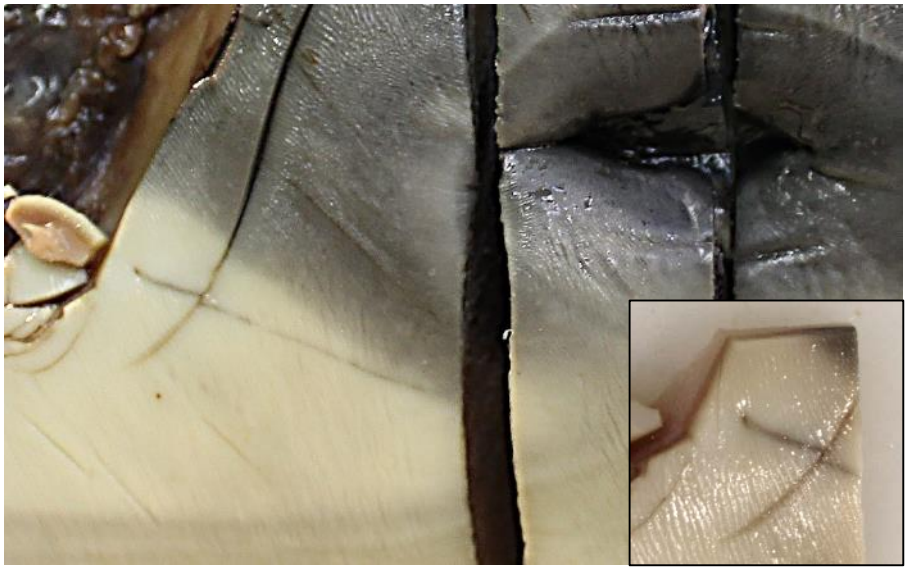

Figure 460. Macroscopic picture of the eye and external ear opening and marked pigmentation of a striped dolphin (ID5386).

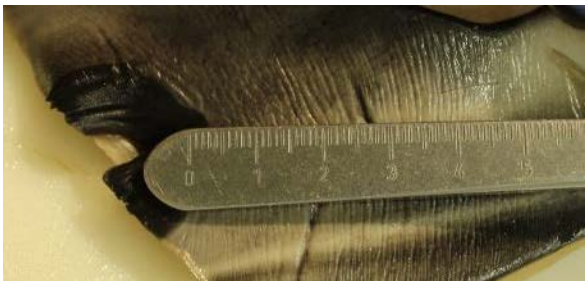

Figure 461. Macroscopic image of the left side of striped dolphin skin at the region of the eye and ear (ID2926). The opening is situated about 2.5-3 cm caudoventral to the posterior eye commissure. Note the vertical ridges in the skin and the shape of the ear opening as a vertical slit due to a combination of dehydration and removal of the skin tension after dissecting the skin.

Figure 462. Macroscopic left lateral image of the ear canal and cartilage, sectioned slightly medial to *Error! Reference source not found.*. ***A triangular shaped connective tissue capsule envelops the external ear canal. On the rostroventral side of the canal, there is a bean-shaped cartilage.***

3.2 Microscopic anatomy

3.2.1 External ear opening

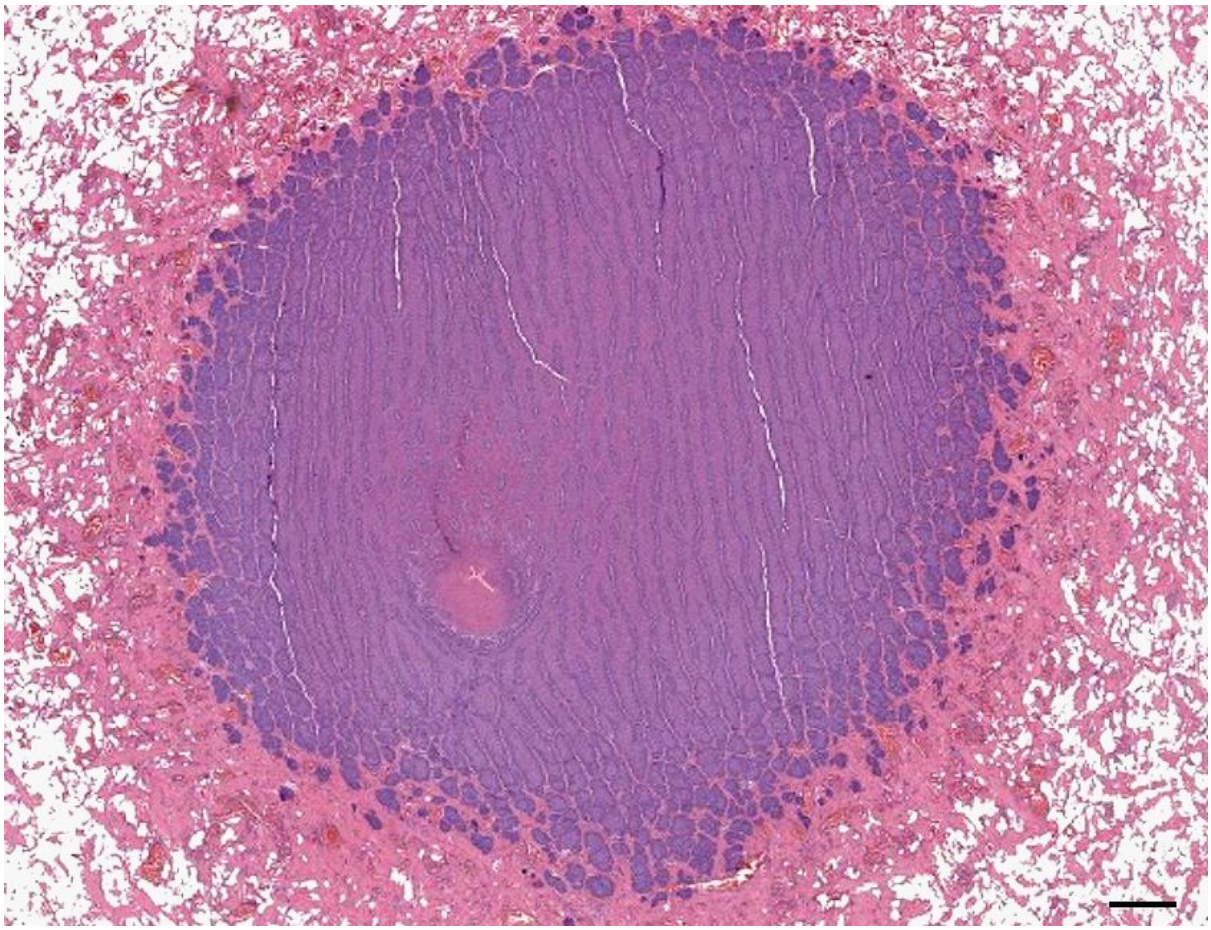

Figure 463. Histological transverse section (HE) of the external ear opening of a striped dolphin on its progression through the skin. Scale bar 0.5 mm.

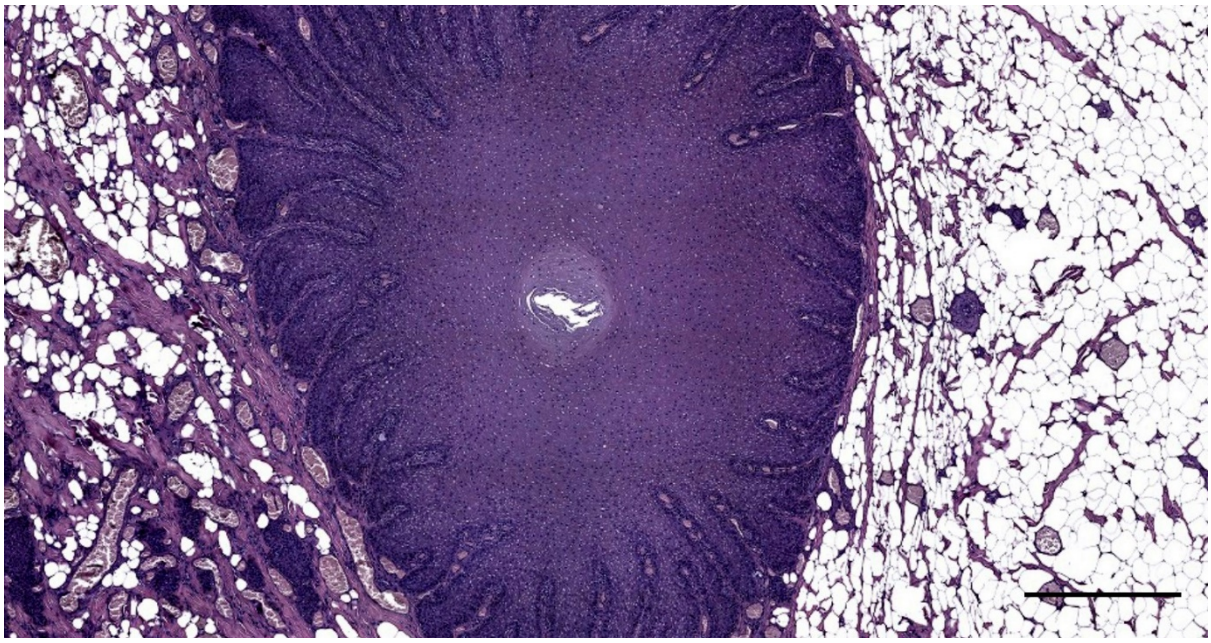

Figure 464. Histological image (HE staining) of a transverse section through the right ear canal of a harbour porpoise at the transition between external ear opening and ear canal (UT1727_R0201). Scale bar 500 µm

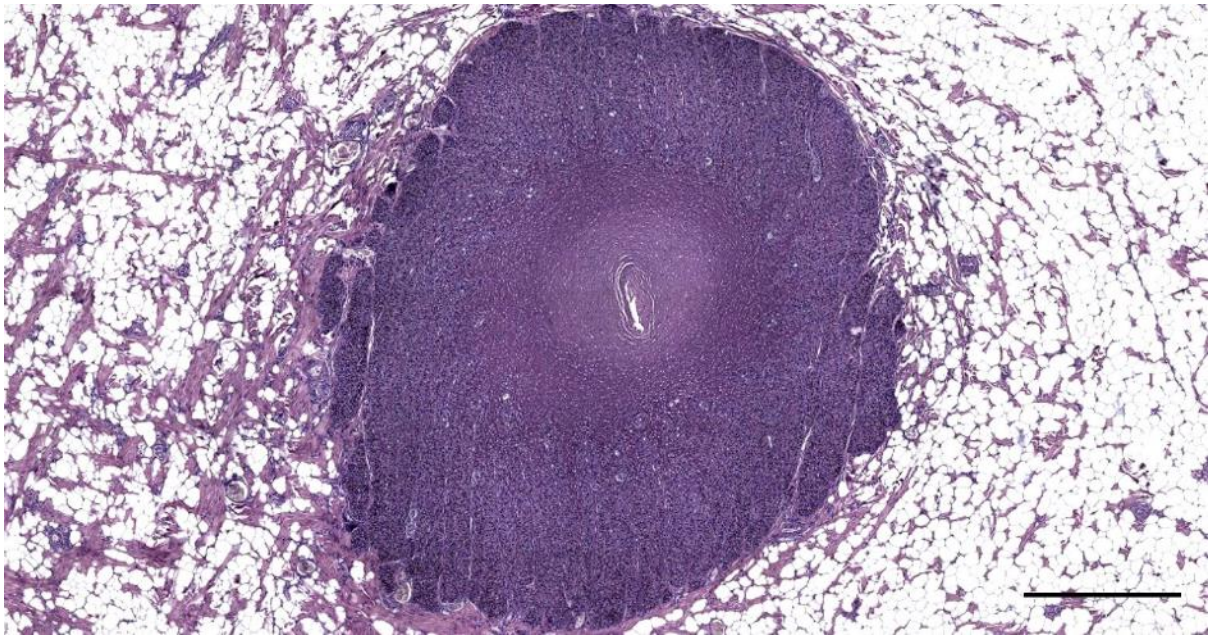

Figure 465. Histological image of a transverse section through the external ear opening in a harbour porpoise (UT1664). Scale bar 500 µm

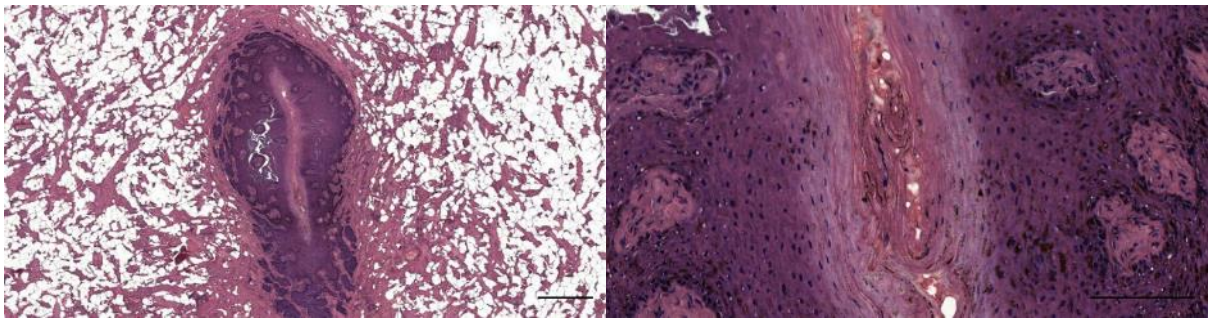

Figure 466. Two magnifications of a histological transverse section (HE staining) through the ear canal of a striped dolphin (ID292/18) at the level of the proximal end of the external ear opening. Note the extremely small lumen, filled with red blood cells. Scale bar left 0.5 mm, right 100 µm

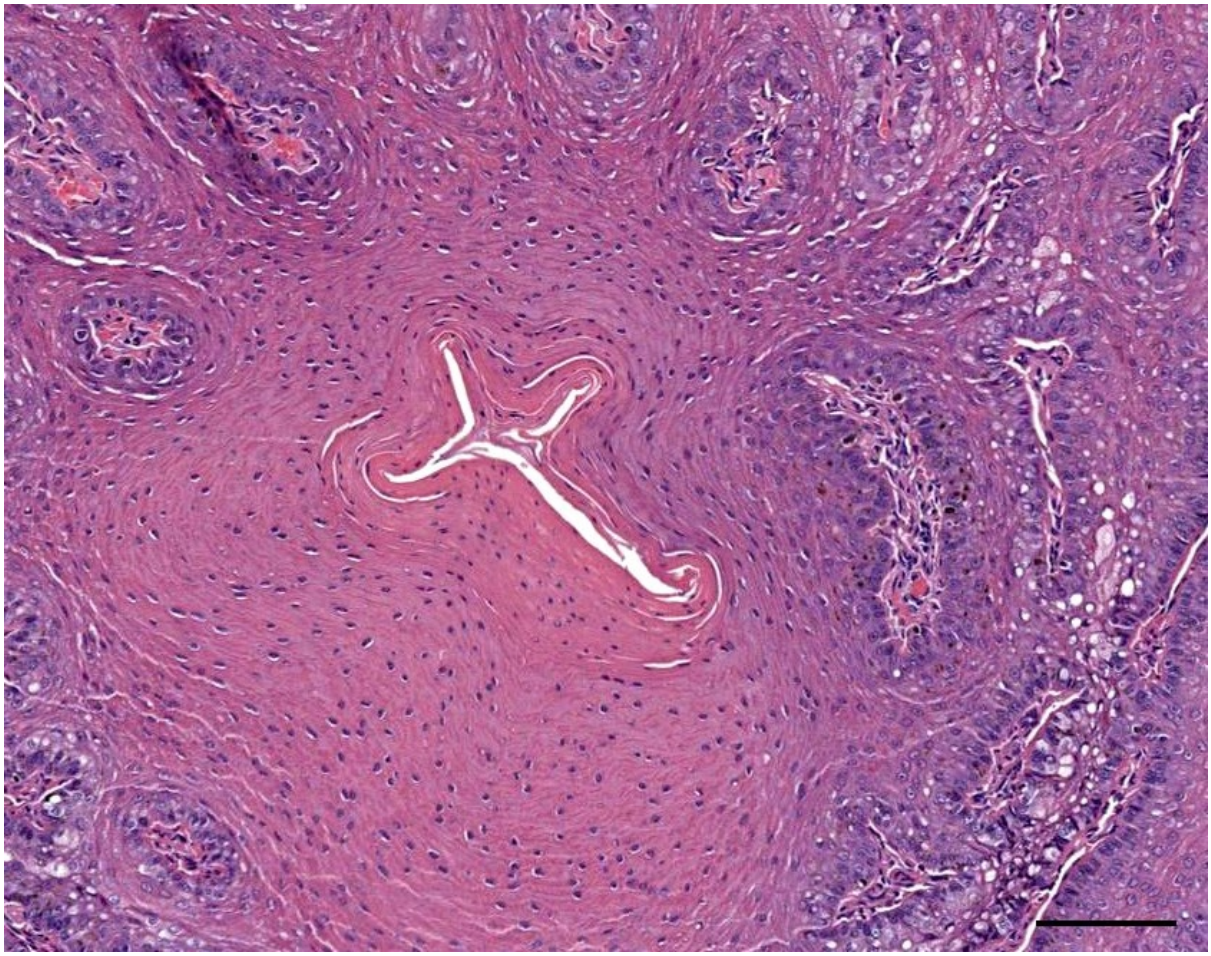

Figure 467. Detail of Figure 463. Histological transverse section (HE) of the medial end of the external ear opening. Note the very small lumen. Scale bar 0.1 mm.

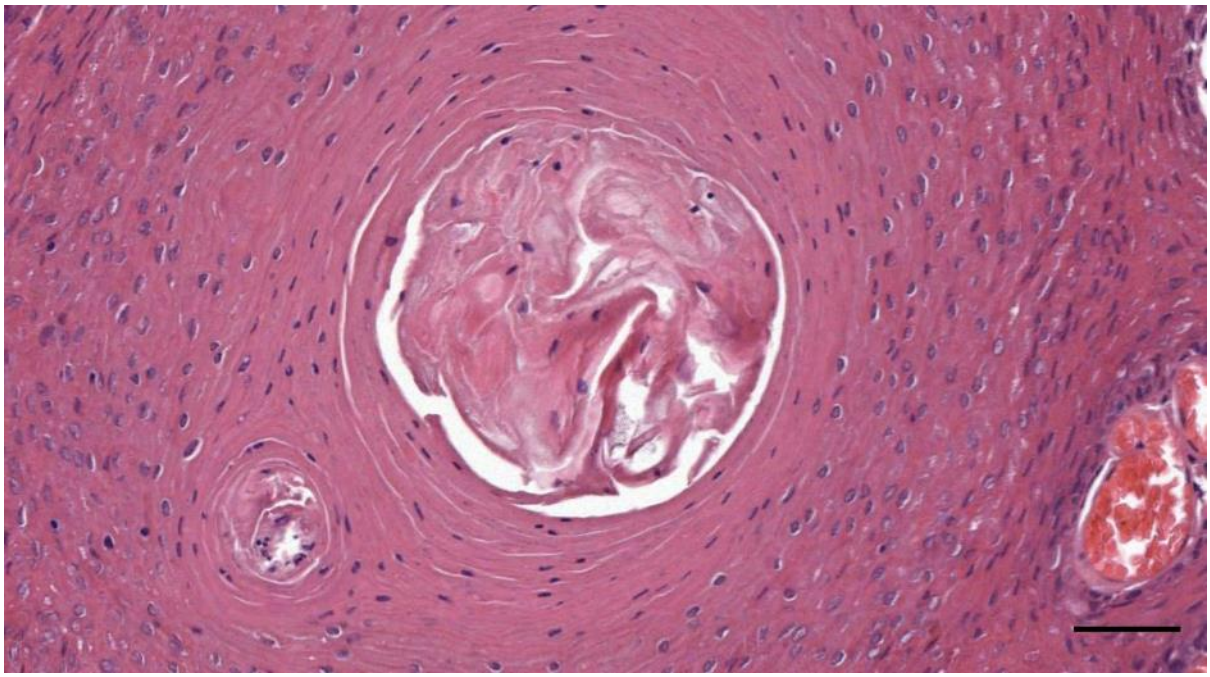

Figure 468. (274/18_L1) Artificial lumen filled with desquamated epithelial cells. Scale bar 50 µm

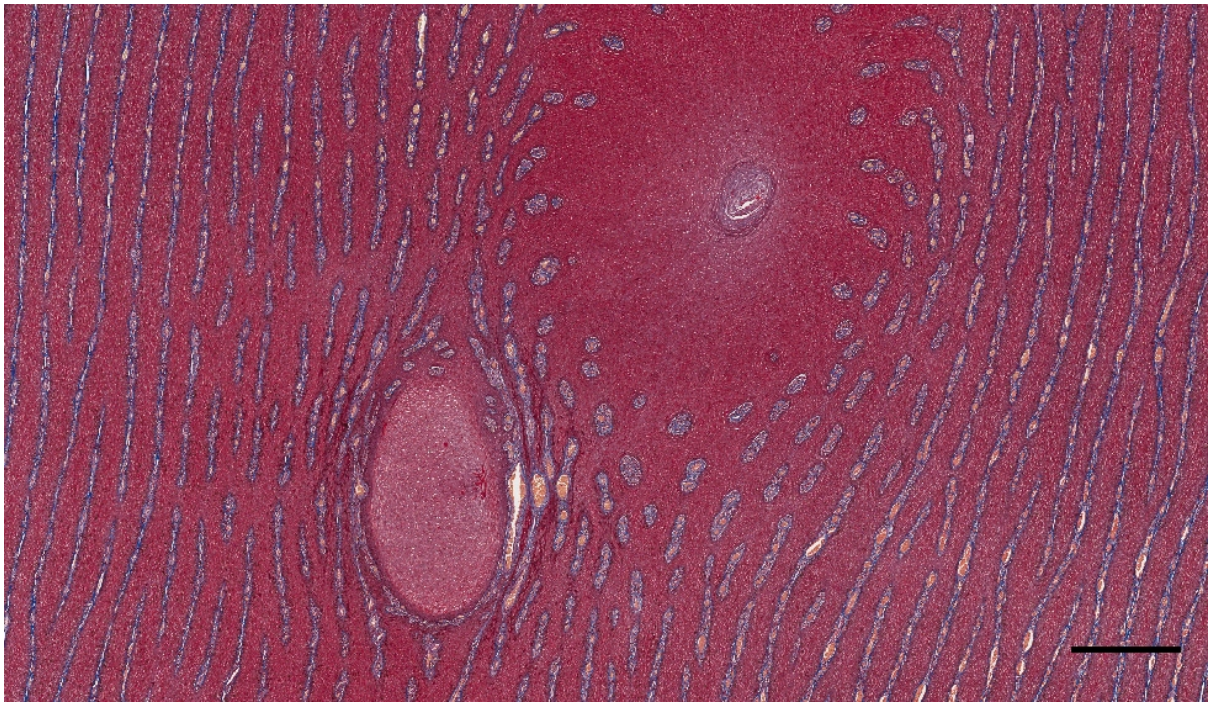

Figure 469. Histological image (Masson´s trichrome) of a transverse section through the right external ear opening in a harbour porpoise (UT1728R_0501). Scale bar 500 µm

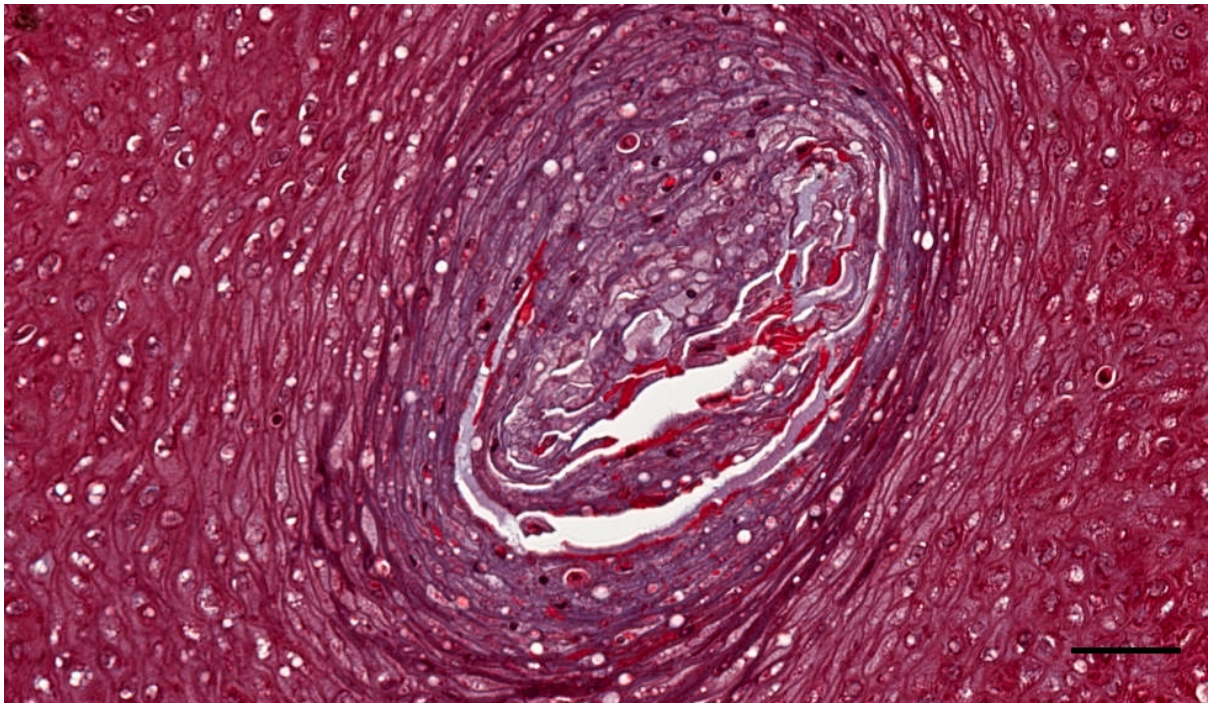

Figure 470. Detail of Figure 469. Histological image (Masson´s trichrome) of a transverse section through the right external ear opening in a harbour porpoise (UT1728R_0501). Scale bar 50 µm

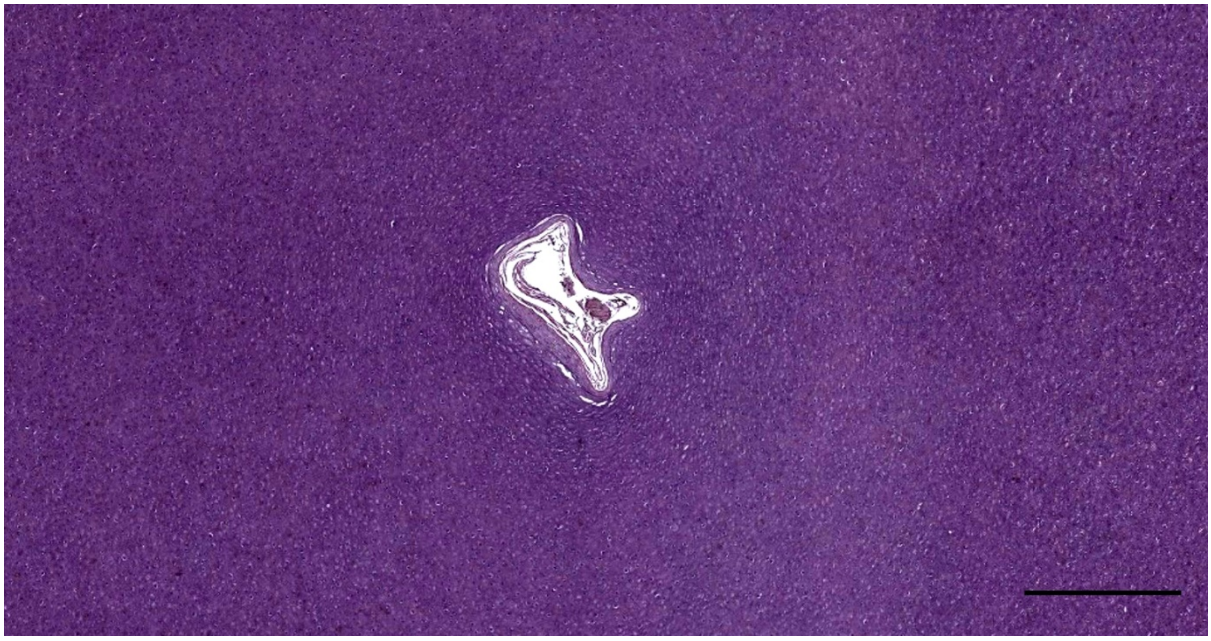

Figure 471. Histological image (HE) of a transverse section through the external ear opening of a harbour porpoise (UT1718_L0101). Scale bar 500 µm

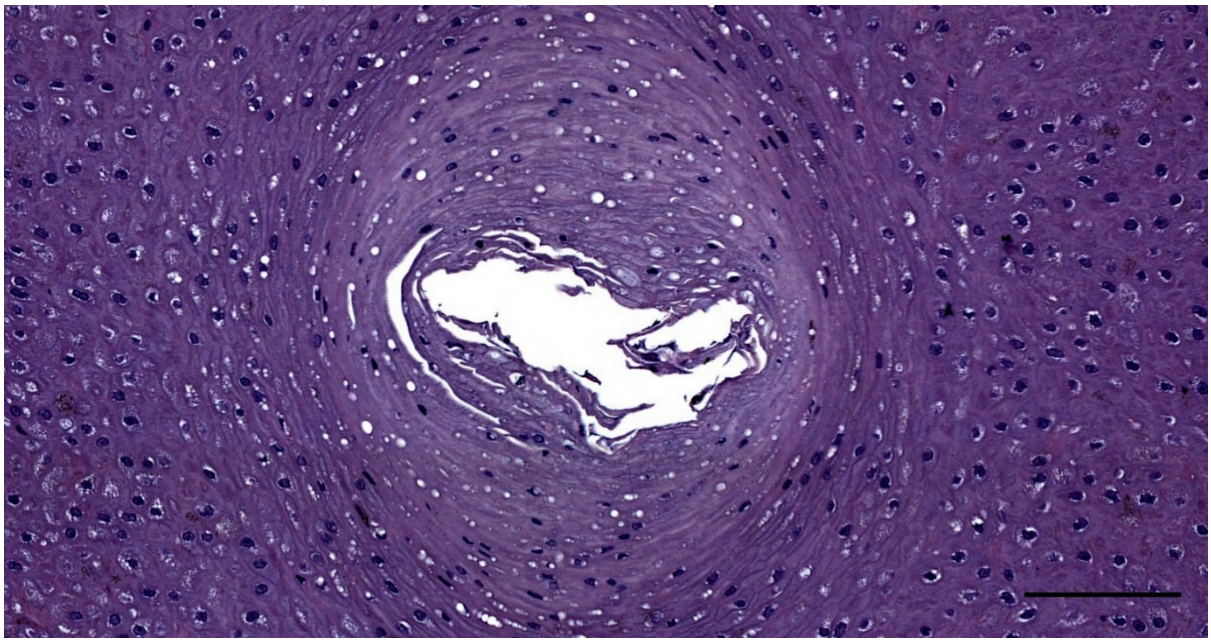

Figure 472. Detail ogf Figure 464. Small ear opening. Scale bar 100 µm

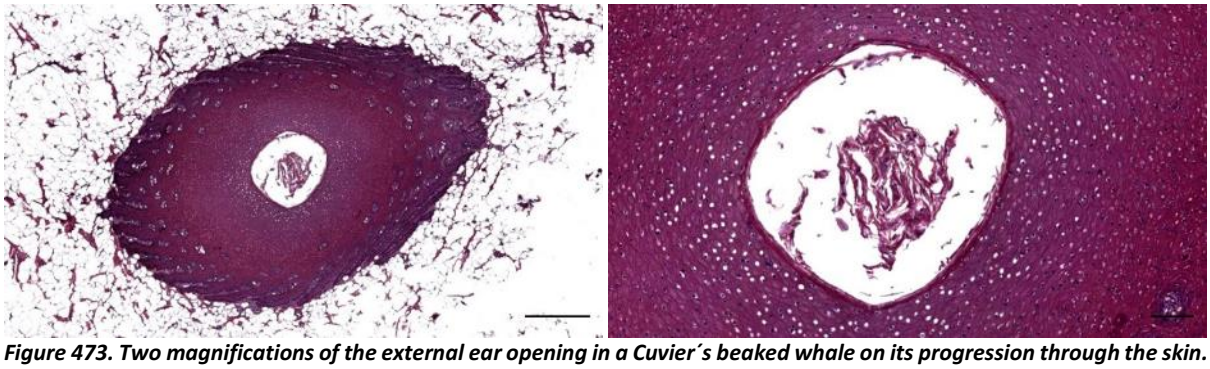

Figure 473. Two magnifications of the external ear opening in a Cuvier´s beaked whale on its progression through the skin. The lumen contains desquamated epithelial cells. Scale bars 500 µm left, 100 µm right

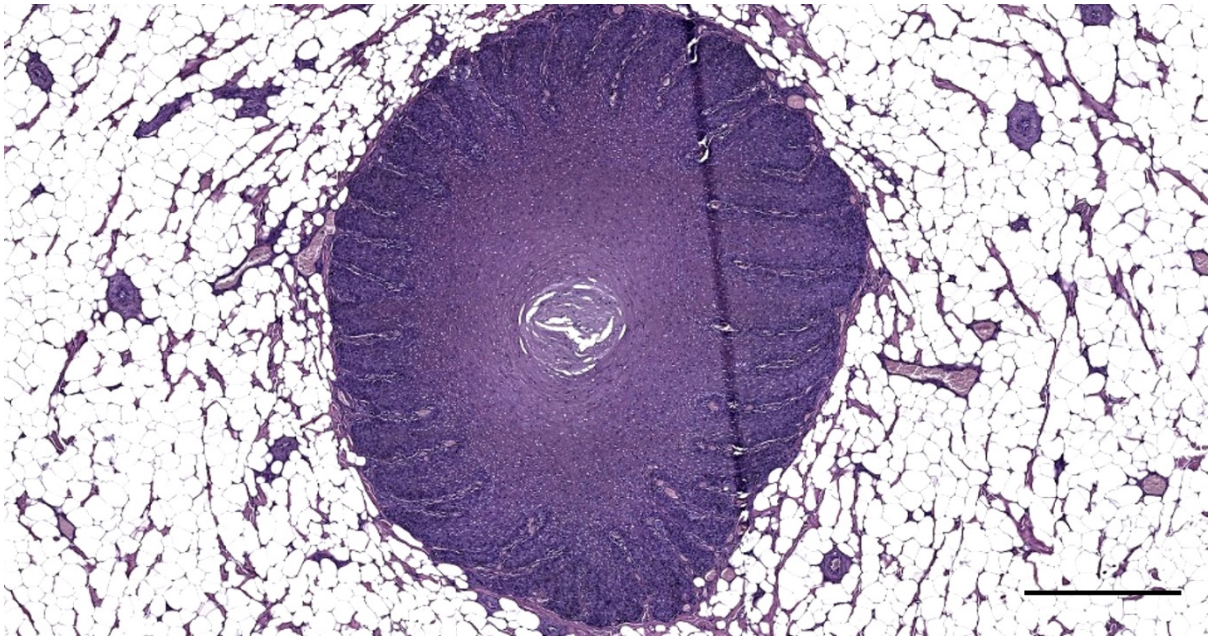

Figure 474. Histological image (HE staining) of a transverse section through the right ear canal of a harbour porpoise about 1 cm beneath the skin (UT1727_R0301). Artefacts in a possible artificial lumen. Scale bar 500 µm

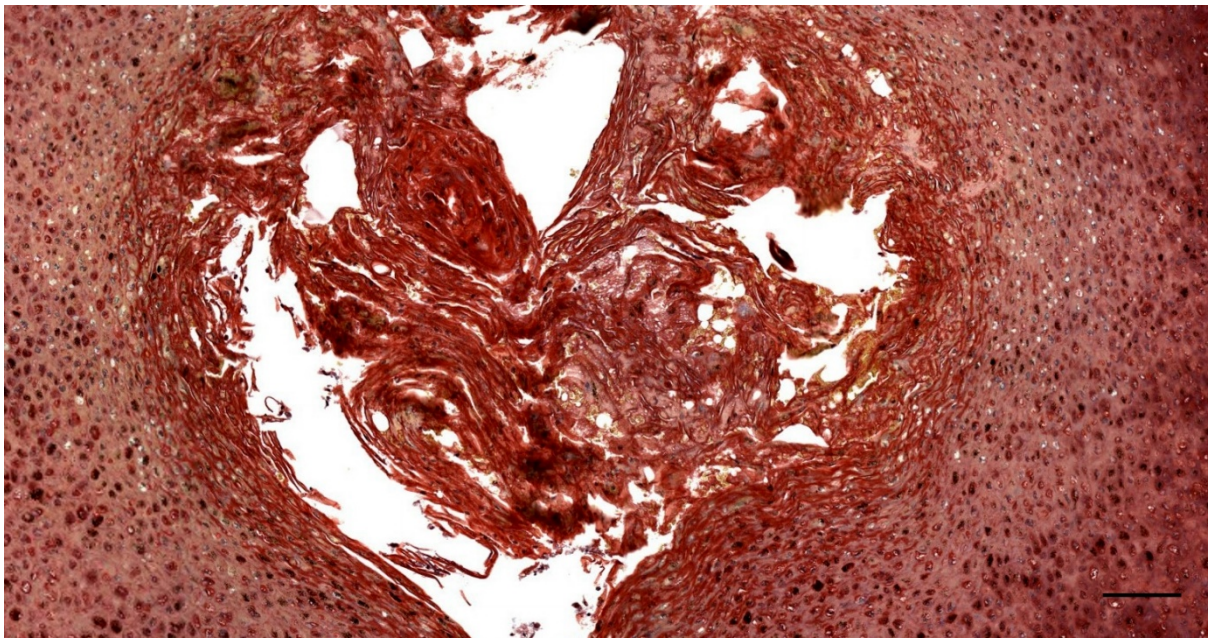

Figure 475. Histological image (Masson´s trichrome) of a transverse section through the external ear opening in a harbour porpoise (UT1711_R01_01). Scale bar 100 µm

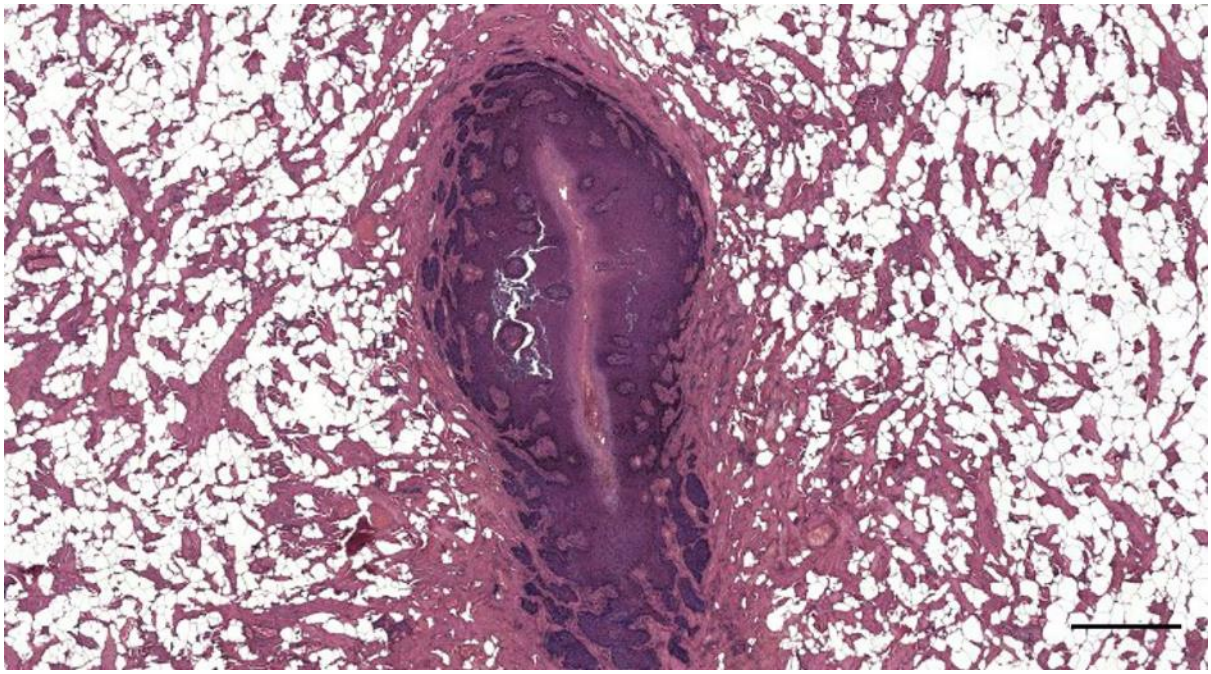

Figure 476. Histological image of a transverse section through the external ear canal in a striped dolphin at about 0.5 cm beneath the skin (ID292/18_L1). Scale bar 0.5 mm

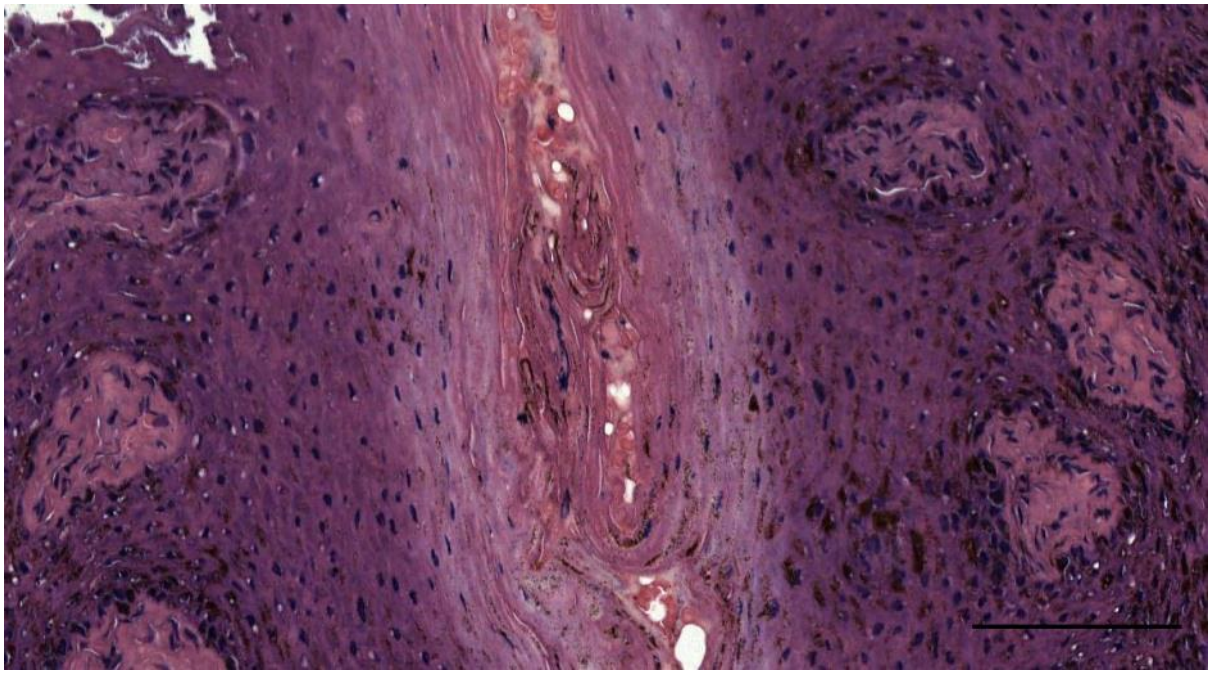

Figure 477. Detail of Figure 476. Note the artificial lumen and the presence of red blood cells. Scale bar 100 µm

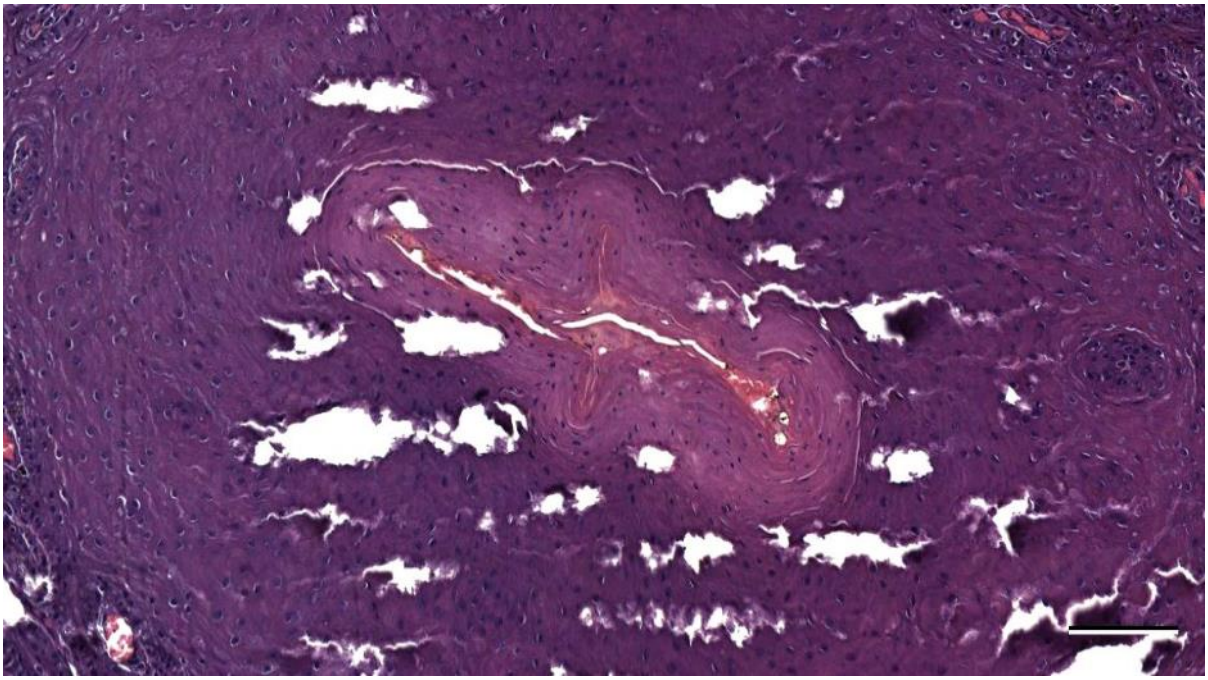

Figure 478. Histological image of a transverse section through the ear canal of a striped dolphin (44/17_R1)(HE staining). Ear canal lumen with red blood cells. Scale bar 100 µm

Figure 479. Histological image of a transverse section through the external ear opening in a striped dolphin (457_R1). Scale bar 100 µm

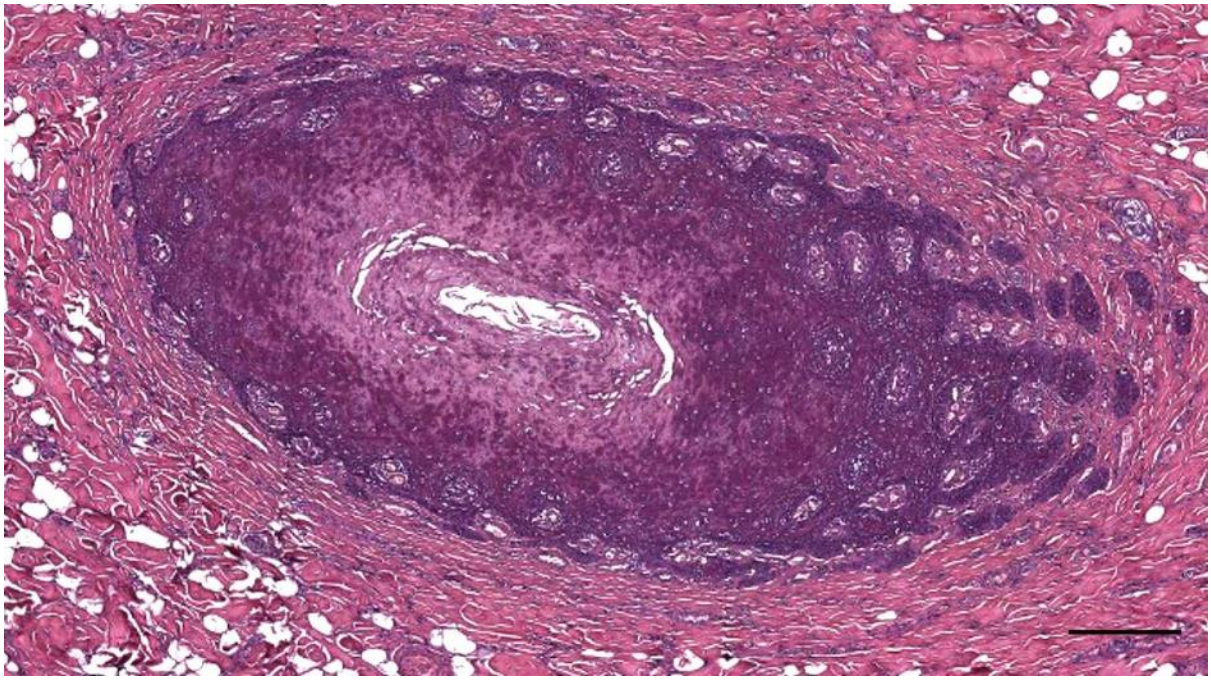

Figure 480. Histological image of a transverse section through the external ear opening in a striped dolphin (457_R2). A section about 5 mm medial to Figure 479. Scale bar 250 µm

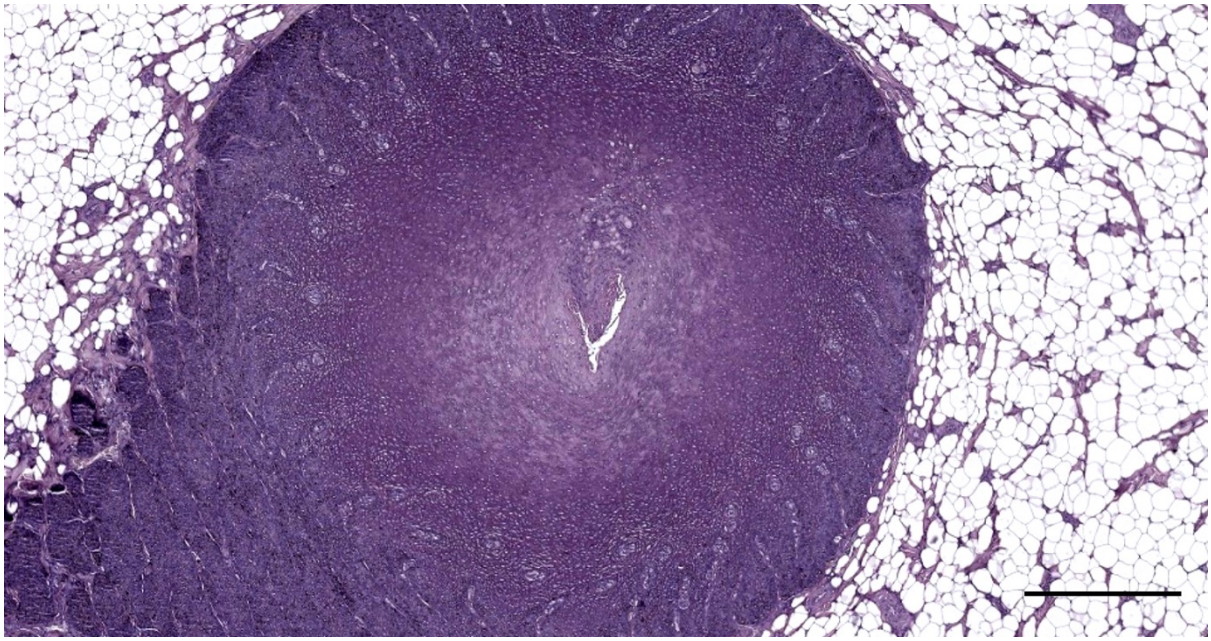

Figure 481. Histological image (HE) of a transverse section through the external ear canal of a harbour porpoise, immediately beneath the skin (UT1718_L0201). Scale bar 500 µm

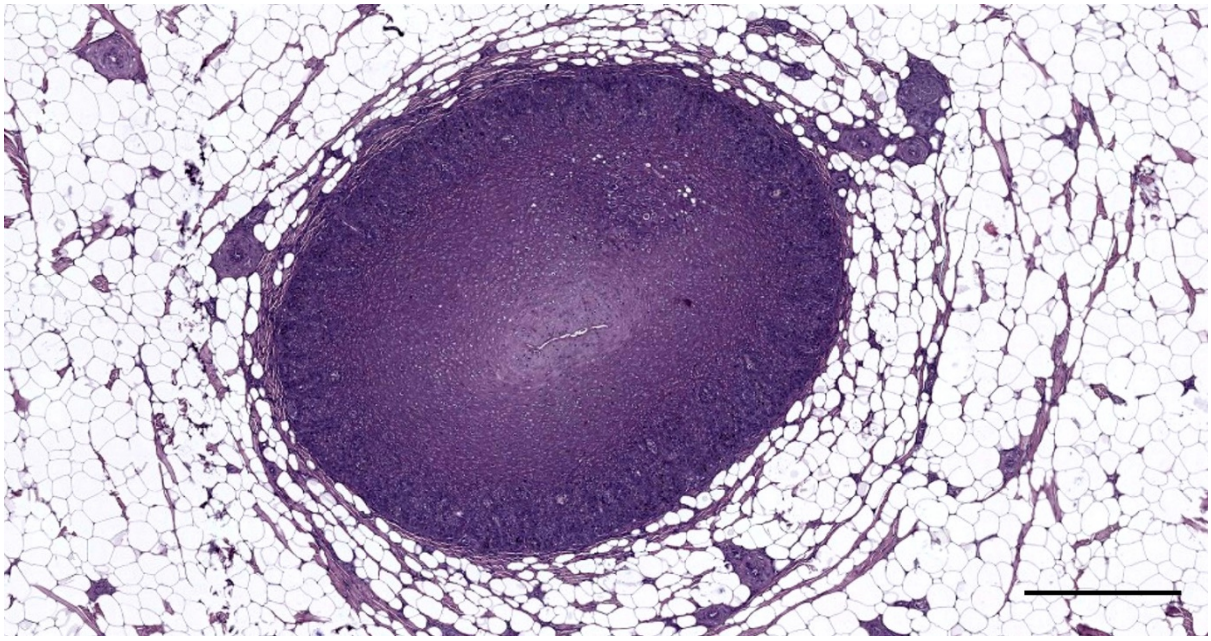

Figure 482. Histological image (HE) of a transverse section through the external ear canal of a harbour porpoise, about 1 cm beneath the skin (UT1718_L0301). Scale bar 500 µm

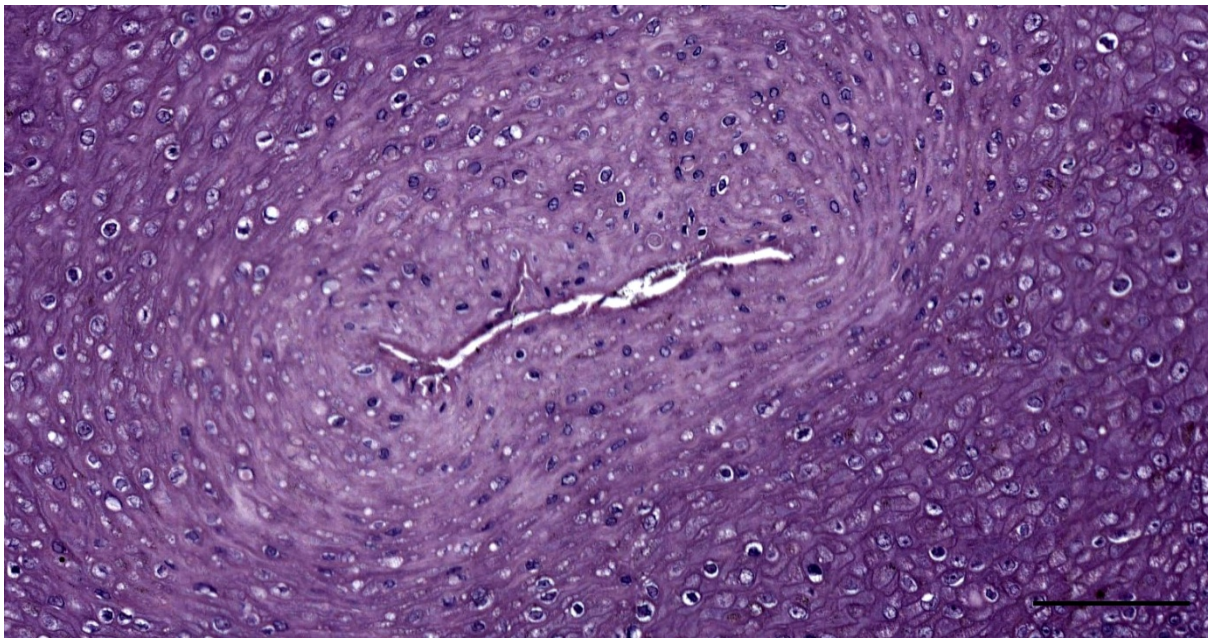

Figure 483. Histological image (HE) of a transverse section through the external ear canal of a harbour porpoise, about 1 cm beneath the skin (UT1718_L0302). Scale bar 100 µm

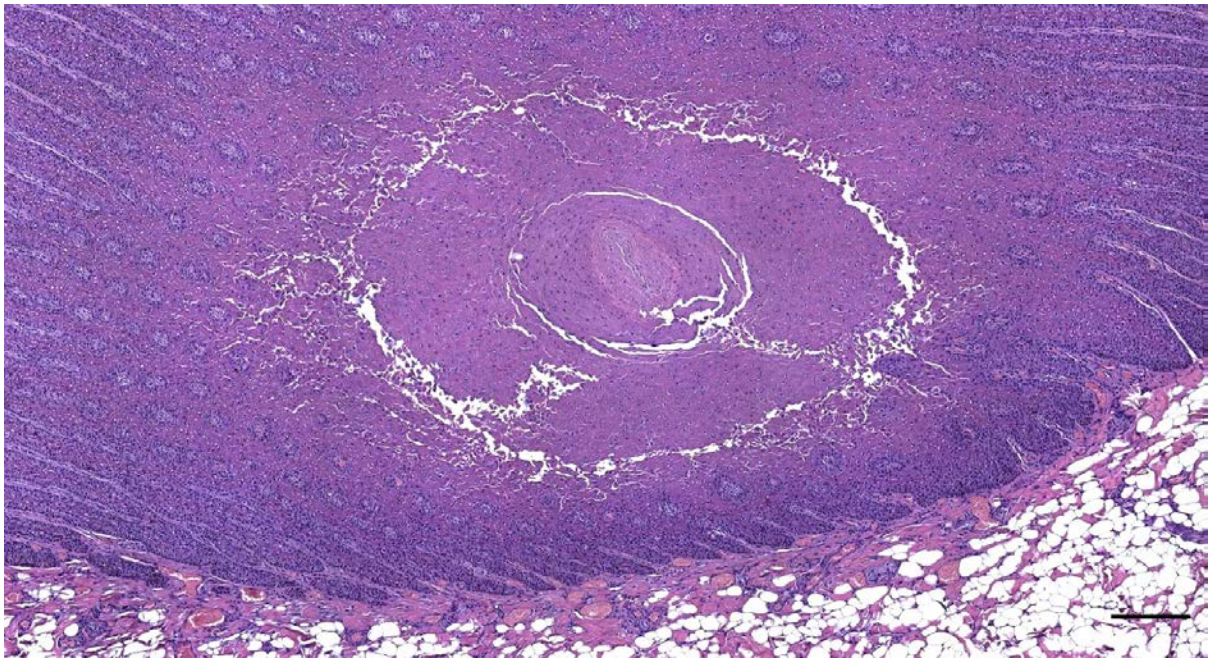

Figure 484. Histological image (HE staining) of a transverse section through the ear canal at the level of the external ear opening in a harbour porpoise (UT1709). Artificial lumen in the skin indent of the external ear opening. Scale bar 200 µm.

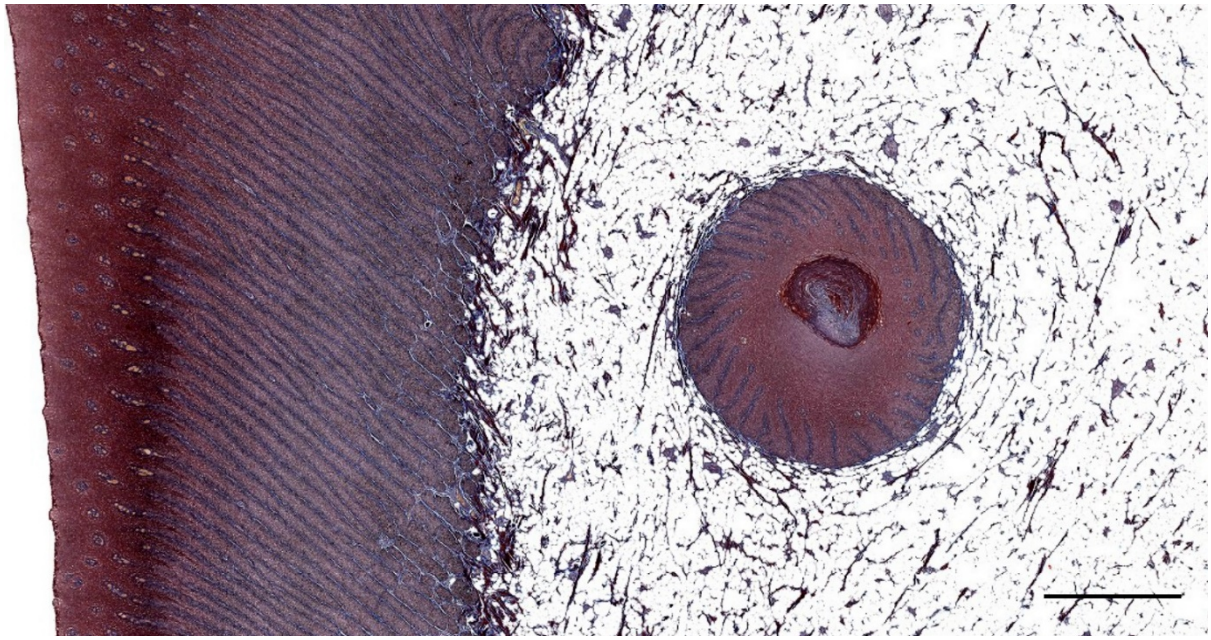

Figure 485. Histological image (Masson´s trichrome) of a transverse section through the external ear opening of a harbour porpoise (UT1718_R020501). Scale bar 1 mm

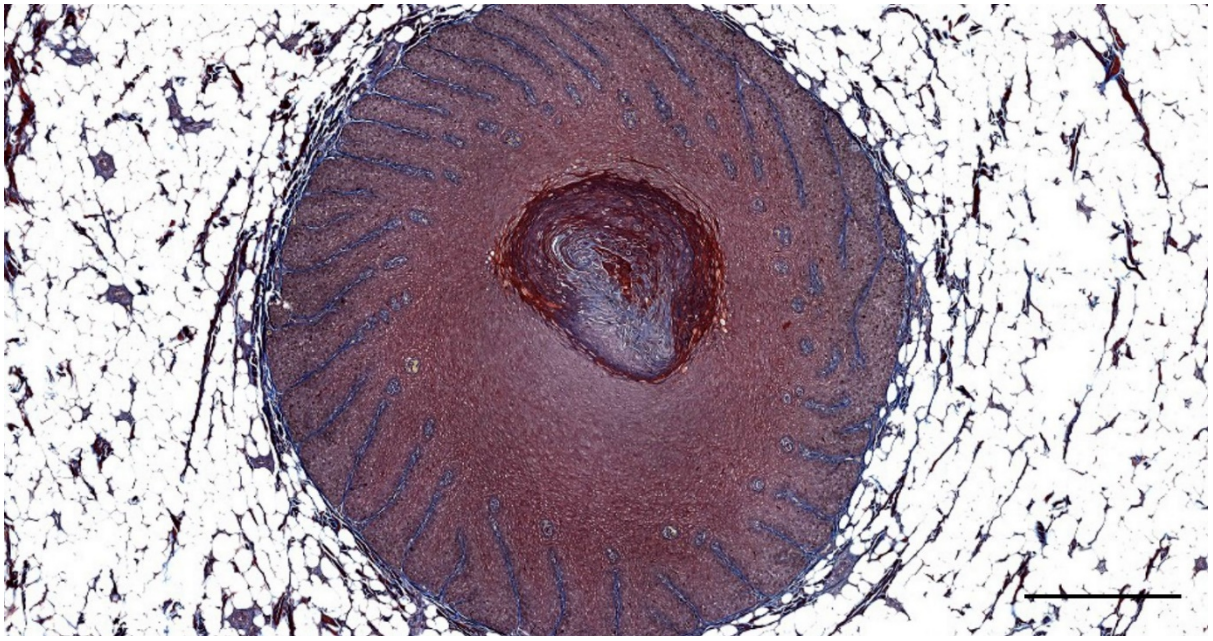

Figure 486. Detail of Figure 485. Histological image (Masson´s trichrome) of a transverse section through the external ear opening of a harbour porpoise (UT1718_R020502). Scale bar 500 µm

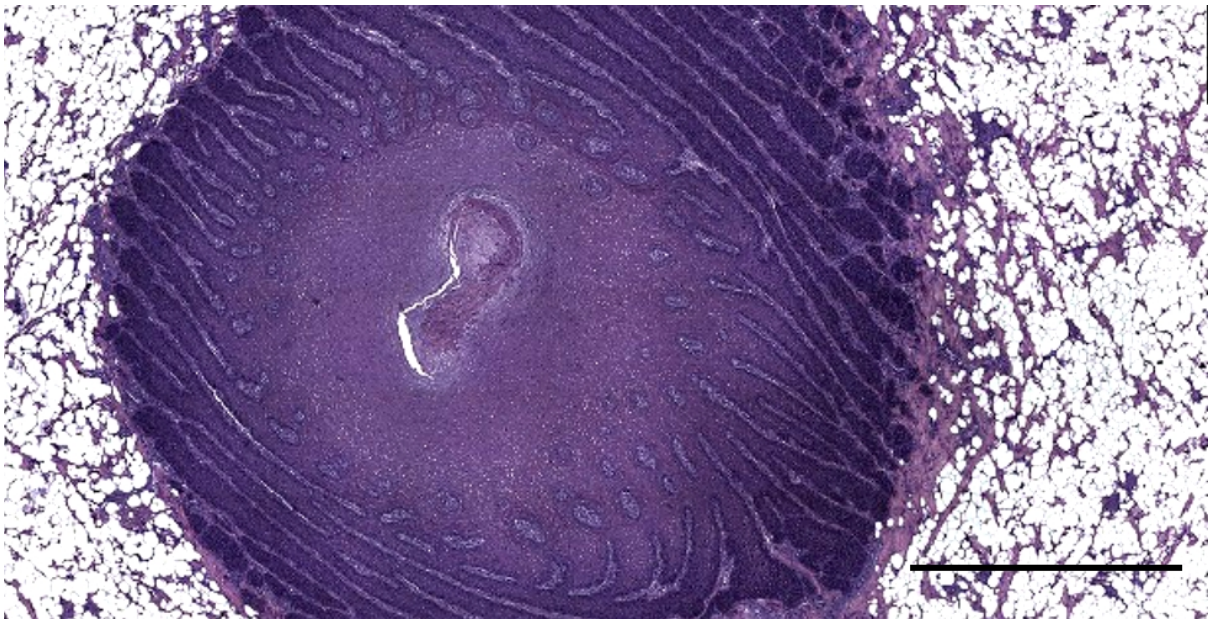

Figure 487. Histological image (HE staining) of a transverse section through the left external ear opening of a harbour porpoise (UT1734_L02). Scale bar 500 µm

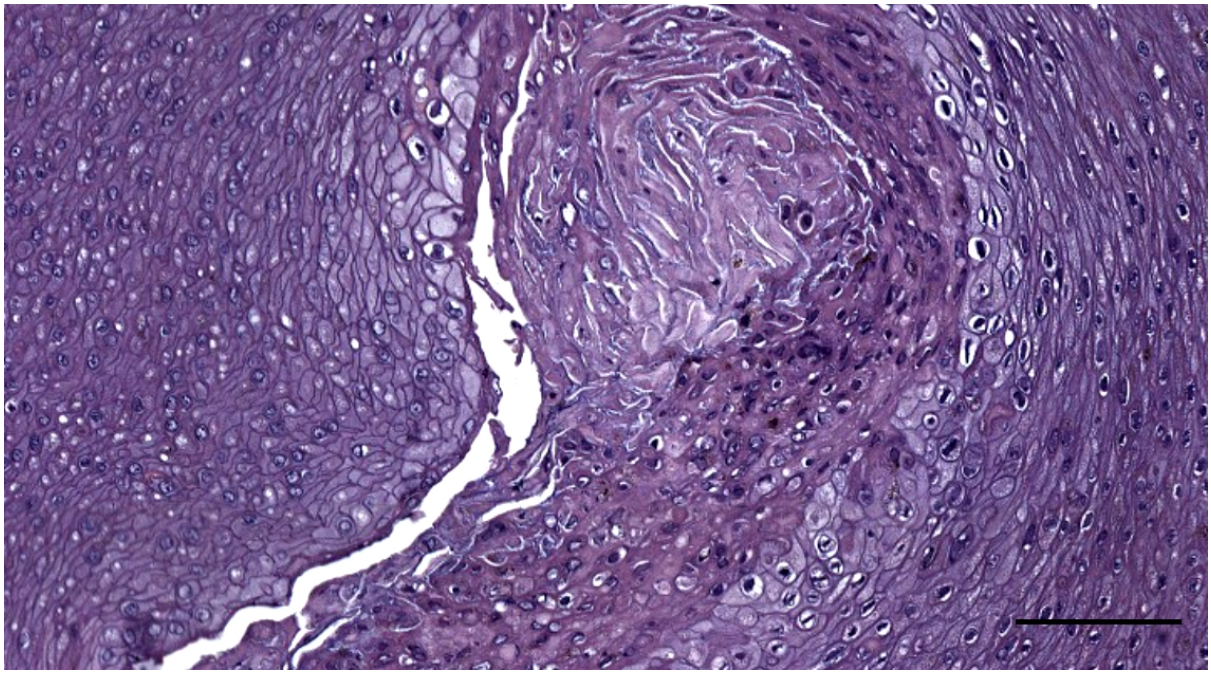

Figure 488. Detail of Figure 487. (UT1734_L02). Scale bar 100 µm

3.2.2 Lumen, content and epithelium

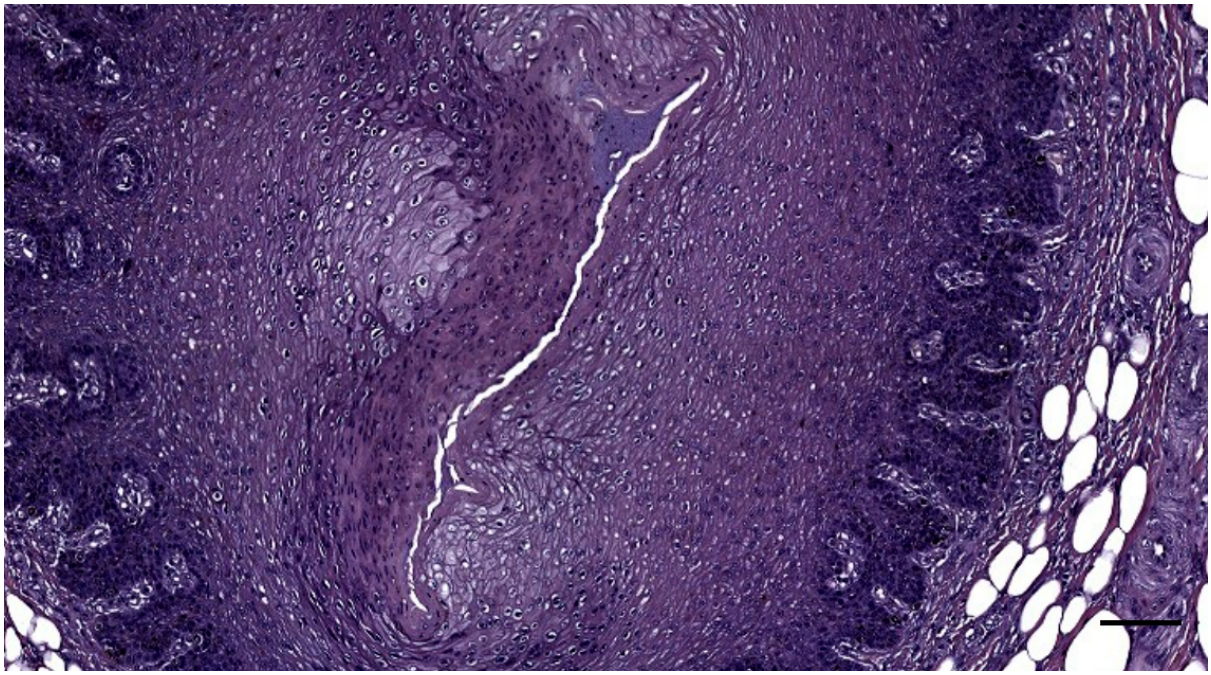

Figure 489. Histological image (HE staining) of a transverse section through the left external ear canal of a harbour porpoise at about 1 cm beneath the skin (UT1734_L03). Scale bar 100 µm

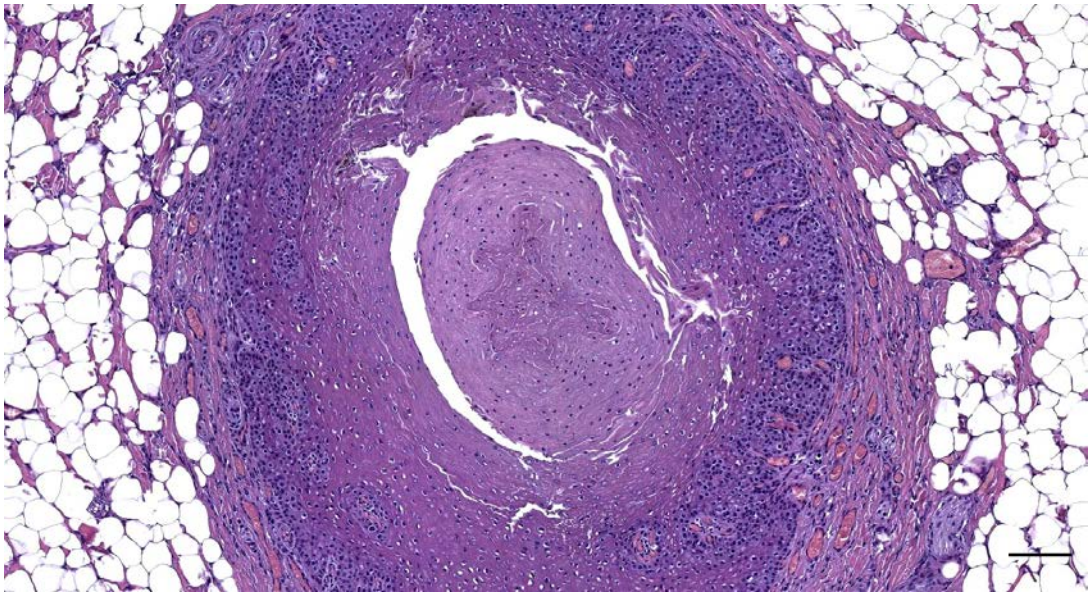

Figure 490. Histological image (HE staining) of a transverse section through the ear canal immediatly beneath the skin in a harbour porpoise (UT1709). Artificial lumen in the superficial blubber layer. Scale bar 100 µm.

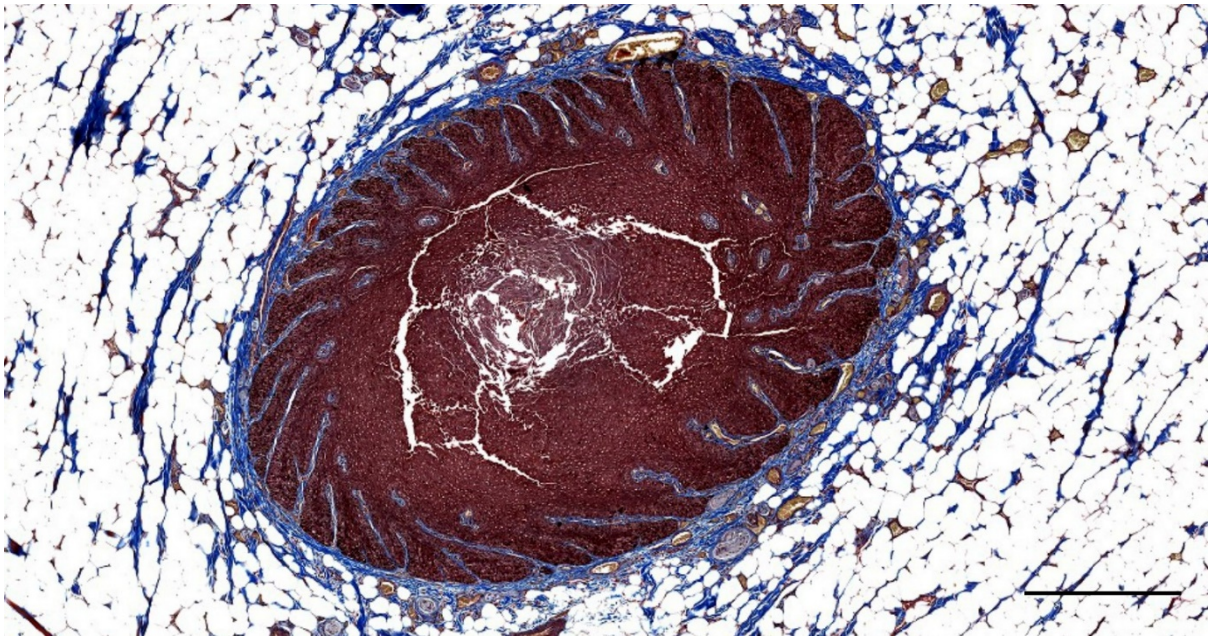

Figure 491. Histological image (Masson´s trichrome) of a transverse section through the external ear ear canal in a harbour porpoise, at about 0.5 cm beneath the skin. Scale bar 500 µm

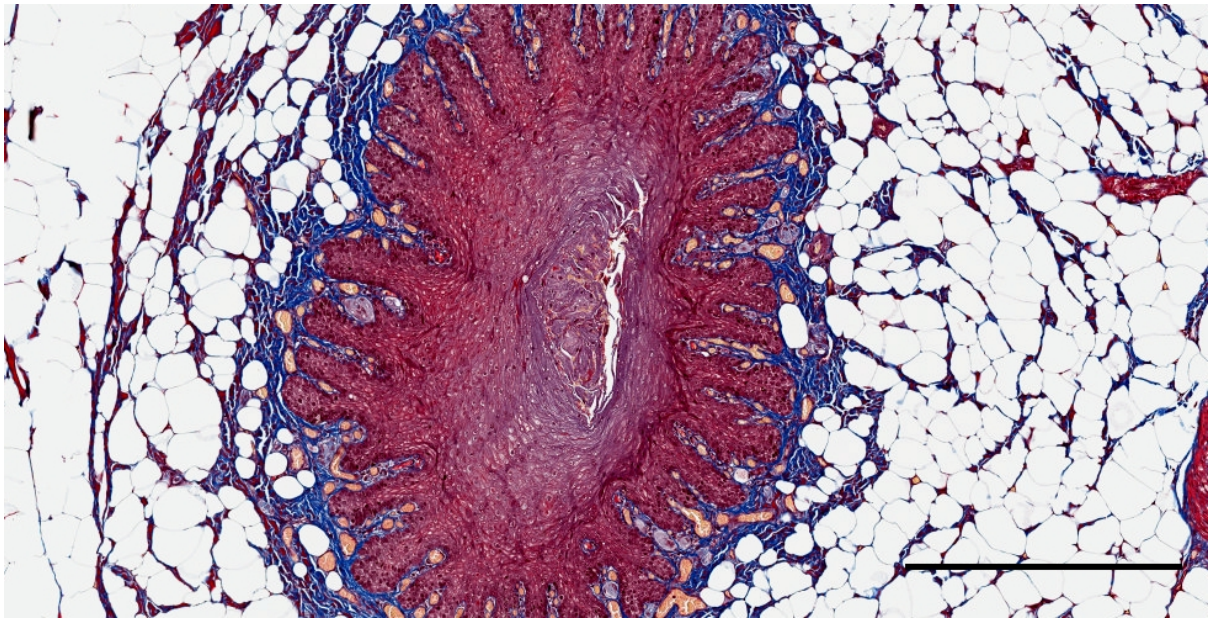

Figure 492. Histological image (Masson´s trichrome) of a transverse section through the right external ear canal in a harbour porpoise, about 0.5 cm beneath the skin (UT1728R_0205). Scale bar 500 µm

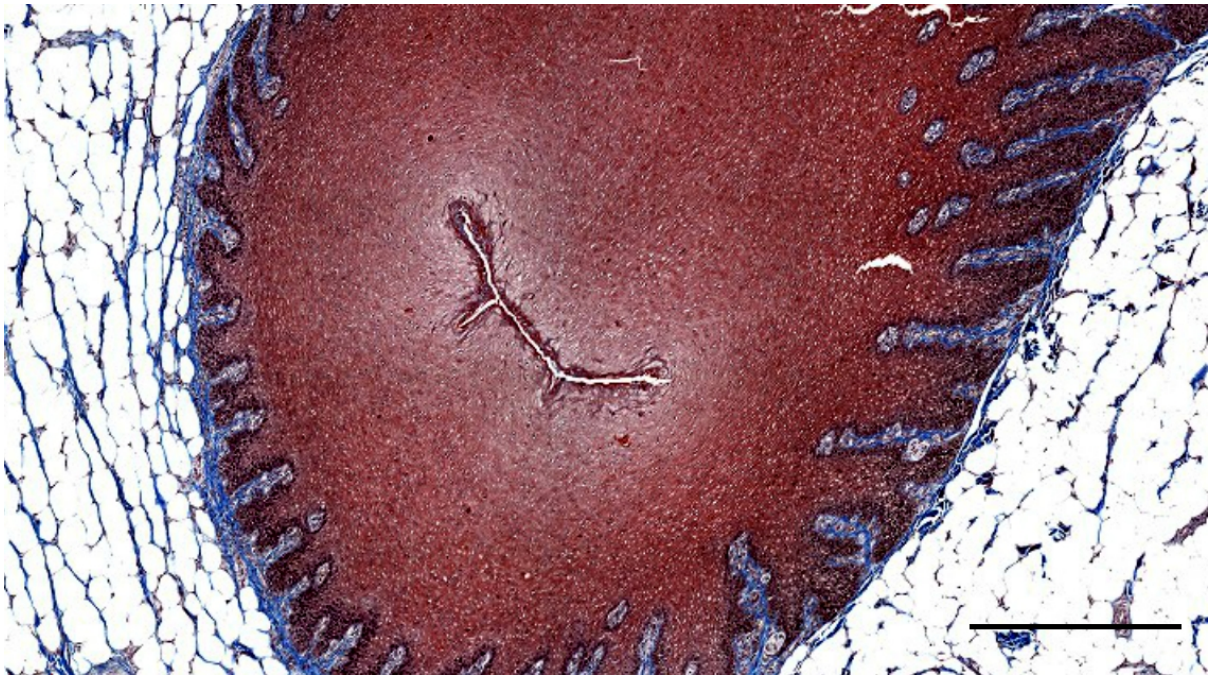

Figure 493. Histoligcal image (Masson´s trichrome) of a transverse section through the right external ear canal of a harbour porpoise at about 1 cm beneath the skin (UT1734_R0301). Scale bar 500 µm

Figure 494. Histological image (HE) of a transverse section through the ear canal of a harbour porpoise at about 0.5 cm beneath the skin (UT1712_R02). Scale bar 500 µm

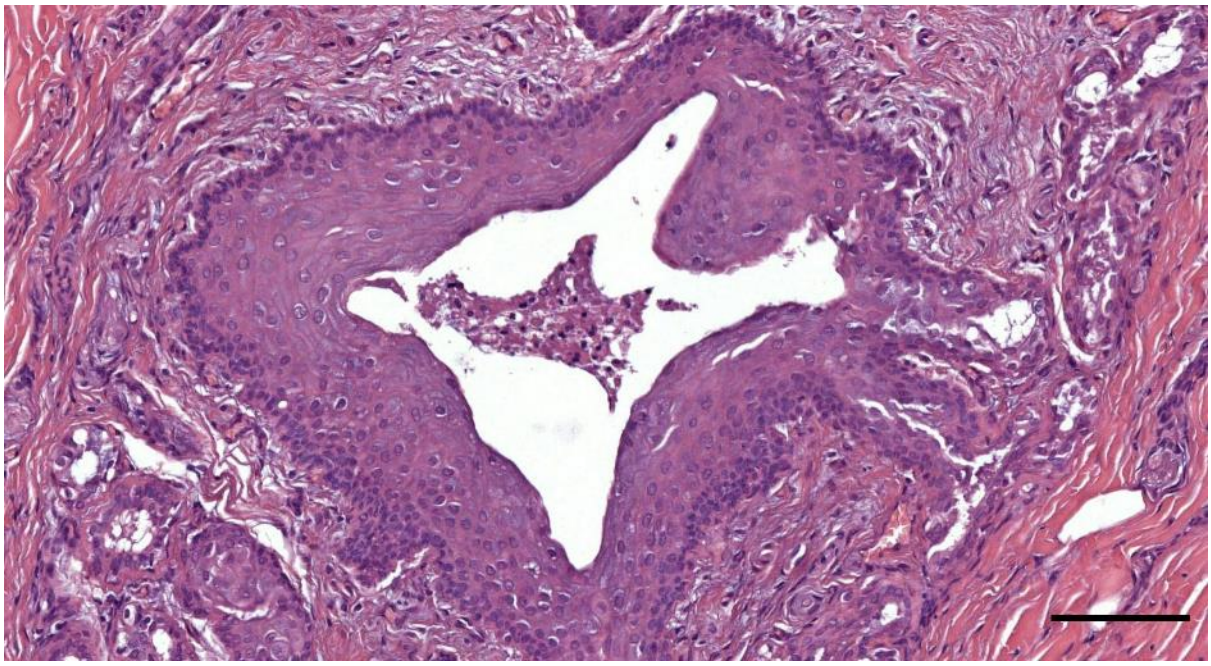

Figure 495. HE staining of a cross-section of the ear canal in a striped dolphin (ID232/17). The content of the ear canal consists of cells with pyknotic nuclei, probably pushed out of the glands and into the canal lumen through manipulation of the tissue or associated with an active stranding event. Scale bar 100 µm

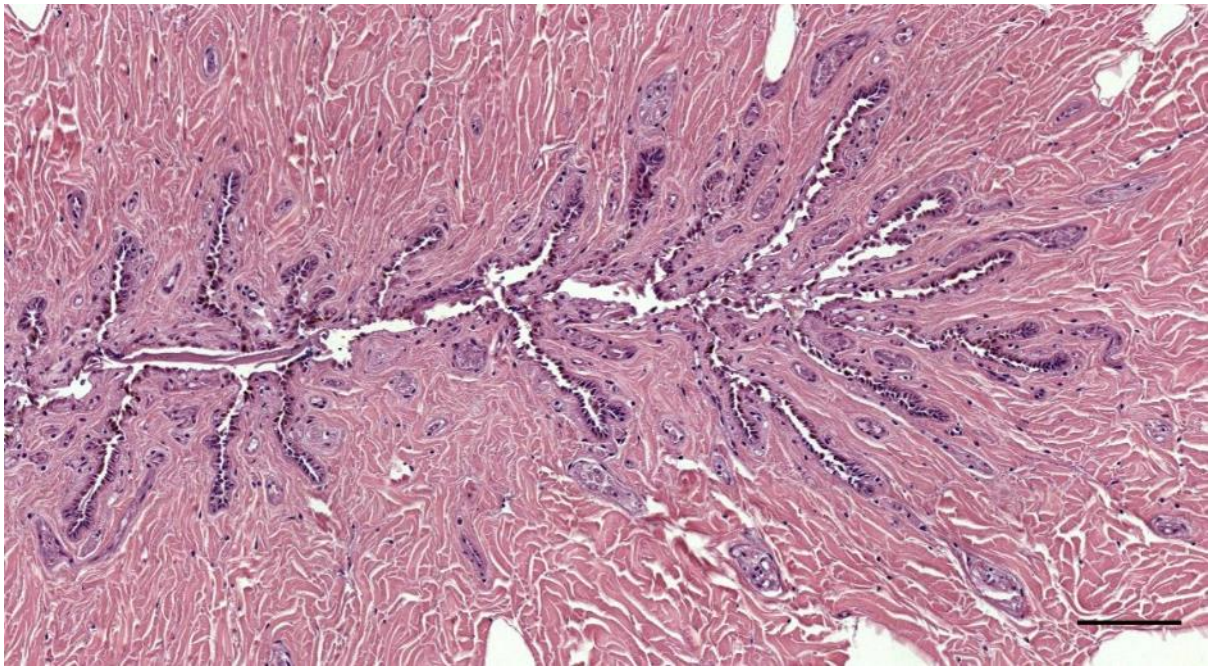

Figure 496. Histological transverse section through the external ear canal of a Cuvier´s beaked whale about 7 cm beneath the skin (177/19). Scale bar 100 µm.

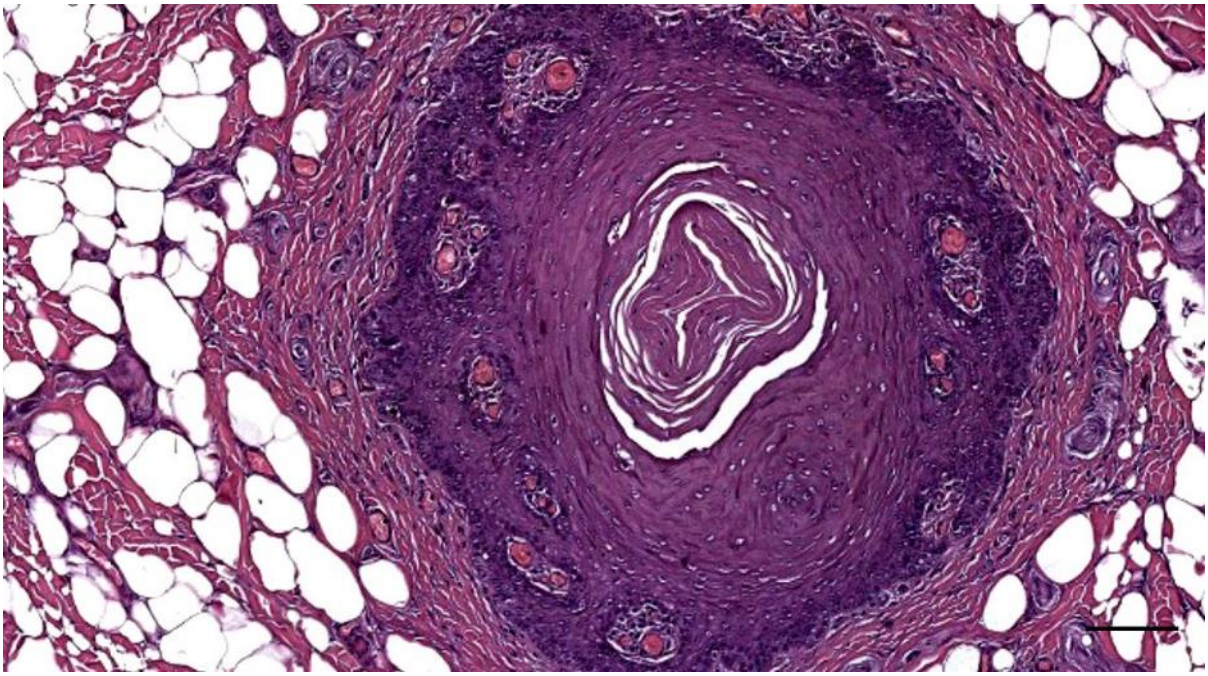

Figure 497. (509/17_L2) Artificial lumen in the superficial part of the blubber layer. Scale bar 100 µm.

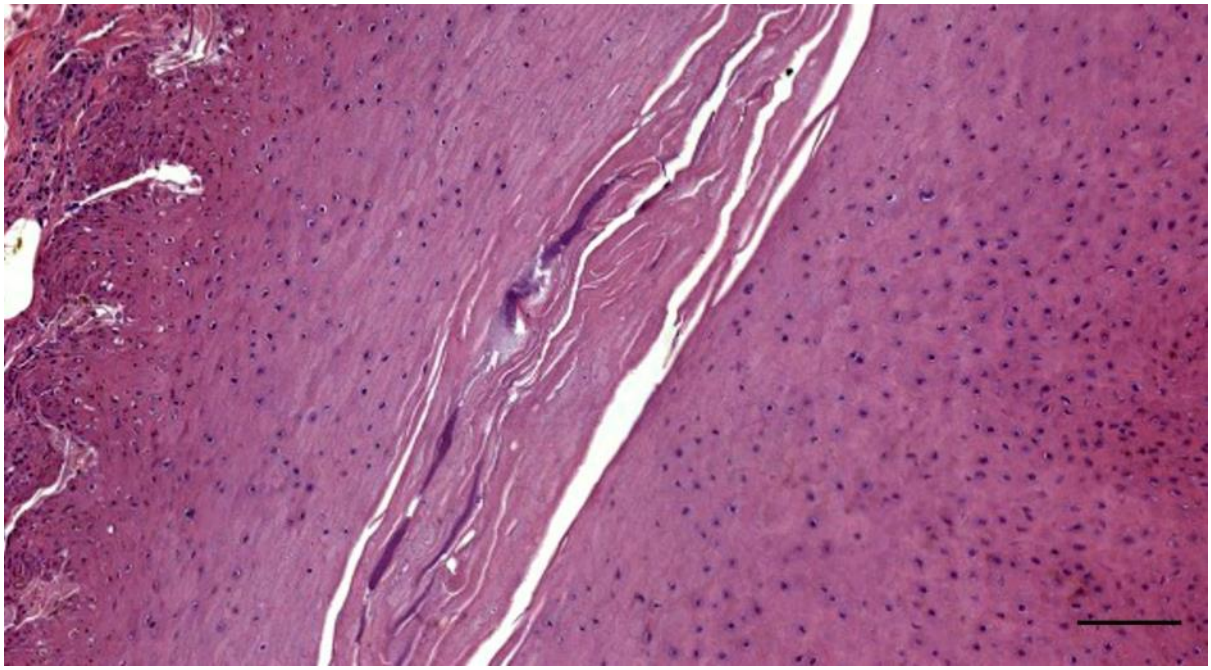

Figure 498. Histological transverse section through the external ear canal of a Cuvier´s beaked whale about 2 cm beneath the skin (177/19). Scale bar 100 µm

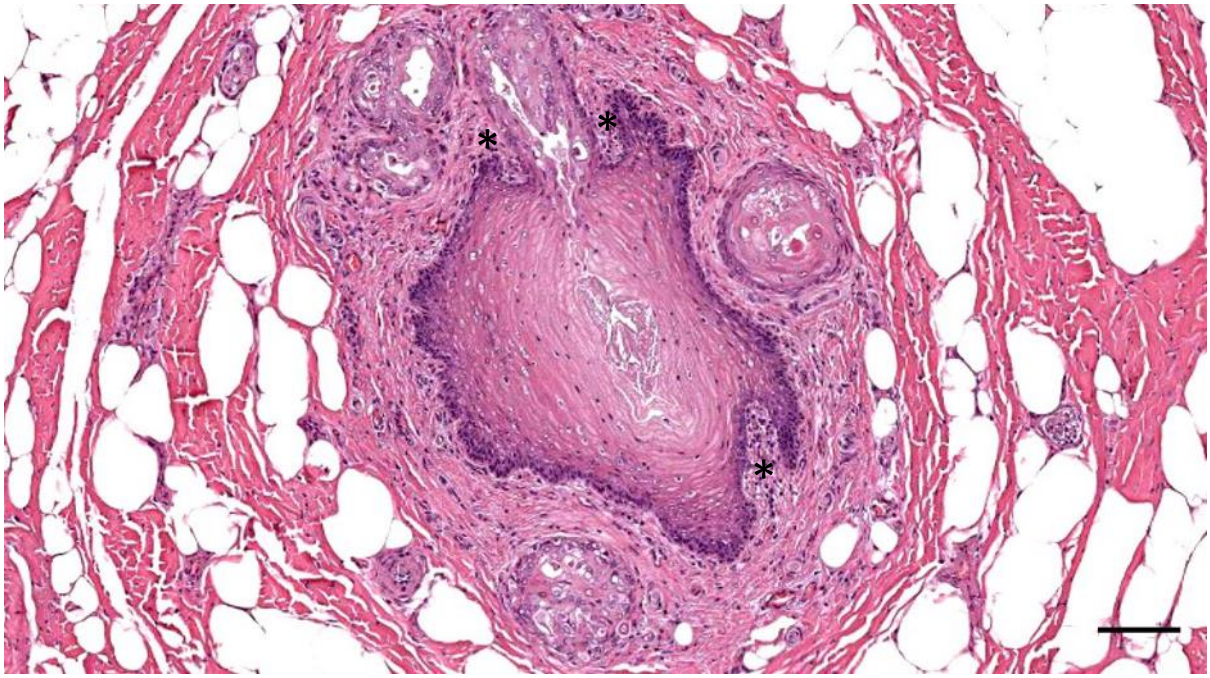

Figure 499. (274/18_L2) Artificial lumen at the level of the distal end of the glands and excretory ducts. Note the presence of mononuclear cells in the subepithelial layer (asterisks). Scale bar 50 µm

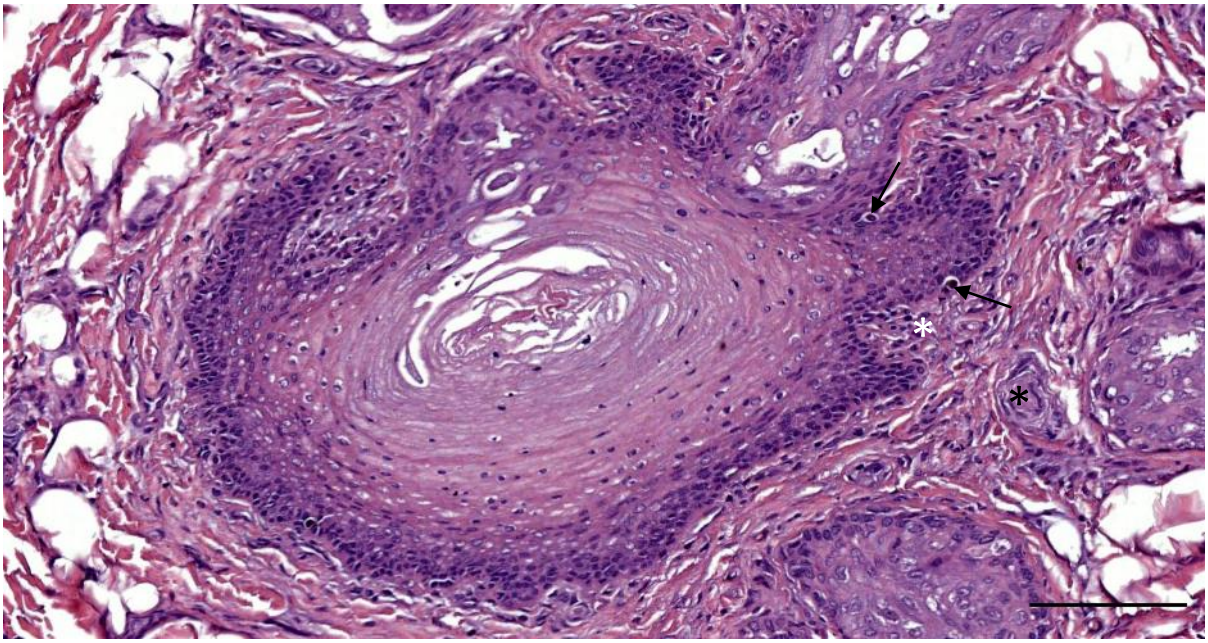

Figure 500. (274/18_R2) Artificial lumen with artefacts. Note the presence of glandular structures and an excretory duct penetrating the epithelium. Note the scant presence of mononuclear cells in the subepithelial layer (white asterisk). A corpuscle (black asterisk). There is also the possible presence of Merkel cells (arrows). Scale bar 100 µm

Figure 501. (77/18_R2) Artificial lumen filled with desquamated epithelial cells, and probable artefactual spaces. Scale bar 200 µm

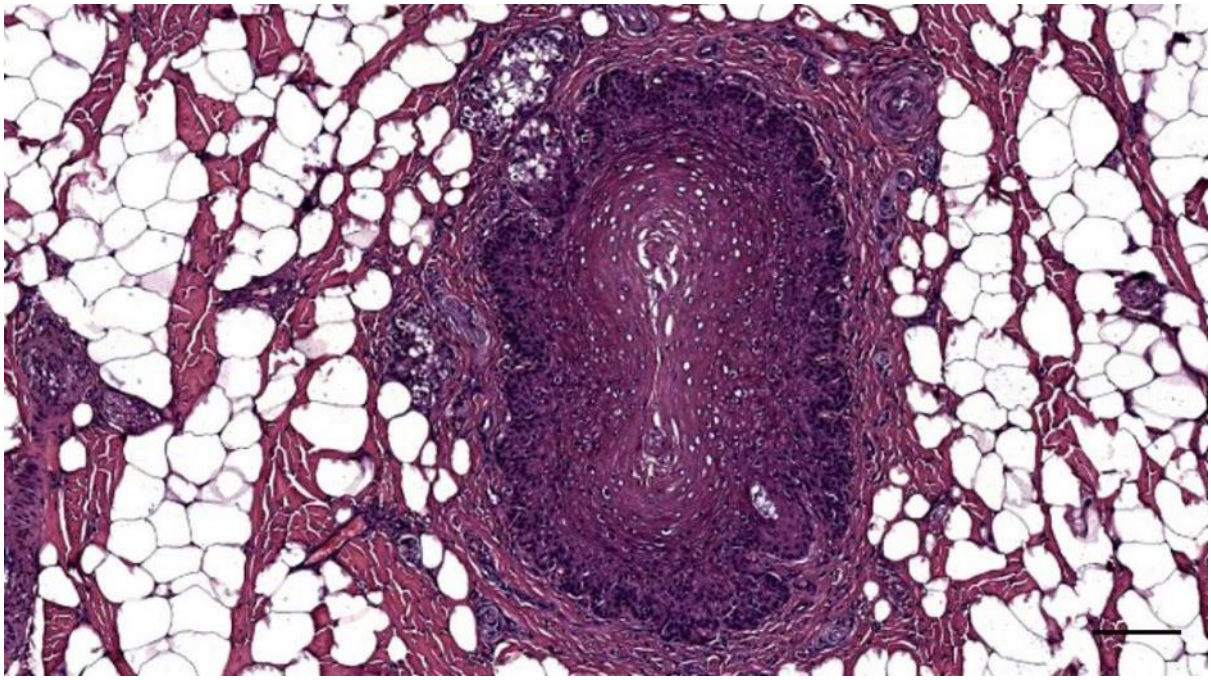

Figure 502. (449_L2) Ear canal cross-section with absent lumen and glands. Scale bar 100 µm

Figure 503. HE stained cross-section of the ear canal of a striped dolphin about 1 cm beneath the surface. The lumen is absent as the space is wholly taken up with stratum superficiale of the epithelium. The white spaces are likely artefacts of the preparation which disrupted the intercellular connections (Cfr. *Error! Reference source not found.* ***Top Middle). Beneath the epithelium, there is a loose connective tissue layer comprising lamellar corpuscles, and surrounding that there is a denser connective tissue layer containing fat cells, larger blood vessels, and nerves. Scale bar 100 µm***

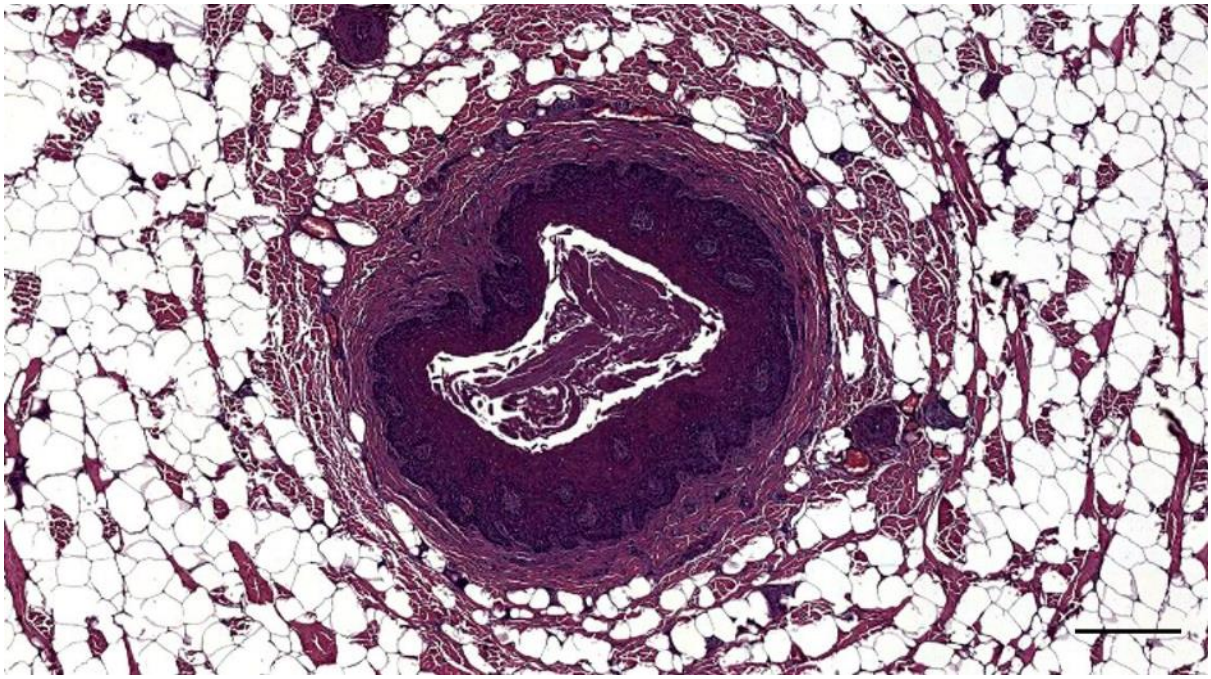

Figure 504. (44/17_L2, HE) Ear canal with intraluminal desquamated nucleated epithelial cells. Scale bar 100 µm

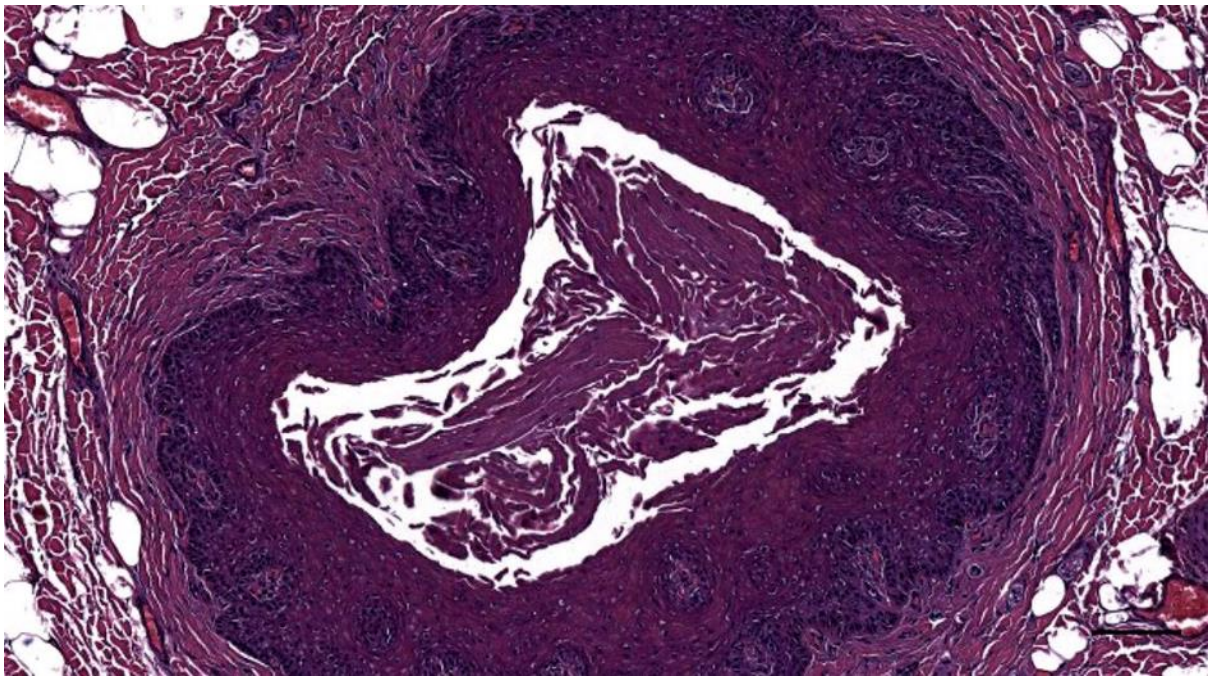

Figure 505. (44/17_L2, HE) Ear canal with intraluminal desquamated nucleated epithelial cells. Scale bar 100 µm

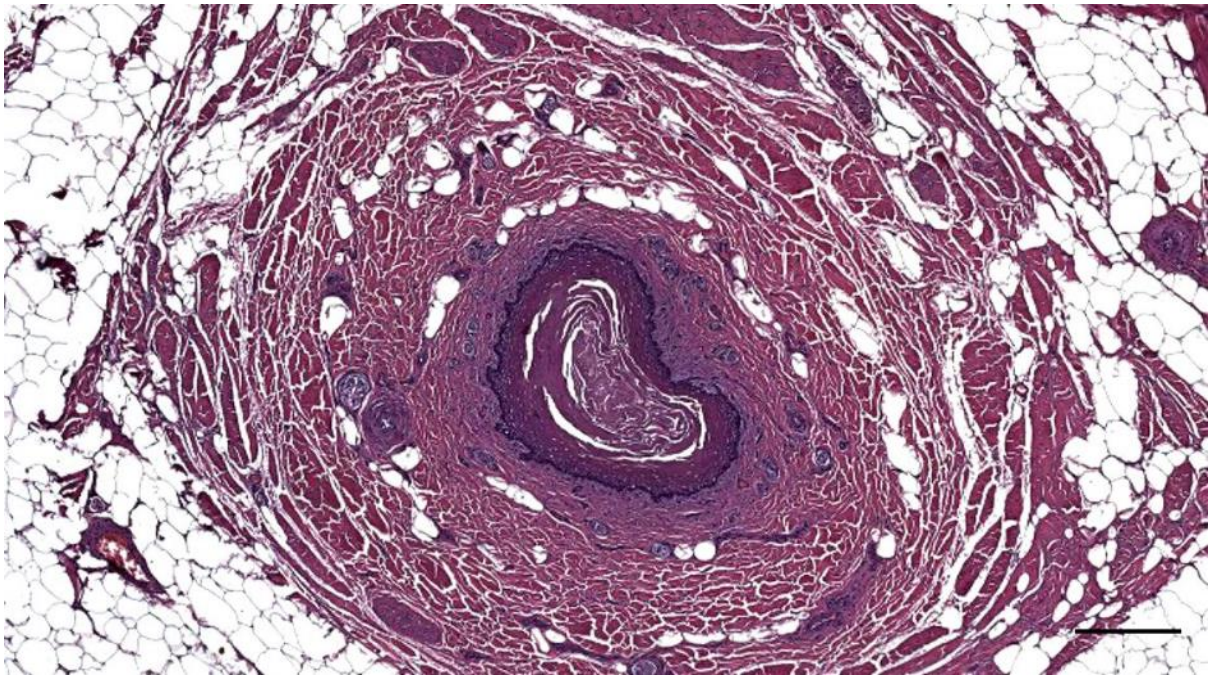

Figure 506. Histological transverse section through the ear canal of a striped dolphin (44/17_L3, HE) on its course through the blubber layer with intraluminal desquamated nucleated epithelial cells. Note the intense vasculature and innervation with the abundant presence of lamellar corpuscles in the superficial propria. The connective tissue around the canal gradually increases in size as the canal progresses towards the middle ear, and striated muscles insert into the connective tissue. Scale bar 100 µm

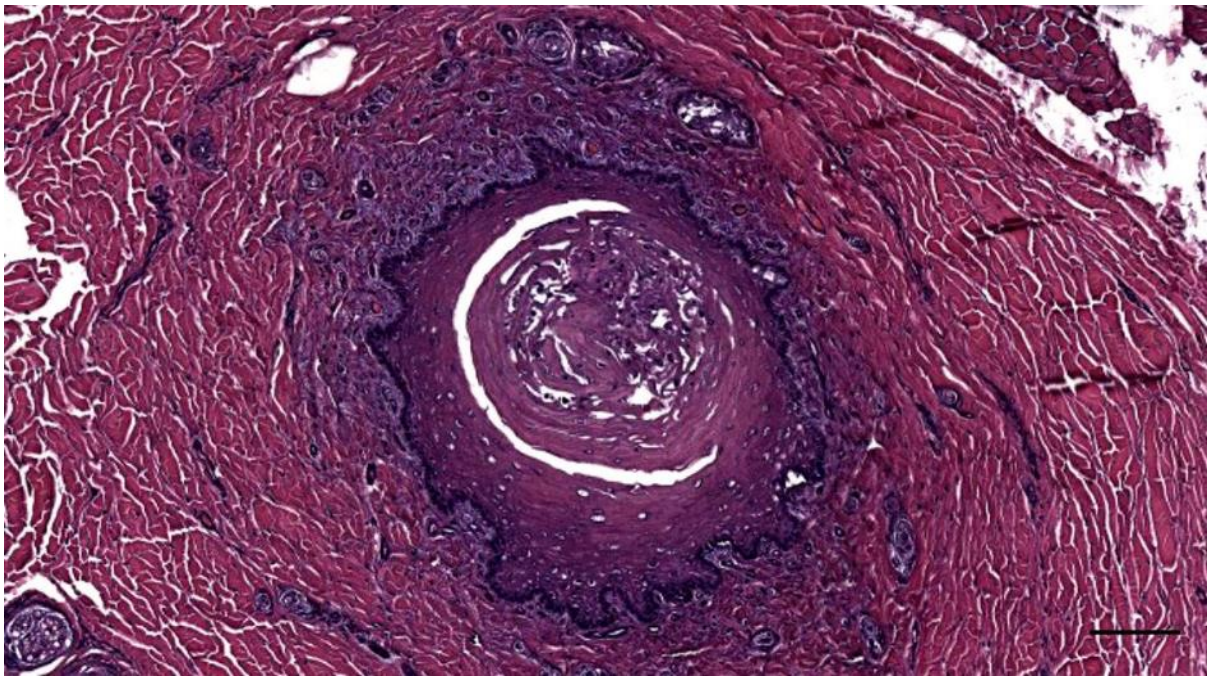

Figure 507. (ID44/17_L4, HE) Ear canal filled with keratine and desquamated epithelial cells. Scale bar 100 µm

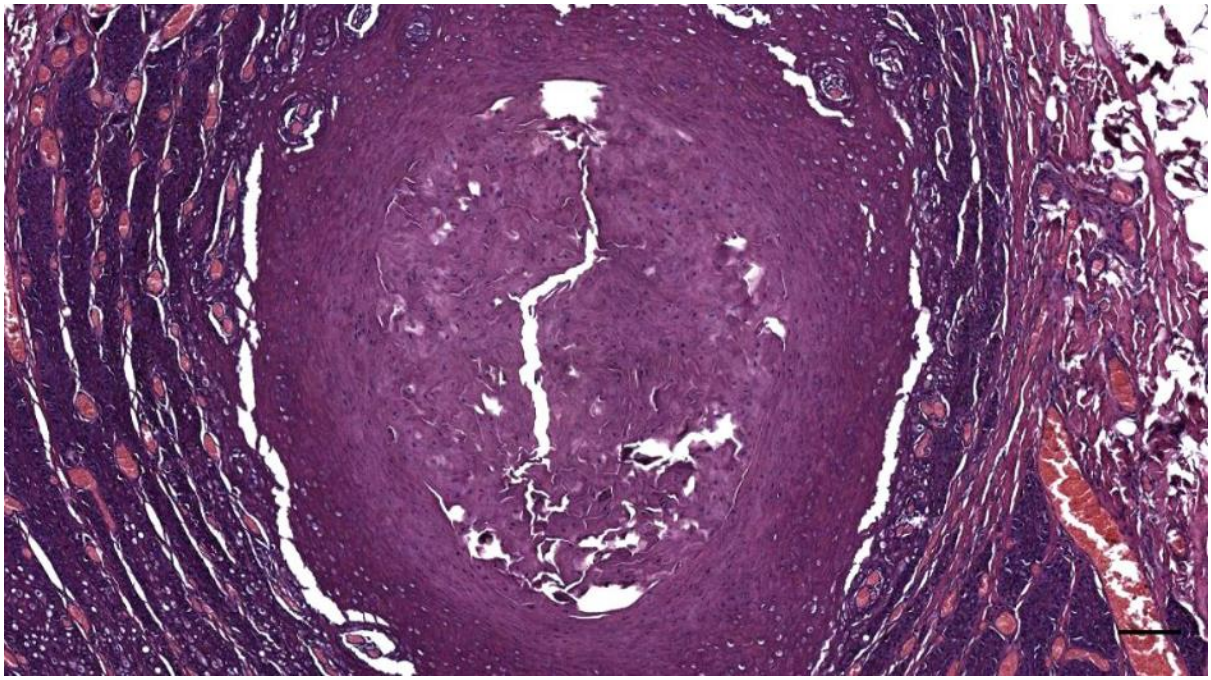

Figure 508. HE staining of a transverse section through the proximal end of the external ear opening of a striped dolphin (ID44/17). The lumen is almost filled with partially desquamated layers of incompletely keratinized epithelial cells. Scale bar 100 µm

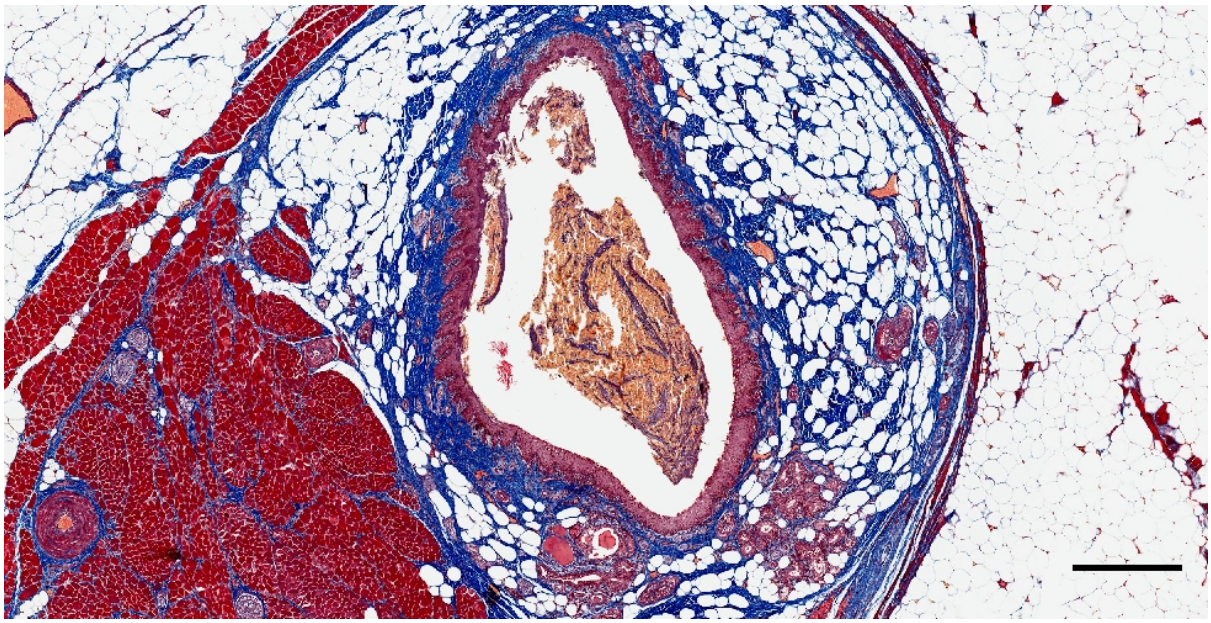

Figure 509. Histological image (Masson´s trichrome) of a transverse section through the right external ear canal in a harbour porpoise, about 1.5 cm beneath the skin (UT1728R_0405). Scale bar 500 µm

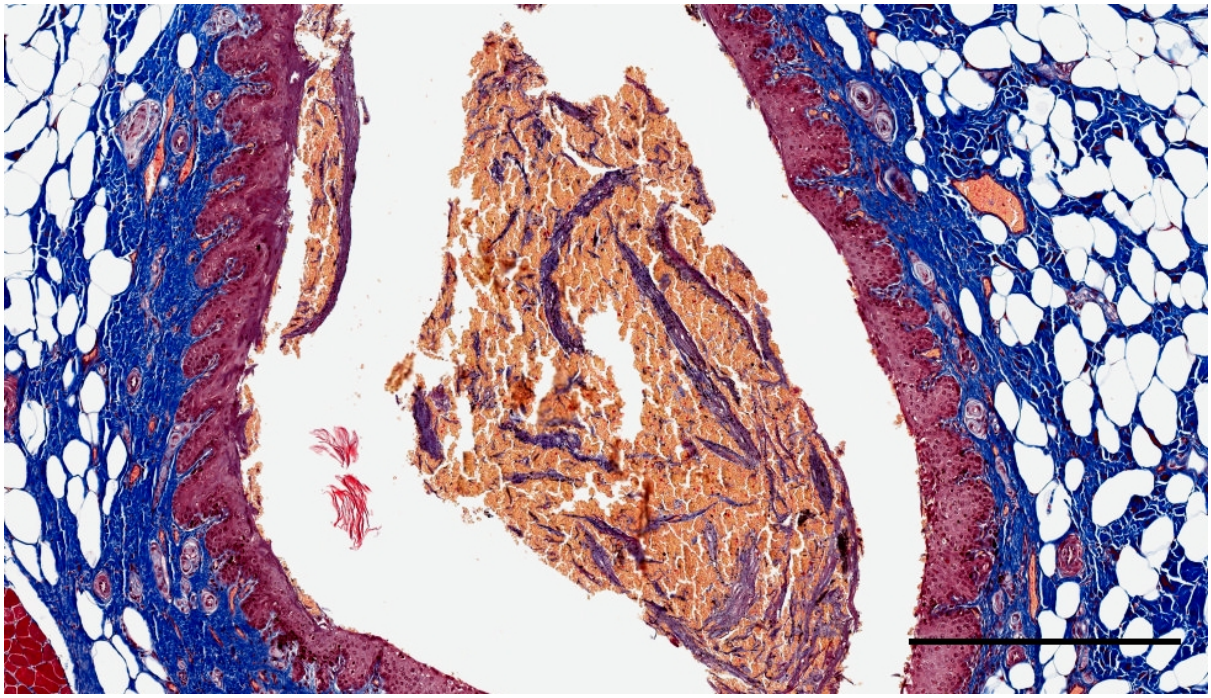

Figure 510. Histological image (Masson´s trichrome) of a transverse section through the right external ear canal in a harbour porpoise, about 1.5 cm beneath the skin (UT1728R_0405). The lumen contains desquamated epithelial cells and red blood cells. Scale bar 500 µm

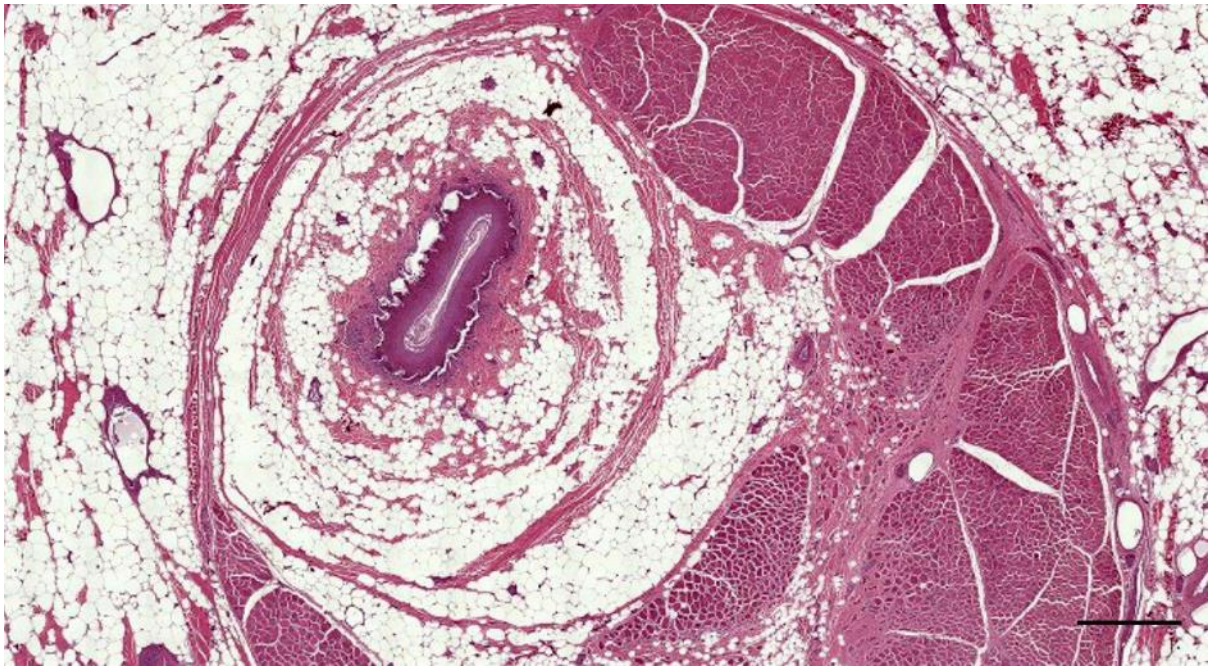

Figure 511. Histological transverse section through the external ear canal of a Cuvier´s beaked whale about 4.5 cm beneath the ski (177/19). Scale bar 1 mm

Figure 512. Histological transverse section through the external ear canal of a Cuvier´s beaked whale about XX cm beneath the ski (177/19)_R04_03_Scale1mm

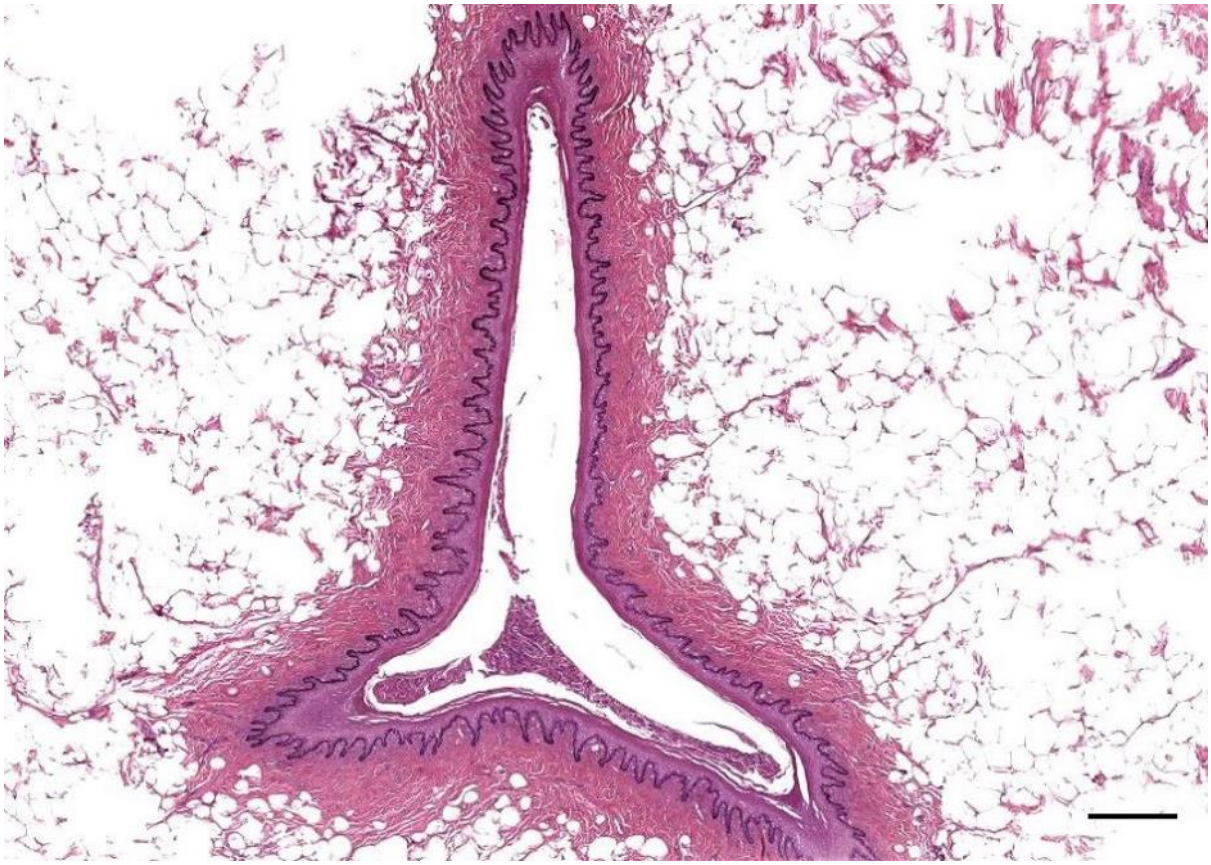

Figure 513. 429_08_3 Lumen shape. Scale bar 0.5mm

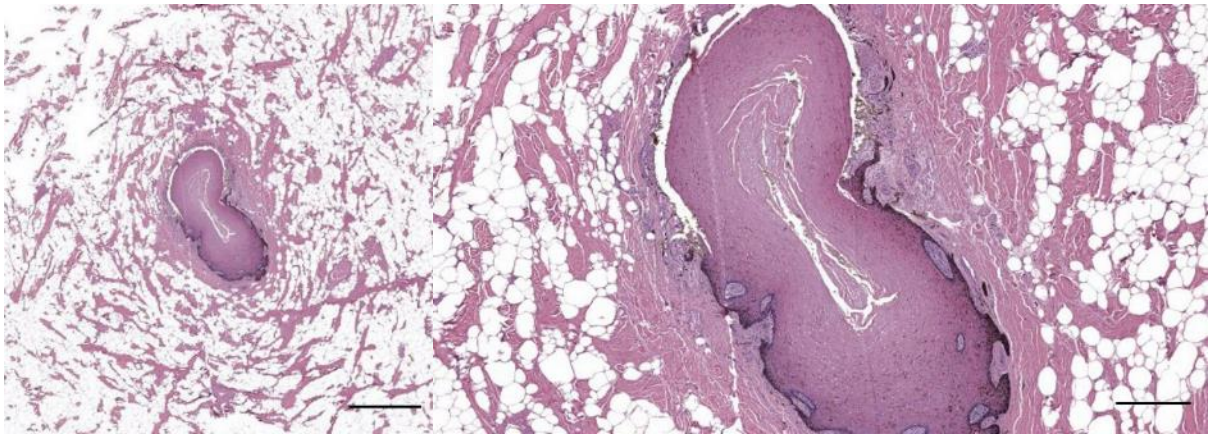

Figure 514. Two magnifications of a histological transverse section through the ear canal of a long-finned pilot whale (ID441) about 2 cm beneath the skin. Scale bar 1mm left, and 300 µm right

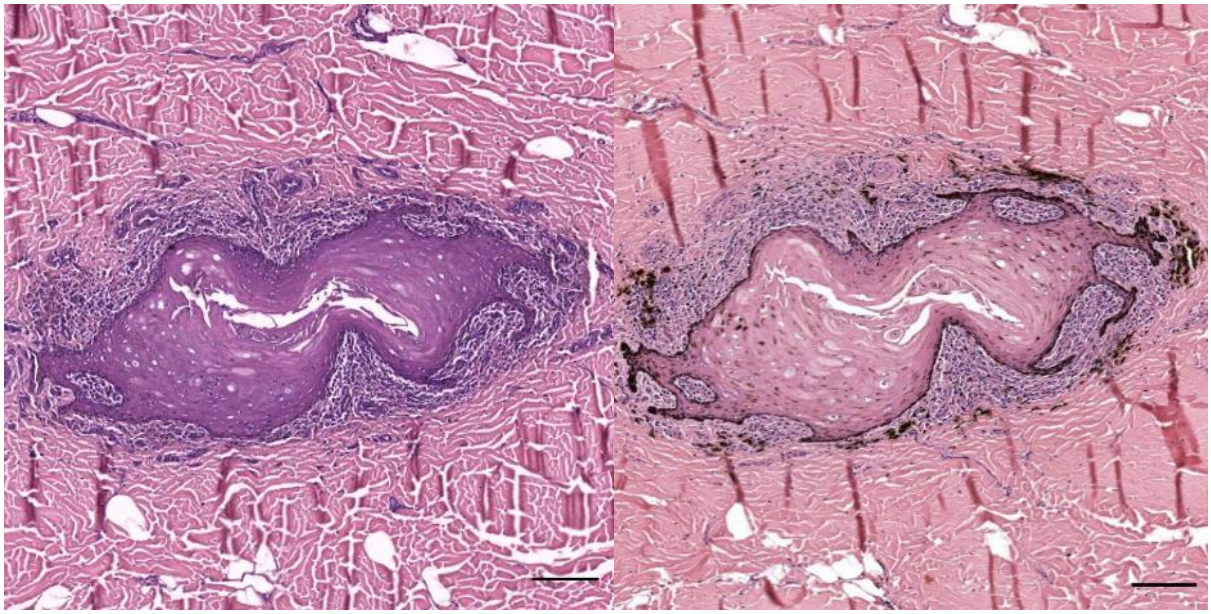

Figure 515. Histological transverse sections through the ear canal of a long-finned pilot whale (ID441) about 3 cm beneath the skin. Left: HE after bleaching; right: normal HE. This confirmed that the dark-coloured material in the subepithelial tissue was melanin. Scale bars 100 µm

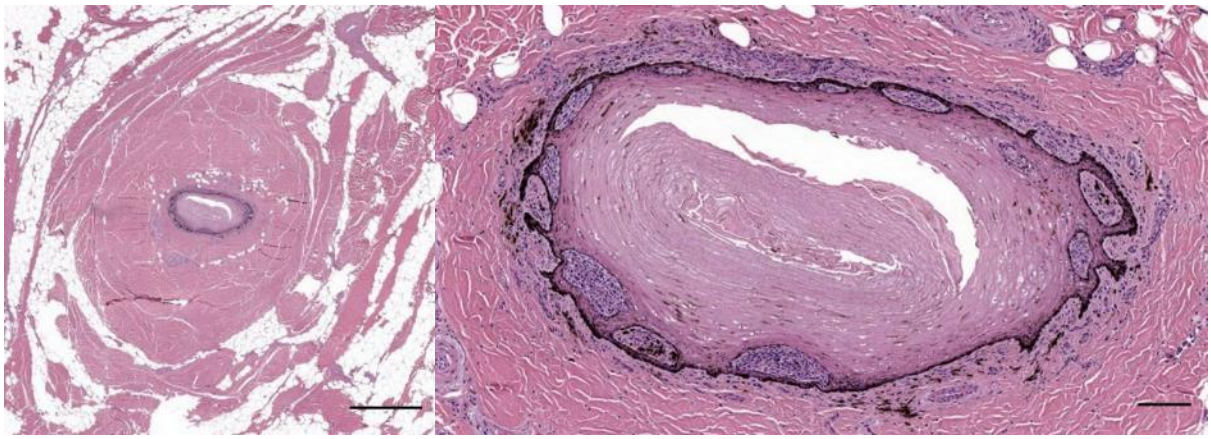

Figure 516. Two magnifications of a histological transverse section through the ear canal of a long-finned pilot whale (ID441)) about 2.5 cm beneath the skin. Scale bars 1 mm left, 100 µm right

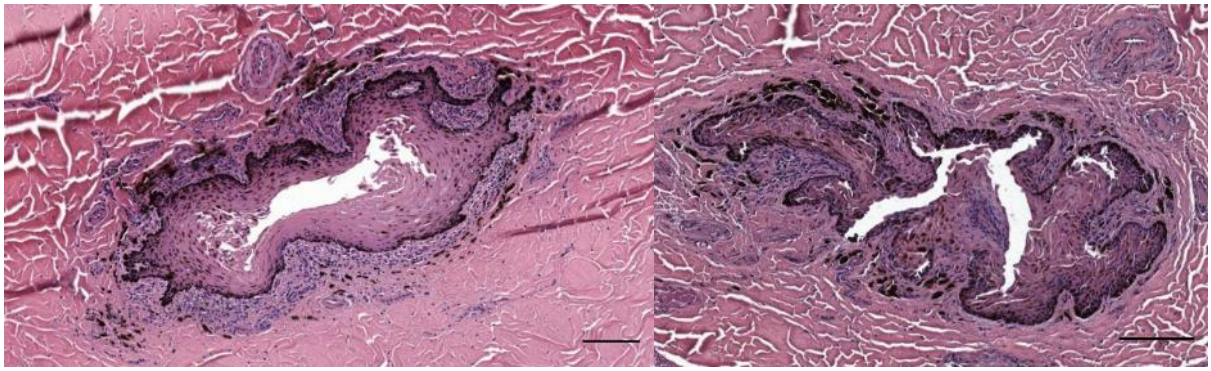

Figure 517. Two histological transverse sections through the ear canal (left is left ear canal, right is right ear canal) of a long-finned pilot whale (ID441) about 3.5 cm beneath the skin. Scale bars 100 µm

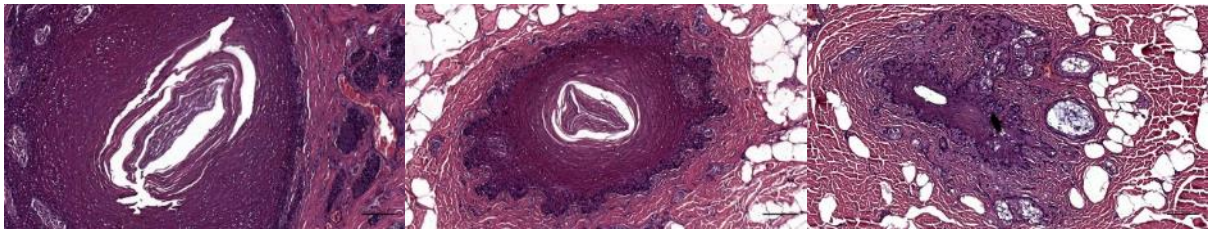

Figure 518. Histological transverse section through the right ear canal of a striped dolphin (ID127565) at about 0.5 cm (left), 1 cm (central) cm, and 1.5 cm (right) beneath the skin. Note the luminal content with epithelial layers in the left and centre image, and the minute size of the lumen in spatial relation with glandular structures in the right image. Scale bars 100 µm

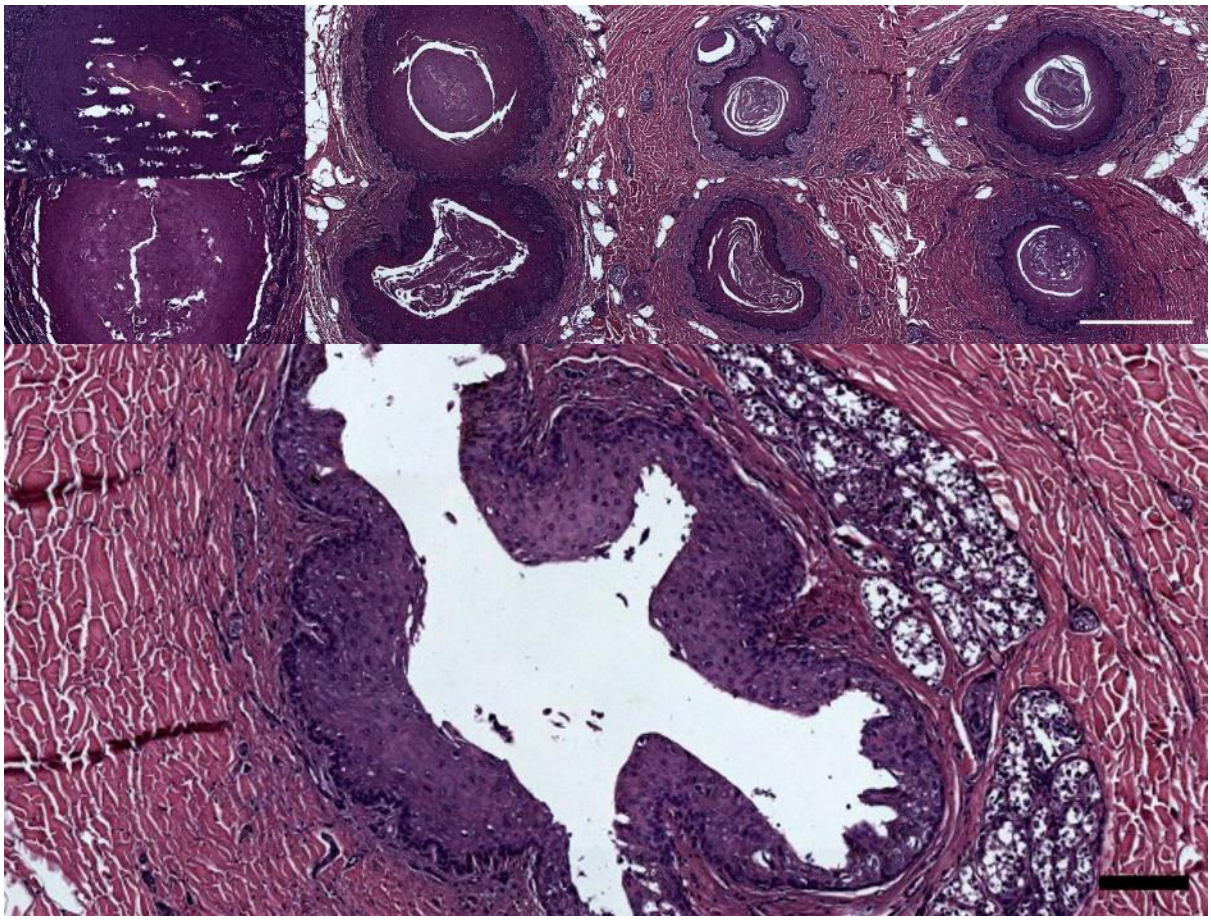

Figure 519. Histological transverse sections through the left (top row) and right (bottom row) ear canal of a striped dolphin at about 1, 1.5, 2 and 2.5 cm beneath the skin, before opening at the level of the glands (bottom image) (left ear canal only as the right side had artefacts)(ID44/17). Scale bar top 500 µm, bottom 100 µm

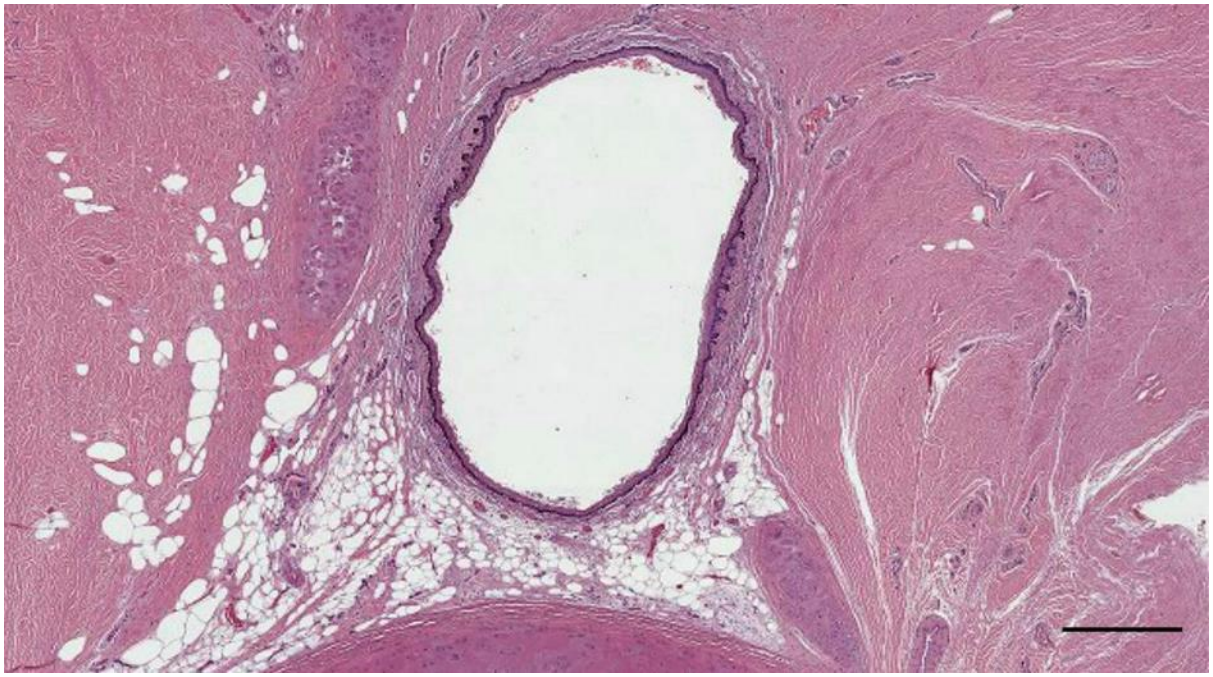

Figure 520. HE stained cross-section of the ear canal (169/17_R10). Scale bar 500 µm

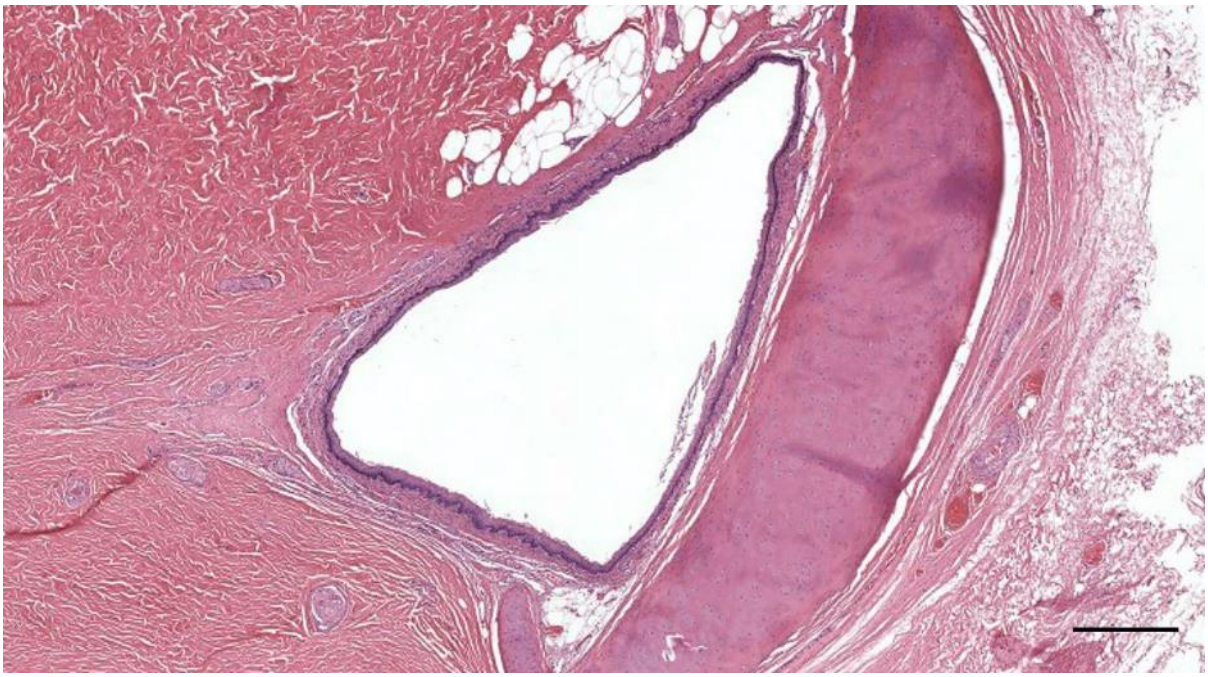

Figure 521. HE stained cross-section of the ear canal with cartilage (293/18_L7). Scale bar 0.5 mm

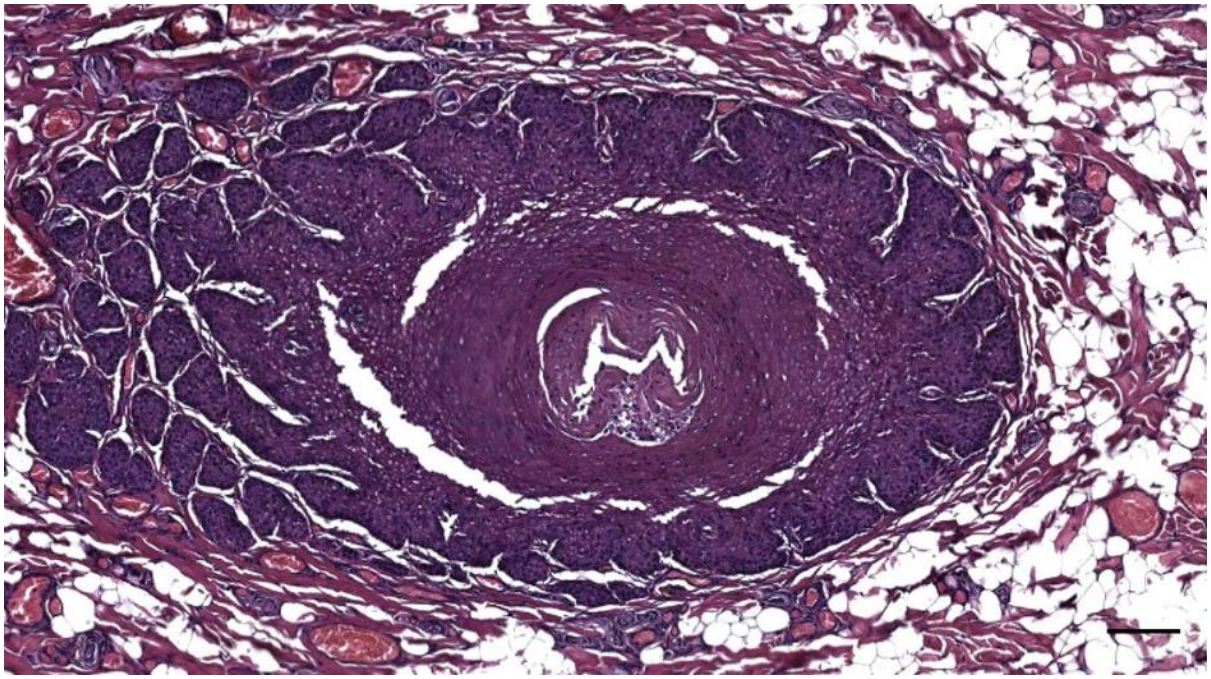

Figure 522. HE-stained cross-section of the ear canal in striped dolphin (ID449_L1) Ear canal cross-section immediately beneath the epidermis filled with epithelial cells and glandular cells with hyperchromatic nuclei. Scale bar 100 µm

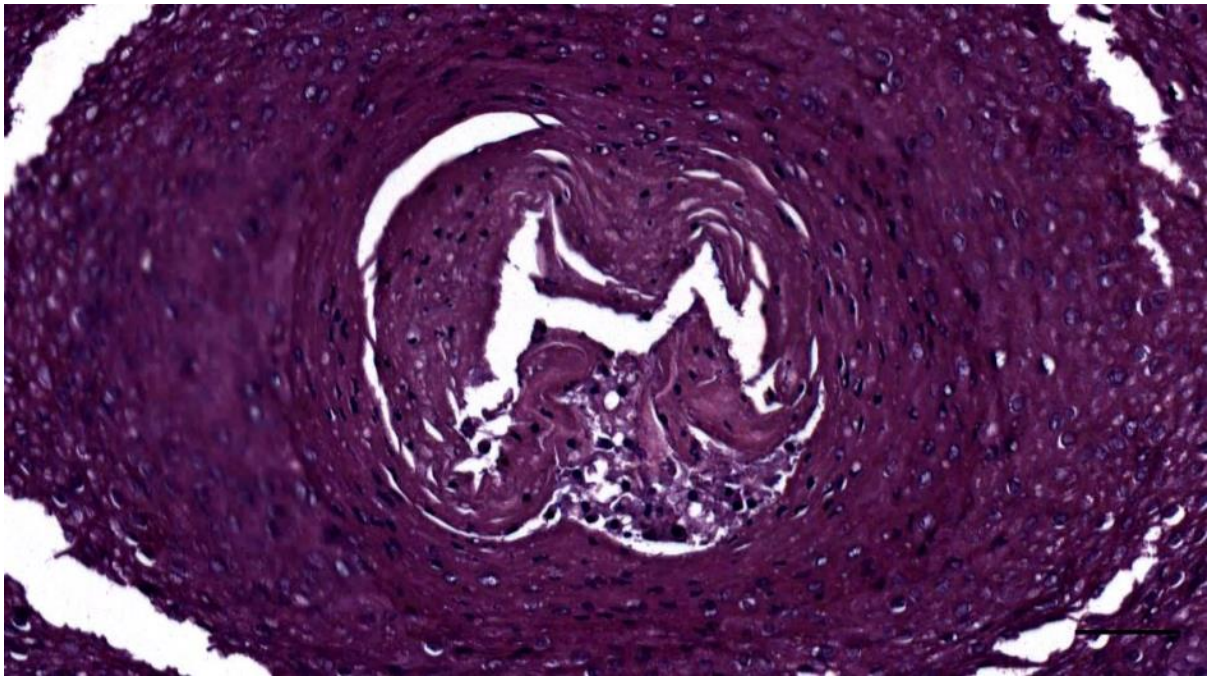

Figure 523. Detail of Figure 522. Ear canal with epithelial and glandular cells with hyperchromatic nuclei. Scale bar 50 µm

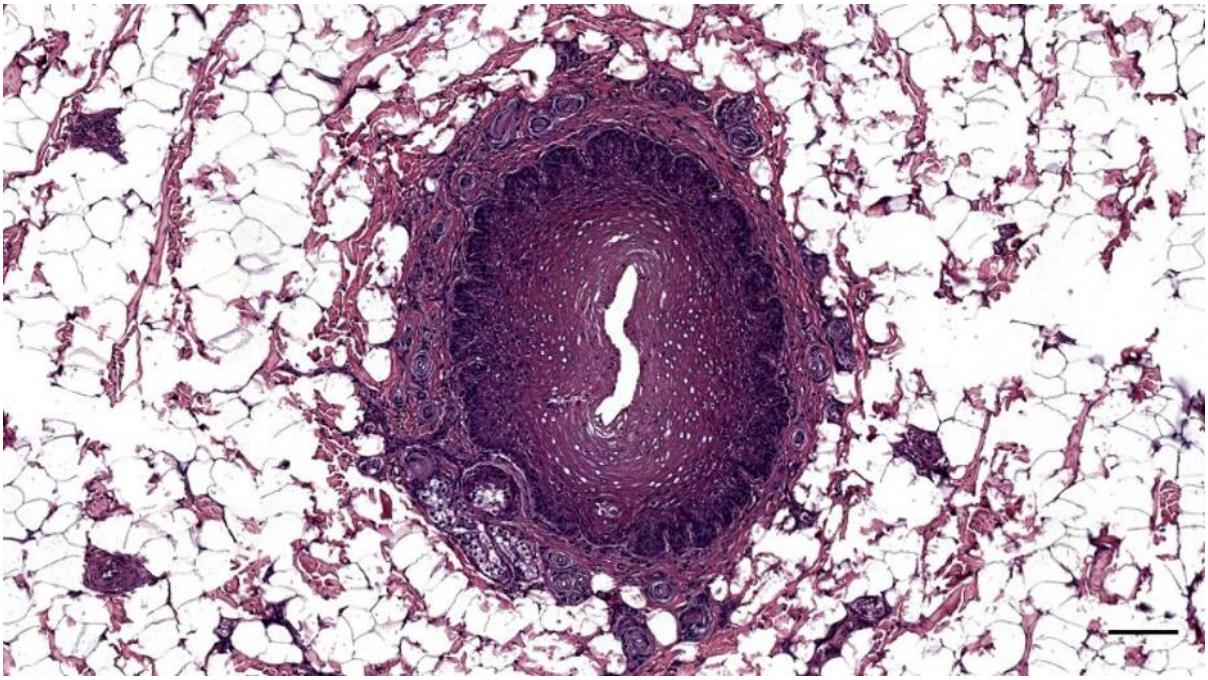

Figure 524. HE-stained cross-section of the right ear canal in striped dolphin (ID449_R2). Cross-section of the ear canal and glands at their lateral end. Scale bar 100 µm

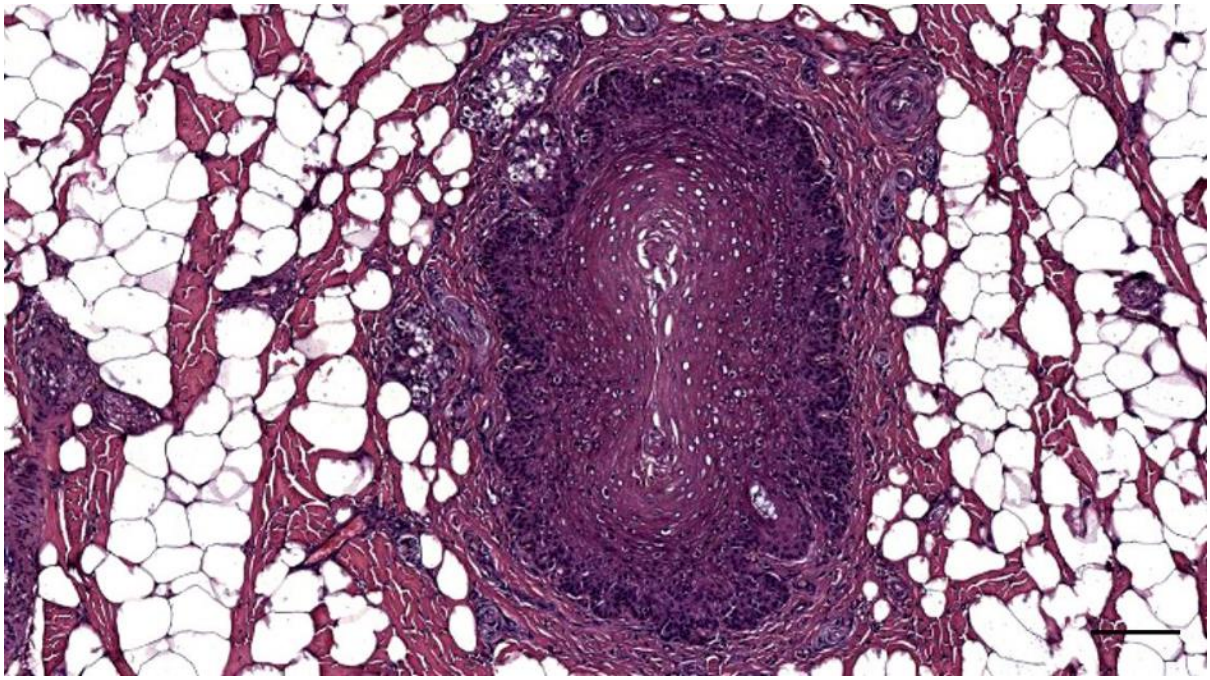

Figure 525. HE-stained cross-section of the left ear canal in striped dolphin (ID449_L2) Ear canal cross-section with artificial lumen and glands. Scale bar 100 µm

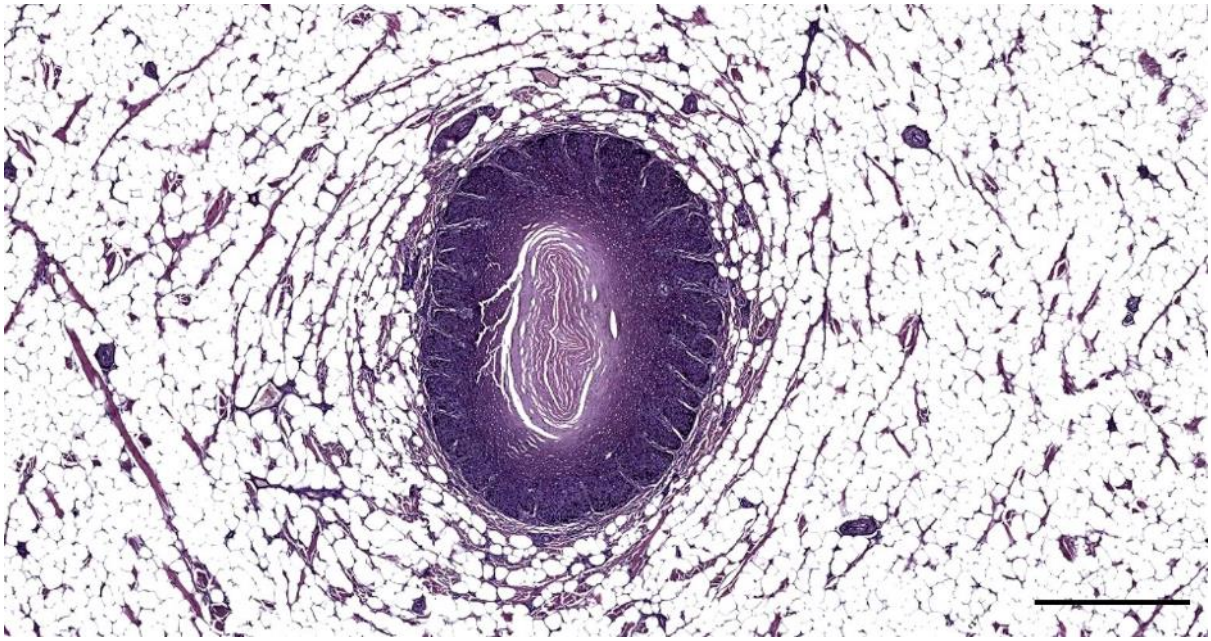

Figure 526. HE-stained cross-section of the right ear canal in harbour porpoise. Note that the lumen is filled with layered epithelial cells (UT1692_R0401). Scale bar 500 µm

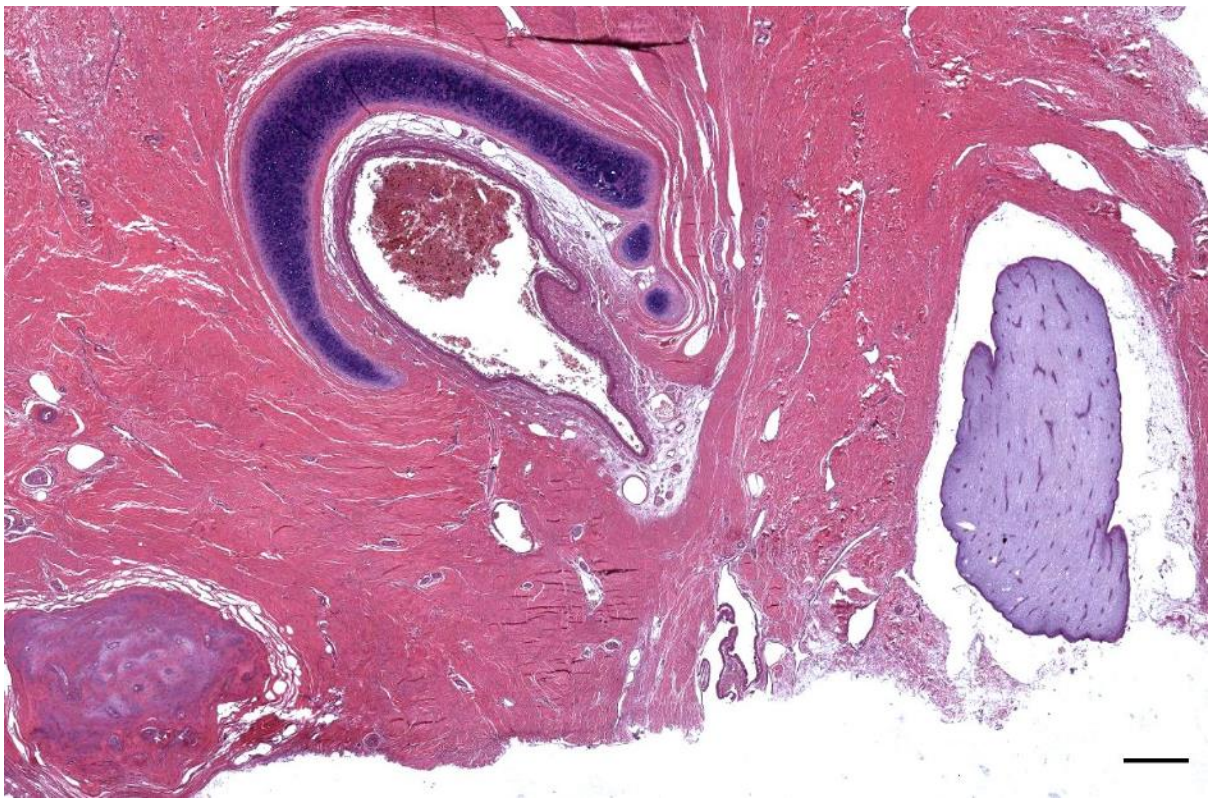

Figure 527. HE-stained cross-section of the right ear canal in striped dolphin (ID449_Rx1)(Decalcified). Note that the lumen contains red blood cells (artefact). Note the nervous ridge, the cartilaginous flangs, and the middle ear bones. Scale bar 0.5 mm

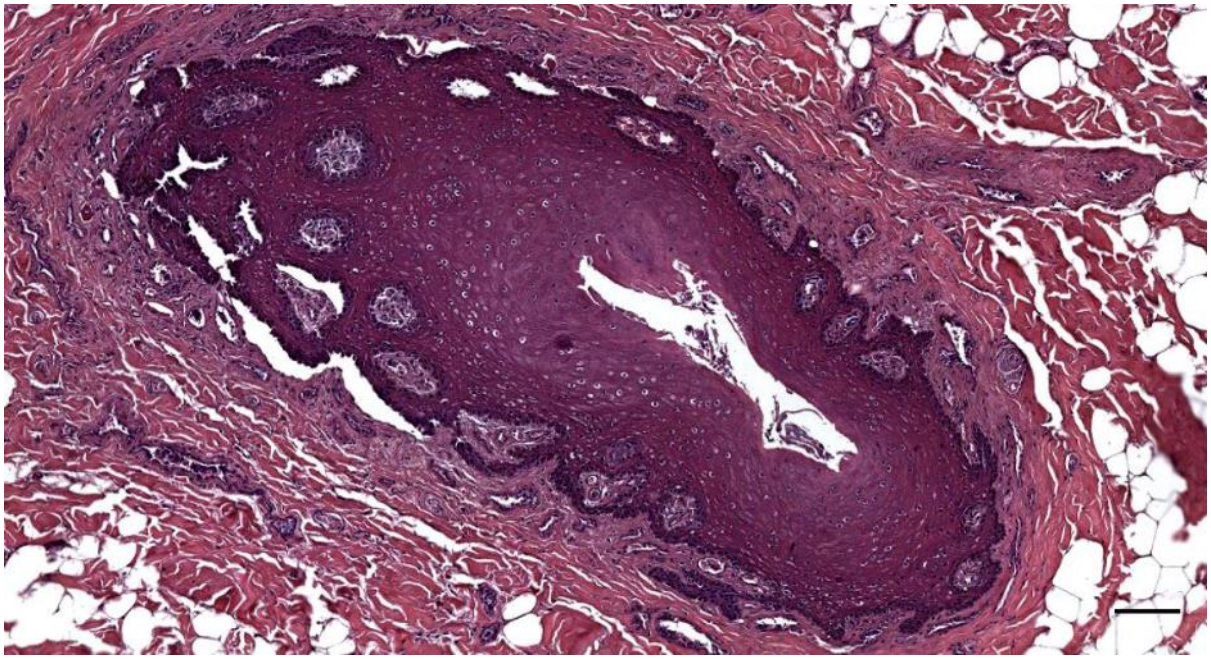

Figure 528. HE-stained cross-section of the right ear canal in a bottlenose dolphin (444_R1). Ear canal at the level of the porus acusticus externus. Scale bar 100 µm

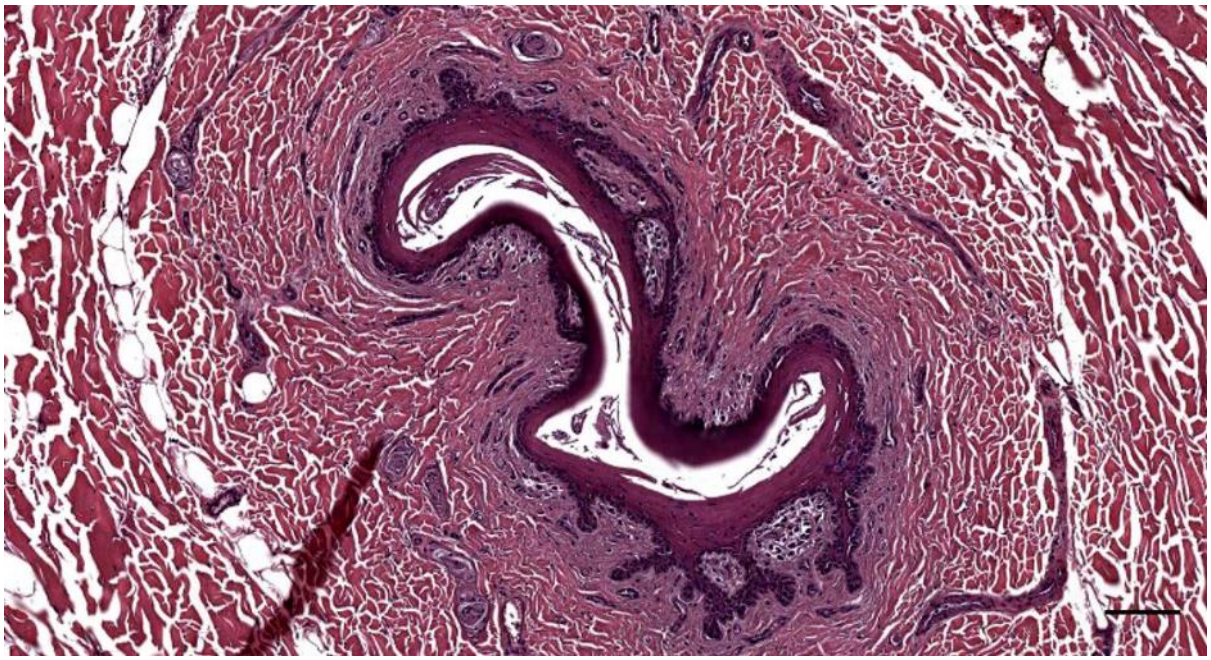

Figure 529. HE-stained cross-section of the right ear canal in a bottlenose dolphin (444_R3). Scale bar 100 µm

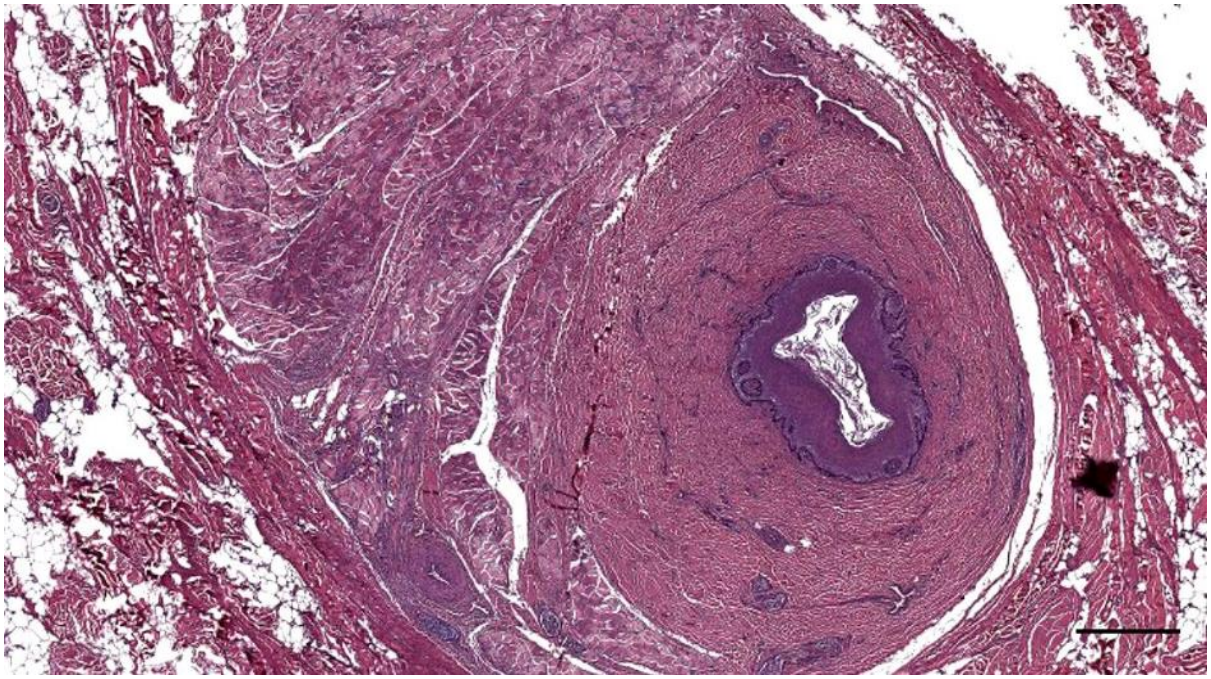

Figure 530. HE-stained cross-section of the right ear canal in a bottlenose dolphin about 2 cm beneath the skin (457_R5). Note the degenerated muscles. Scale bar 500 µm

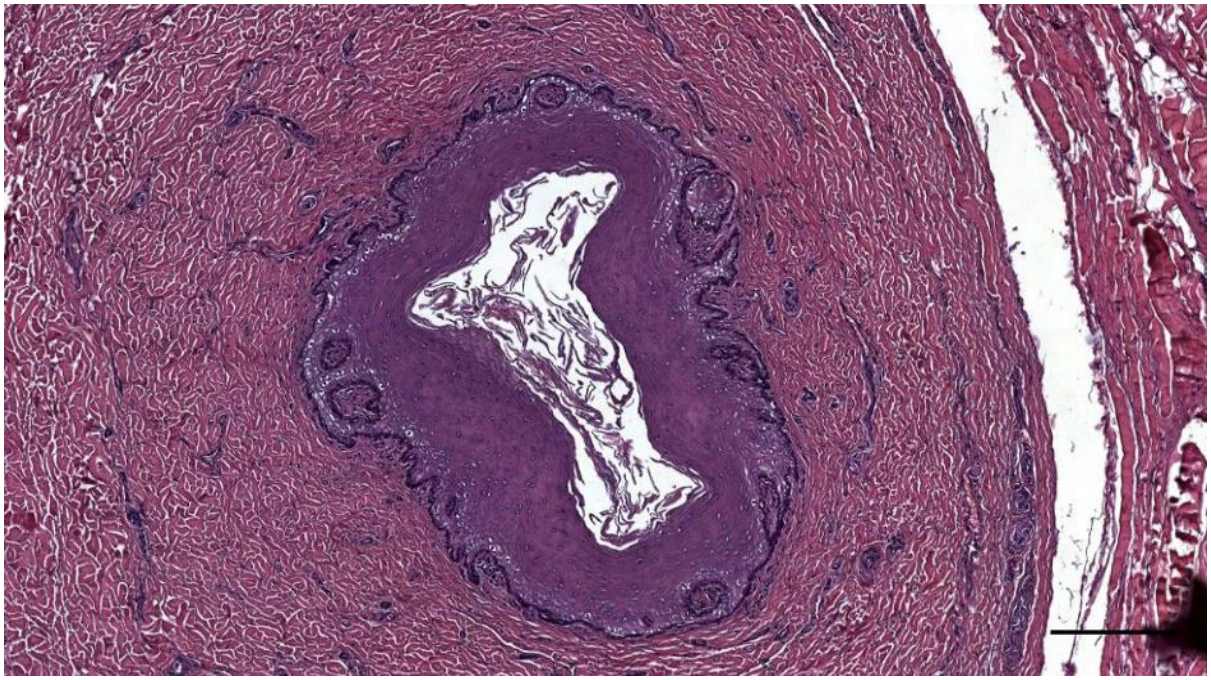

Figure 531. Detail of Figure 530 (457_R5). Ear canal with desquamated epithelial cells in the lumen. Scale bar 250 µm

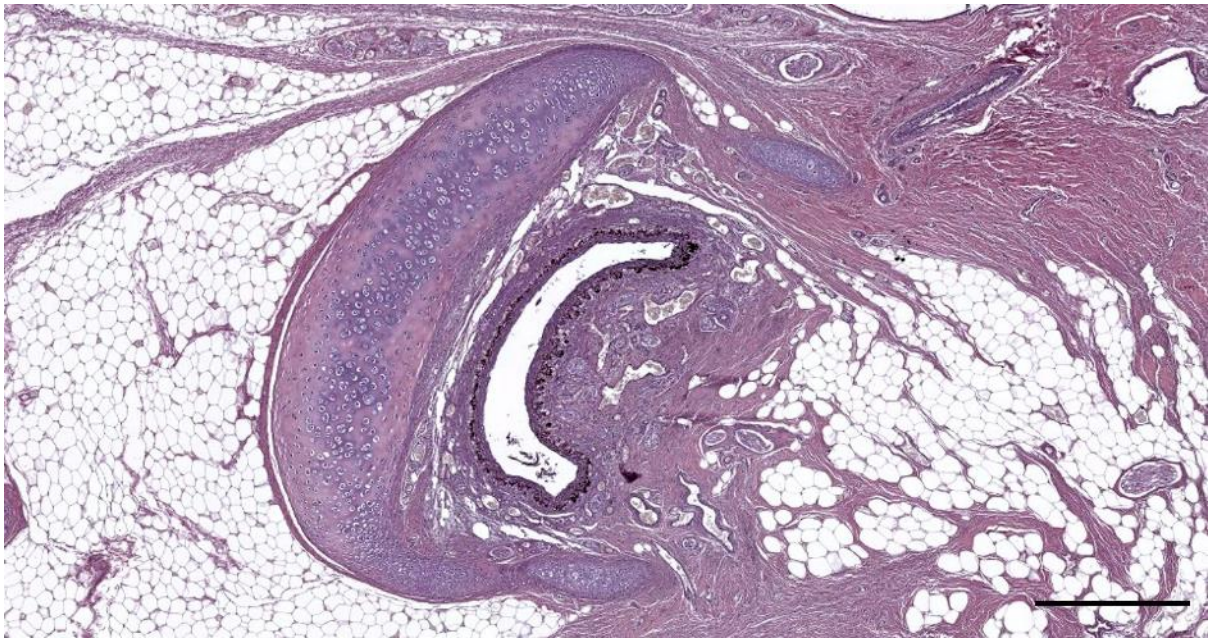

Figure 532. Histological transverse section (HE staining) of the right ear canal of a harbour porpoise (UT1692_Rx1). Note the lunar shape of the lumen of the ear canal. Scale bar 500 µm

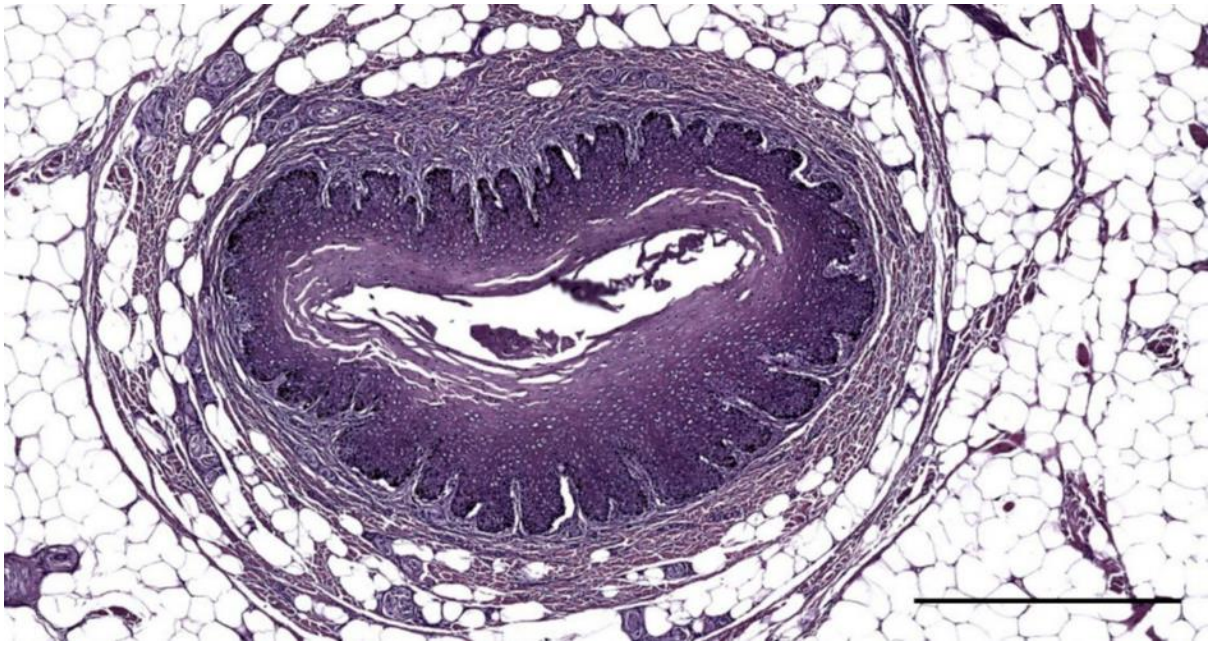

Figure 533. Histological transverse section (HE staining) of the left ear canal of a harbour porpoise at about 1 cm beneath the skin (UT1692_L0201). Scale bar 500 µm

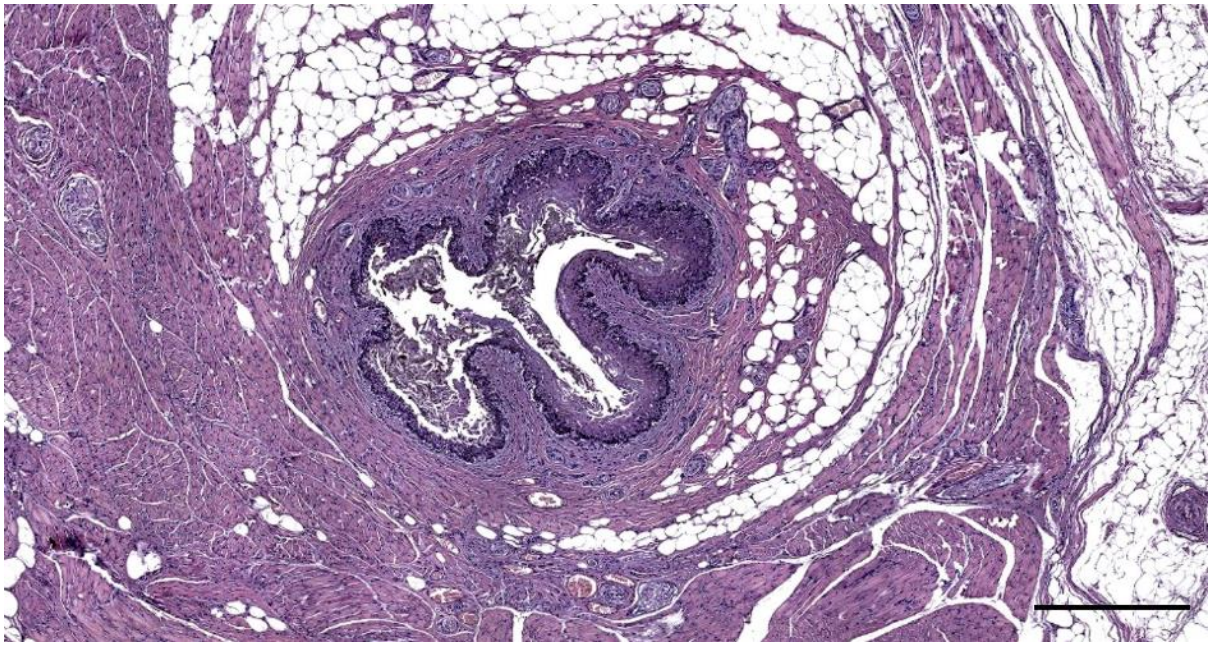

Figure 534. Histological transverse section (HE staining) of the left ear canal of a harbour porpoise at about 2 cm beneath the skin (UT1692_L0401). Note the desquamation of the epithelial layers – possibly a combination of pre- and post-mortem processes. Scale bar 500 µm

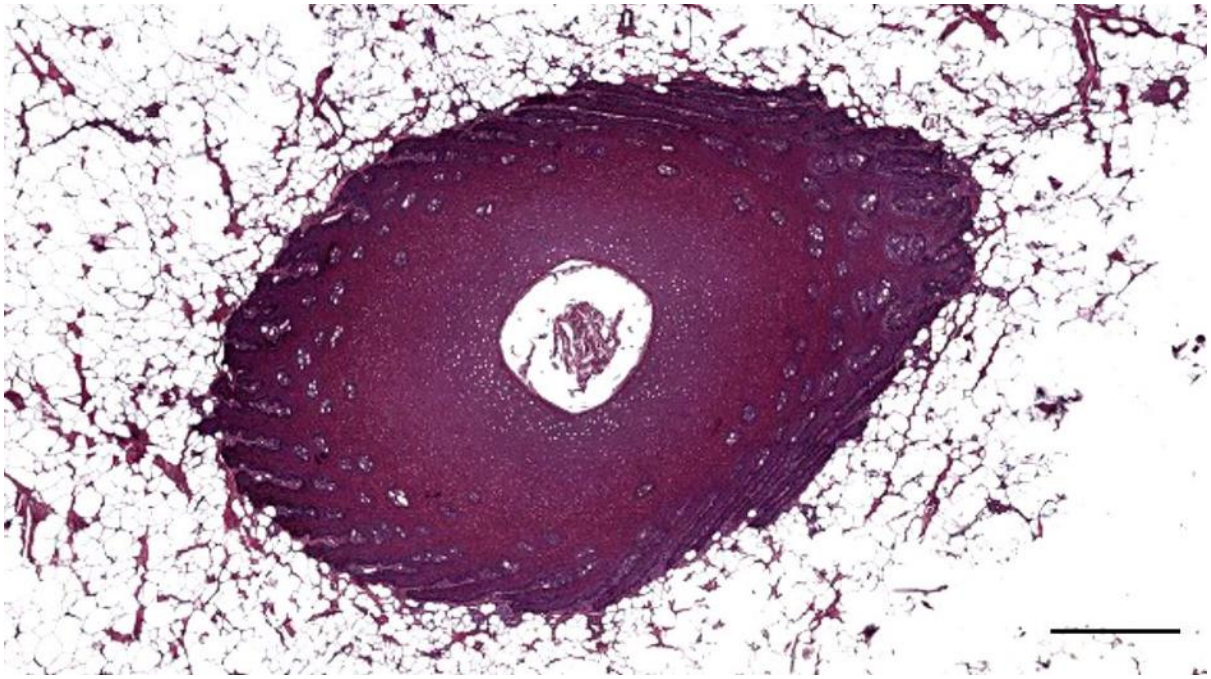

Figure 535. Histological transverse section (HE staining) of the medial end of the external ear opening of a Cuvier´s beaked whale (ID429_01, HE). Scale bar 500 µm

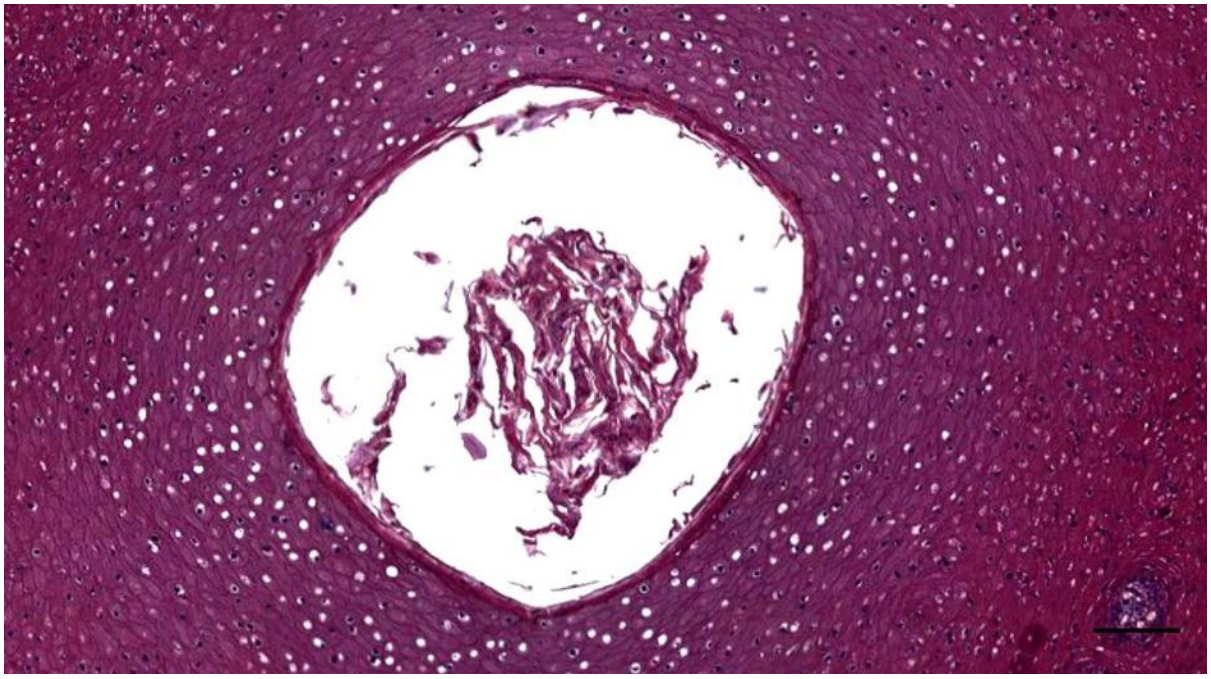

Figure 536. Detail of Figure 473. Histological transverse section (HE staining) of the medial end of the external ear opening of a Cuvier´s beaked whale (ID429, HE). Ear canal lumen with desquamated epithelial cells. Scale bar 100 µm

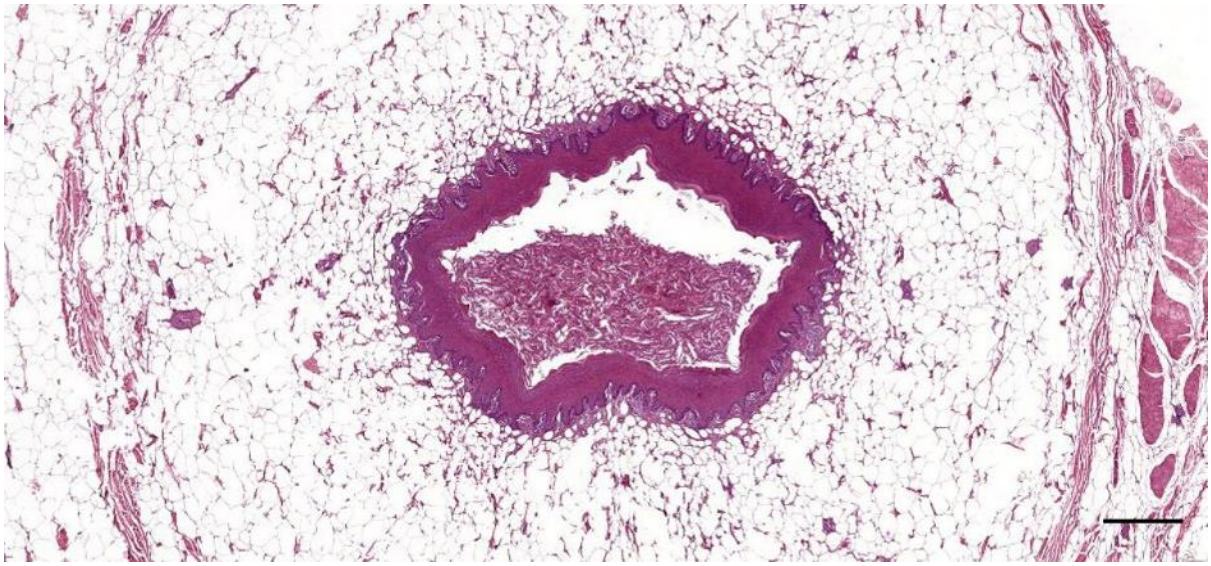

Figure 537. Histological transverse section (HE staining) of the external ear canal in a Cuvier´s beaked whale at about 1 cm beneath the skin (ID429_02, HE). Scale bar 500 µm

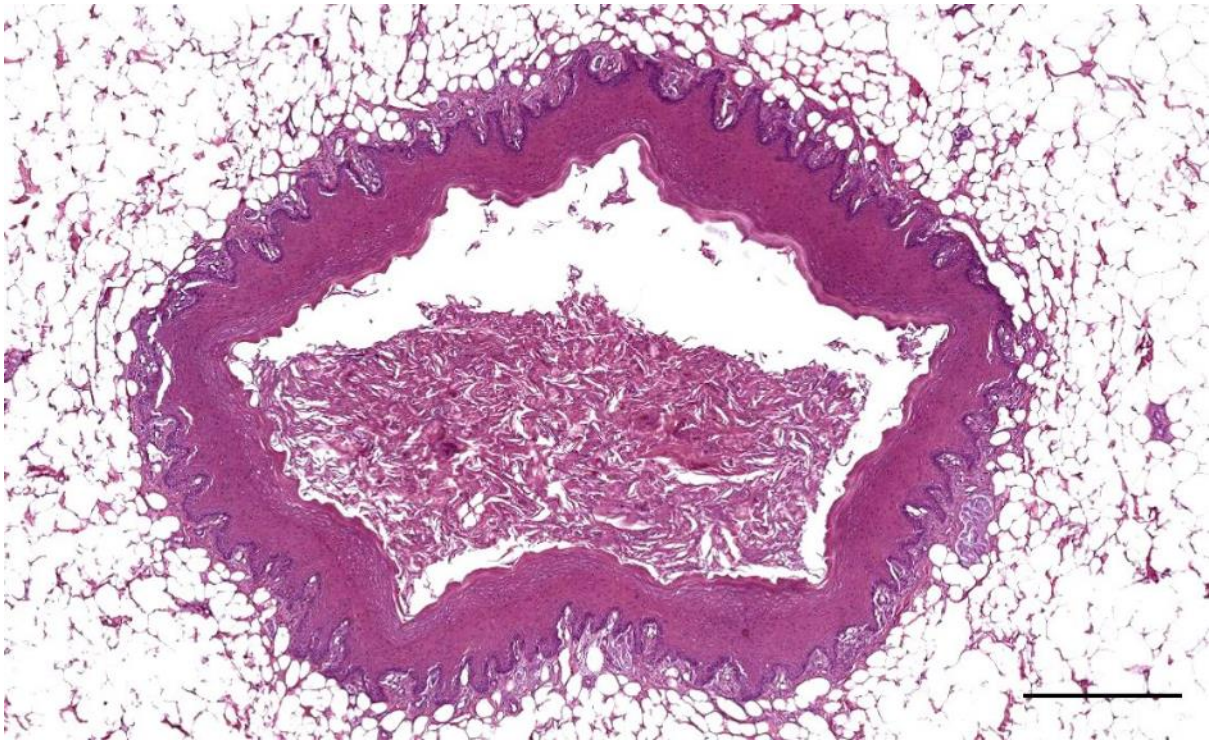

Figure 538. Histological transverse section (HE staining) of the external ear canal in a Cuvier´s beaked whale at about 1 cm beneath the skin (ID429_02, HE) Detail of Figure 537. Ear canal with luminal content. Scale bar 500 µm

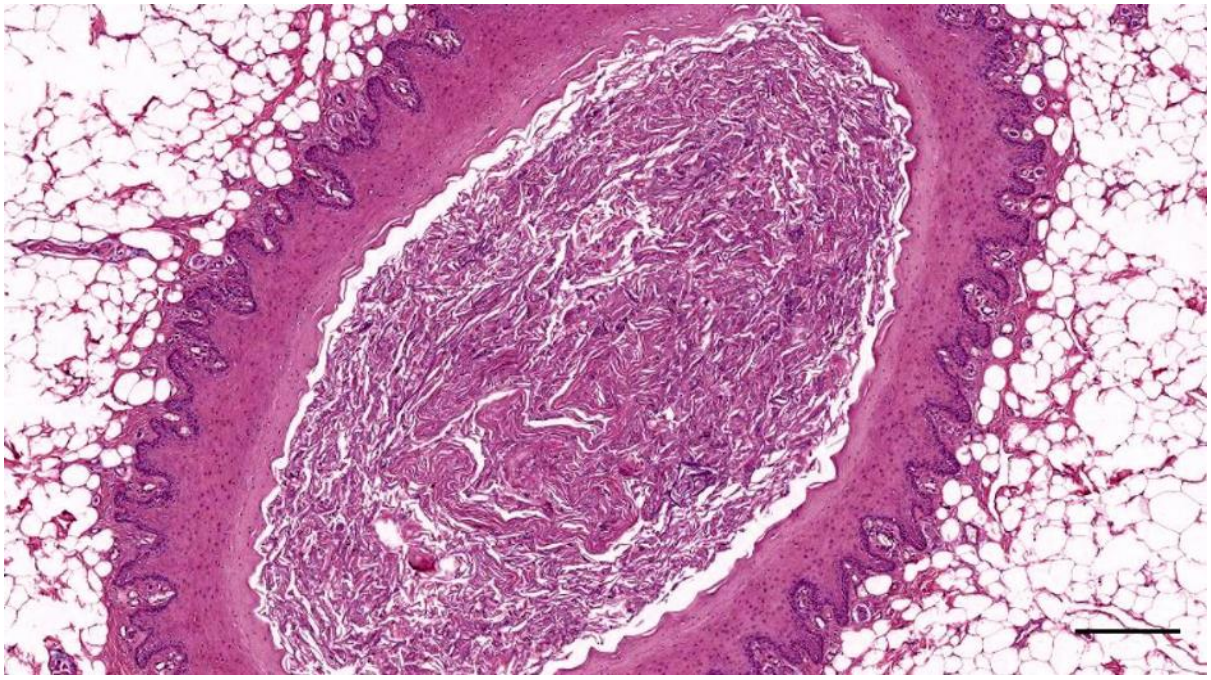

Figure 539. Histological transverse section (HE staining) of the external ear canal in a Cuvier´s beaked whale at about 1.5 cm beneath the skin (ID429_03, HE). Ear canal with content. Scale bar 300 µm

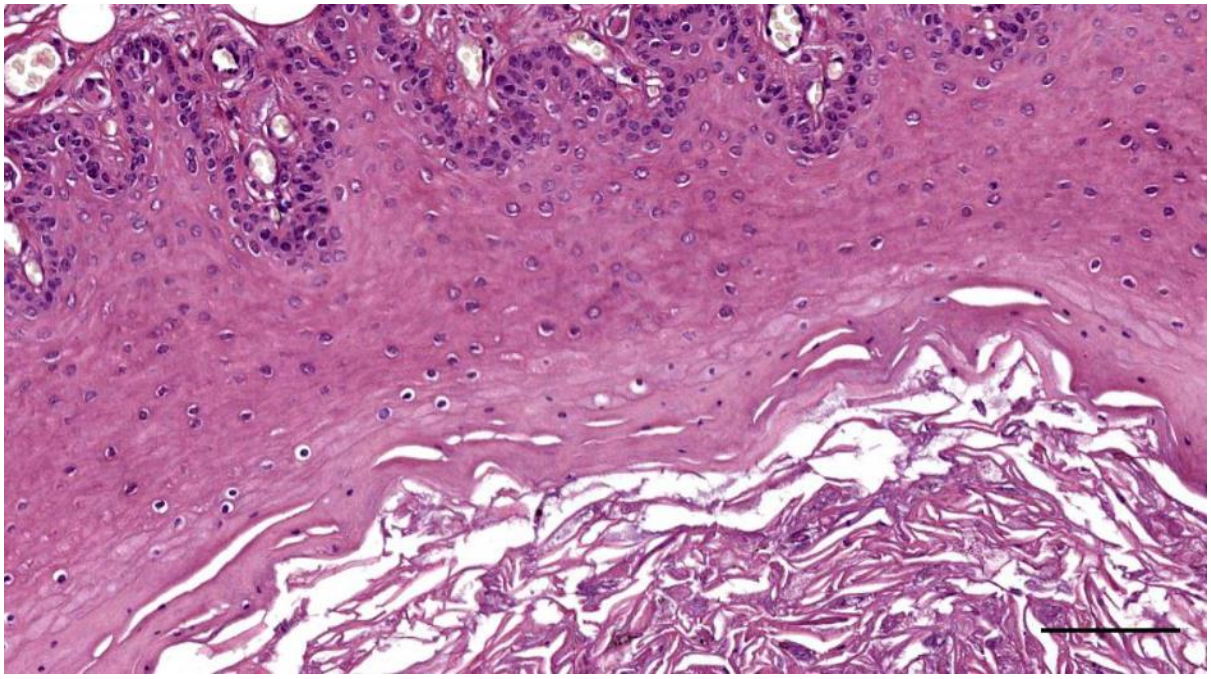

Figure 540. Histological transverse section (HE staining) of the external ear canal in a Cuvier´s beaked whale at about 1.5 cm beneath the skin (ID429_03, HE). Ear canal epithelium. Scale bar 100 µm

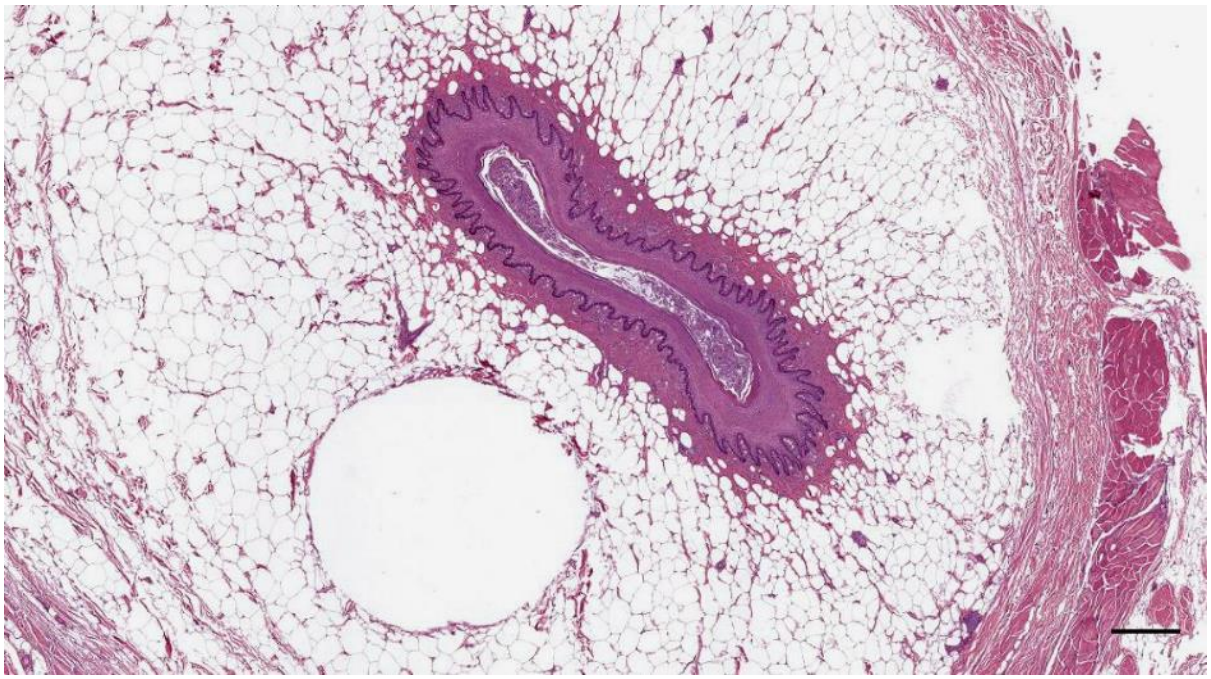

Figure 541. Histological transverse section (HE staining) of the external ear canal in a Cuvier´s beaked whale at about 2.5 cm beneath the skin (ID429_05) Ear canal with an adjacent gas bubble in the fat tissue situated within the connective tissue capsule. Scale bar 500 µm

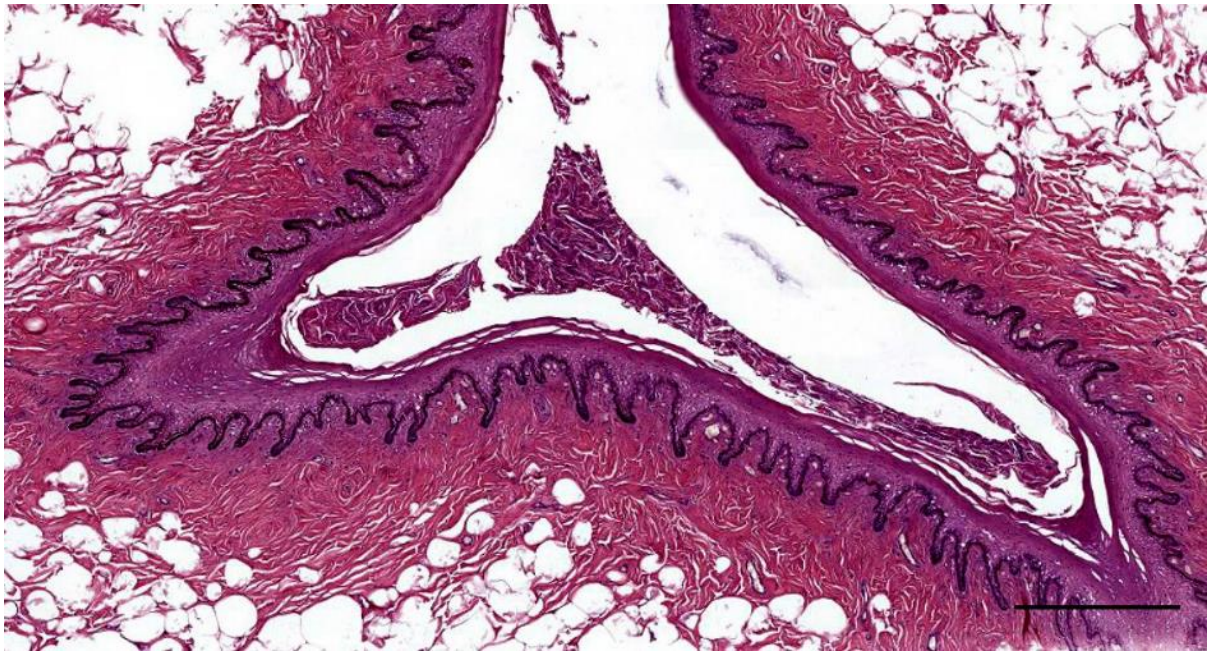

Figure 542. Histological transverse section (HE staining) of the external ear canal in a Cuvier´s beaked whale at about 4 cm beneath the skin (ID429_08) Ear canal. Scale bar 500 µm

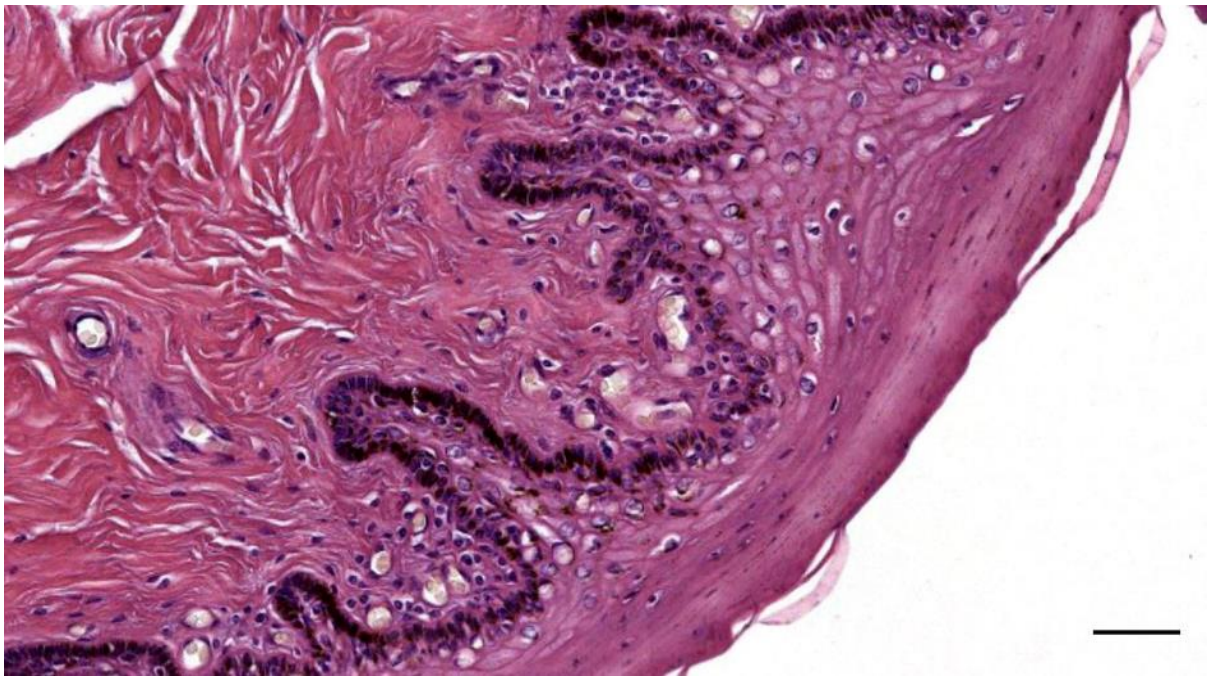

Figure 543. Detail of Figure 542 (ID429_08) Ear canal epithelium with lymphocytic infiltration in the lamina propria. Scale bar 50 µm

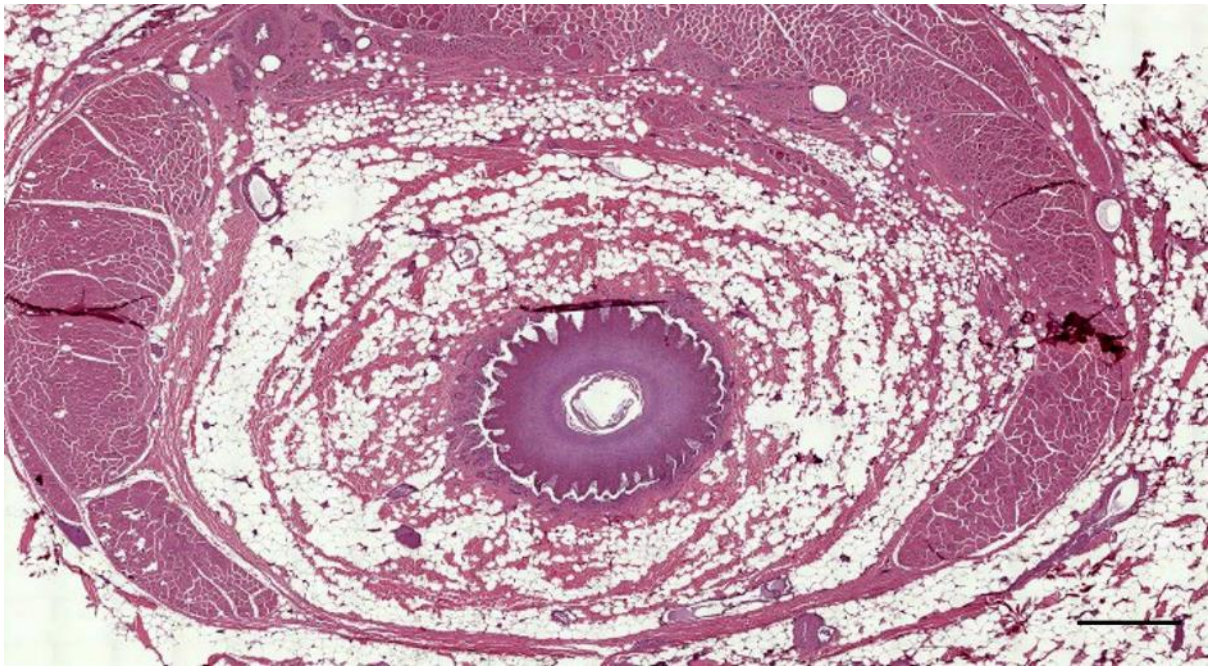

Figure 544. Histological transverse section (HE staining) through the external ear canal of a Cuvier´s beaked whale about 1.5 cm beneath the ski (ID177/19). Scale bar 1 mm

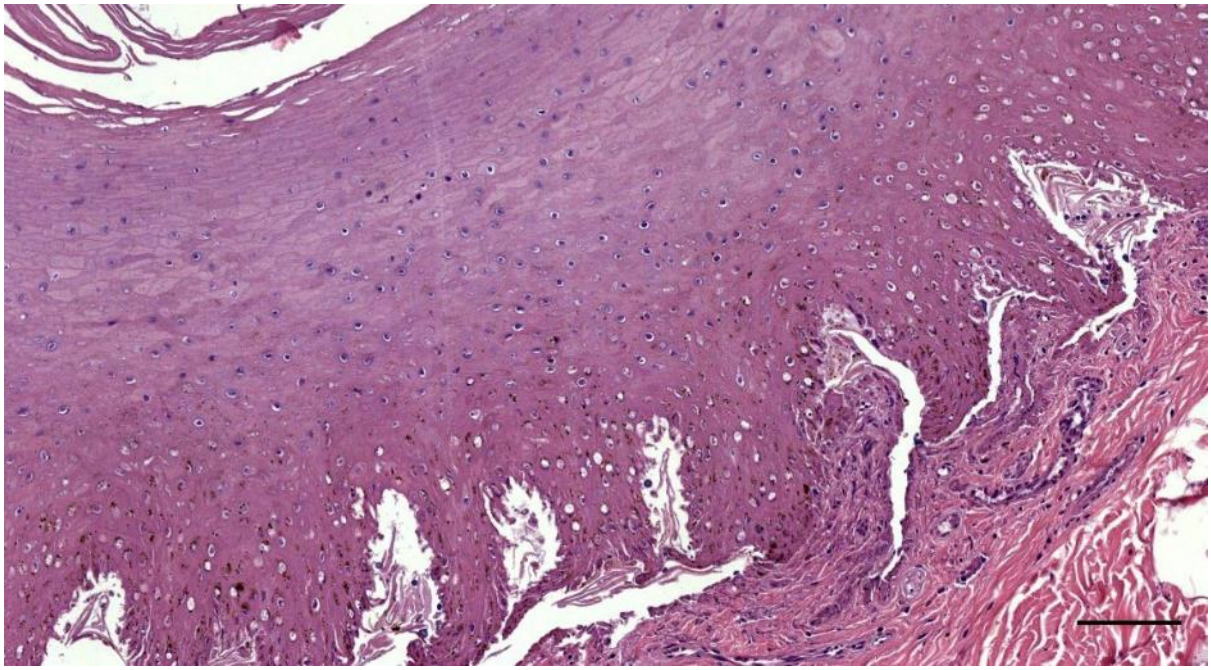

Figure 545. Histological transverse section (HE staining) through the external ear canal of a Cuvier´s beaked whale about 1.5 cm beneath the skin (177/19). Scale bar 100 µm

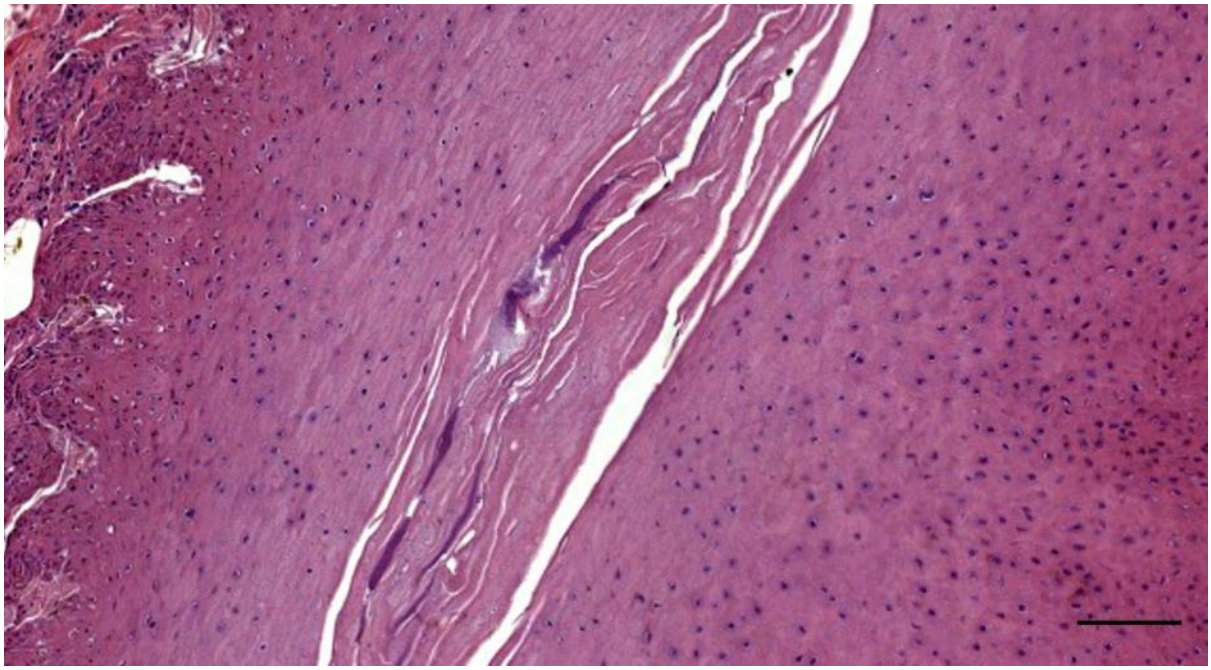

Figure 546. Histological transverse section (HE staining) through the external ear canal of a Cuvier´s beaked whale about 3 cm beneath the skin (177/19. Scale bar 100 micron

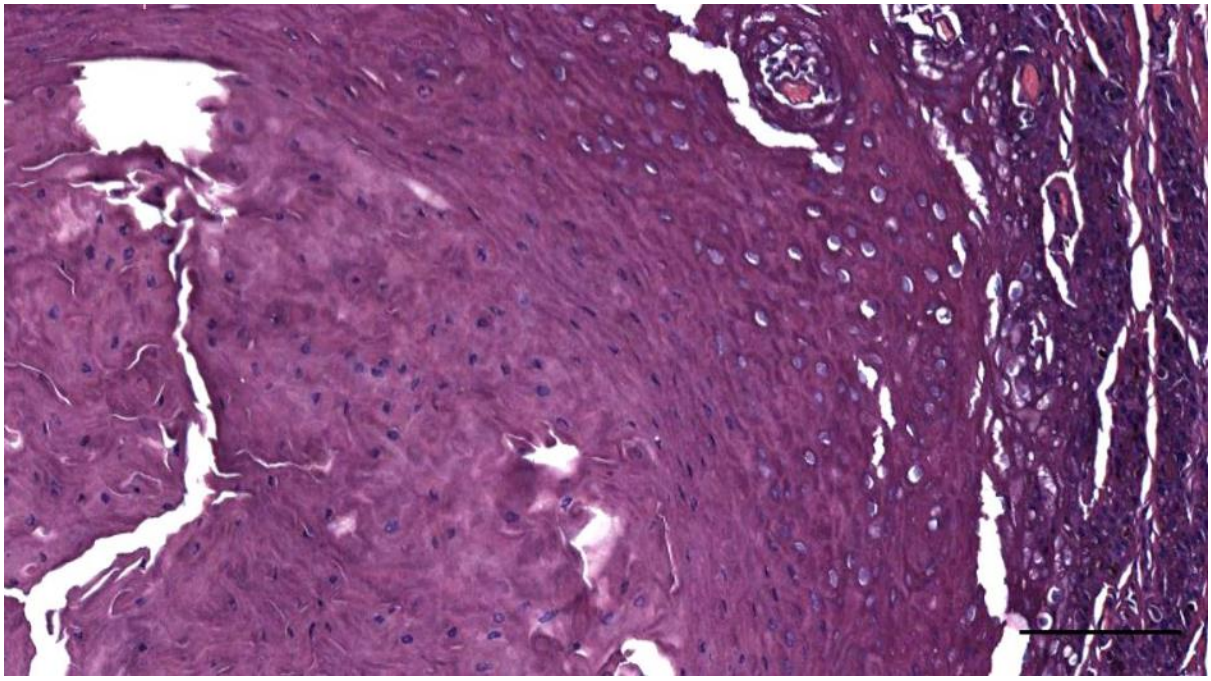

Figure 547. Detail of Figure 508. Note the basophilic nuclei in all layer of the epithelium. Scale bar 100 µm

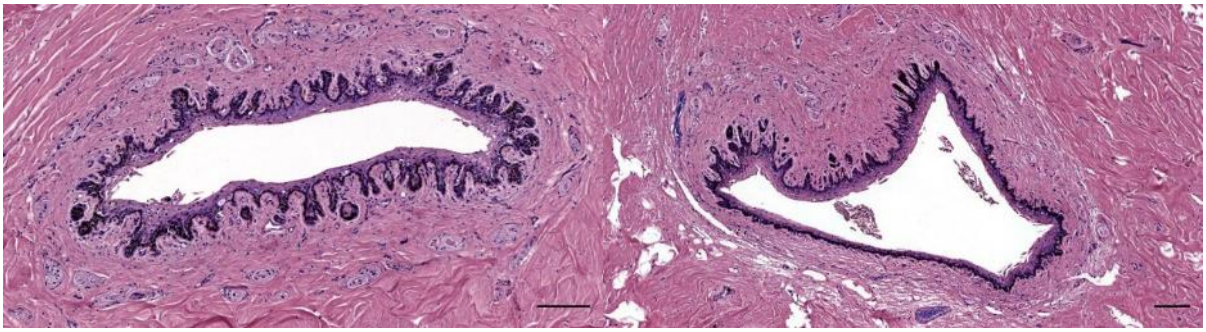

Figure 548. Histological transverse section (HE staining) through the ear canal of a bottlenose dolphin (ID444) at about 3 cm (left) and 5 cm (right) beneath the skin. Note the intricate relation between epithelium and subepithelial tissue, around the ear canal in the left image and on one side of the ear canal in a tissue bulge in the right image. Scale bars 100 µm

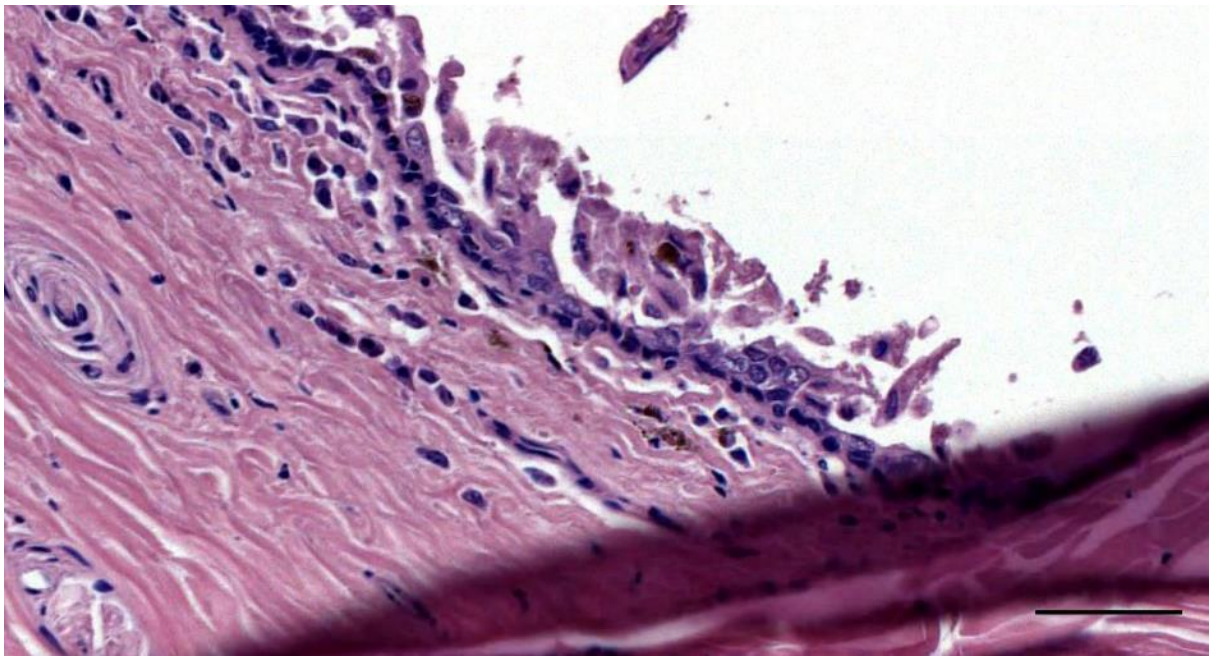

Figure 549. Histological transverse section (HE staining) through the left ear canal of a bottlenose dolphin (444_L5) Melanocytes in the subepithelial tissue. Scale bar 50 µm

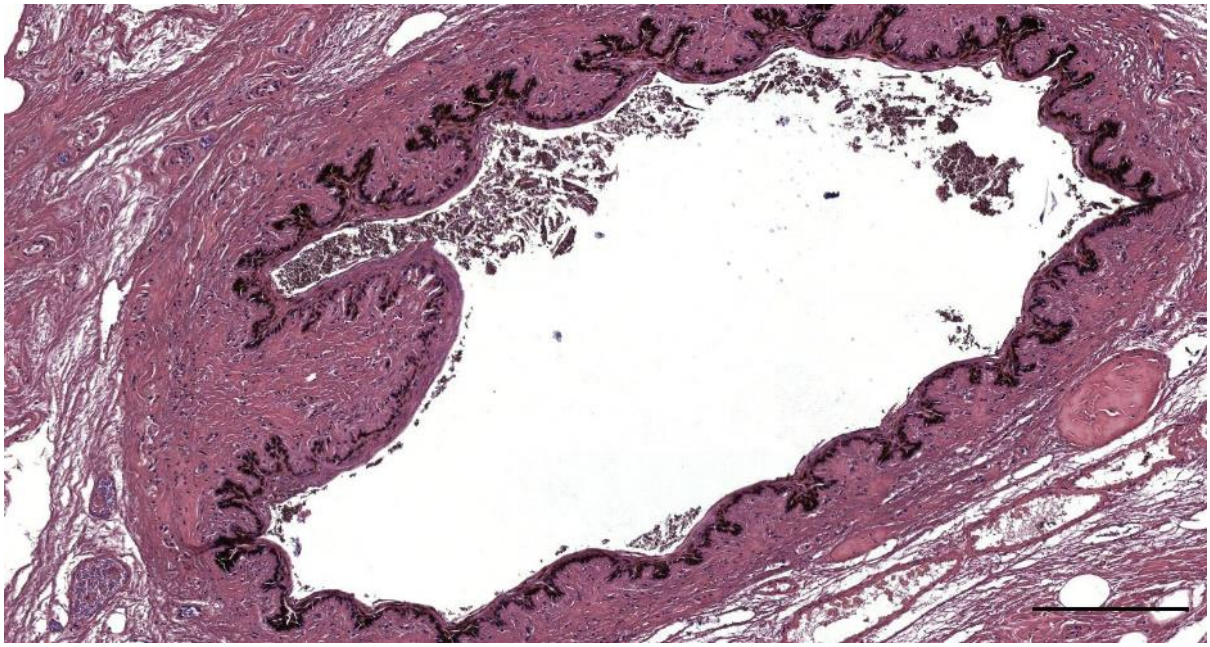

Figure 550. Histological transverse section (HE staining) through the ear canal of a pilot whale (441_R19). Ear canal with nervous tissue ridge. Scale bar 200 µm

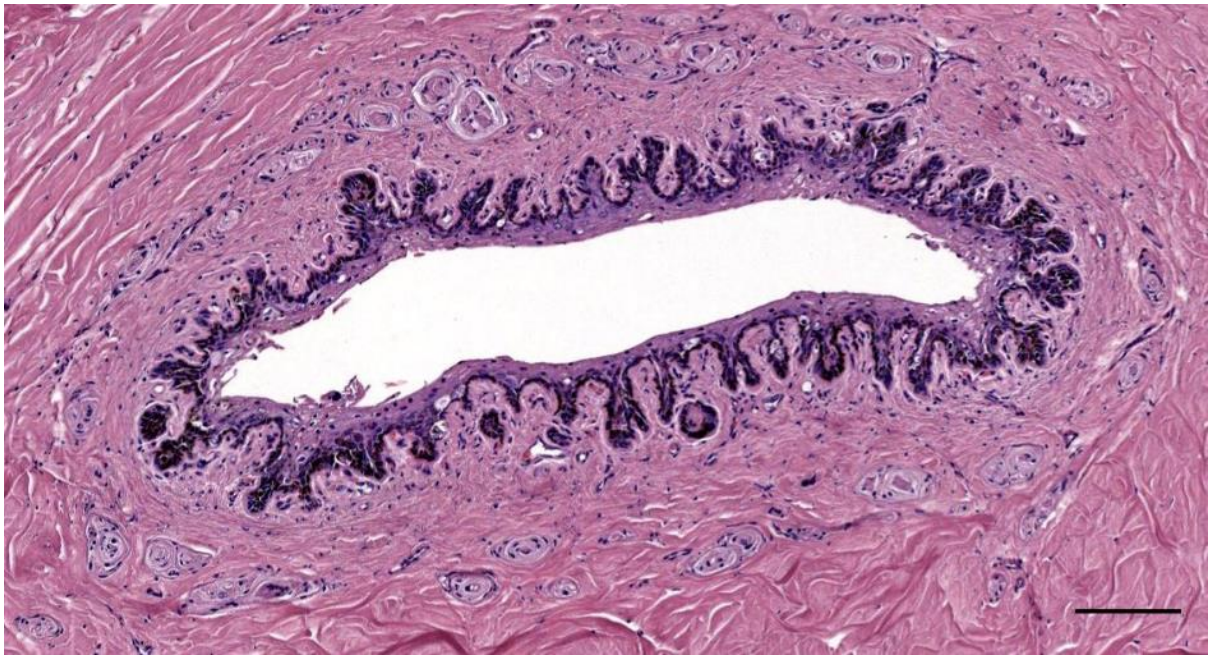

Figure 551. Histological transverse section (HE staining) through the ear canal of a bottlenose dolphin (444_L10). Note the elaborate epithelial subepithelial interaction. Scale bar 100 µm

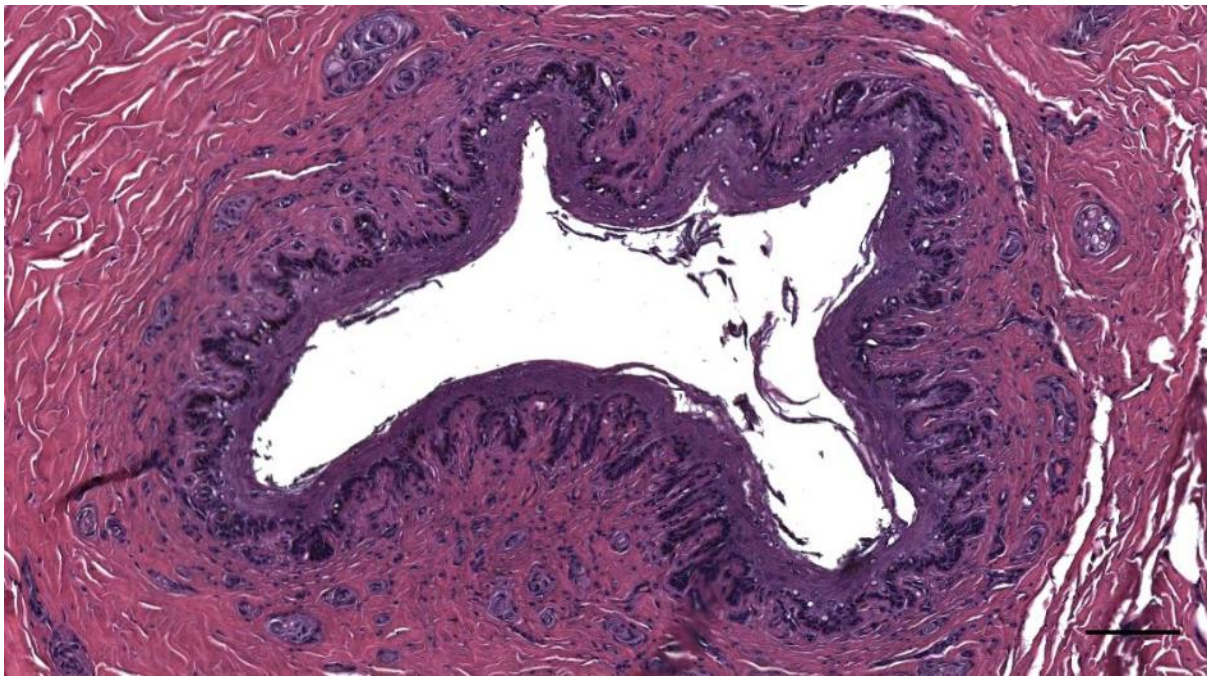

Figure 552. Histological transverse section (HE staining) through the ear canal of a bottlenose dolphin (457_R8). Scale bar 100 µm

Figure 553. Histological transverse section (HE staining) through the ear canal of a harbour porpoise at about 1 cm beneatah the skin. Scale bar 500 µm

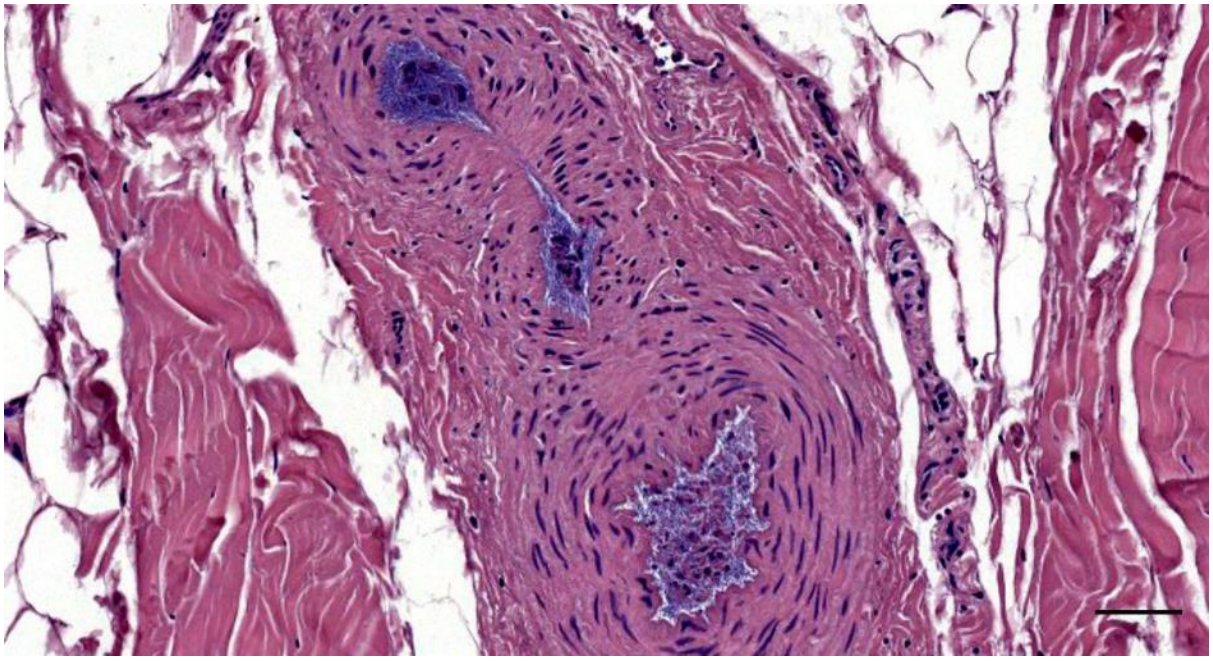

Figure 554. HE staining of small arteria presented leucocytosis in a bottlenose dolphin (444_L5). Scale bar 50 µm

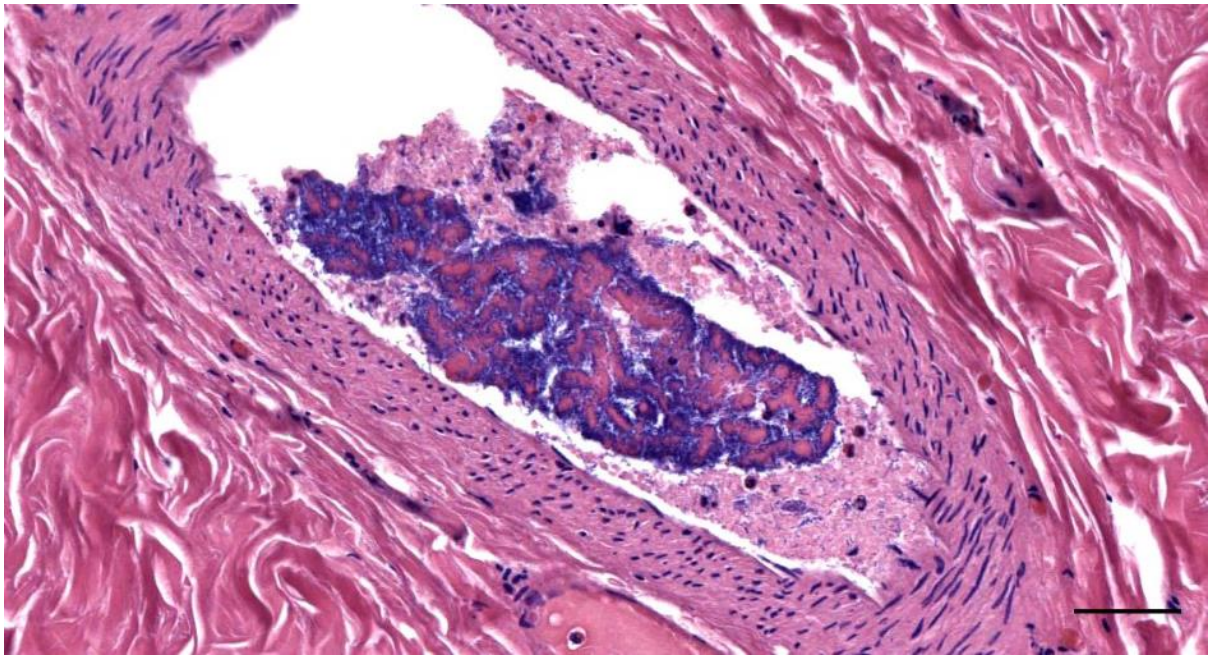

Figure 555. HE staining of a small arteria presented leucocytosis in a bottlenose dolphin (444_L12) Leukocytosis. Scale bar 50 µm

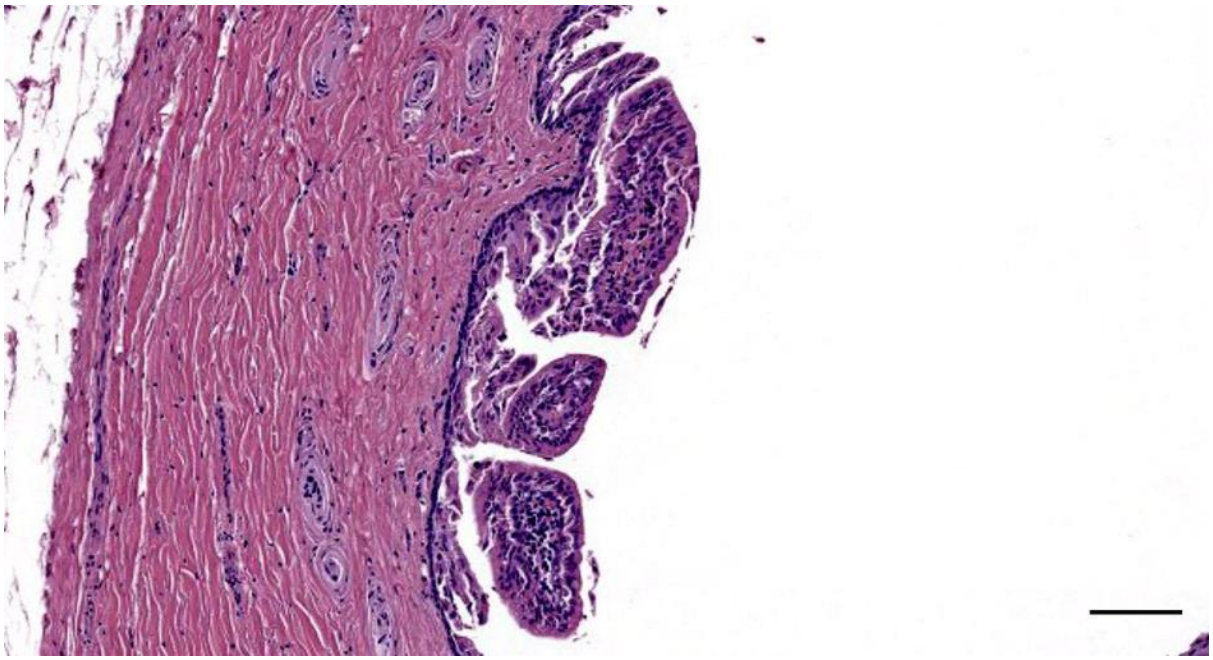

Figure 556. Histological transverse section (HE staining) of the ear canal in a bottlenose dolphin (444_L5) with eroded epithelium except for few papillae with likely glandular epithelium. Scale bar 100 µm

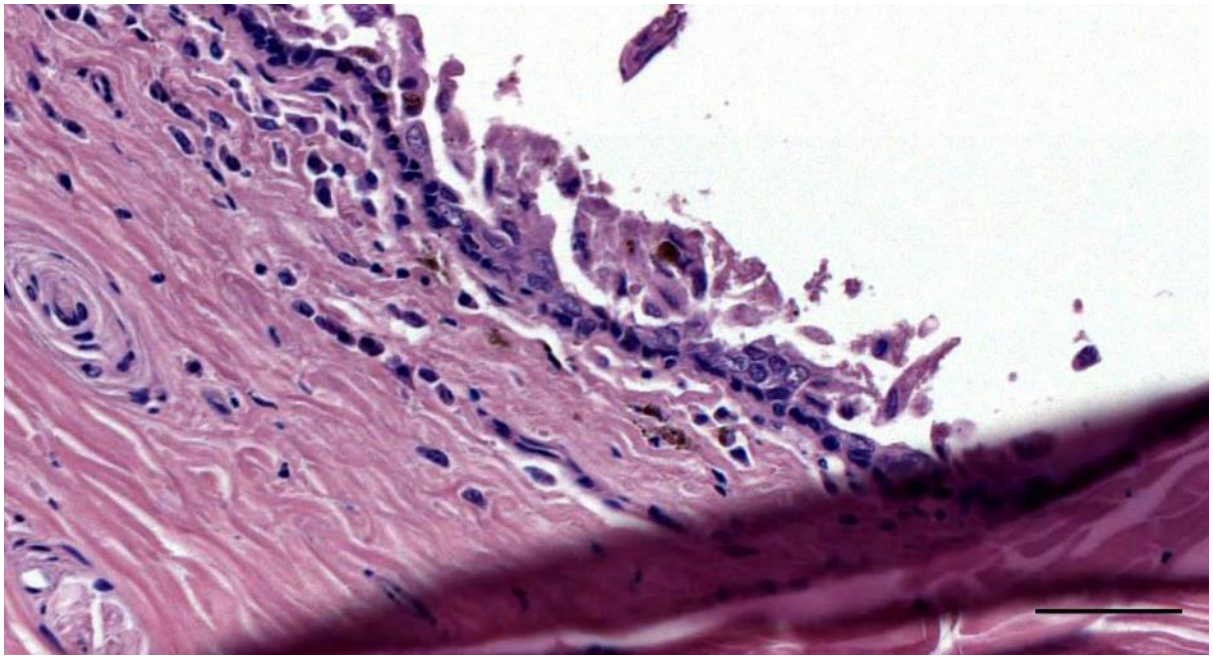

Figure 557. Histological transverse section (HE staining) of the ear canal in a bottlenose dolphin (444_L5) with melanin in the subepithelial tissue. Scale bar 50 µm

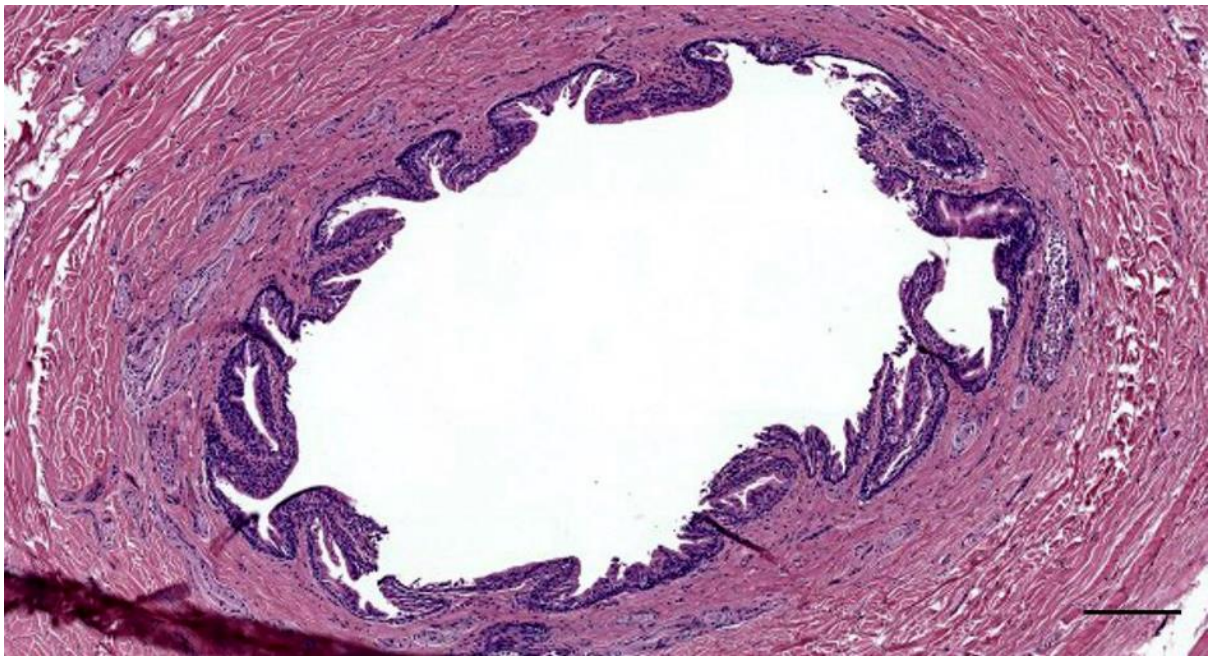

Figure 558. Histological transverse section (HE staining) of the ear canal in a bottlenose dolphin (444_L6). Ear canal and glands/glandular epithelium. Scale bar 200 µm

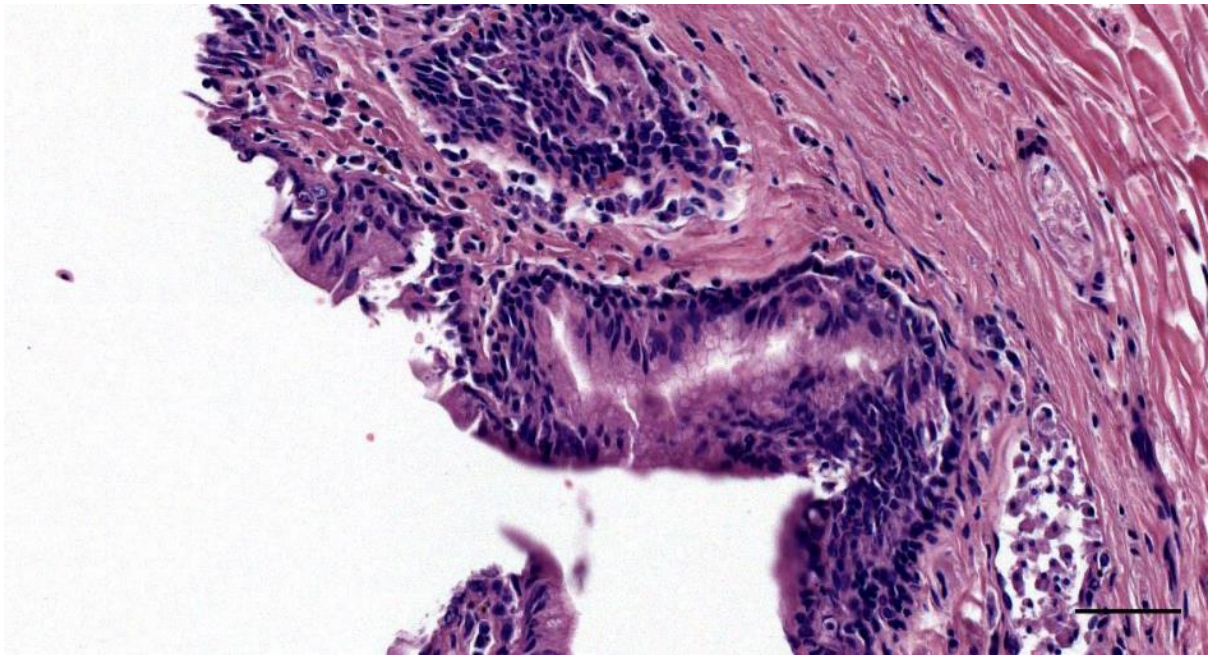

Figure 559. Detail of Figure 339 (444_L6). Ear canal and glands/glandular epithelium. Scale bar 50 µm

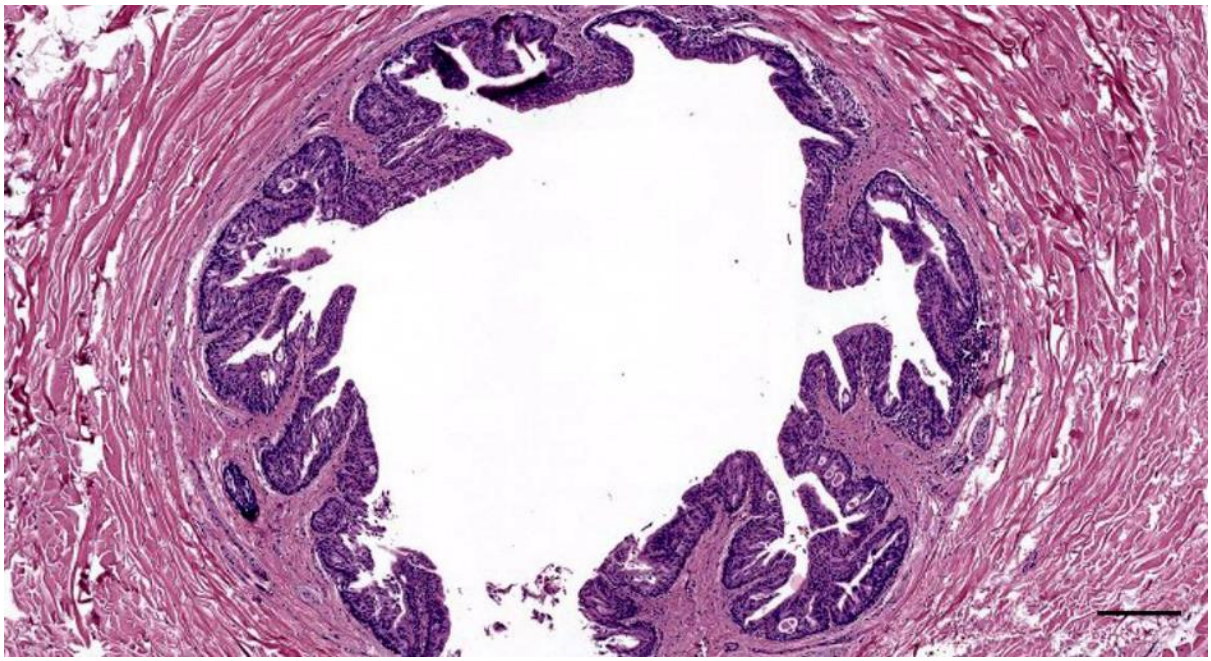

Figure 560. Histological transverse section (HE staining) of the ear canal in a bottlenose dolphin (444_L7). Ear canal and glands/glandular epithelium. Scale bar 200 µm

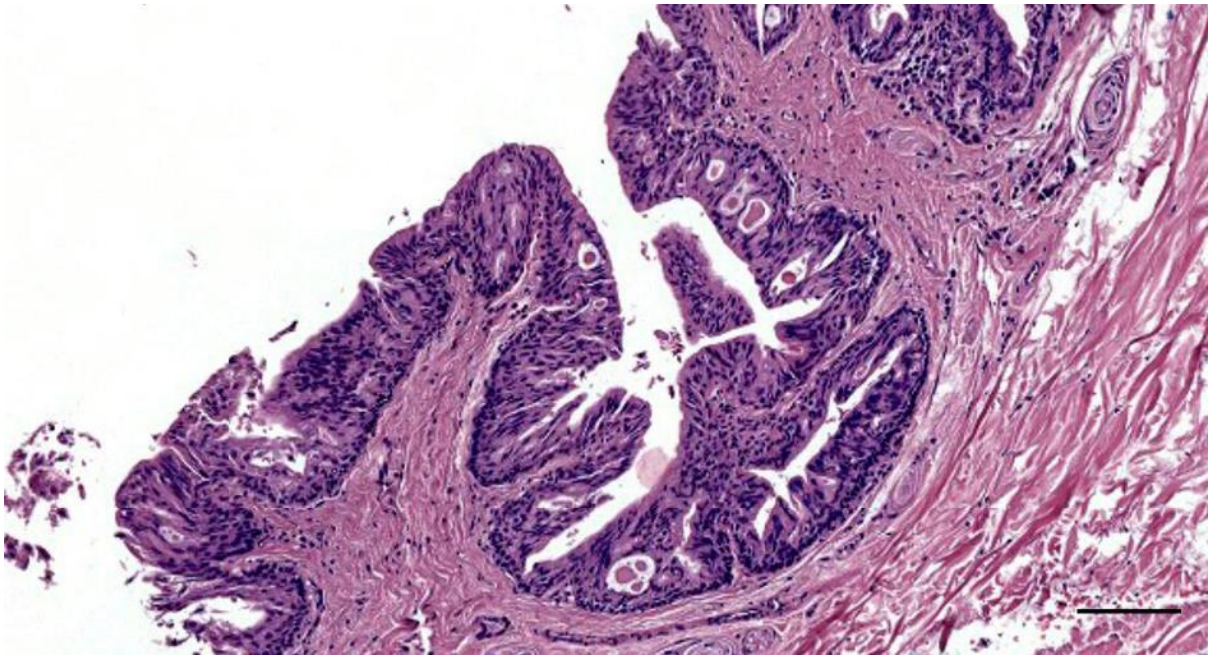

Figure 561. Detail of Figure 560 (444_L7). Note the apoptotic changes in the glandular epithelium. Scale bar 100 µm

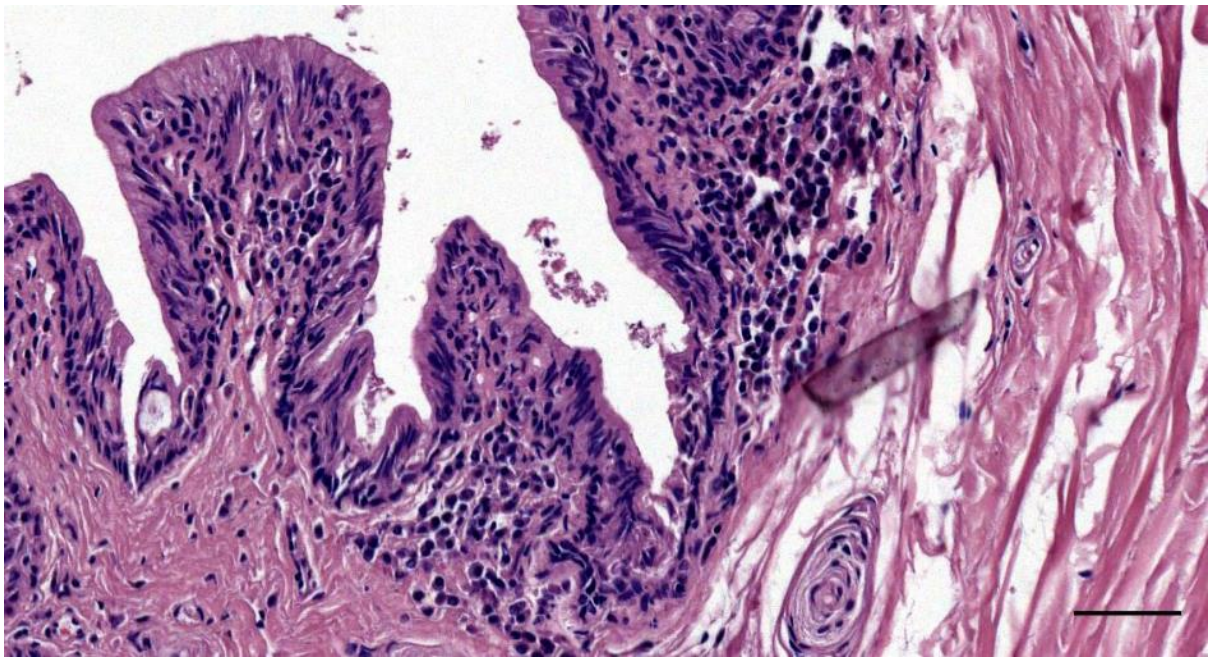

Figure 562. Detail of Figure 560 (444_L7). Note the mononuclear infiltrate in the superficial propria. Scale bar 100 µm

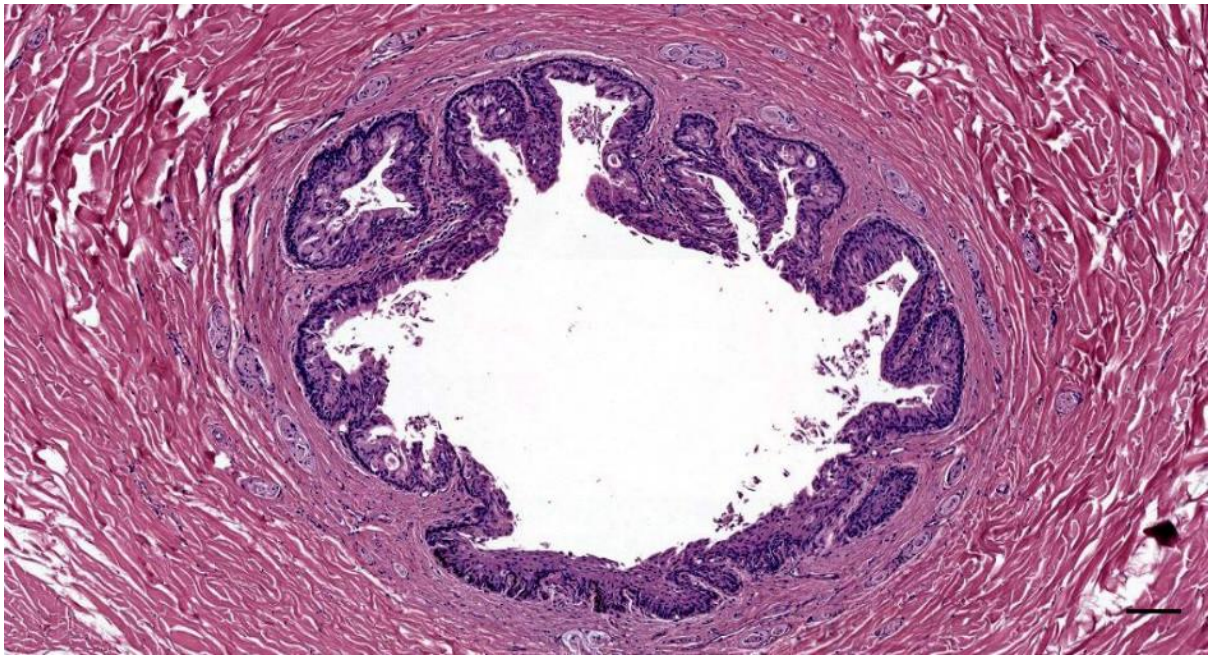

Figure 563. Histological transverse section (HE staining) of the ear canal in a bottlenose dolphin (444_L8). Ear canal and glands. Scale bar 100 µm

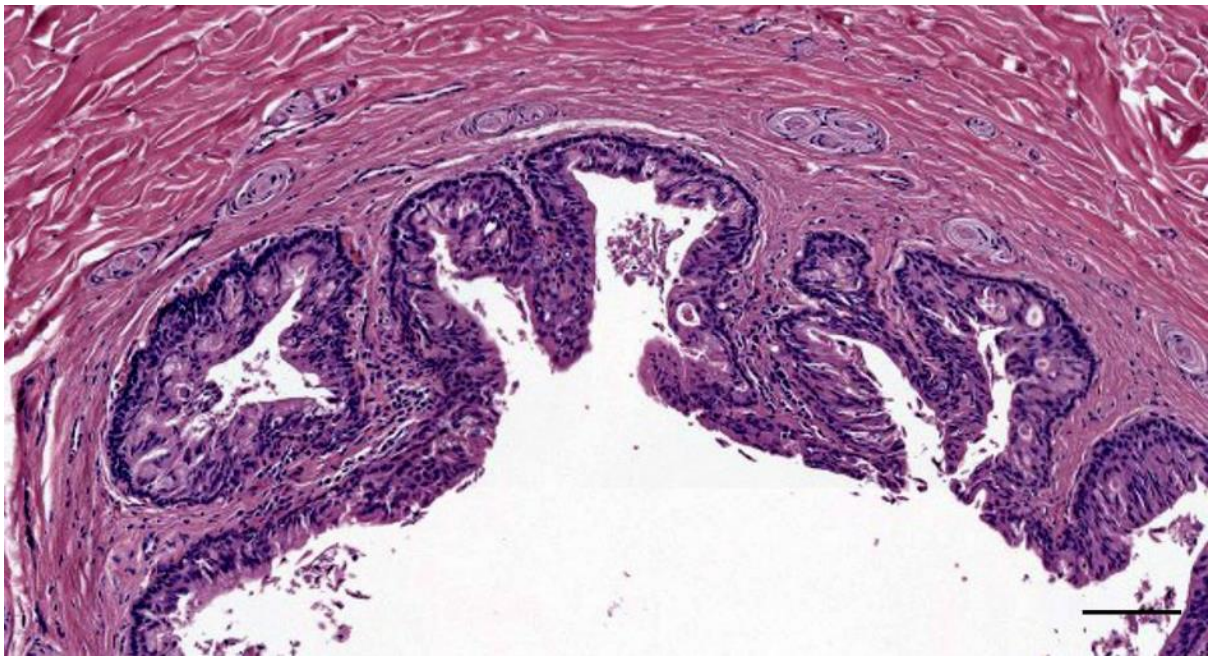

Figure 564. Detail of Figure 345 (444_L8) Ear canal and glands, note the lamellar corpuscles and the lymphocytic infiltrate in the superficial lamina propria. Scale bar 100 µm

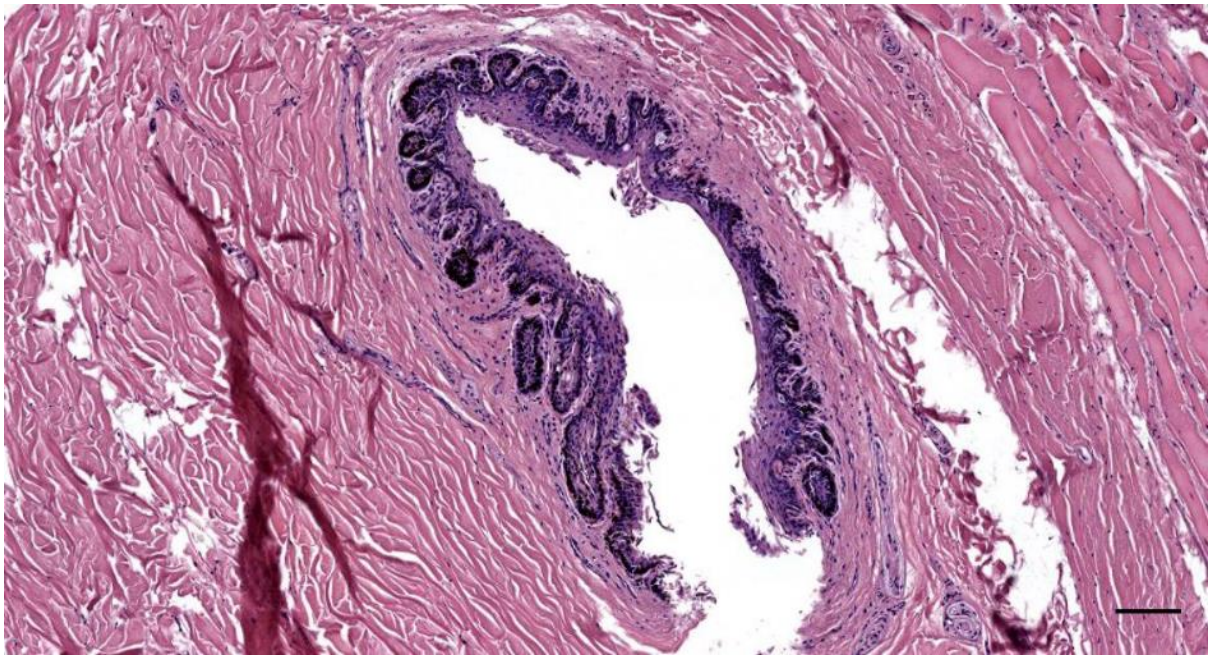

Figure 565. Histological transverse section (HE staining) of the ear canal in a bottlenose dolphin (444_L9). Ear canal with squamous epithelium. Scale bar 100 µm

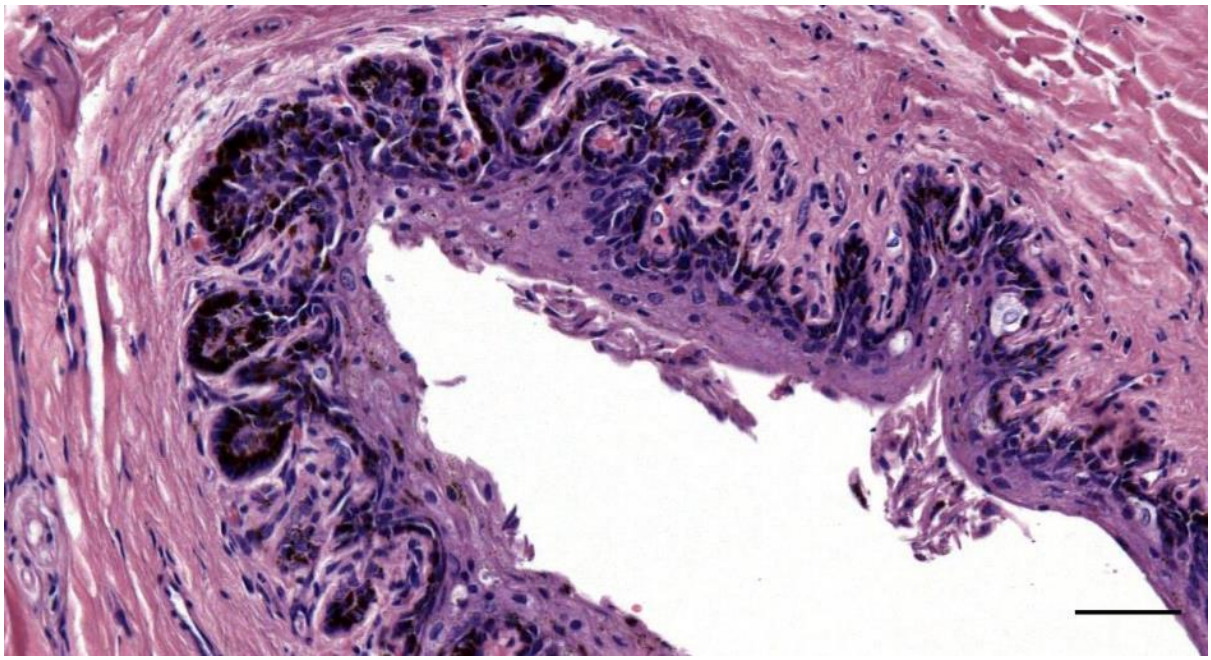

Figure 566. Detail of Figure 565 (444_L9). Ear canal with squamous epithelium. Scale bar 50 µm

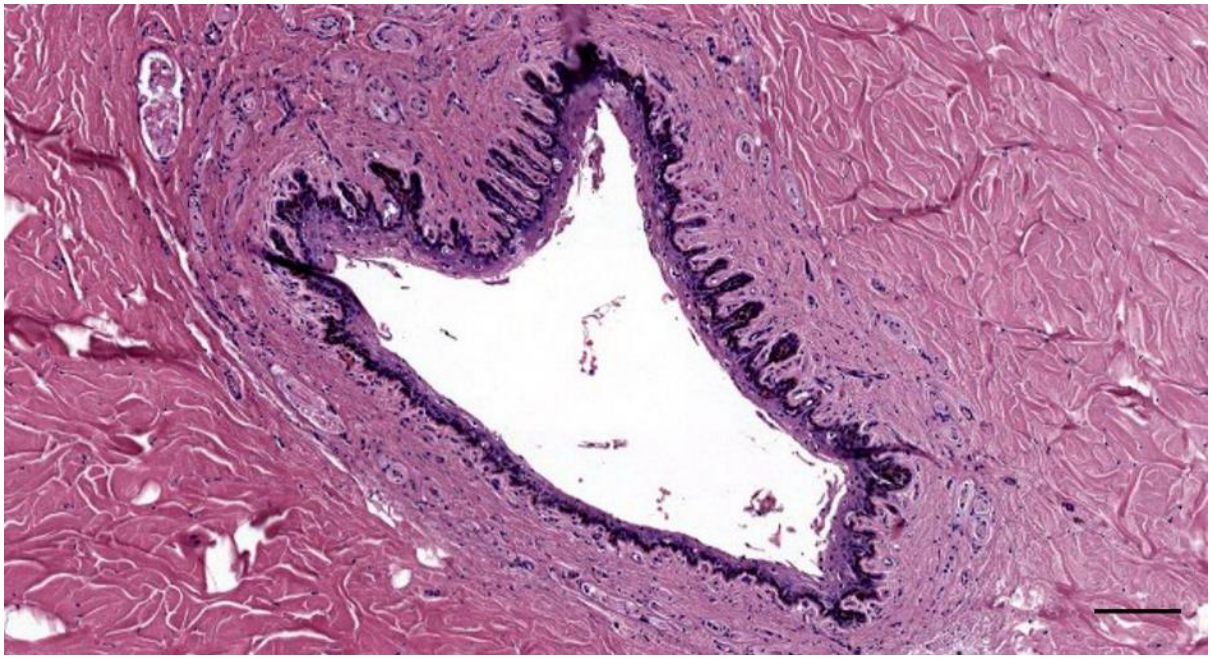

Figure 567. Histological transverse section (HE staining) of the ear canal in a bottlenose dolphin (444_L12). Note the nervous tissue ridge(s) and the difference in the papillary layer at the nervous tissue ridge and the tissue closer to the cartilage (bottom). Scale bar 100 µm

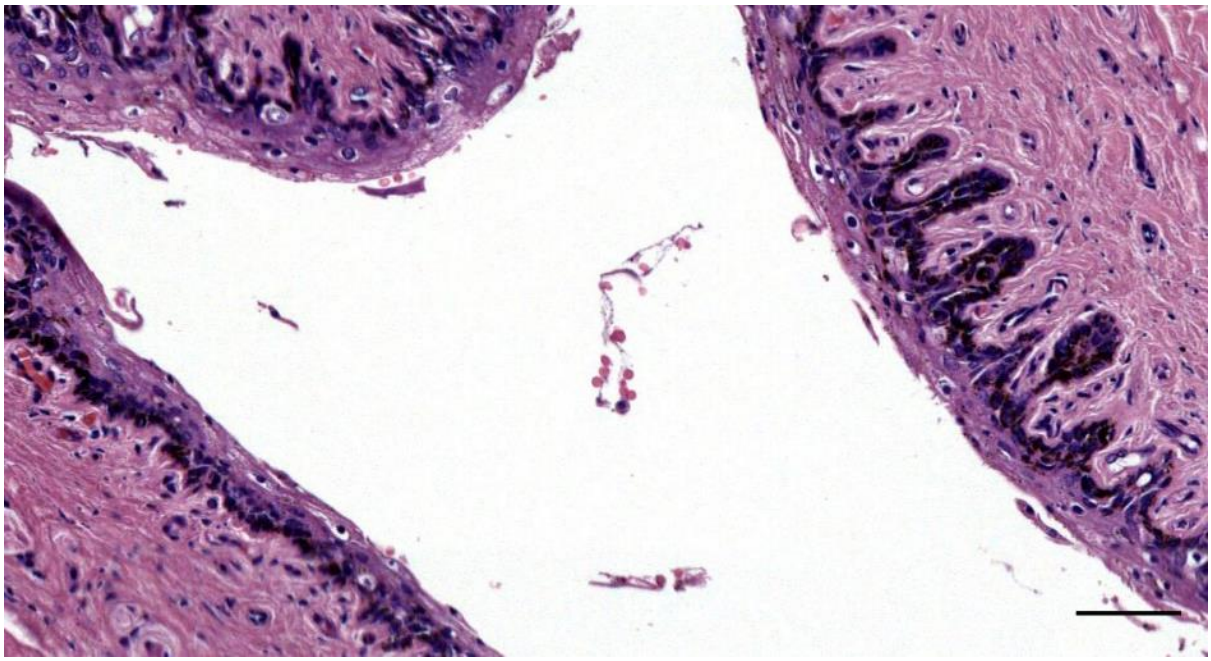

Figure 568. Detail of Figure 567 (444_L12). Ear canal with red blood cells in the lumen. Scale bar 50 µm

3.2.2.1 Transmission Electron Microscopy

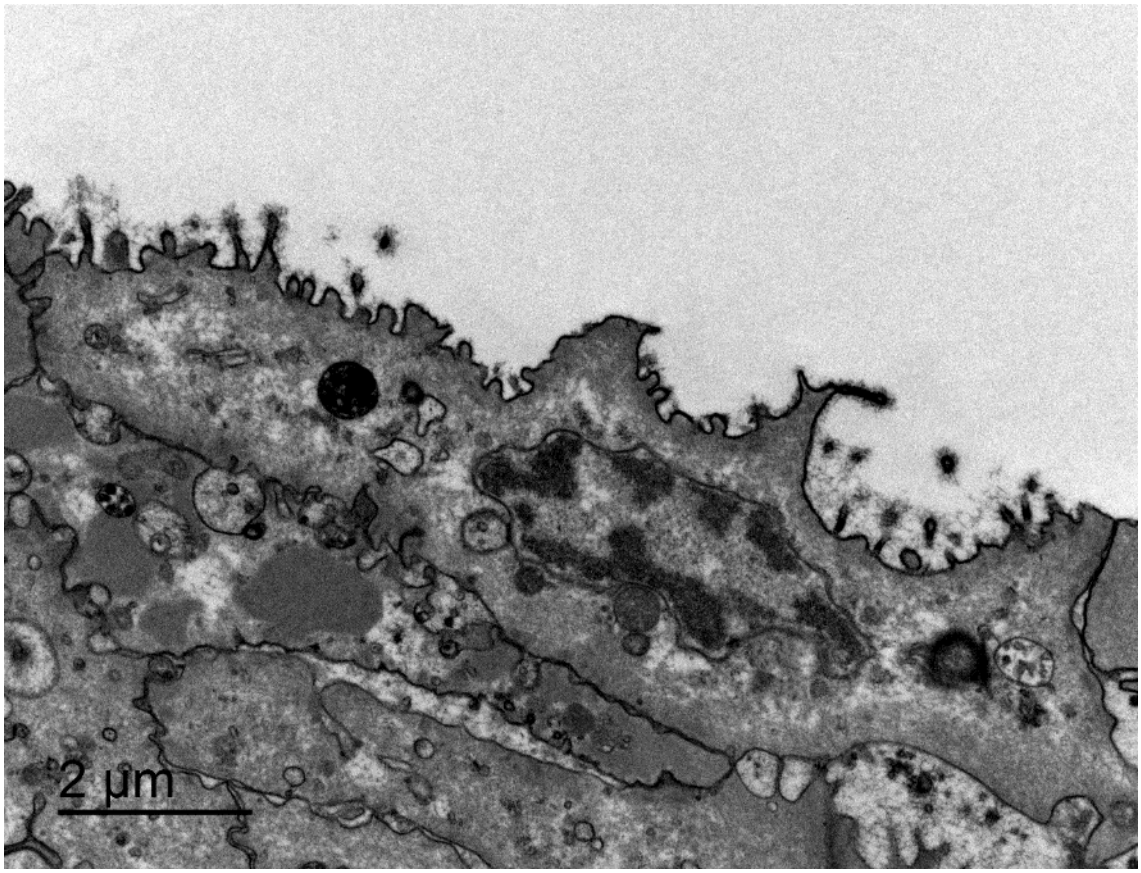

Figure 569. TEM detail image of an apical epithelial cell with nucleus with eu- and heterochromatin, electron-lucid to electron-dense dense intracellular vesicles. (TEM x 15.000)

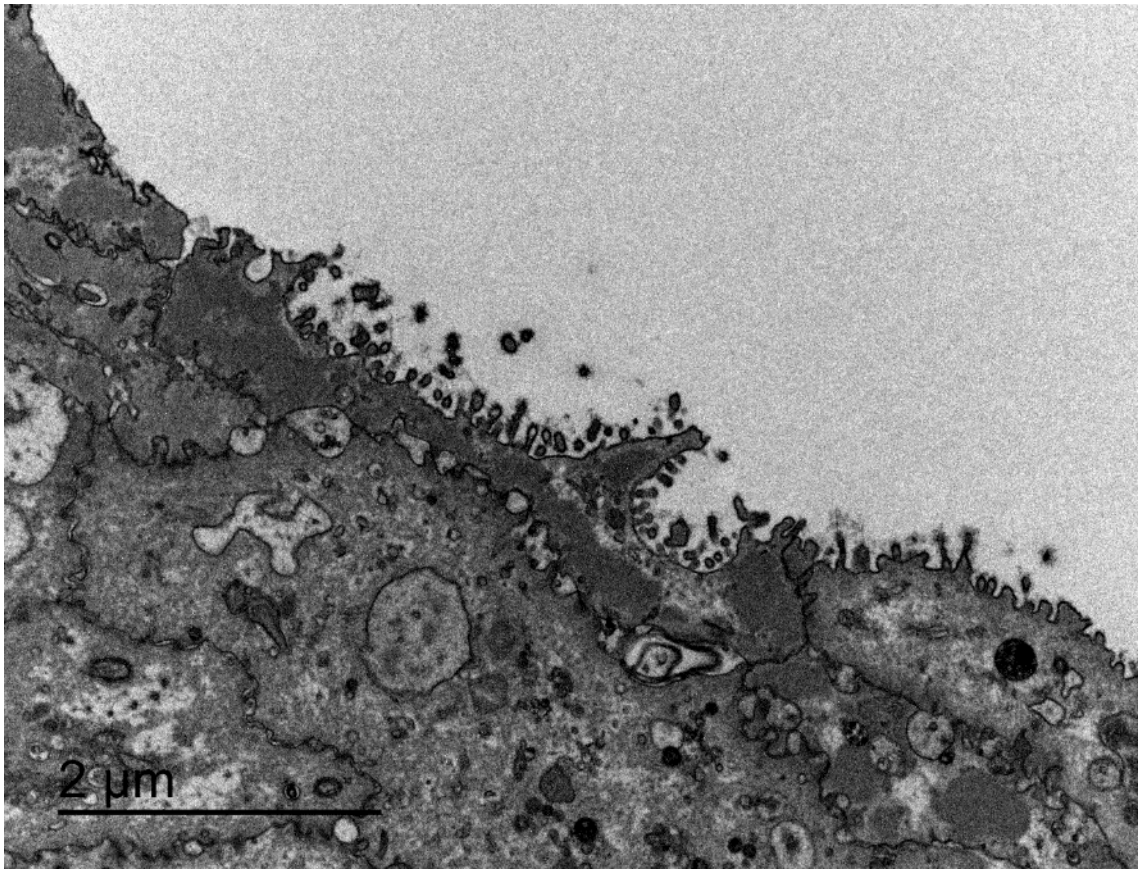

Figure 570. TEM detail image of an apical epithelial cell. (TEM x 10.000)

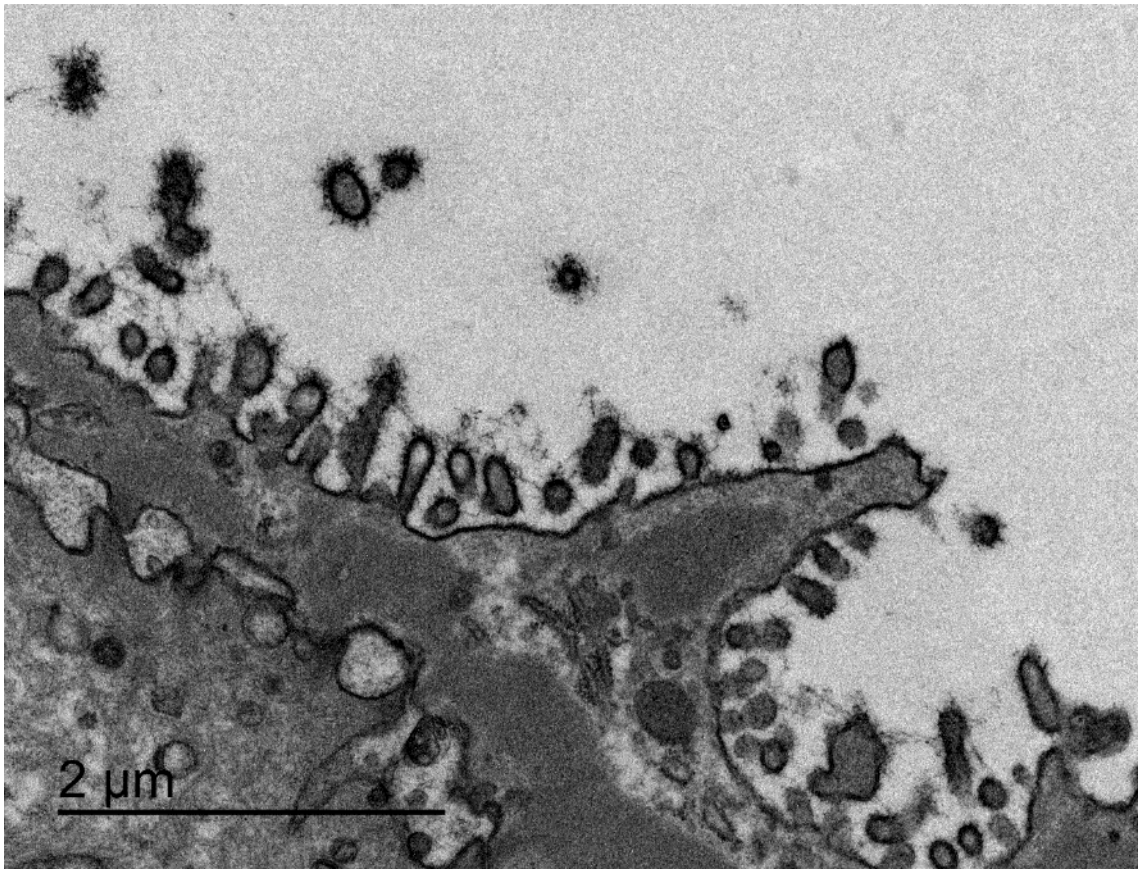

Figure 571. TEM detail image of an apical epithelial cell. (TEM x 30.000)

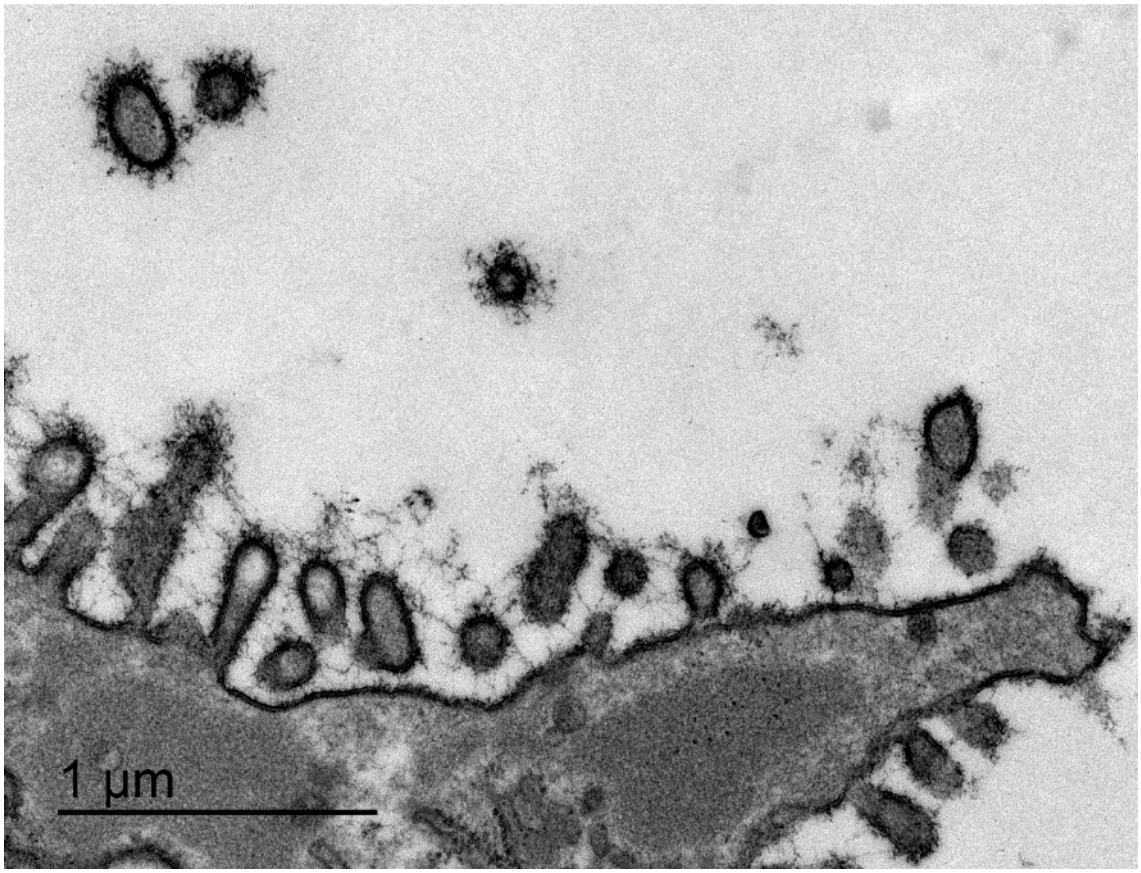

Figure 572. TEM detail image of an apical epithelial cell. (TEM x 50.000)

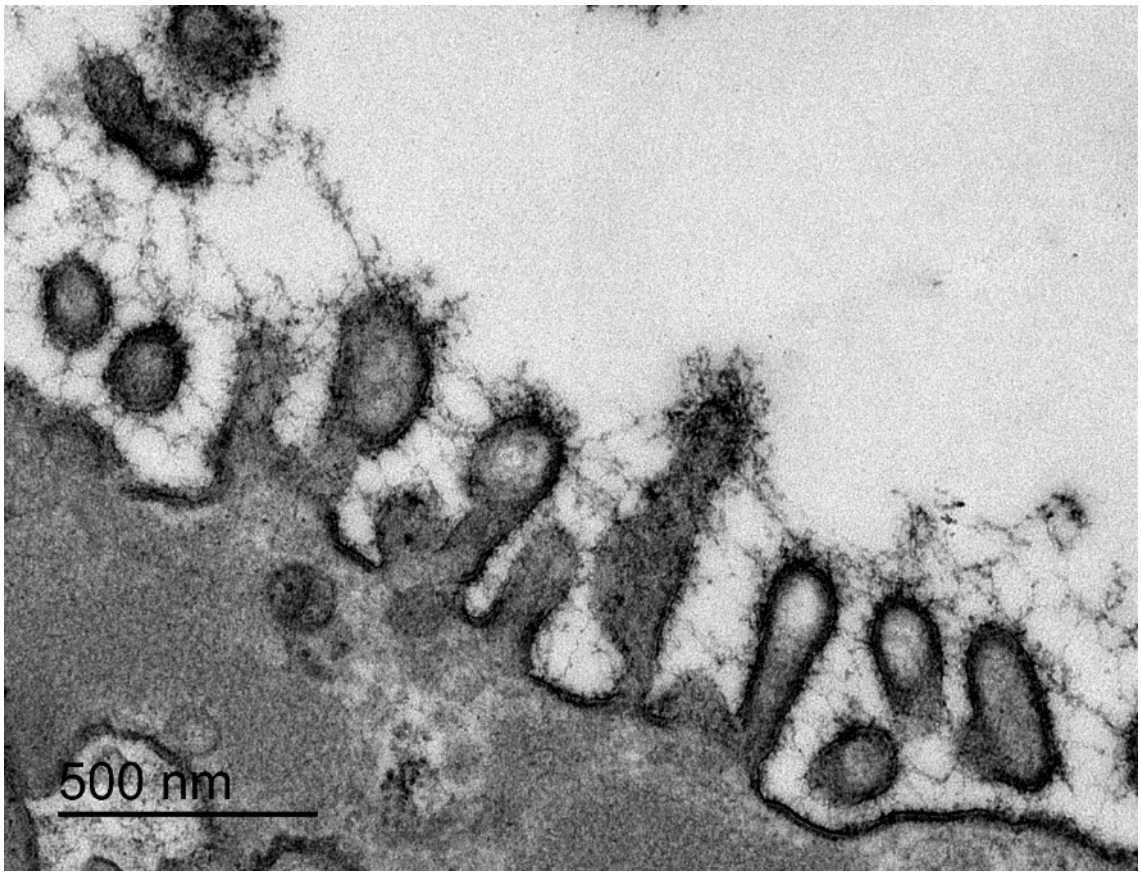

Figure 573. TEM detail image of an apical epithelial cell. (TEM x 80.000)

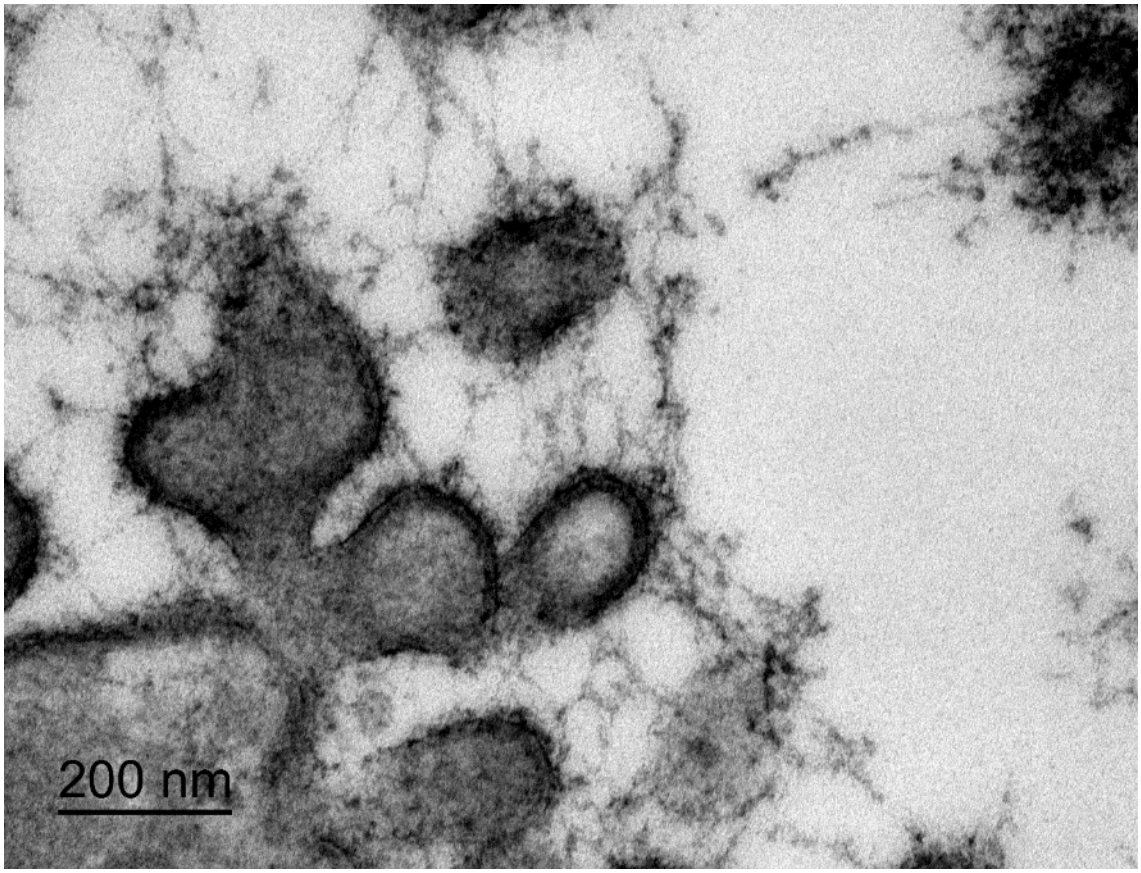

Figure 574. Detail image of exocytotic (or endocytic) protrusions on the apical cell membrane of an epithelial cell (E) in the ear canal of a striped dolphin. There is an extensive glycocalyx connecting and interconnecting the vesicles. The content of the vesicles is relatively clear in comparison with the plasma membrane, which is electron-dense. (TEM x 150.000)

3.2.1 Glands

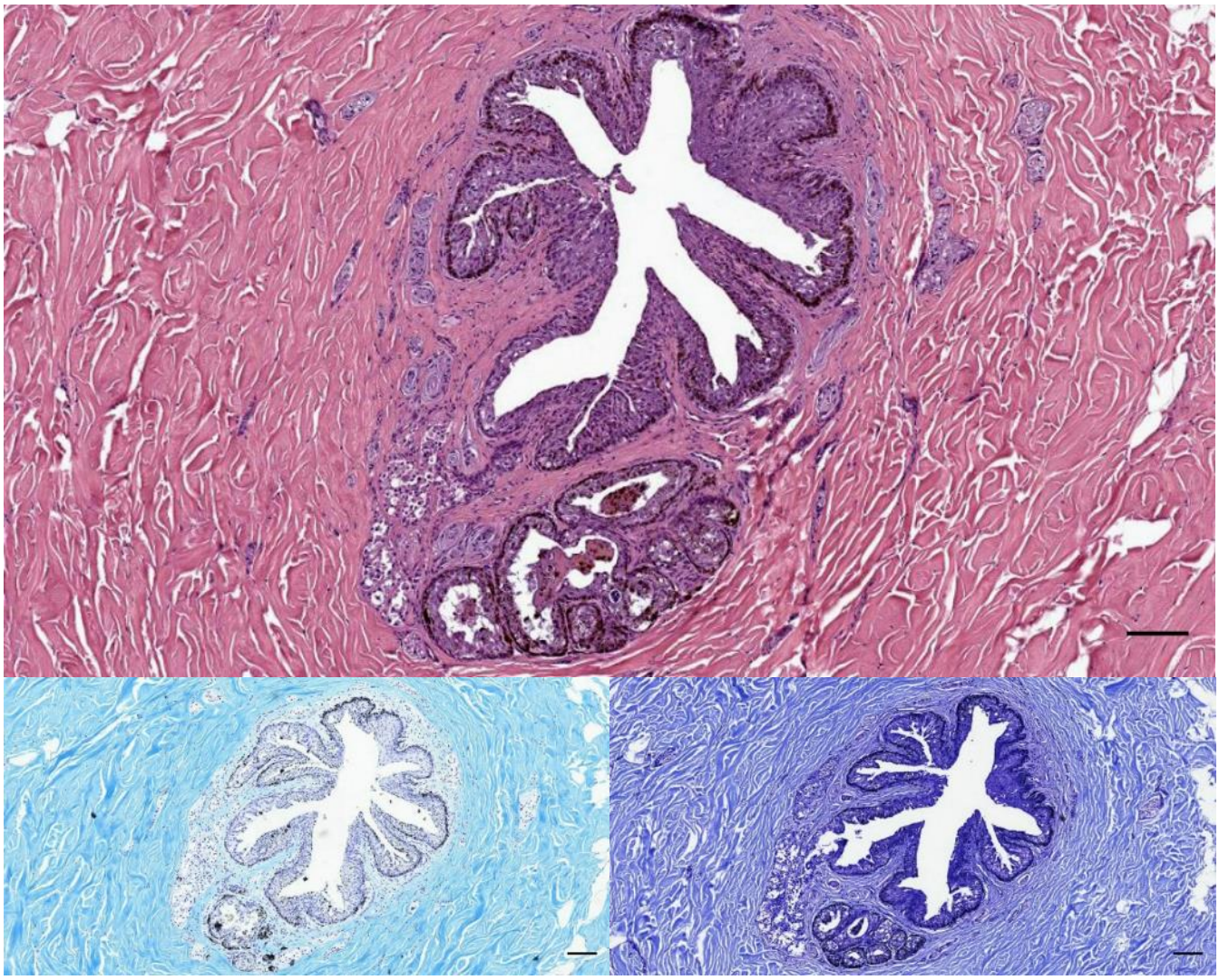

Figure 575. HE-stained cross-section (Top), and two Luxol Fast Blue stains (with different stain times)(Bottom) of the ear canal and associated glands of a striped dolphin about 0.5 cm beneath the surface. Scale bar 100 µm.

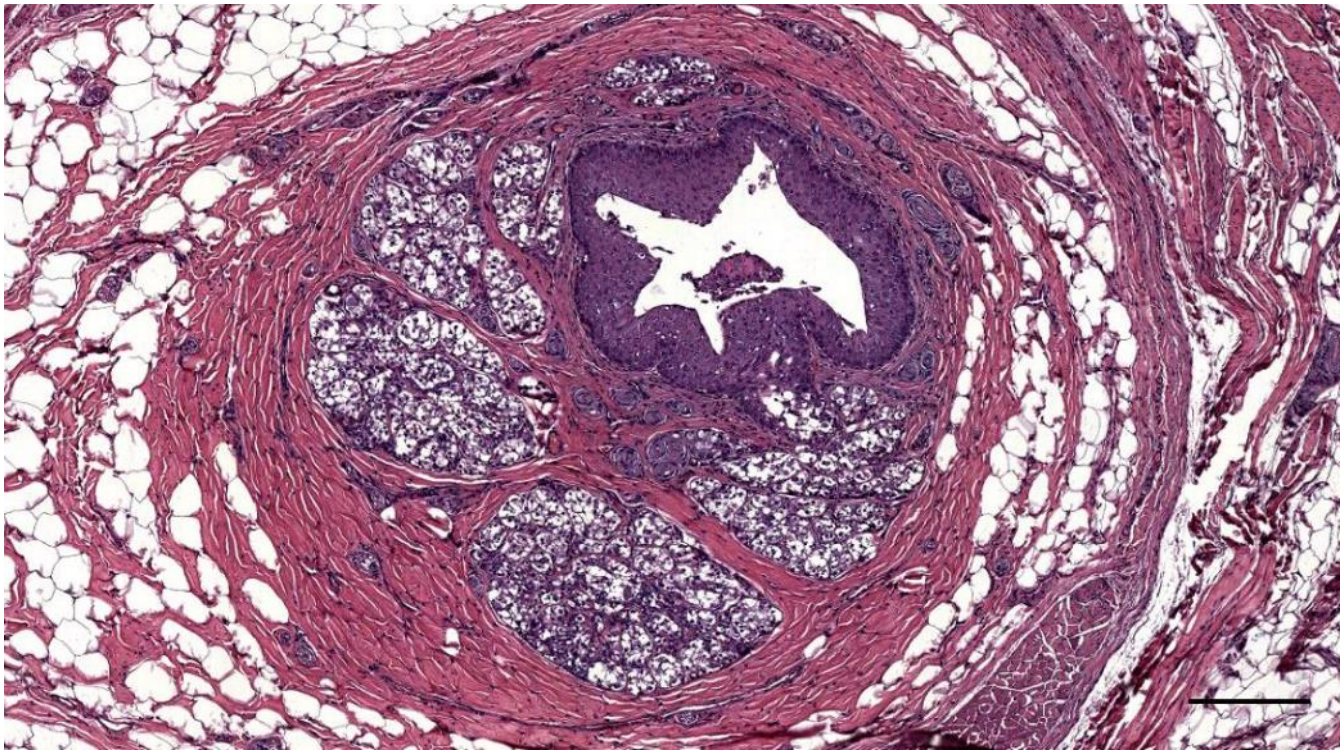

Figure 576. HE-stained cross-section of the ear canal and associated glands of a striped dolphin about 1 cm beneath the surface. Scale bar 200 µm

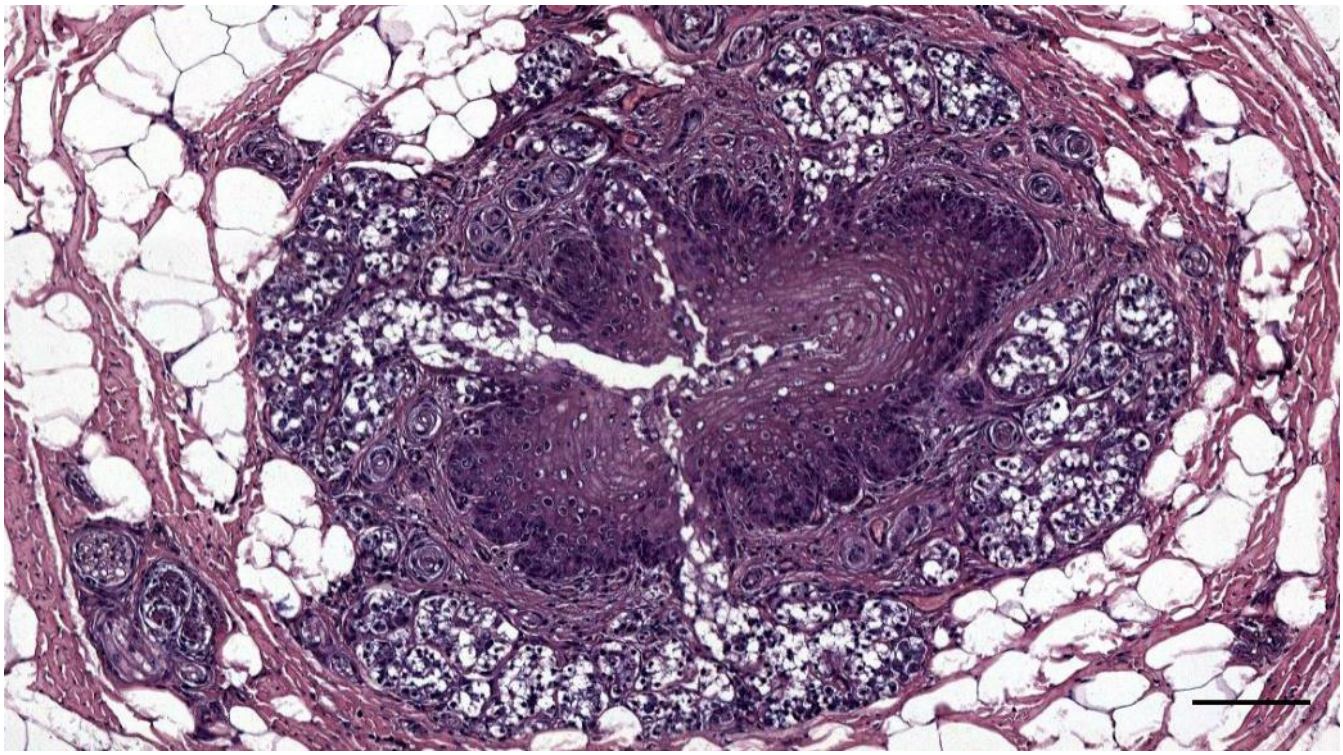

Figure 577. HE-stained cross-section of the ear canal and glands in striped dolphin, about 0.5 cm beneath the skin. Scale bar 200 µm

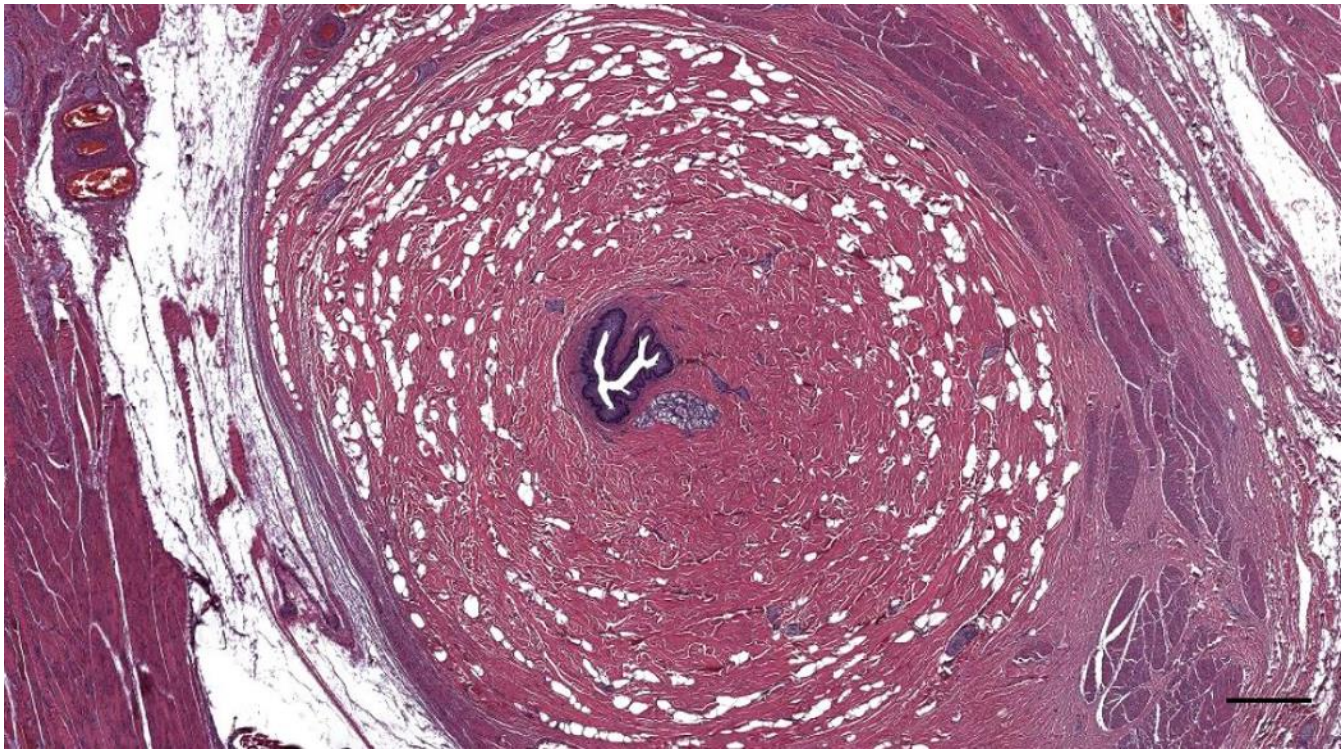

Figure 578. Same animal as in Figure 16, but a cross-section slightly deeper (about 1.5cm beneath the surface). There are still glands associated with the ear canal. The adipoconnective tissue sheath is larger, and the muscles are associated with it in the periphery. Around the sheath, there is still some fat tissue, but a lot more connective tissue as in the distal section.

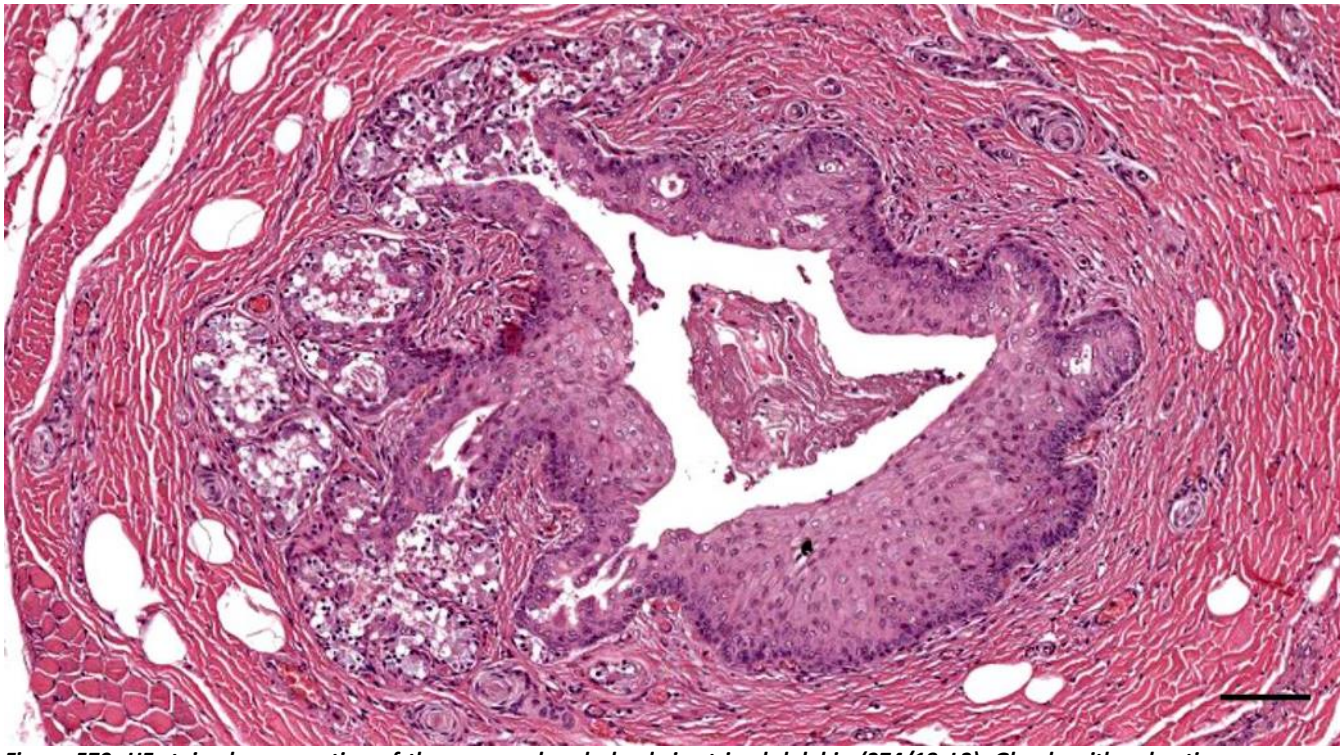

Figure 579. HE-stained cross-section of the ear canal and glands in striped dolphin (274/18_L3). Glands with pyknotic nuclei. Scale bar 100 µm

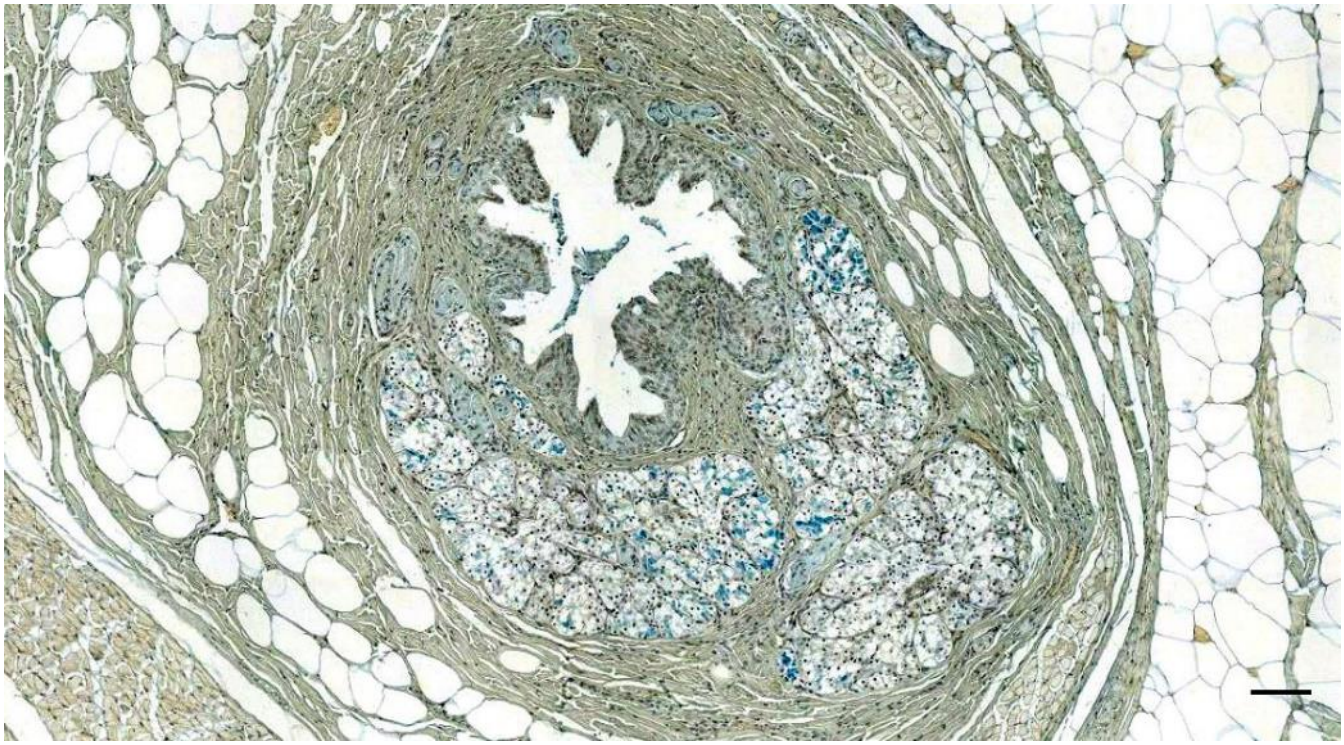

Figure 580. Alcian blue staining of a transverse section through the ear canal and glands about 1.5cm beneath the surface. Scale bar 100 µm

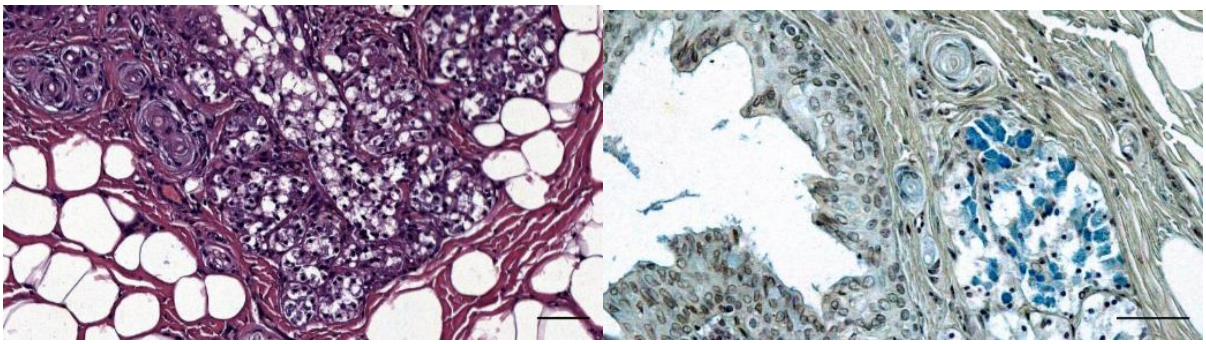

Figure 581. Left: (Detail of Figure 576) HE-stained histological detail of glandular structures and lamellar corpuscles in the adipoconnective tissue around the external ear canal. Right: (Detail of Figure 580). Alcian blue-stained detail of the epithelium of the ear canal, glands, and lamellar corpuscles in the subepithelial tissue. Scale bars 50 µm

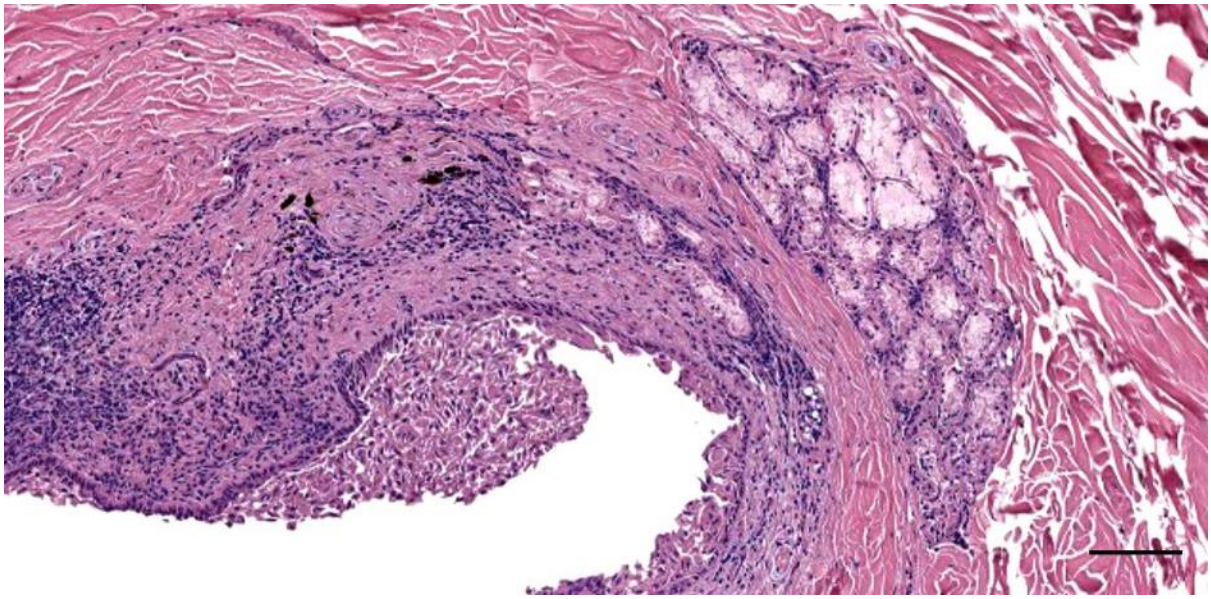

Figure 582. Histological transverse section (HE staining) through the ear canal of a long-finned pilot whale at about 5 cm beneath the skin (441_L12). Scale bar 100 µm

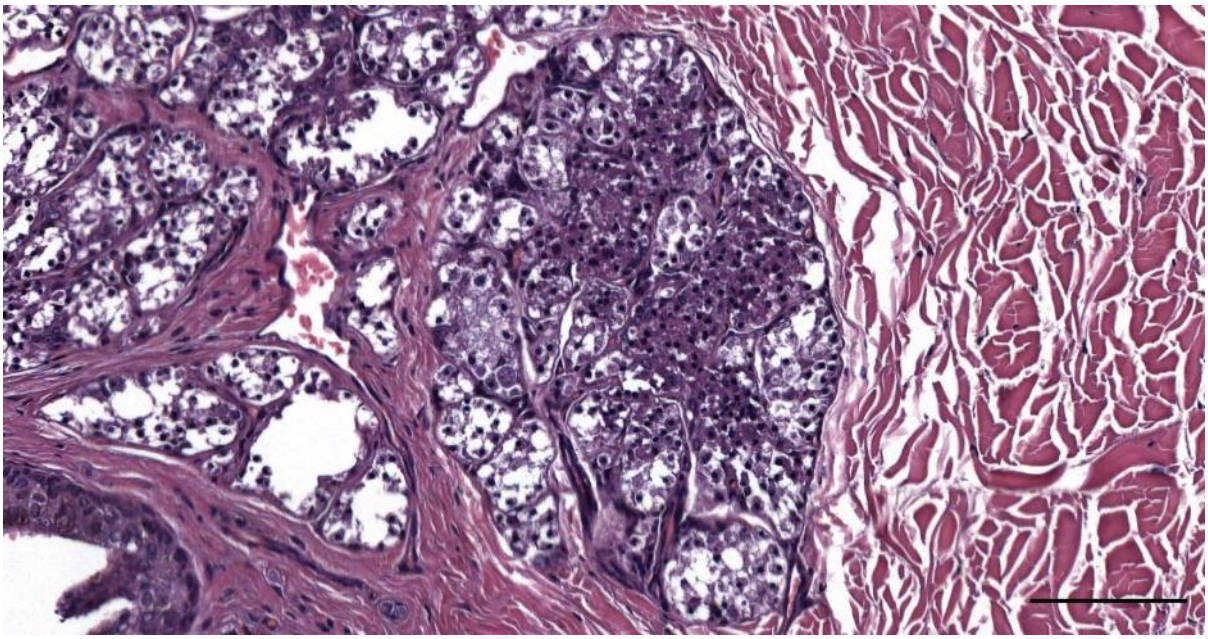

Figure 583. Histological detail image of a striped dolphin ear canal glands with pyknotic nuclei, at about 3 cm beneath the skin (44/17_R6). Scale bar 100 µm

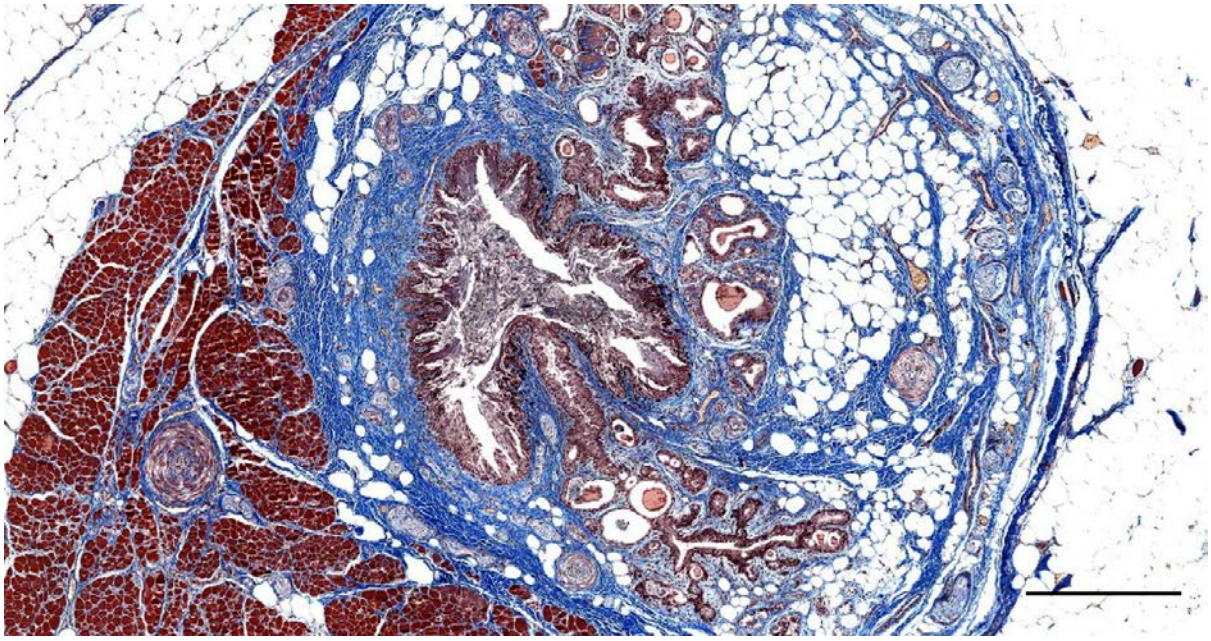

Figure 584. Histological image (Masson´s trichrome) of a transverse section through the external ear canal in a harbour porpoise, at about 1.5 cm beneath the skin (UT1711_R0601). Note the glands and excretory ducts that lead to the ear canal lumen, in which there is glandular content and epithelial cells. Note the impacted content in the glands. Scale bar 500 µm

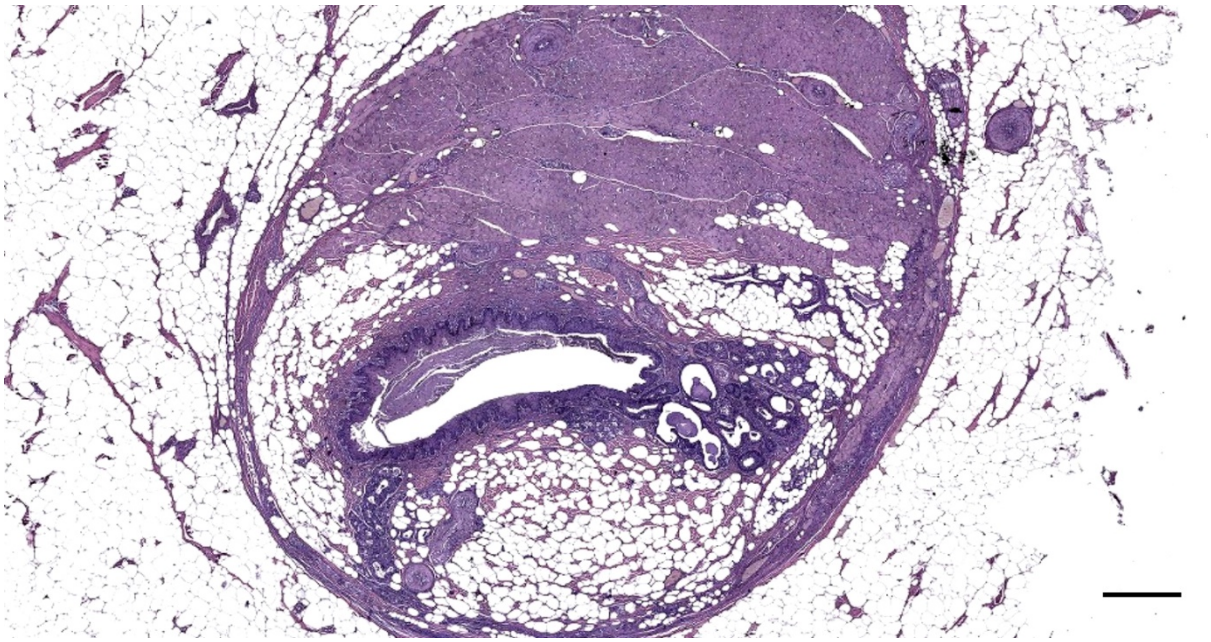

Figure 585. Histological image (HE staining) of a transverse section through the right ear canal of a harbour porpoise about 1.5 cm beneath the skin (UT1727_R0501). Lumen and glands. Scale bar 500 µm

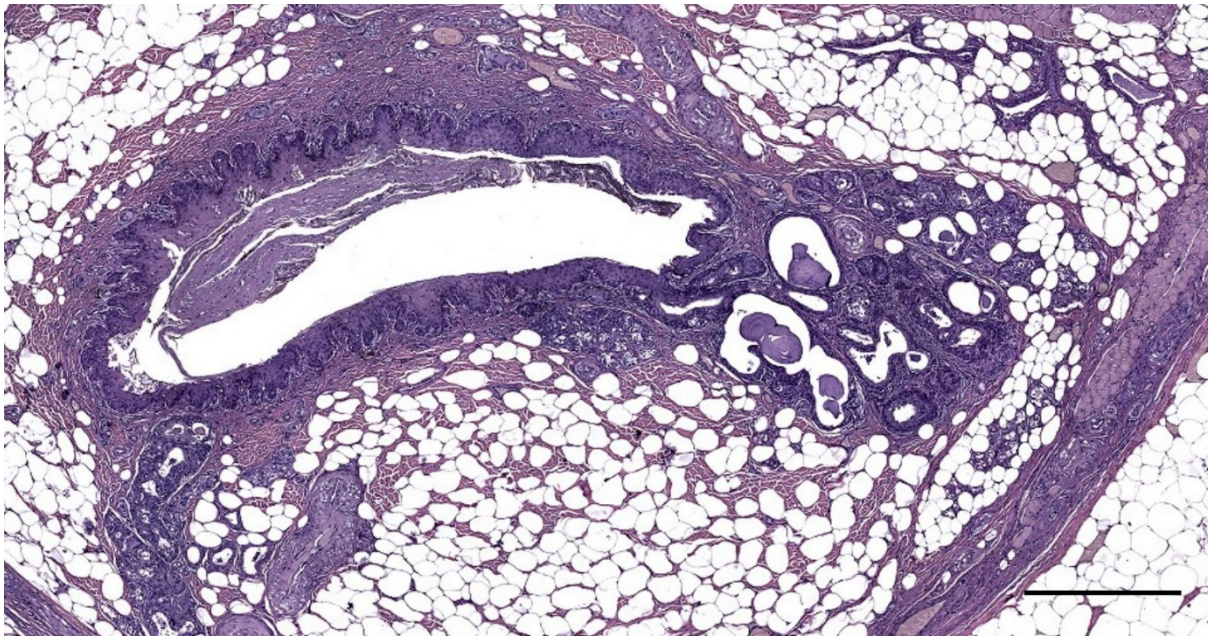

Figure 586. Detail of Figure 585. Histological image (HE staining) of a transverse section through the right ear canal of a harbour porpoise about 1.5 cm beneath the skin (UT1727_R0502). Note the impacted content in the glands. Scale bar 500 µm

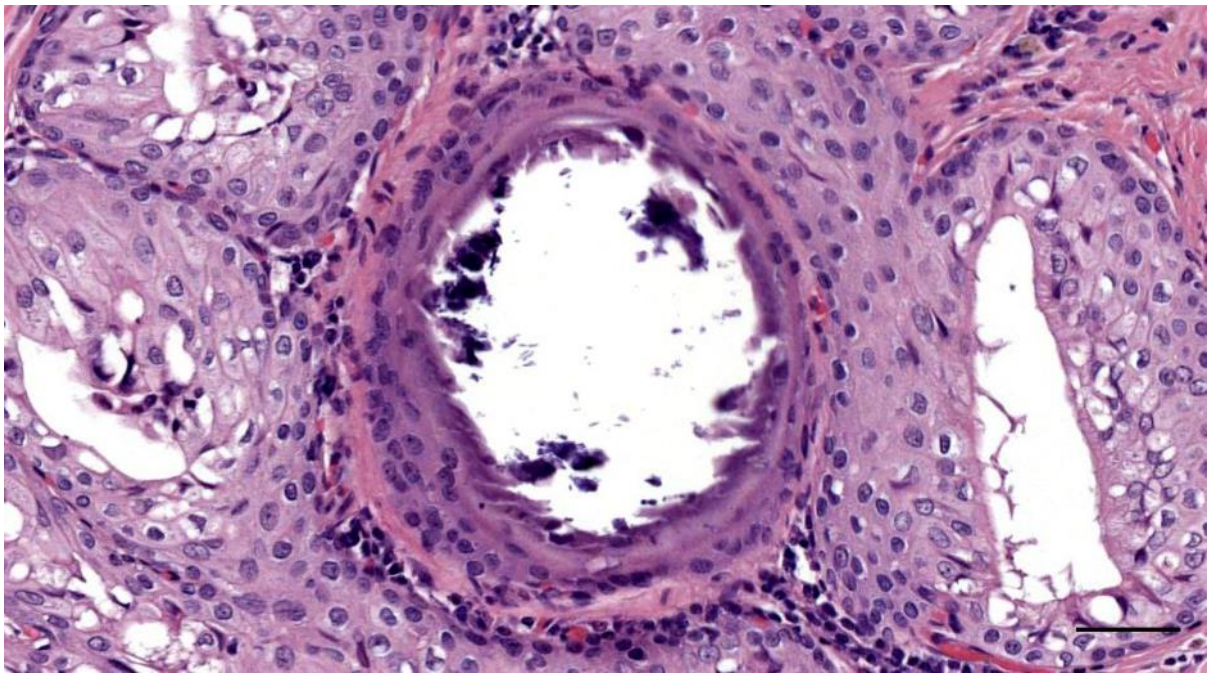

Figure 587. HE stained detail image of a round structure with mineralized content, indicative of a process of stasis. (169/17_R3). Scale bar 50 µm

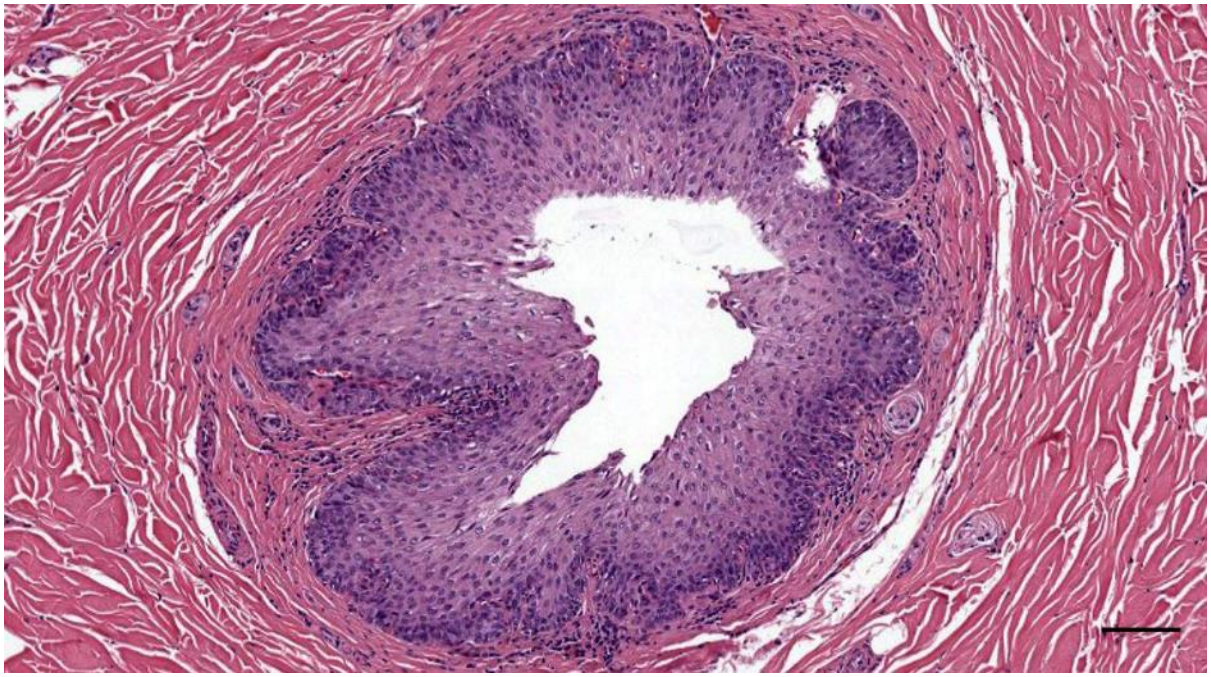

Figure 588. Histological image (HE staining) of a transverse section through the right ear canal of a common dolphin at about 2.5 cm beneath the skin, medial to the glandular structures (169/17_R5). Scale bar 100 µm

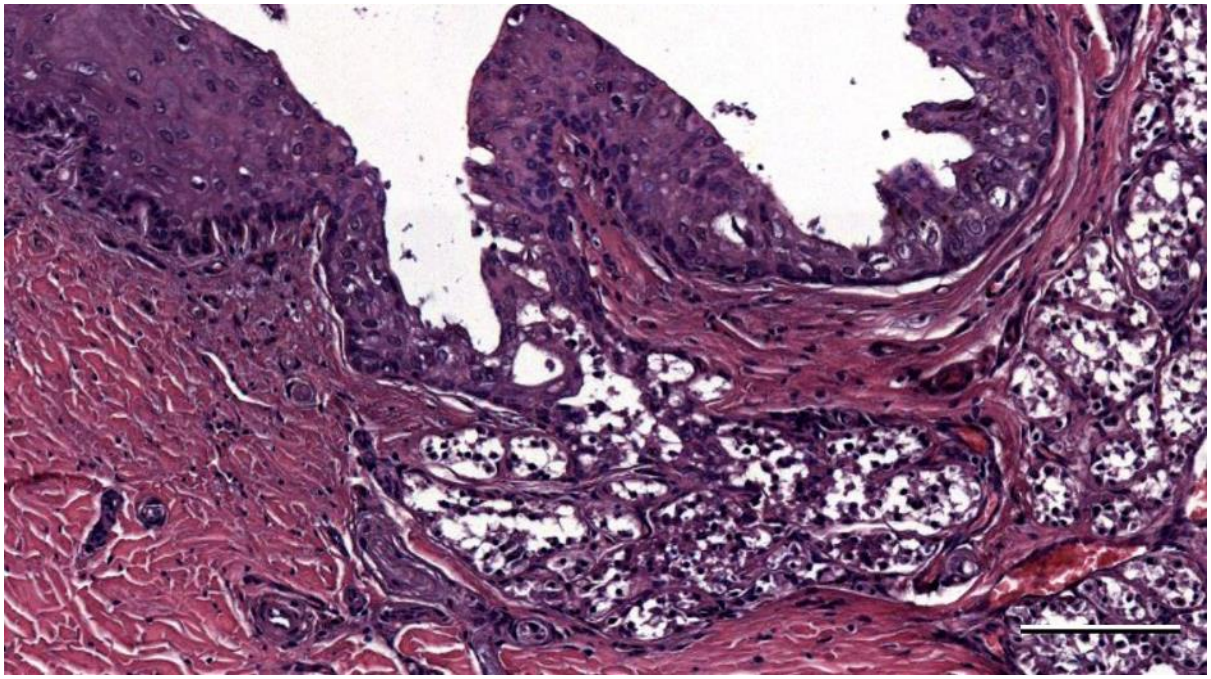

Figure 589. Histological image (HE staining) of a transverse section through the left ear canal of a striped dolphin at about 2.5 cm beneath the skin (44/17_L5, HE). Ear canal glands with excretory duct. Scale bar 100 µm

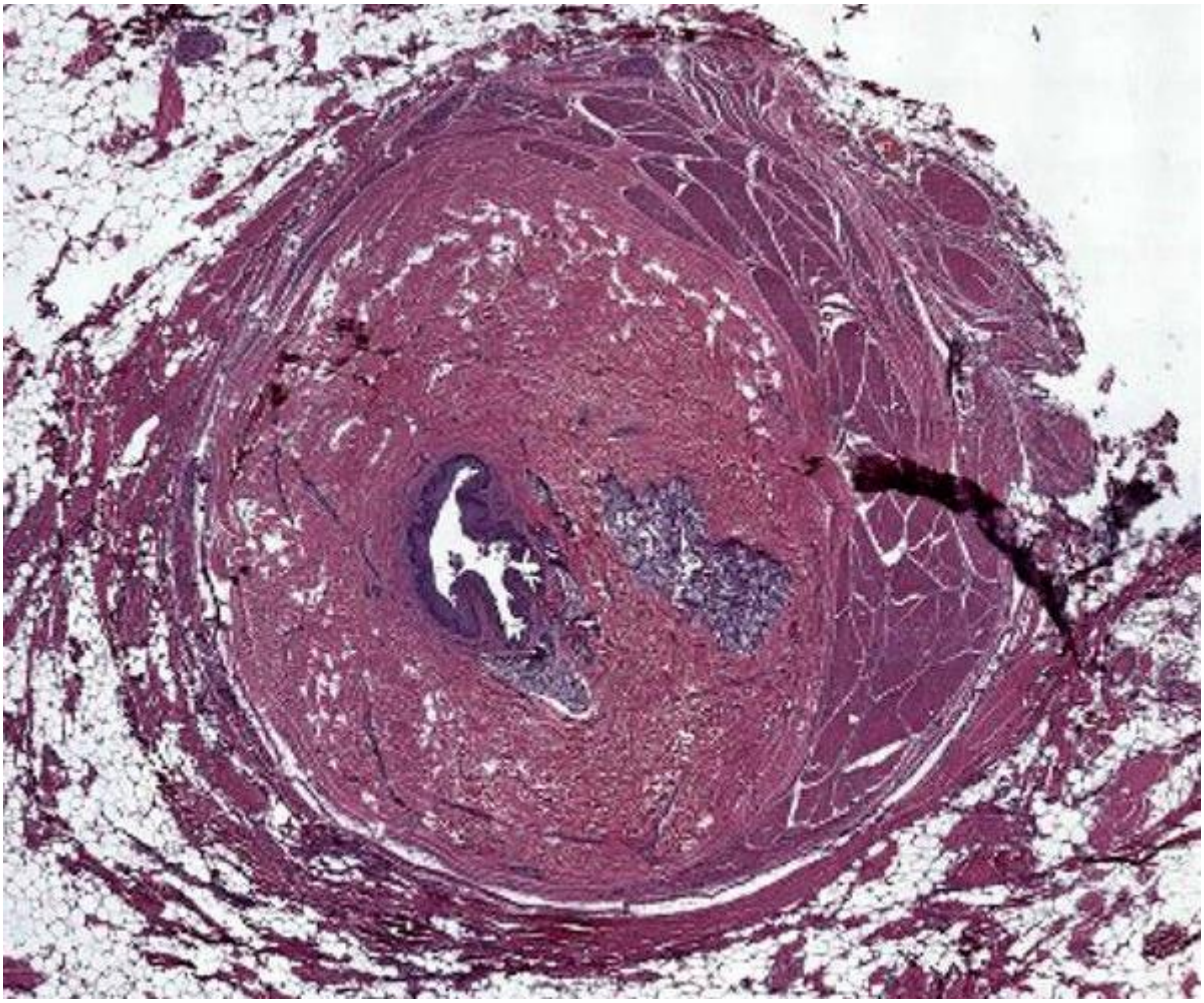

Figure 590. Histological image (HE staining) of a transverse section through the left ear canal of a striped dolphin at about 3 cm beneath the skin (44/17_L6, HE) Ear canal surrounded by glands, adipoconnective tissue and striated muscles. Scale bar 500 µm

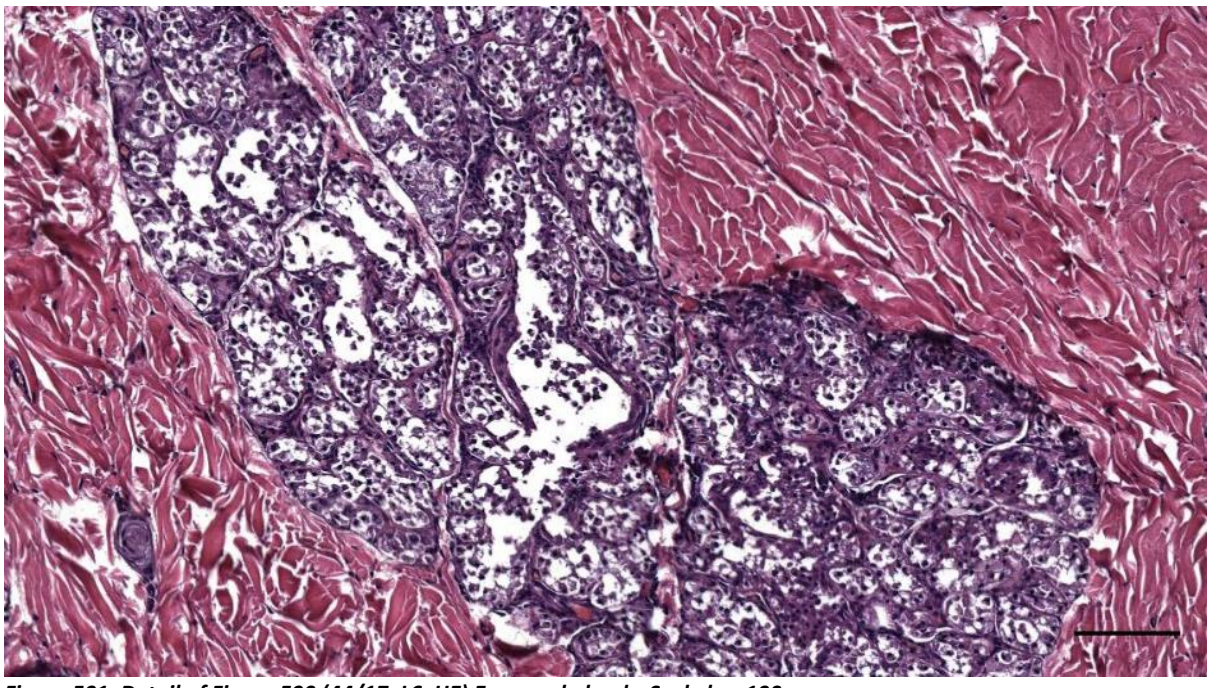

Figure 591. Detail of Figure 590 (44/17_L6, HE) Ear canal glands. Scale bar 100 µm

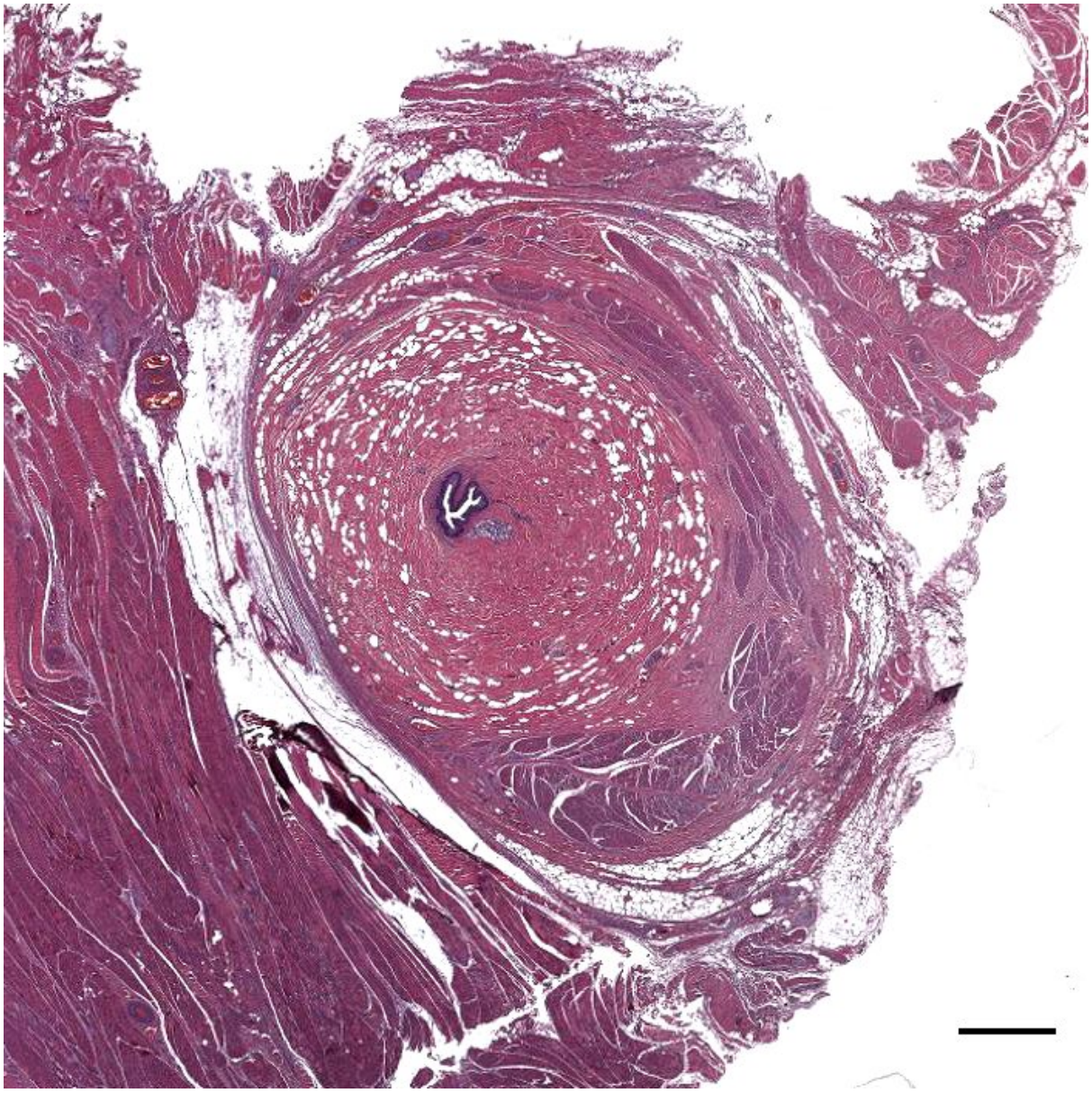

Figure 592. Histological image (HE staining) of a transverse section through the left ear canal of a striped dolphin at about 3.5 cm beneath the skin (44/17_L7, HE) Ear canal. Scale bar 500 µm

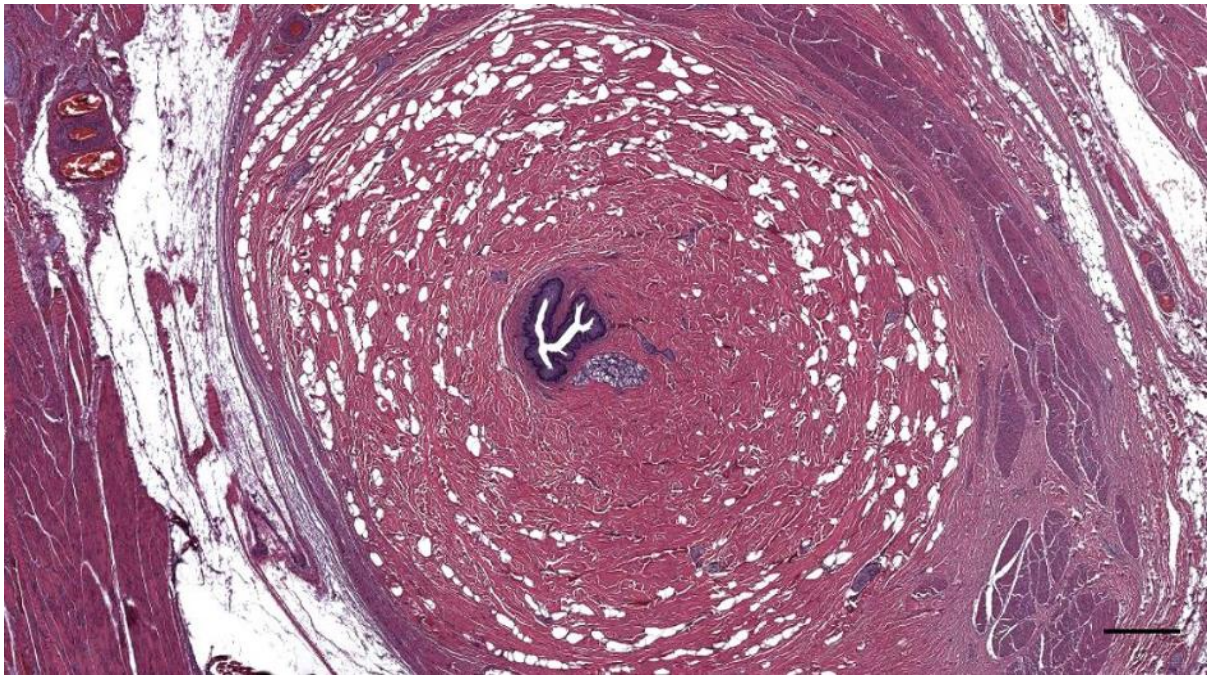

Figure 593. Histological image (HE staining) of a transverse section through the left ear canal of a striped dolphin at about 3.5 cm beneath the skin (44/17_L7, HE). Scale bar 500 µm

Figure 594. Detail of Figure 593 (44/17_L7, HE). Scale bar 100 µm

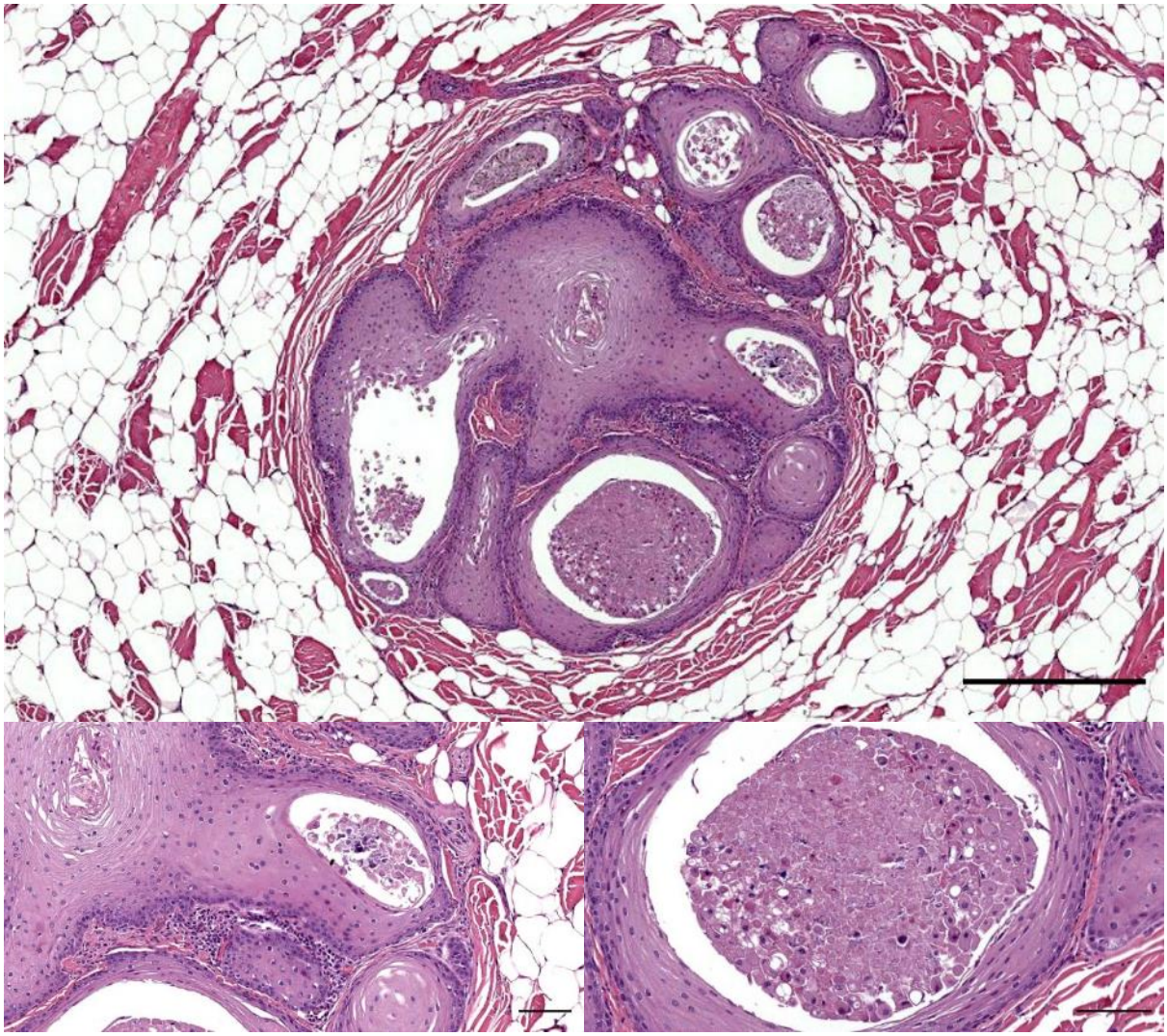

Figure 595. Histological image (HE staining) of a transverse section through the right ear canal of a common dolphin at about 1 cm beneath the skin (169_17_R2). Note the glands, excretory ducts, and impacted content. Scale bars 200 µm top, and 100 µm bottom

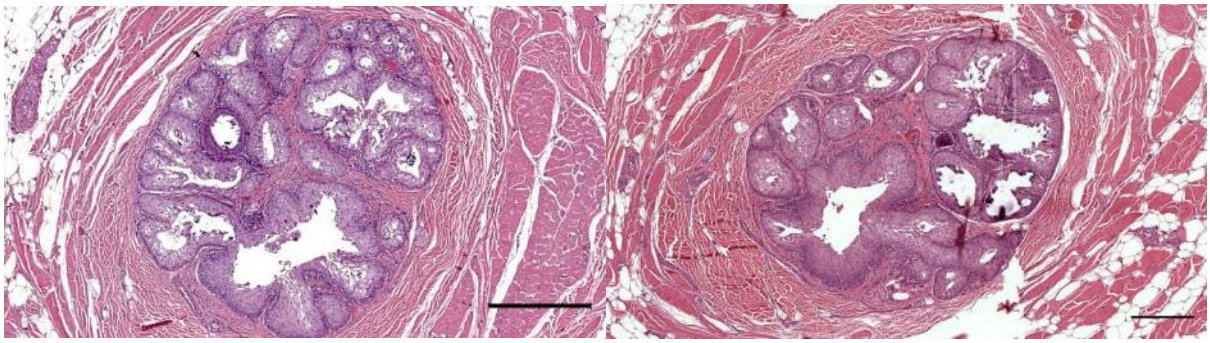

Figure 596. HE-stained cross-sections of the external ear canal in a common dolphin, at about 1 and 1.5 cm beneath the surface of the skin. The distinction between the ear canal and glands is not clear. Scale bar 500 µm

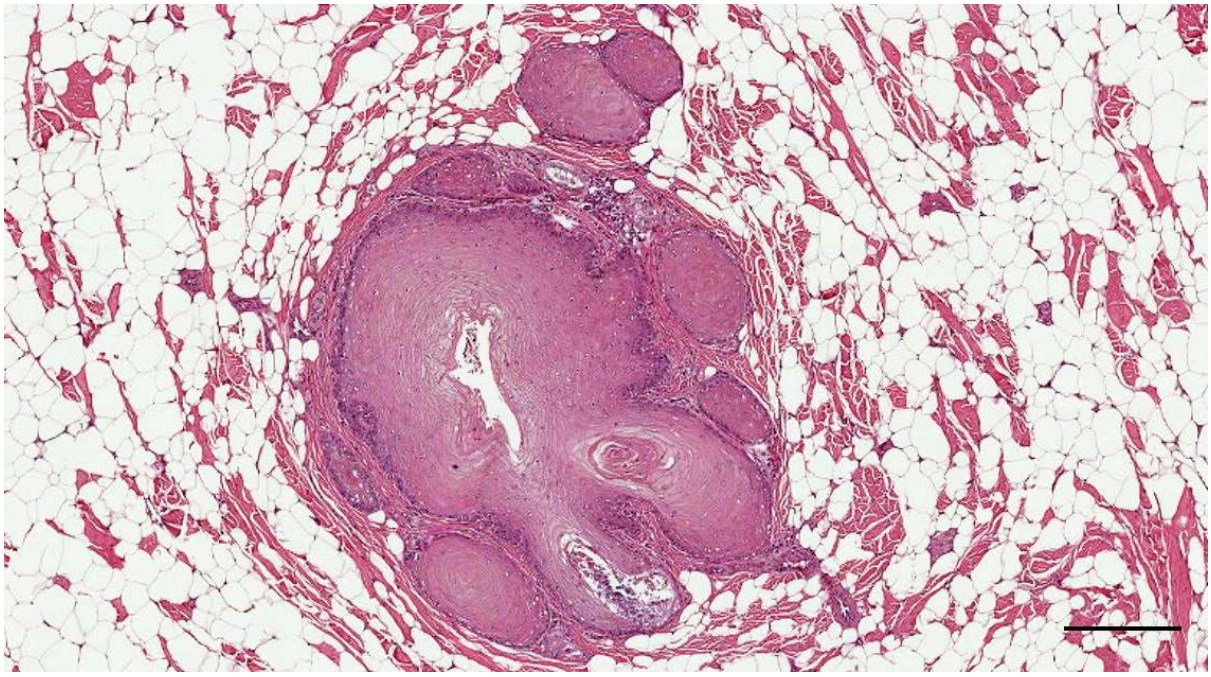

Figure 597. Histological image (HE staining) of a transverse section through the left ear canal of a common dolphin at about 1 cm beneath the skin (169_17_L2). Note the glands and excretory ducts. Scale bar 300 µm

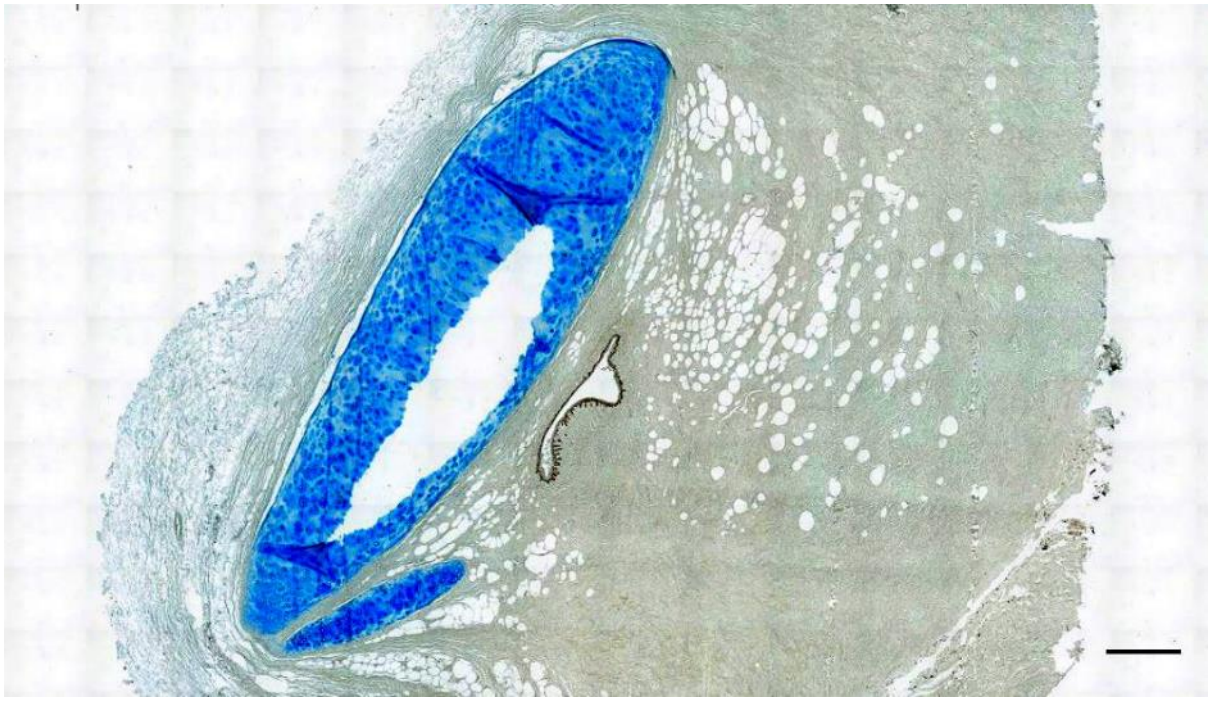

Figure 598. Histological image (Alcian blue staining) of a transverse section through the ear canal of a bottlenose dolphin at about 4 cm beneath the skin (ID444_eam2_9_AB_1). Note the intense blue staining of the cartilage. Scale bar 500 µm

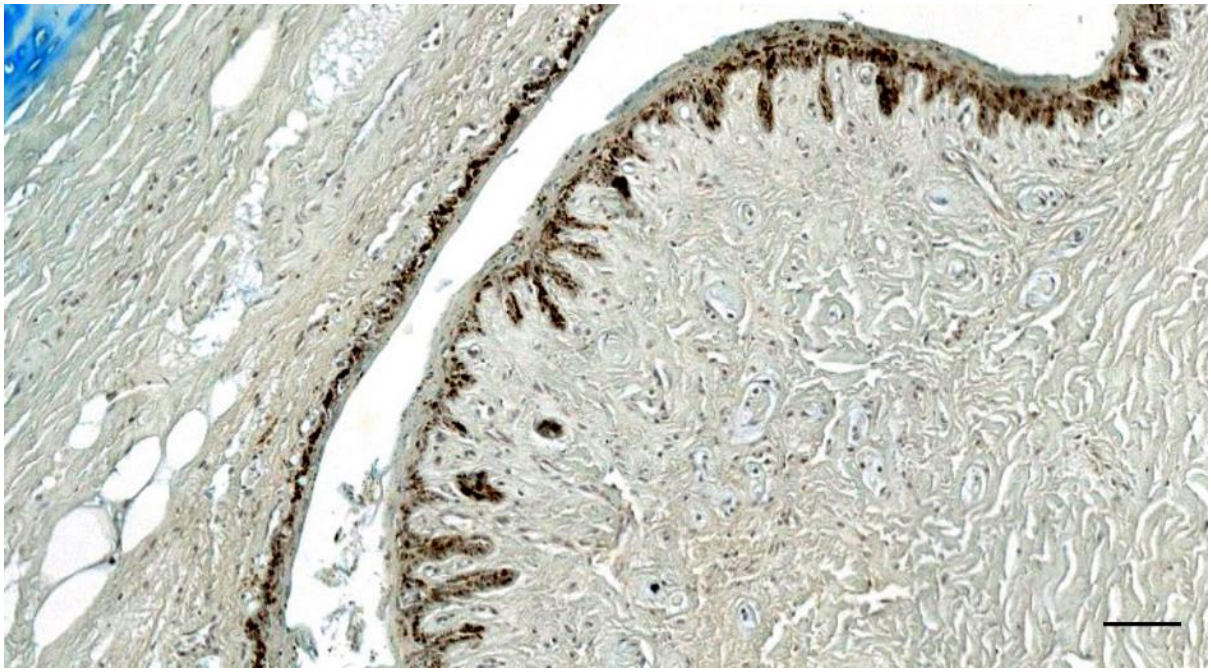

Figure 599. Histological image (Alcian blue staining) of a transverse section through the ear canal of a bottlenose dolphin at about 4 cm beneath the skin (ID444_eam2_9_AB_2). Detail image of the sensory ridge with many nervous structures. Scale bar 50 µm

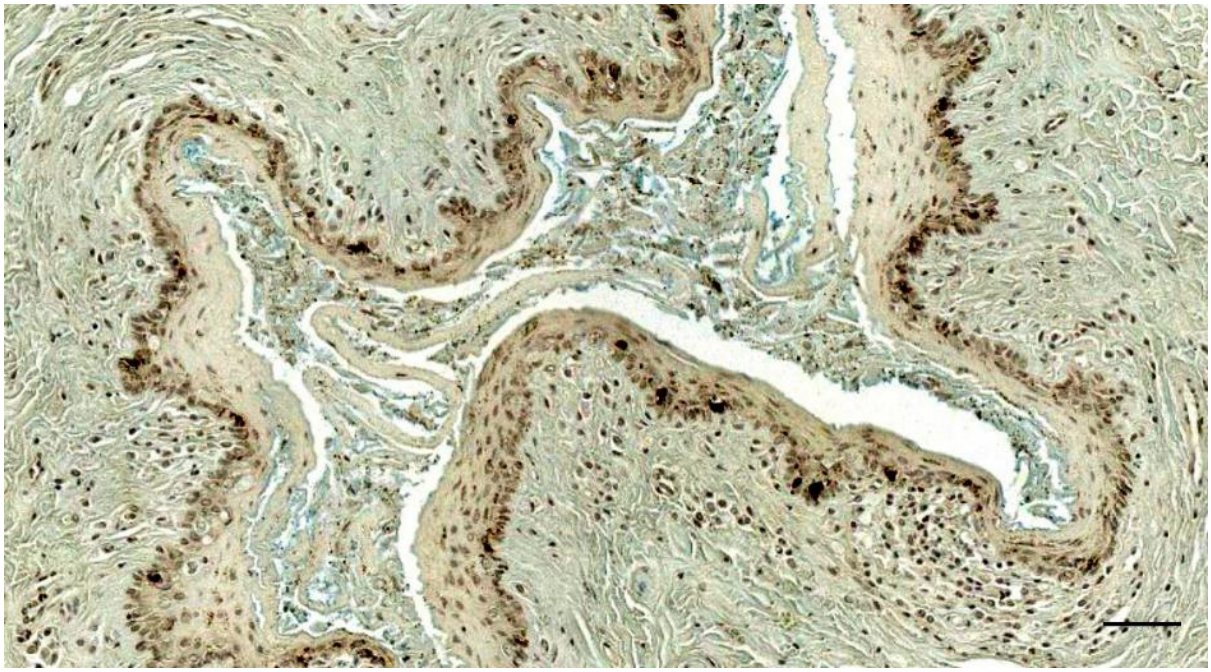

Figure 600. Histological image (Alcian blue staining) of a transverse section through the ear canal of a bottlenose dolphin at about 2 cm beneath the skin (ID444_eam2_4_AB_1). Scale bar 50 µm

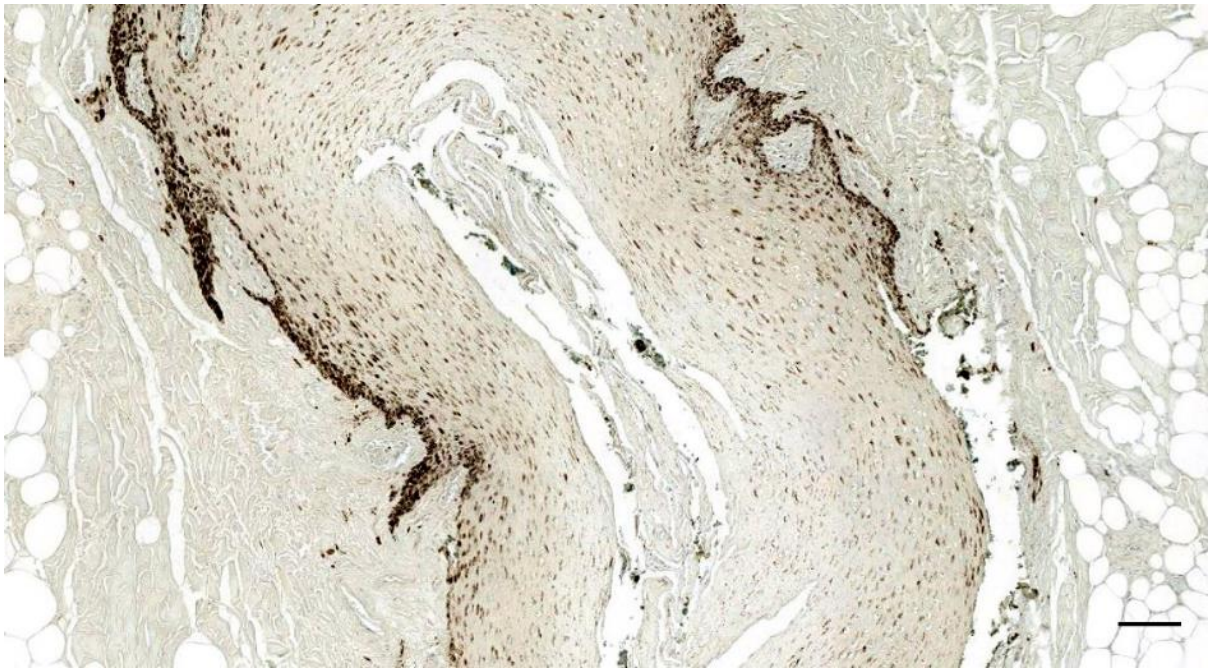

Figure 601. Histological image (Alcian blue staining) of a transverse section through the ear canal of a long-finned pilot whale at about 1 cm beneath the skin (441_eamL2_AB). Scale bar 100 µm

Figure 602. Histological detail image (Alcian blue staining) of a transverse section through the ear canal of a striped dolphin at about 2 cm beneath the skin (419/16_4_AB_1). Scale bar 50 µm

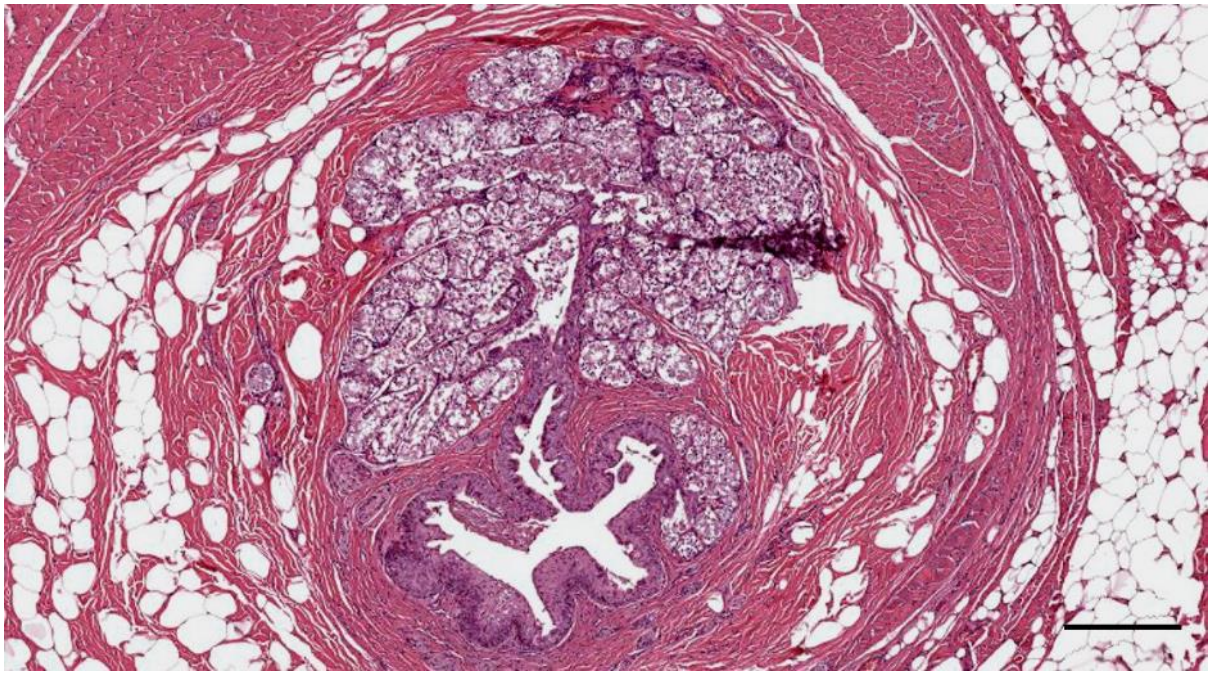

Figure 603. Histological transverse section (HE staining) through the ear canal of a striped dolphin at about 2 cm beneath the skin (274_18_L4). Scale bar 300 µm

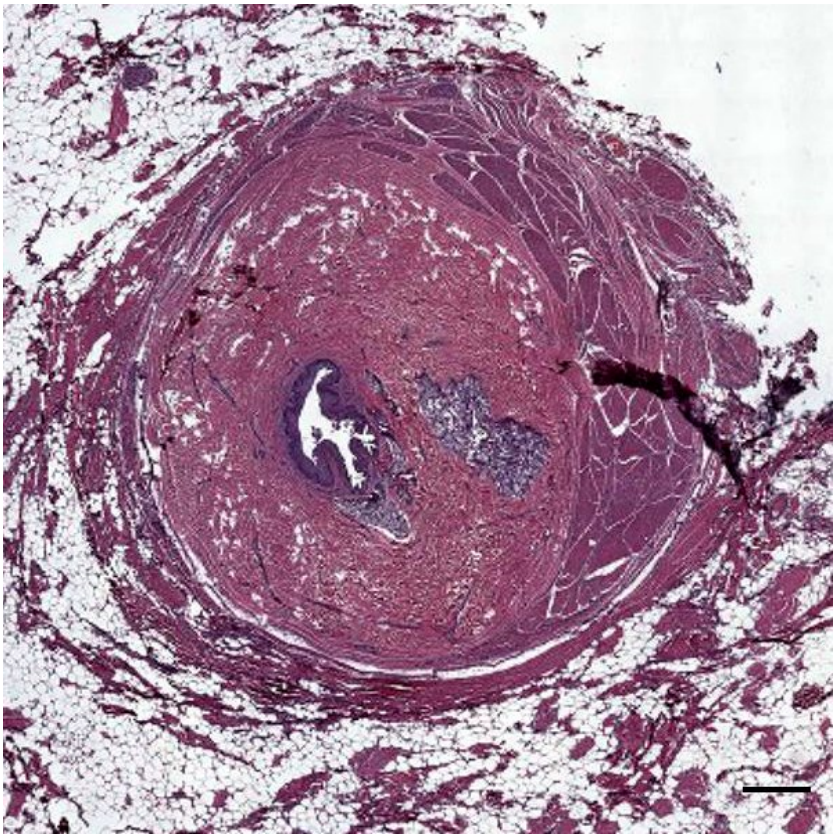

Figure 604. Histological transverse section (HE staining) through the ear canal of a striped dolphin at about 3 cm beneath the skin (44/17_L6, HE). Ear canal surrounded by glands, adipoconnective tissue and striated muscles. Scale bar 500 µm

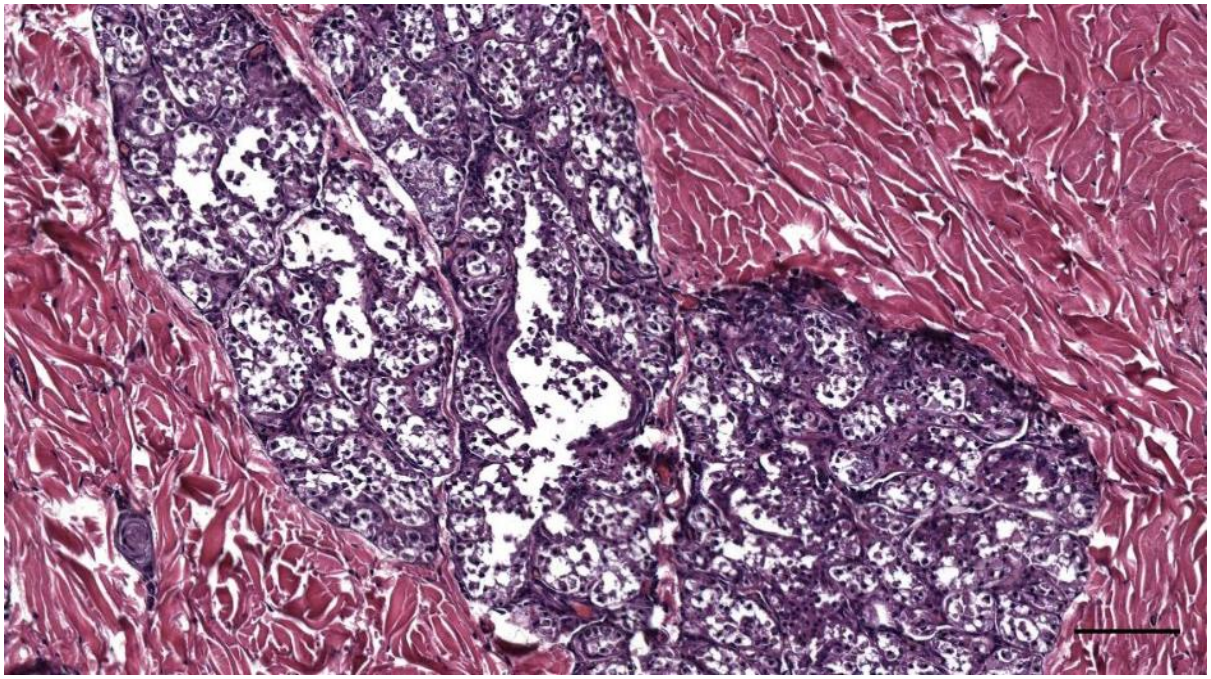

Figure 605. Histological detail (HE staining) of the auricular glands of a striped dolphin at about 3 cm beneath the skin (44/17_L6, HE). Scale bar 100 µm

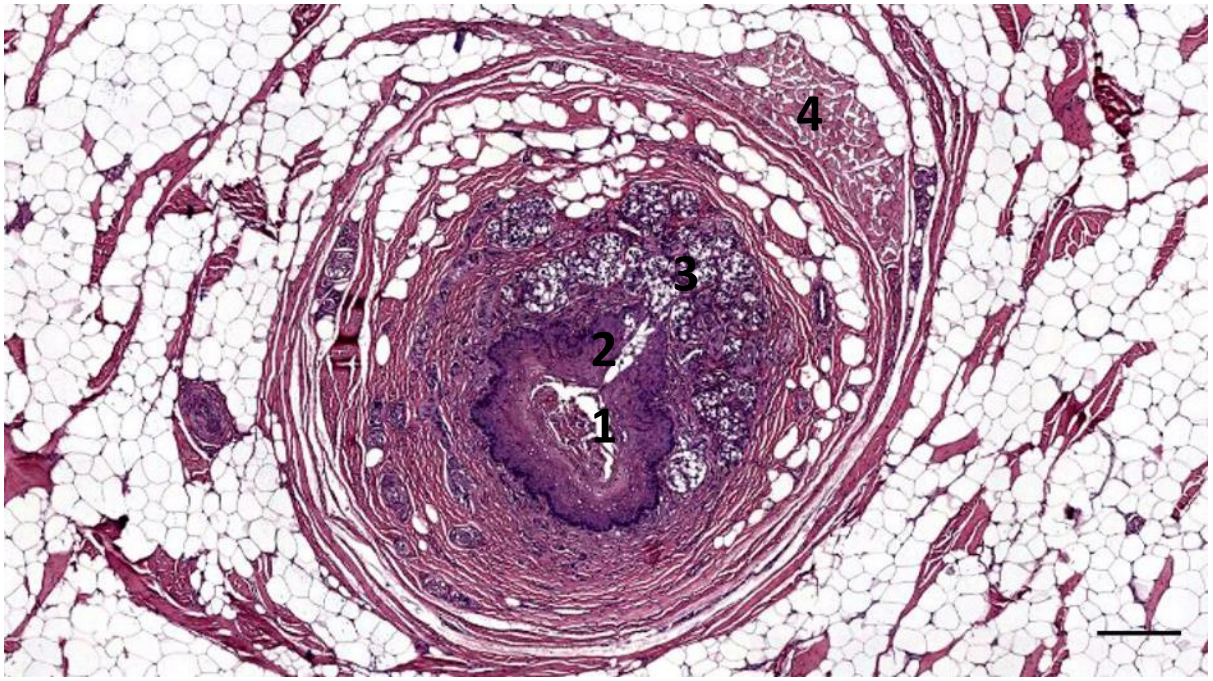

Figure 606. Histological transverse section through the external ear canal of a striped dolphin (ID449) at the level of the glands, about 2 cm beneath the skin. 1. Ear canal lumen; 2. Glandular excretory duct; 3. Glands; 4. Striated muscle inserting into the fibro-elastic tissue capsule. Scale bar 200 µm

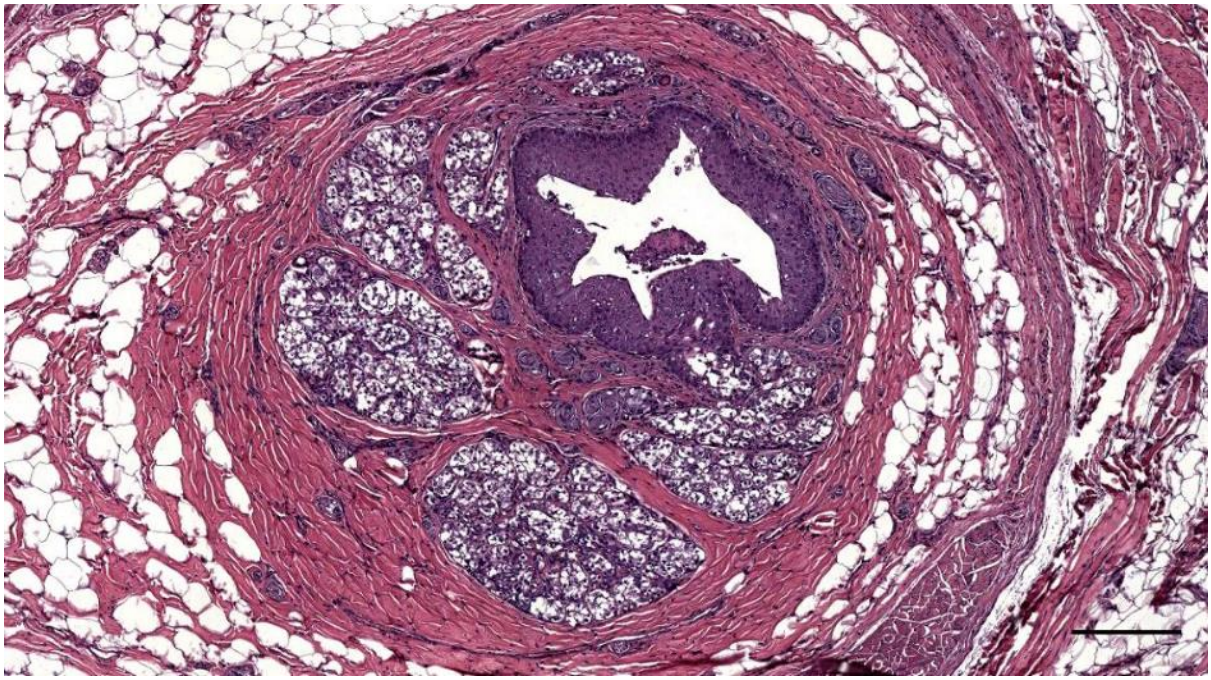

Figure 607. Histological transverse section through the ear canal of a striped dolphin at about 2 cm beneath the skin (449_L04). Scale bar 200 µm

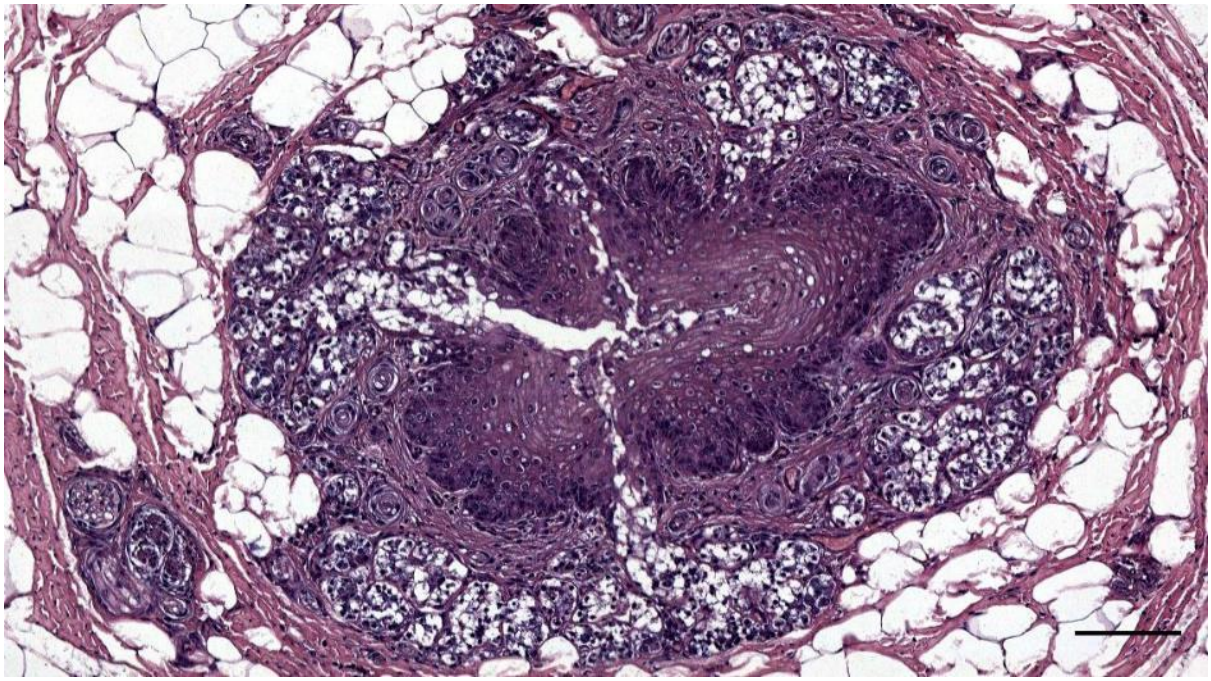

Figure 608. Histological transverse section through the ear canal of a striped dolphin at about 2 cm beneath the skin (449_R3). Scale bar 200 µm

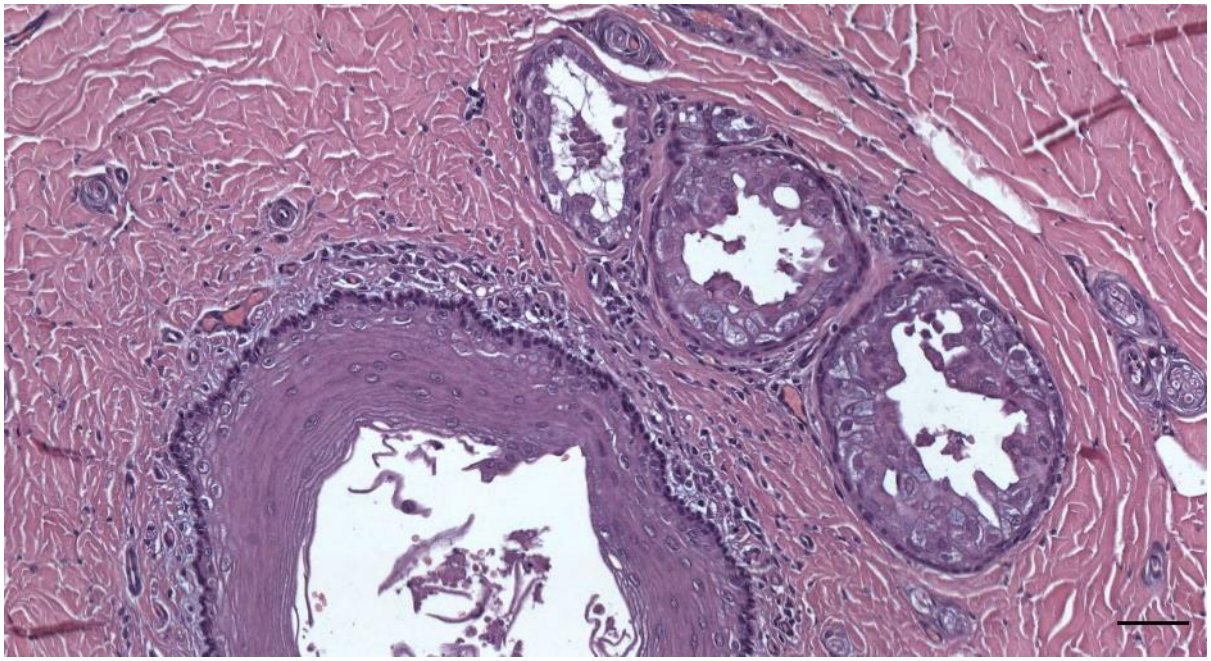

Figure 609. The distinction between excretory and secretory cells is not clear due to postmortem degeneration and apoptosis (620/17_L5). Scale bar 50 µm

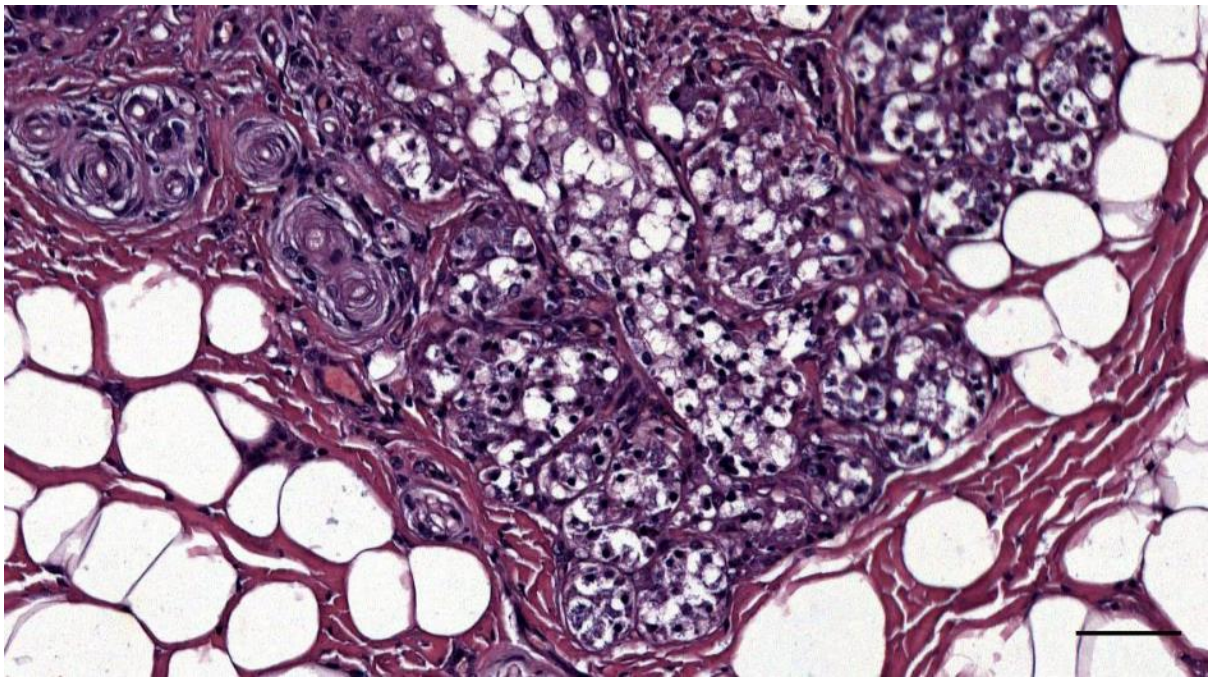

Figure 610. Histological transverse section through the ear canal of a striped dolphin at about 1.5 cm beneath the skin (449_L03). Pyknotic nuclei in the glands. Scale bar 50 µm

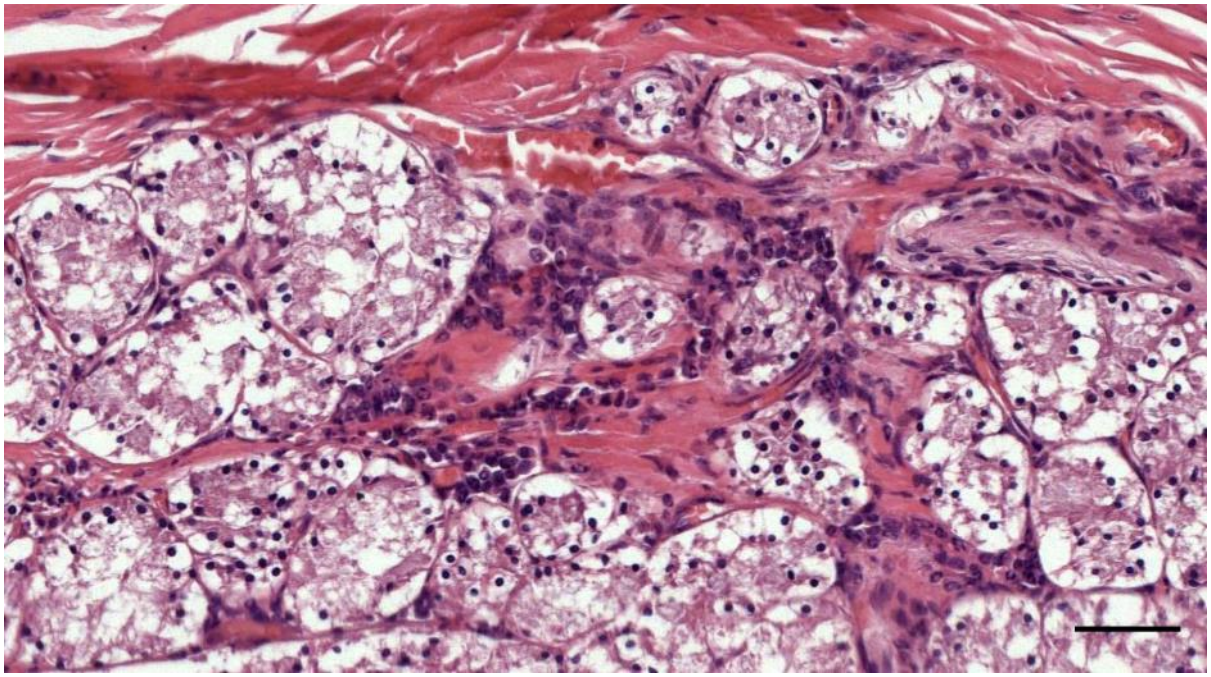

Figure 611. (L4) Mononuclear cells (lymphocytes, and few plasmacells and macrophages) associated with the glands in a superficial section through the ear canal. Scale bar 50 µm

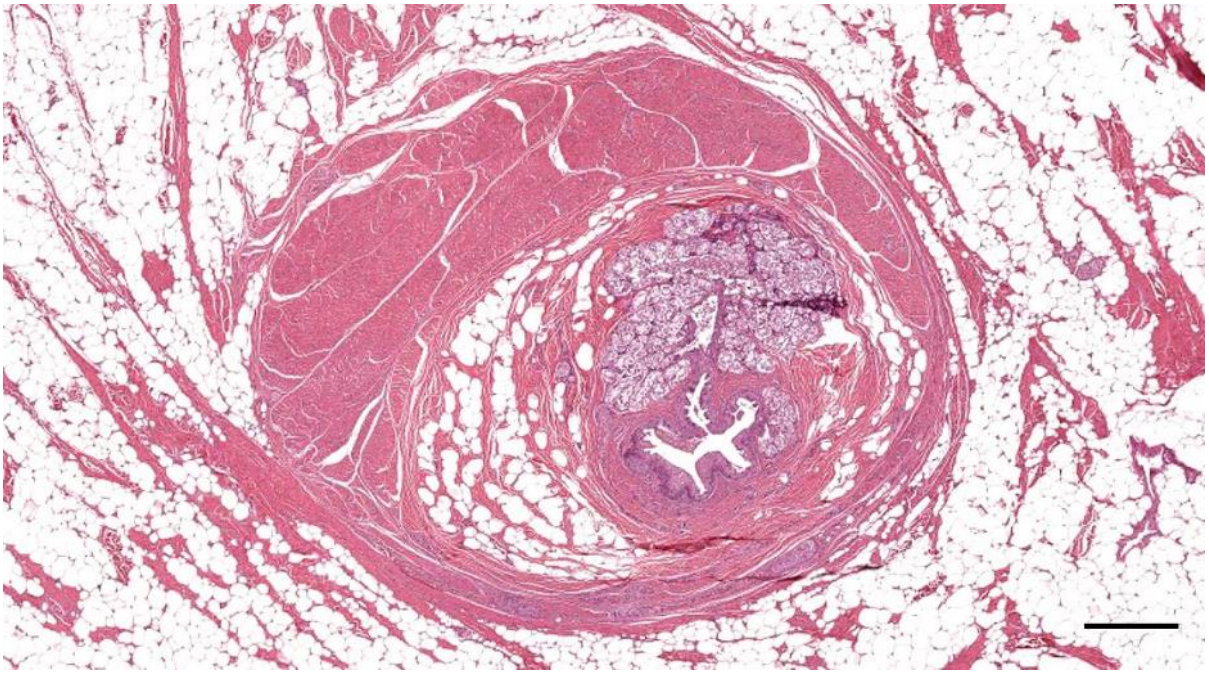

Figure 612. (274/18_L4) Section through the ear canal with glands and adipose tissue surrounded by a combination of a capsule of fibro-elastic tissue that contains nerve bundles on one side, and muscle tissue that runs parallel to the ear canal on the other side. The muscle tissue inserts into the capsule. Scale bar 0.5 mm

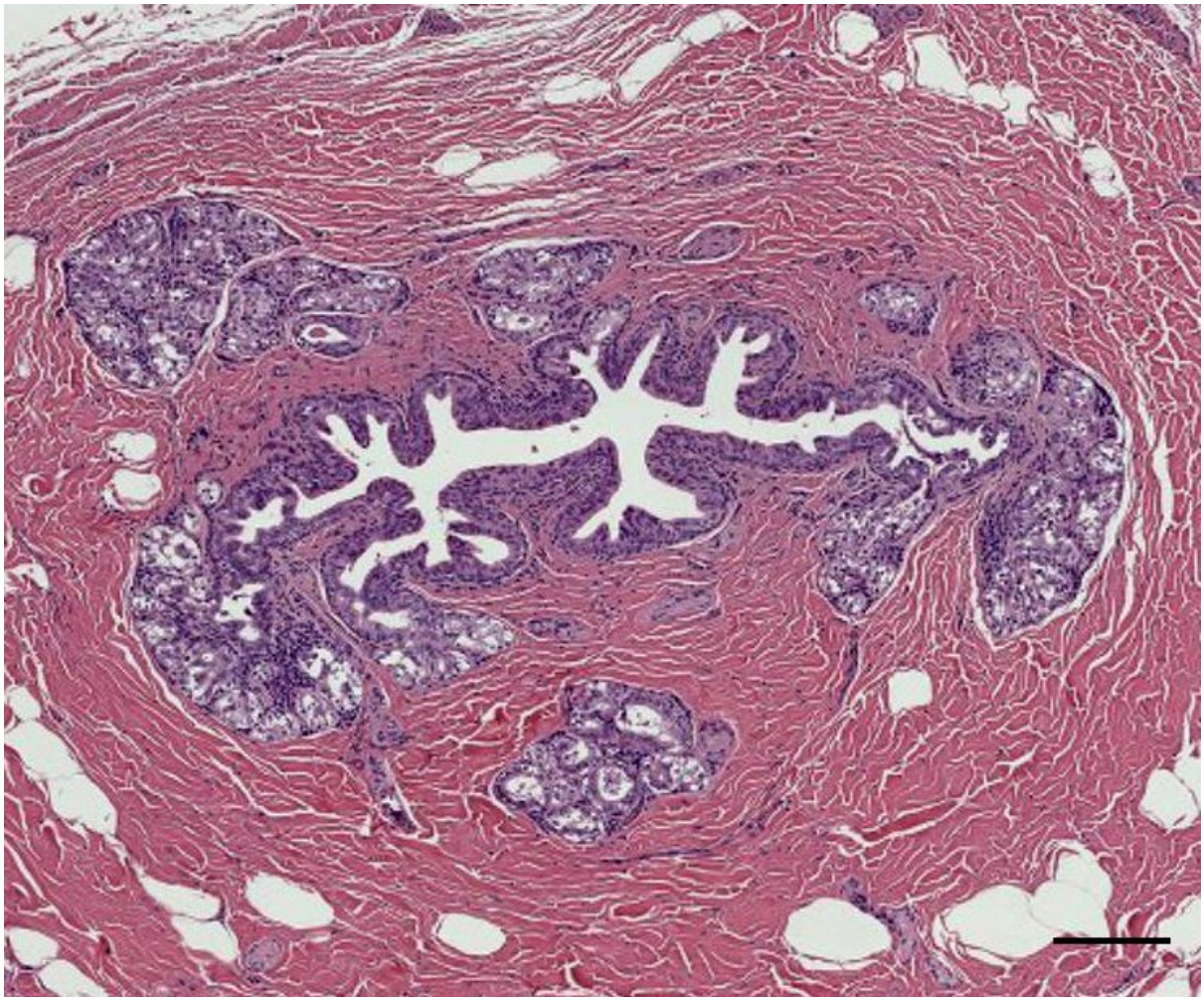

Figure 613. Histological transverse section through the ear canal of a striped dolphin at about 2 cm beneath the skin (168_17_4). Scale bar 200 µm

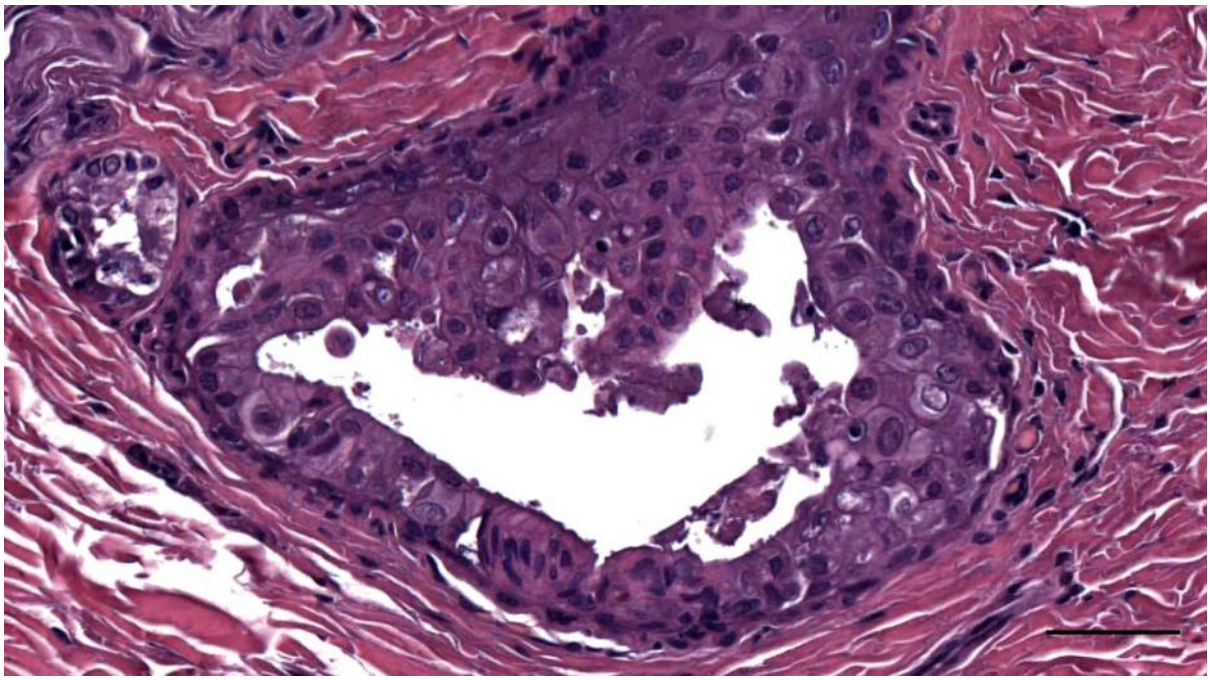

Figure 614. Detail histological image (HE stain) of a possible glandular excretory duct in a bottlenose dolphin (ID457). Scale bar 50 µm

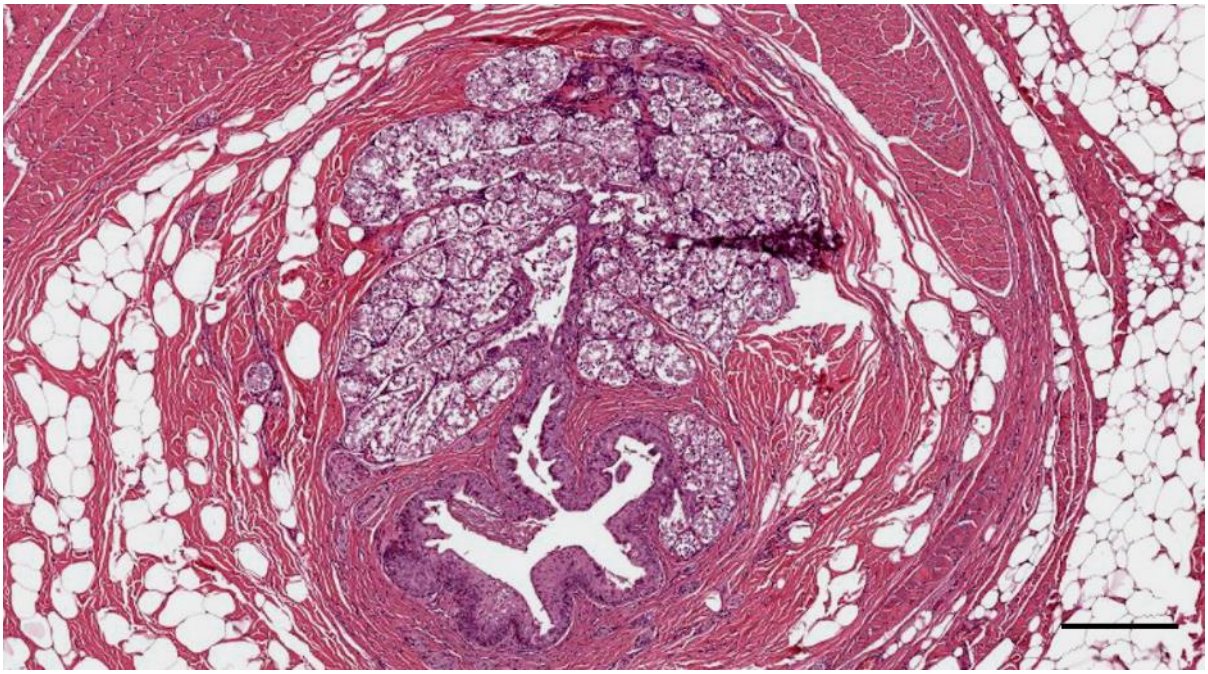

Figure 615. (274/18_L4). Ear canal and glands

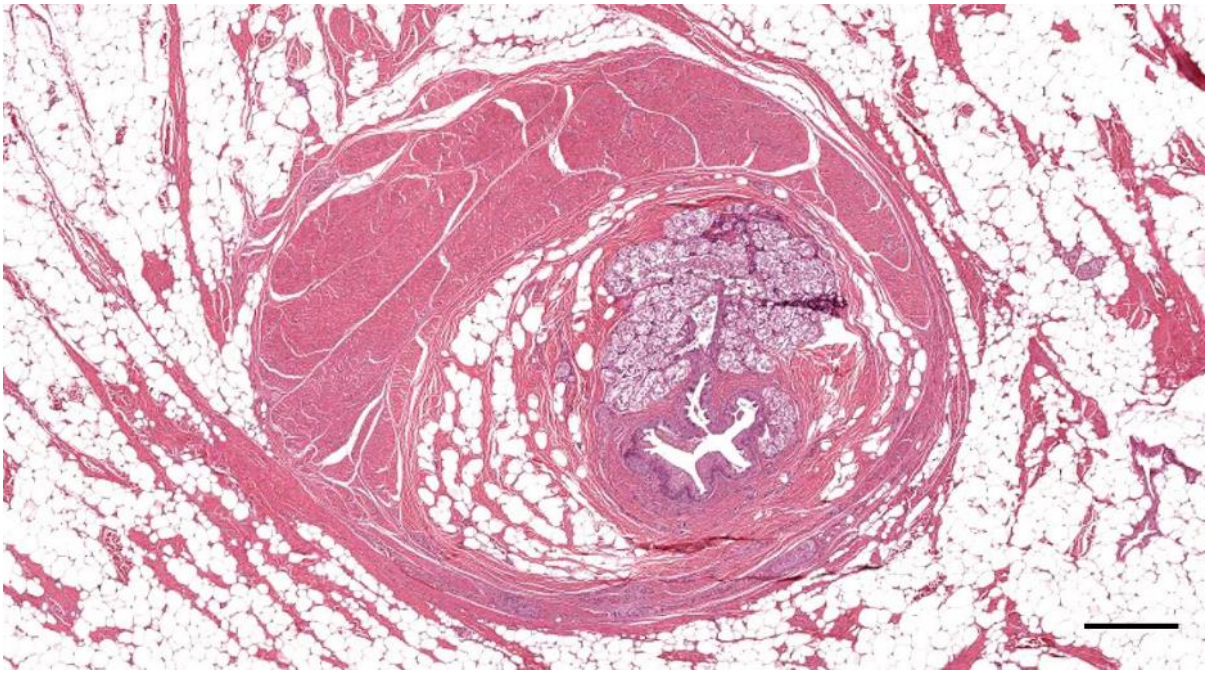

Figure 616. (274/18_L4) Section through the ear canal with glands and adipose tissue surrounded by a combination of a capsule of fibro-elastic tissue that contains nerve bundles on one side, and muscle tissue that runs parallel to the ear canal on the other side. The muscle tissue inserts into the capsule. Scale bar 0.5 mm

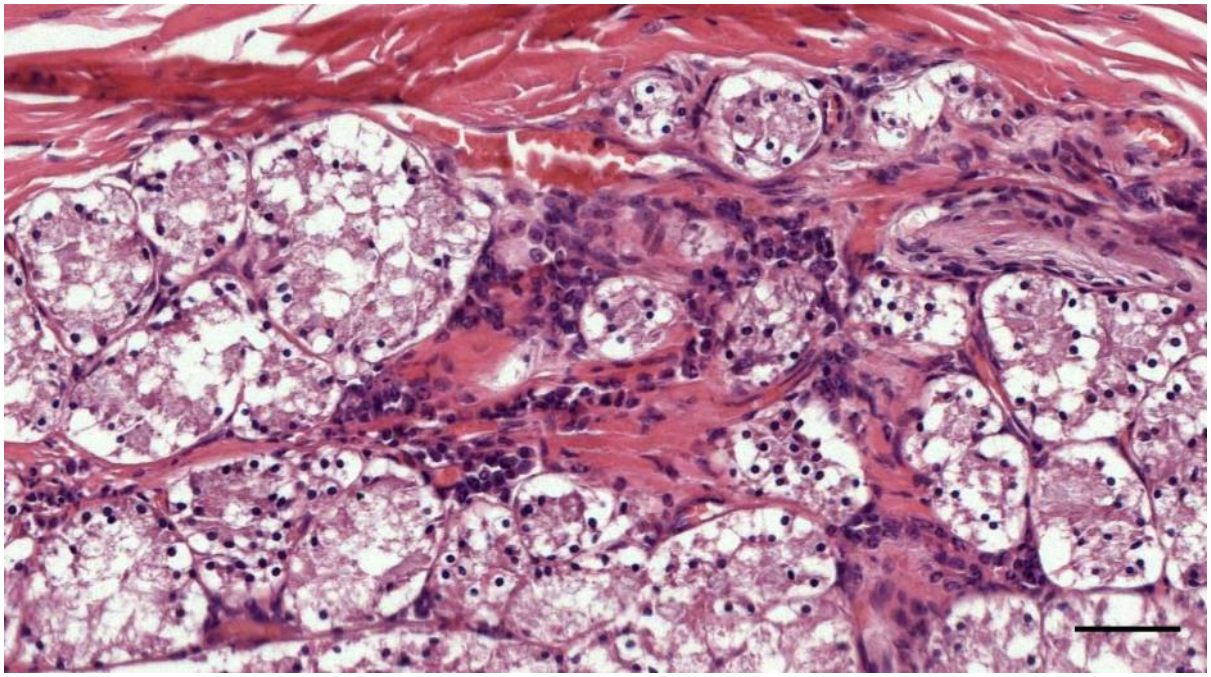

Figure 617. (274/18_L4) Mononuclear cells (lymphocytes, and few plasmacells and macrophages) associated with the glands in a superficial section through the ear canal. Scale bar 50 µm

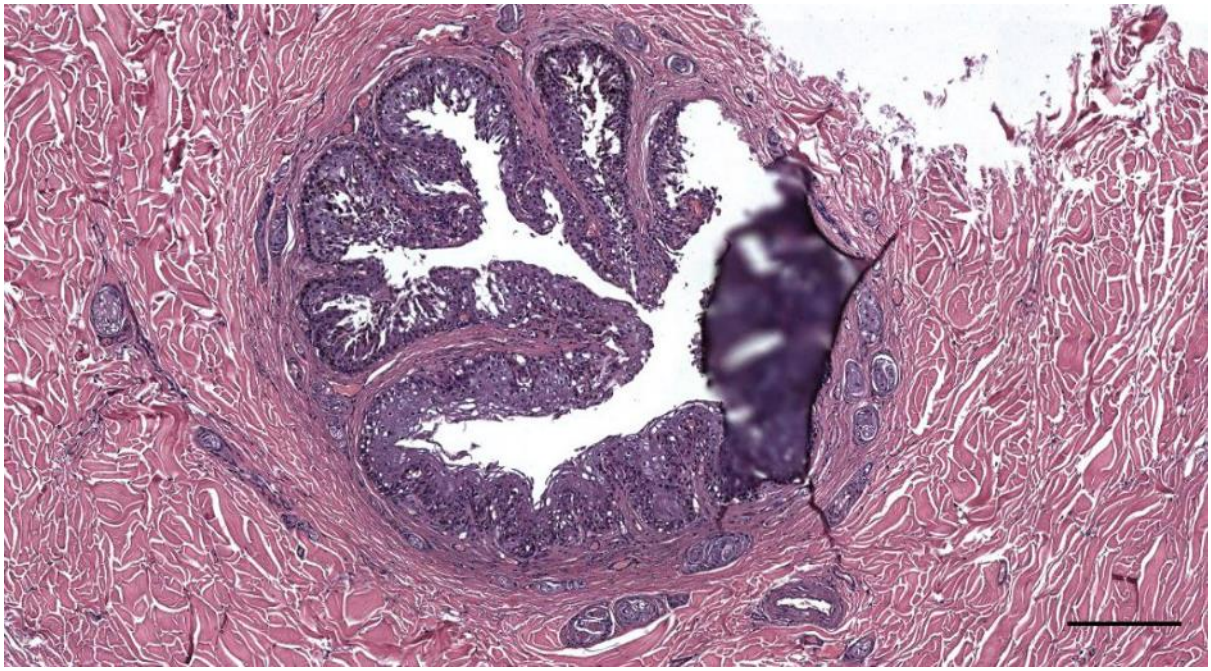

Figure 618. (292/18_L5) Ear canal with possible glands, sharing the same lumen. Scale bar 200 µm

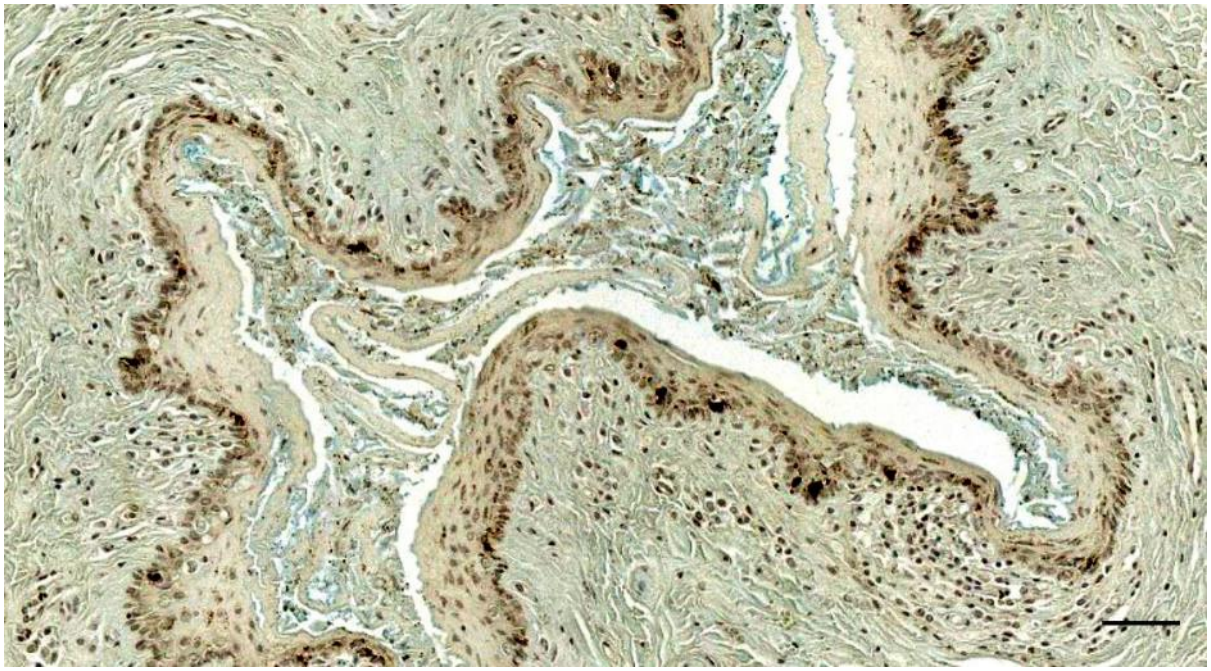

Figure 619. Alcian blue-stained cross-section of the right ear canal in a bottlenose dolphin (444_R4). Scale bar 50 µm

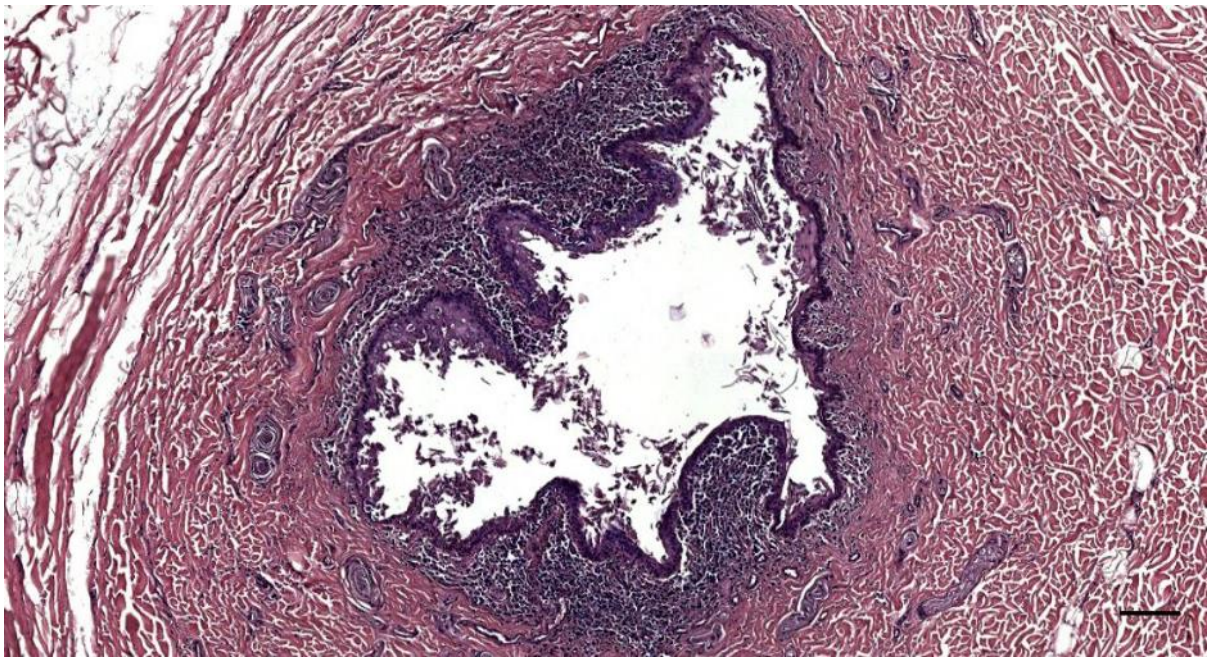

Figure 620. HE-stained cross-section of the right ear canal in a bottlenose dolphin (444_R5). Note the inflammation. Scale bar 100 µm

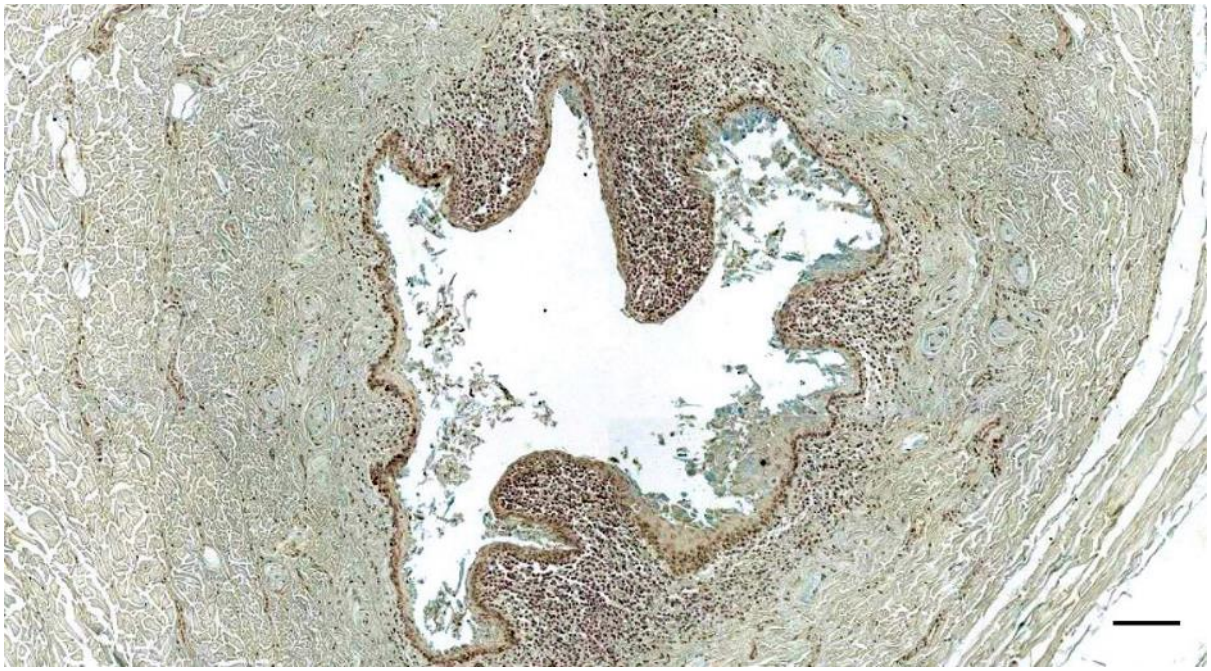

Figure 621. Alcian blue-stained cross-section of the right ear canal in a bottlenose dolphin (444_R5). Note the inflammation. Scale bar 100 µm

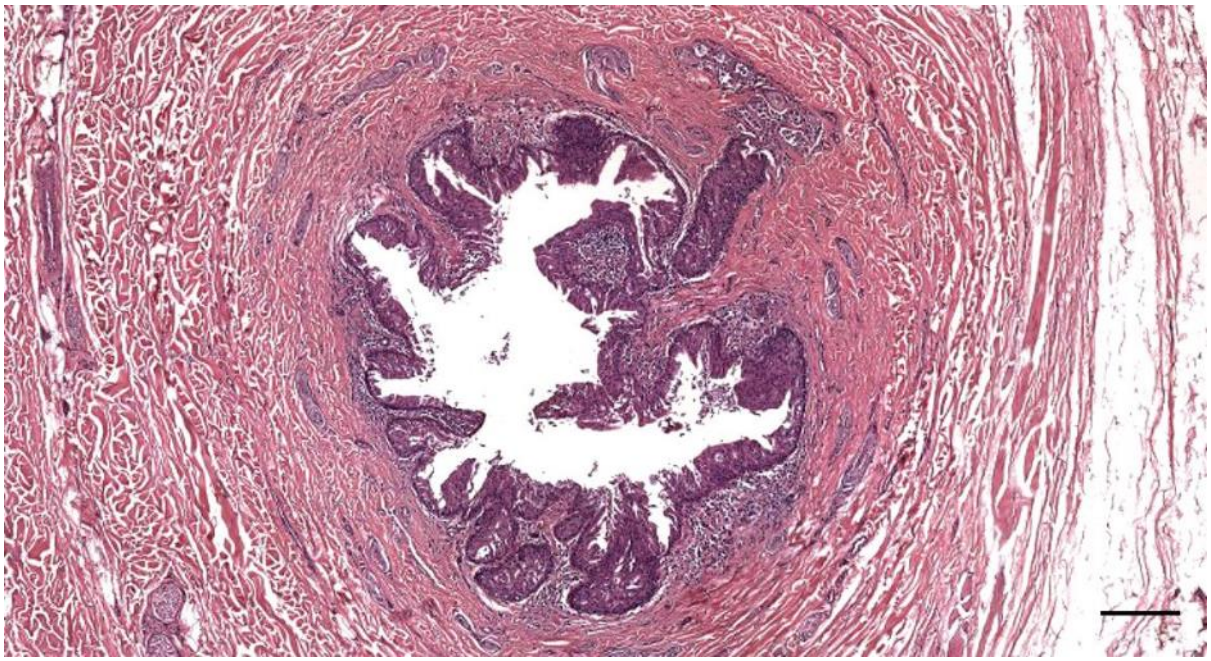

Figure 622. HE-stained cross-section of the right ear canal in a bottlenose dolphin (444_R6). Note the glands and excretory duct. Scale bar 200 µm

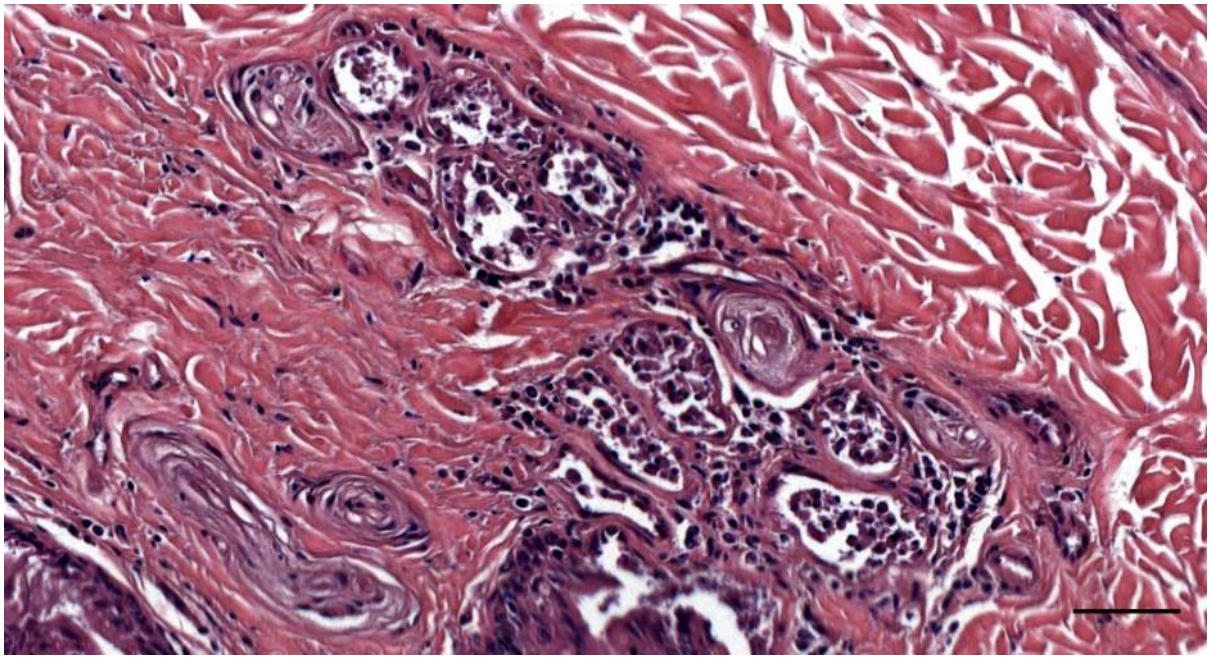

Figure 623. Detail of Figure 354 (444_R6) Ear canal glands with cells with pyknotic nuclei. Scale bar 50 µm

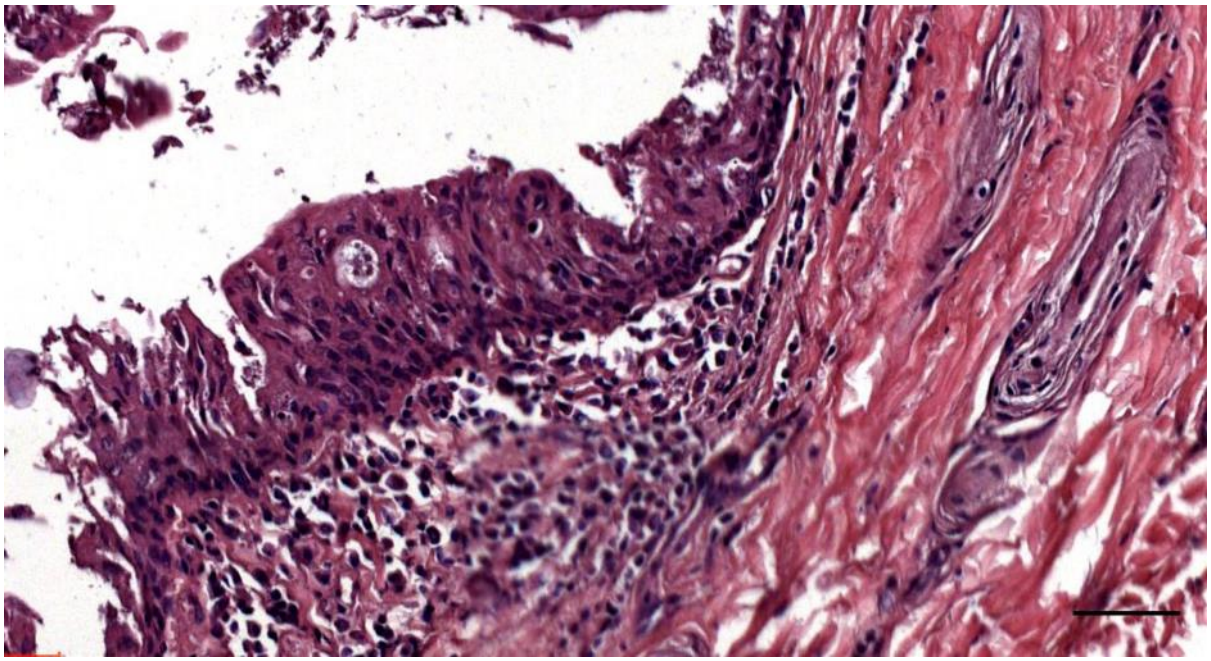

Figure 624. Detail of Figure 354 (444_R6) Ear canal with indications of a pseudostratified epithelium with many artefacts. Scale bar 50 µm

Figure 625. Alcian blue-stained cross-section of the right ear canal in a bottlenose dolphin (444_R6). Glands and inflammation. Scale bar 200 µm

Figure 626. HE-stained cross-section of the right ear canal in a bottlenose dolphin (444_R7). Note the glands and excretory duct. Scale bar 100 µm

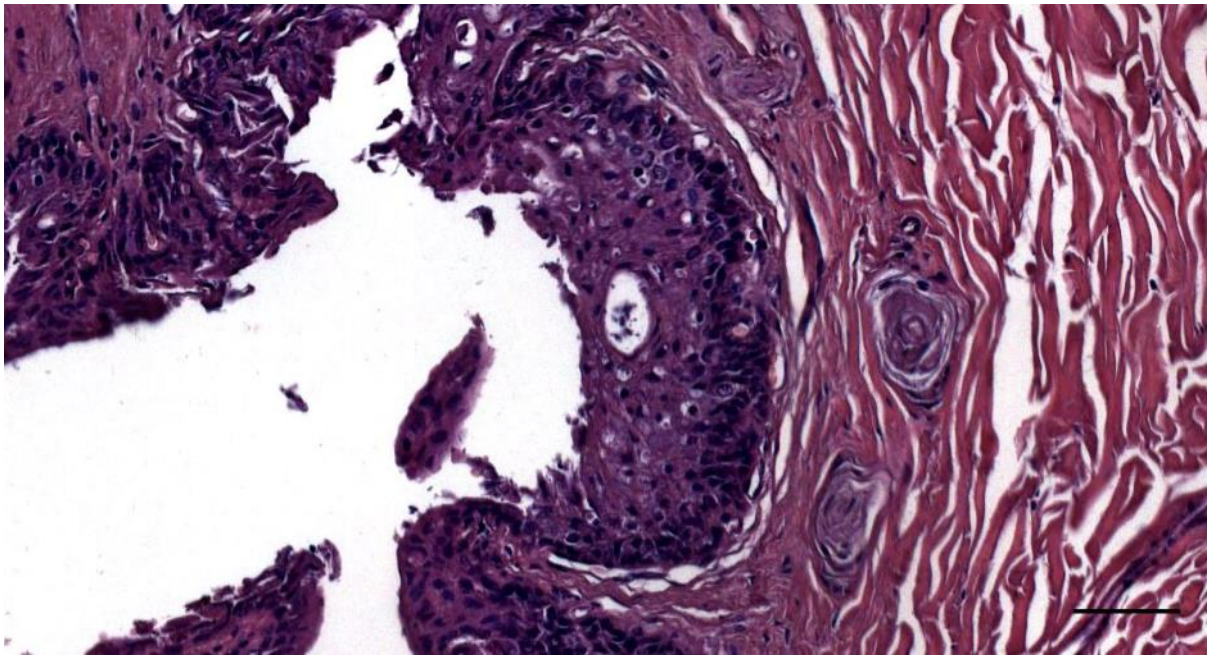

Figure 627. Detail of the ear canal epithelium in Figure 357 (444_R7). Scale bar 50 µm

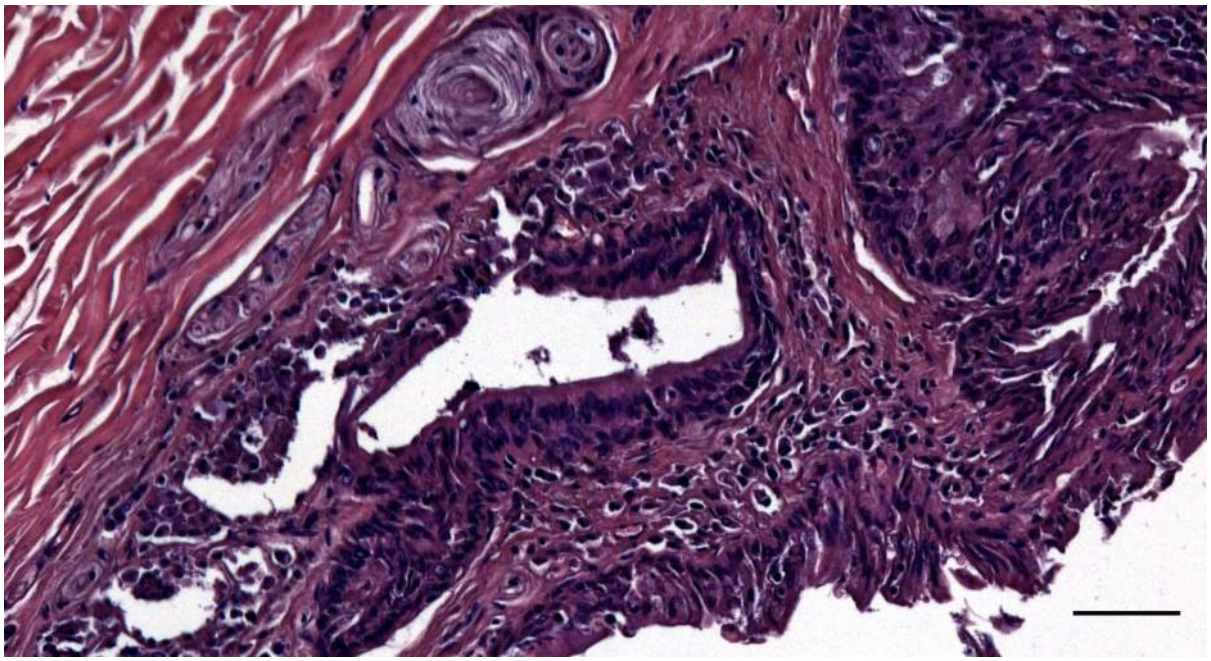

Figure 628. Detail of Figure 357 (444_R7) Indications of a double layered epithelium in a possible glandular structure. Scale bar 50 µm

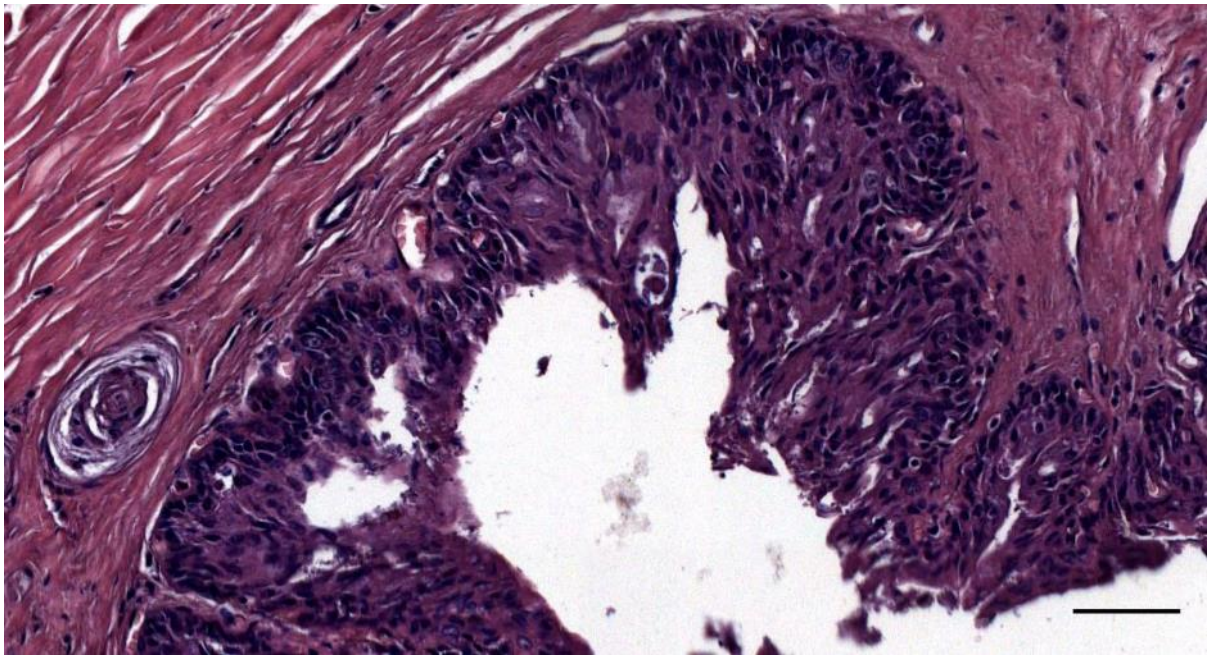

Figure 629. Detail of the ear canal epithelium in Figure 357 (444_R7). Scale bar 50 µm

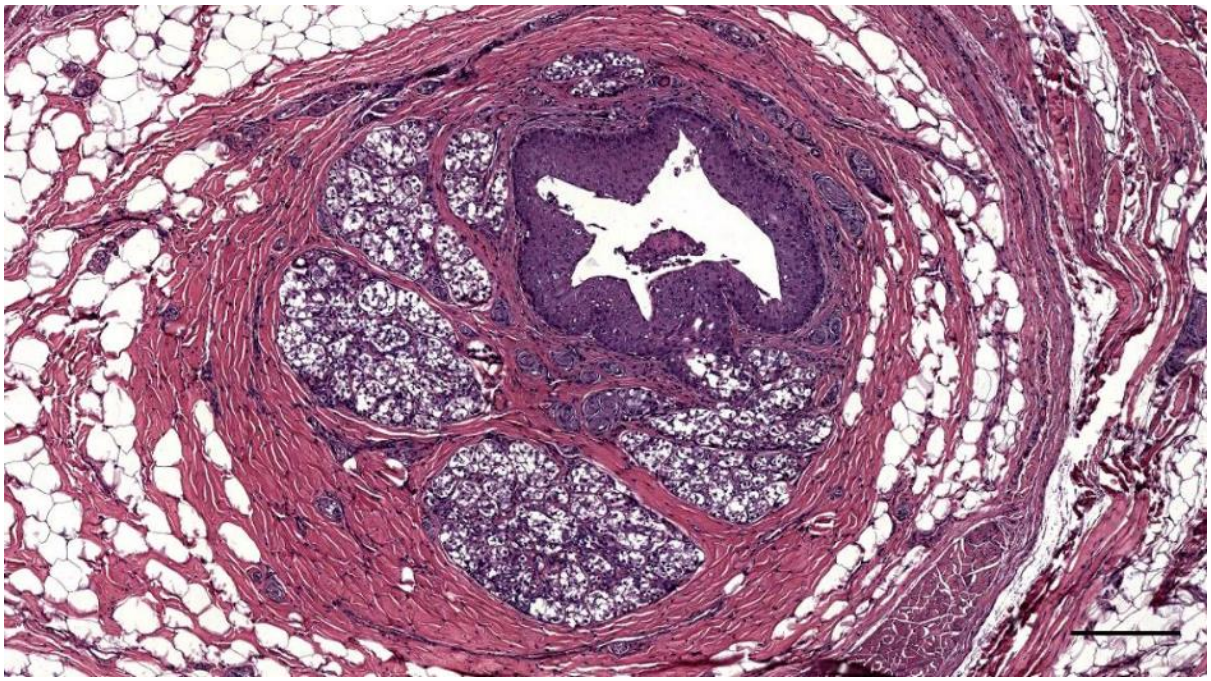

Figure 630. (ID449) Stenella coeruleoalba. (449_L3) Ear canal cross-section with glands. Scale bar 200 µm

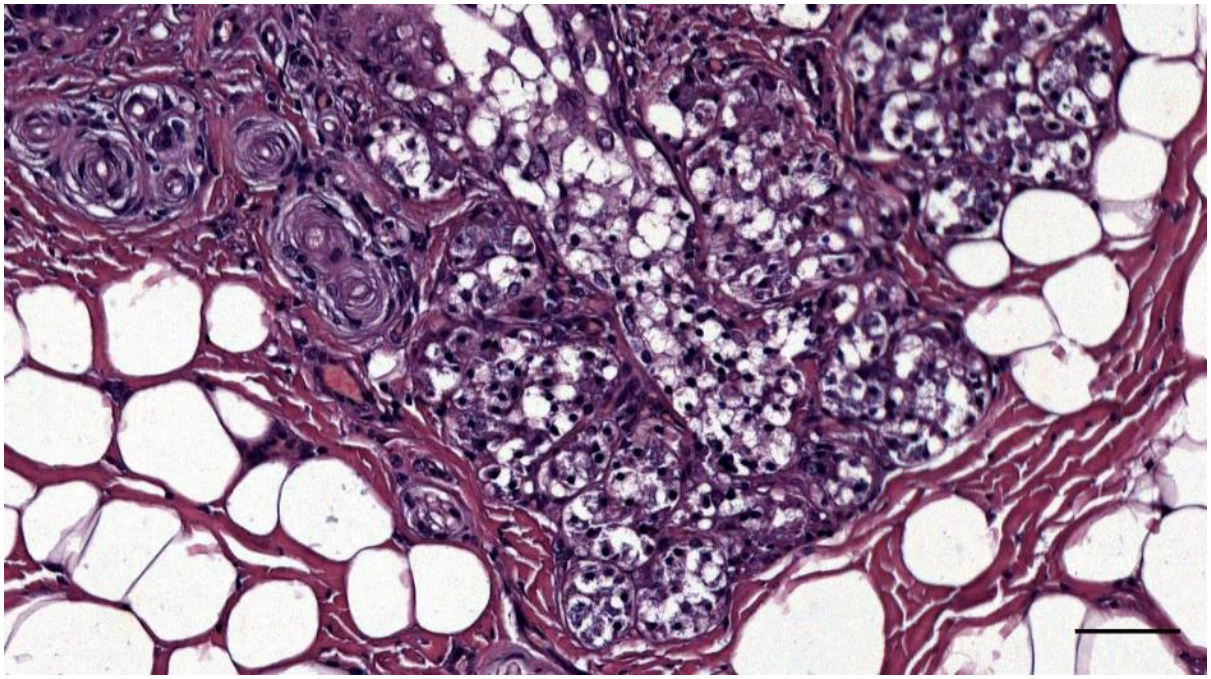

Figure 631. (ID449) Stenella coeruleoalba. (449_L3) Detail of Figure 630. Ear canal glands. Scale bar 50 µm

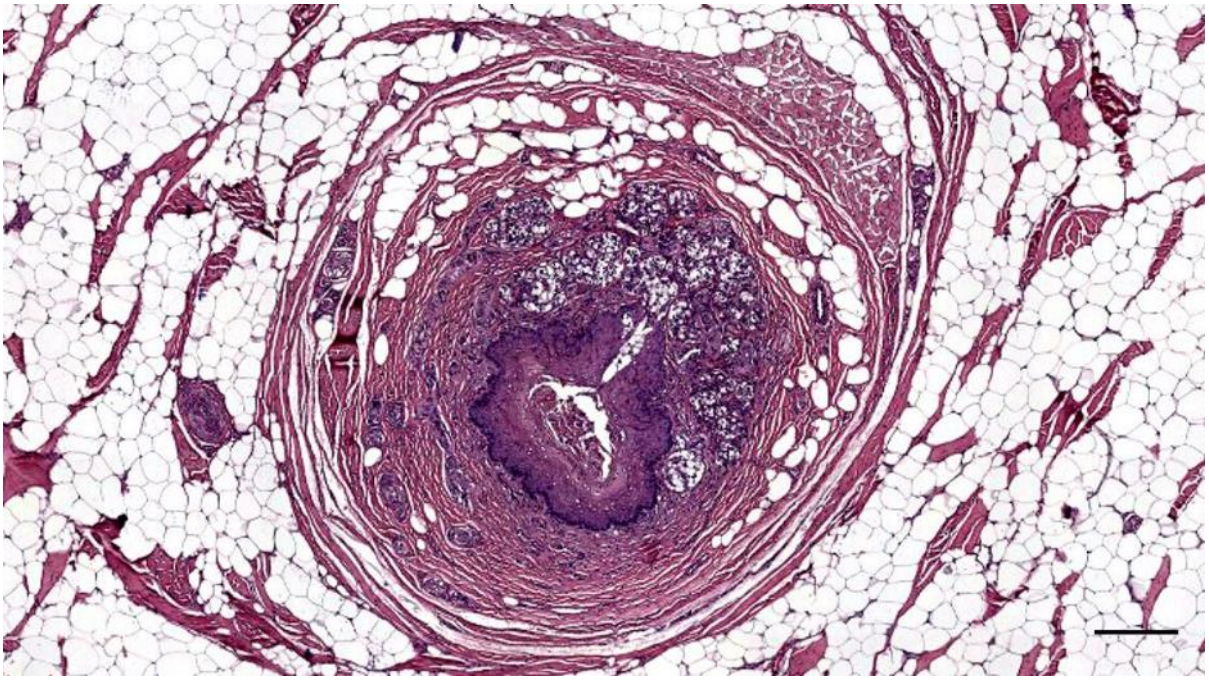

Figure 632. (ID449) Stenella coeruleoalba. (449_R4) Cross-section of the ear canal and glands. Scale bar 200 µm

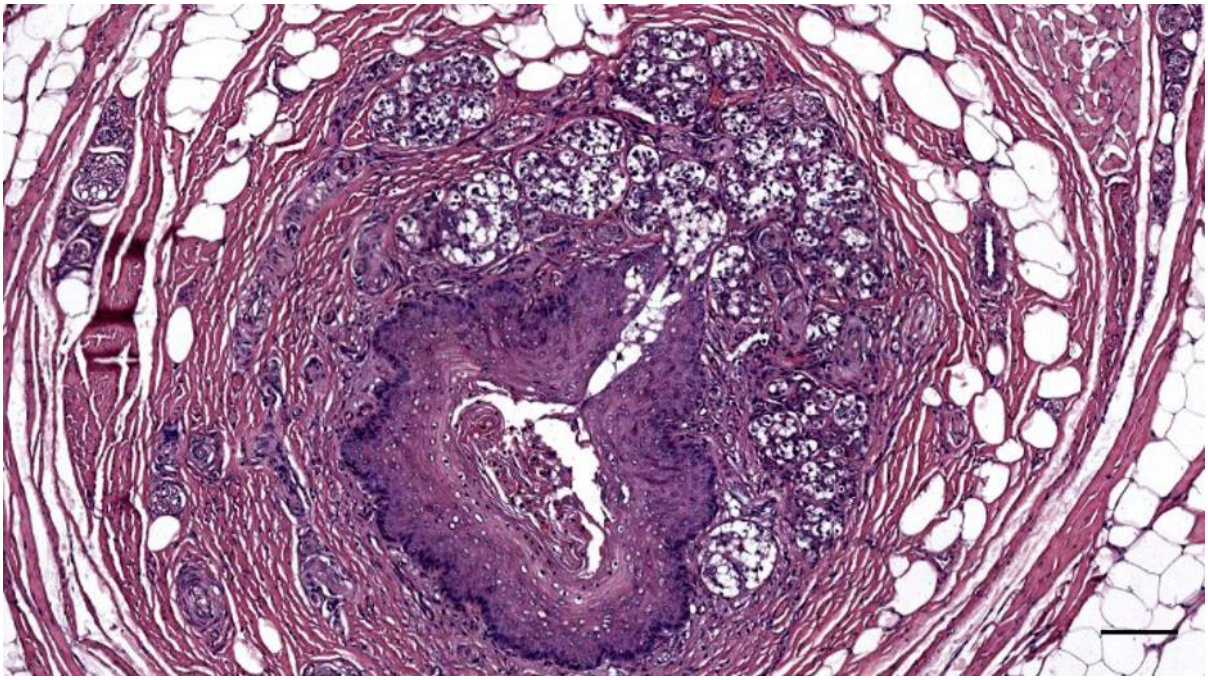

Figure 633. (ID449) Stenella coeruleoalba. (449_R4) Detail of Figure 632. Cross-section of the ear canal and glands with excretory duct. Scale bar 100 µm

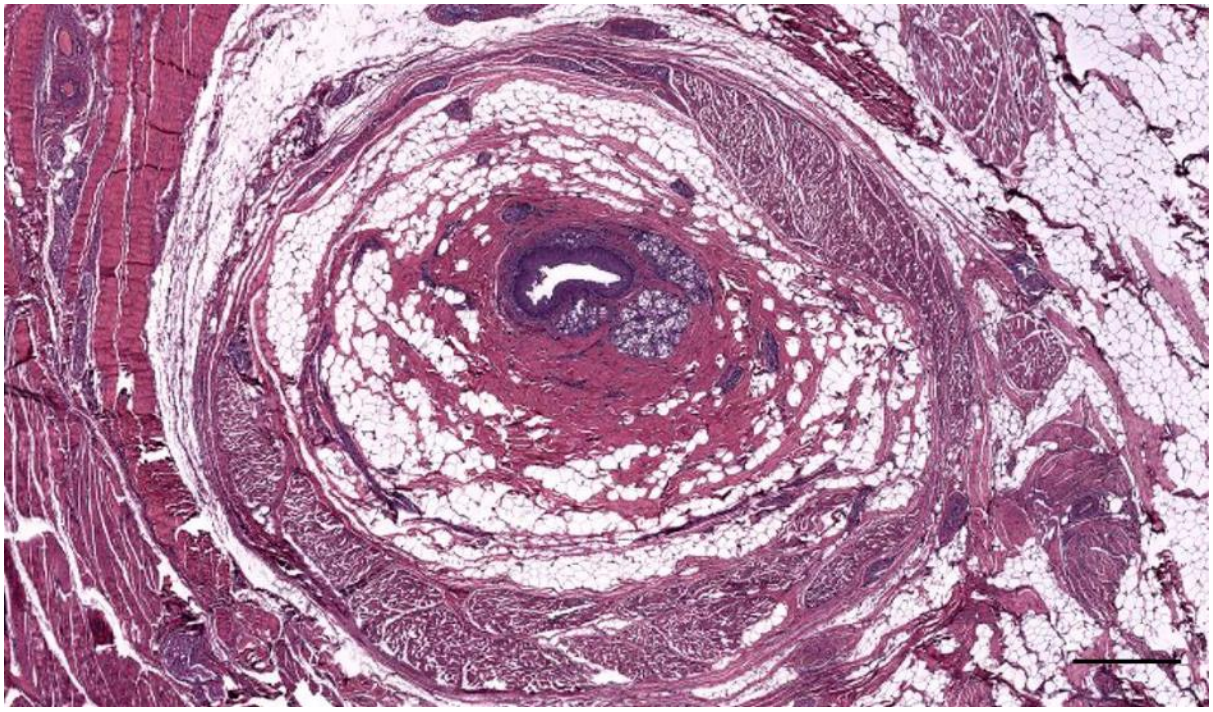

Figure 634. (ID449) Stenella coeruleoalba. (449_R5) Cross-section of the ear canal and glands, surrounded by connective tissue and fat, a muscular layer, and more fat and connective tissue. Scale bar 500 µm

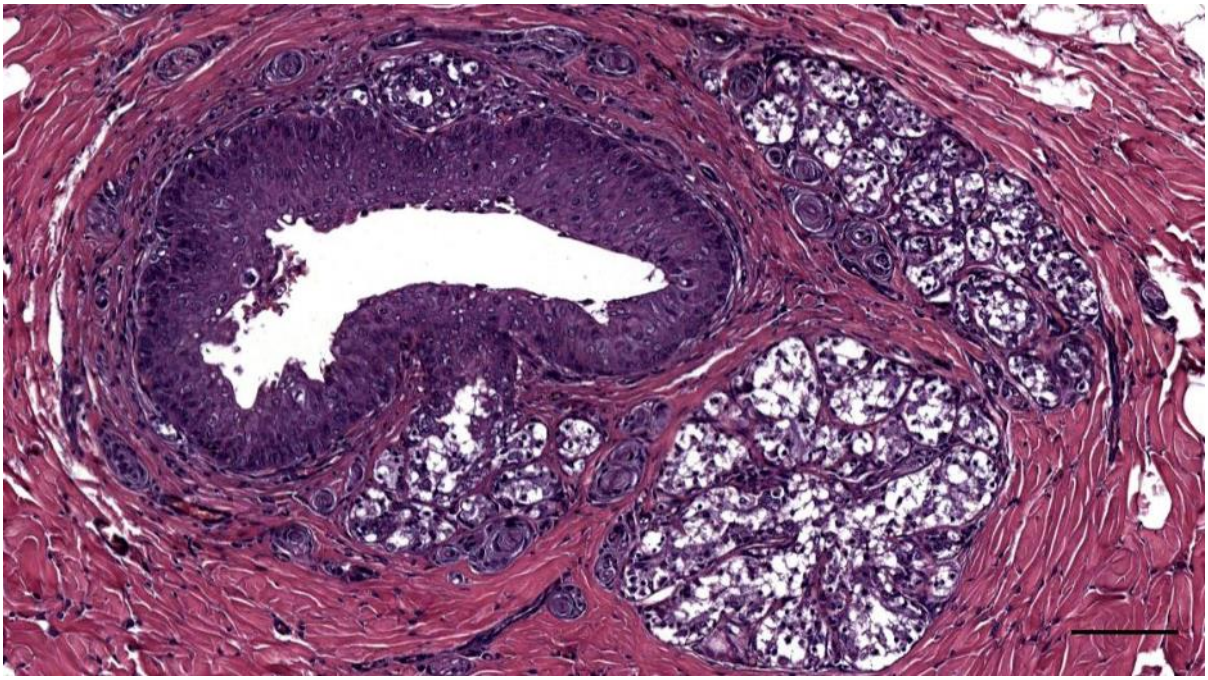

Figure 635. (ID449) Stenella coeruleoalba. (449_R5) Detail of Figure 634. Ear canal and glands. Scale bar 100 µm

3.2.1 Connective and adipose tissue

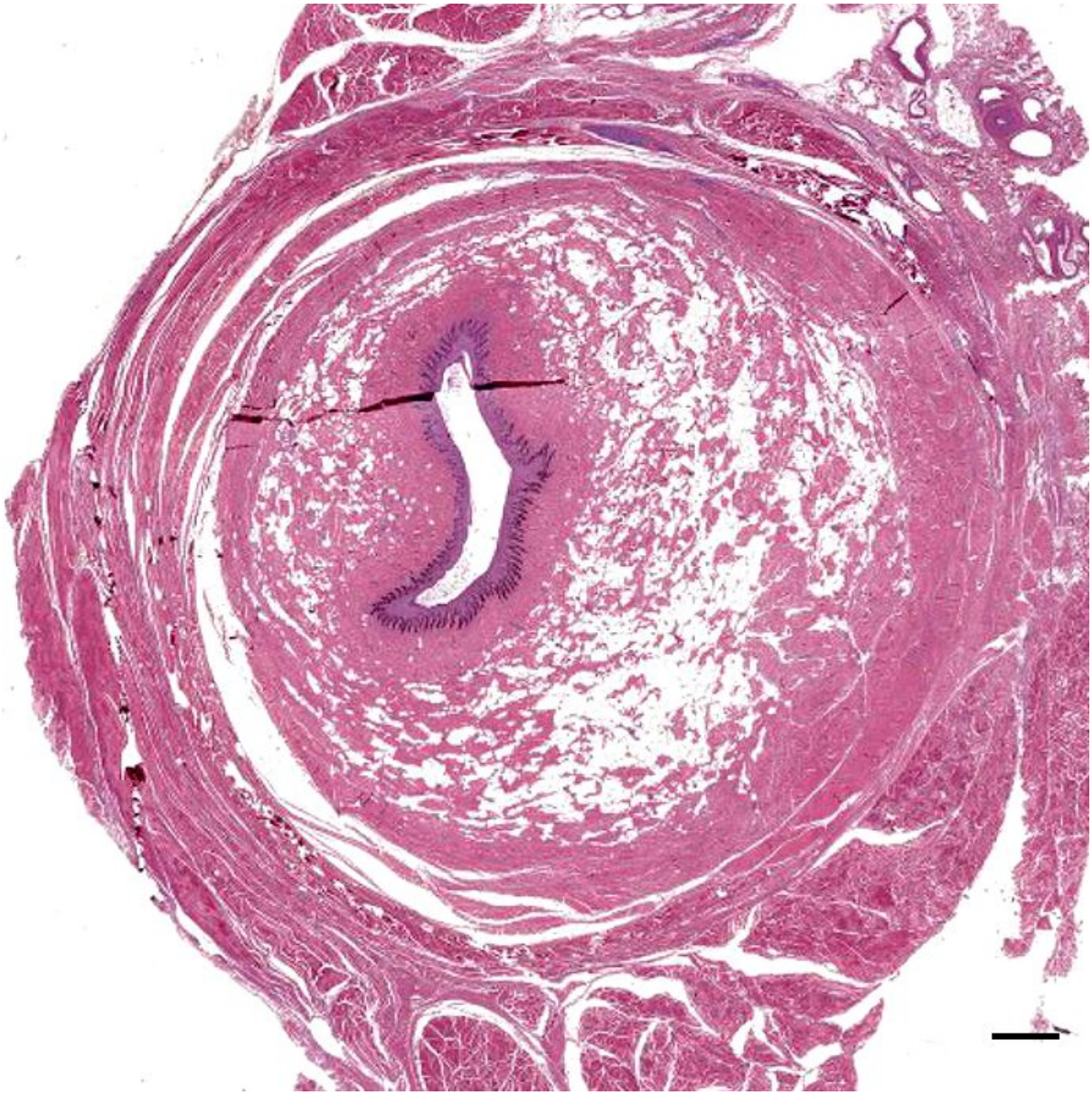

Figure 636. Histological cross-section (HE staining) of the ear canal in Cuvier´s beaked whale (ID429_11). Ear canal within the adipoconnective tissue, surrounded by a circular organization of connective and muscle tissue. Scale bar 1 mm

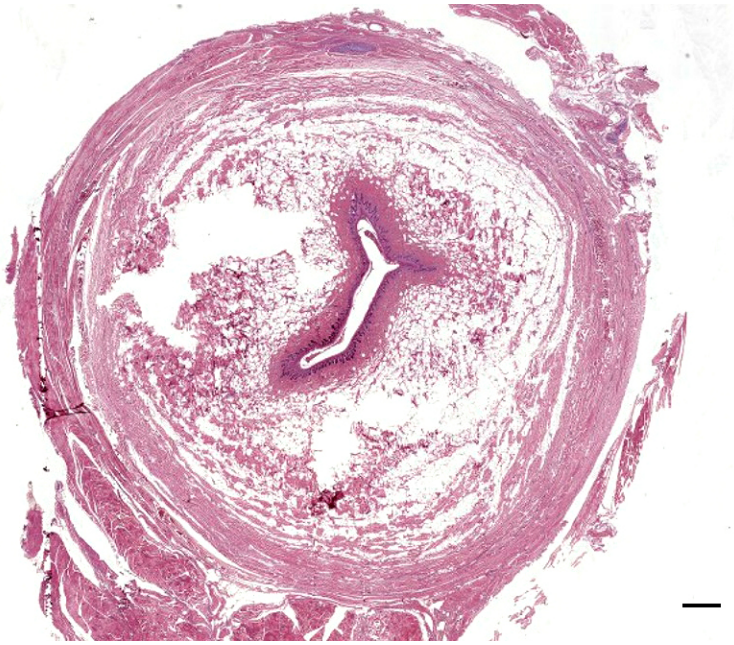

Figure 637. Histological image (HE staining) of a transverse section through the ear canal of a Cuvier's beaked whale at about 6 cm from the surface. (HE staining). Meatus lumen; Connective tissue capsule; Muscle tissue, circular, longitudinally oriented.

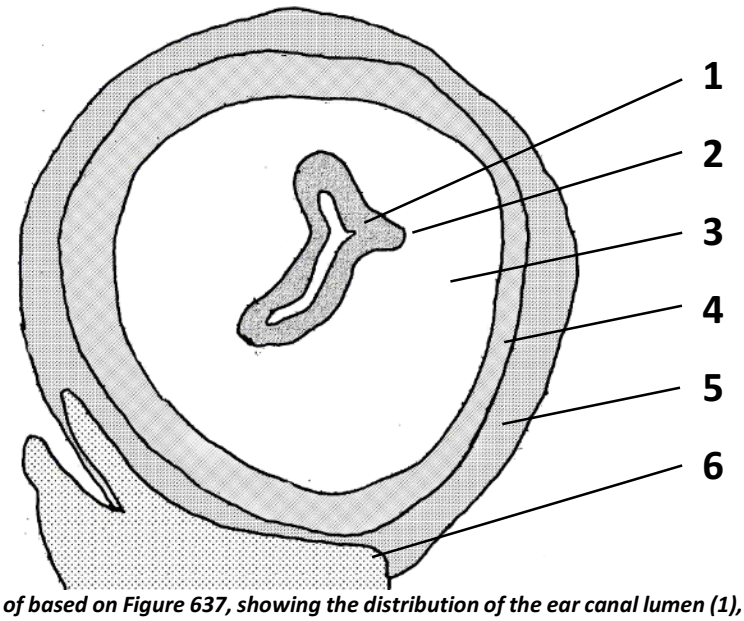

Figure 638. Schematic drawing of based on Figure 637, showing the distribution of the ear canal lumen (1), epithelium and the superficial subepithelial layer with connective tissue (2), subepithelial layer with mainly fatty tissue (3), connective tissue capsule (4), muscle tissue with circular orientation (5), muscular tissue with longitudinal orientation (6).

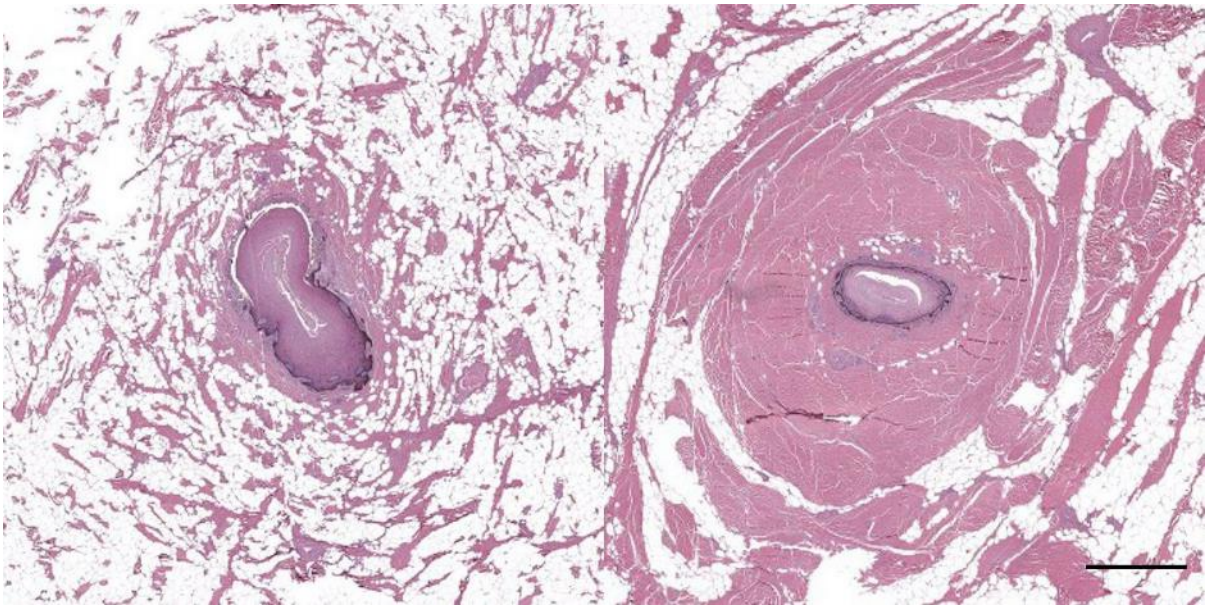

Figure 639. Two histological images (HE staining) of transverse sections through the ear canal of a long-finned pilot whale at two different depths (about 1 and 2 cm) beneath the skin. Note the difference in ration fat vs. connective tissue. Scale bar 1 mm

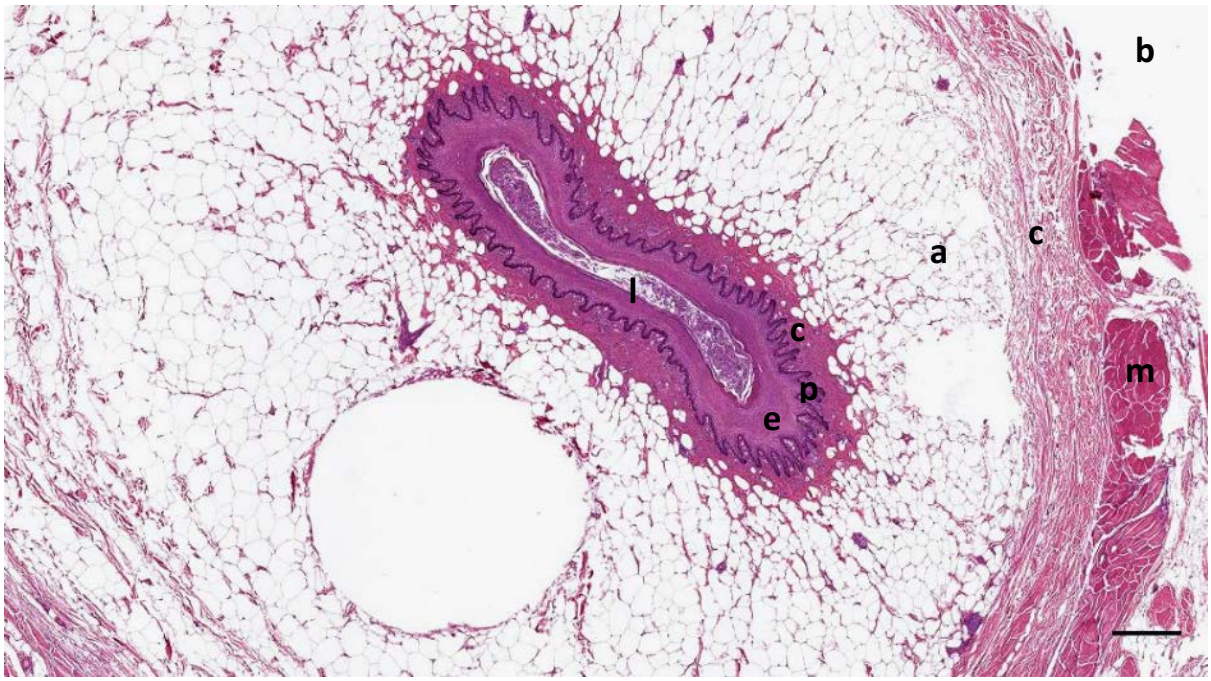

Figure 640. Histological image (HE staining) of a transverse section through the ear canal of a Cuvier's beaked whale (429_05) at about 2 cm beneath the skin. The ear canal is surrounded by a thin layer of connective tissue, a thicker layer of adipocytes (a) interweaved with fine strands of connective tissue, and which are separated from the blubber (at the location of b) by a connective tissue capsule (c) with circularly orientated collagen fibres, in which muscles (m) insert. The adipocytes, together with the surrounding connective tissue (c) form the adipoconnective tissue sheath as in other animals, although in beaked whale there the two components a and c are clearly separated, at least in the distal third of the ear canal. Scale bar 0.5mm

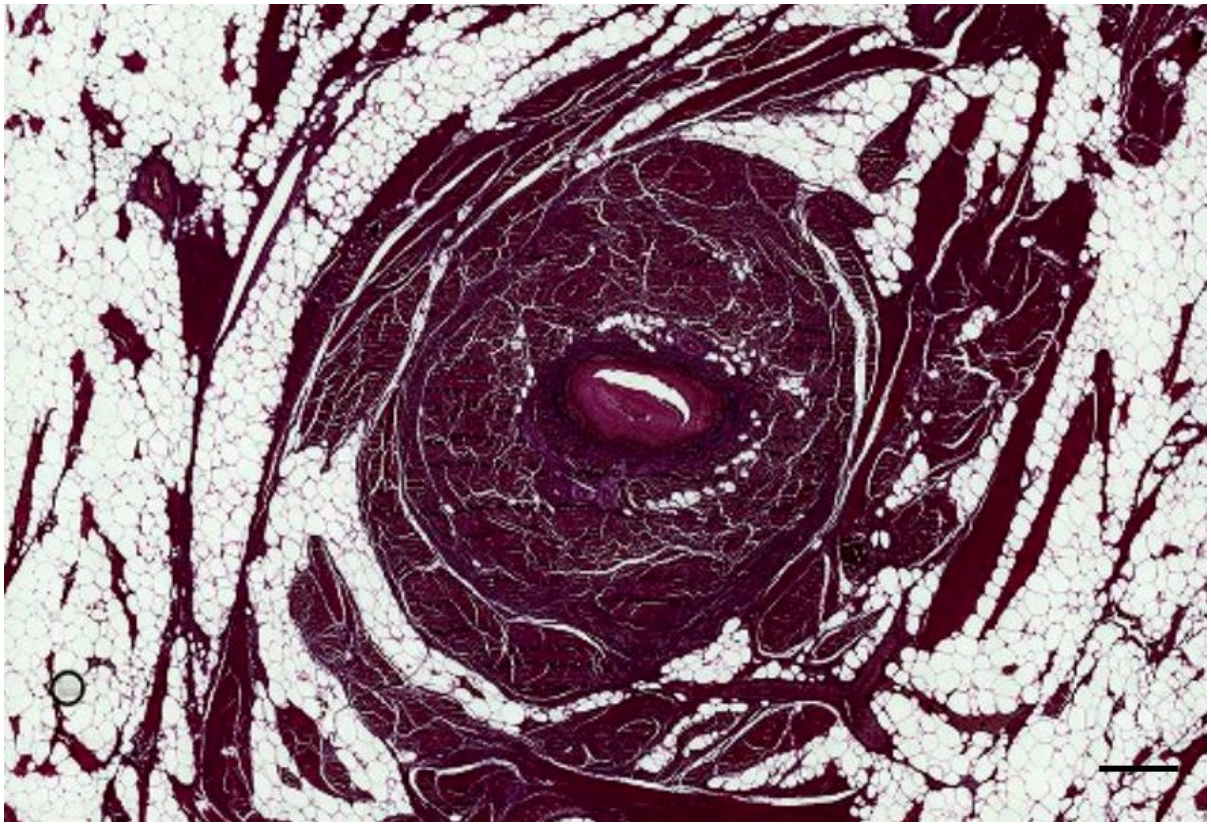

Figure 641. Histological transverse section (Weigert´s elastic staining) of the ear canal in a striped dolphin at about 1 cm beneath the skin (Sc1_02). No elastic fibres were noted in the adipoconnective tissue close to the ear canal. Scale bar 50 µm

Figure 642. Histological transverse section (Weigert´s elastic staining) of the ear canal in a striped dolphin at about 5 cm beneath the skin (5386_L10). Ear canal and cartilage, embedded in connective tissue. See Figure 643 for a drawing of the location of the elastic fibres. Scale bar 500 µm

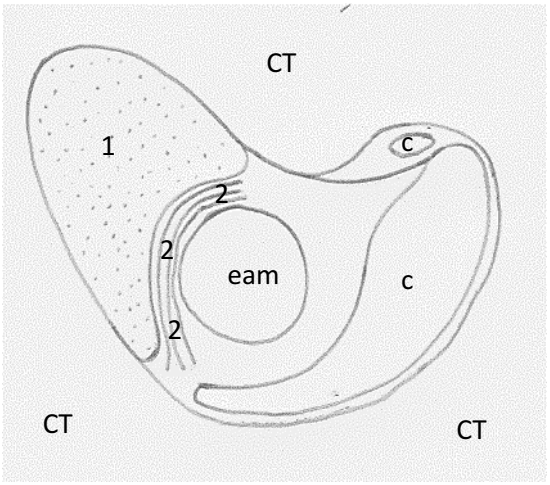

Figure 643. Drawing Figure 642, showing the location and orientation of elastic fibres associated with the ear canal (eam) in a section with cartilage (c). The fibres are orientated parallel (1) and transverse (2) to the direction of the ear canal.

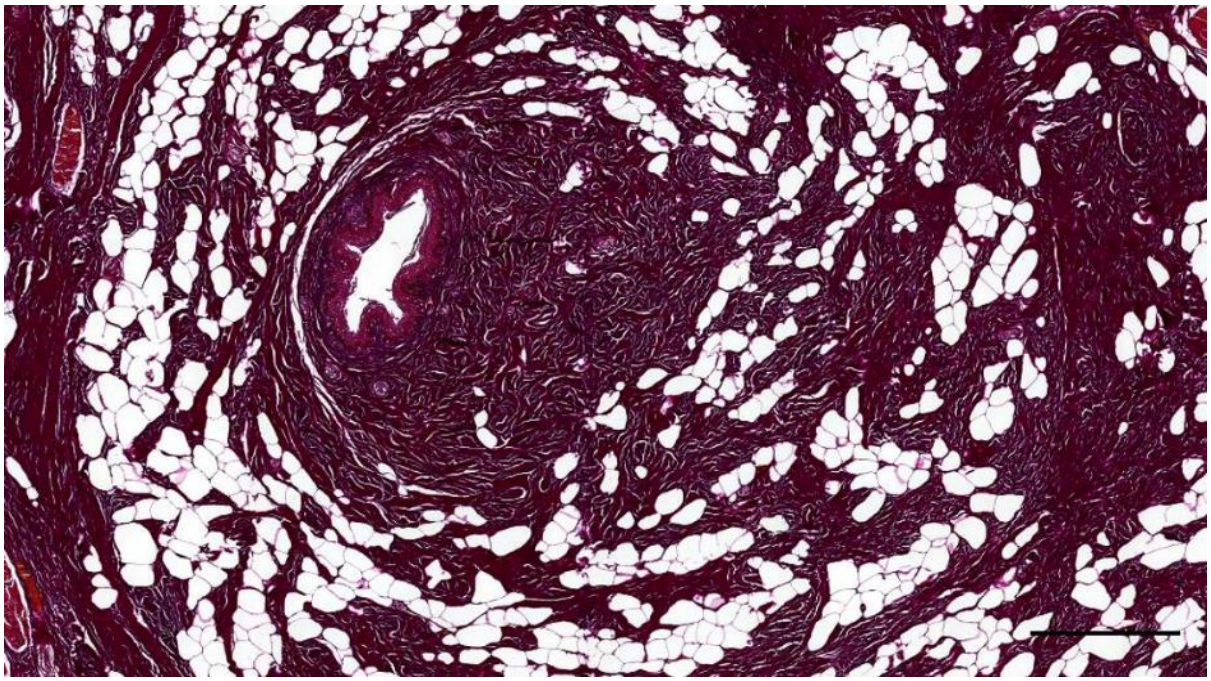

Figure 644. Histological transverse section (Weigert´s elastic staining) of the ear canal in a striped dolphin at about 1 cm beneath the skin (Sc1_02). No elastic fibres in the adipoconnective tissue close to the ear canal. Scale bar 500 µm

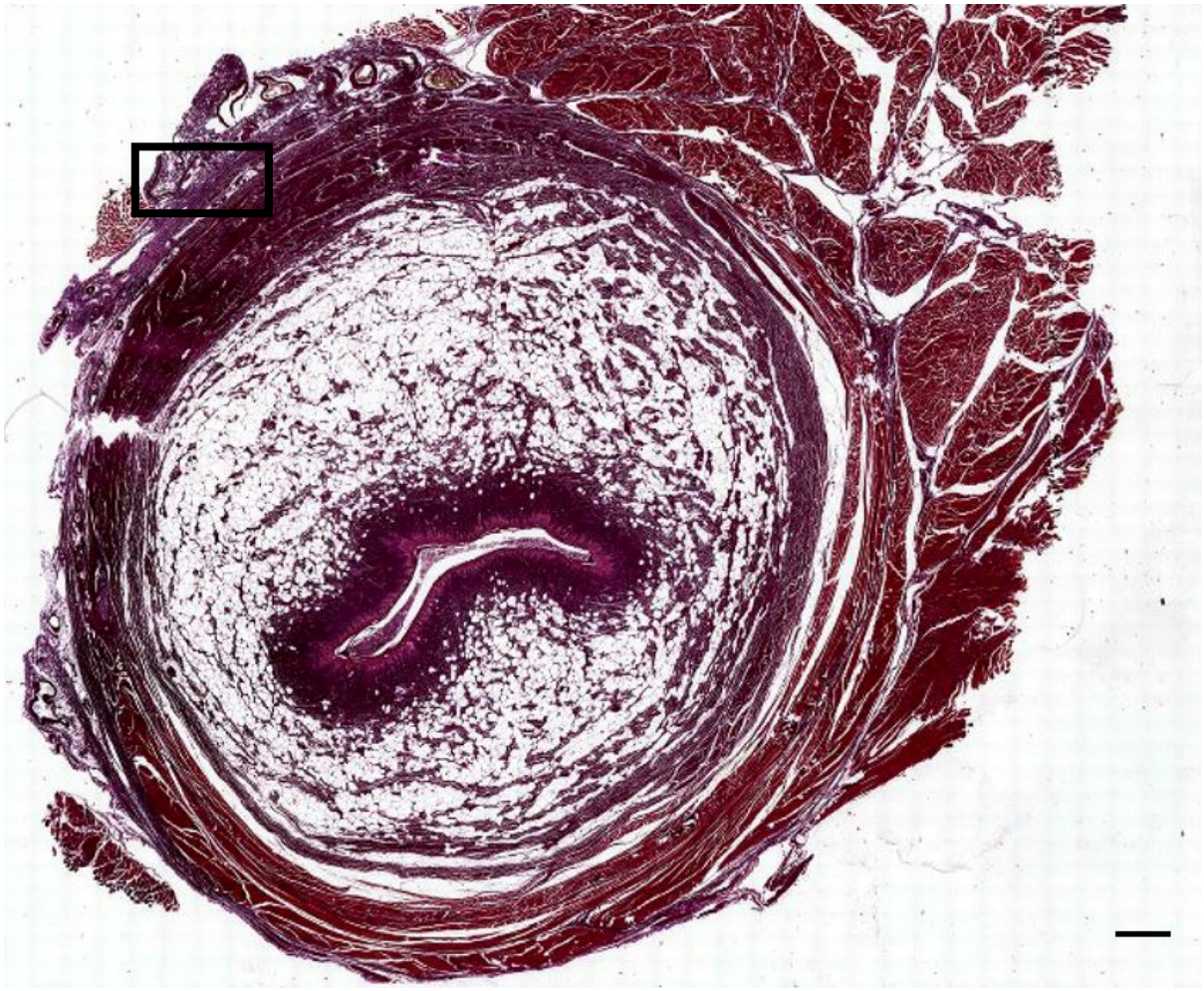

Figure 645. Histological transverse section (Weigert´s elastic staining) of the ear canal in a Cuvier´s beaked whale at about 5 cm beneath the skin (429_10). Elastic fibres are situated peripheral to the circular capsule of connective tissue and musculature. The frame indicates the location of Figure 646. Scale bar 1 mm

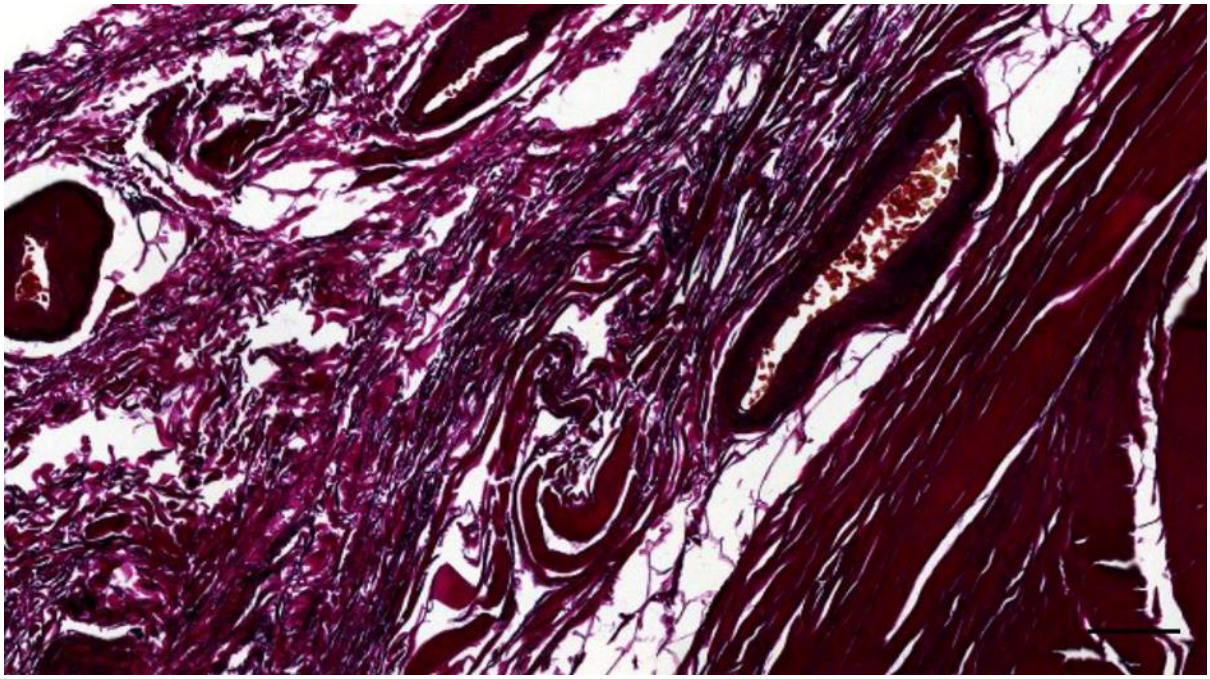

Figure 646. Detail of Figure 645 (Ziphius cavirostris, 429_10, Weigert). Elastic fibres are situated peripherally to the circular capsule of connective tissue and musculature (bottom right). Scale bar 100 µm

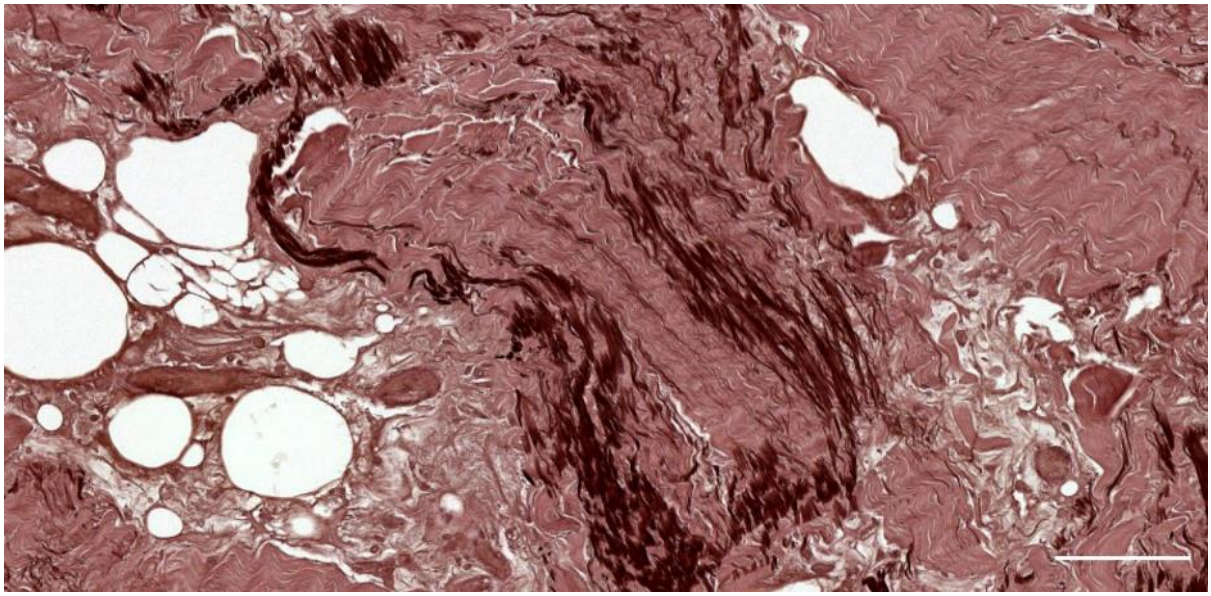

Figure 647. Detail of *Error! Reference source not found.* ***Elastic fibres in the distant connective tissue. Scale bar 100 µm***

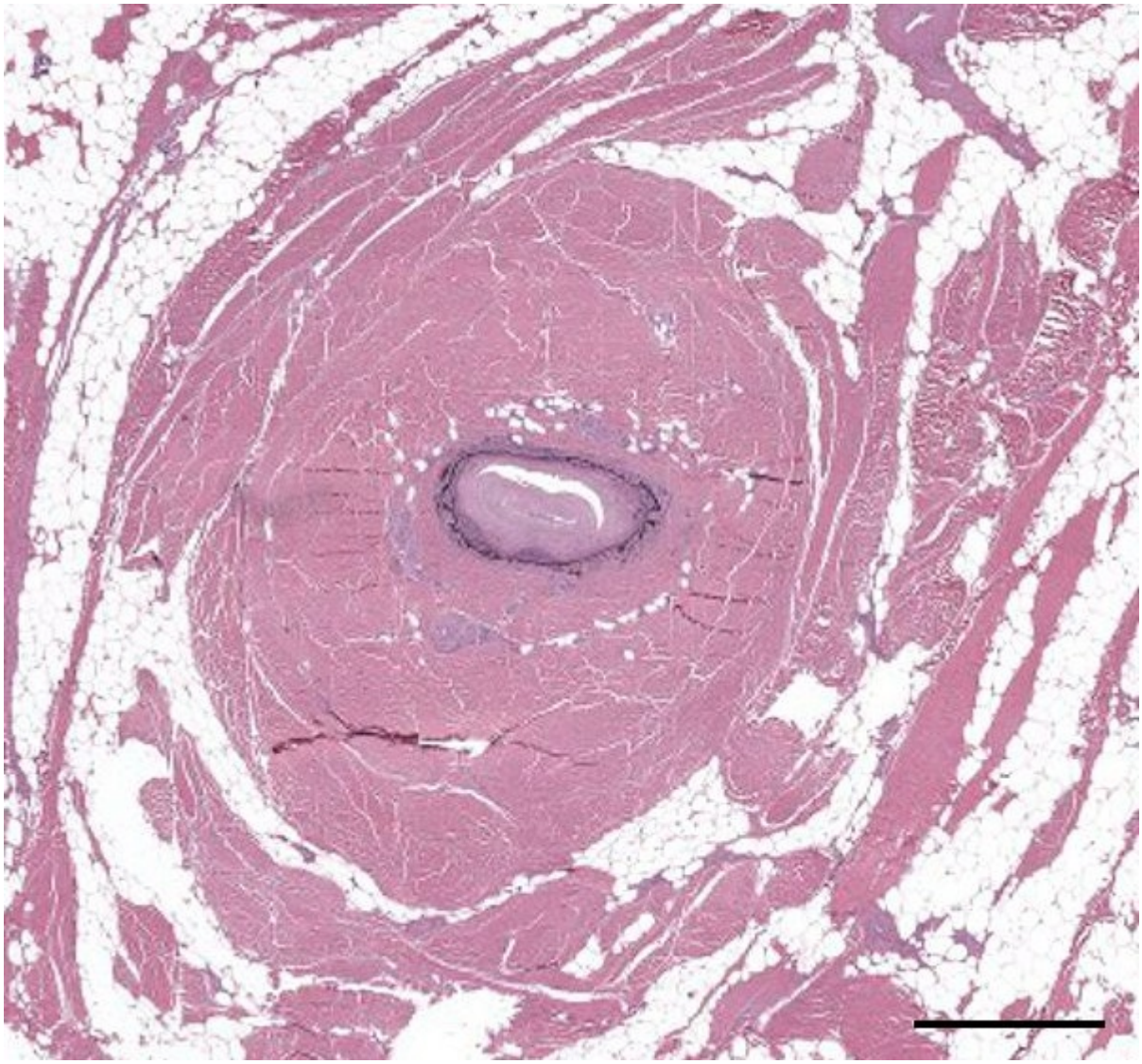

Figure 648. Histological transverse section through the ear canal in a long-finned pilot whale at about 2 cm beneath the skin (441_L4). The ear canal is embedded in connective tissue and surrounded by connective tissue and fat. Scale bar 1 mm

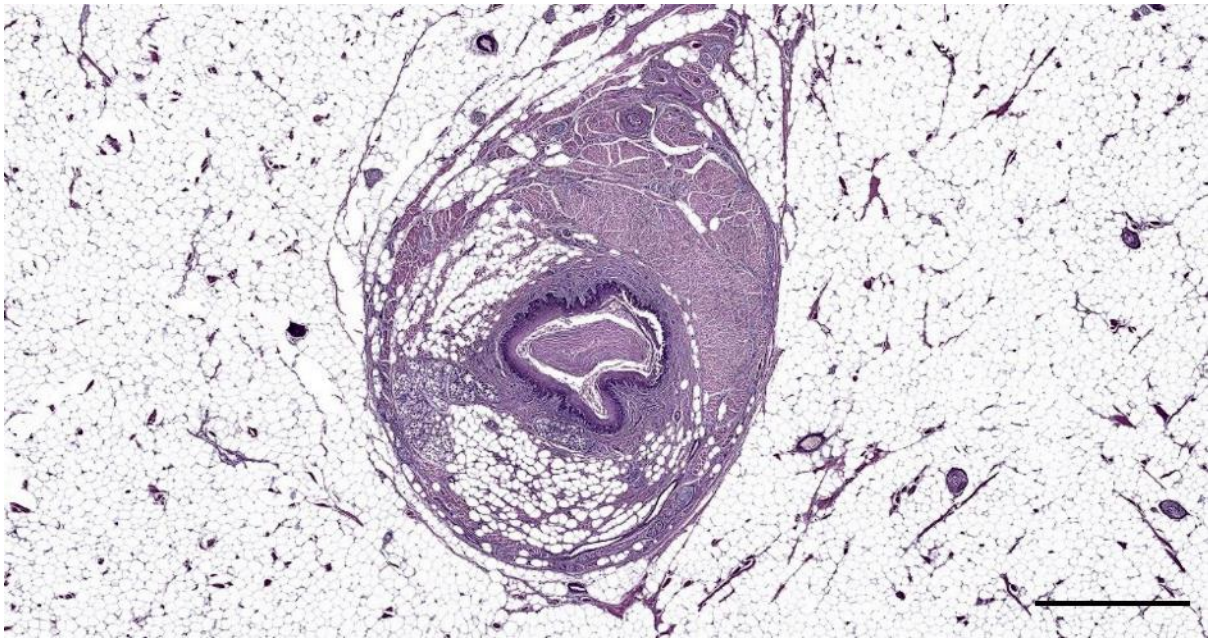

Figure 649. Histological transverse section through the ear canal in a harbour porpoise at about 1 cm beneath the skin (UT1692_L0301). Note the adipoconnective tissue capsule. Scale bar 1mm

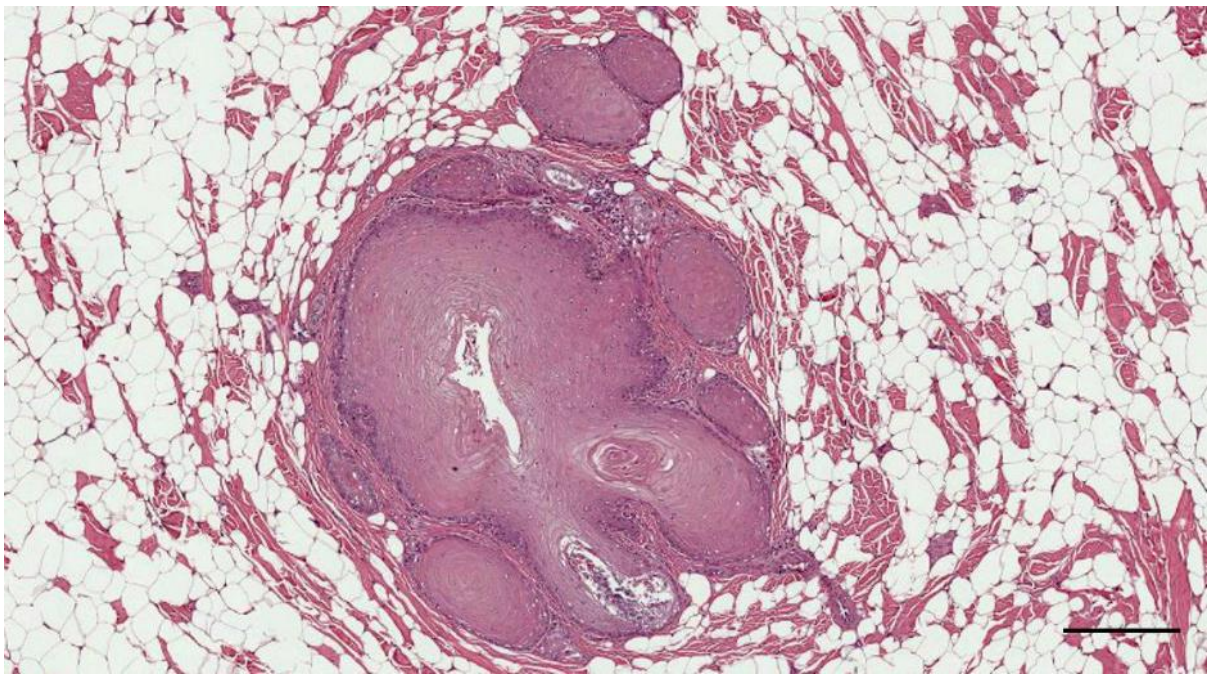

Figure 650. Histological transverse section (HE staining) through the ear canal of a common dolphin at about 1 cm beneath the skin (169/17_L2). Note the ear canal with glands and glandular excretory ducts of which only one has a true lumen with degenerated epithelial cells while the others do not have a lumen. Scale bar 300 µm

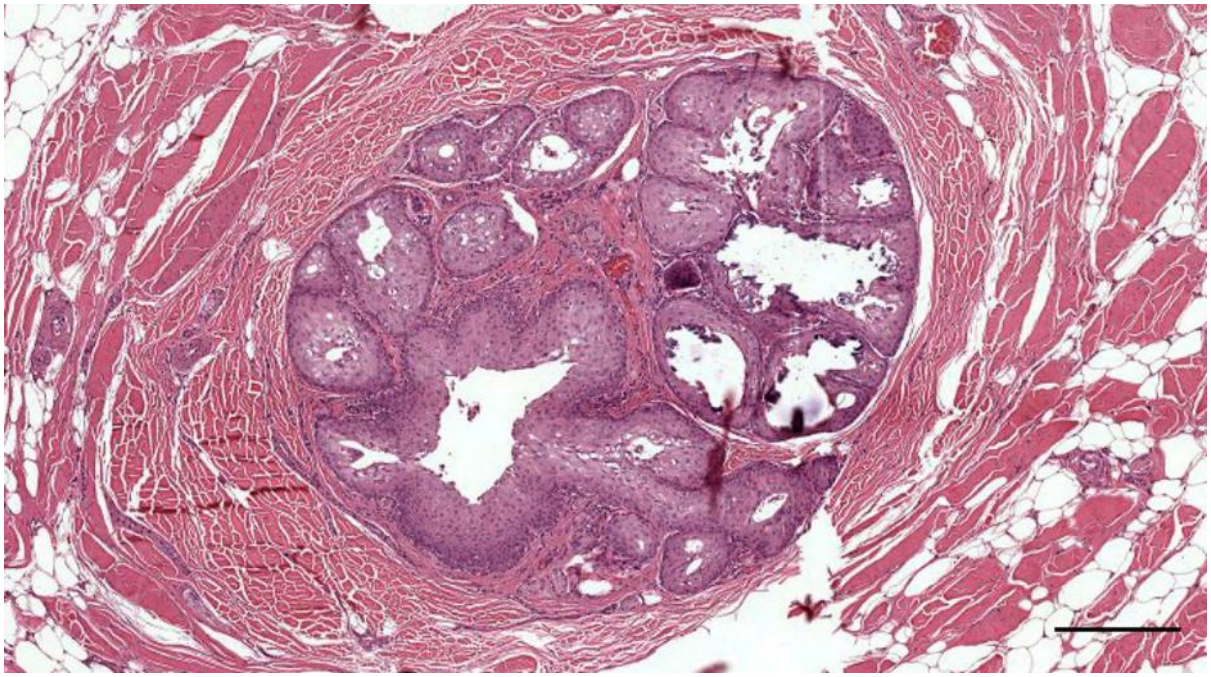

Figure 651. Histological transverse section (HE staining) through the ear canal of a common dolphin at about 1.5 cm beneath the skin (169/17_L3). Ear canal with glandular structures. Scale bar 300 µm

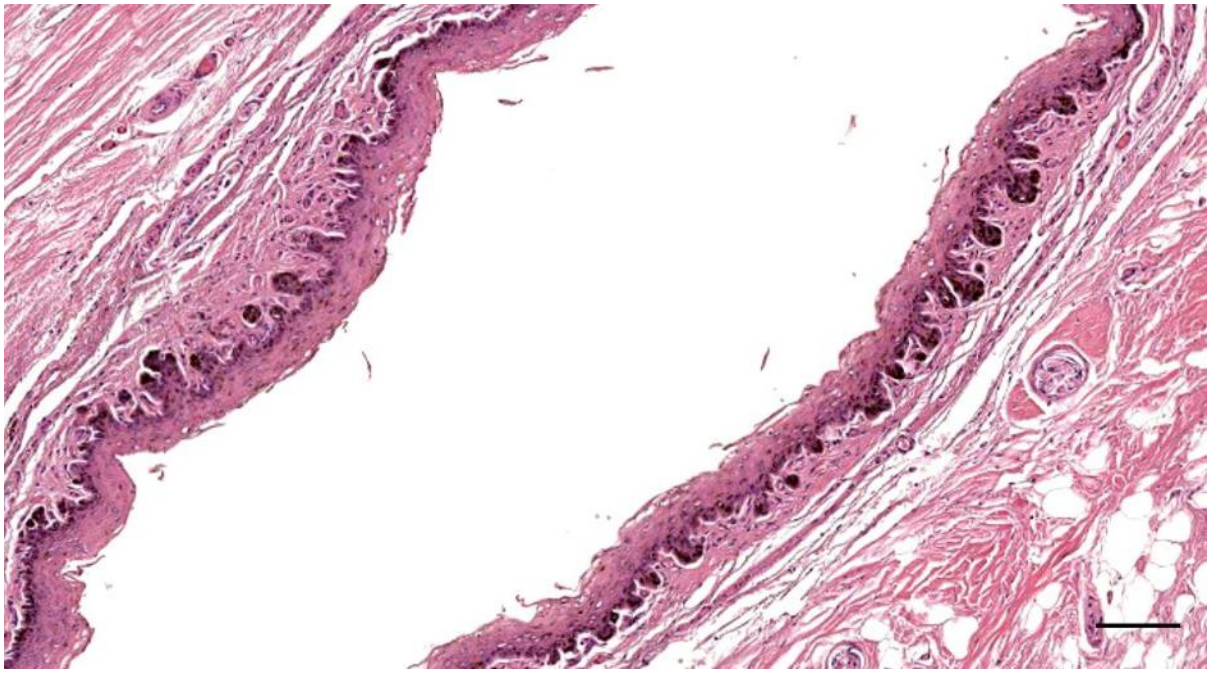

Figure 652. Histological transverse section (HE staining) through the ear canal of a common dolphin at about 3.5 cm beneath the skin (169/17_L7). Scale bar 100 µm

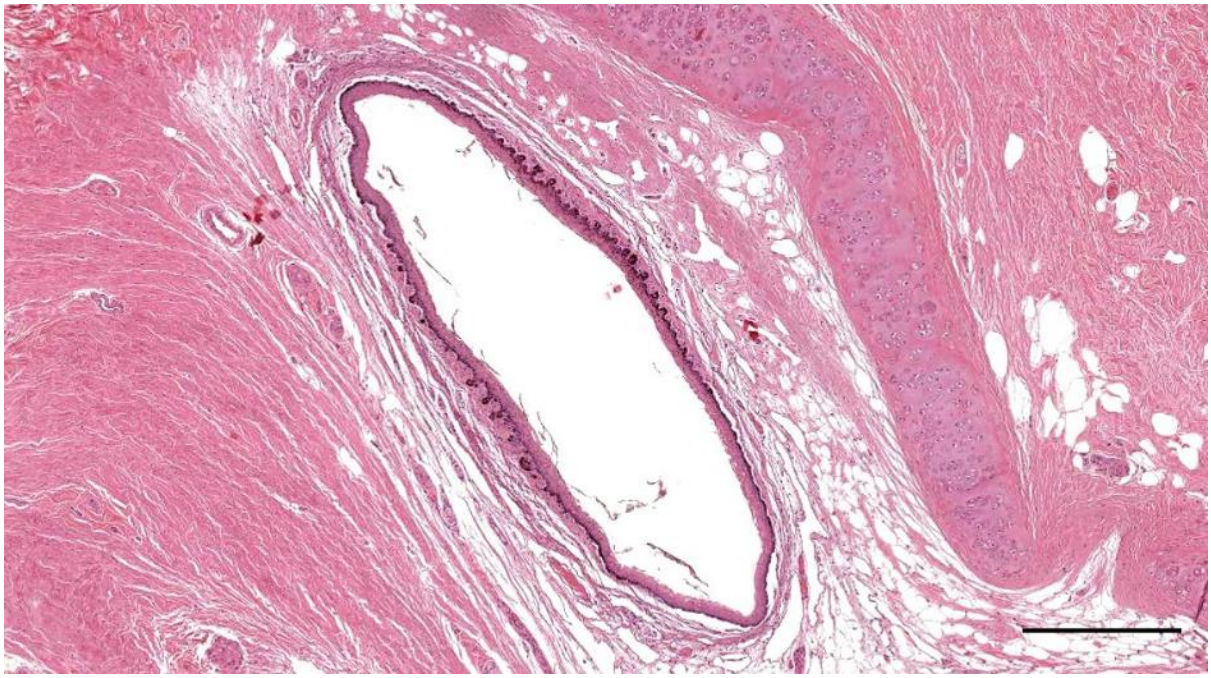

Figure 653. Histological transverse section (HE staining) through the ear canal of a common dolphin at about 4 cm beneath the skin (169/17_L8). Scale bar 500 µm

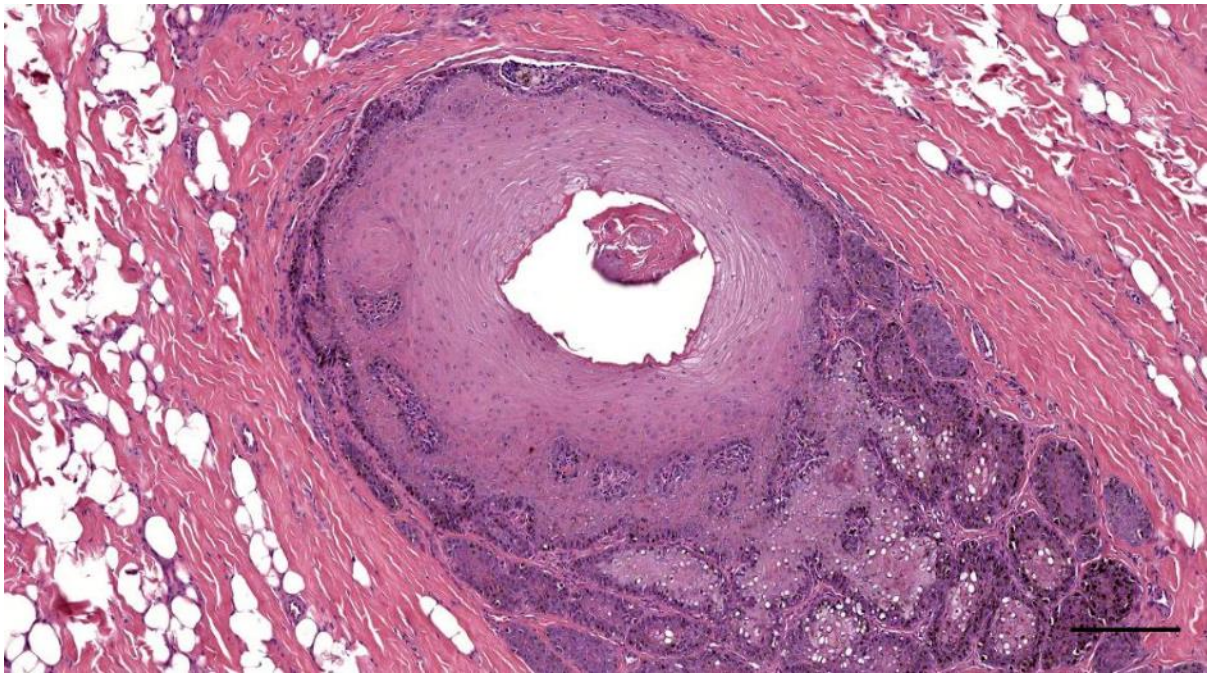

Figure 654. Histological transverse section (HE staining) through the ear canal of a common dolphin at the external ear opening (169/17_R1). Note the lumen size and dermal papillae. Scale bar 200 µm

3.2.1 Musculature

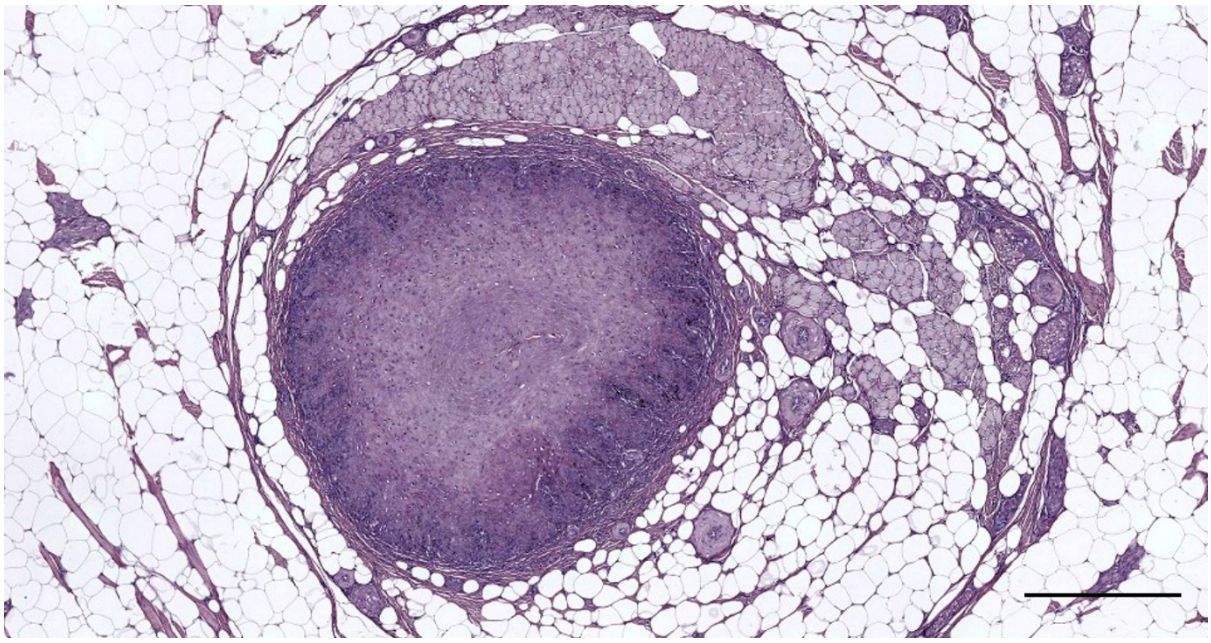

Figure 655. Histological image (HE) of a transverse section through the external ear canal of a harbour porpoise, about 1.5 cm beneath the skin (UT1718_L0401). Scale bar 500 µm

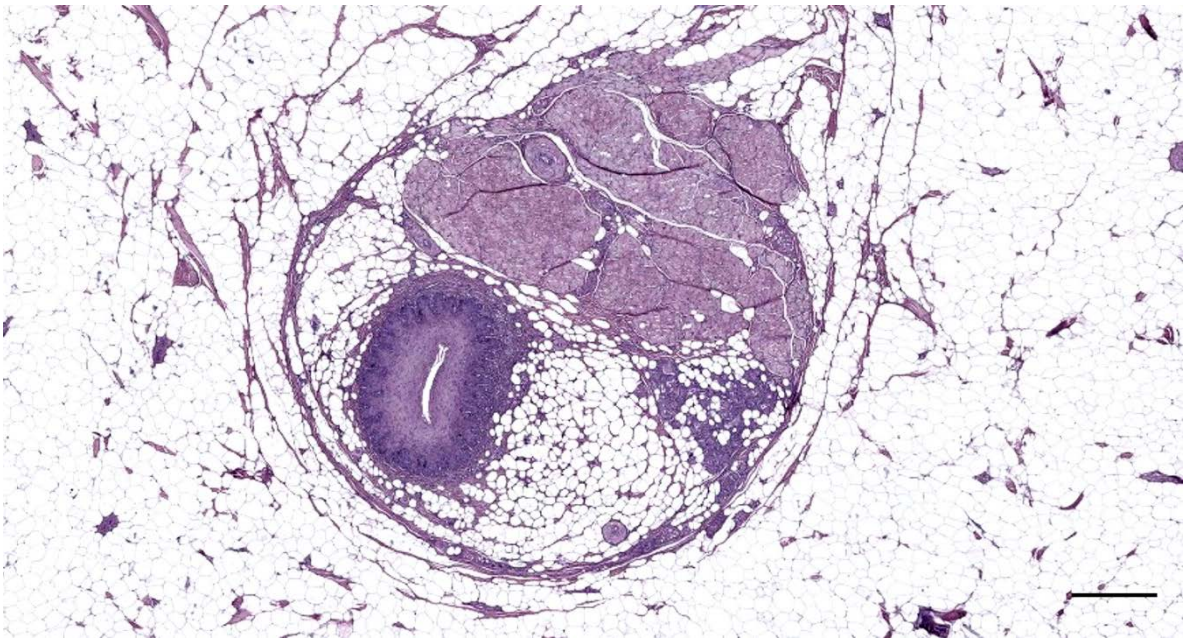

Figure 656. Histological image (HE) of a transverse section through the external ear canal of a harbour porpoise, about 2 cm beneath the skin (UT1718_L0501). Scale bar 500 µm

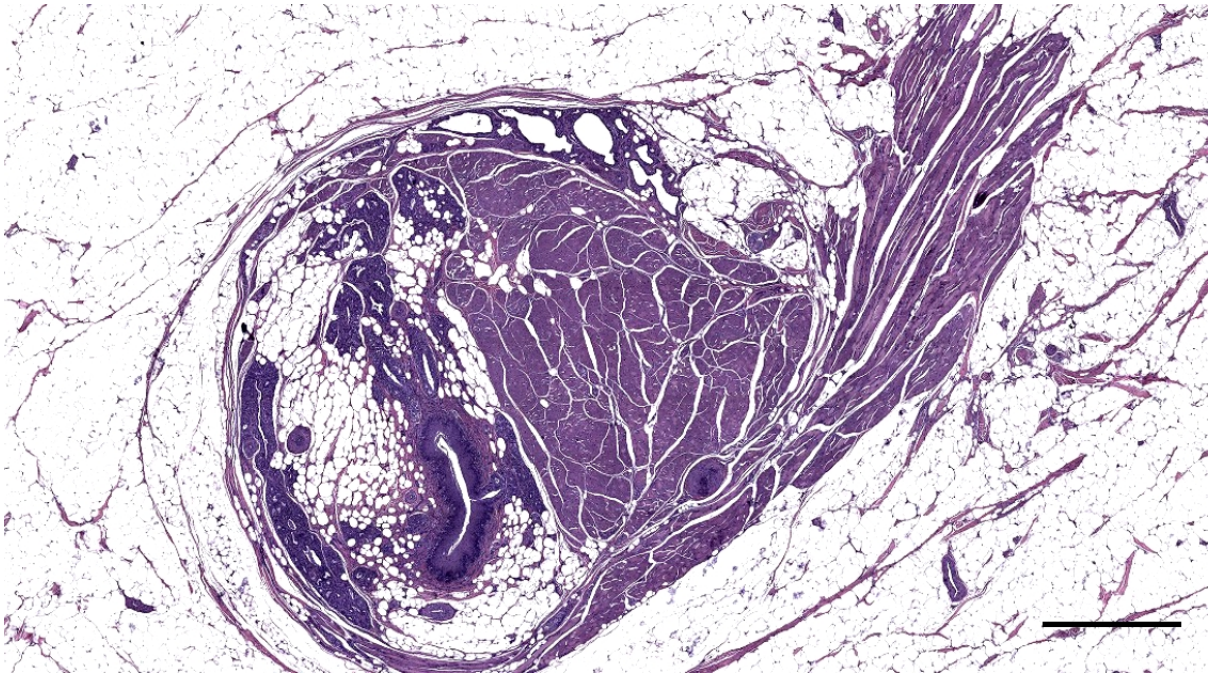

Figure 657. Histological image (HE staining) of a transverse section through the left external ear canal of a harbour porpoise at about 2 cm beneath the skin (UT1734_L06). Muscles and glands. Scale bar 1 mm

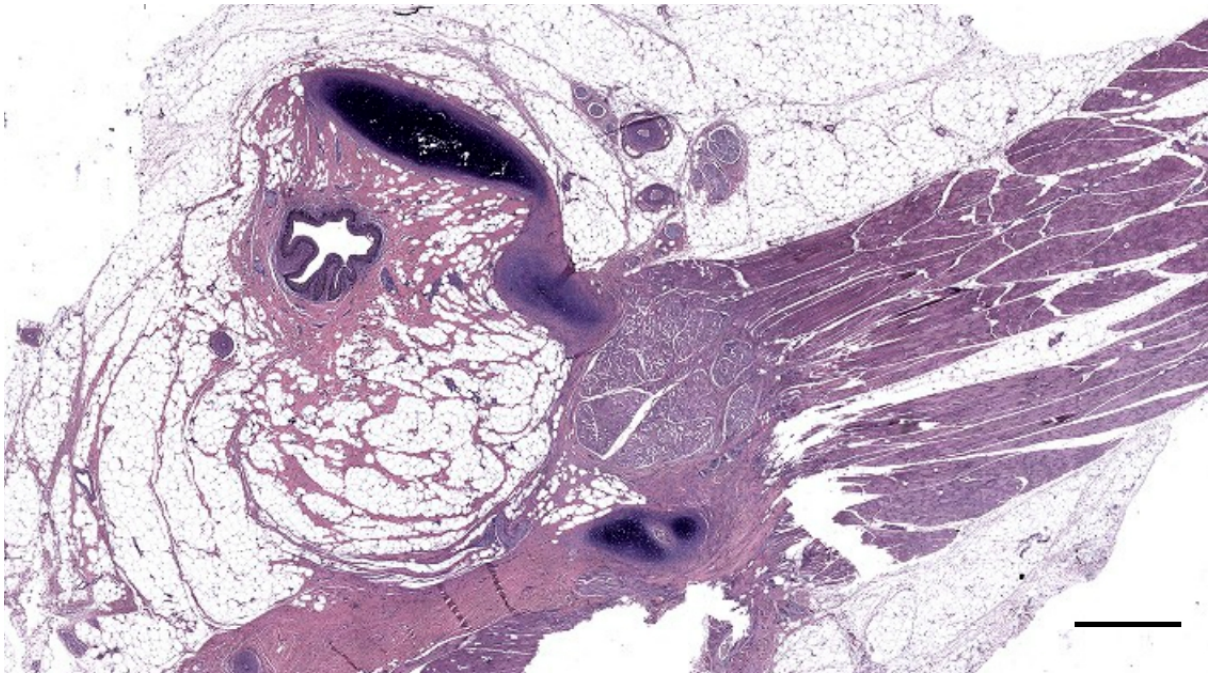

Figure 658. Histological image (HE staining) of a transverse section through the left external ear canal of a harbour porpoise at about 3 cm beneath the skin (UT1734_L10). Scale bar 1mm

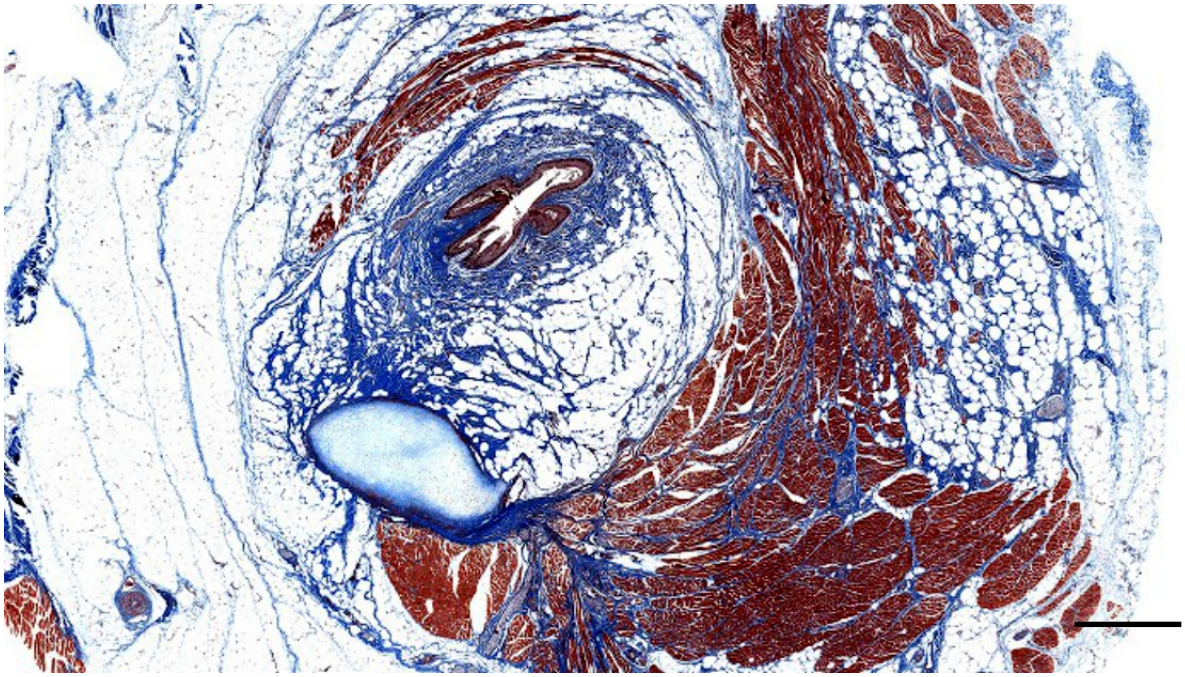

Figure 659. Histoligcal image (Masson´s trichrome) of a transverse section through the right external ear canal of a harbour porpoise at about 2 cm beneath the skin (UT1734_R0601). Scale bar 1 mm

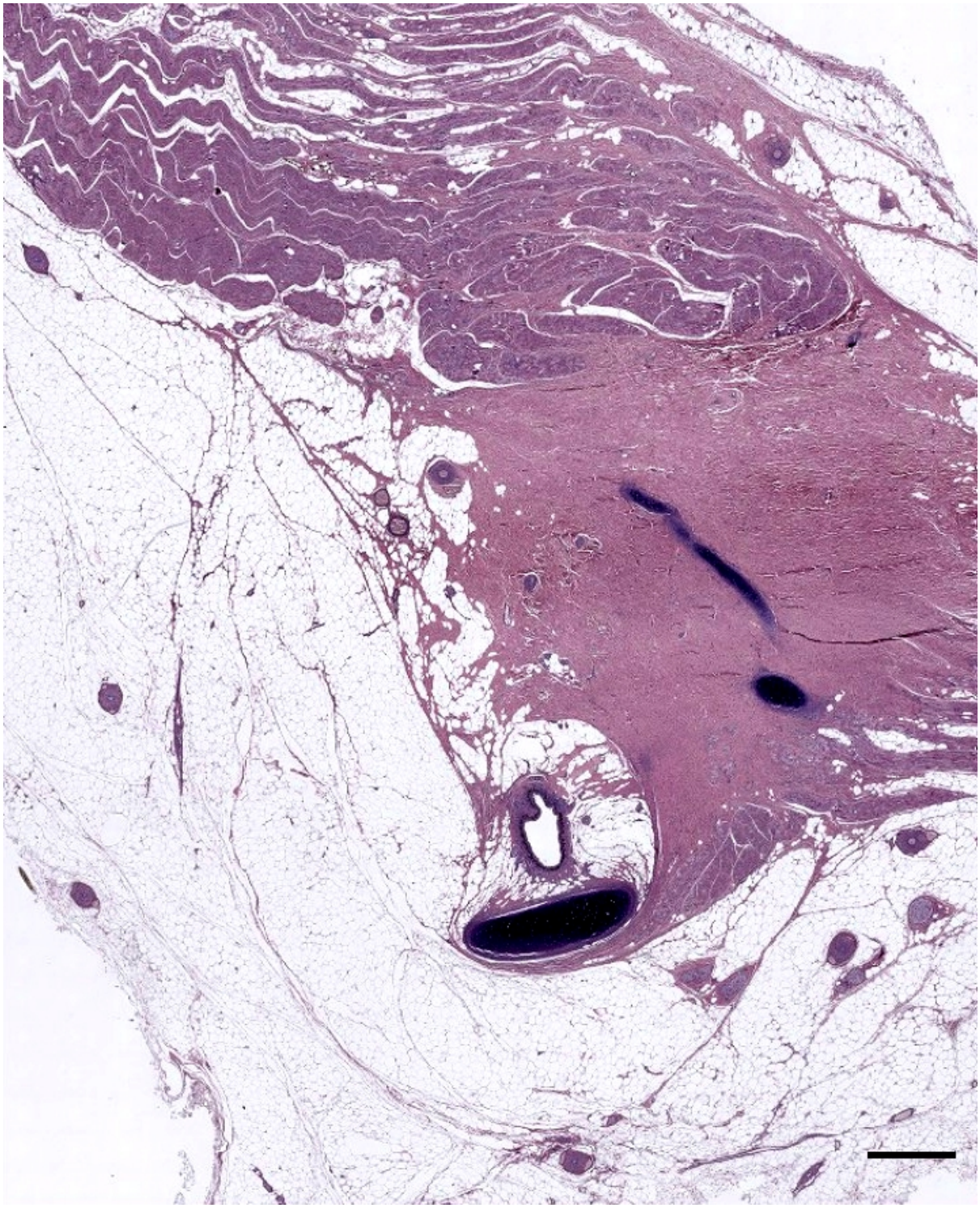

Figure 660. Histological image (HE) of a transverse section through the external ear canal of a harbour porpoise, about 3.5 cm beneath the skin (UT1718_L1002). Scale bar 1 mm

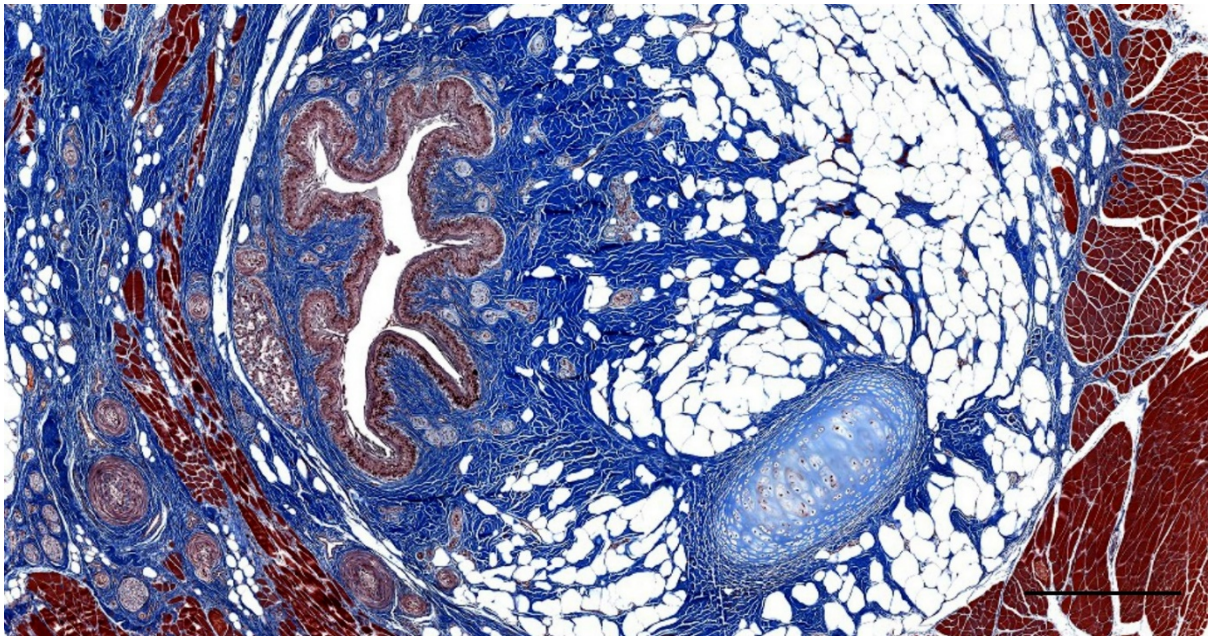

Figure 661. Histological image (Masson´s trichrome) of a transverse section through the ear canal of a harbour porpoise at about 2.5 cm beneath the skin, at the top of the ventral curvature (UT1712_L07). Scale bar 500 µm

3.2.2 Cartilage

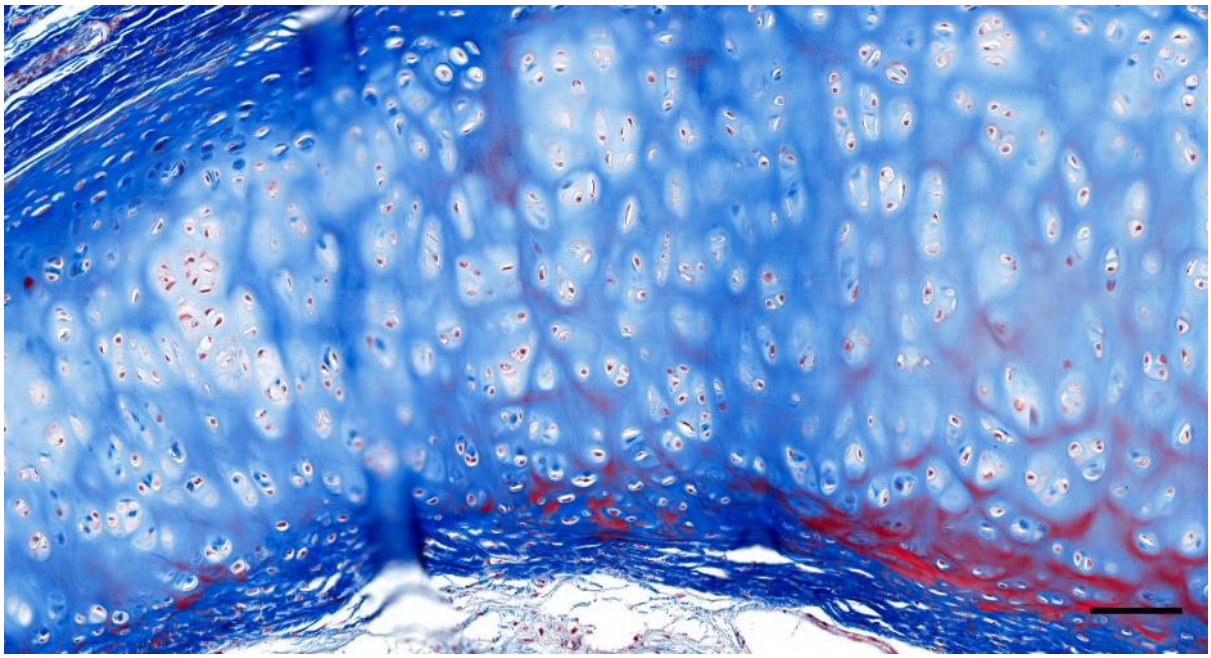

Figure 662. Histological image of the cartilage associated with the ear canal in a striped dolphin (127565_1609)(Masson´s trichrome). Scale bar 100 µm

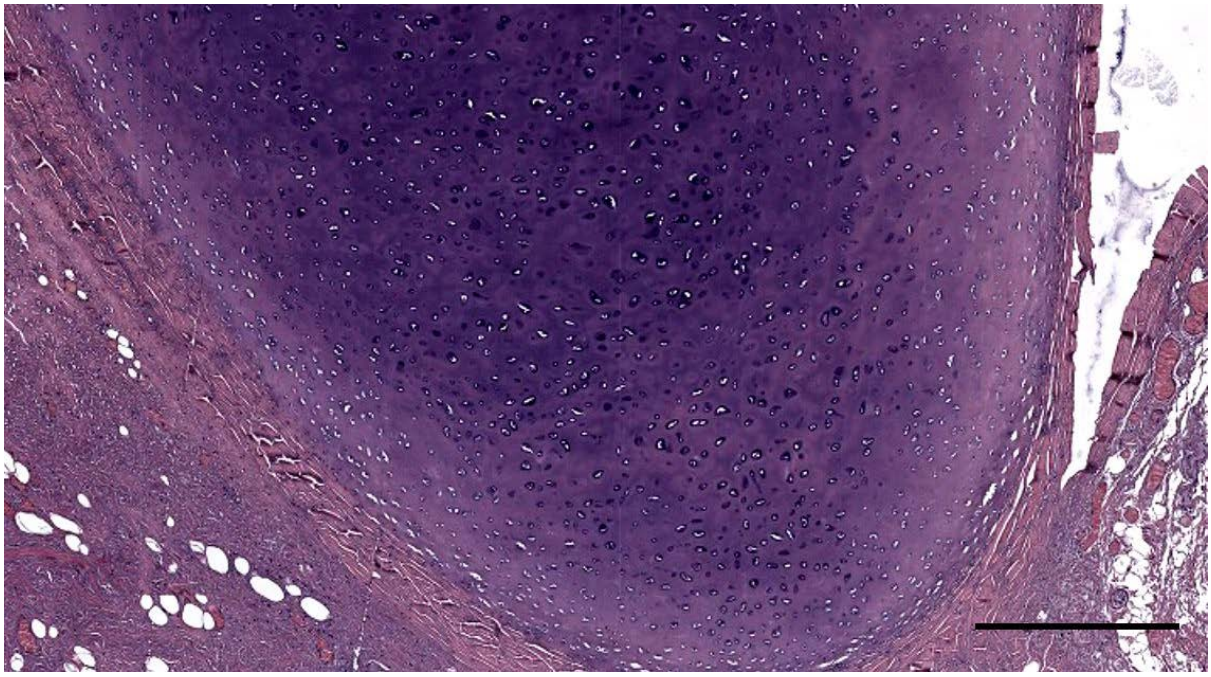

Figure 663. Histological detail image of the cartilage in the trachea of a bottlenose dolphin (ID493). Scale bar 500 µm

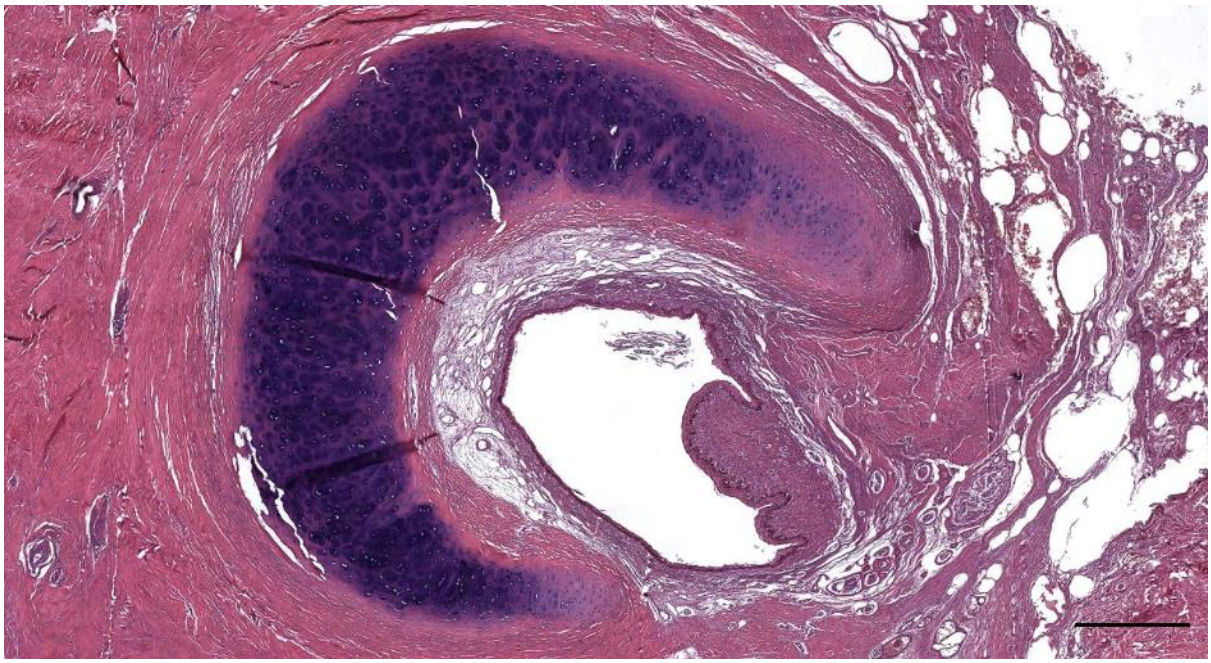

Figure 664. HE-stained cross-section of the ear canal and cartilage of a striped dolphin (ID509/17_Lx1), close to the TP complex. Scale bar 0.5 mm

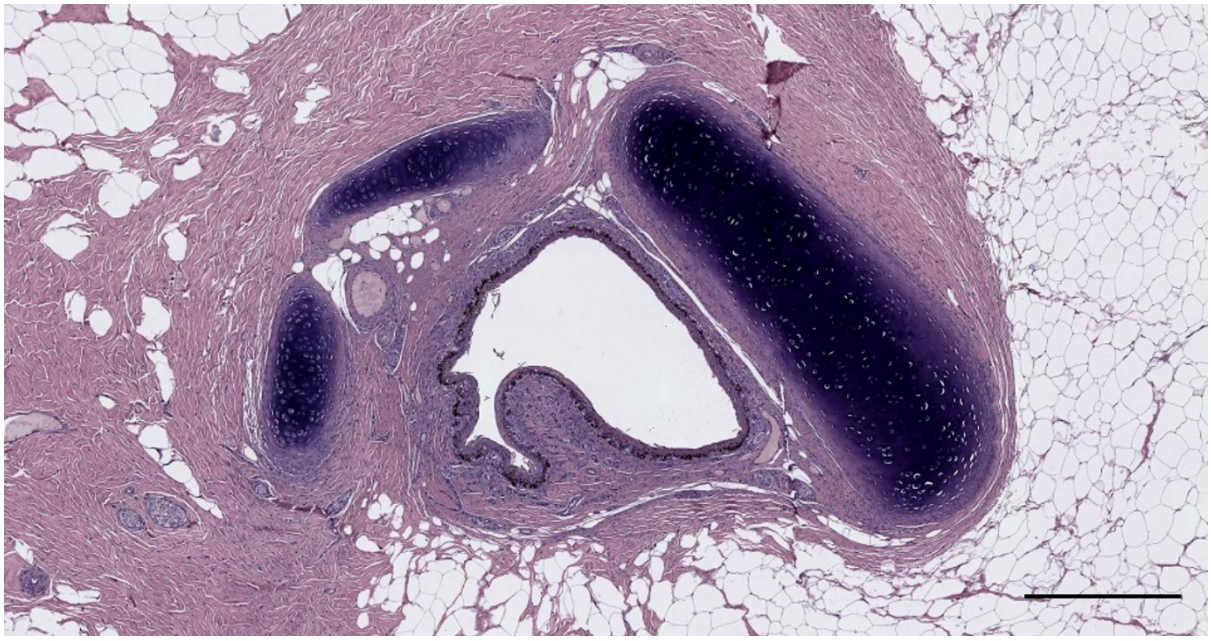

Figure 665. Histological image (HE) of a transverse section through the external ear canal of a harbour porpoise, about 4 cm beneath the skin (UT1718_L1201). Scale bar 500 µm

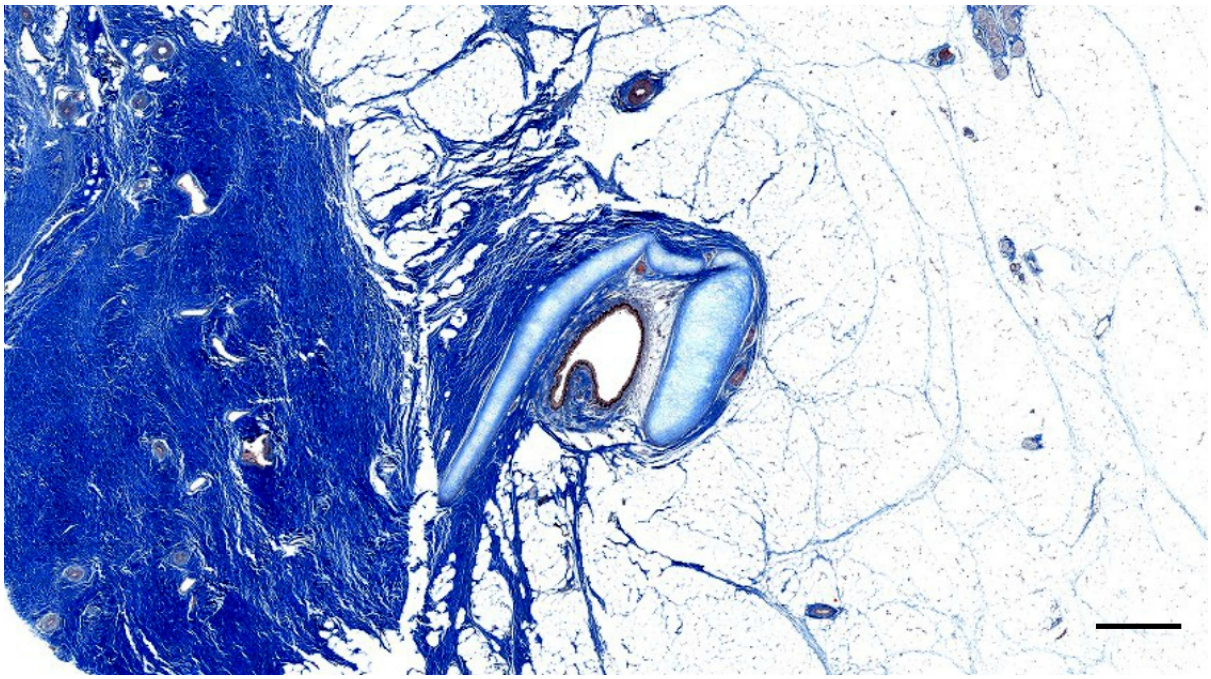

Figure 666. Histoligcal image (Masson´s trichrome) of a transverse section through the right external ear canal of a harbour porpoise at about 3 cm beneath the skin (UT1734_R0801). Scale bar 1mm

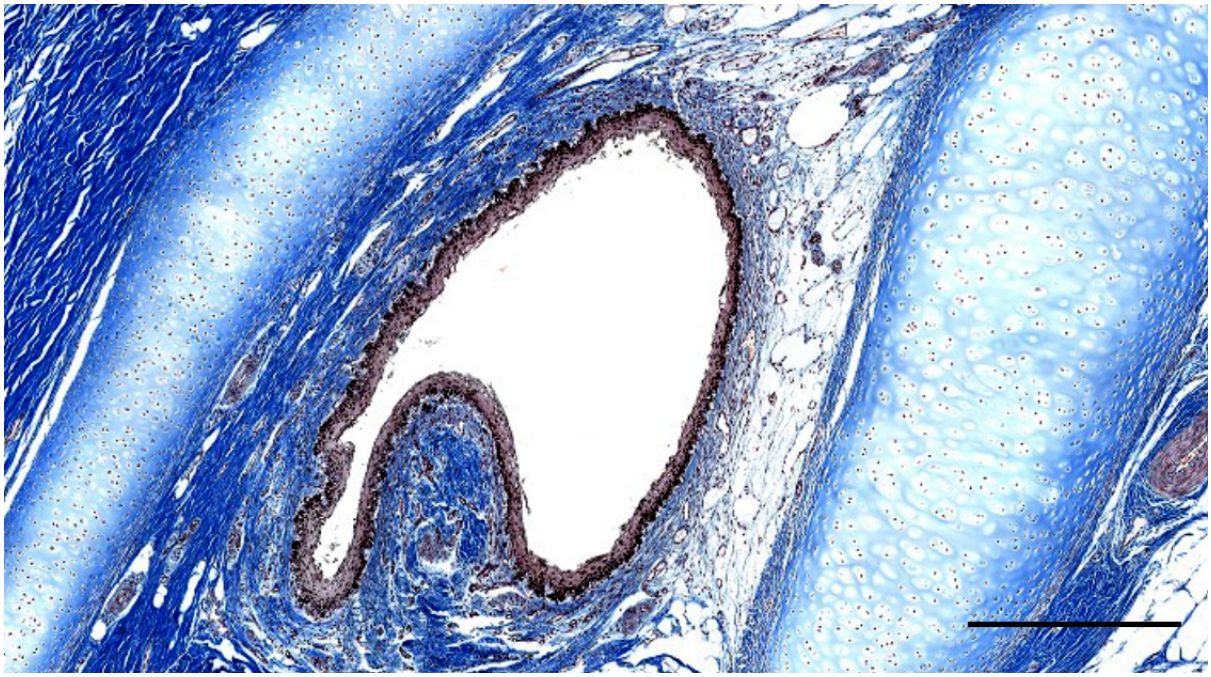

Figure 667. Detail of Figure 666 (UT1734_R0801). Scale bar 500 µm

Figure 668. Histological transverse section through the ear canal of a striped dolphin at about 5 cm beneath the skin (274/18). Horseshoe-shaped cartilage with an additional flange, and the ear canal with a subtle nervous tissue ridge, and vascular sinuses. Scale bar 1 mm

Figure 669. Histological transverse section (HE-staining) through the ear canal of a Cuvier´s beaked whale at about 6 cm beneath the skin (ID429_14) Ear canal and cartilage embedded within dense connective tissue, and surrounded by muscle and connective tissue. Scale bar 1 mm

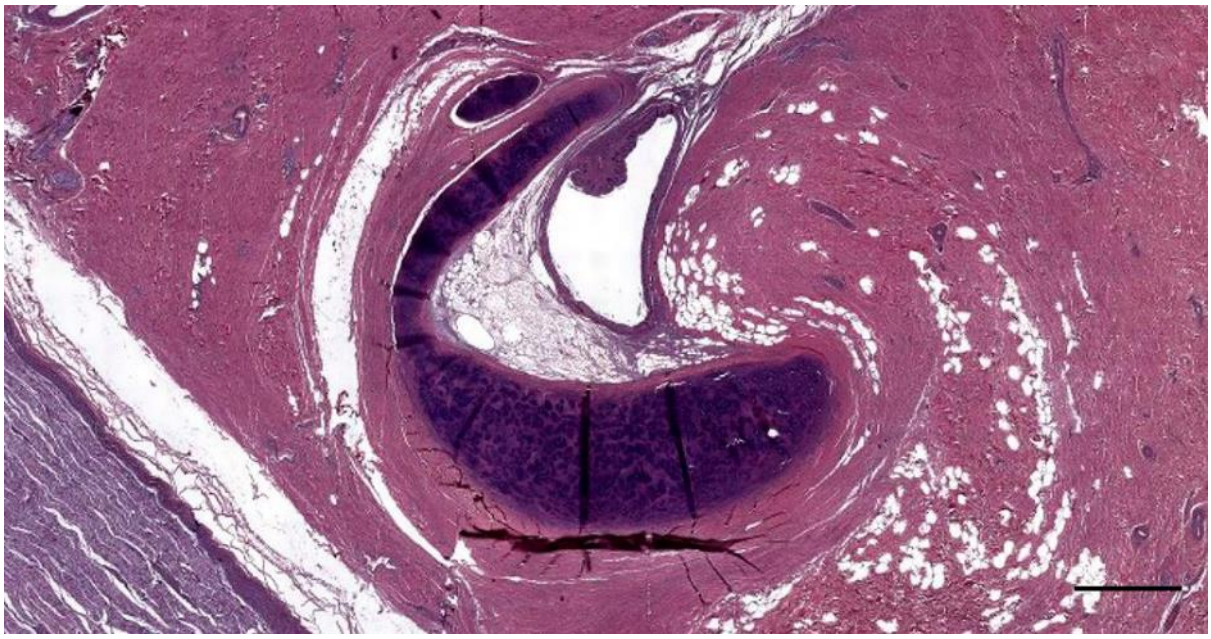

Figure 670. Histological transverse section (HE staining) through the ear canal of a bottlenose dolphin (457_R14) at about 6 cm beneath the skin. Note the facial nerve, the bifurcated cartilage, the nervous tissue ridge, vascular lacunae, and dense connective with adipocytes. Scale bar 1 mm.

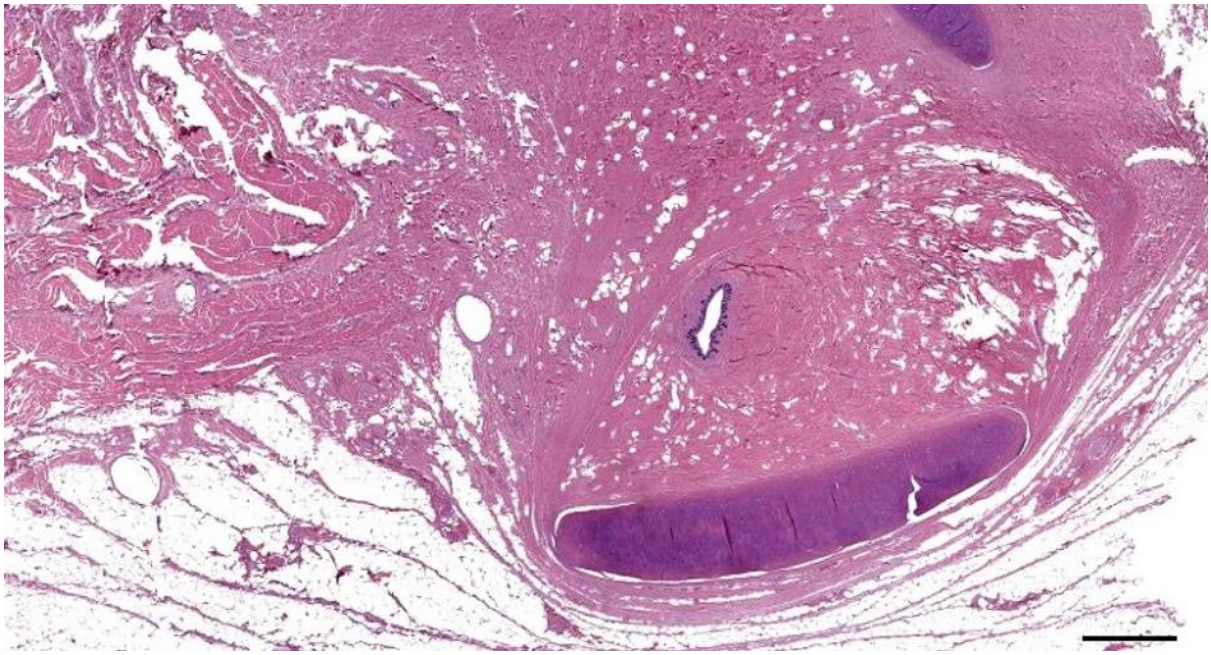

Figure 671. Histological transverse section (HE staining) through the left ear canal of a bottlenose dolphin (444_L11) at about 5 cm beneath the skin. Scale bar 1 mm

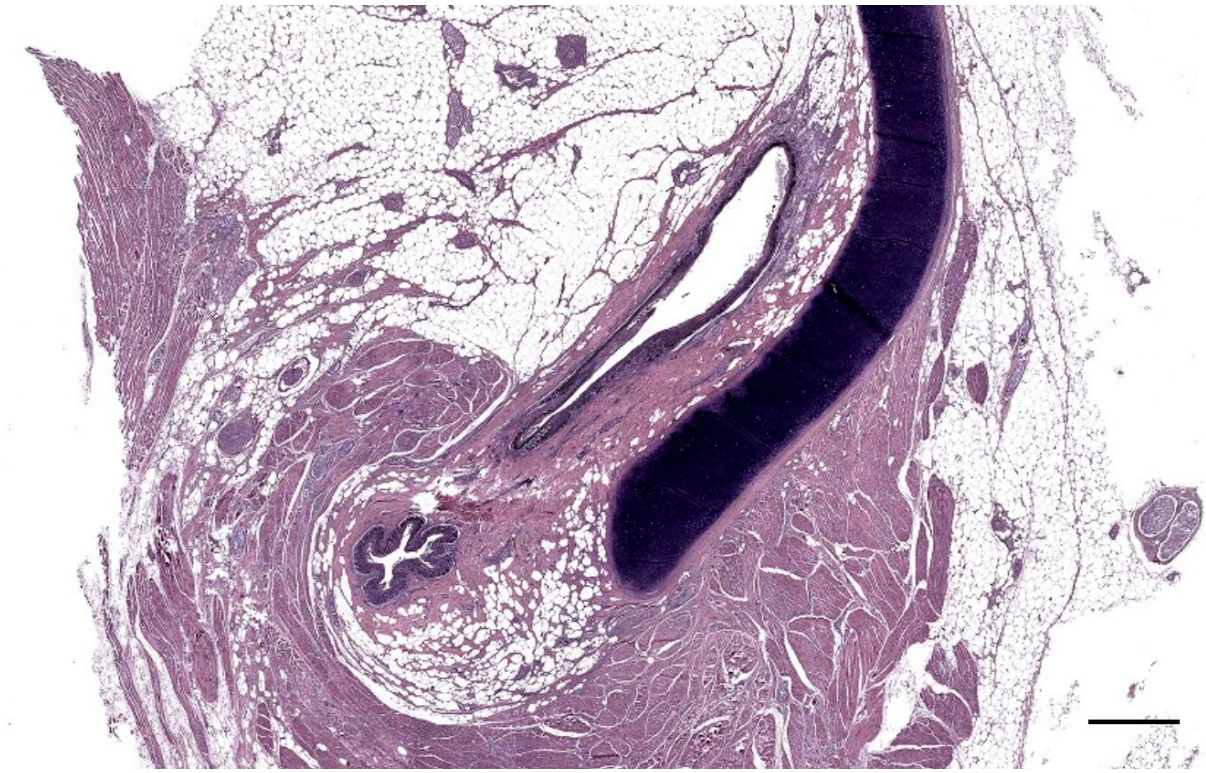

Figure 672. Histological image (HE staining) of a double section through the external ear canal in a harbour porpoise, at about 3.5 cm beneath the skin (UT1771_R1101). Scale bar 1 mm

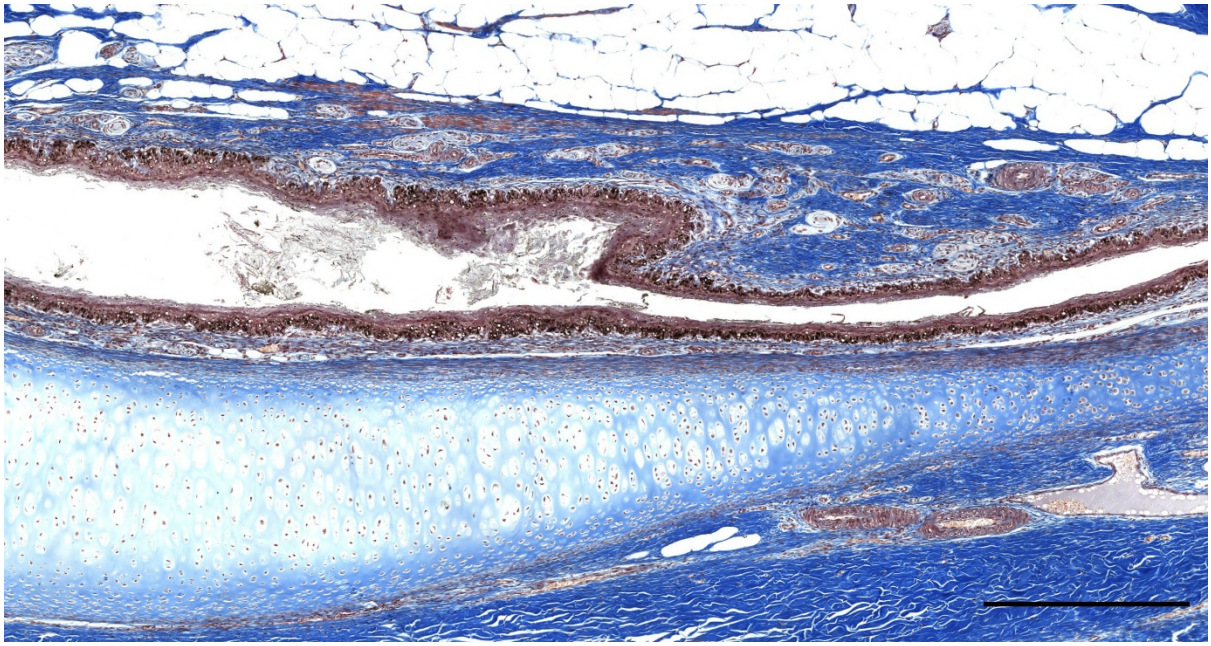

Figure 673. Histological image (Masson´s trichrome) of an oblique section through the right external ear canal and cartilage of a harbour porpoise, at the level of the ventral curvature (UT1740_R0801). Scale bar 500 µm

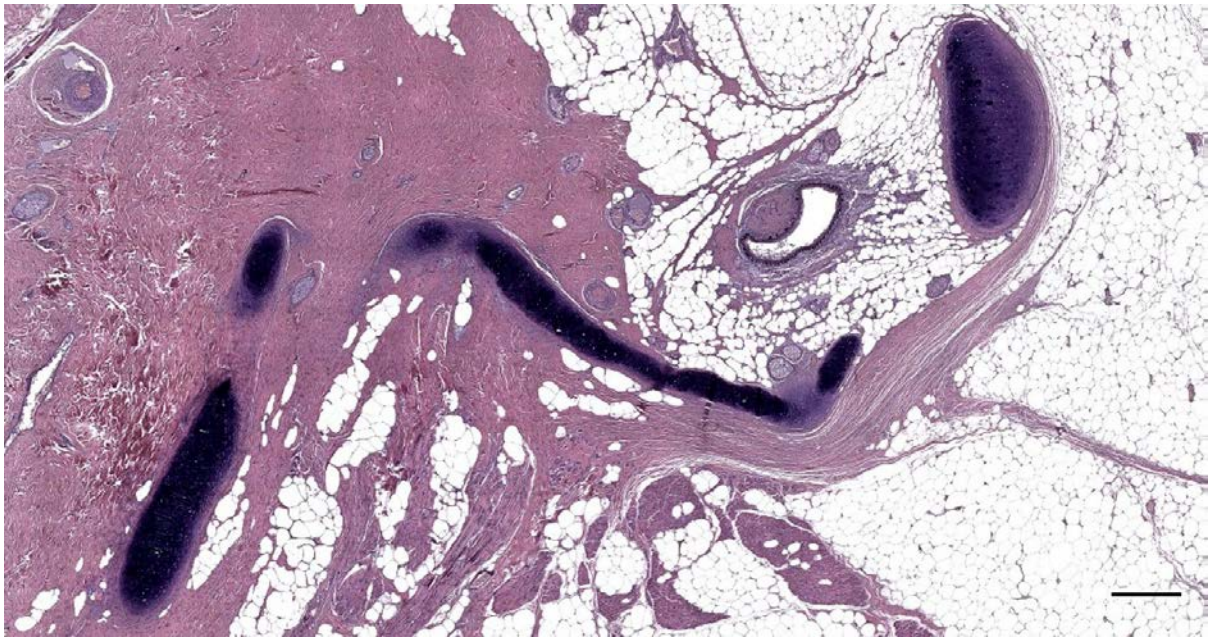

Figure 674. Histological image (HE staining) of a transverse section through the external ear canal in a harbour porpoise, at about 4 cm beneath the skin (UT1711_R1201). Scale bar 500 µm

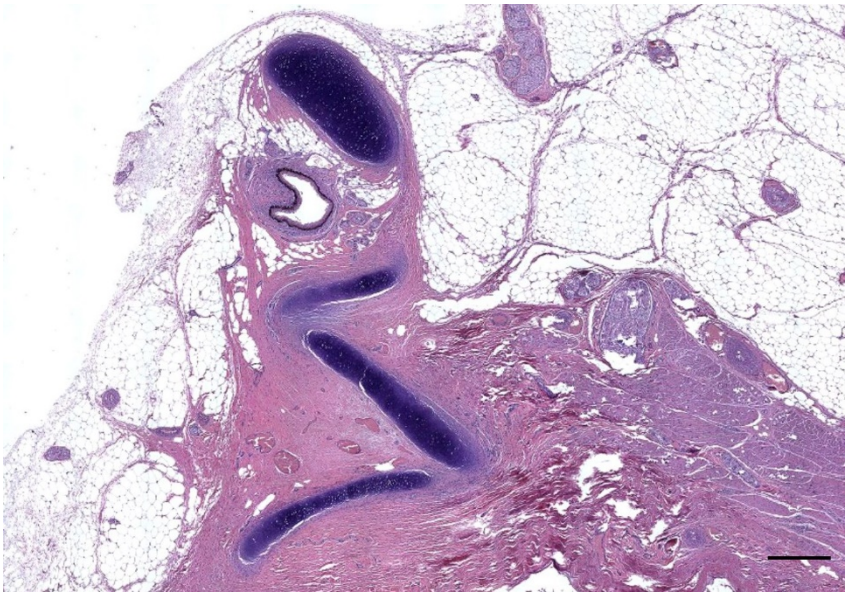

Figure 675. Histological image (HE staining) of a transverse section through the ear canal at the bottom of the ventral curvature in a harbour porpoise (UT1709) Bottom is lateral, Left is ventral. Muscles attaching to the cartilage in the curvature section of the canal. Scale bar 500 µm.

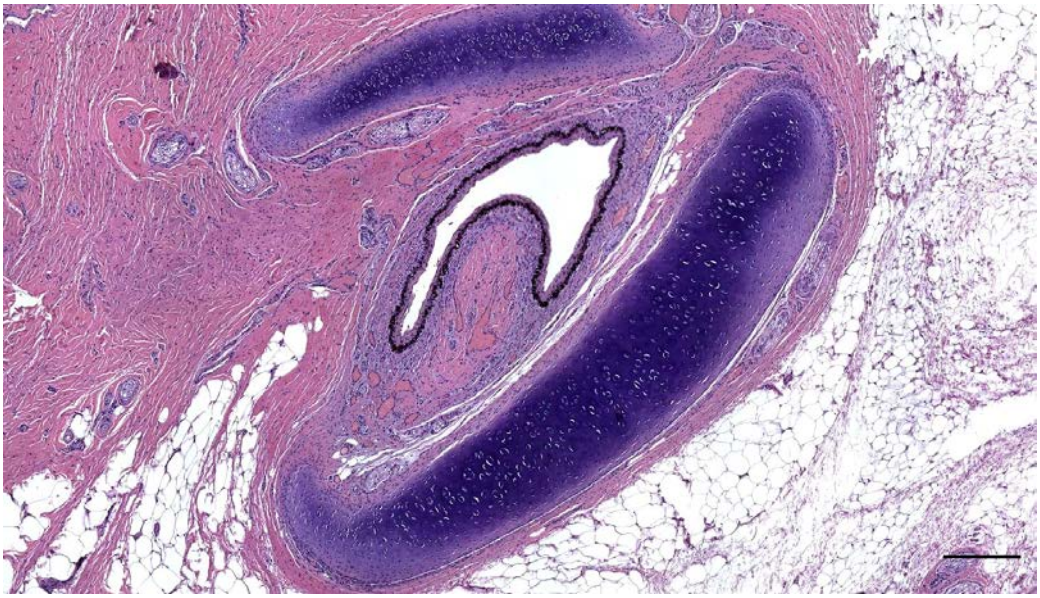

Figure 676. Histological image (HE staining) of a transverse section through the ear canal at the bottom of the ventral curvature in a harbour porpoise (UT1709_09). Scale bar 250 µm.

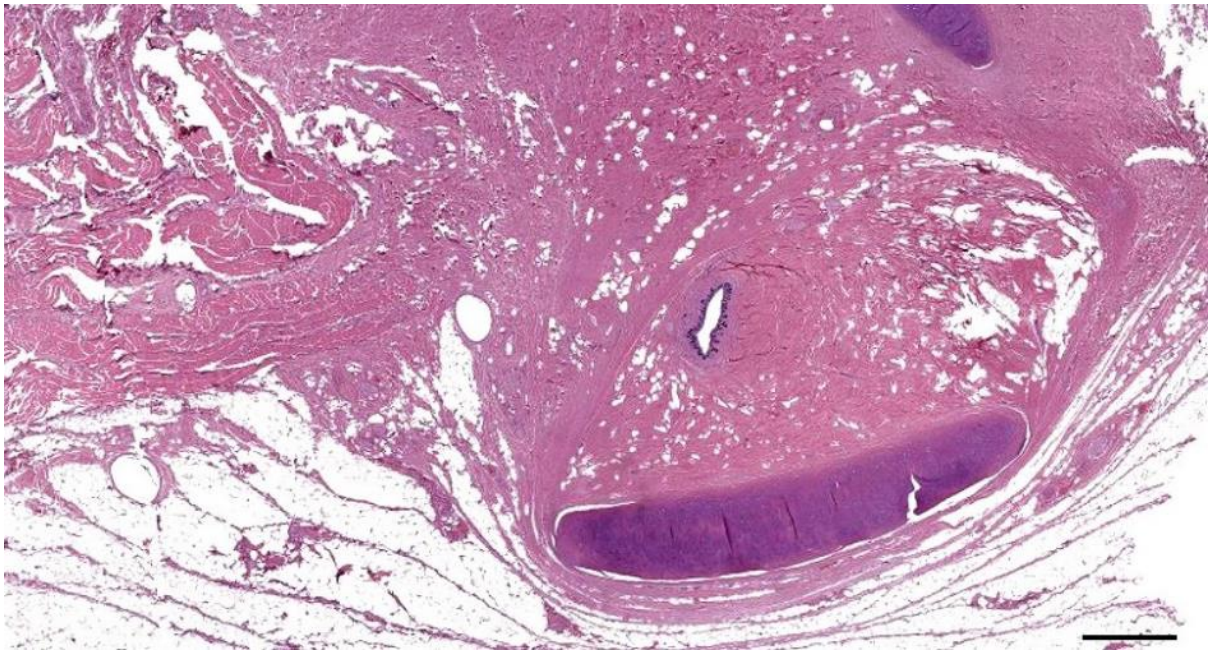

Figure 677. Histological cross-section (HE staining) of the left ear canal of a bottlenose dolphin at the level of the ventral curvature (ID444_L11). Scale bar 1 mm

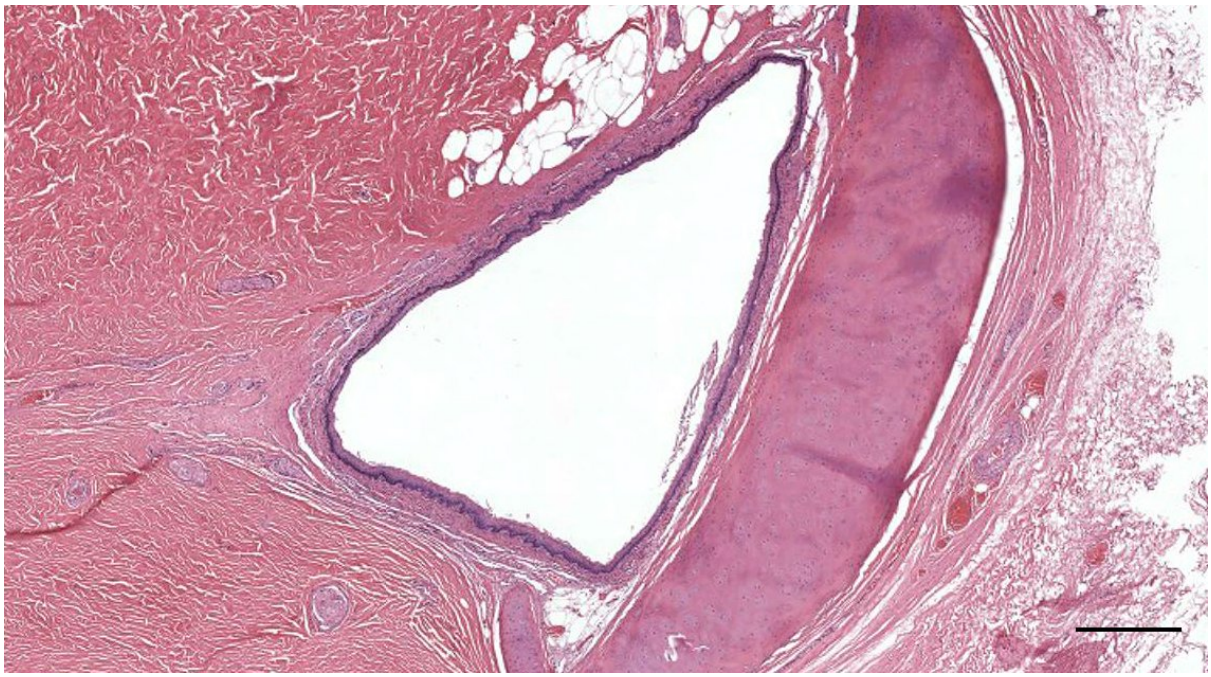

Figure 678. Histological image (HE staining) of the external ear canal and cartilage in a striped dolphin at about 3.5 cm beneath the skin (293_18_L7). Scale bar 0.5 mm

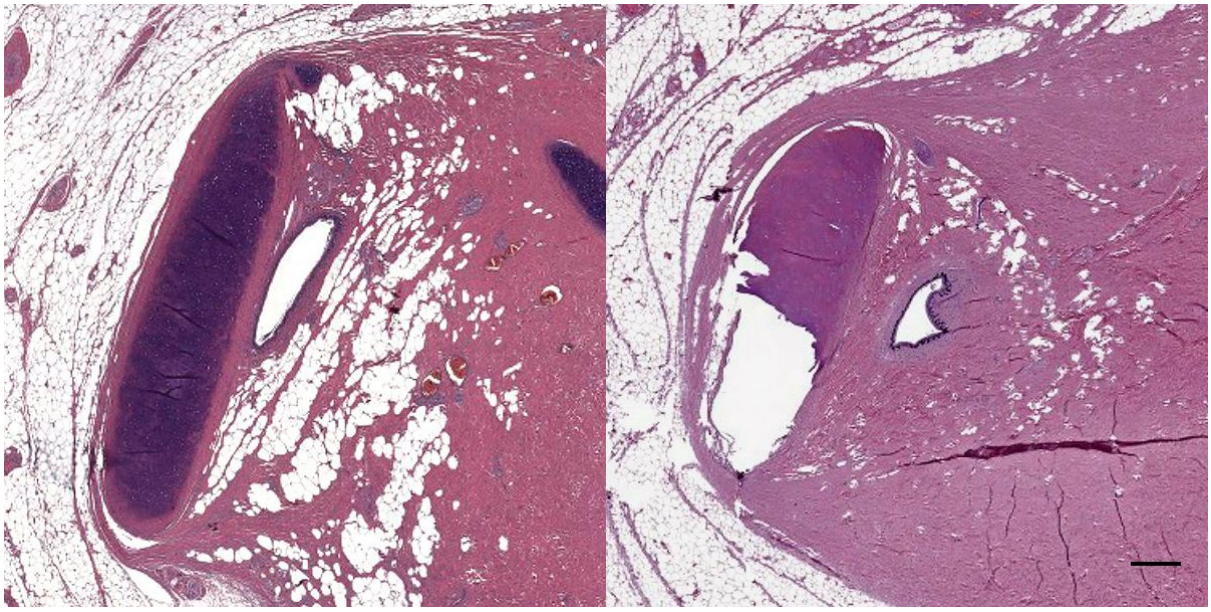

Figure 679. Histological images (HE staining) of the external ear canal and cartilage in a striped dolphin (127565_R7; Left) and bottlenose dolphin (444_R09; Right). Scale bar 500 µm

- *Vascular lacunae*

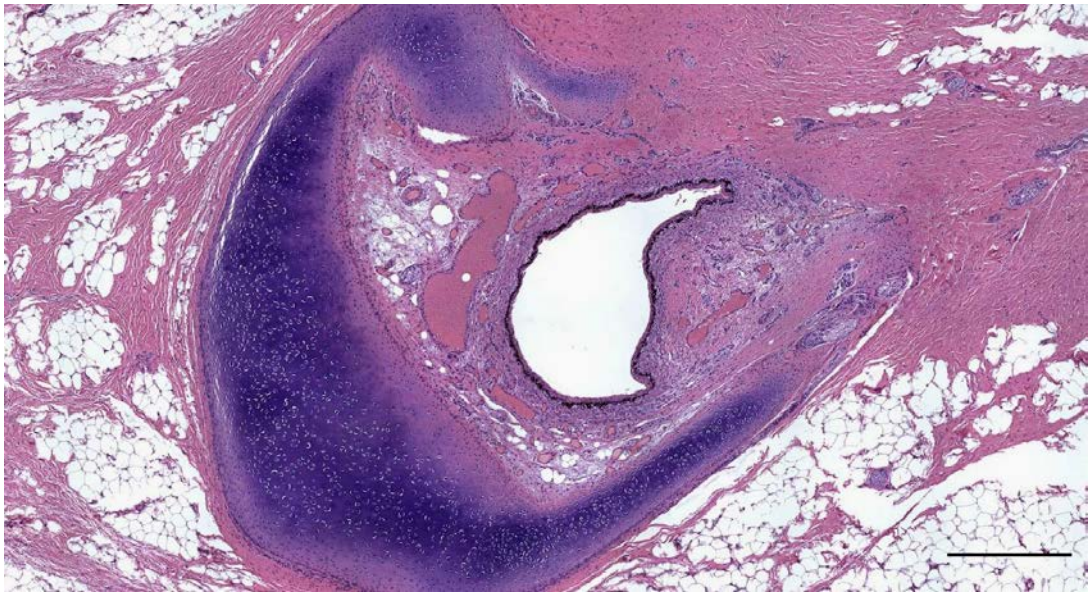

Figure 680. Histological image (HE staining) of a transverse section through the external ear canal of a harbour porpoise (UT1709) at about 4 cm beneath the skin. Note the cartilage and the vascular lacunae. Scale bar 500 µm.

3.2.3 Lymphoid tissue

3.2.3.1 At the level of the glands

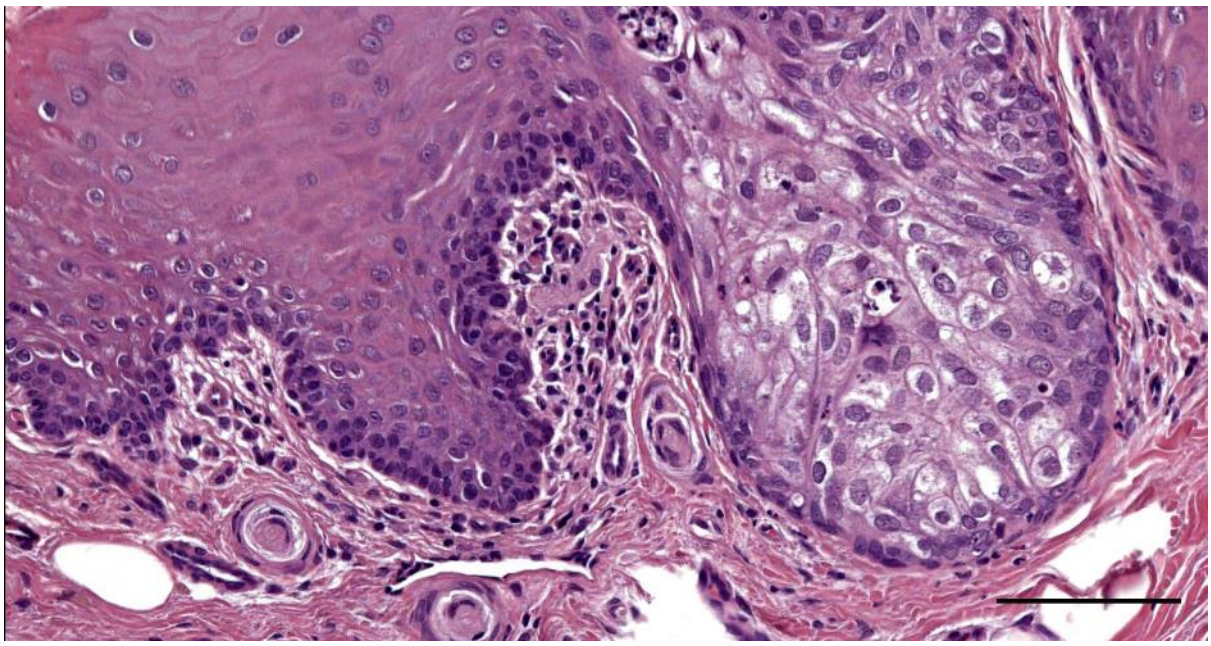

Figure Histological image (HE staining) of the mononuclear cells in the auricular subepithelial tissue in a striped dolphin (168_17_3). Note the lamellar corpuscles, and the glandular epithelium in continuation with the ear canal epithelium. Scale bar 100 µm

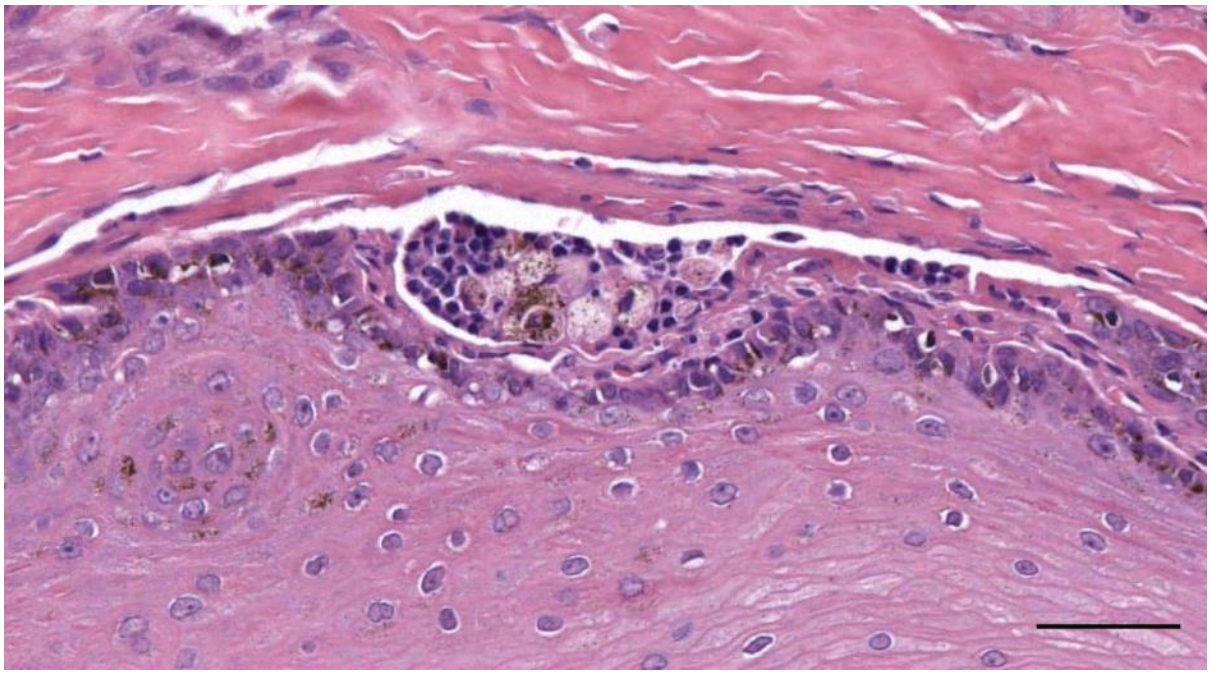

Figure 681. Detail of Figure 654 (169/17_R1). Mononuclear cells (mainly lymphocytes, and few plasmacells) immediately below the epithelium. Scale bar 50 µm

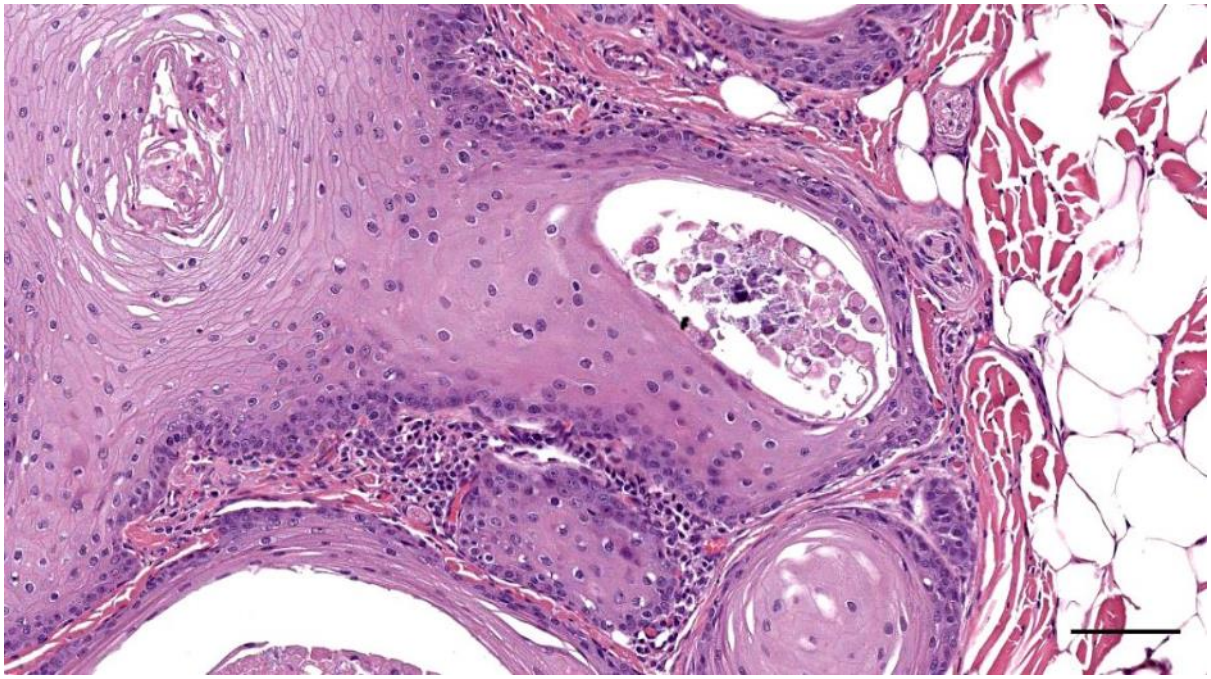

Figure 682. Detail of *Error! Reference source not found.* ***(169/17_R2). Mononuclear cells in the subepithelial tissue situated between the ear canal and glandular structures. Scale bar 100 µm***

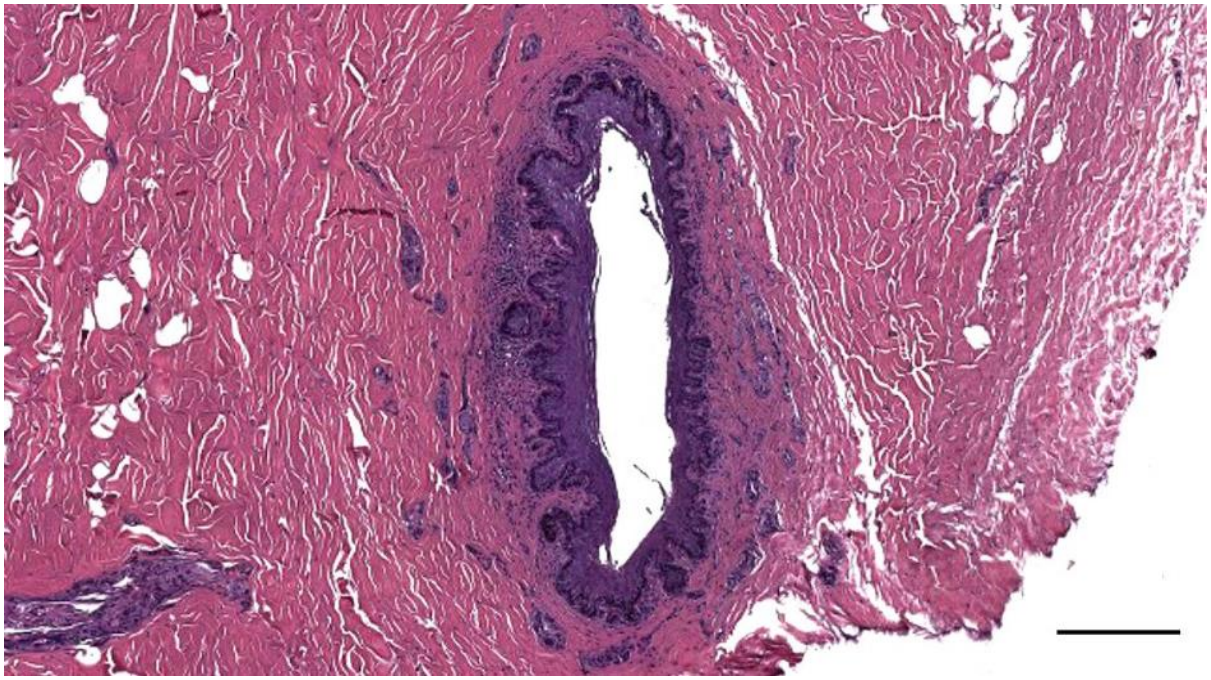

Figure 683. Histological cross-section (HE staining) of the ear canal with mononuclear infiltration in a bottlenose dolphin, at about 3 cm beneath the skin (457_R7). Scale bar 250 µm

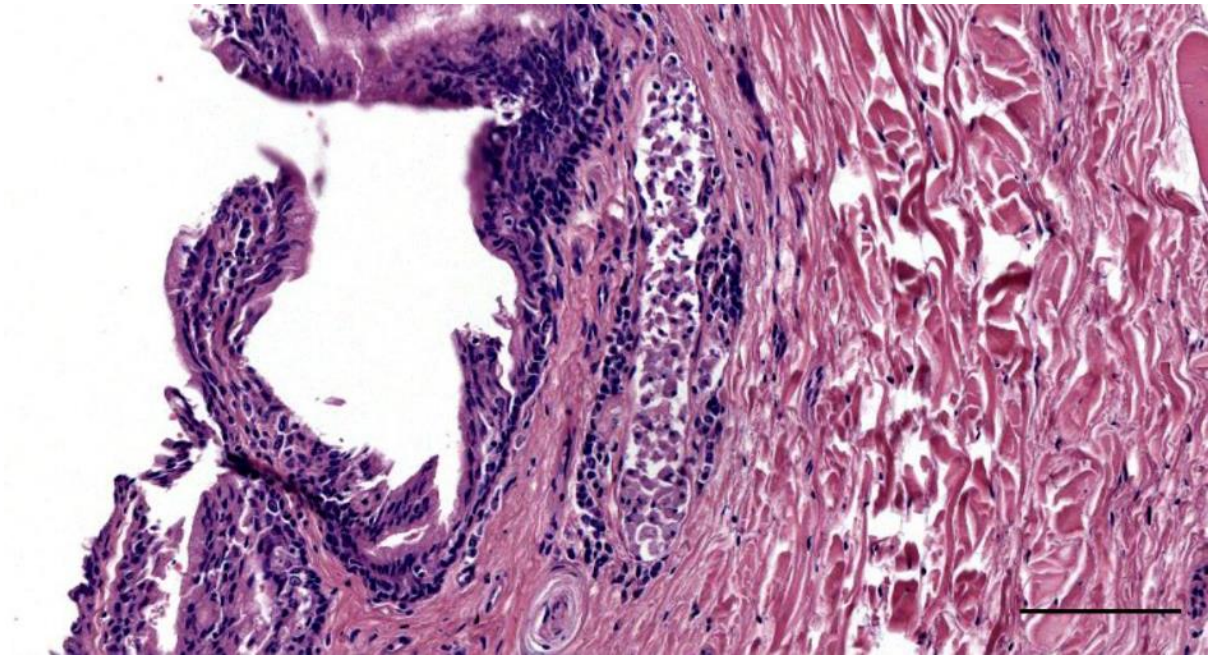

Figure 684. Histological detail (HE staining) of the ear canal and glands in a bottlenose dolphin (444_L6). Note the glands/glandular epithelium and mononuclear cells in the subepithelial tissue and around the glands. Scale bar 100 µm

3.2.3.2 Between ear canal and cartilage

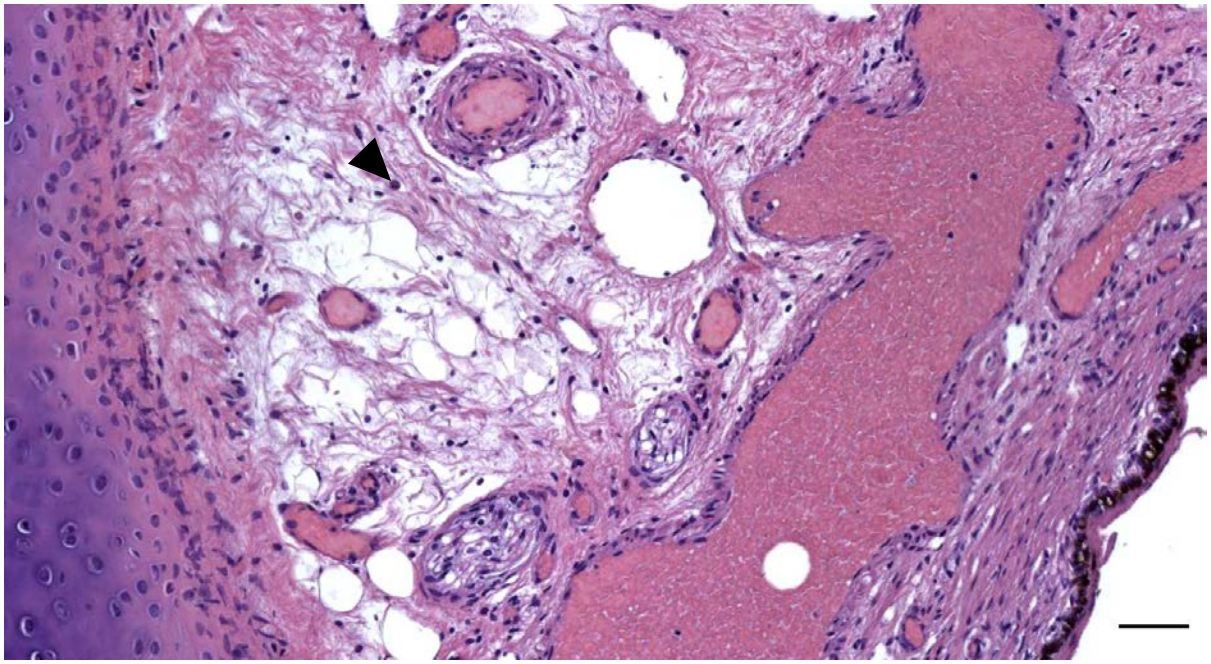

Figure 685. Detail of Figure 680. Histological image (HE staining) of a transverse section through the external ear canal of a harbour porpoise (UT1709) at about 4 cm beneath the skin. There are scant mononuclear cells in the loose connective tissue between ear canal and cartilage. The cellular composition consists mainly of lymphocytes with few macrophages (arrowhead). Scale bar 50 µm

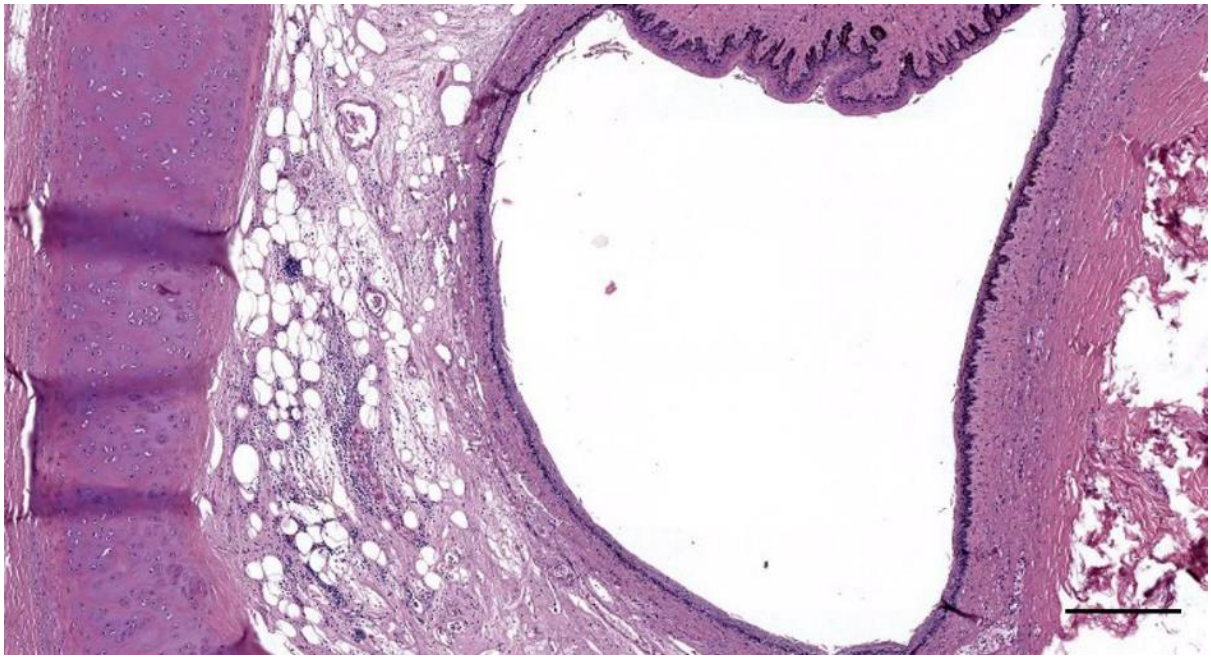

Figure 686. Histological detail (HE staining) of the left ear canal of a bottlenose dolphin, with a mononuclear infiltrate between ear canal and cartilage, in a bottlenose dolphin ear canal (444_L18). Scale bar 300 µm

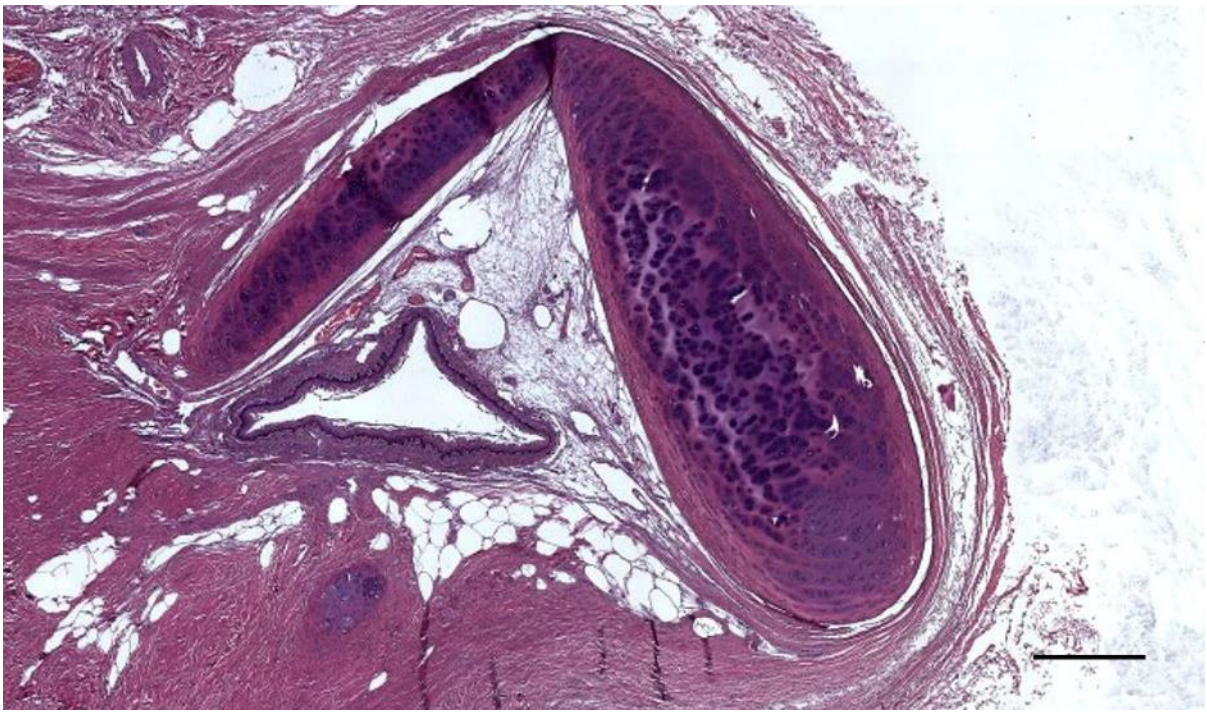

Figure 687. (77/18_R12). Scale bar 0.5 mm

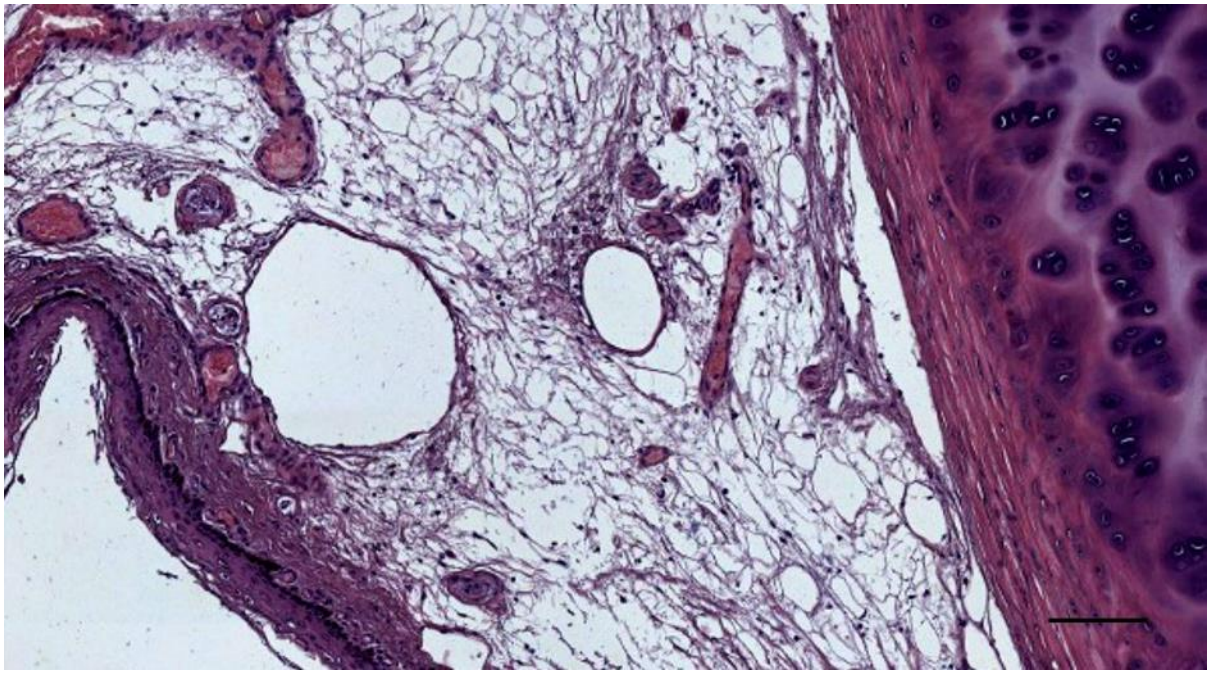

Figure 688. (77/18_R12) Detail of Figure 687. Mononuclear cells situated between ear canal and cartilage. Scale bar 100 µm

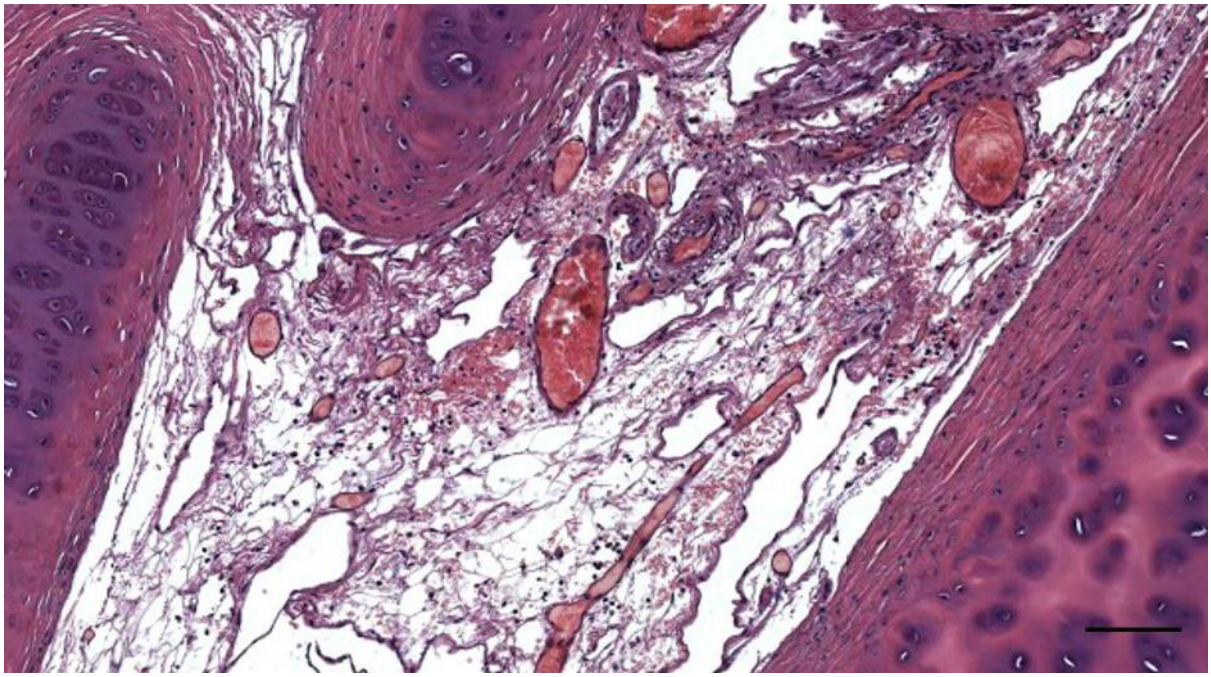

Figure 689. (292/18_L11) Mononuclear cells (lymphocytes) between ear canal and cartilage, situated in the reticular connective tissue network with vascular lacunae. Scale bar 100 µm

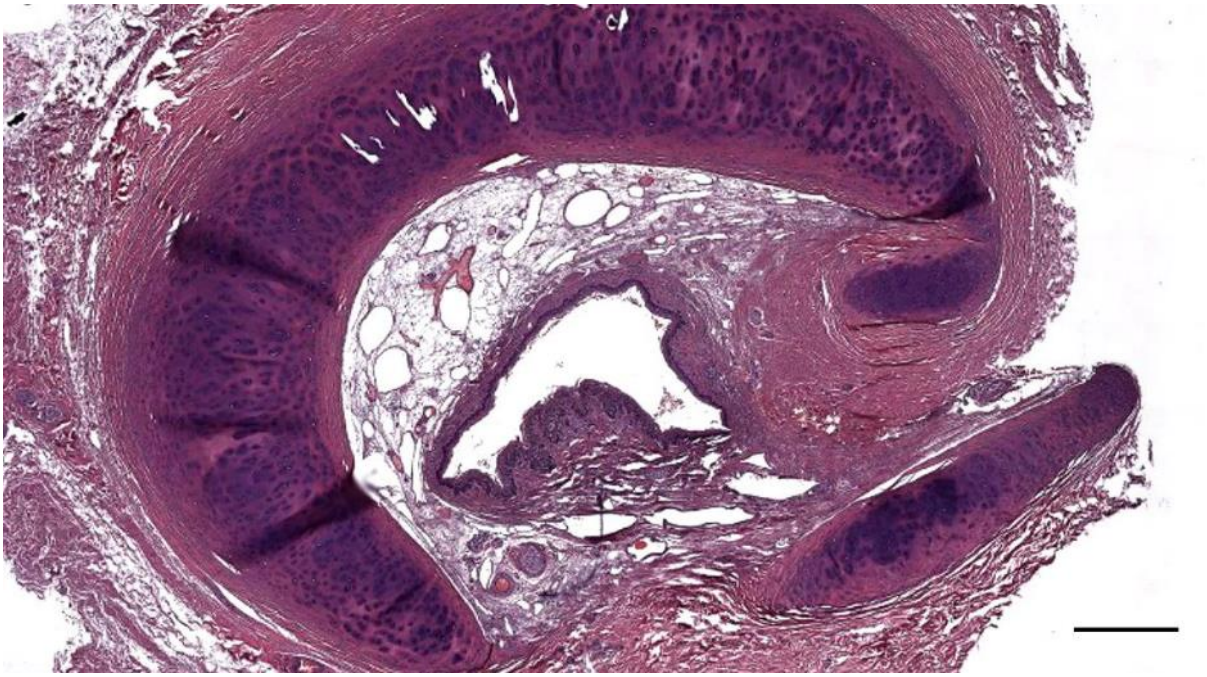

Figure 690. (292/18_L12) Overview of the ear canal with nervous tissue ridge and cartilage medial to the curvature of the canal. Scale bar 100 µm

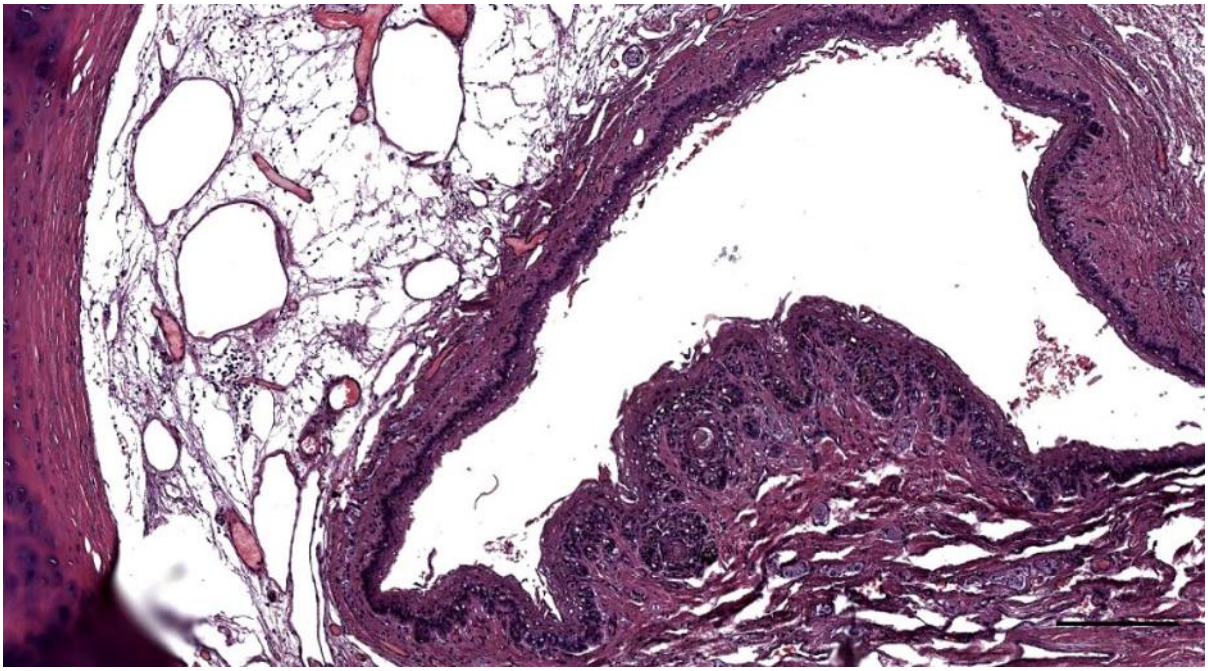

Figure 691. (292/18_L11) Mononuclear cells (lymphocytes) between ear canal and cartilage, situated in the reticular connective tissue network with vascular lacunae. Note the nervous tissue ridge bulging into the ear canal lumen. Scale bar 200 µm

3.2.3.3 Nodular tissue

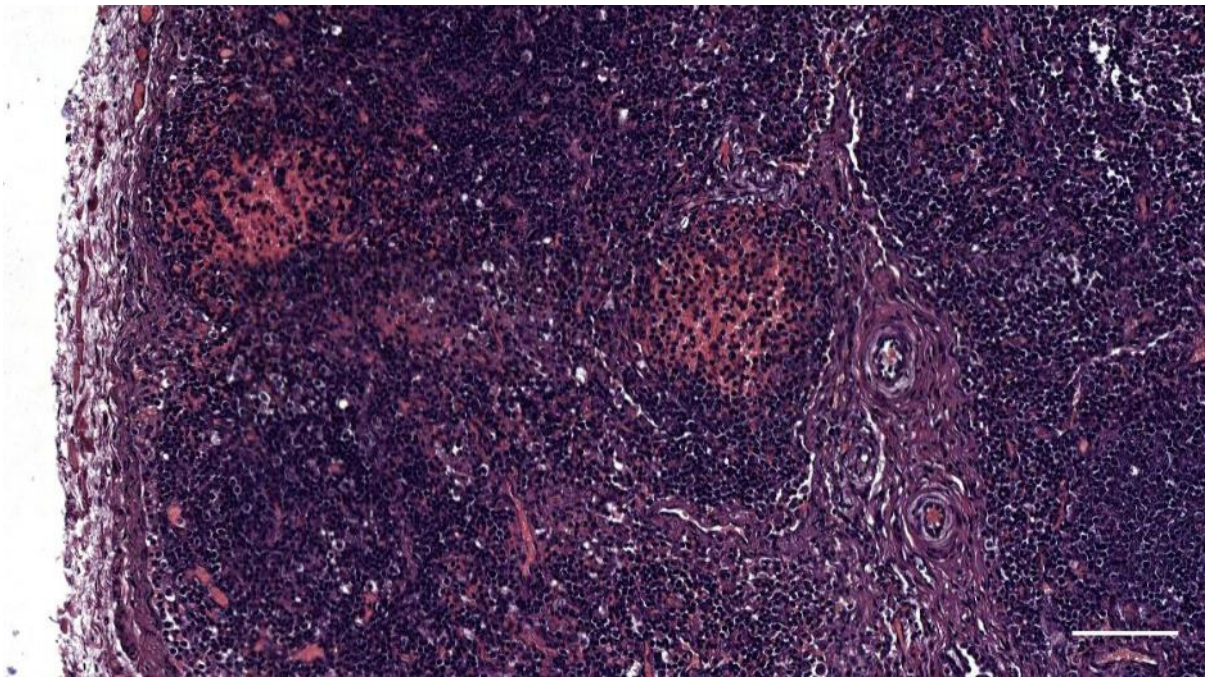

Figure 692. (ID449) Stenella coeruleoalba. (449_R8) Detail of *Error! Reference source not found.* ***. Lymphoid tissue. Scale bar 100 µm***

3.2.4 Medial end of the external ear canal

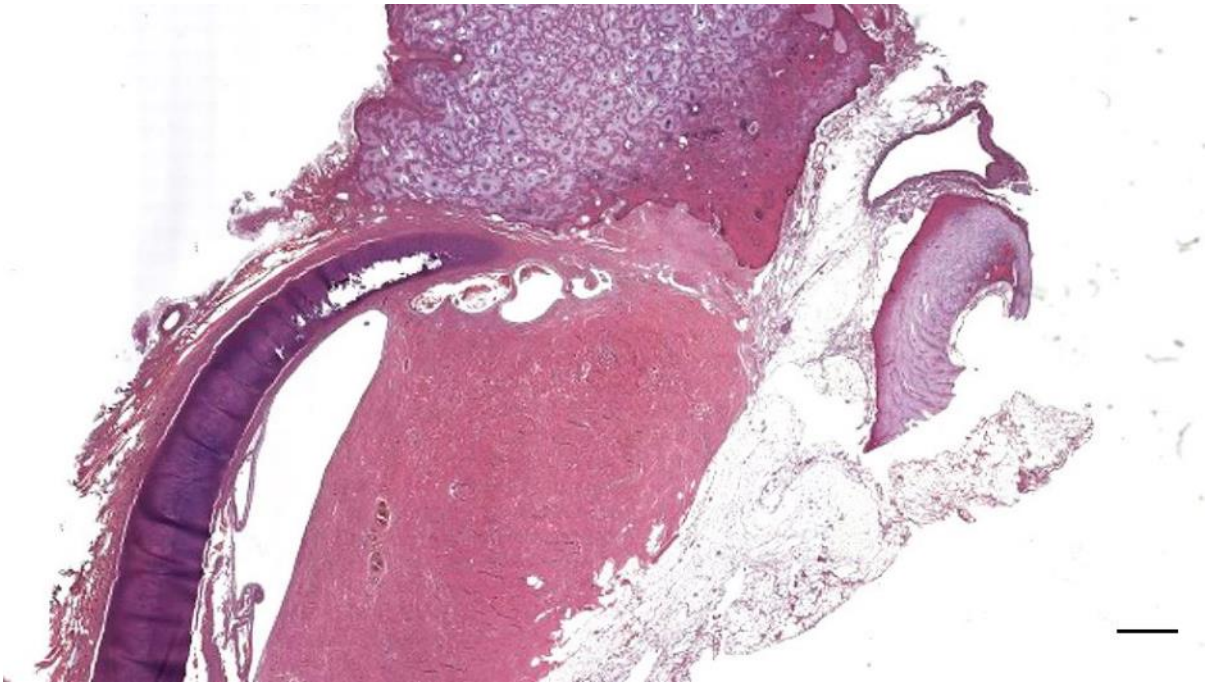

Figure 693. HE section of the right ear canal (1) entering the TP complex. Scale bar 0.5 mm

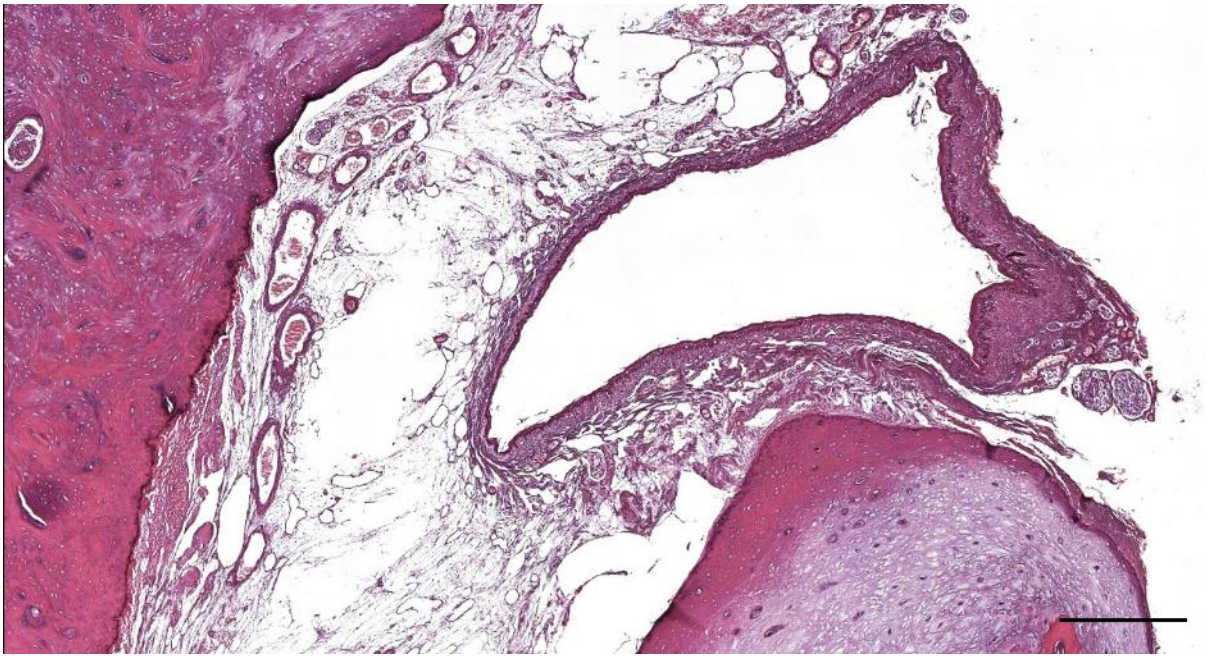

Figure 694. Detail of Figure 693. HE section of the right ear canal (1) entering the TP complex. Scale bar 0.5 mm

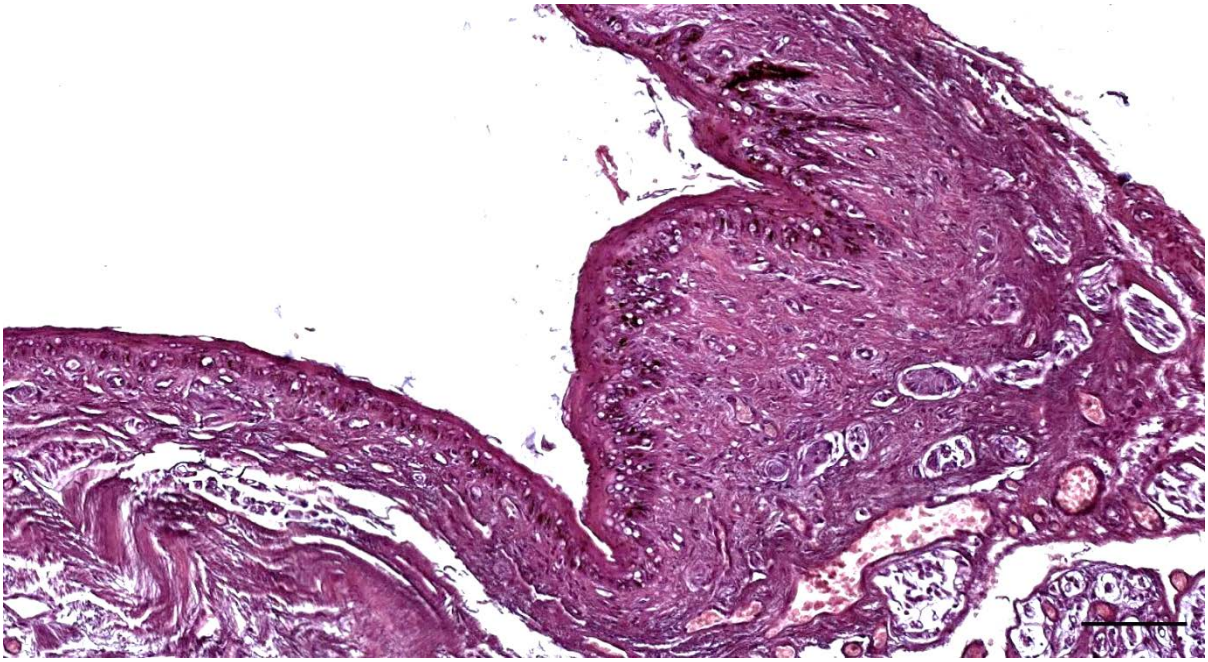

Figure 695. Detail of Figure 693. Note the tissue bulge with many corpuscles and small nerve fibres projecting into the canal lumen. Scale bar 100 µm

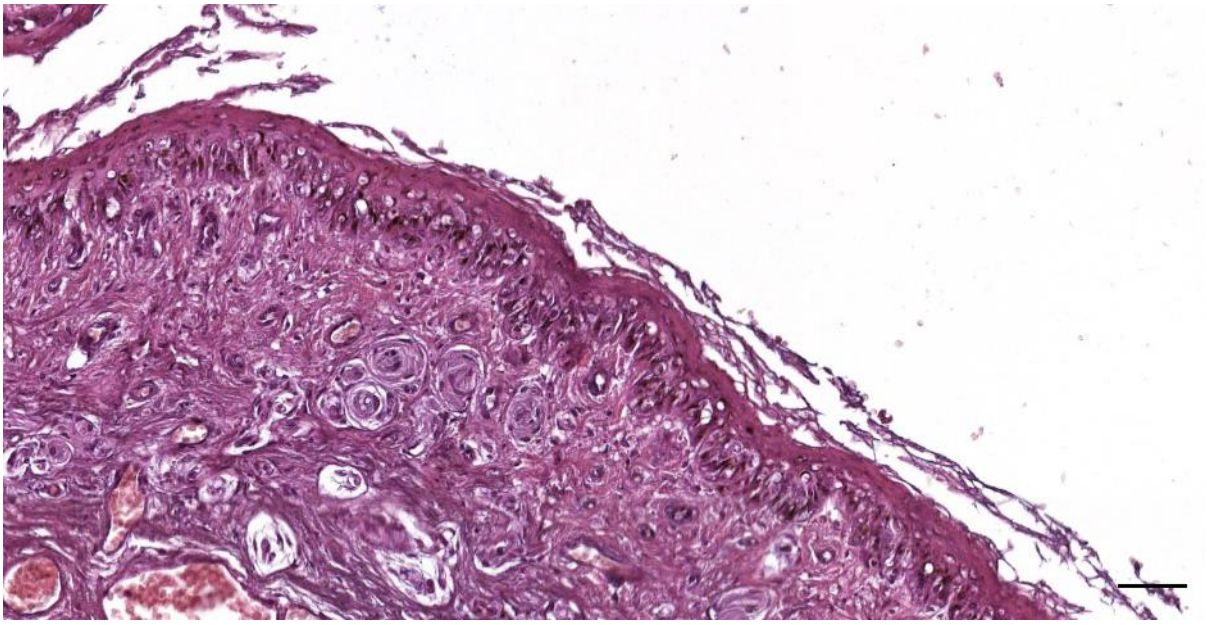

Figure 696. Histological image (HE stain) showing the dense subepithelial innervation with small nerves and lamellar corpuscles. Scale bar 50 µm

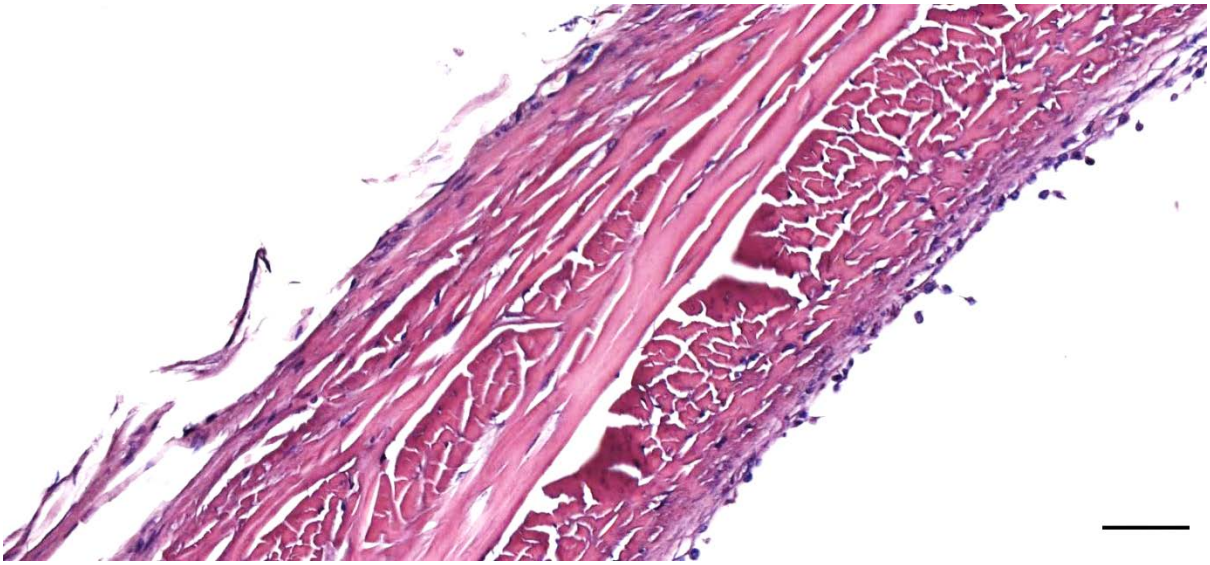

Figure 697. Histological image (HE stain) of the tympanic membrane. Scale bar 50 µm

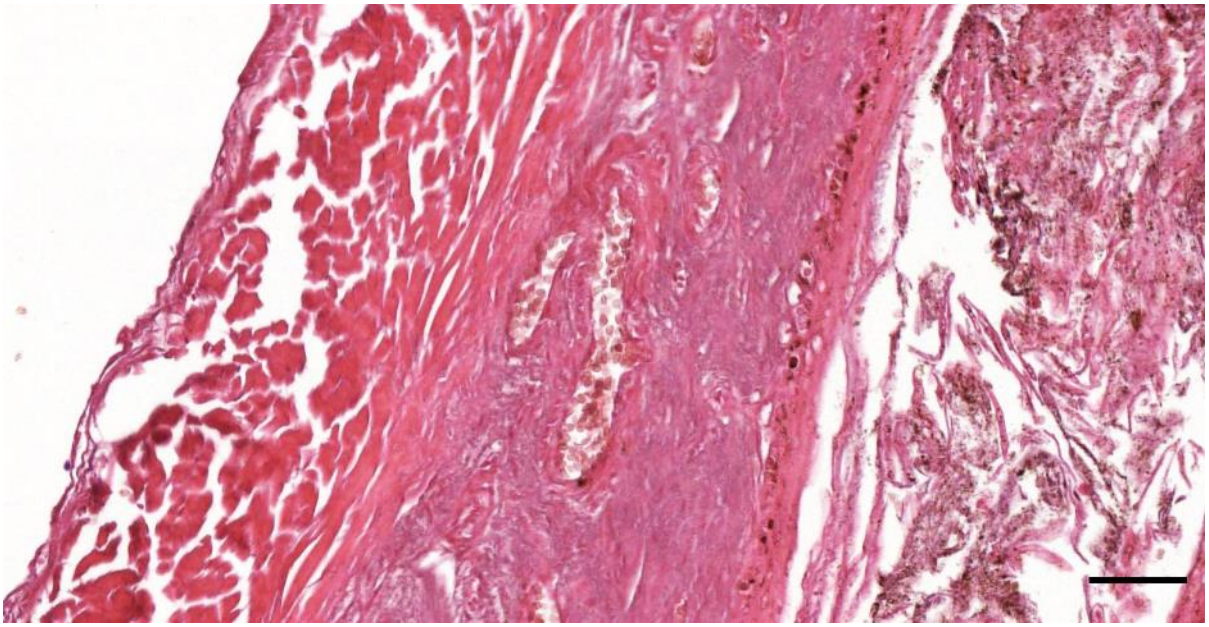

Figure 698. Histological detail image (HE stain) of the tympanic membrane in the centre with the ear canal with cellular content on the right and tympanic cavity on the left. Scale bar 50 µm

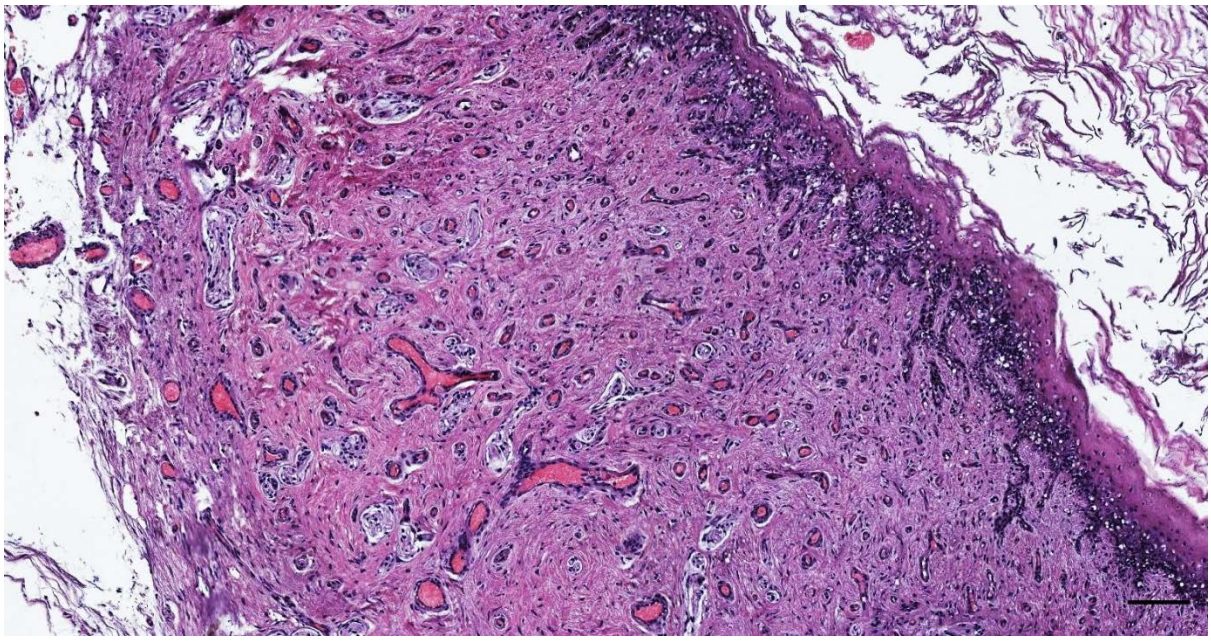

Figure 699. HE staining of the nervous tissue ridge. Scale bar 100 µm.

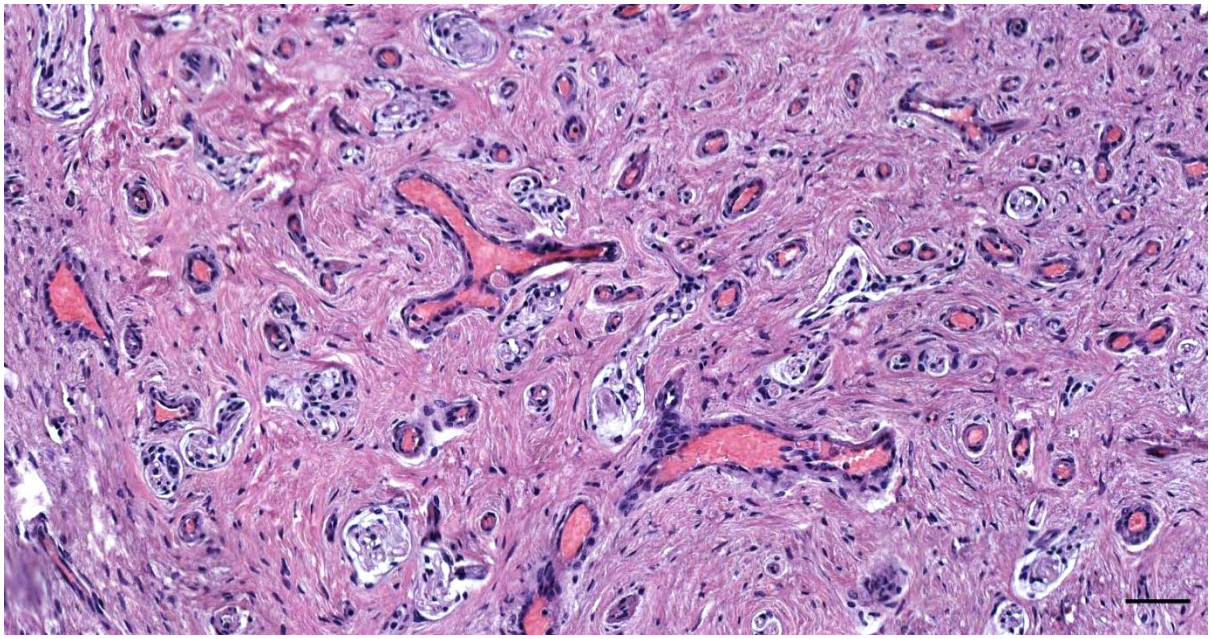

Figure 700. HE staining of the nervous tissue ridge. Scale bar 50 µm.

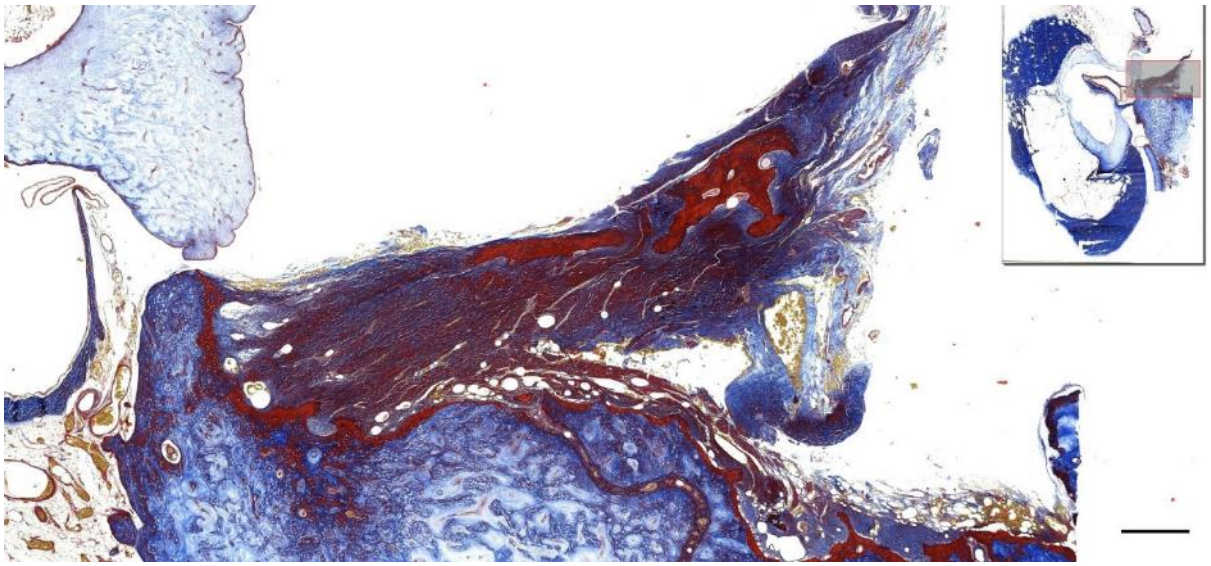

Figure 701. Detail of the suspension ligament attaching to the posterior process of the tympanic (insert). Scale bar 0.5 mm. These ligaments connect the TP complex to the bones of the skull, and keep the former suspended in the peribullar sinus. This allows for the TP complex to be acoustically isolated from the other bones (Reysenbach De Haan, 1957; Ketten and Wartzok, 1990; Cranford et al., 2008).

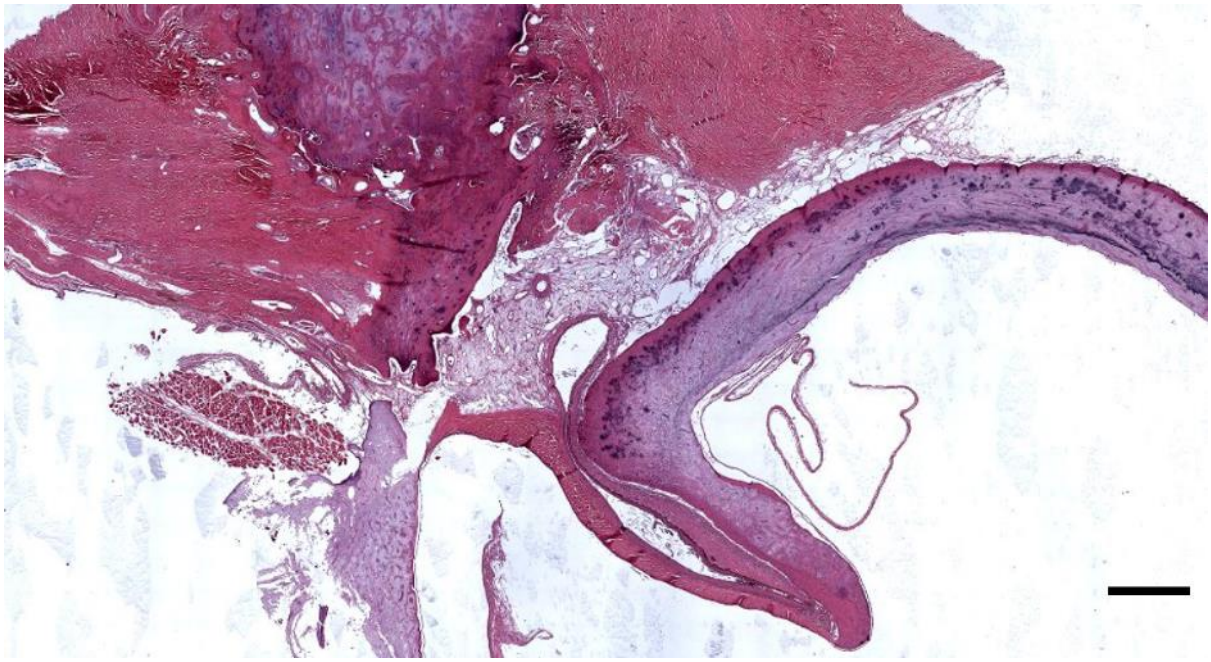

Figure 702. Histological image (HE stain) of the ear canal turning around the sigmoid process. Also note the tympanic membrane (509_17_Lx2). Scale bar 1 mm

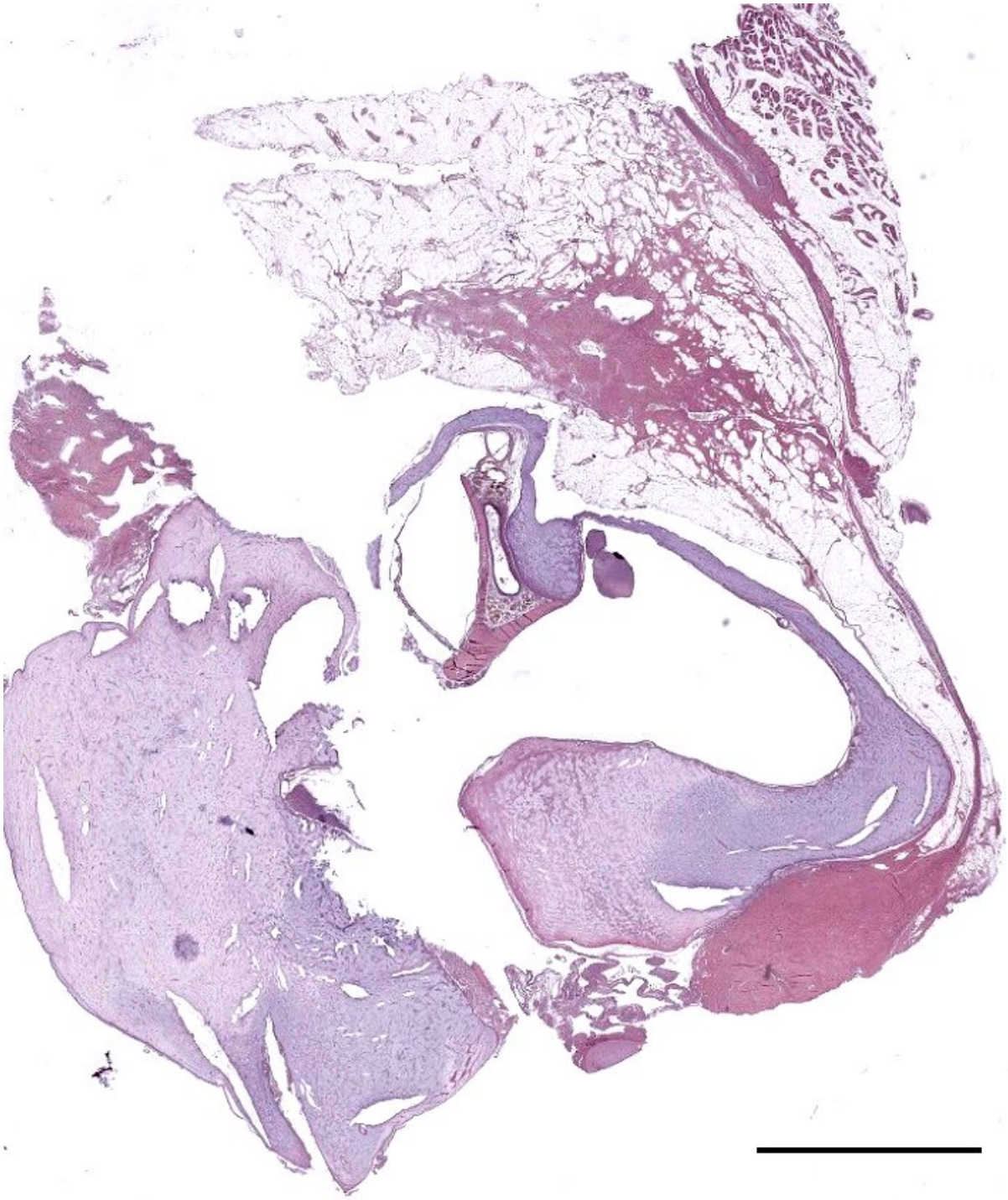

Figure 703. HE stained decalcified section of the medial end of the ear canal with tympanic membrane and part of tympanic conus in a harbour porpoise (UT1692_Rx4). Scale bar 5 mm

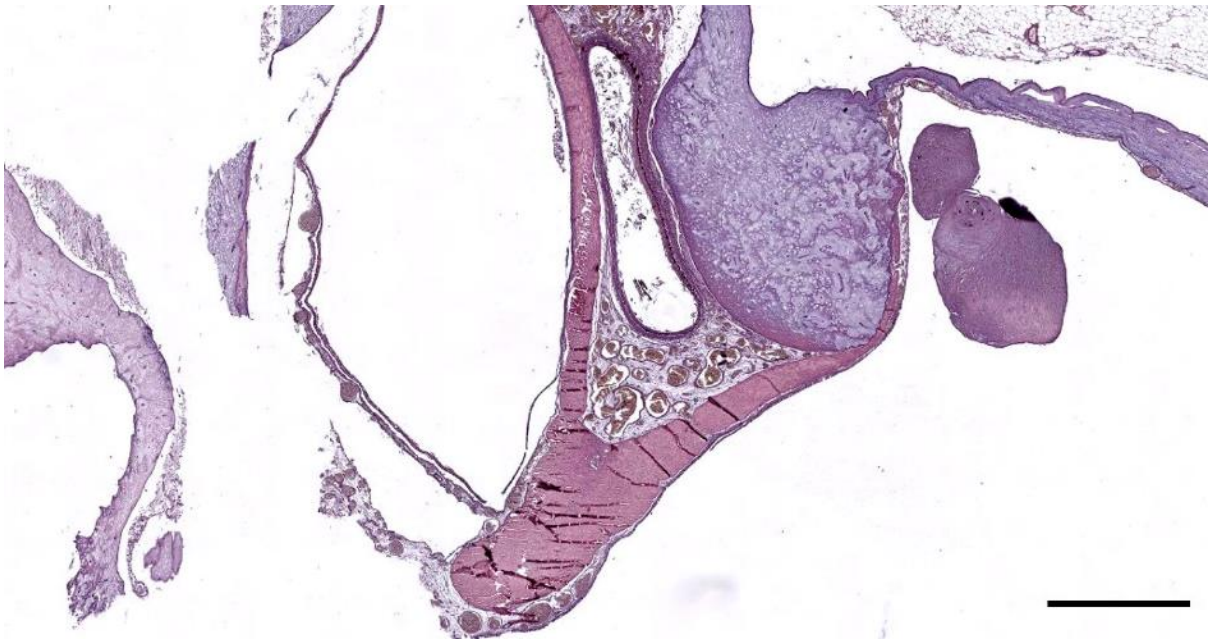

Figure 704. Detail of Figure 703 ear canal and tympanic conus.Scale bar 1 mm

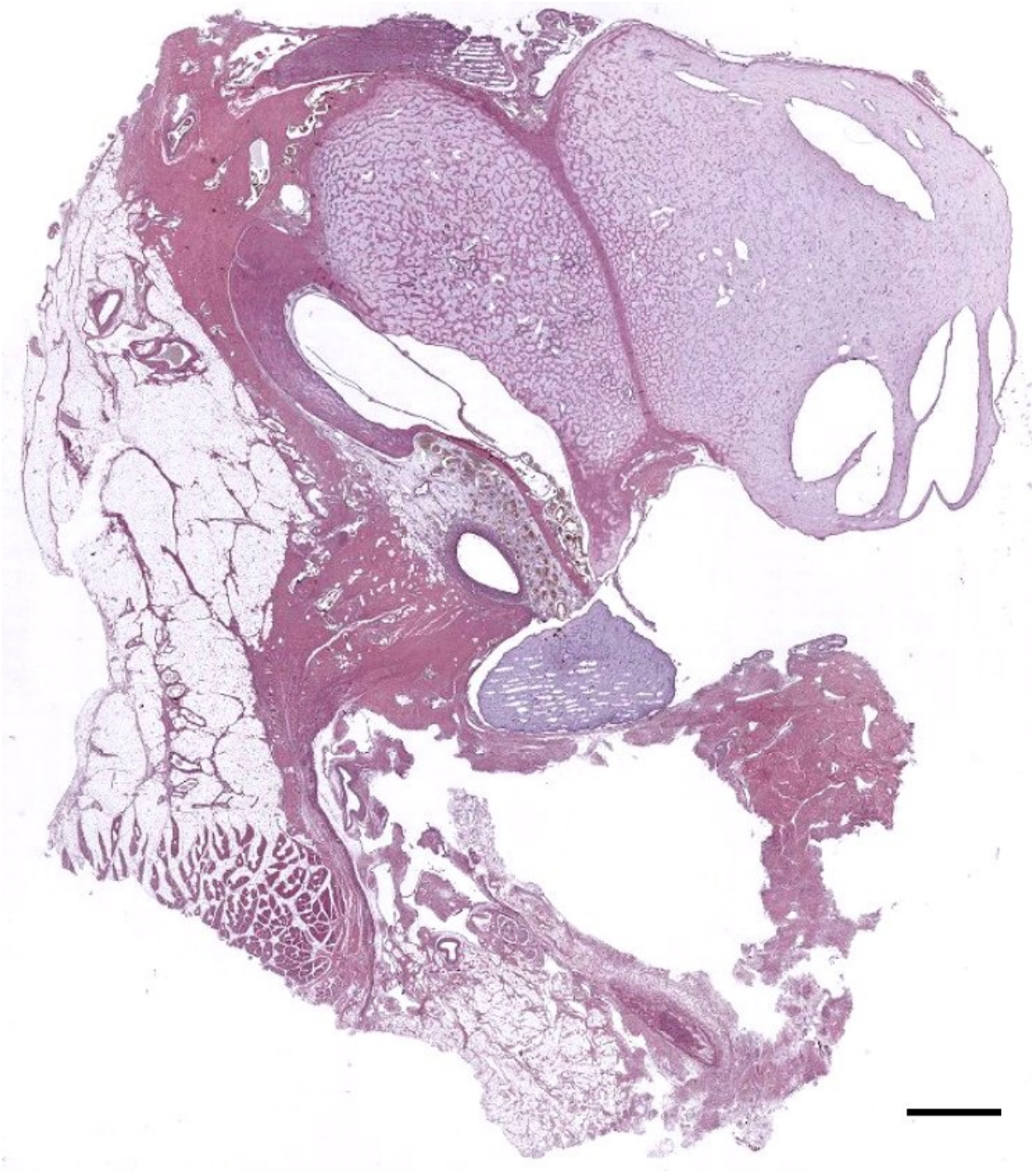

Figure 705. HE stained decalcified section of the medial end of the ear canal on enterin the TP complex. Scale bar 1mm

3.2.5 *Mononuclear infiltrate*

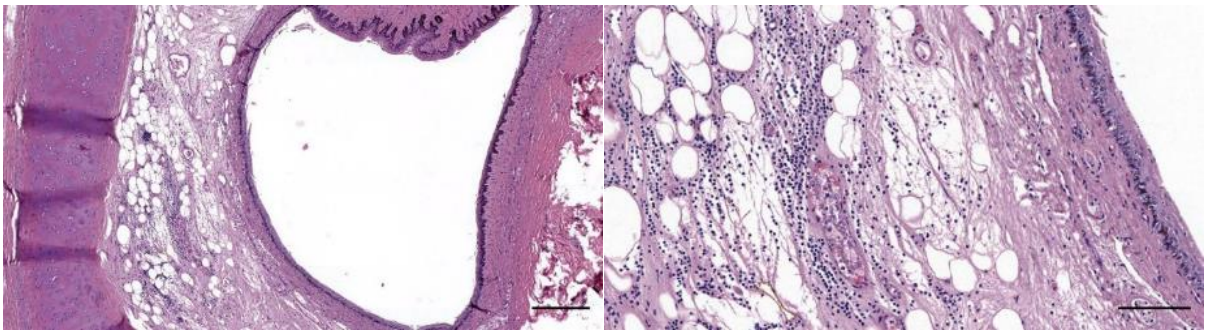

Figure 706. Histological cross-section (HE staining) of the left ear canal of a bottlenose dolphin, close to the middle ear (ID444_L18). There is a mononuclear infiltrate between the ear canal and cartilage. Scale bar left 300 µm, and right 100 µm

3.2.6 *Nodular lymphoid tissue*

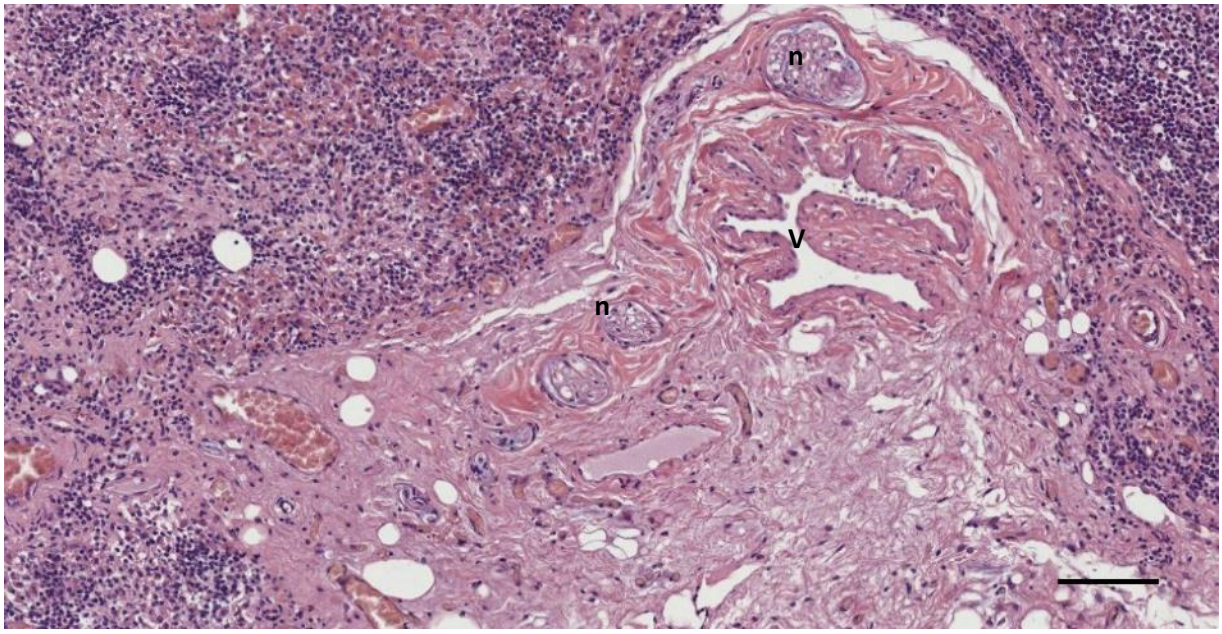

Figure 707. (274/18_R9) Stroma surrounding the lymphoid tissue. n: nerves; v: a vascular structure with red blood cells and lymphocytes in the lumen; all are embedded in loose connective tissue and scant adipocytes. Scale bar 100 µm

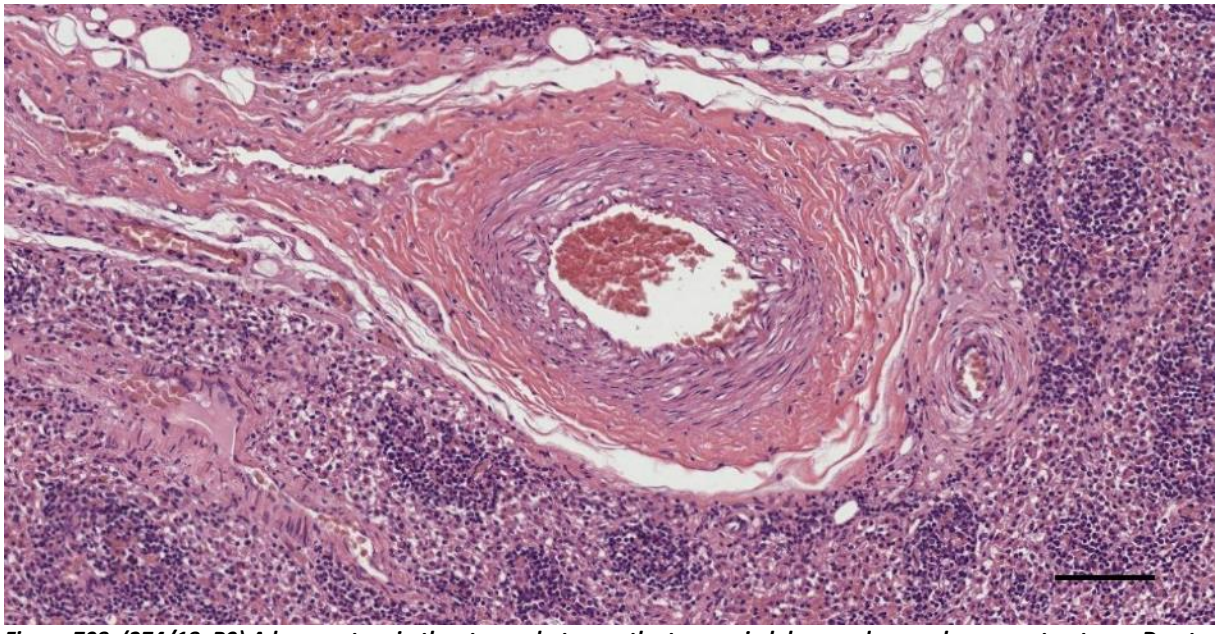

Figure 708. (274/18_R9) A large artery in the stroma between the two main lobes, and several venous structures. Due to its location and size, this could be the main artery supplying the lymphoid tissue. Scale bar 100 µm

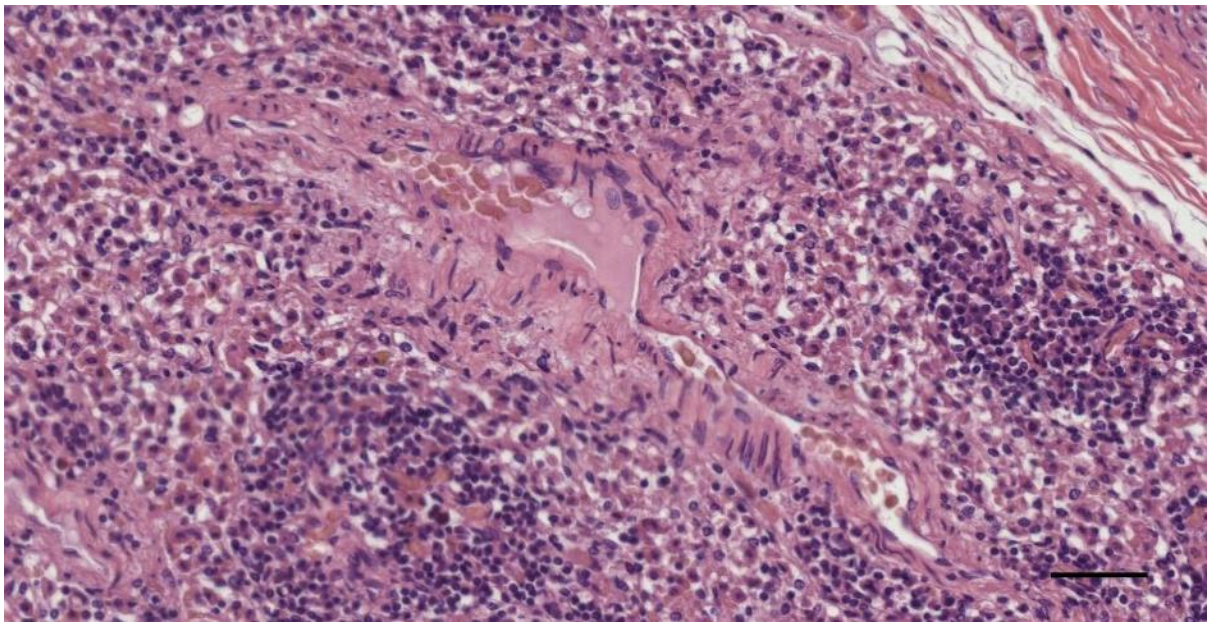

Figure 709. (274/18_R9) Endothelial lined structure with red blood cells and plasma. Scale bar 50 µm

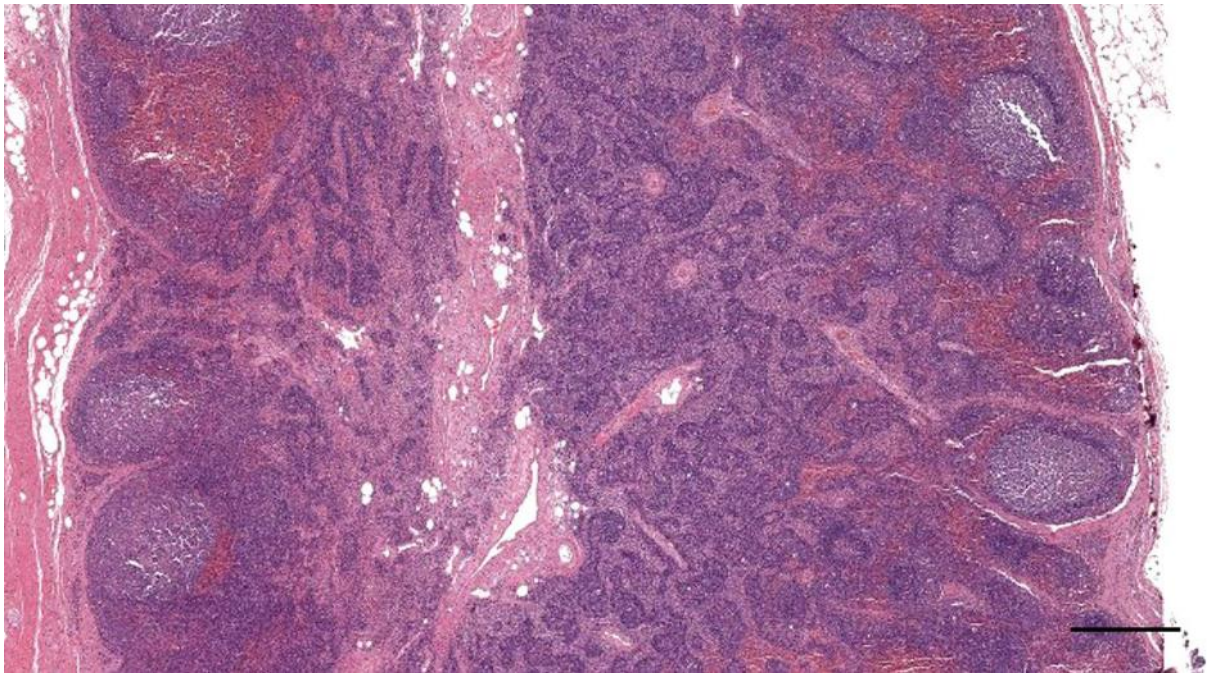

Figure 710. (274/18_L9) Detail of lymphoid tissue with septum. Scale bar 0.5 mm

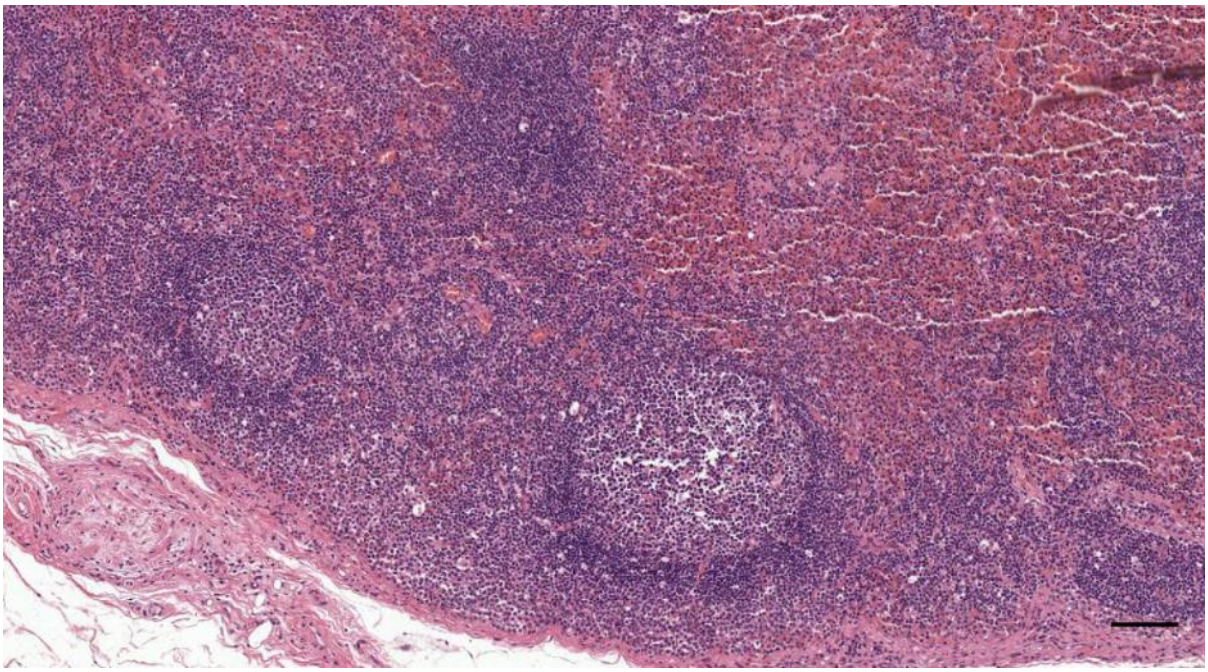

Figure 711. (274/18_L9) Detail of lymphoid tissue. Scale bar 100 µm

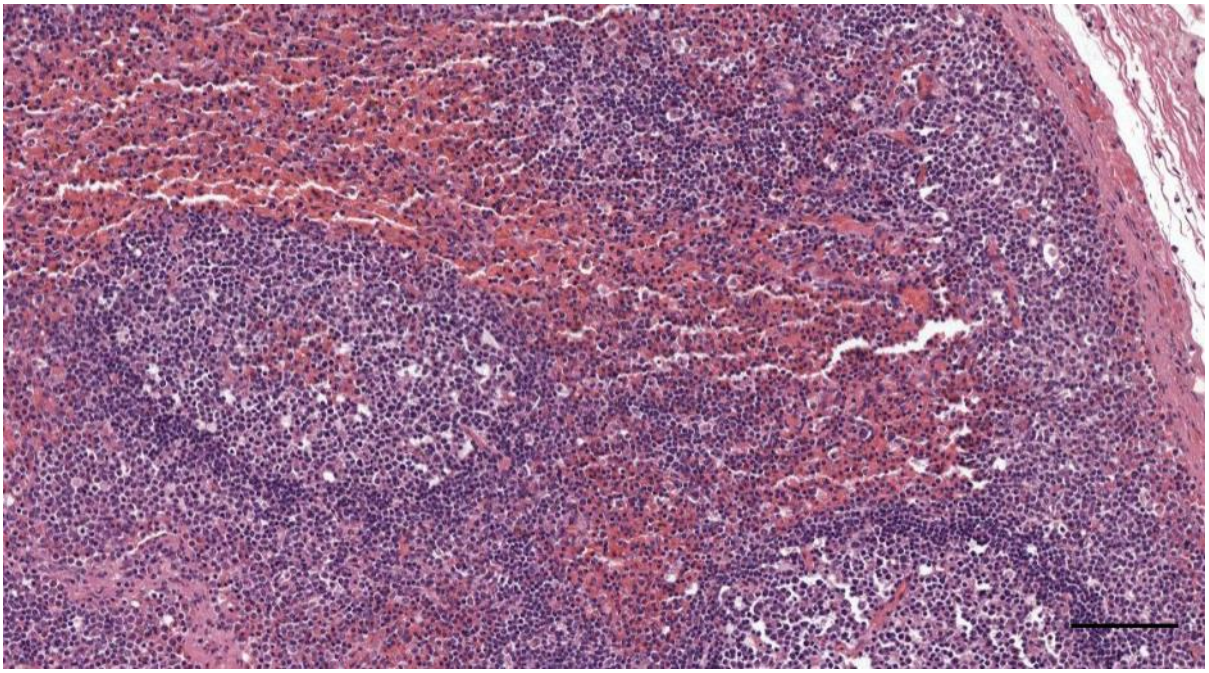

Figure 712. (274/18_L9) Detail of lymphoid tissue. Scale bar 100 µm

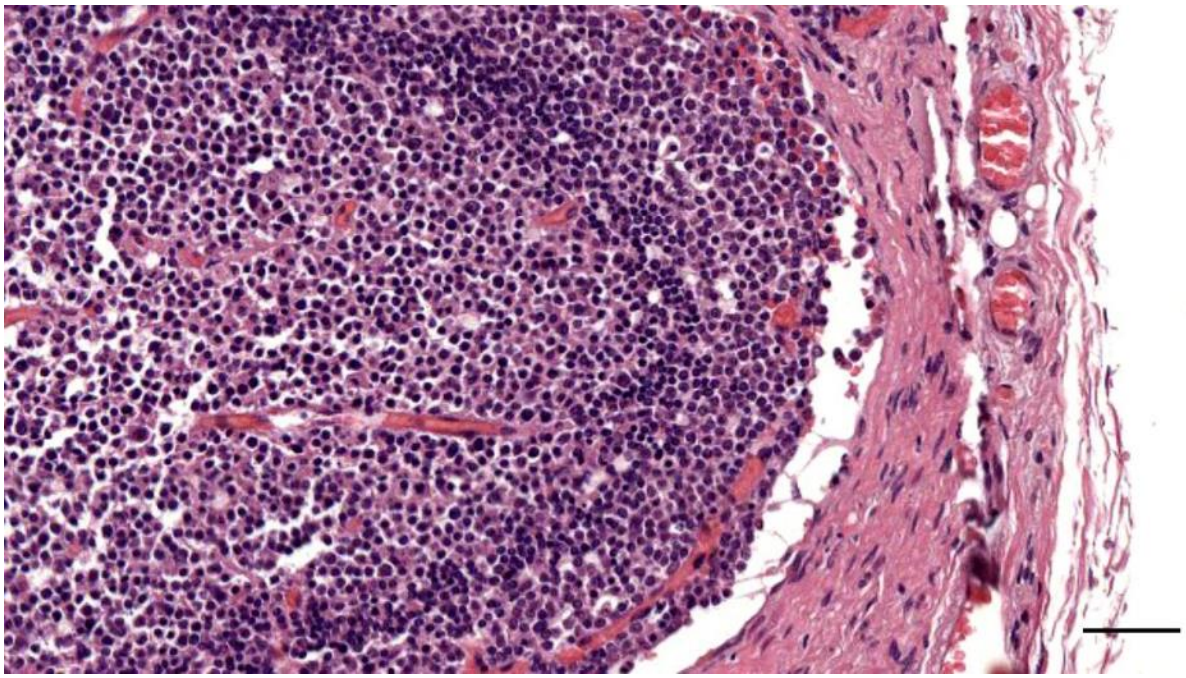

Figure 713. (274/18_L9) Detail of lymphoid tissue. Scale bar 50 µm

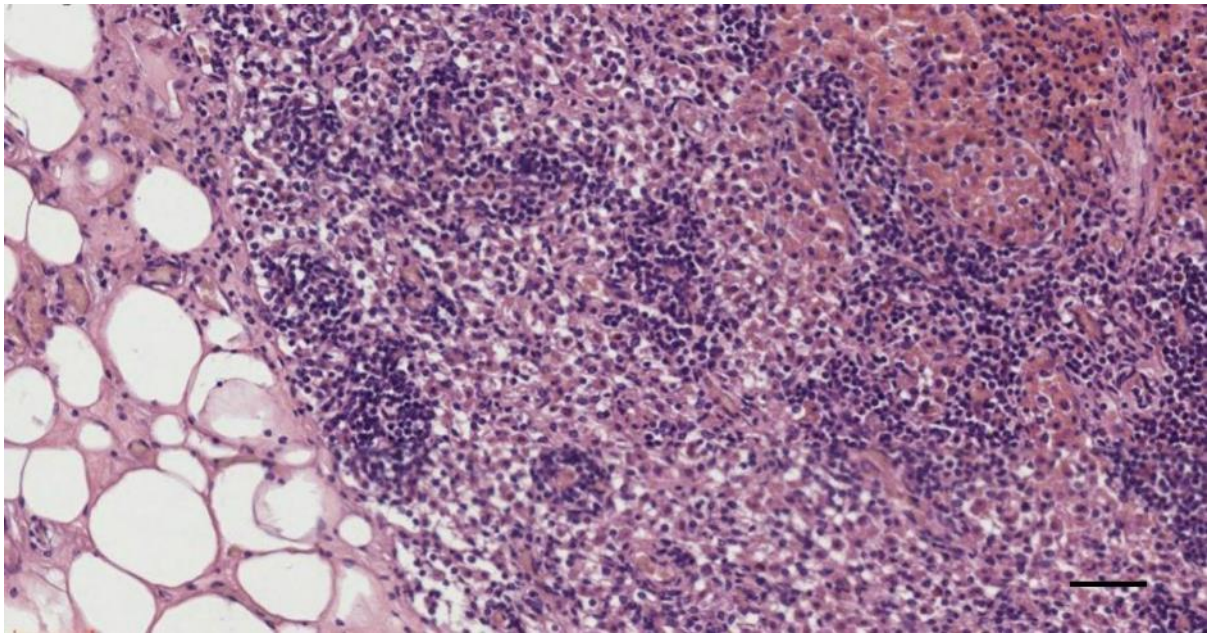

Figure 714. (274/18_R9) Edge of the lymphoid tissue, with from left to right, adipose tissue in direct contact with the lymphoid tissue; parafollicular tissue with patched concentrations of lymphocytes and dispersed erythrocytes; and deeper, more parafollicular tissue but with the intense presence of erythrocytes. Scale bar 50 µm

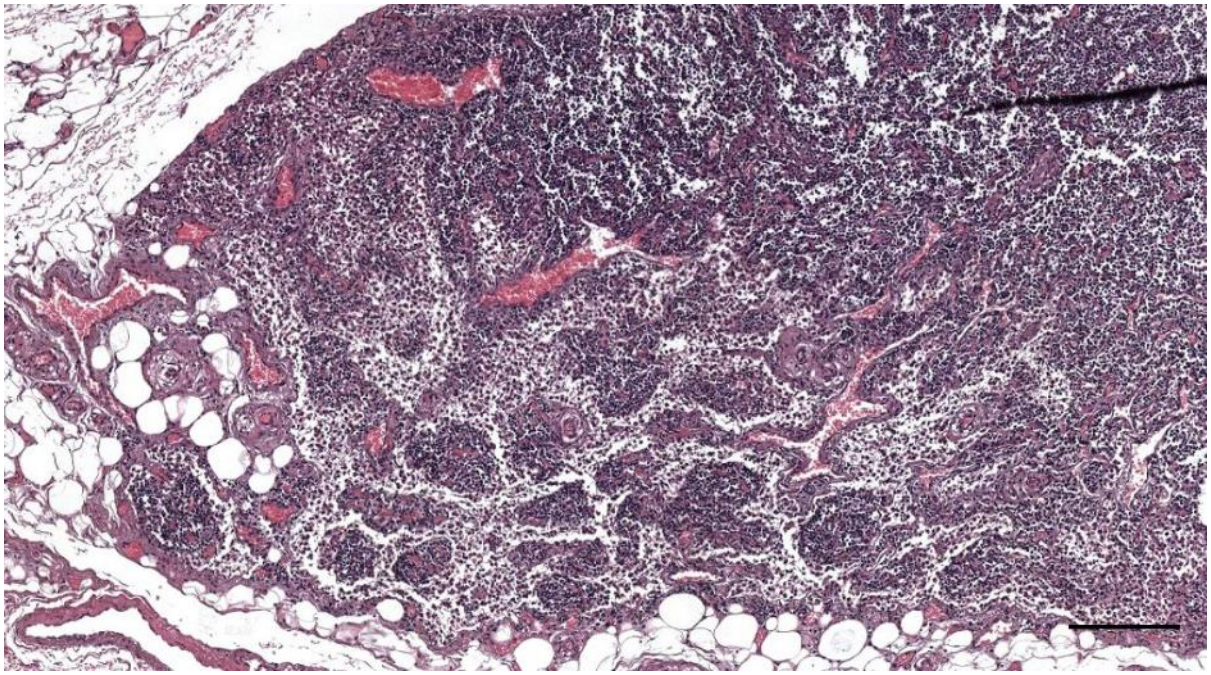

Figure 715. (362/18_L11) Lymphoid associated tissue. Scale bar 200 µm

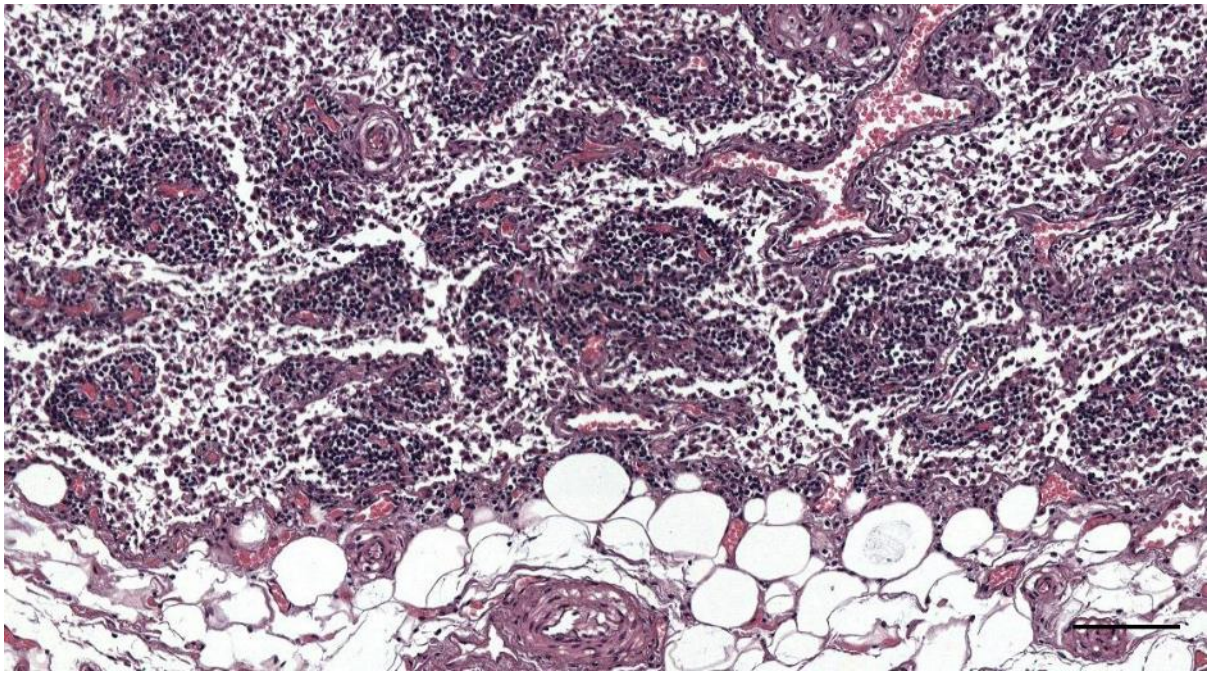

Figure 716. (362/18_L11) EAM associated lymphoid tissue. Scale bar 100 µm

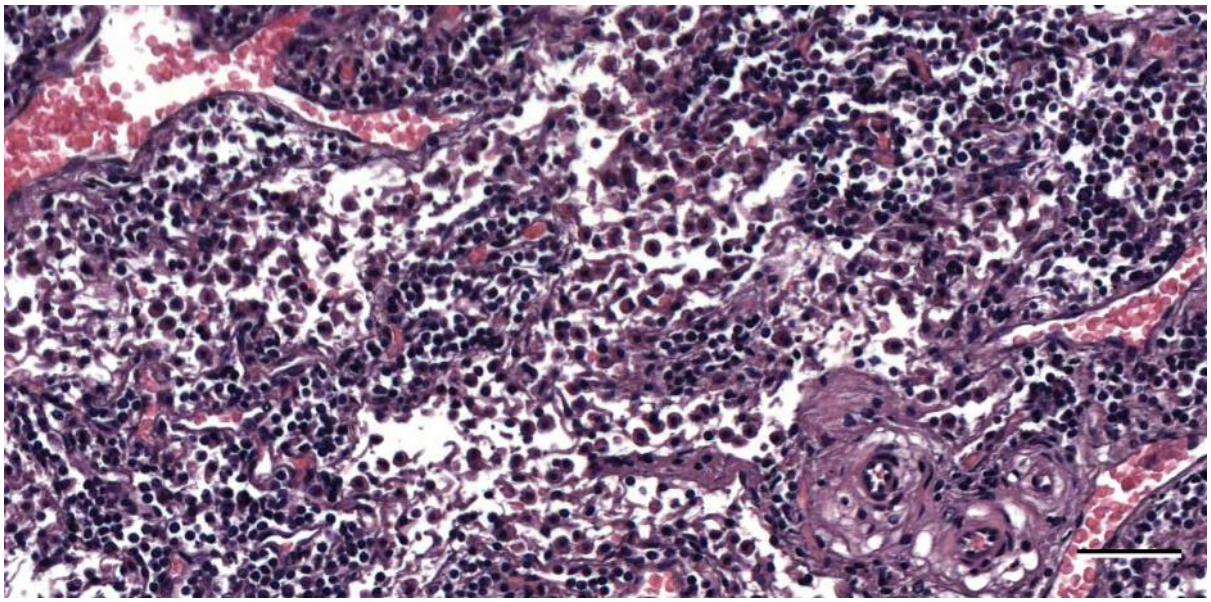

Figure 717. (362/18_L11) EAM associated lymphoid tissue. Scale bar 50 µm

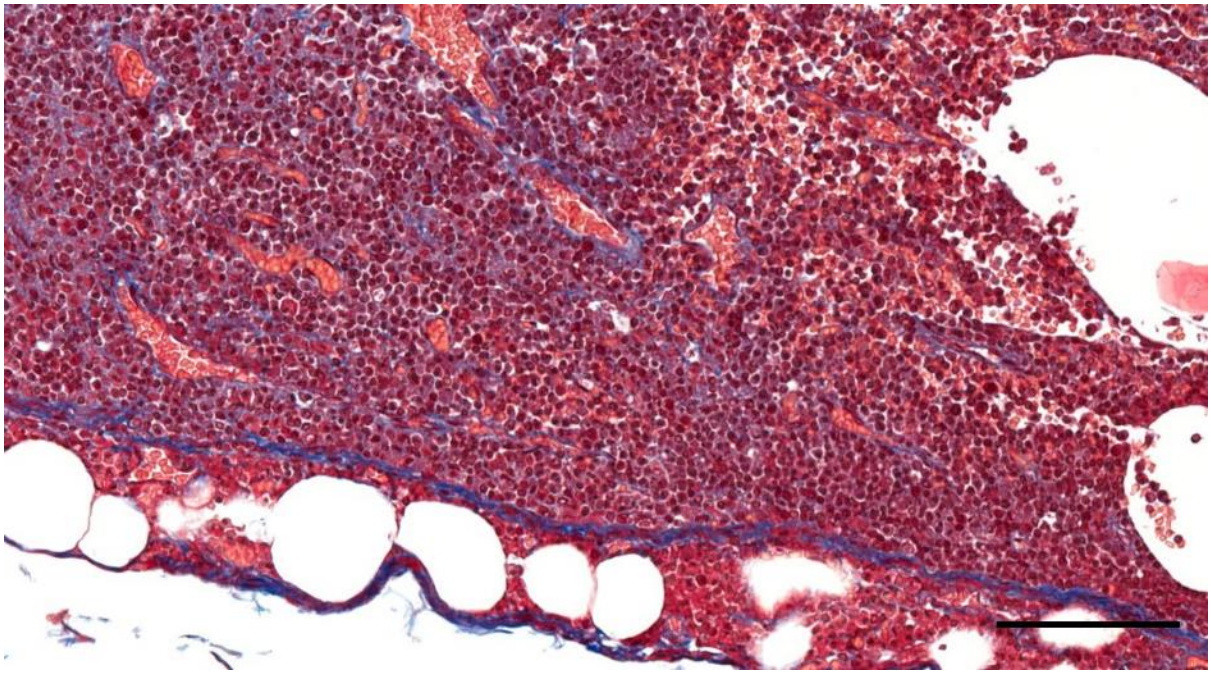

Figure 718. Detail of *Error! Reference source not found.*. ***(Striped dolphin 127565) Lymph node subcapsular sinus. Scale bar 100 µm***

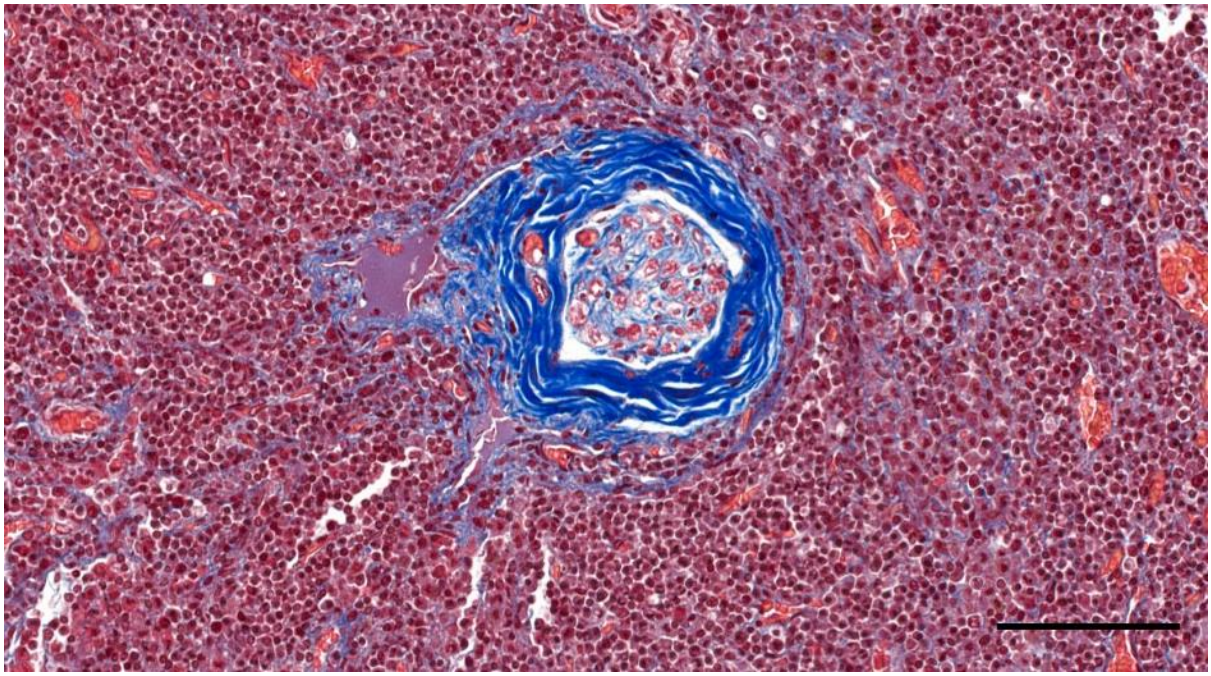

Figure 719. Detail of *Error! Reference source not found.*. ***(Striped dolphin 127565) Nerve inside the lymph node. Scale bar 100 µm***

3.2.7 Medial end of the ear canal

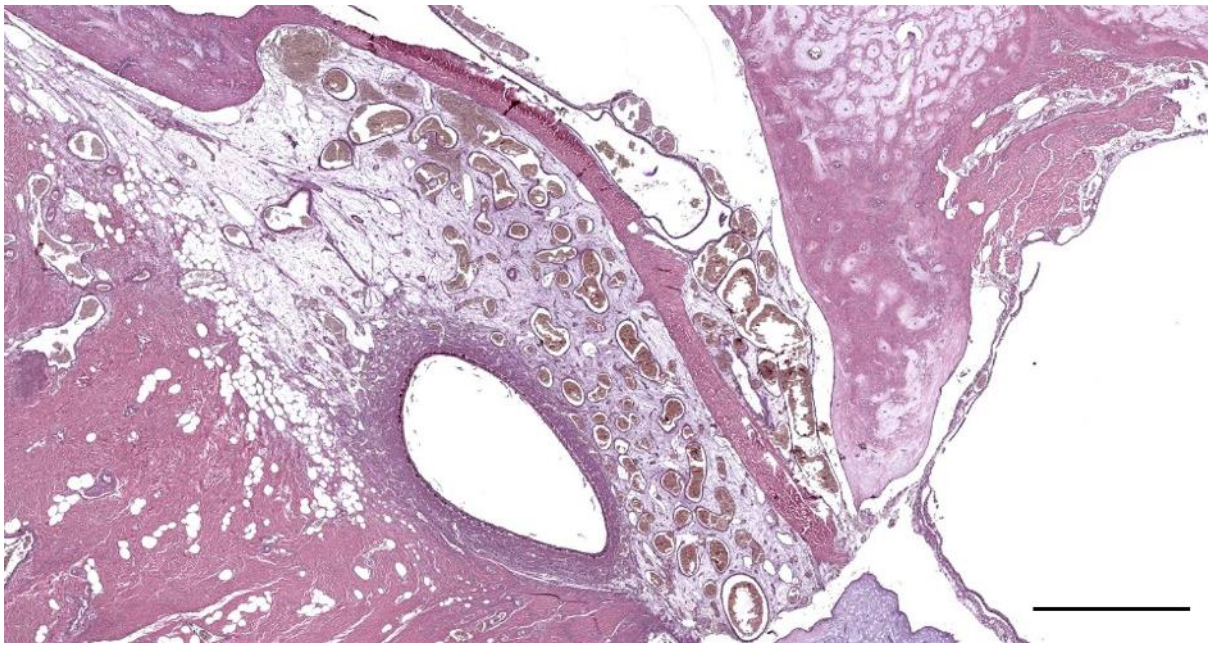

Figure 720. UT1692_Rx3_b_scale1mm

Figure 721. Right ear canal (1) and tympanic membrane (2) and ligament (2') suspended between the sigmoid process (3) and the malleus (4). 5. Posterior process (Up is ventral - Left is rostral). Scale bar 1 mm.

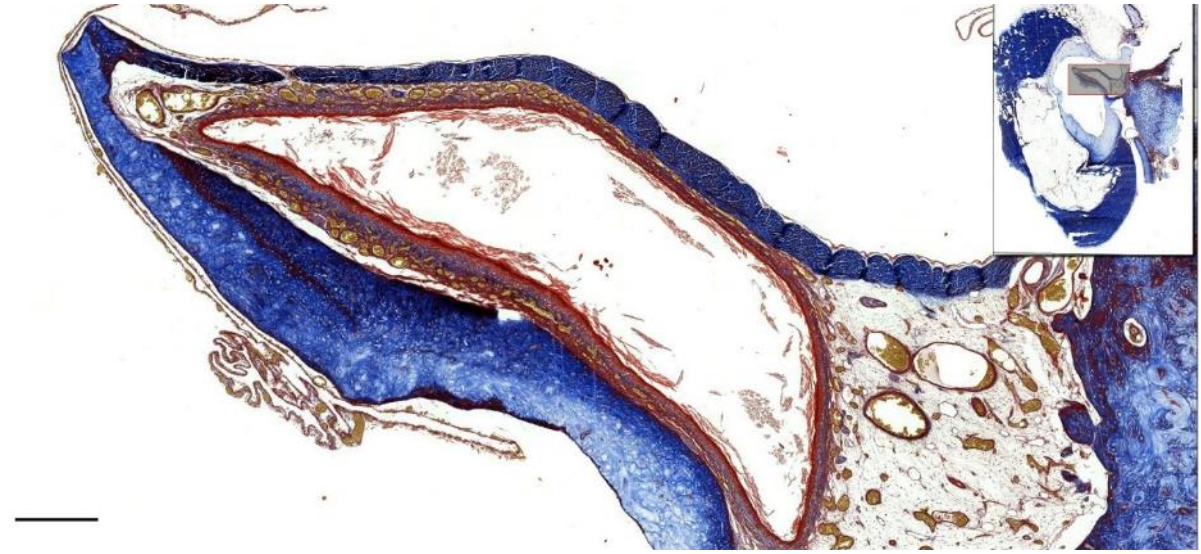

Figure 722. Detail of the ear canal in *Error! Reference source not found.* ***(insert). Scale bar 0.5 mm.***

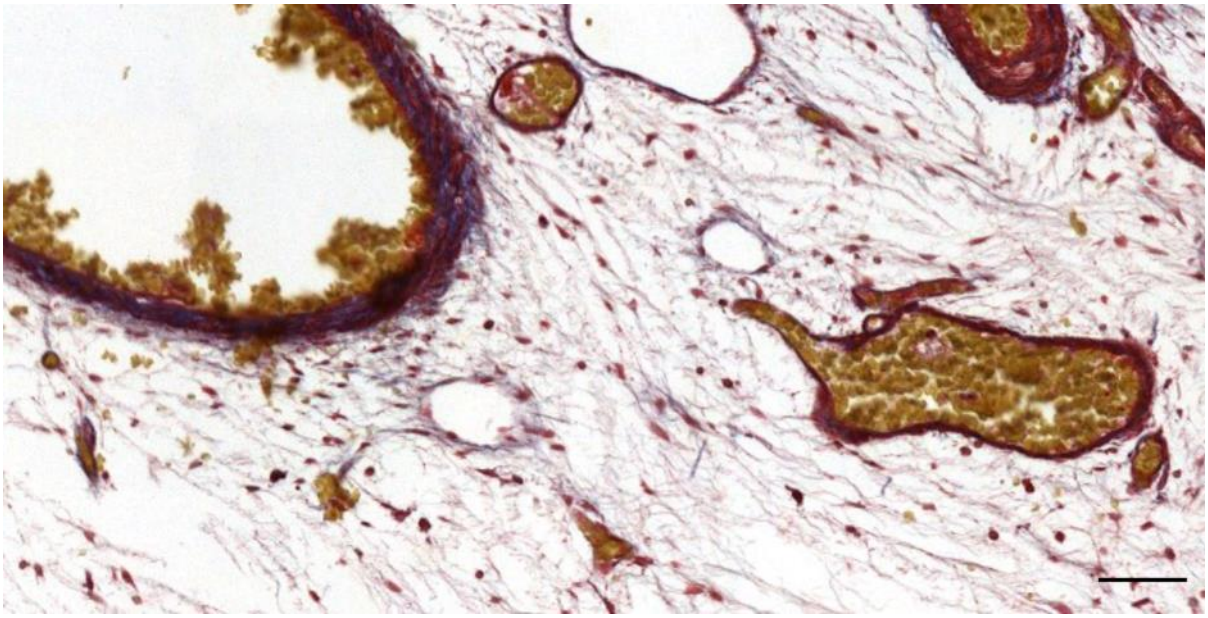

Figure 723. Detail of Figure 722. Histological detail of the vascular plexus and embedded in a reticular connective tissue network. Scale bar 50 µm

3.2.8 Foetus

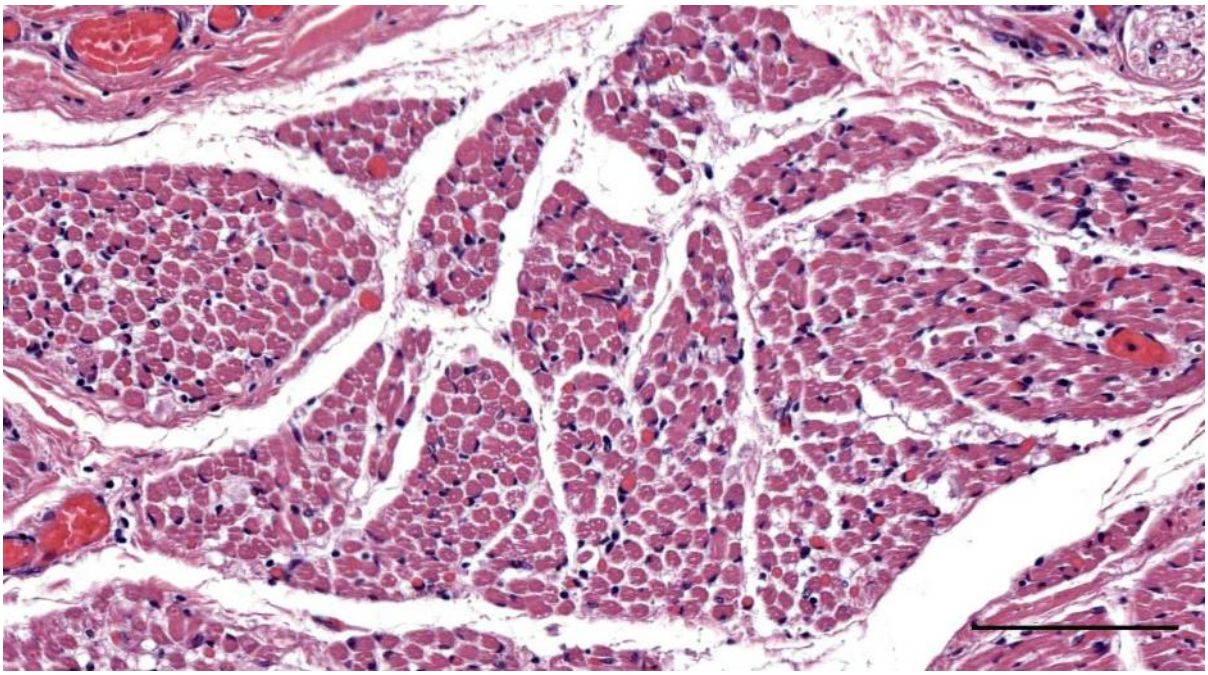

Figure 724. (293/18_foetus_L3) Detail of the muscles around the ear canal. Note the small diameter of the muscle fibres, and the relative large amount of connective tissue between fibres (similar to endomysial fibrosis). Scale bar 100 µm

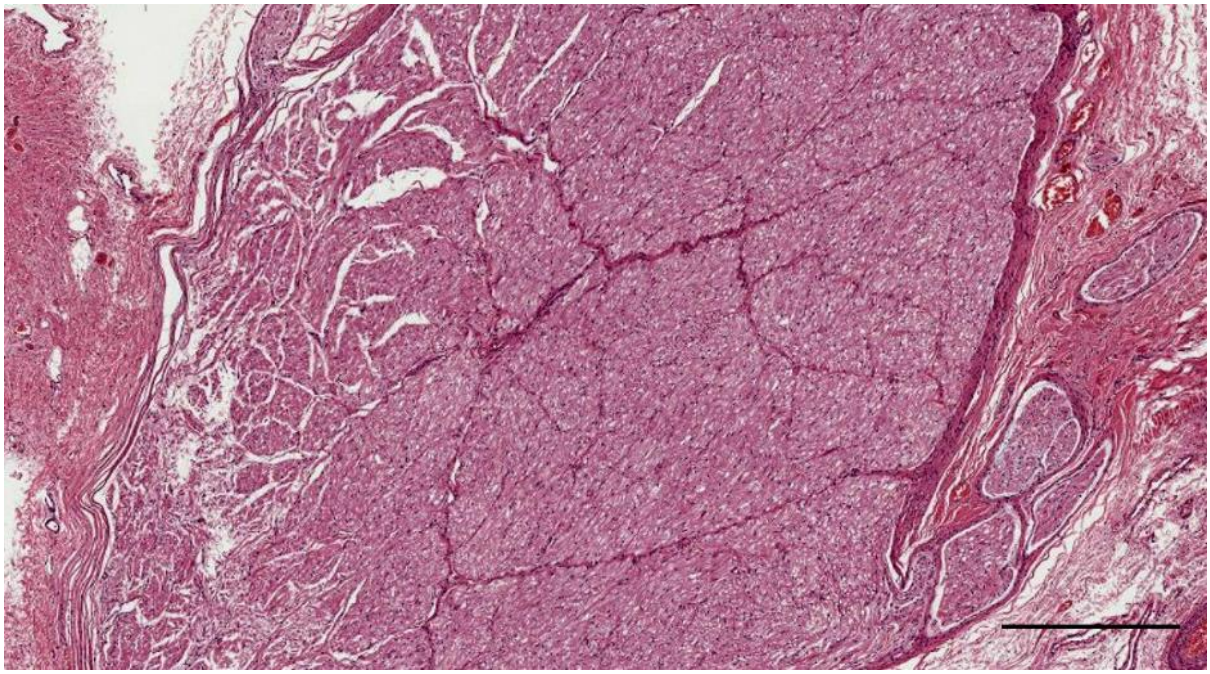

Figure 725. (293/18_foetus_L6) Facial nerve with branches of smaller nerves. Scale bar 0.5 mm

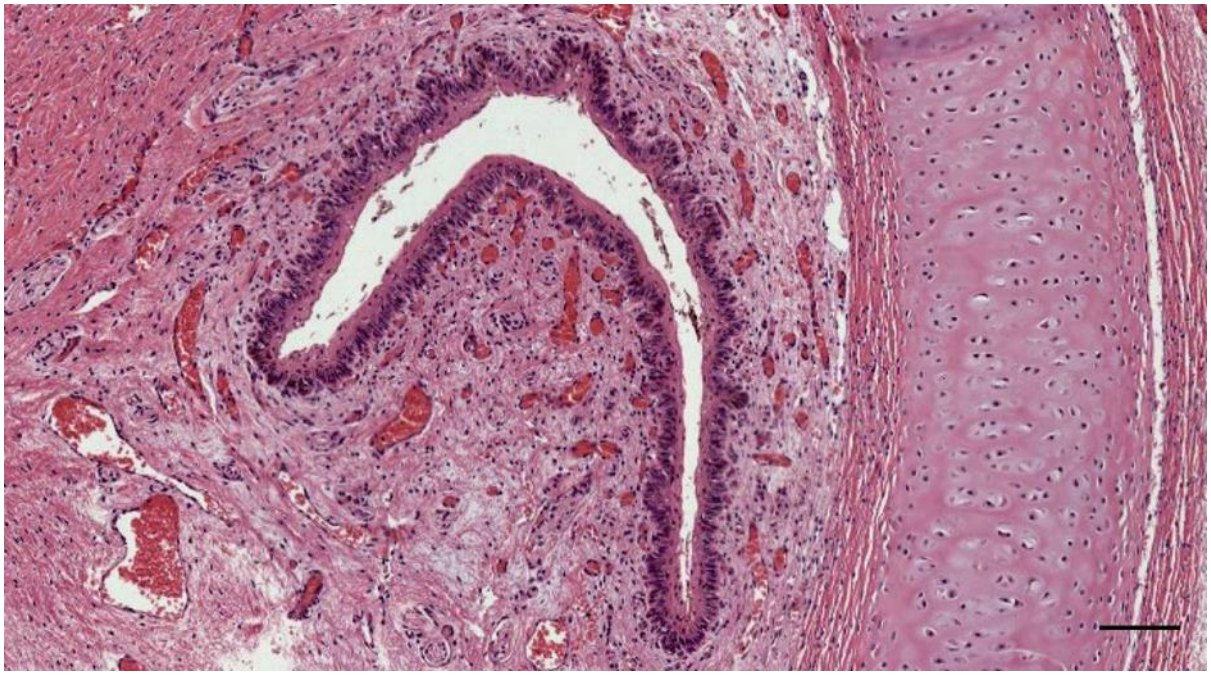

Figure 726. Histological image (HE stain) of Ear canal with a semilunar shape in association with the cartilage(293/18_foetus_L6). Scale bar 50 µm

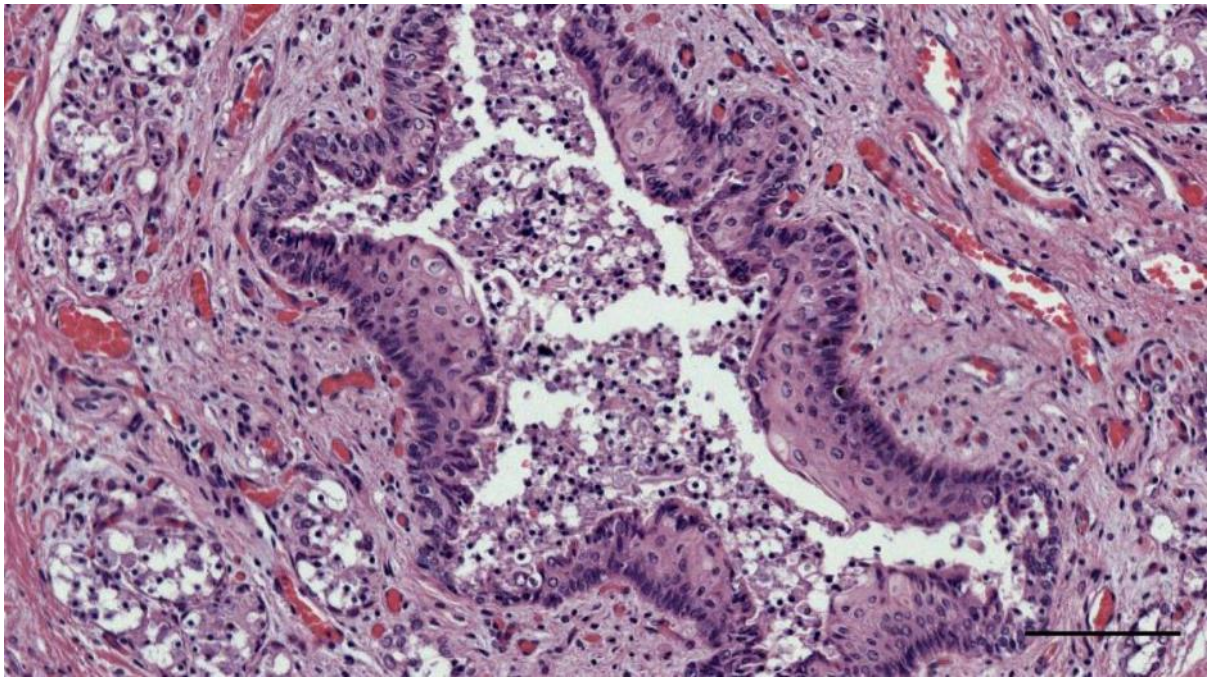

Figure 727. (293/18_foetus_L3) Detail of the ear canal with cellular content coming from the glands. Scale bar 100 µm

3.3 Innervation

3.3.1 Lamellar corpuscles

3.3.1.1 Circummeatal

Figure 728. HE-stained cross-section through the ear canal of a striped dolphin (ID 12691), ± 1cm below the skin surface. Note the abundance of lamellar corpuscles and small nerve fibres in the subepithelial tissue surrounding the entire canal. Scale bar = 100 µm

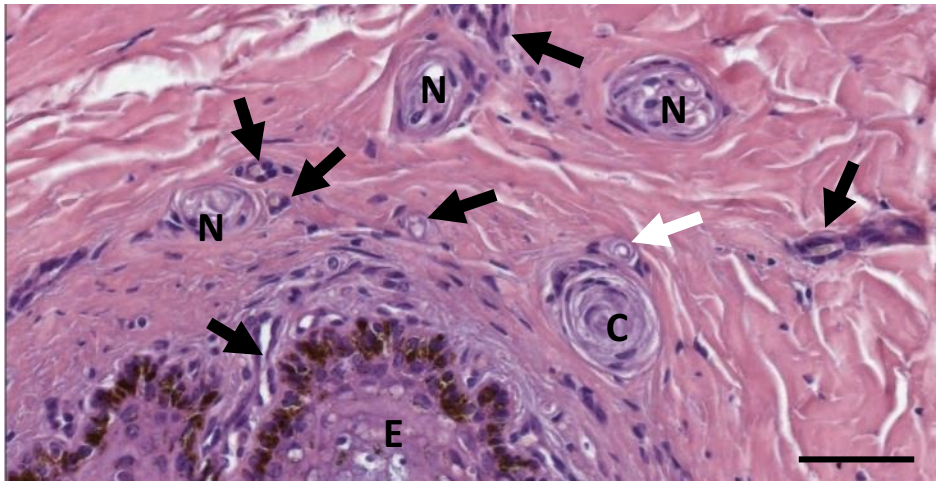

Figure 729. HE staining of nervous and vascular structures in the subepithelial tissue of the external ear canal; e: epithelium; c: lamellar corpuscle; n: small nerve bundle; black arrows: vascular structures; white arrows: vascular structure or small myelinated nerve fibres. The white areas between connective tissue (collagen fibres) are artefacts of the tissue preparation (De Vreese et al., 2020a).

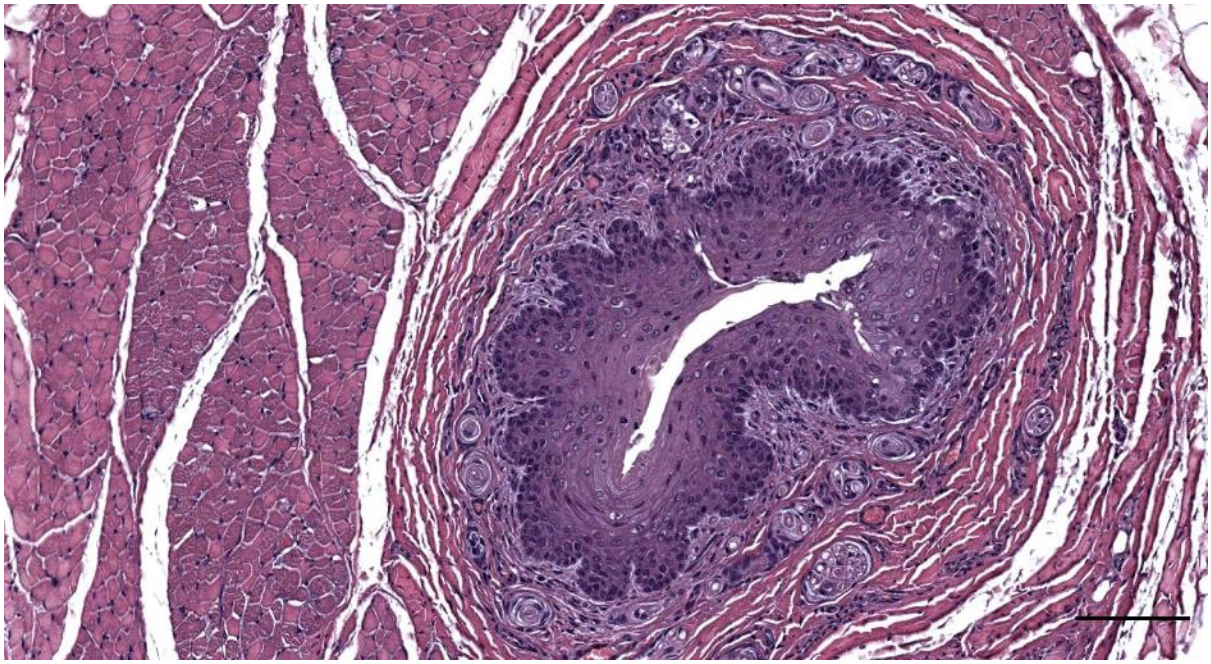

Figure 730. Histological image (HE staining) of corpuscles in the subepithelial tissue in a transverse section through the ear canal of a striped dolphin (ID419/16) at about 2 cm beneath the skin. There is a small amount of glandular tissue with indications of excretory ducts. Scale bar 100 µm.

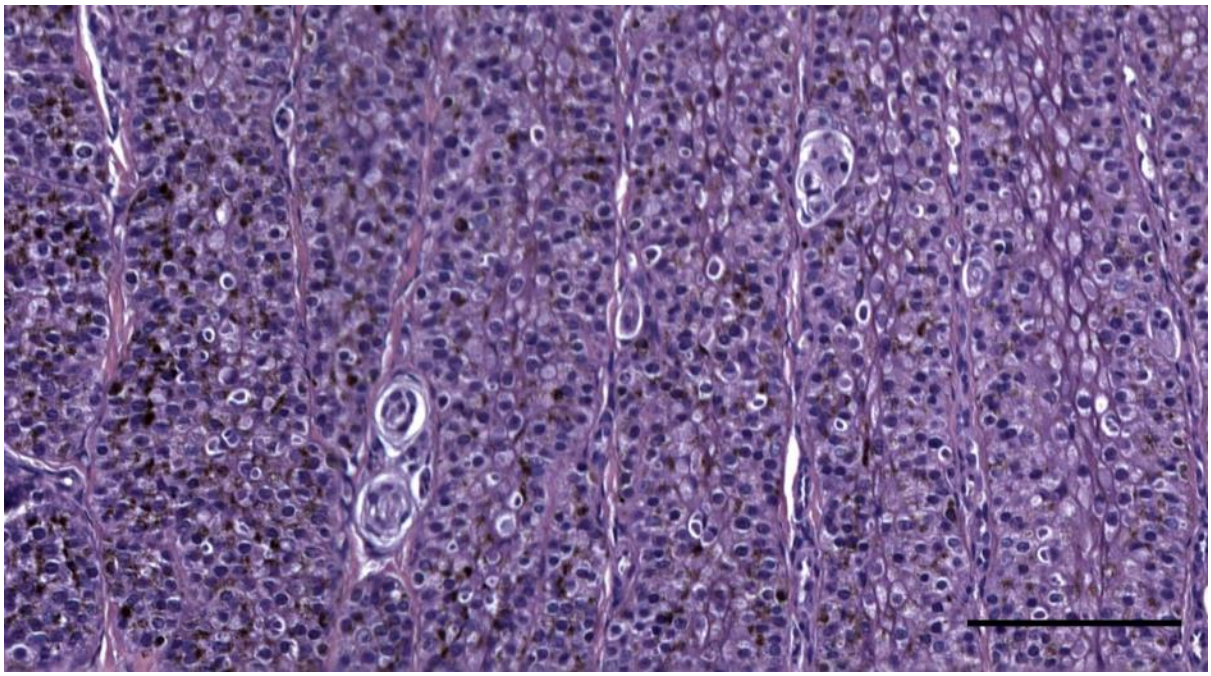

Figure 731. HE stained histological images of lamellar nervous structures in the dermal papillae close to the external ear opening in a harbour porpoise. Scale bar 100 µm

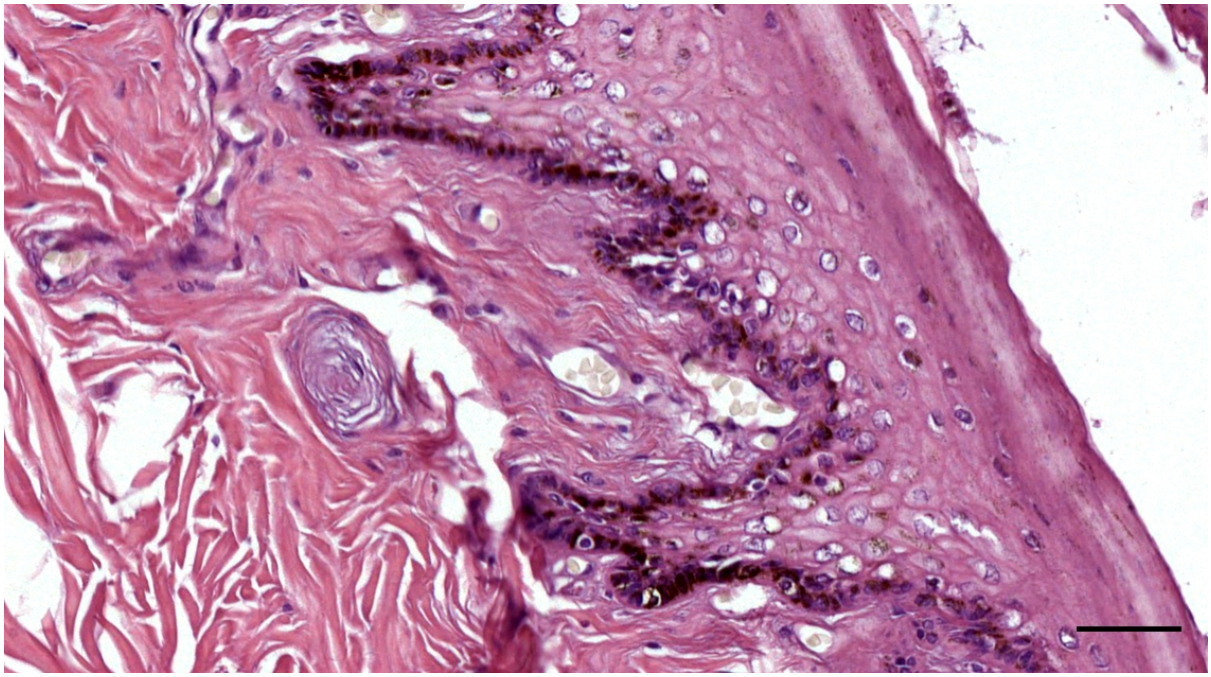

Figure 732. Histological detail image (HE staining) of a lamellar corpuscle in the subepithelial tissue of a Cuvier´s beaked whale ear canal (ID429). Scale bar 50 µm

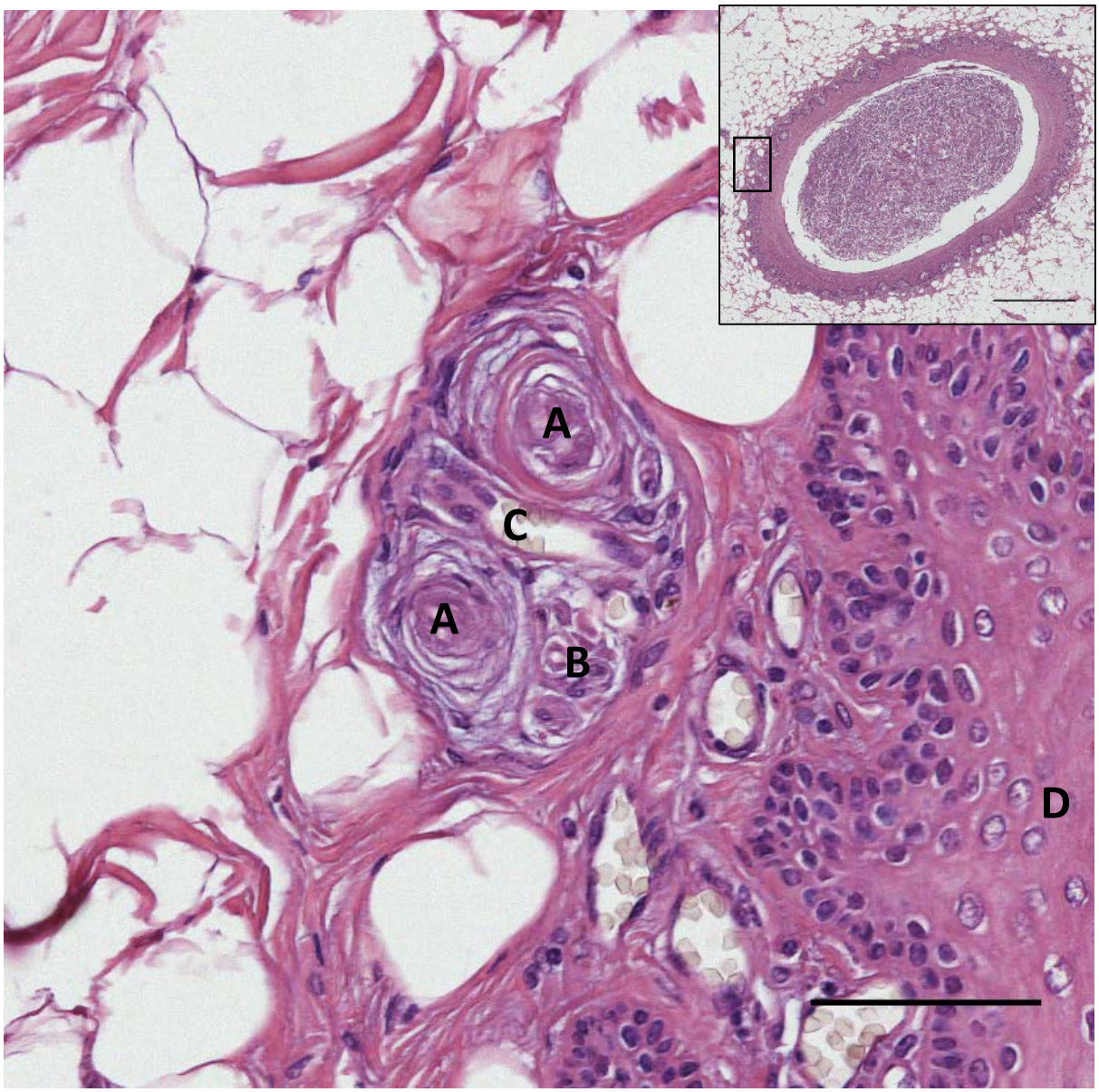

Figure 733. Histological detail (HE staining) of a lamellar corpuscle complex in the vicinity of the ear canal epithelium (D) in Cuvier´s beaked whale. The complex constitutes at least two cross-sections through lamellar corpuscles (A), a nerve (B) and a blood vessel (C). Scale bar 0.1 mm. The image on the top right depicts an overview section and the location of the detail section. Scale bar 1 mm.

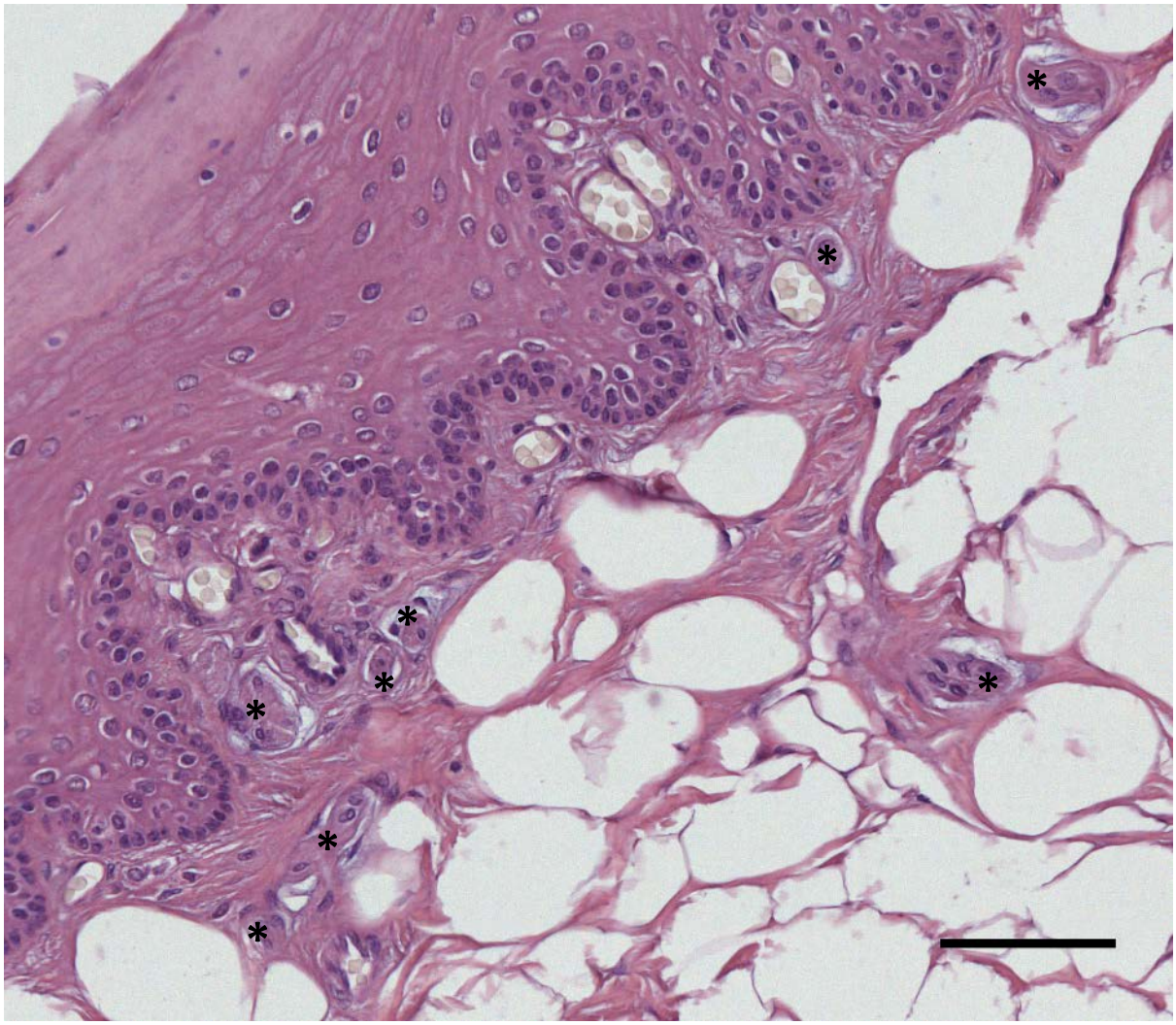

Figure 734. Histological detail (HE staining) of eight probable nervous structures (*) in the vicinity of the ear canal in Cuvier´s beaked whale. Scale bar 0.1 mm.

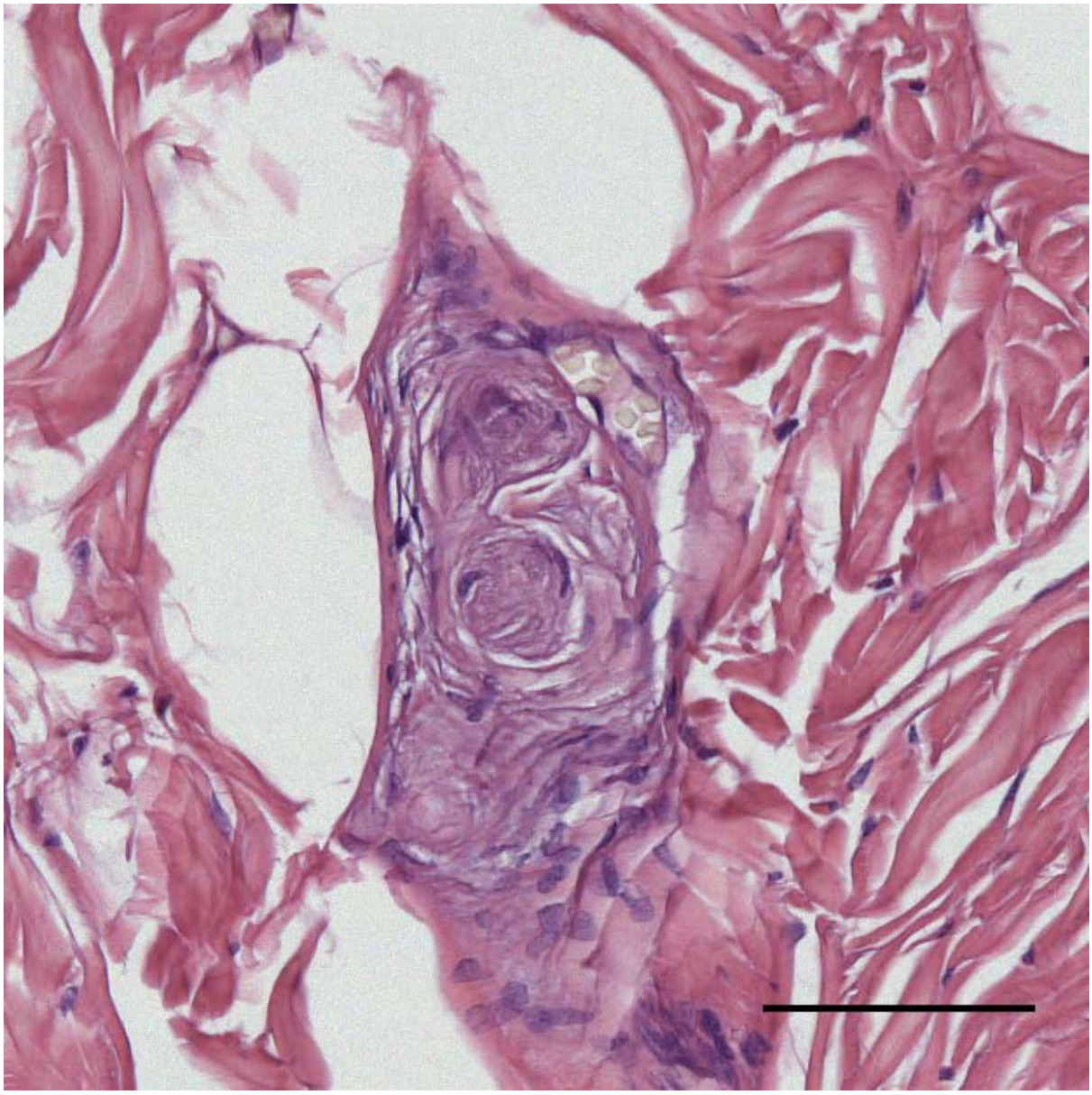

Figure 735. Detail image (HE staining) of a corpuscle complex in Cuvier´s beaked whale (ID429 – block 10) with at least two lamellar corpuscles and one blood vessel. Scale bar 100 µm.

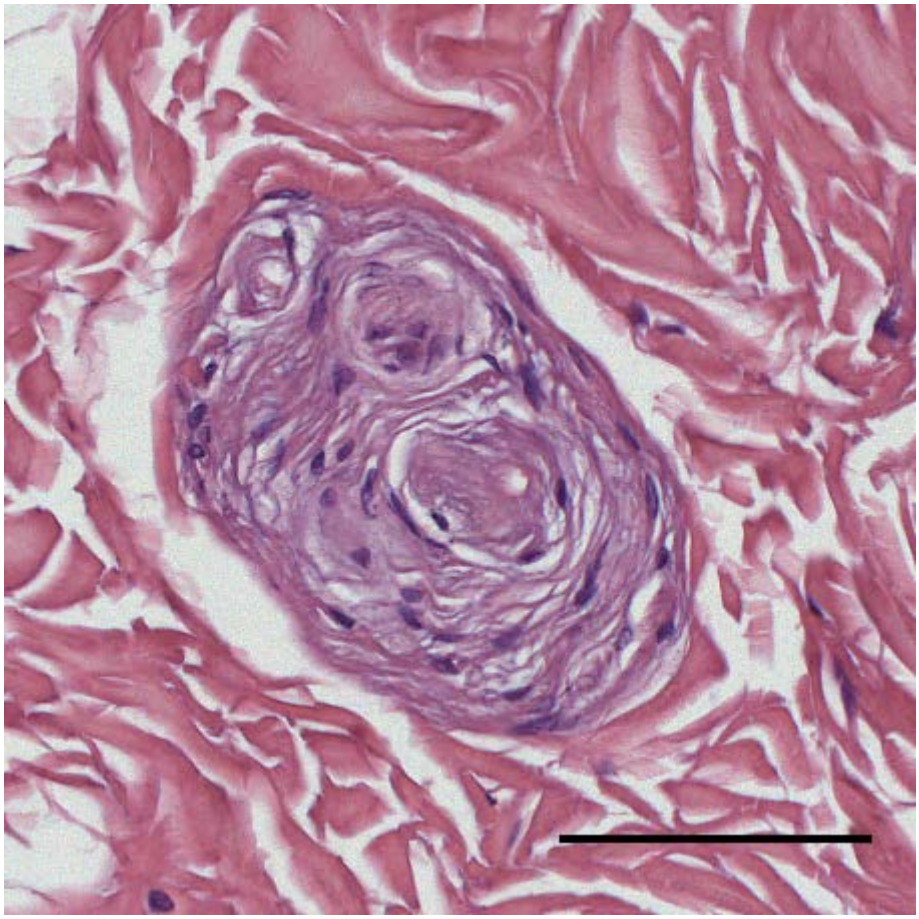

Figure 736. Detail of a corpuscle complex in Cuvier´s beaked whale (ID429 – block 10) with at least two lamellar corpuscles. The smaller lamellar structure could be a third corpuscle or a blood vessel. HE stain. Scale bar 100 µm.

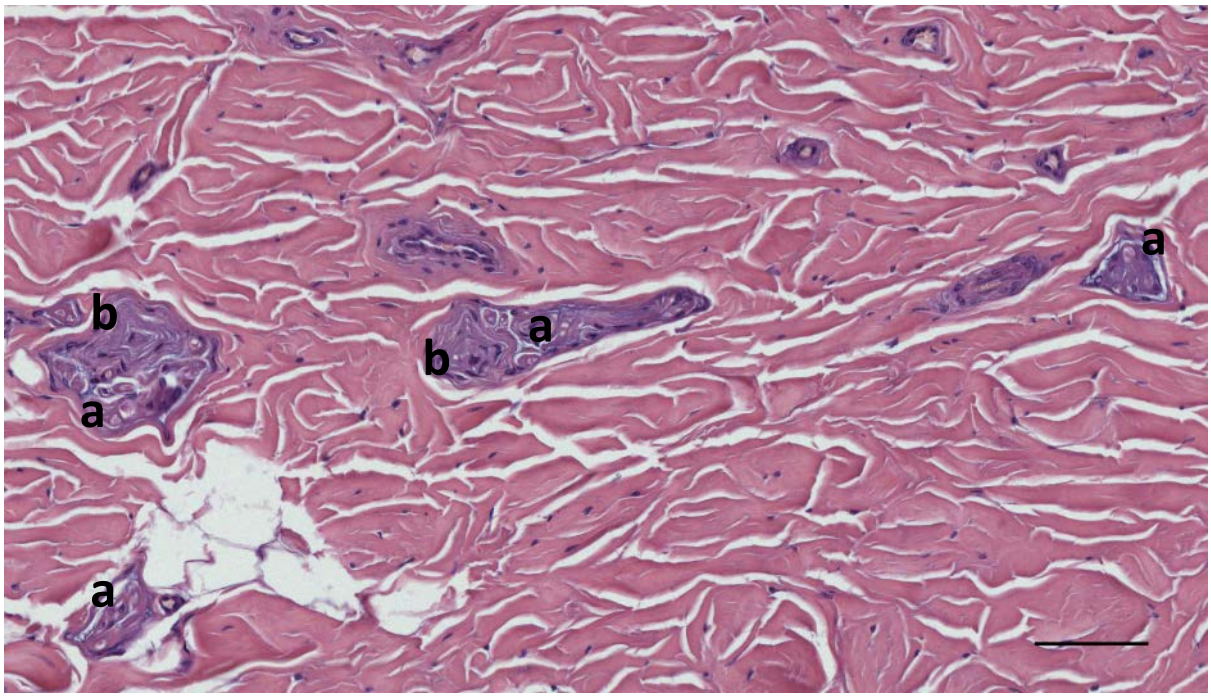

Figure 737. Detail of a likely continuation of a nerve (a) and corpuscle (b) within the same capsule in Cuvier´s beaked whale (ID429 – block 14a). These might be several sections through the same structure. HE stain. Scale bar 100 µm.

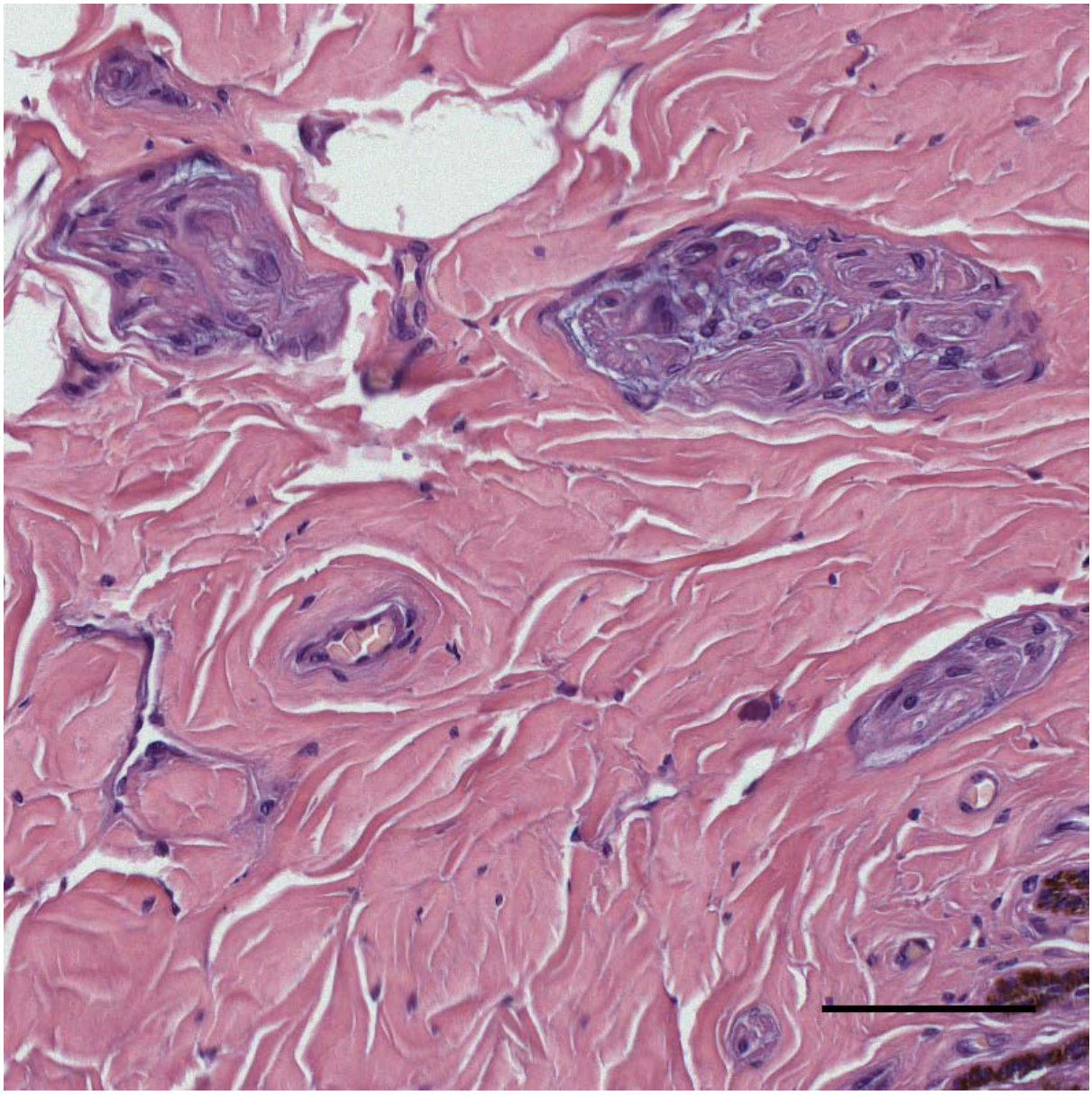

Figure 738. Detail of several nervous structures in the subepithelial tissue of the ear canal of a Cuvier´s beaked whale (ID429 – block 14b). The largest structure on the top right comprises at least two lamellar corpuscles within a nerve fibre. The structure on the top left has indications of being a complex corpuscle, although not certain. Two smaller structures on the bottom right, close to the basement membrane of the epithelium are small nerve fibres or corpuscles, although not certain. HE stain. Scale bar 100 µm.

3.3.1.1.1 In spatial association with blood vessels

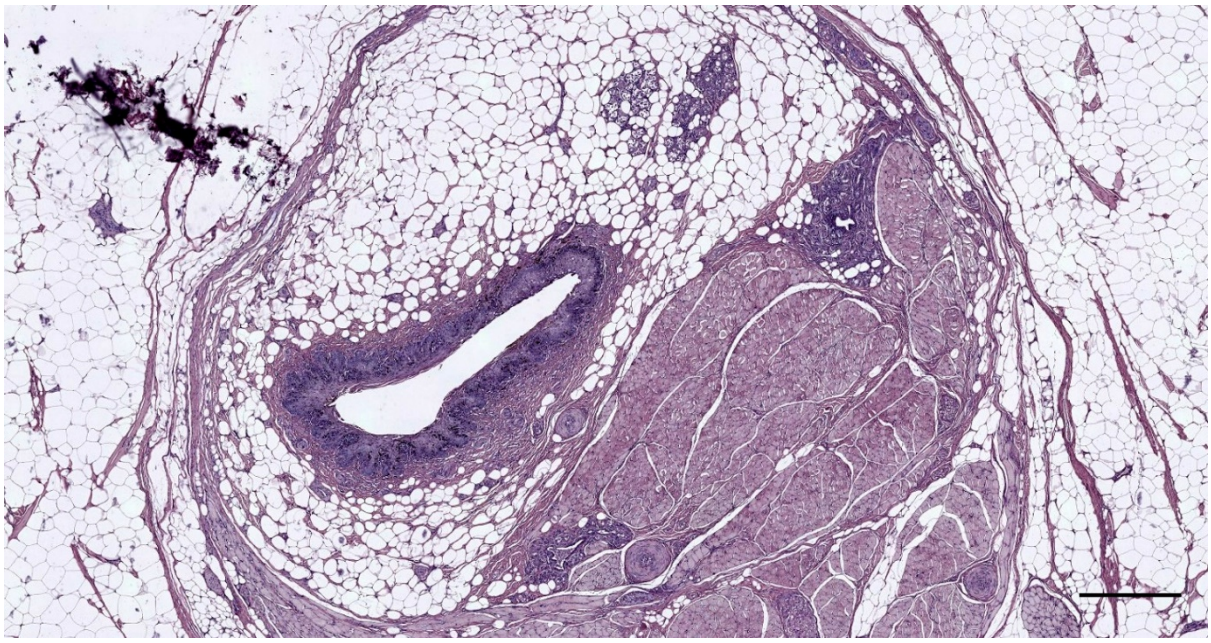

Figure 739. Histological image (HE staining) of a transverse section through the external ear canal of a harbour porpoise, about 2 cm beneath the skin (UT1718_L0601). Scale bar 500 µm

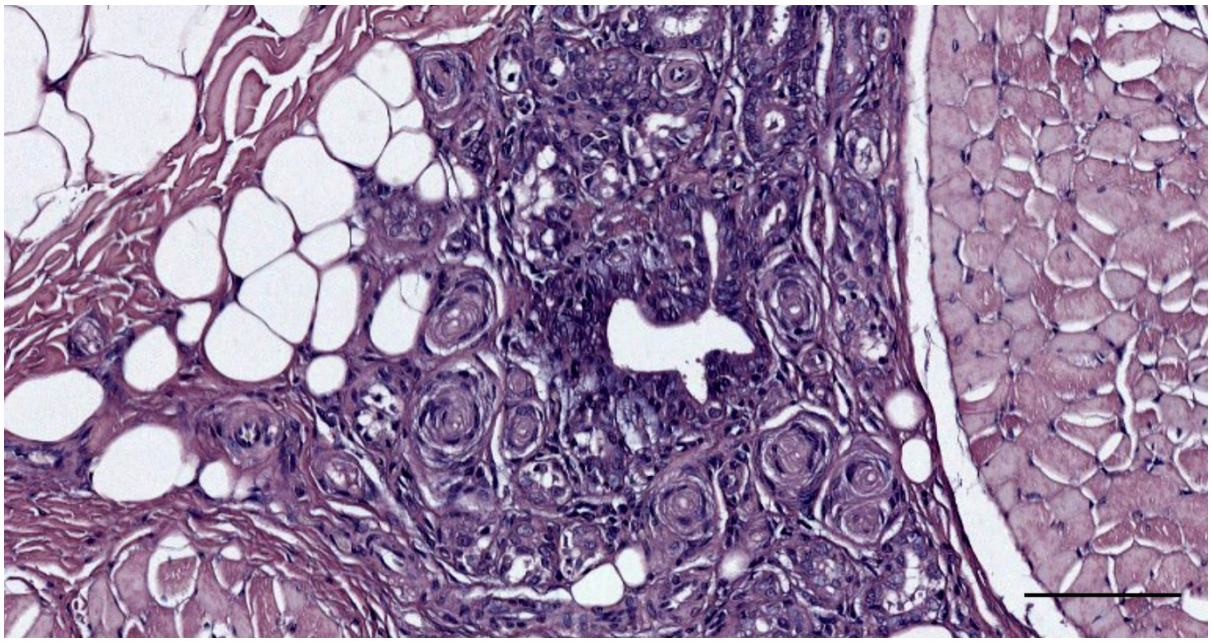

Figure 740. Detail of Figure 739. Histological image (HE) of a transverse section through the external ear canal of a harbour porpoise, about 1 cm beneath the skin (UT1718_L0602). Lamellar corpuscles spatially associated with a vascular structure, and in between muscle tissue. Scale bar 100 µm

3.3.1.2 Nervous tissue ridge

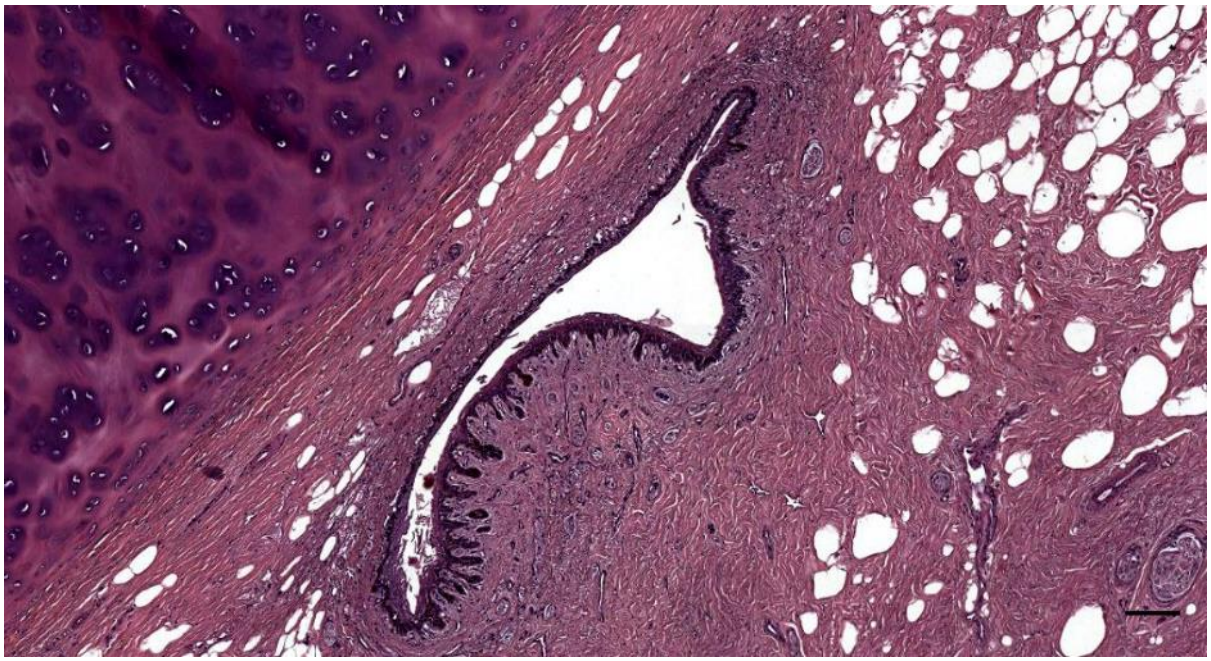

Figure 741. Histological image (HE staining) of the right ear canal of a bottlenose dolphin at about 4 cm beneath the skin (444_R9). Note the ear canal with nervous tissue ridge opposite the cartilage. Scale bar 100 µm

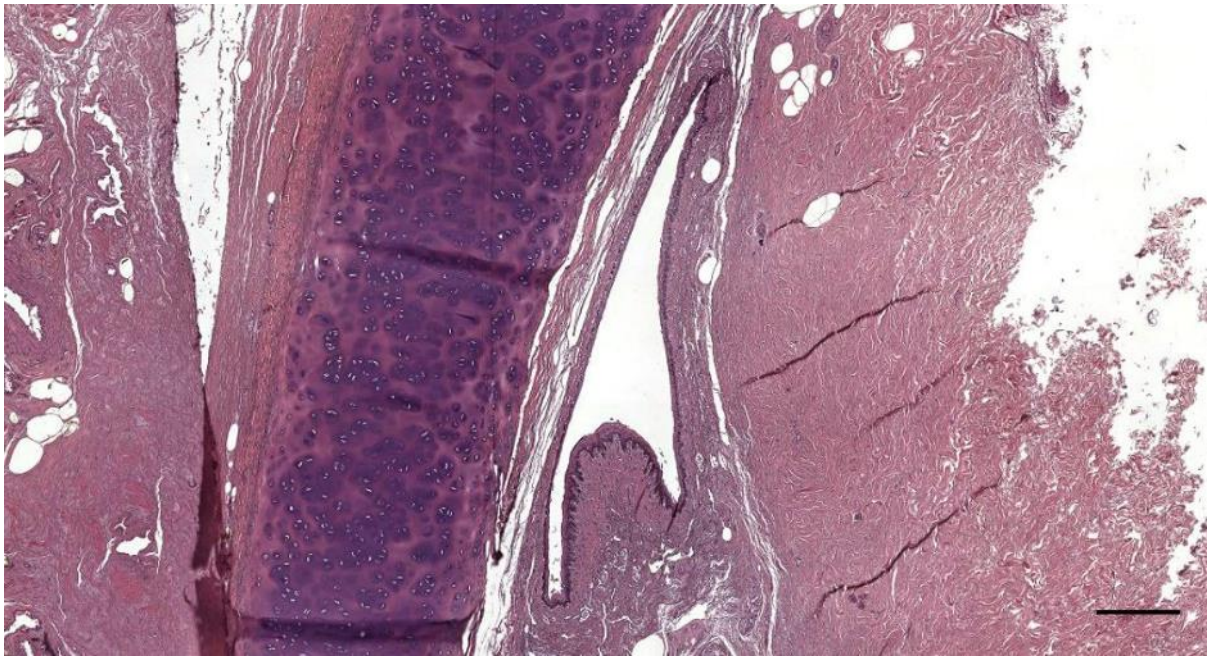

Figure 742. Histological image (HE staining) of the right ear canal of a bottlenose dolphin at about 5.5 cm beneath the skin (444_R12). Note the ear canal with a nervous tissue ridge. Scale bar 300 µm

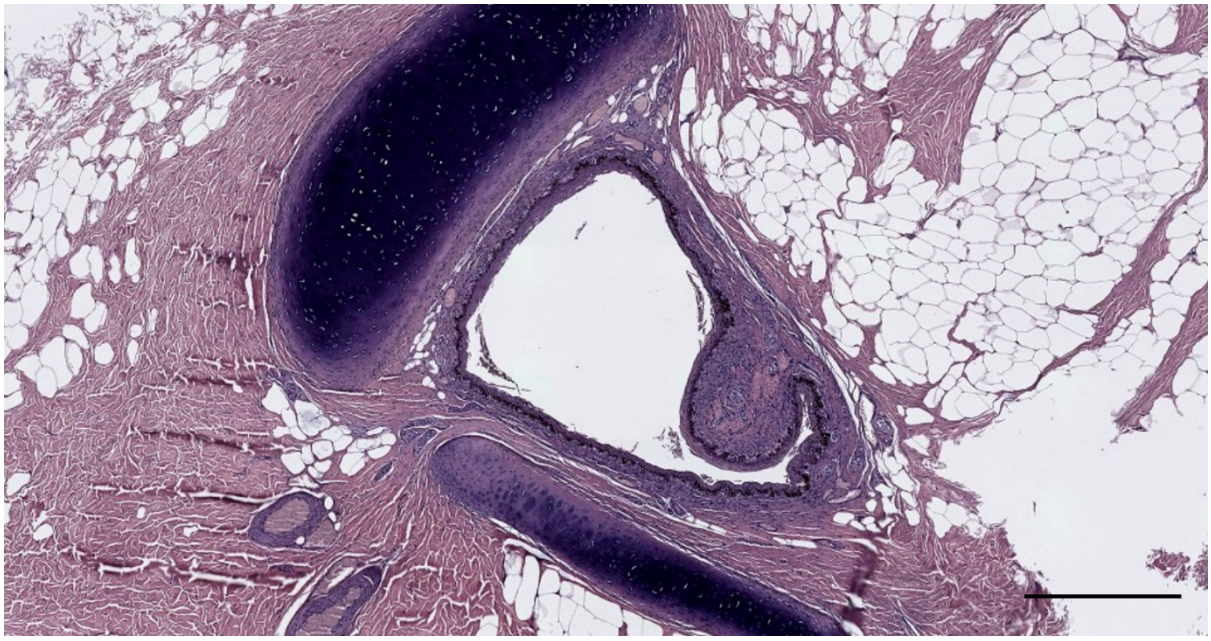

Figure 743. Histological image (HE staining) of a transverse section through the left external ear canal of a harbour porpoise, about 4.5 cm beneath the skin (UT1718_L1301). Scale bar 500 µm

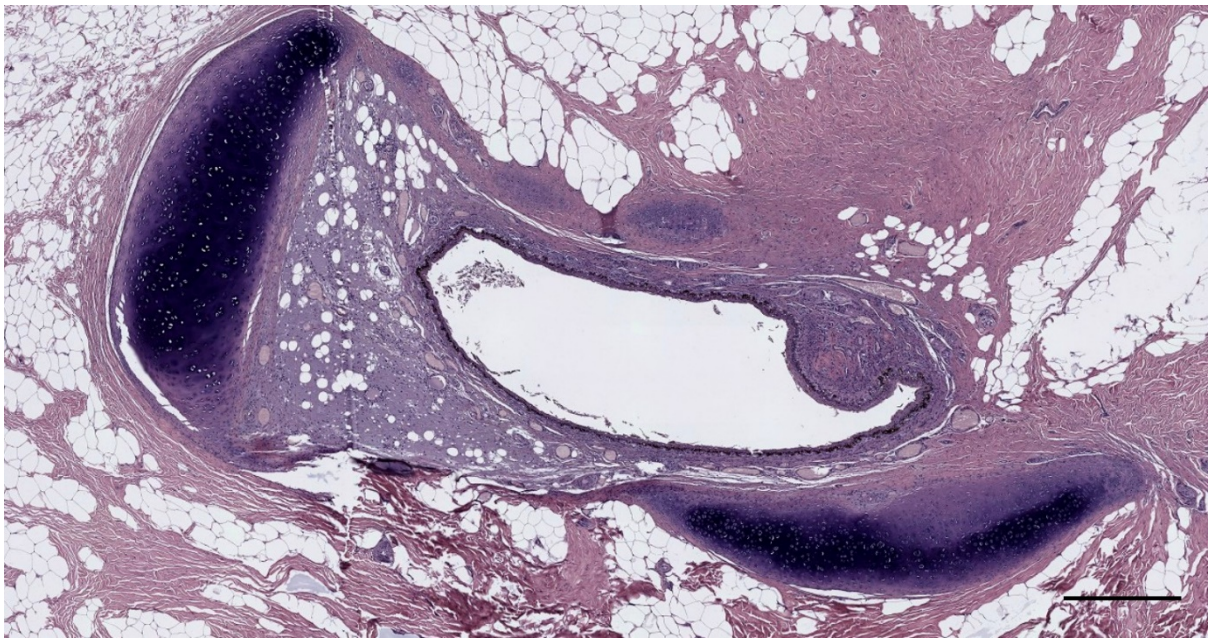

Figure 744. Histological image (HE staining) of a transverse section through the left external ear canal of a harbour porpoise, about 5 cm beneath the skin (UT1718_L1402). Note the ear canal with sensory ridge, and the cartilage flanges. Scale bar 500 µm

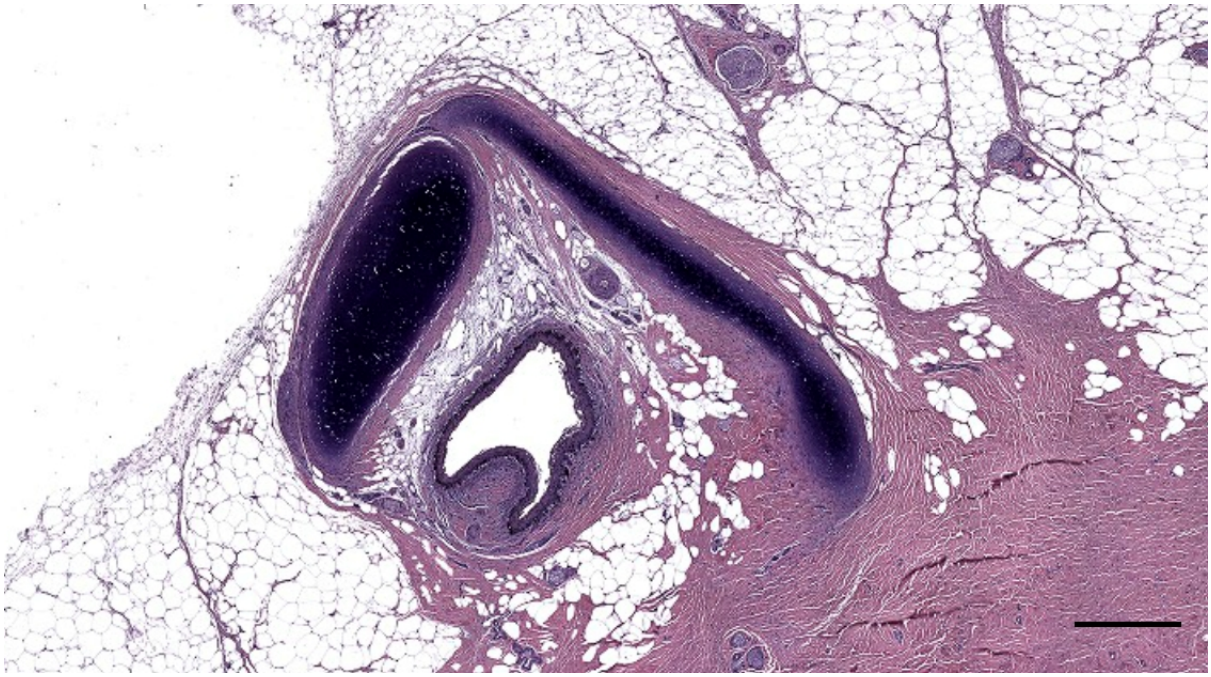

Figure 745. Histological image (HE staining) of a transverse section through the left external ear canal of a harbour porpoise at about 4 cm beneath the skin (UT1734_L12). Scale bar 500 µm

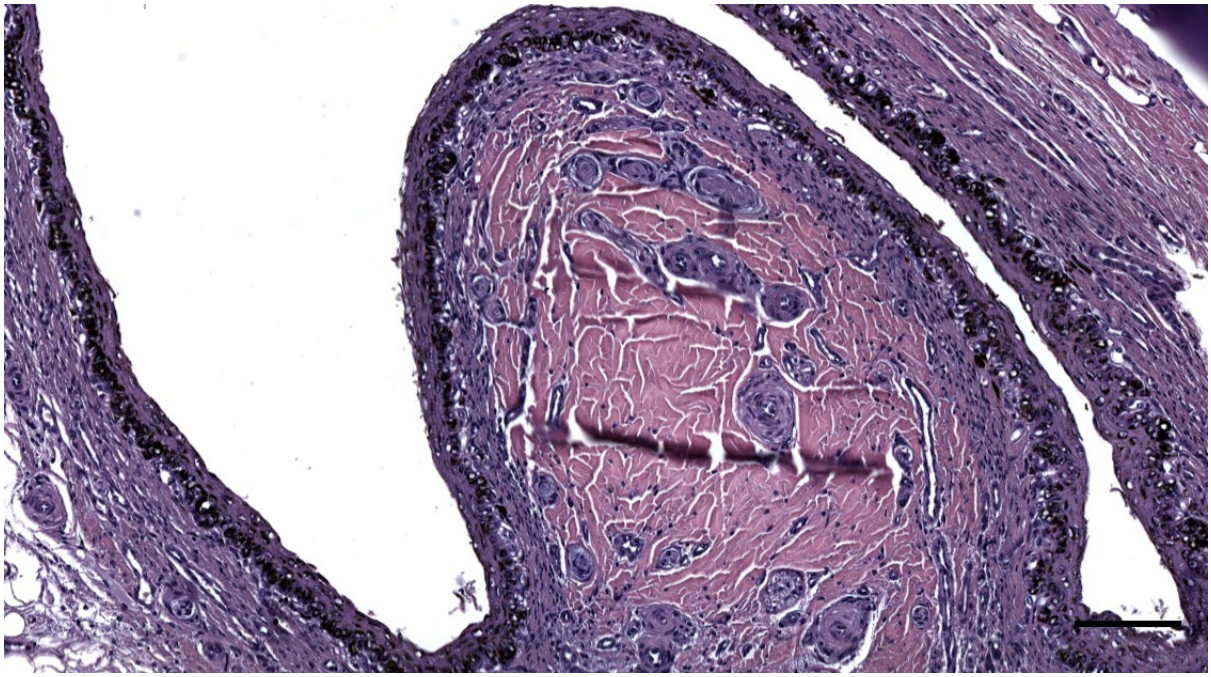

Figure 746. Histological detail (HE staining) of the sensory ridge protruding into the ear canal of a harbour porpoise, at about 5 cm beneath the skin (UT1734_L14). Scale bar 100 µm

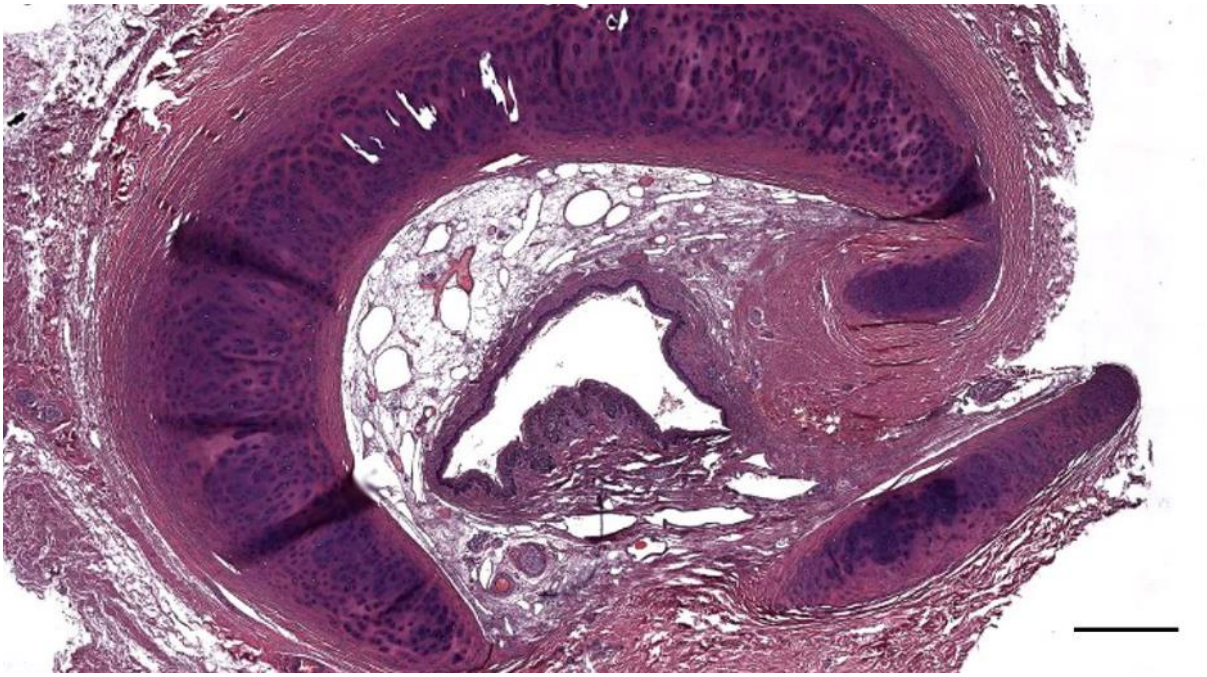

Figure 747. Histological image (HE staining) of the external ear canal and cartilage main body and flanges in a striped dolphin, at about 5.5 cm beneath the skin (292/18_L12). Note the ear canal with nervous tissue ridge opposite the main cartilage. Scale bar 100 µm

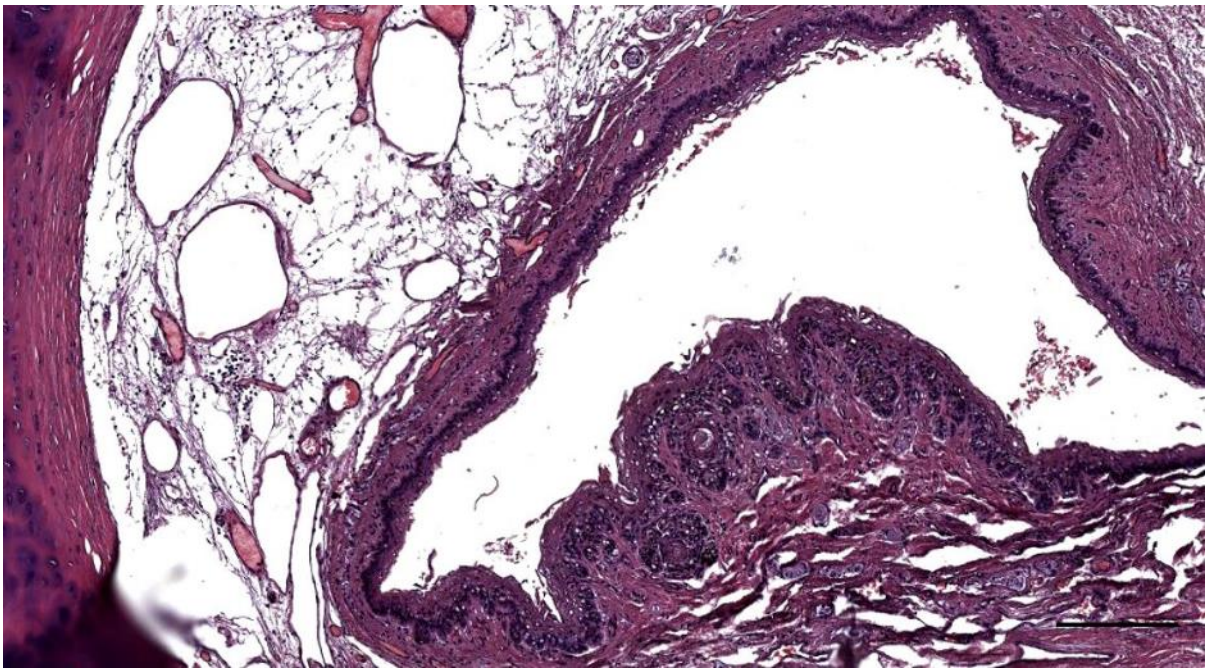

Figure 748. Detail of Figure 747. Mononuclear cells (lymphocytes) between the ear canal and cartilage, situated in the reticular connective tissue network with vascular lacunae. Note the nervous tissue ridge bulging into the ear canal lumen. Scale bar 200 µm

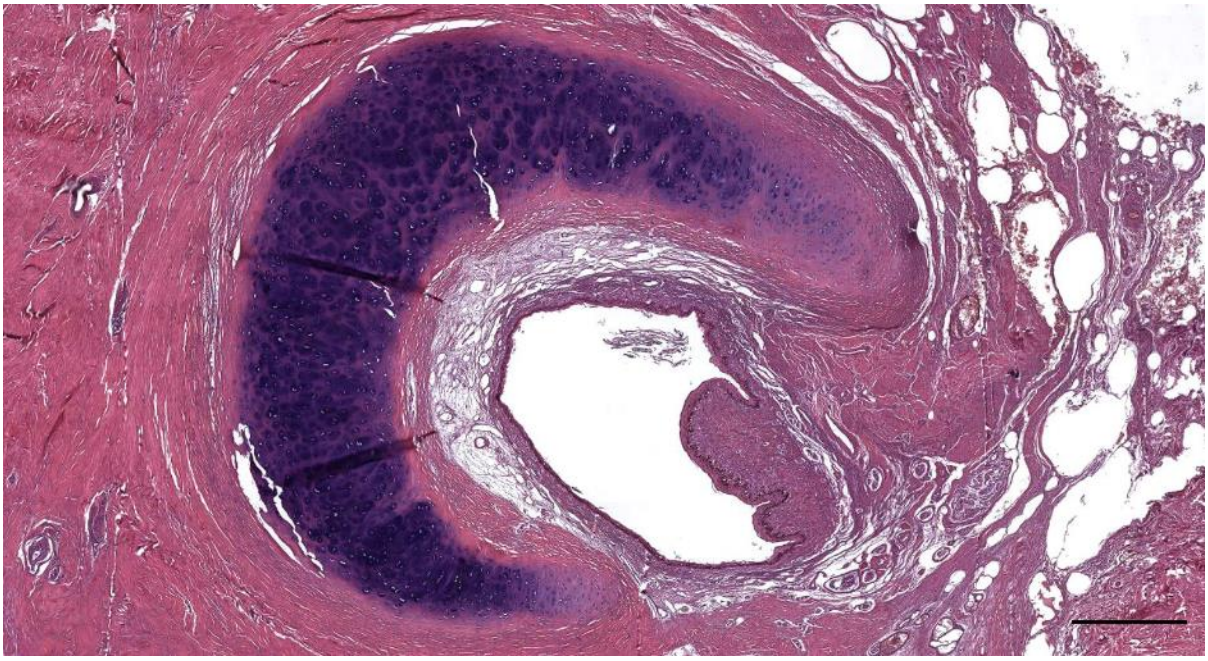

Figure 749. Histological image (HE staining) of the external ear canal and cartilage in a striped dolphin (509/17_Lx1), close to the TP complex. Scale bar 0.5 mm

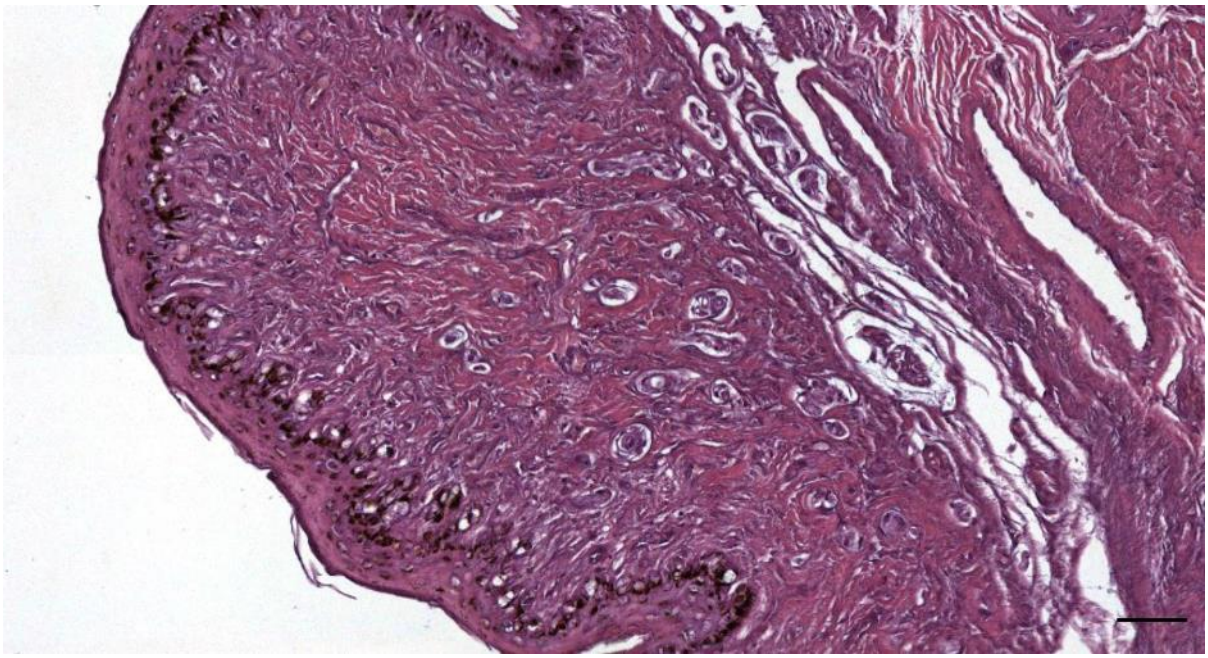

Figure 750. Detail of the nervous tissue ridge in Figure 749. Note the abundance of nervous structures. Scale bar 50 µm.

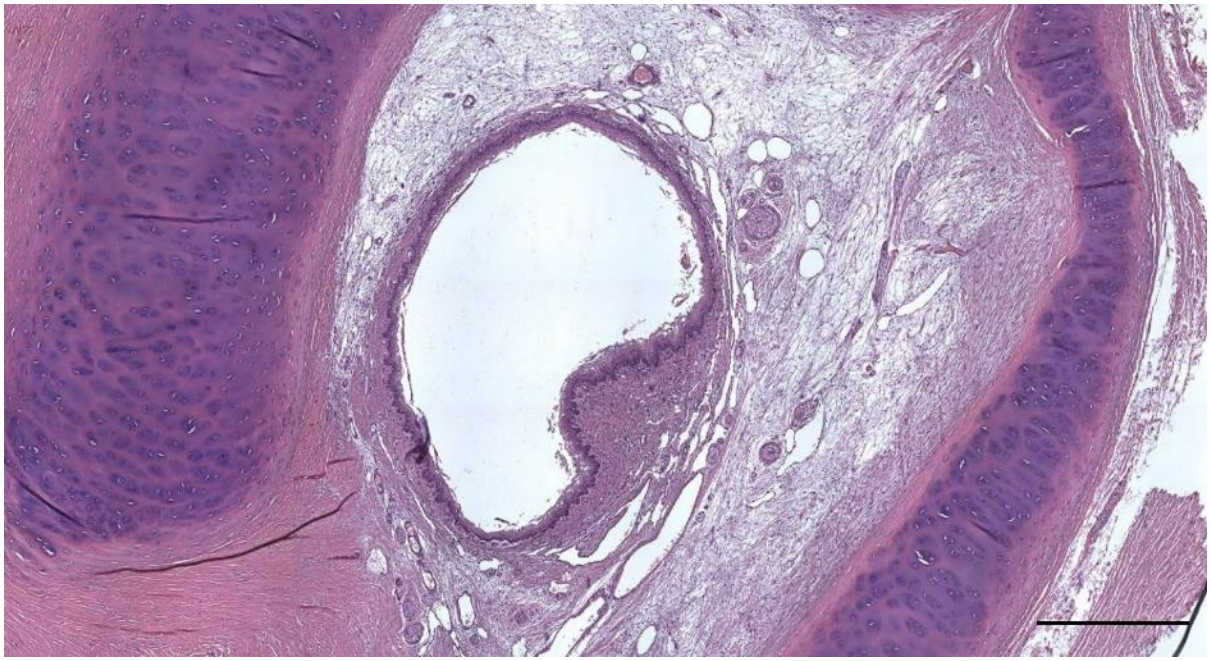

Figure 751. Histological images of the ear canal in a striped dolphin (620/17_L15). Note the ear canal with nervous tissue ridge, embedded in a web of loose (reticular) connective tissue, and surrounded by the horseshoe-shaped cartilage. Scale bar 0.5 mm

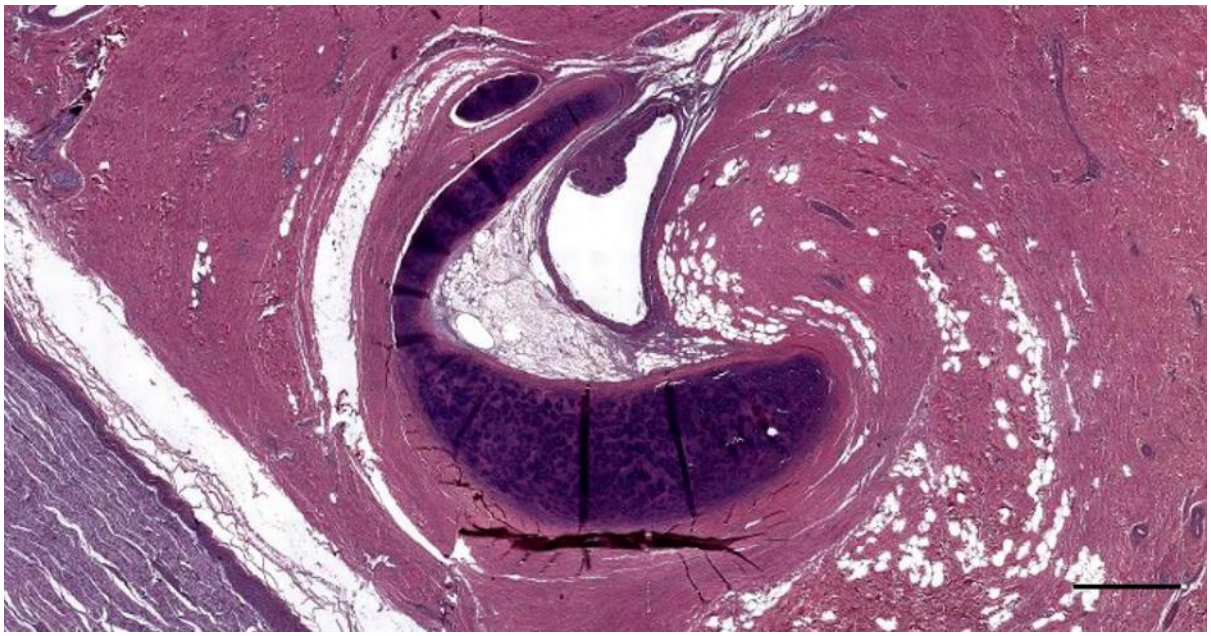

Figure 752. Histological cross-section (HE staining) of the ear canal of a bottlenose dolphin (457_R14) with prominent nervous tissue ridge and vascular lacunae, horseshoe-shaped cartilage with an additional flange, and facial nerve running ventral to the ear canal. Scale bar 1 mm

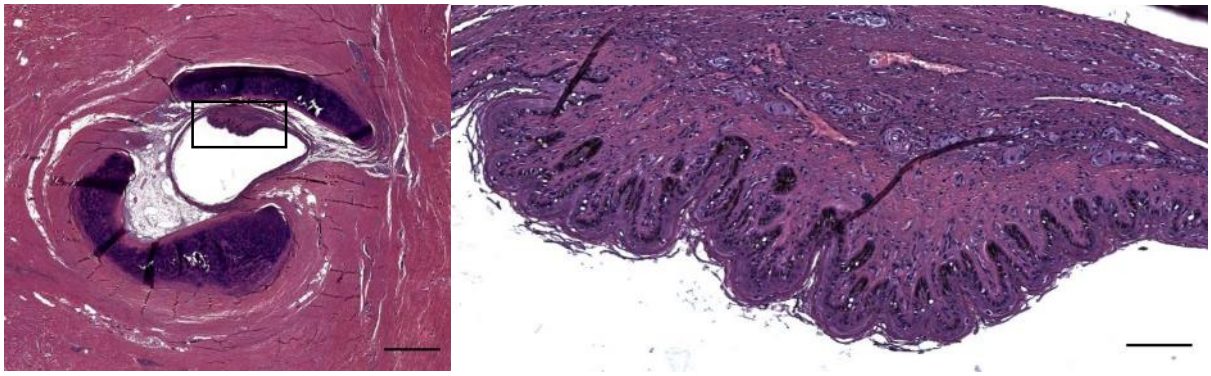

Figure 753. Histological cross-section (HE staining) of the ear canal of a bottlenose dolphin (457_R15). Note the bifurcated cartilage at the proximal end of the ear canal. Right is a detail image of the nervous tissue ridge (inset in the left image) with extensive papillary layer bulging into the canal´s lumen. Scale bar 1 mm left, 100 µm right)

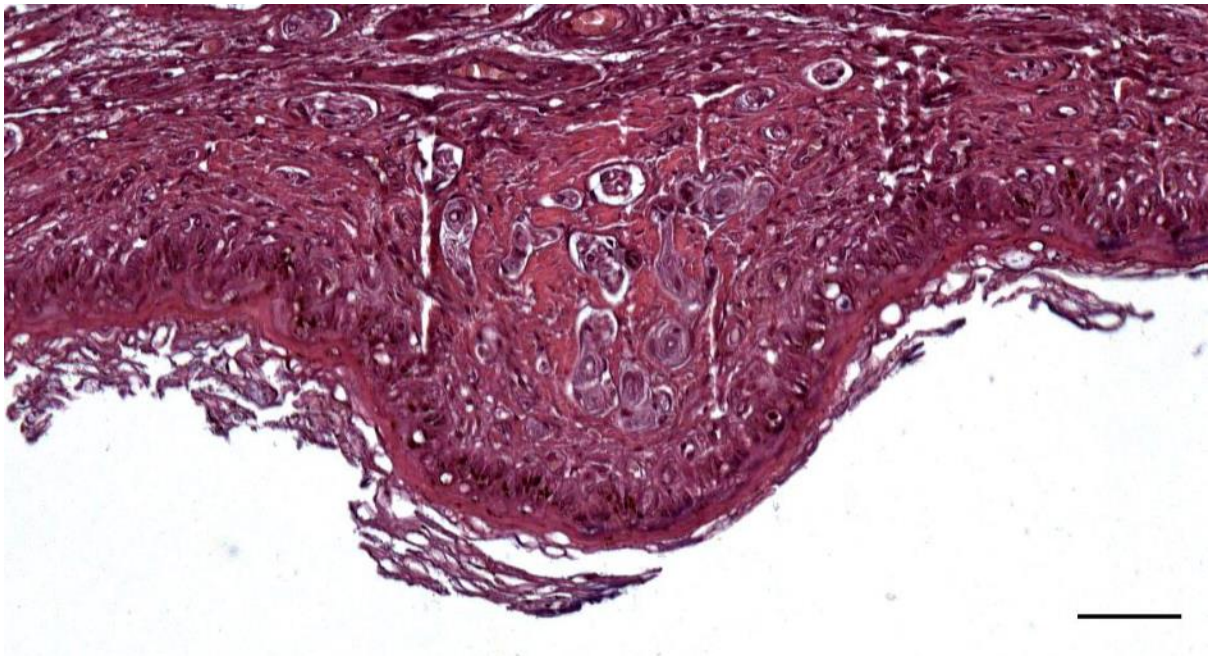

Figure 754. Histological detail image (HE staining) of the ear canal nervous tissue ridge in a decalcified block of a striped dolphin (274/18_Lx1). Scale bar 50 µm

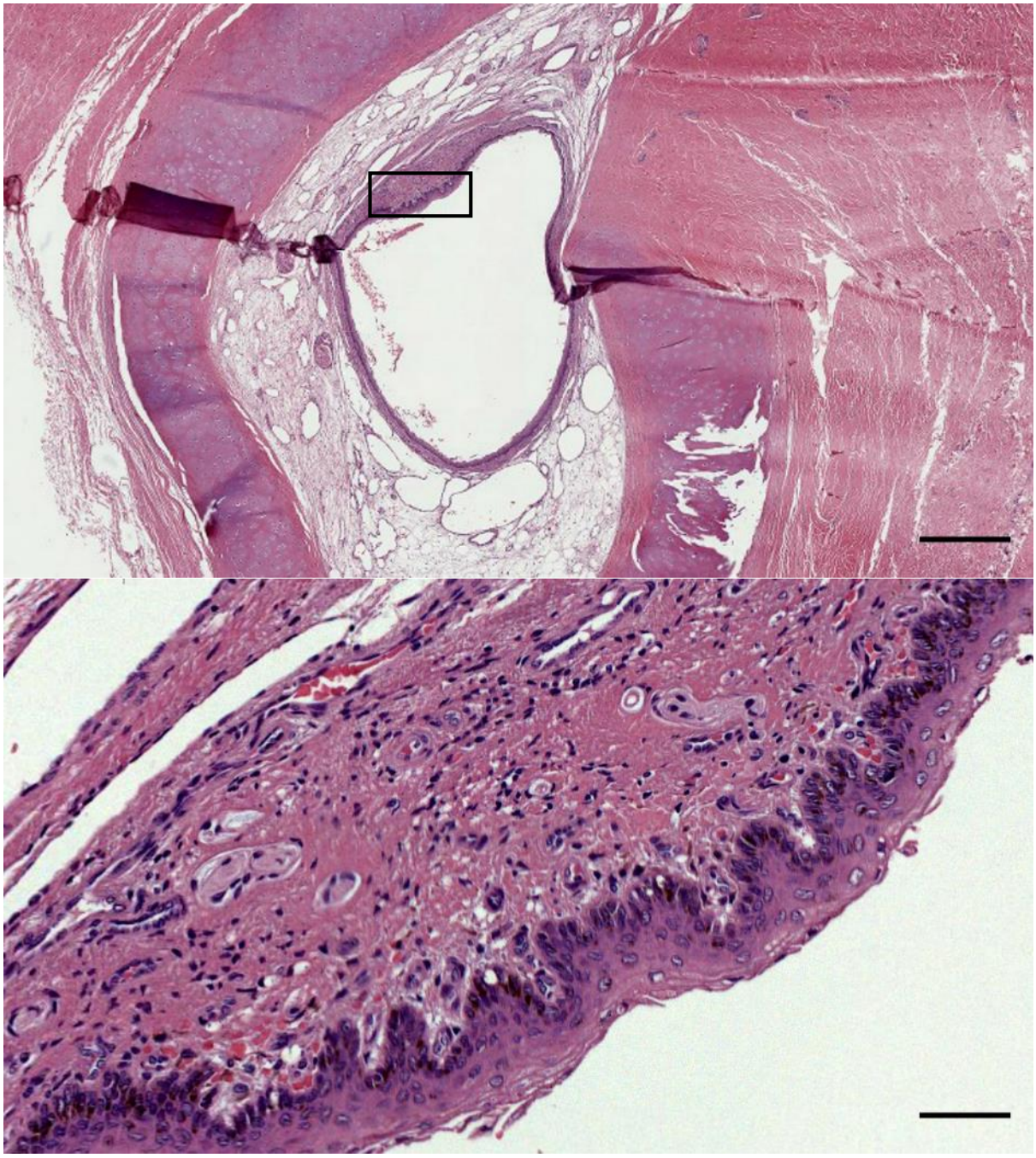

Figure 755. Histological image (HE staining) of the ear canal in a striped dolphin (168_17_9). The bottom image is a higher magnification of the insert in the top image. Scale bars 500 (top) and 50 (bottom) micron

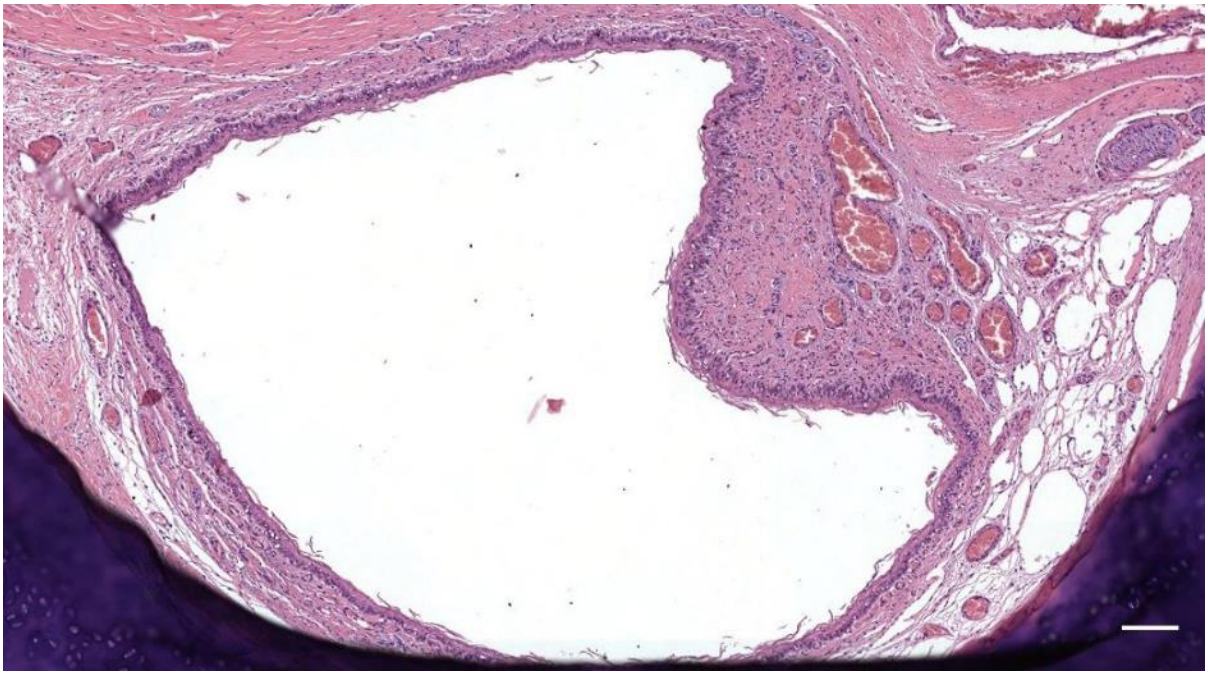

Figure 756. Histological image (HE staining) of the ear canal in a striped dolphin (274/18_R13). Ear canal with well-vascularized nervous tissue ridge. Scale bar 100 µm

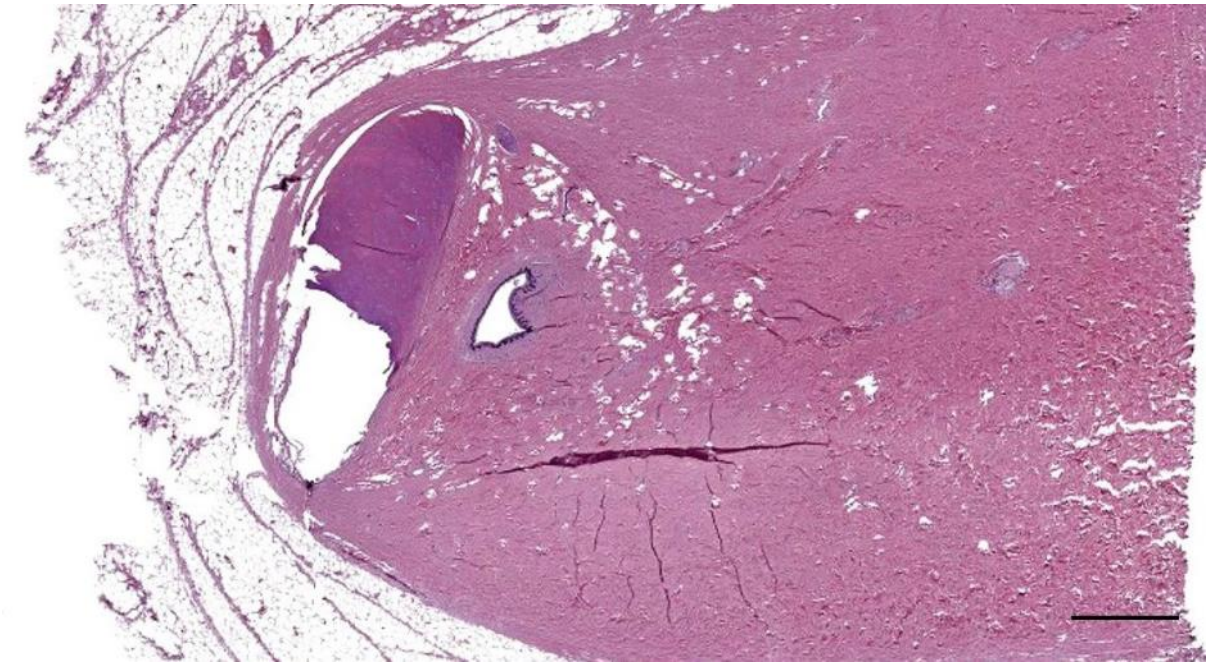

Figure 757. Histological image (HE staining) of the ear canal in a bottlenose dolphin (444_L13). Ear canal with nervous tissue ridge opposite the cartilage. Scale bar 1 mm

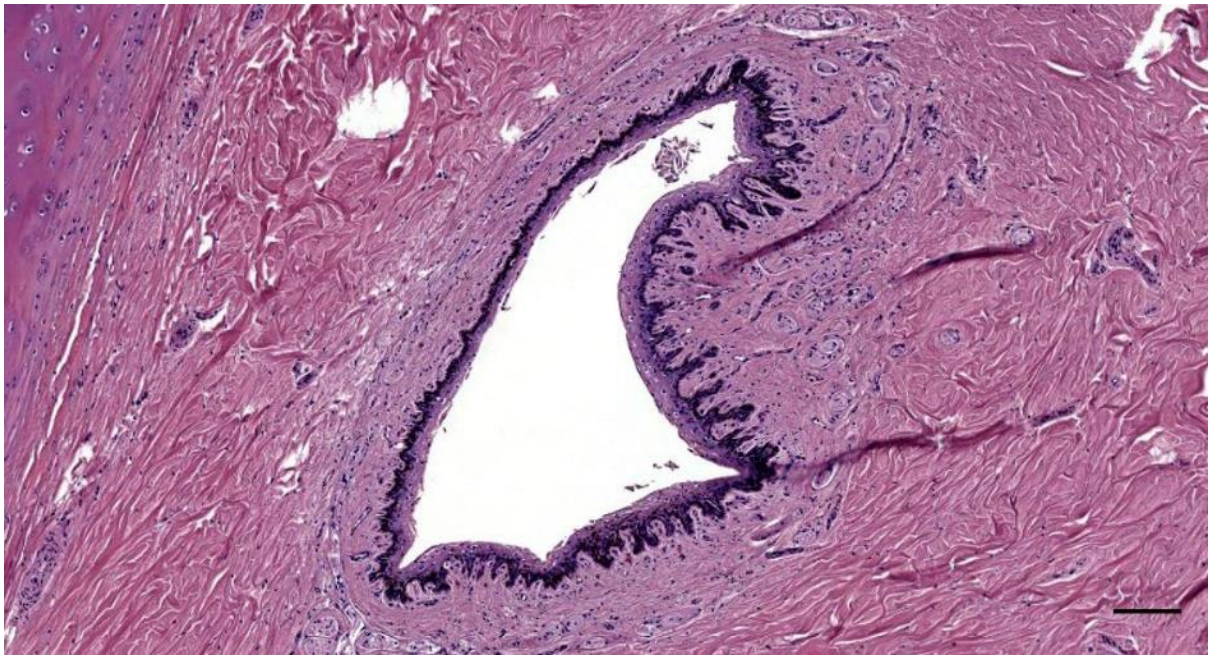

Figure 758. Histological detail of Figure 757 (444_L13). Ear canal with nervous tissue ridge. Scale bar 100 µm

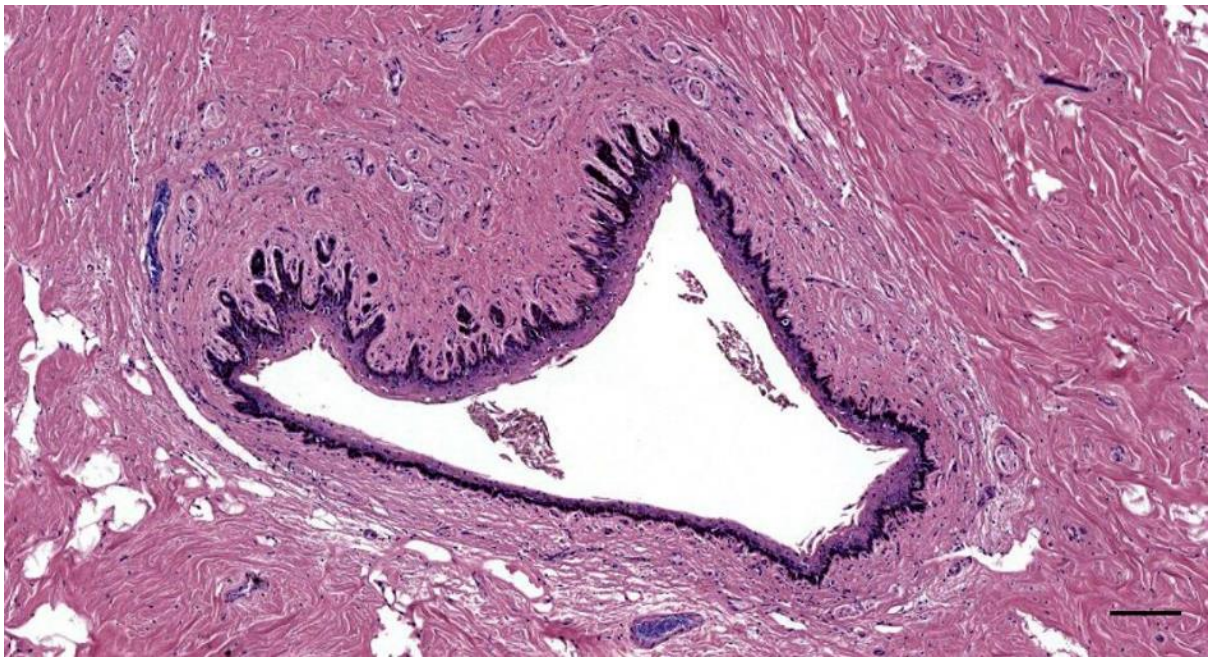

Figure 759. Histological image (HE staining) of the ear canal in a bottlenose dolphin (444_L14). Ear canal with nervous tissue ridge. Scale bar 100 µm

3.3.1.3 Morphology corpuscles

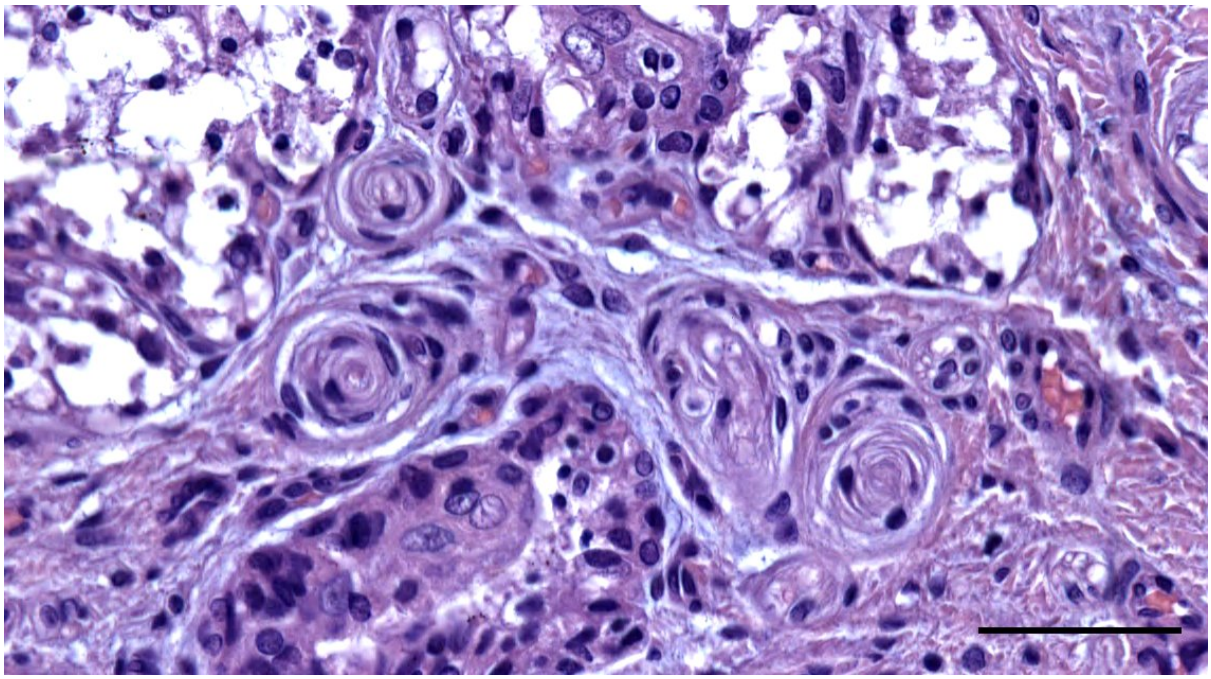

Figure 760. Histological detail (HE staining) of lamellar corpuscles associated with the auricular glands in a harbour porpoise (UT1709_R4). Scale bar 50 µm

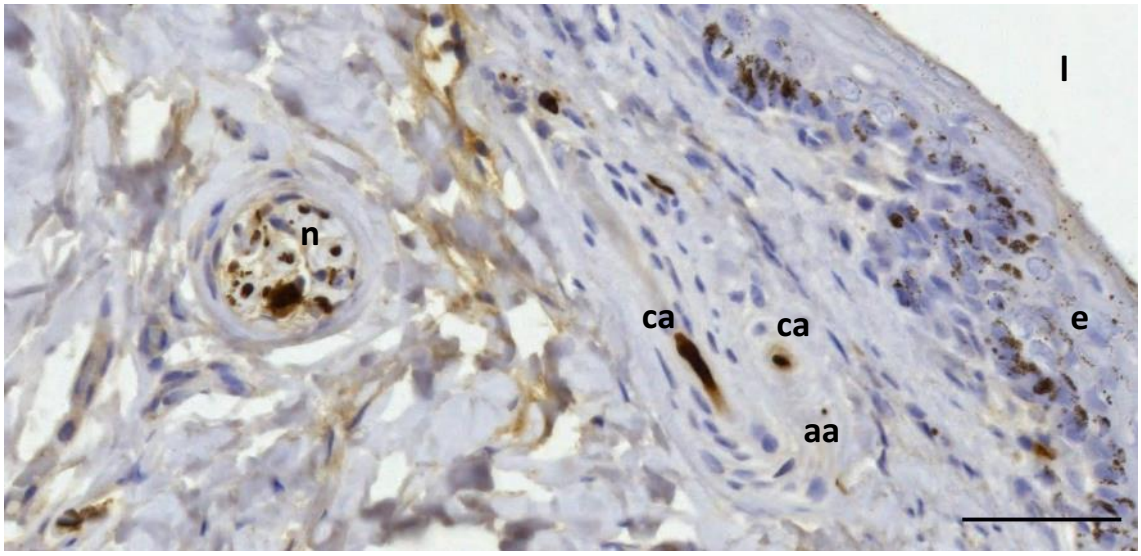

Figure 761. Anti-NF staining of the subepithelial tissue in a striped dolphin ear canal. Section through a small nerve fascicle (n) and two adjacent lamellar corpuscles: one corpuscle with a transversely cut central axon (ca) and a small accessory axon (aa) in the periphery, and one obliquely cut corpuscle. l: lumen of the ear canal; e: epithelium. Scale: 50 µm

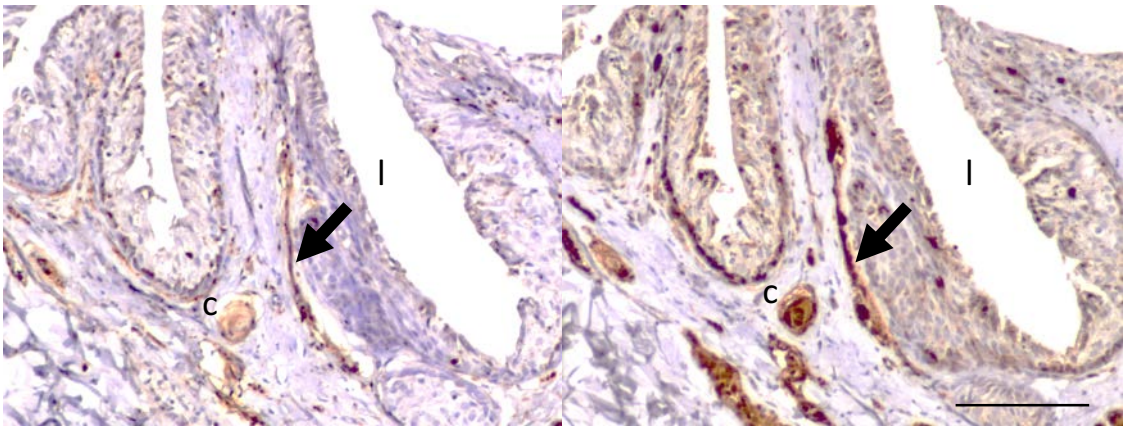

Figure 762. Anti- PGP 9.5 (left) and anti- NF (right) staining of the subepithelial tissue in a striped dolphin ear canal. Note the IR below the basement membrane and an intrapapillary myelinated nerve fibre stained by both antibodies (arrows). c: lamellar corpuscle. l: ear canal lumen. Scale: 100 µm

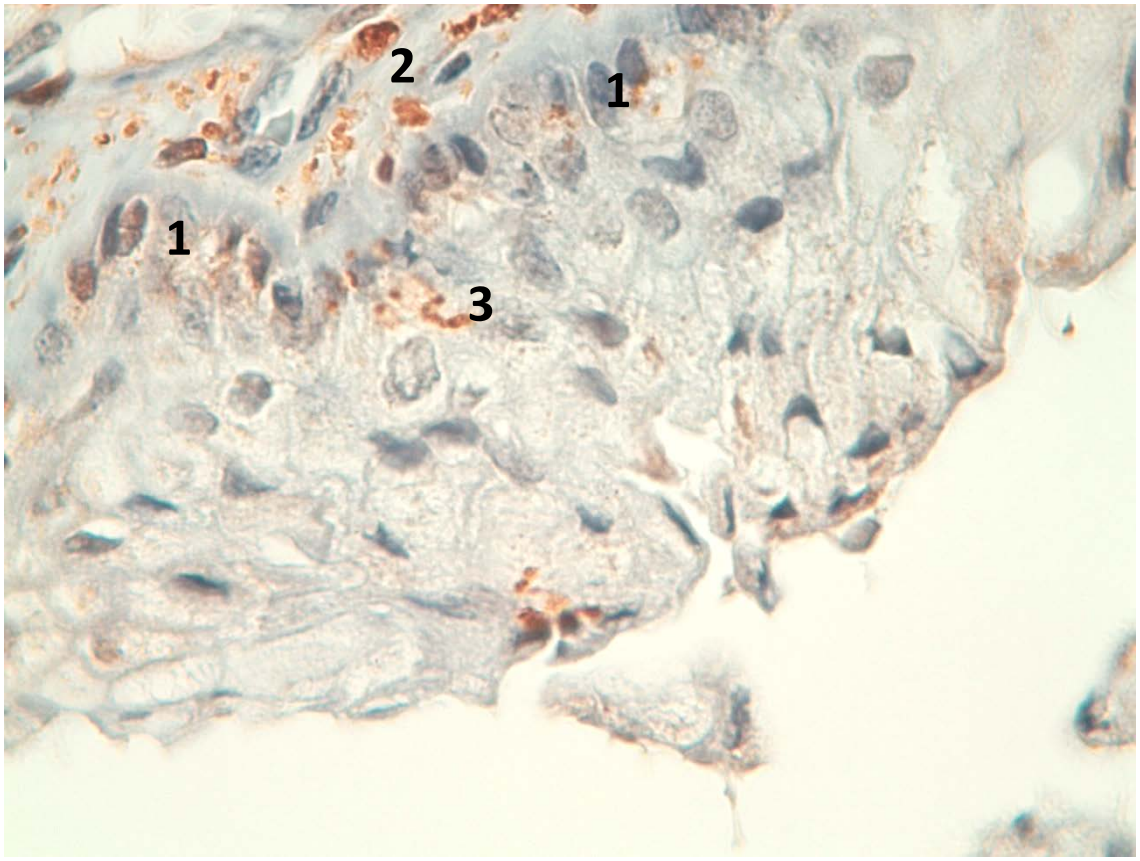

Figure 763. Histological detail of the auricular epithelium, stained with anti-PGP 9.5 (1:500, block, melanin bleaching). Positivity within the epithelium, indicating intraepithelial nerve fibres. 1. Germinal layer; 2. Subepithelial immunoreaction; 3. Intraepithelial nerve ending

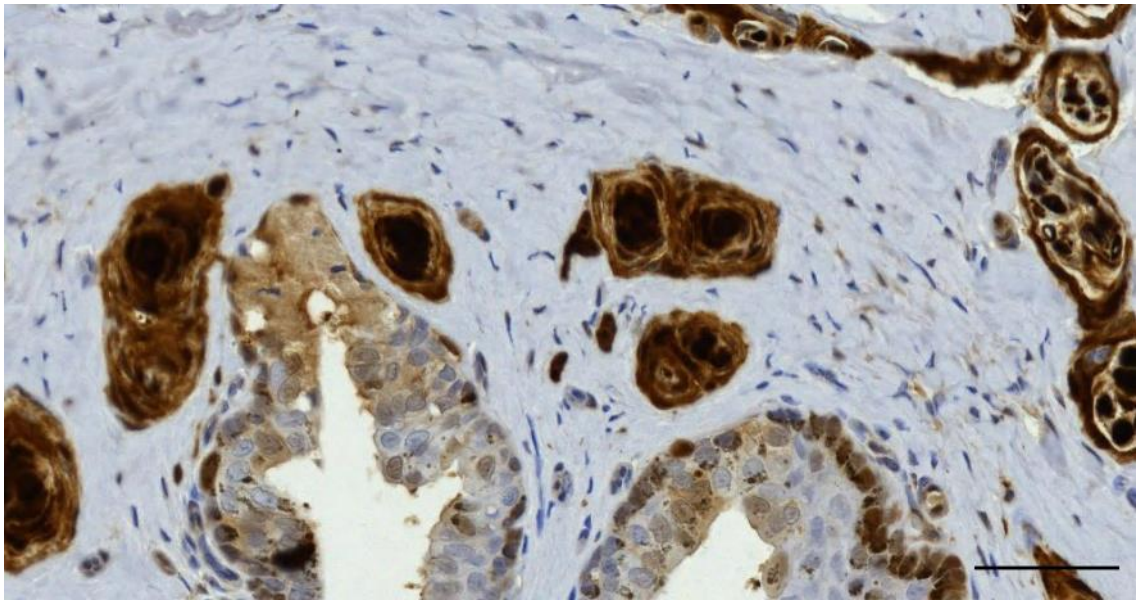

Figure 764. Histological image of lamellar corpuscles associated with the ear canal in a striped dolphin, IHC stain with anti-S-100 (S. coeruleoalba). Note the more intense staining of the central lamellae in comparison to the peripheral layer. Scale bar 50 µm.

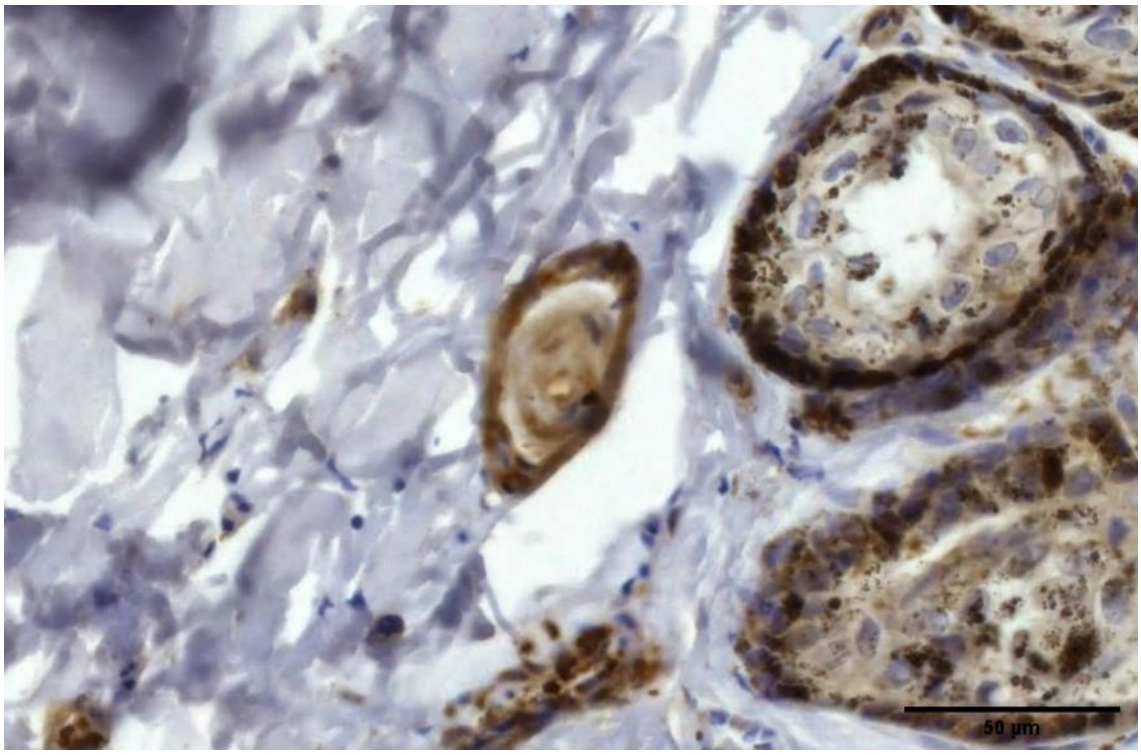

Figure 765. Immunohistochemical stain with anti-NSE in blocking diluent shows immunoreactivity of the peripheral layer of the corpuscles surrounding less intense staining of the central lamellae (in contrast with S100 reactivity, e.g. Figure 764). Scale bar 50 µm

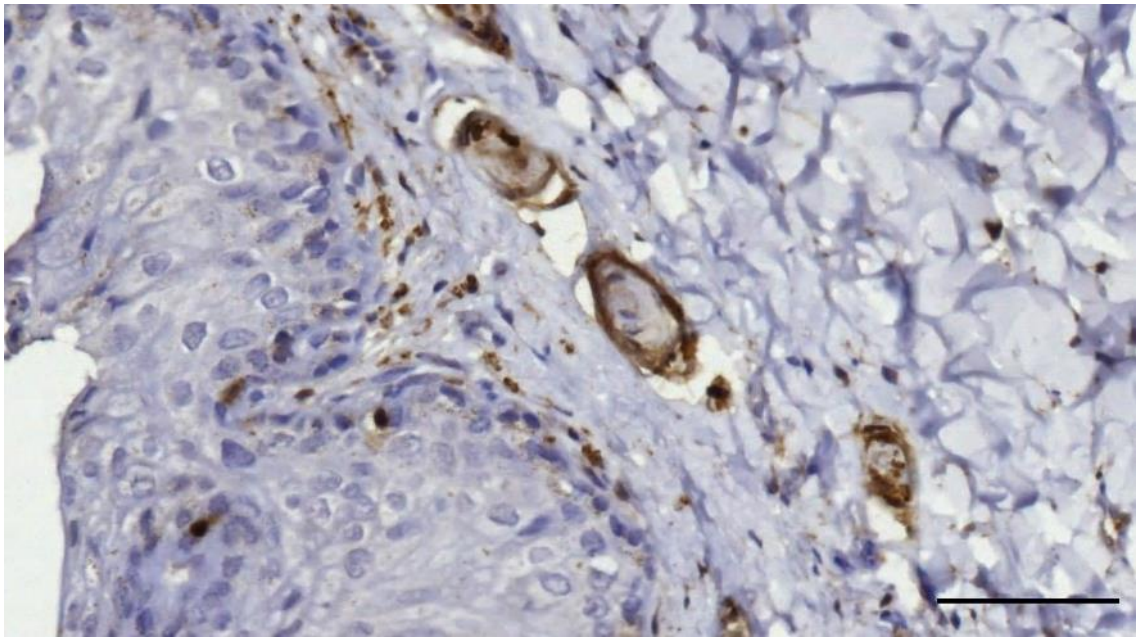

Figure 766. IHC stain with anti-PGP 9.5 (1:2k, blocking diluent). Note the immunoreactivity of the peripheral layer of the corpuscles (in contrast with S100 reactivity, e.g. Figure 764) and the positive reaction in the tissue beneath the epithelium. Scale bar 50 µm

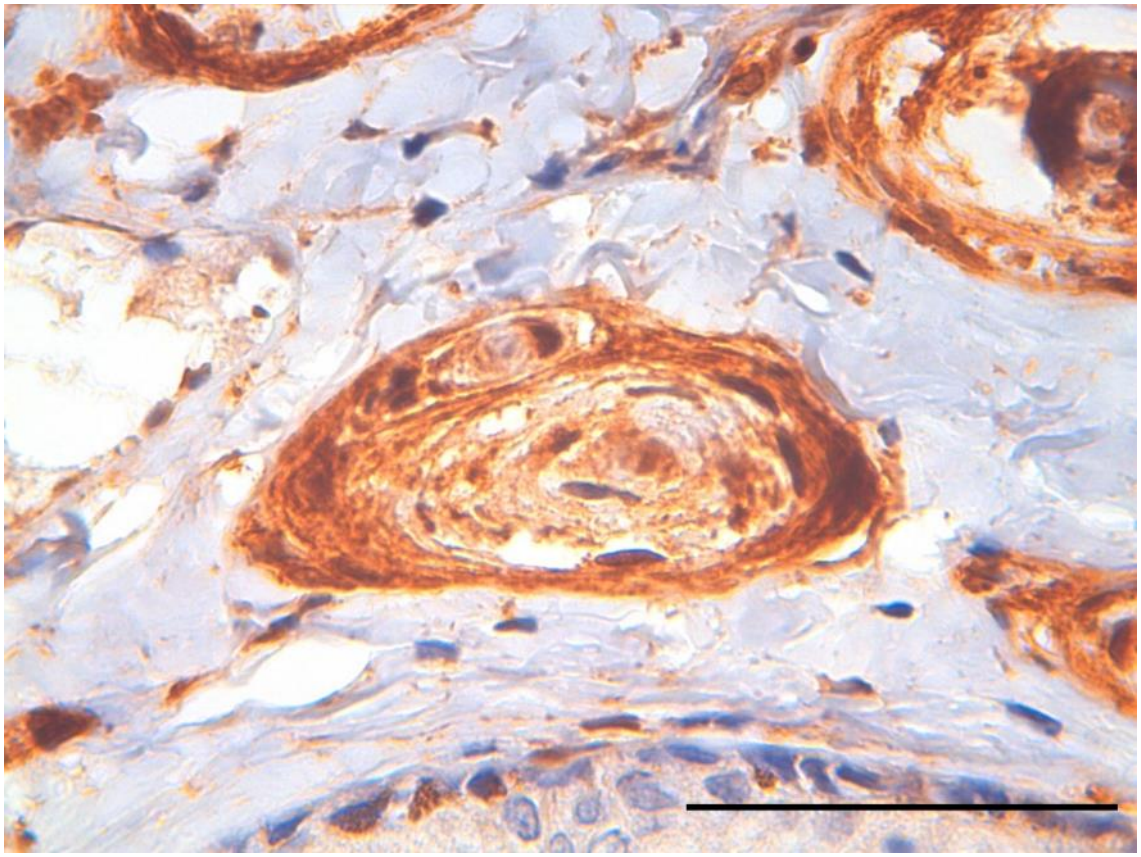

Figure 767. Detail of a corpuscle stained with anti-PGP 9.5 (S. coeruleoalba). Scale bar 50 µm.

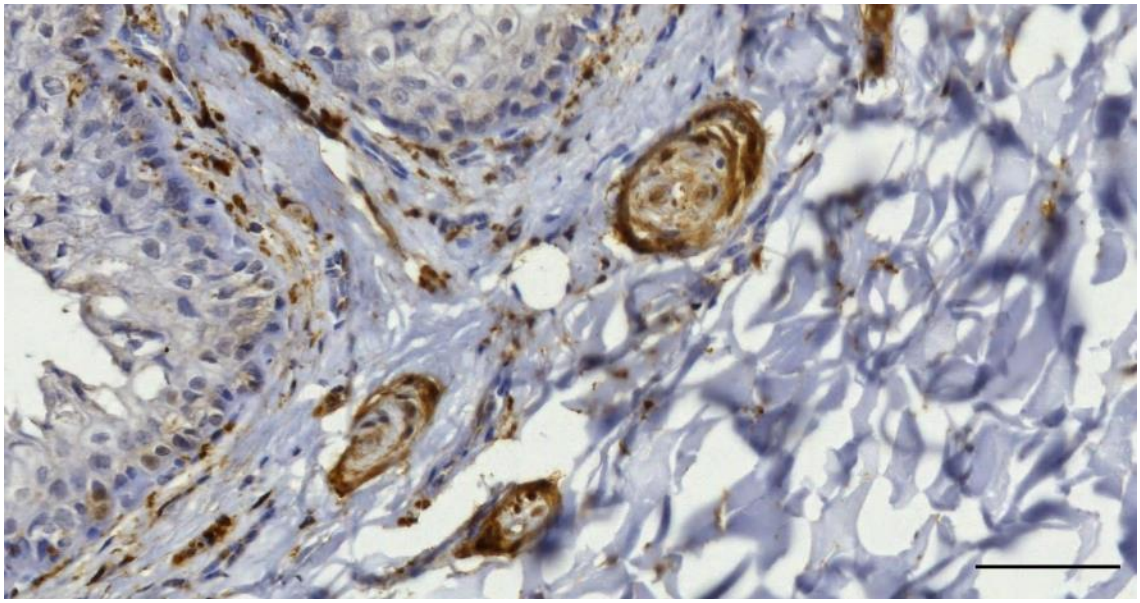

Figure 768. IHC stain with anti-PGP9.5 (S. coeruleoalba). Note the positivity of the most peripheral layers of the corpuscles. Scale bar 50 µm.

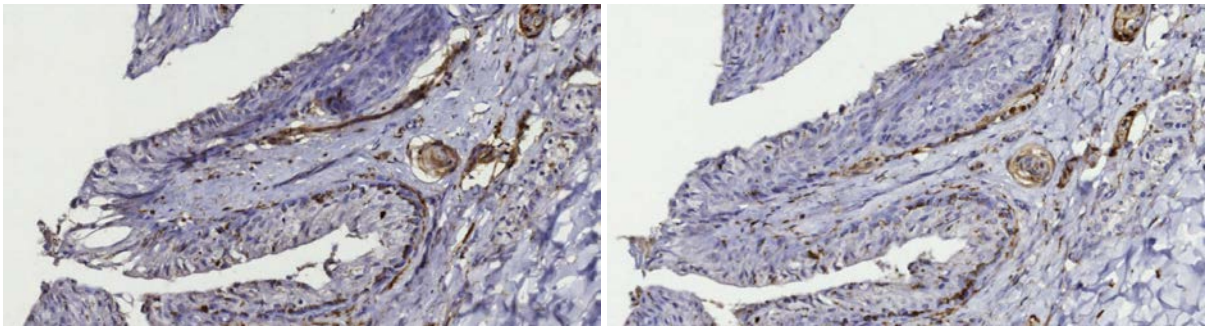

Figure 769. IHC stain with anti-PGP 9.5 (dilution 1:2k, no blocking; two adjacent cross-section of the ear canal of striped dolphin with different melanin bleaching times). The distinction between true positivity and melanin pigmentation in the epithelium was based on the granular aspect of the latter. Note the IR in the dermal papilla in both sections, which might be a nerve fibre entering the dermal papilla. Scale bar 25 µm

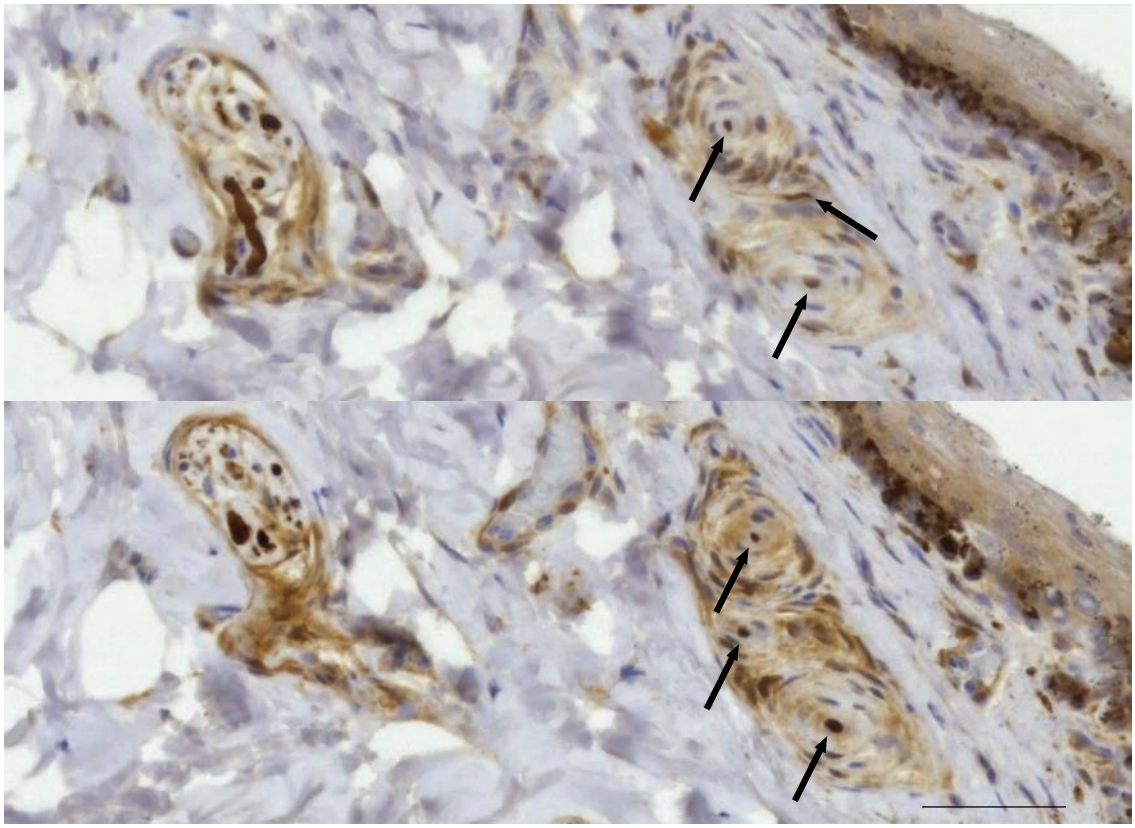

Figure 770. Immunohistochemical stain for anti-NSE (with blocking diluent) shows immunoreactivity of the axons in a composite lamellar corpuscle and a nerve bundle in two sections that are separated by 8 µm between the centres of the sections (S. coeruleoalba). Note the course of an axon in between two corpuscles (of the same corpuscle complex) that forms a third, small lamellar core in the bottom section. There are less intense colourations of the perineurium and about half of the nuclei in the corpuscles. Scale bar 50 µm.

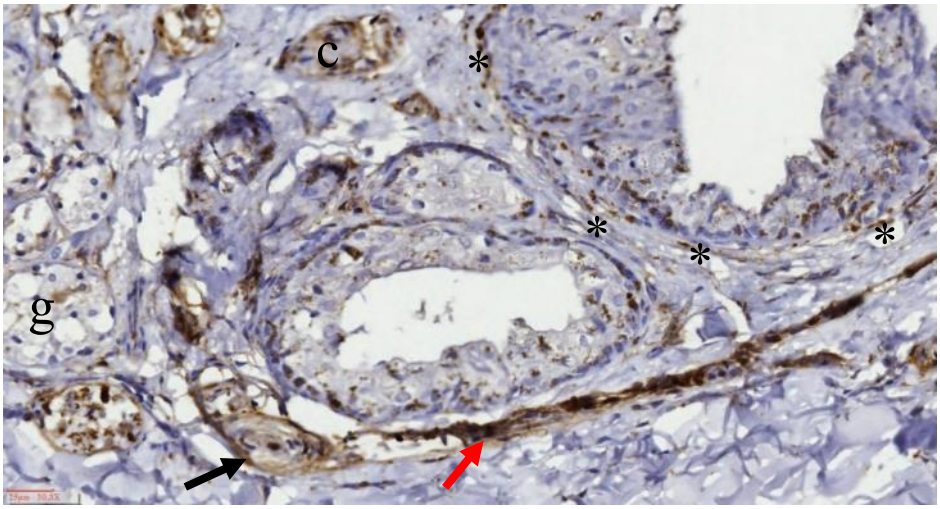

Figure 771. IHC stain with anti-PGP 9.5 (Dilution 1:2000; no blocking; melanin bleaching) Small nerves and corpuscles in the vicinity of the ear canal (l) and associated glandular structures (g). Note the association of a corpuscle, with a positively stained axon and outer layer (black arrow), with a single nerve fibre (longitudinal cut) (red arrow). N: nerve bundles; c: corpuscle; asterisks: multifocal positivity below the basement membrane.

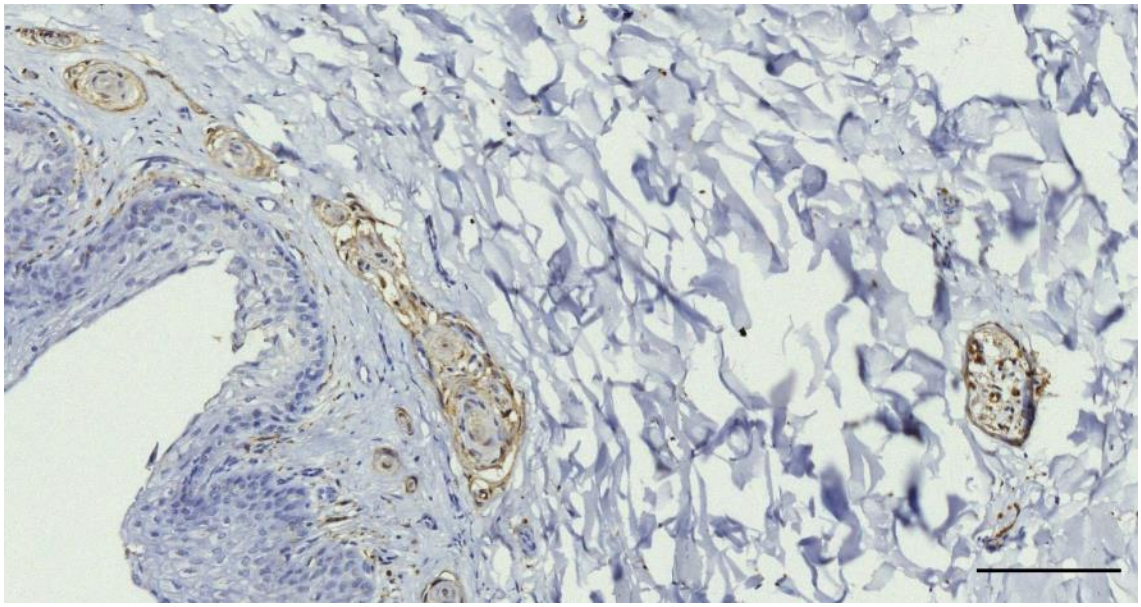

Figure 772. IHC stain with anti-PGP 9.5 (Dilution 1:2000; no blocking; melanin bleaching).

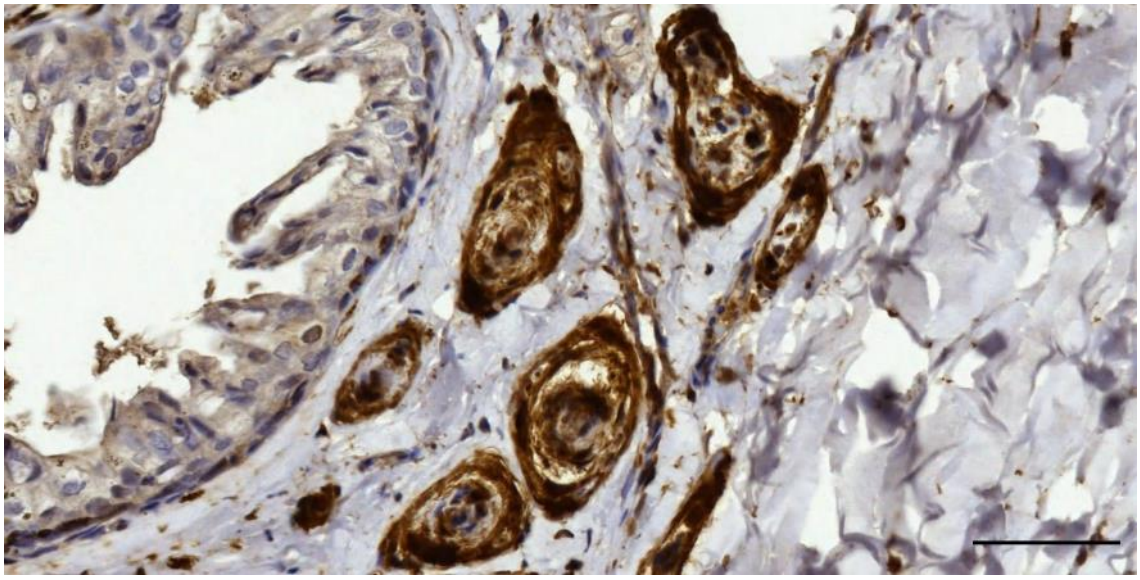

Figure 773. IHC image with anti-PGP9.5 (dilution 1:500). Nerves and corpuscles, immunoreactivity in the axons and perineurium and peripheral layer in corpuscles. Scale bar 50 µm

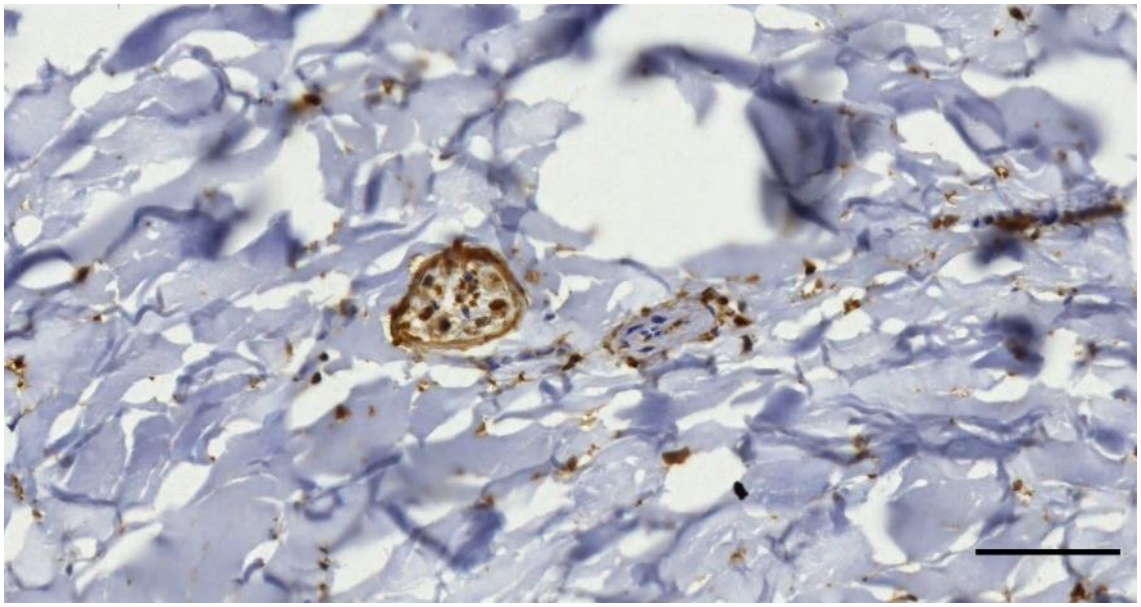

Figure 774. PGP 9.5 (1:500, block, melanin bleaching). A small nerve fascicle and arteriole located in the connective tissue around the ear canal. Axons stains positive, the endoneurium stains negative, and the perineurium stains positive. The artery wall is negative for PGP 9.5 but the tunica externa (adventitia) stains positive due to the presence of nervi vasorum.

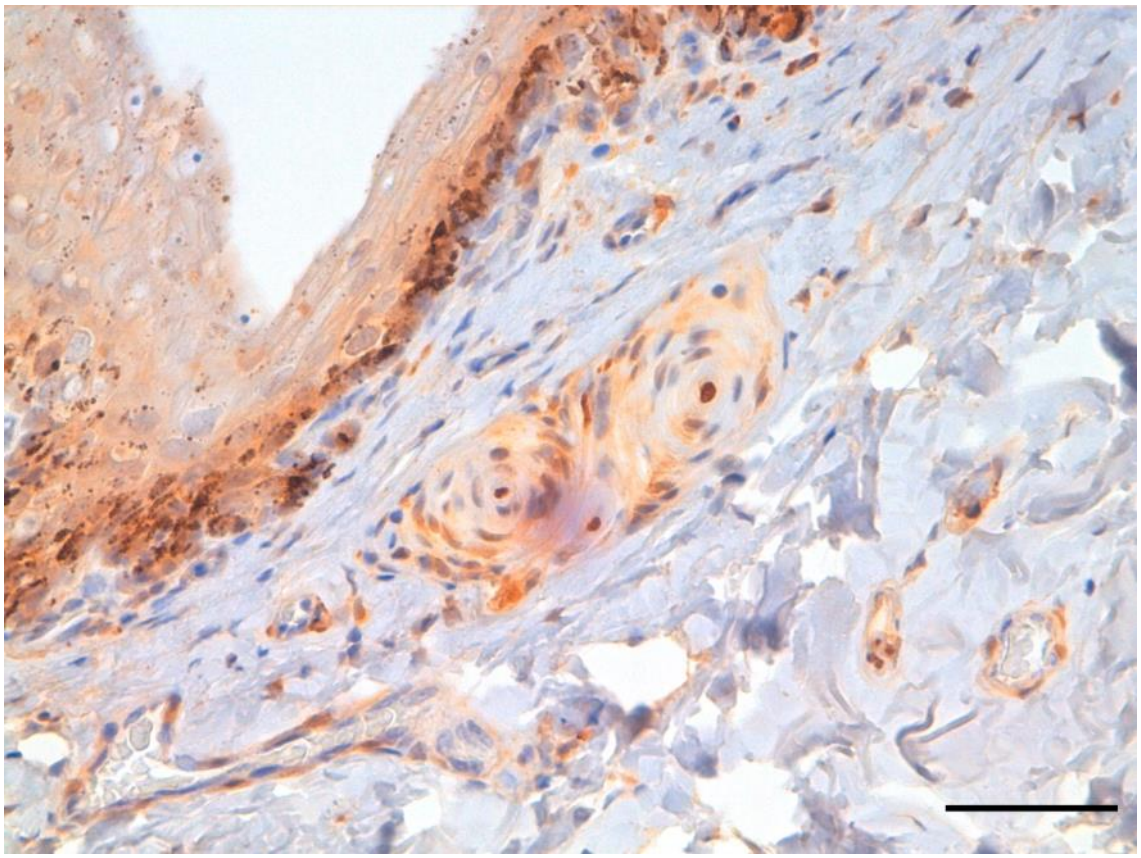

Figure 775. Immunohistochemical stain for anti-NSE (with blocking diluent). Note in the immunoreactivity of the central axon and the cytoplasm of the lamellae with most intense positivity in the peripheral layer. Scale bar 50 µm

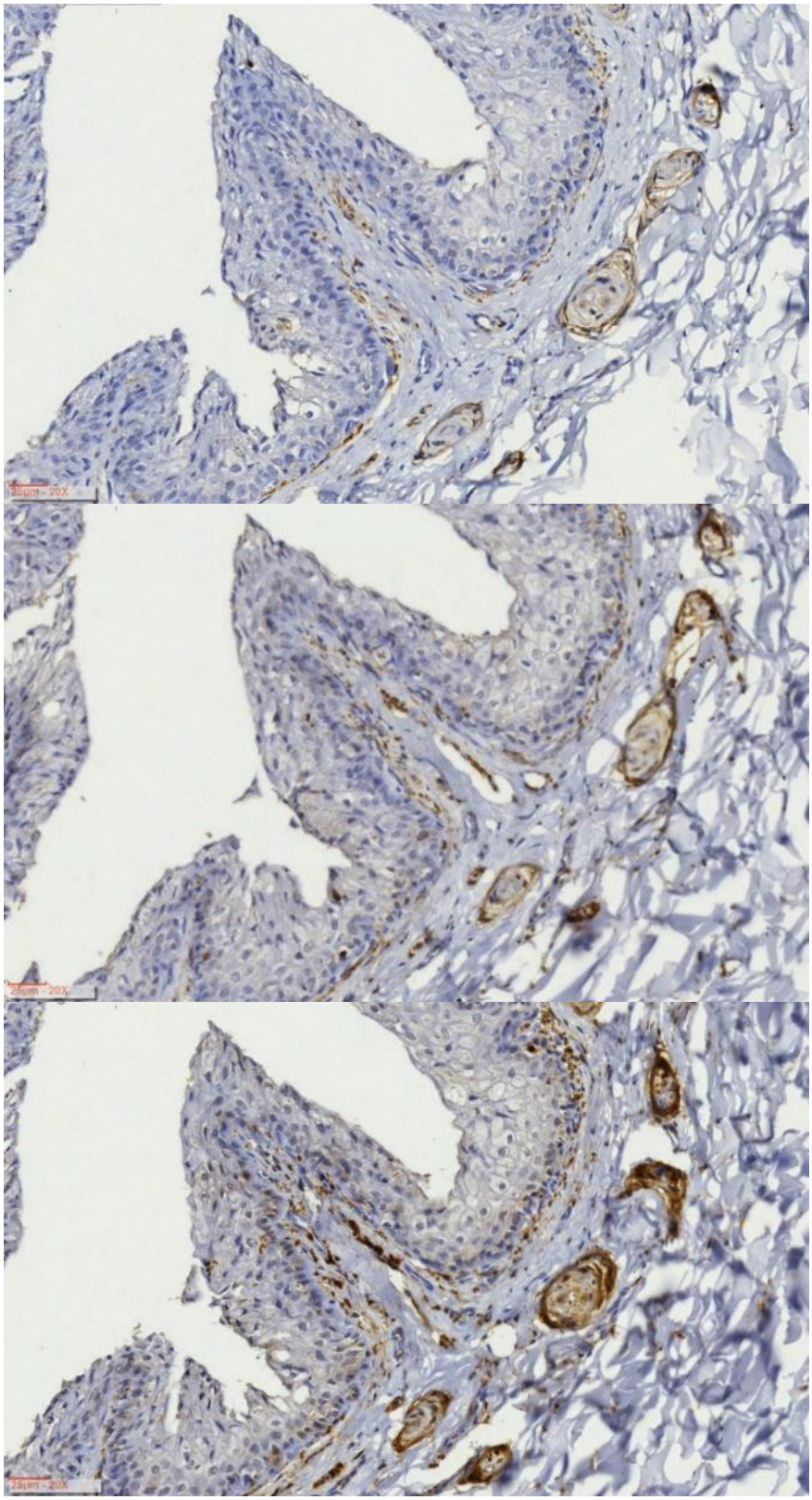

Figure 776. IHC staining of three consecutive sections with anti-PGP 9.5. Top: dilution 1:2000, blocking, melanin bleaching; Middle: dilution 1:2000, no blocking, melanin bleaching; Bottom: dilution 1:500, blocking, melanin bleaching.

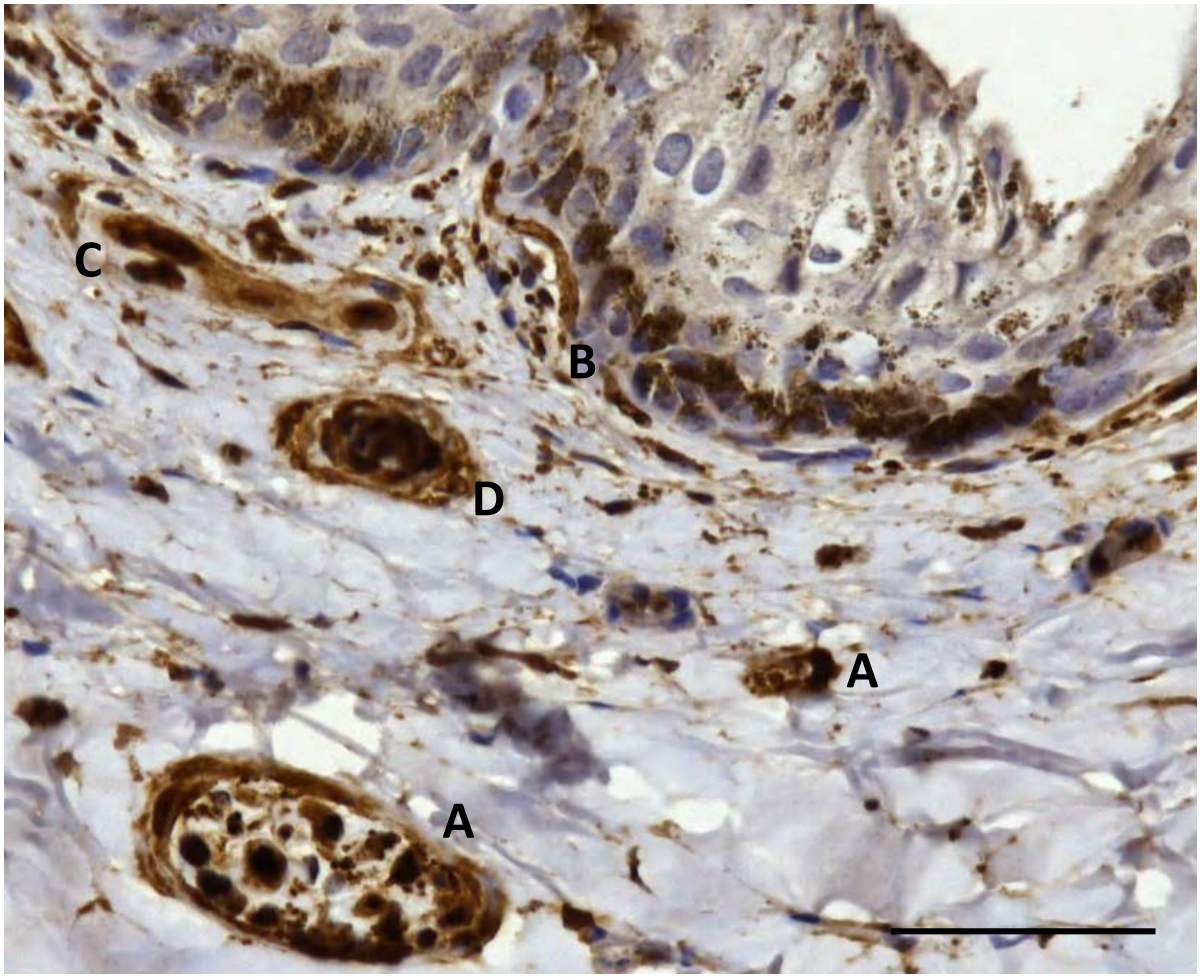

Figure 777. IHC staining of nervous structures beneath the epithelium, stained with anti-PGP 9.5. A: small nerve; B: axon running along the basilar membrane, entering a small dermal papilla; C: oblique section of a simple lamellar corpuscle with multiple sections through the axon; D: transverse section of a simple lamellar corpuscle. Scale bar 50 µm

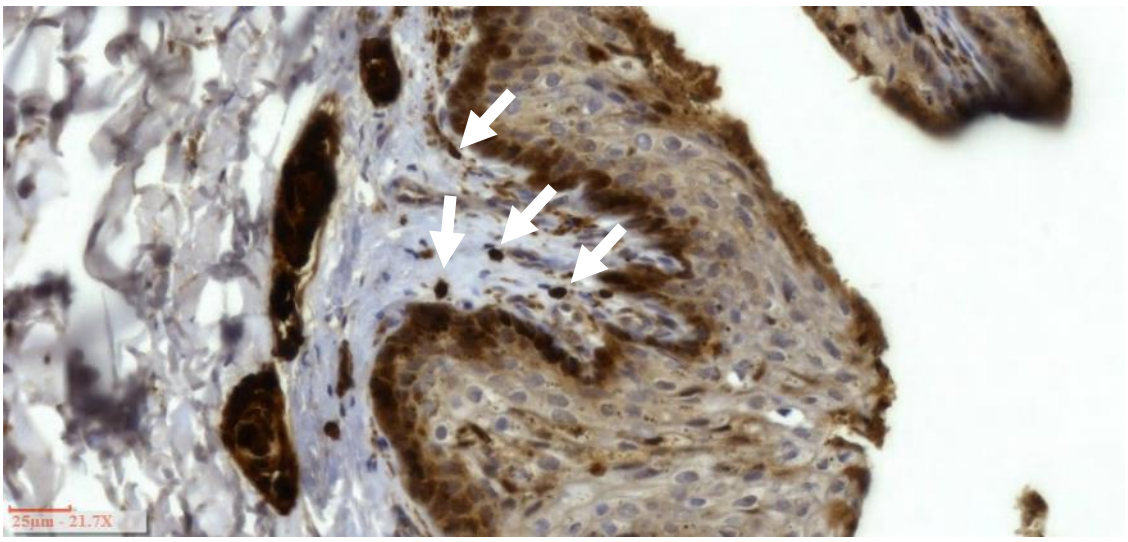

Figure 778. IHC stain with anti-S-100. The distinction between nerves and corpuscles is not clear as both structures can appear as intensely stained ´blobs´. There is a positive reaction in the tissue below the basement membrane, indicating the presence of small myelinated nerve fibres entering the dermal papillae (most clearly identifiable at the top of the image).

.

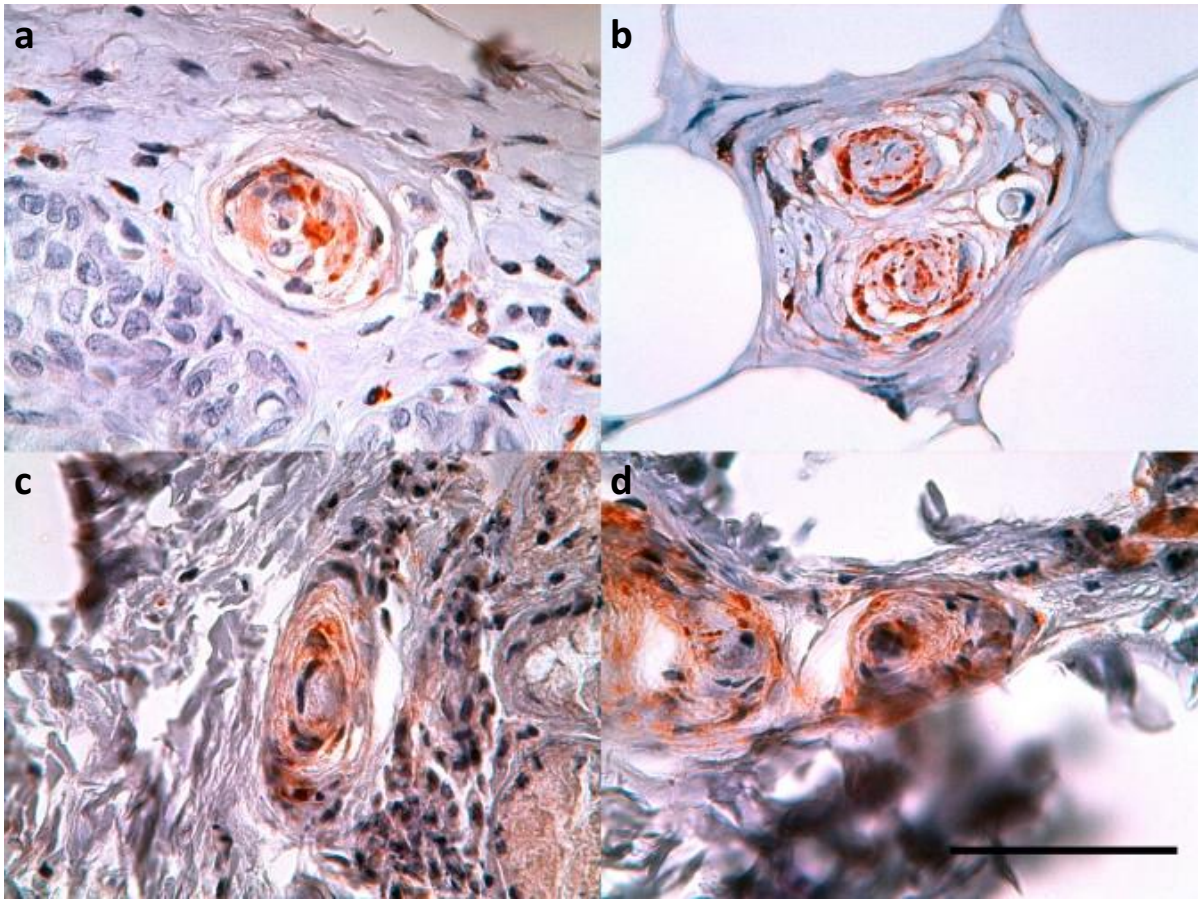

Figure 779. PGP 9.5 (1:500, block, no bleaching). Immunoreactive lamellar corpuscles in the vicinity of the ear canal in common dolphin (a), Cuvier's beaked whale (b), long-finned pilot whale (c), and bottlenose dolphin (d). Scale bar 50 µm (De Vreese et al., 2020).

3.3.2 TEM Corpuscles and Nerves

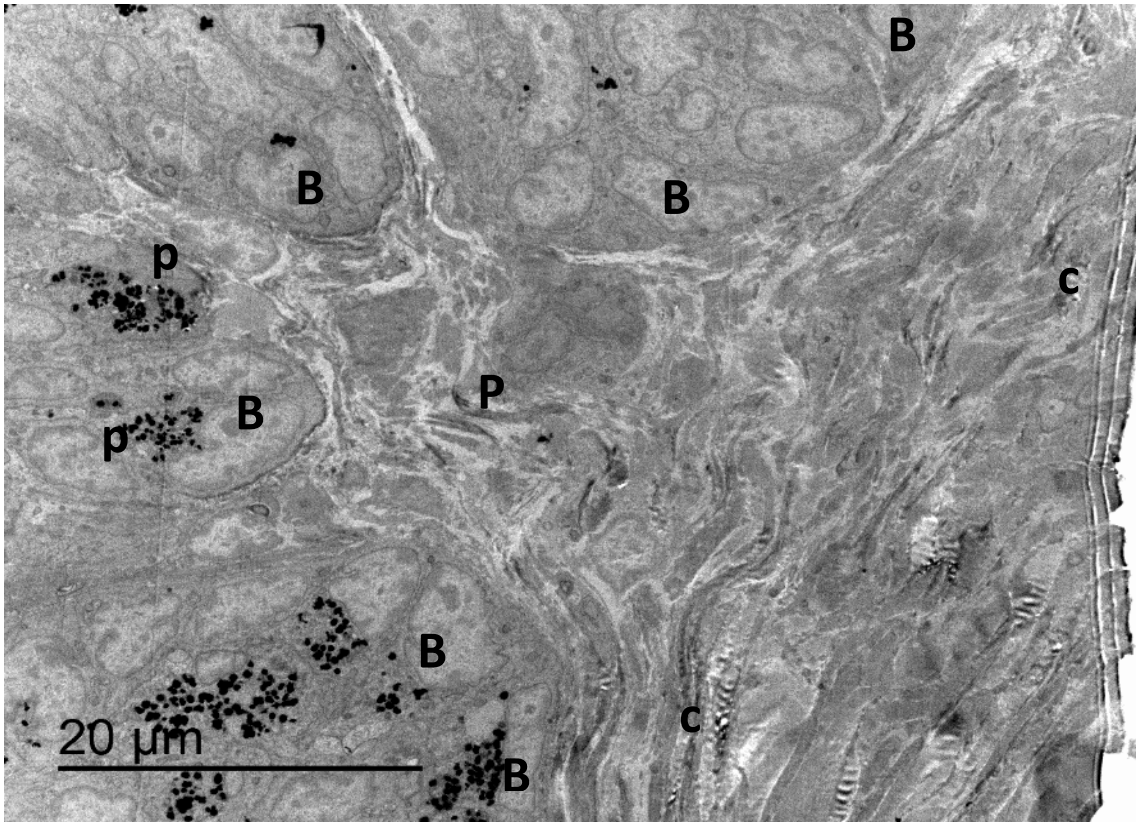

Figure 780. Epithelium and underlying subepithelial tissue B: stratum basale; p: melanin pigment; c: collagen fibres. (TEM x 3000)

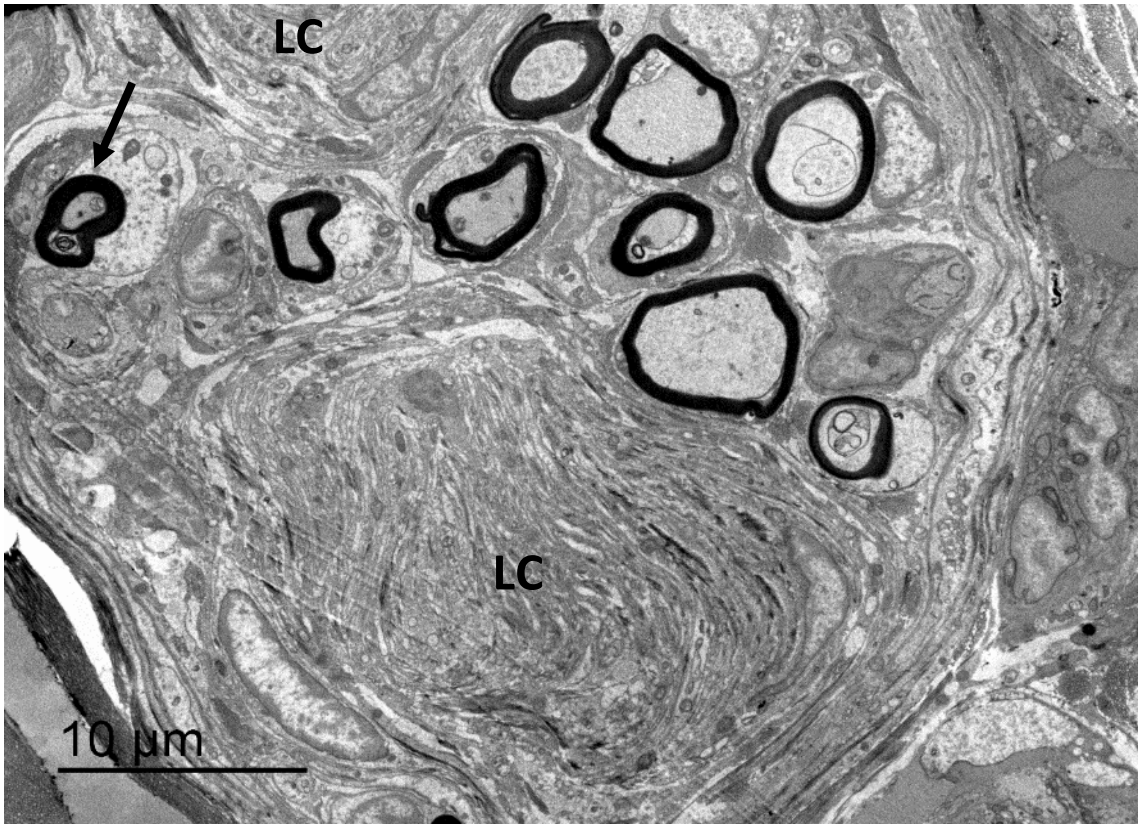

Figure 781. Oblique section through a lamellar corpuscle (LC) and several myelinated nerve fibres embedded within the same perineurial capsule; Arrow: myelin infolding and partitioning

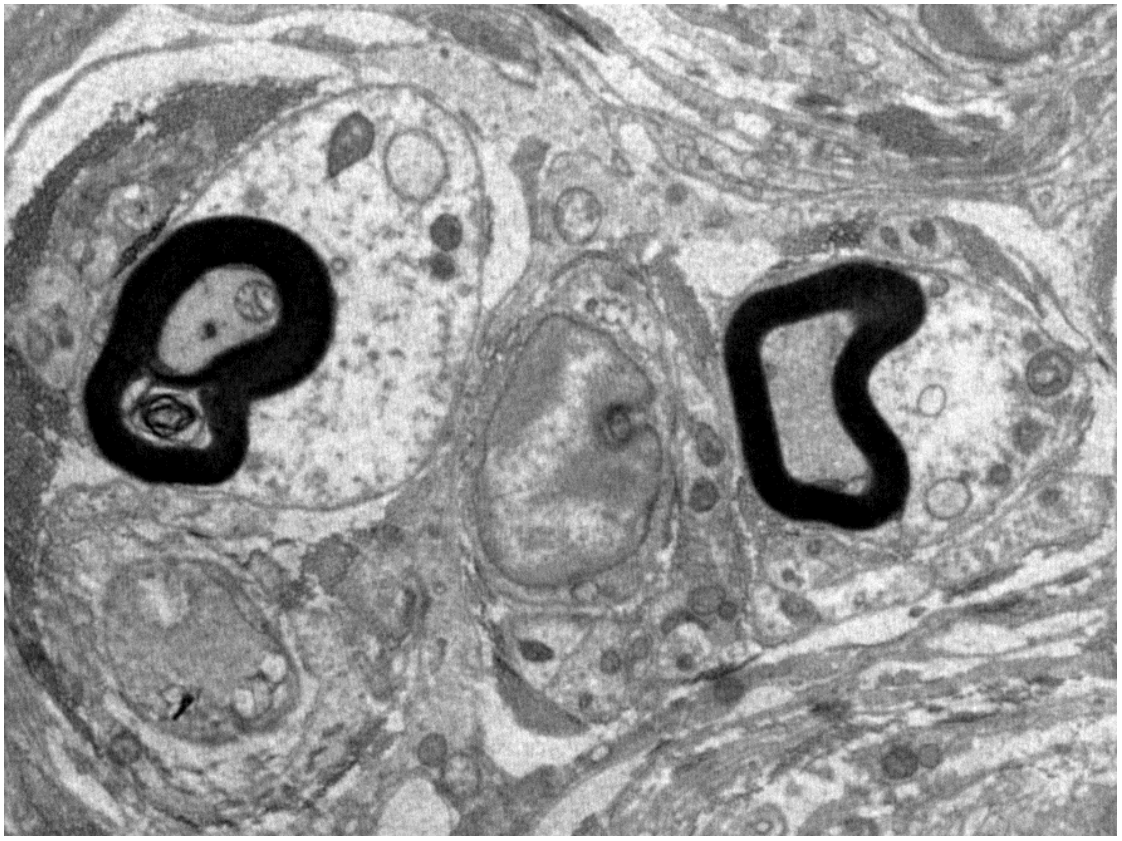

Figure 782. Detail of the previous image, showing the possible lymphocytes in between two myelinated nerve fibres. The nucleus of these cells is slightly indented and contains a substantial amount of heterochromatin.

Figure 783. Overview of a nerve fascicle with myelinated and unmyelinated nerve fibres. (TEM x 8000)

Figure 784. TEM images of a glandular duct and two myelinated nerve fibres.

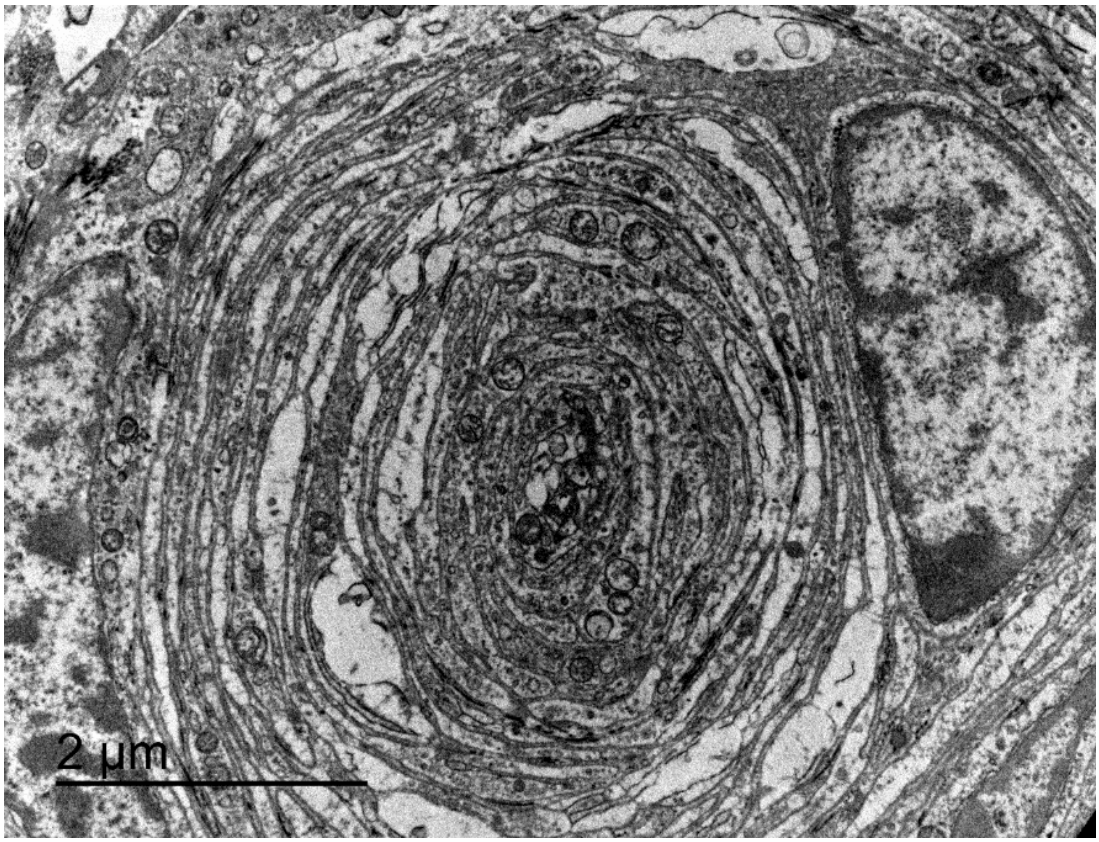

Figure 785. TEM image of a lamellar corpuscle, very similar in structure to a 'corpuscular ending' in the dermis from the opossum snout (Munger, 1971, Fig 10b)

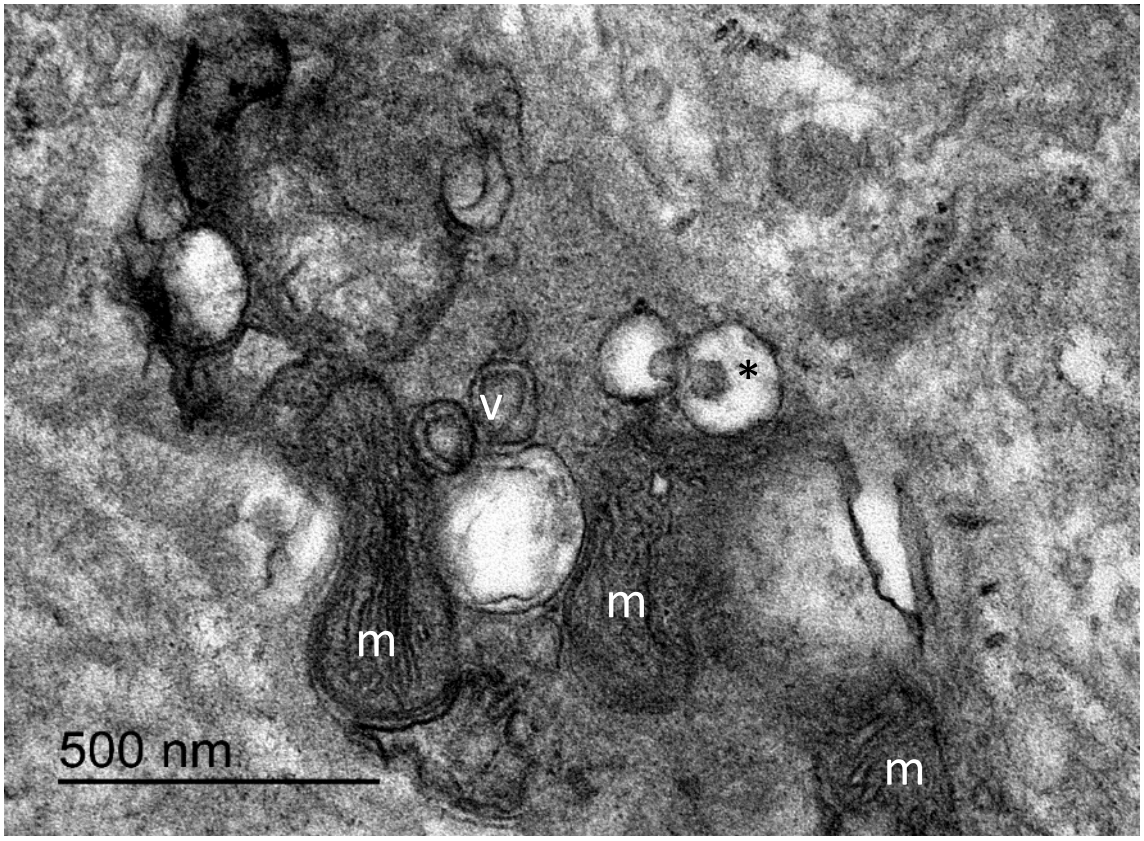

Figure 786. Detail of** Error! Reference source not found.**. The axon terminal with mitochondria (m), vesicles (v), and unknown structures (*).

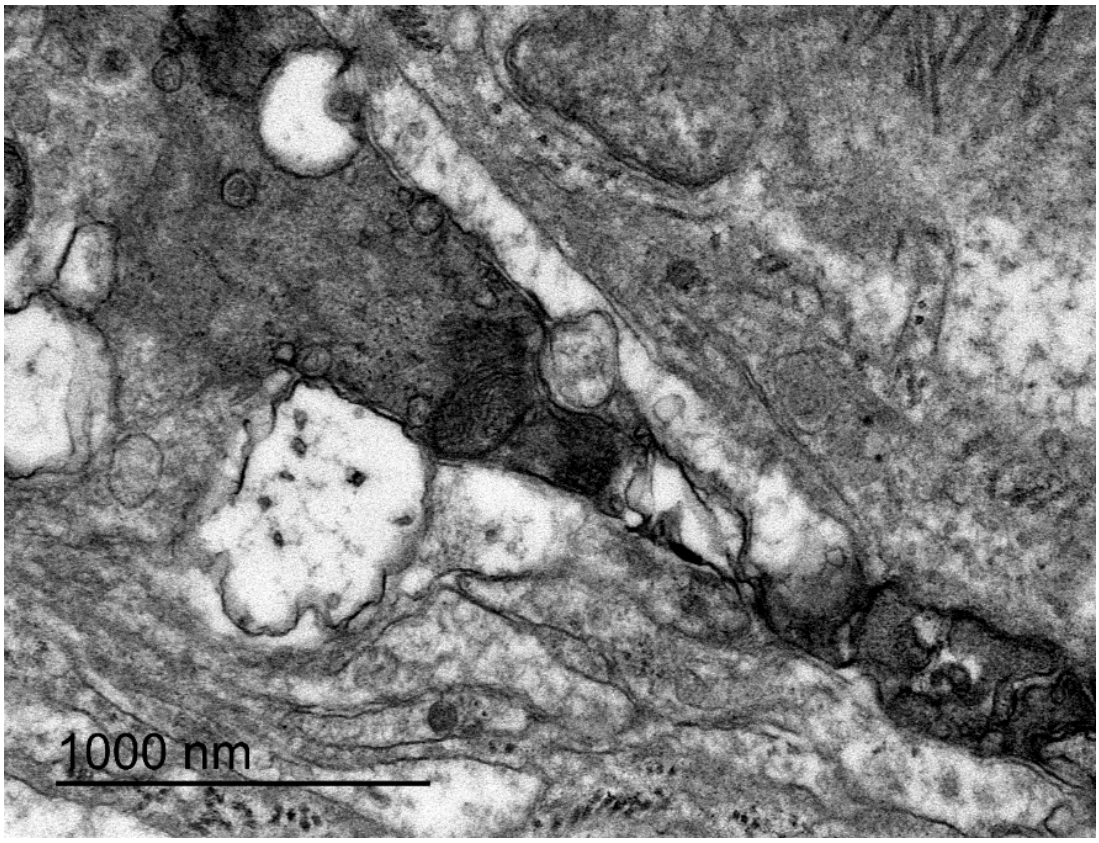

Figure 787. Detail of** Error! Reference source not found.**. The axon terminal pole.

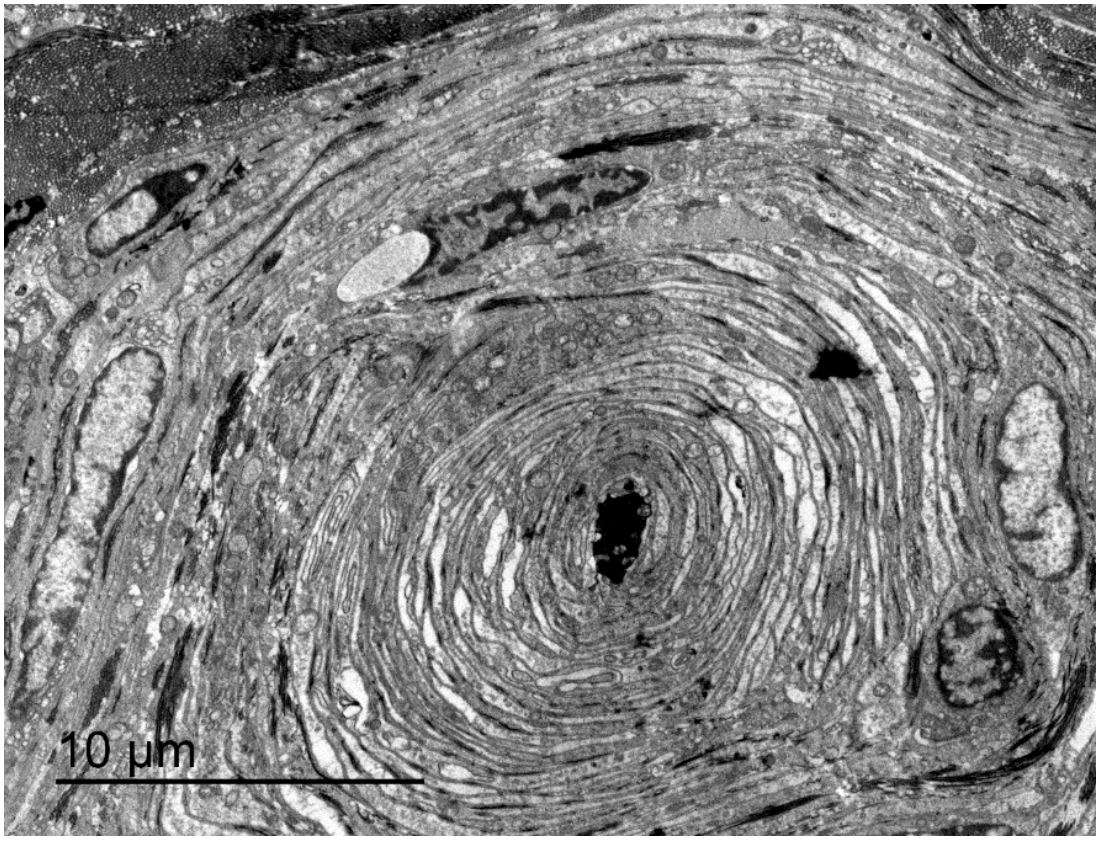

Figure 788. Different view of the same corpuscles as in *Error! Reference source not found*.**.**

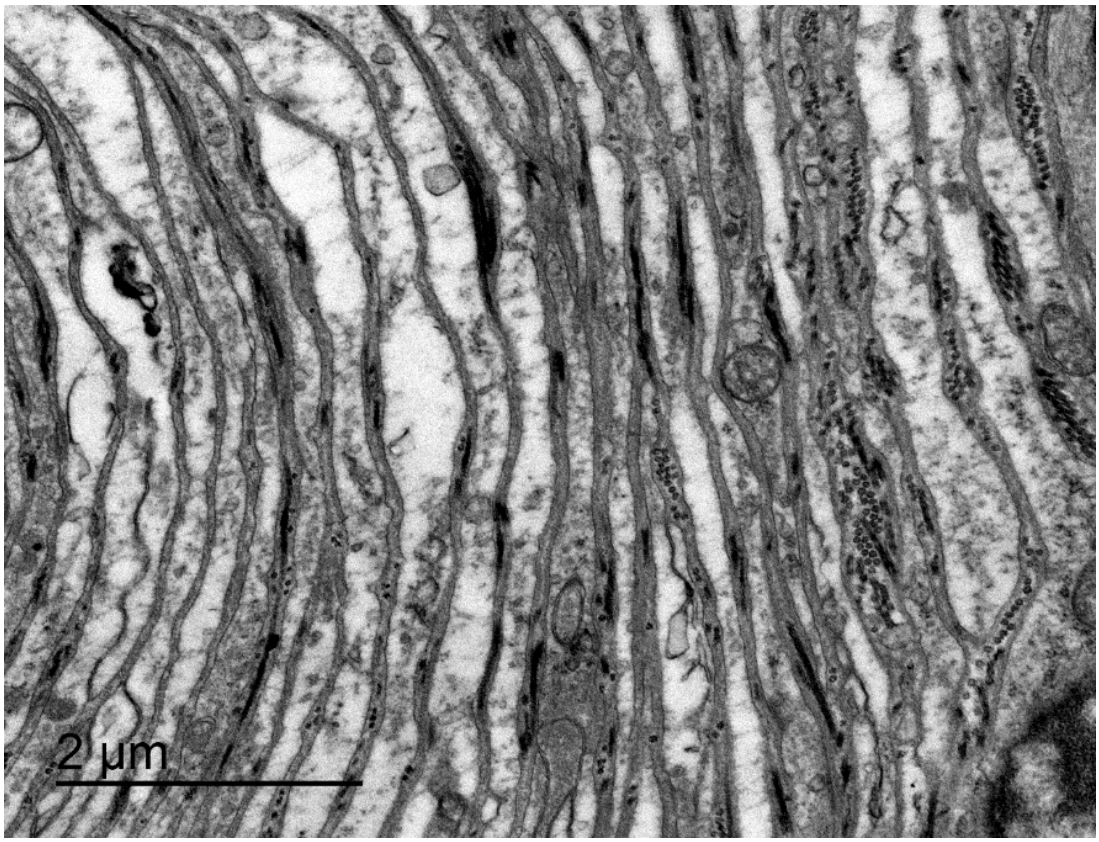

Figure 789. Detail of Figure 788, showing the lamellar structure. The lamellae consist of adjoining plasma membrane and little amount of cytoplasm. There are… Collagen fibres in the extracellular spaces are oriented in two main directions and are section longitudinally and transversely in this transversely sectioned corpuscle.

3.3.3 Facial nerve

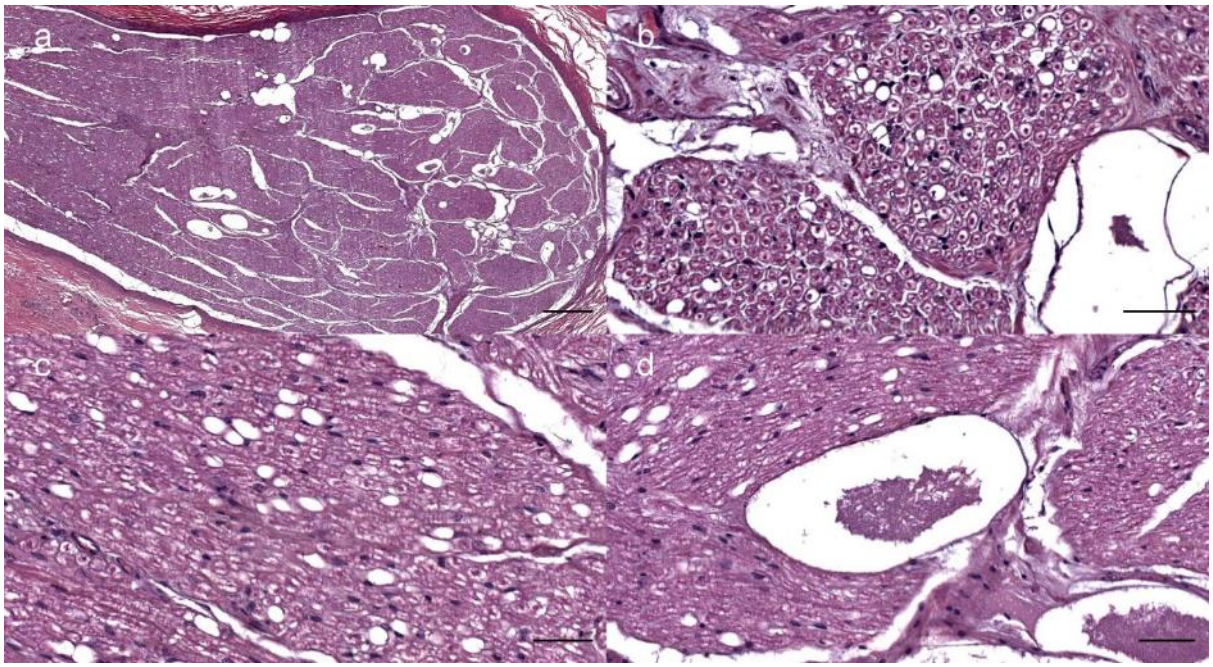

Figure 790. Histological images (HE staining) of the facial nerve near the external ear canal in a striped dolphin (509/17_L14). Facial nerve. Overview (a) and detail (b,c,d) histological images. Scale bars 500 µm (a), 50 µm (b,c,d)).

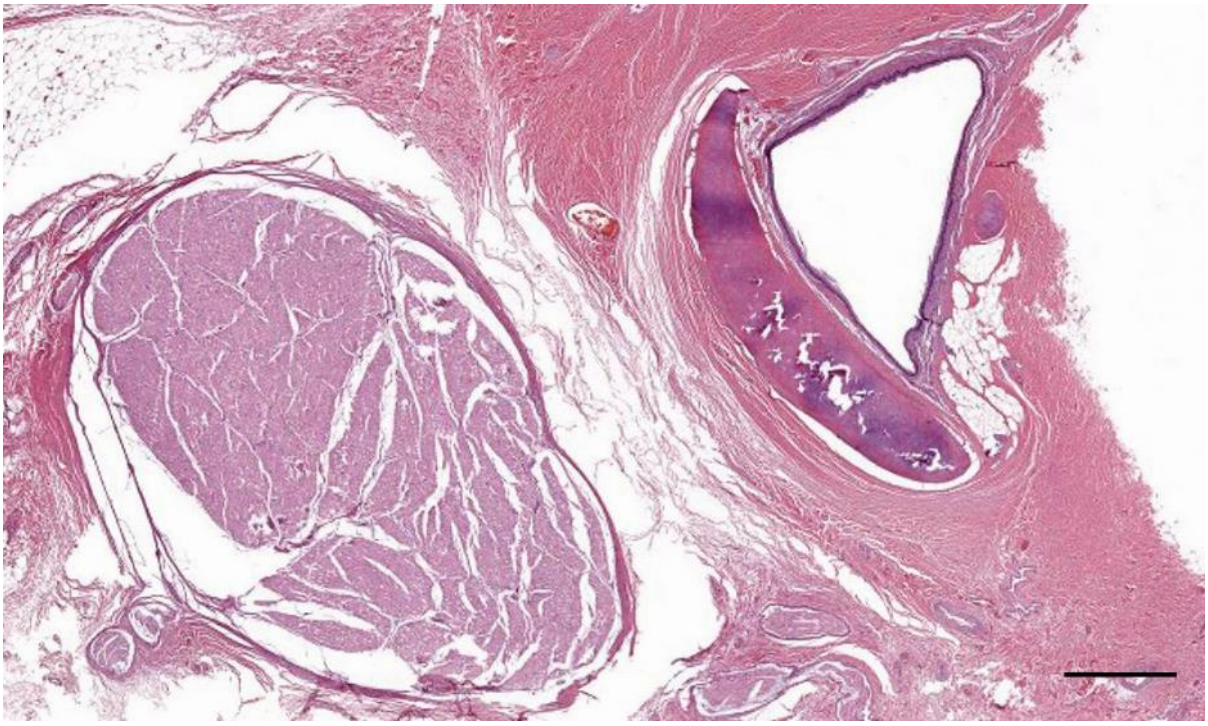

Figure 791. Histological image (HE staining) of the facial nerve near the external ear canal in a striped dolphin (293/18_L8). Scale bar 1 mm

Figure 792. Histological image (HE staining) of the facial nerve near the left external ear canal in a long-finned pilot whale. (441_L16). Scale bar 200 µm

Figure 793. Histological image (HE staining) of the facial nerve near the external ear canal in a bottlenose dolphin (444_L18). Scale bar 500 µm

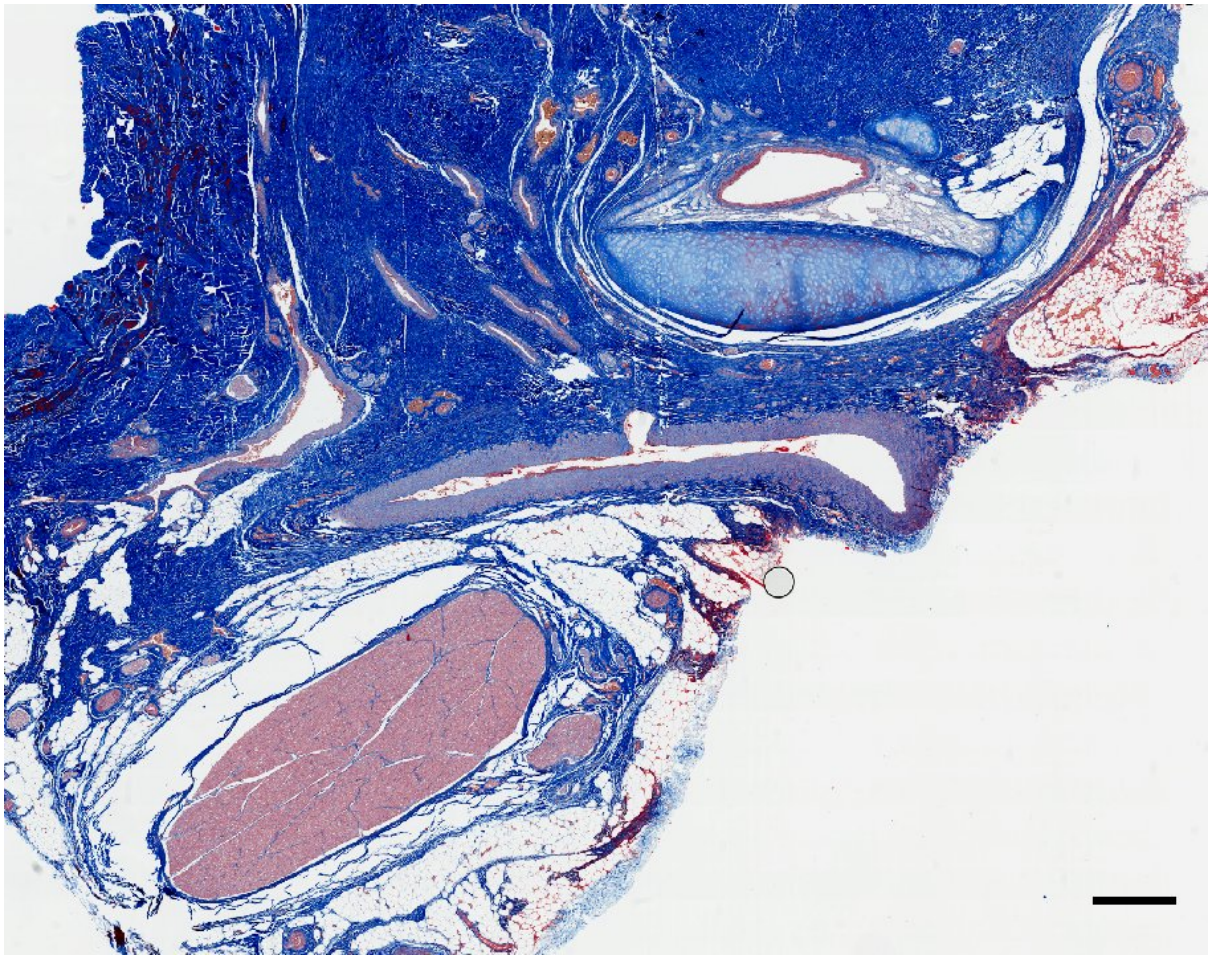

Figure 794. Histological image (Masson's trichrome staining) of the facial nerve near the external ear canal in a striped dolphin (127565_L1409_01). Scale bar 1mm

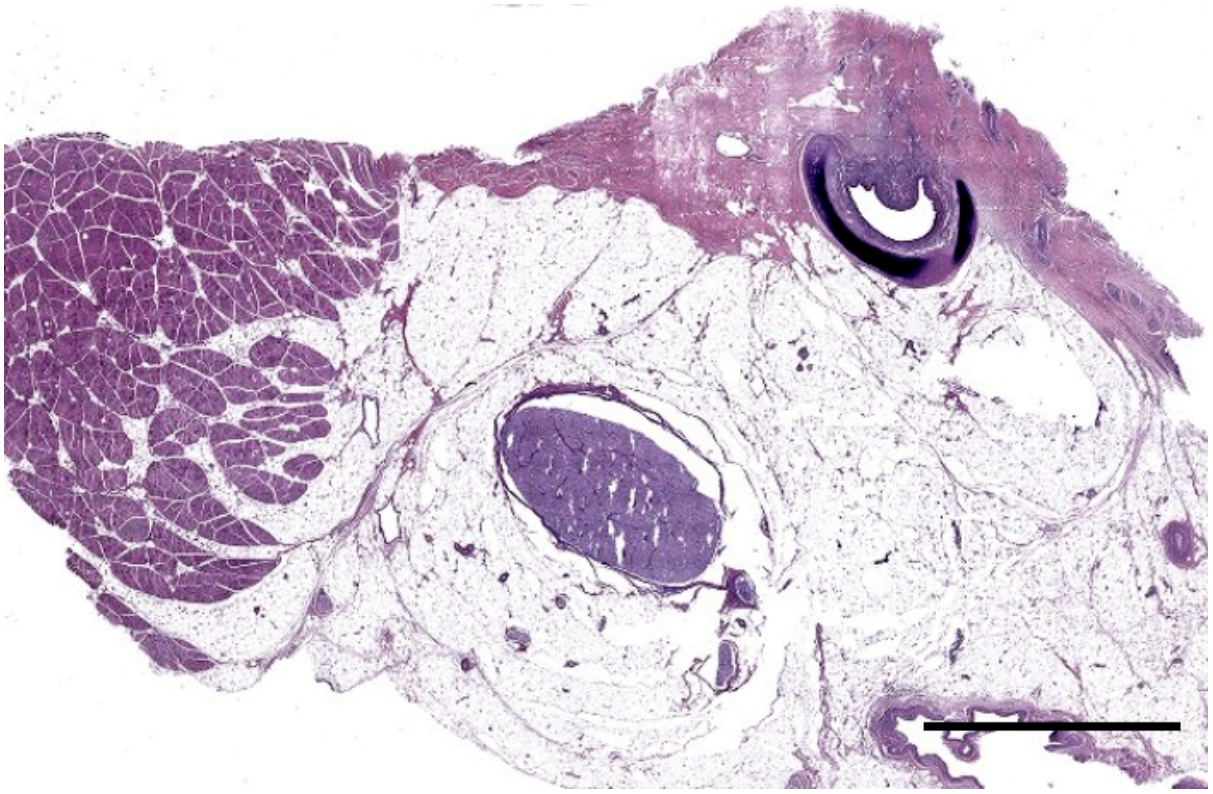

Figure 795. Histological image (HE staining) of a transverse section through the right ear canal of a harbour porpoise about 5 cm beneath the skin (UT1727_R15). Ear canal with nervous ridge and cartilage. Note the facial nerve, ventral to the ear canal, in the fat tissue. Scale bar 5 mm

3.3.4 Terrestrial mammals

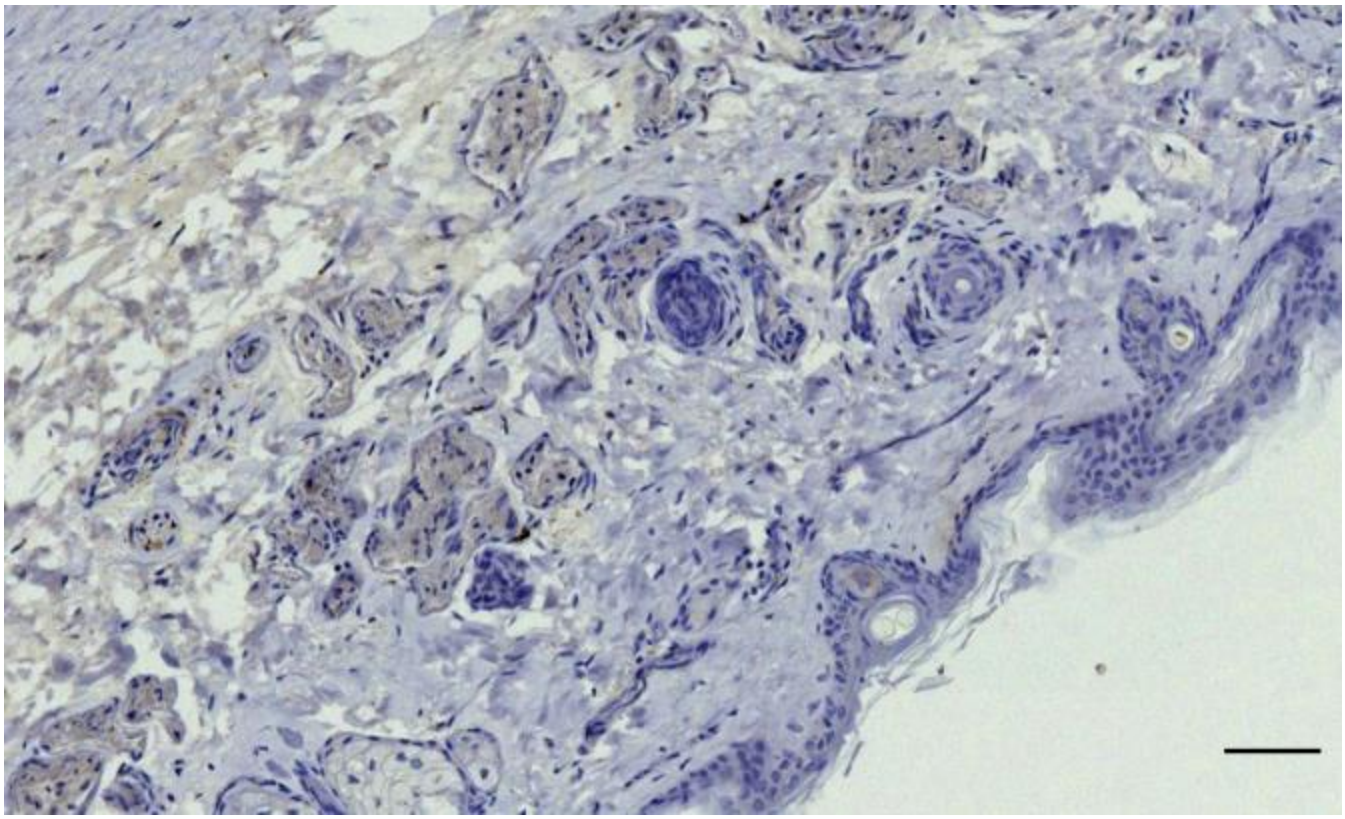

Figure 796. IHC image (anti-NSE) of the auricular dermis in a roe deer. Dermis and epidermis show no reactivity. There is unspecific staining of the glands. This image is representative for all terrestrial mammals in this study. Scale bar 100 µm (De Vreese et al., 2020).

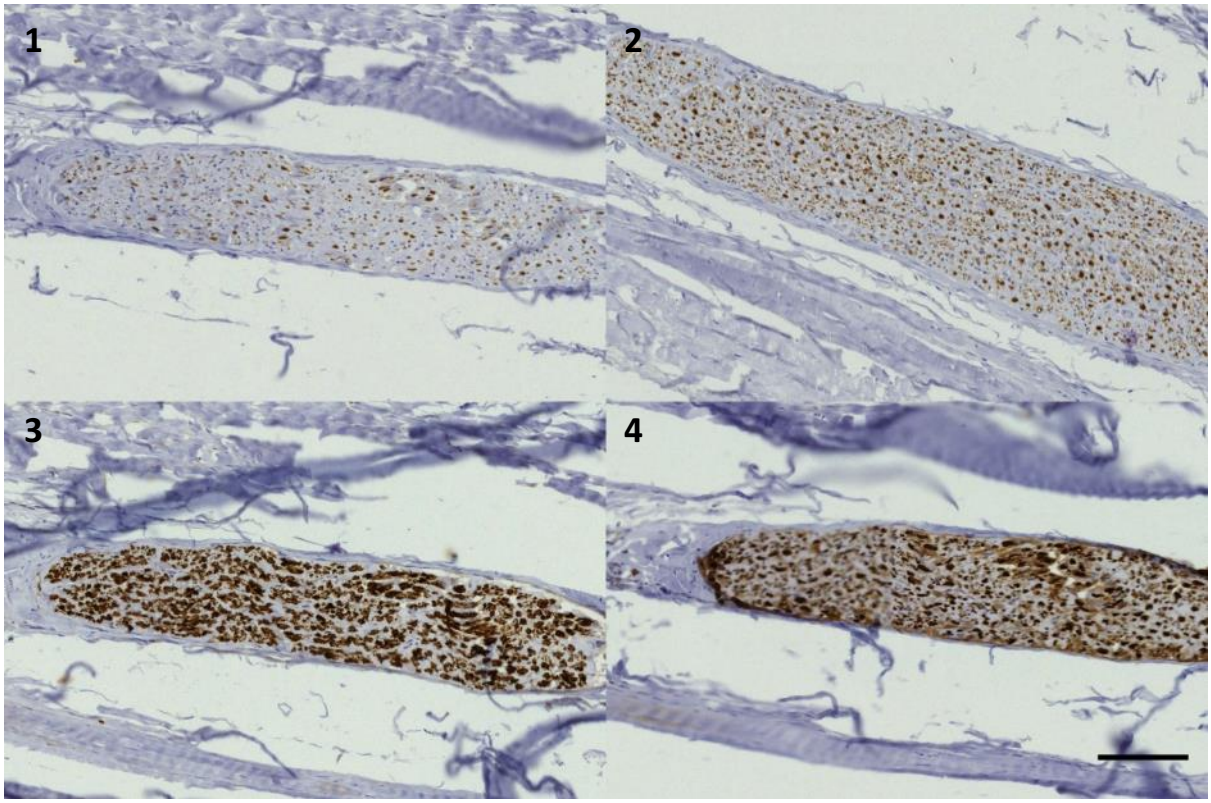

Figure 797. Montage image of nerve bundles of a northern giraffe showing immunoreactivity to anti-NSE (1), anti-PGP 9.5 (2), anti-S100 (3), and anti-NF (4). Scale: 100 µm

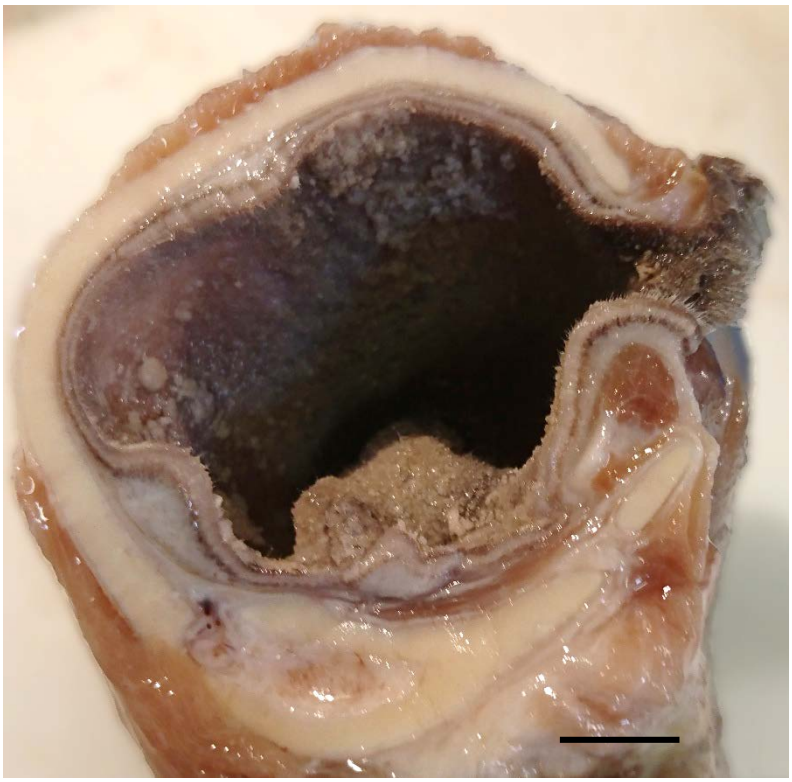

Figure 798. Macroscopic picture of a transverse section through the right ear canal of a giraffe. Right side is rostral. Scale bar 1 cm

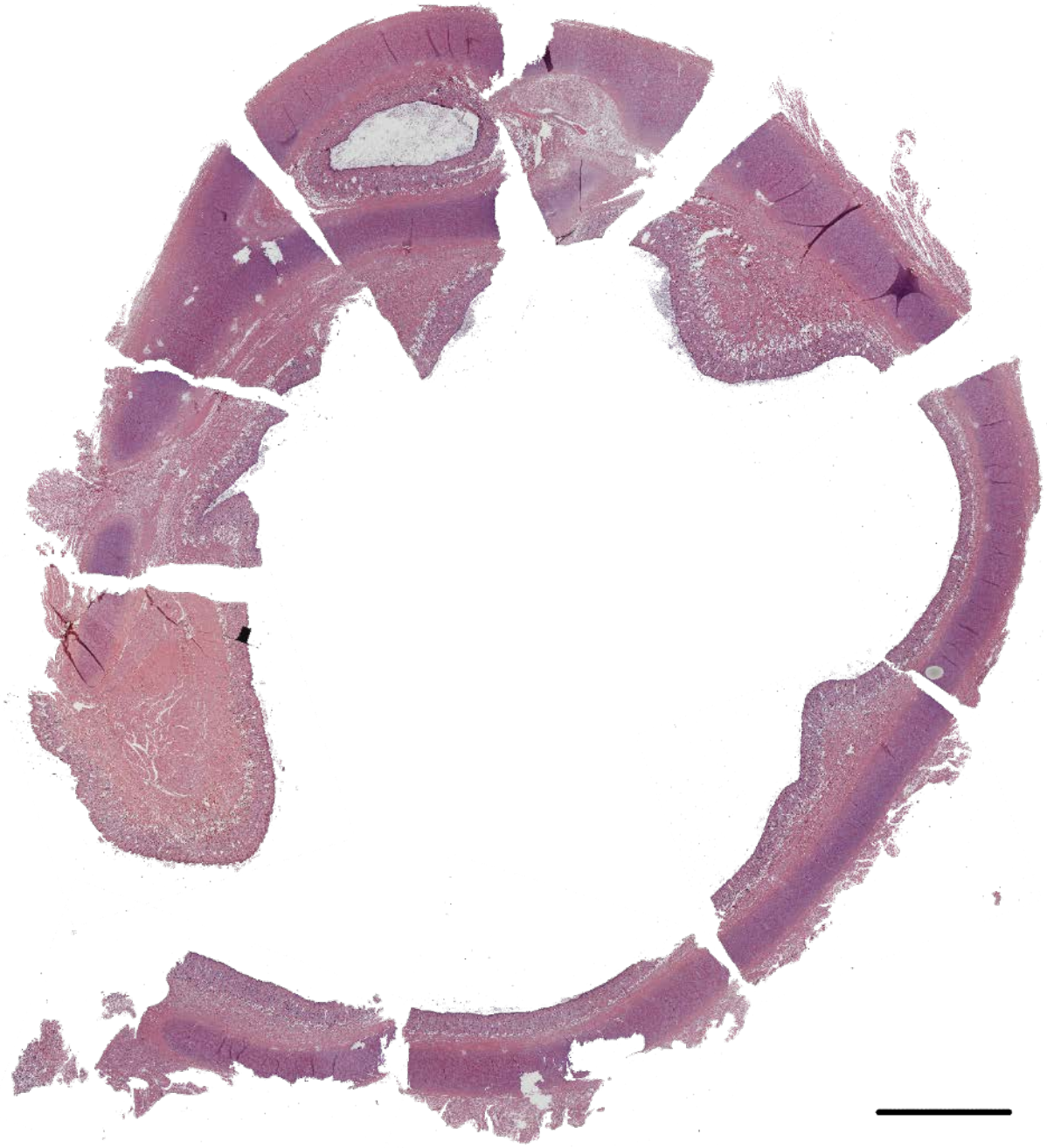

Figure 799. Histological reconstruction of a transverse section through the ear canal of a giraffe about 1 cm medial to the external ear opening. (Left is rostral). The lumen on the dorsal side that is situated between two cartilage rims, is a inlet of the ear canal lined with the same epithelium and subepithelial structures such as glands. Scale bar 1cm.

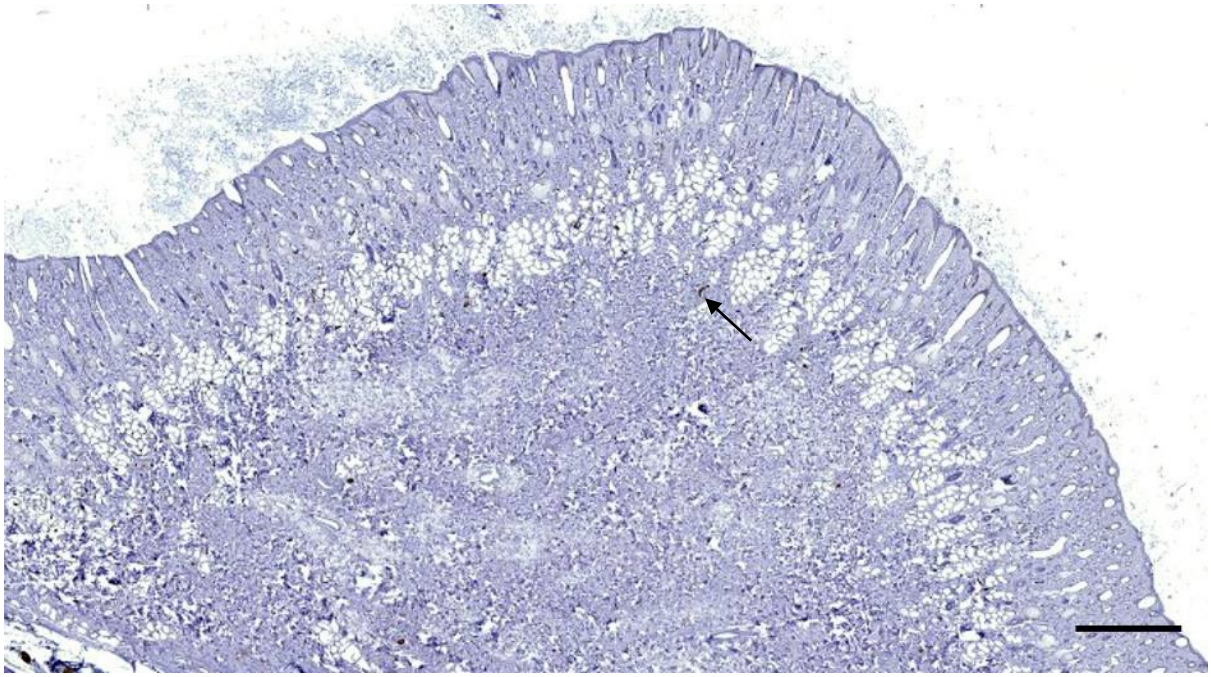

Figure 800. Immunohistological image of a part of the ear canal of a northern Giraffe, stained with anti-NF. There are no immunoreactions except for few small nerve fibres (e.g. arrow). Scale bar 1 mm

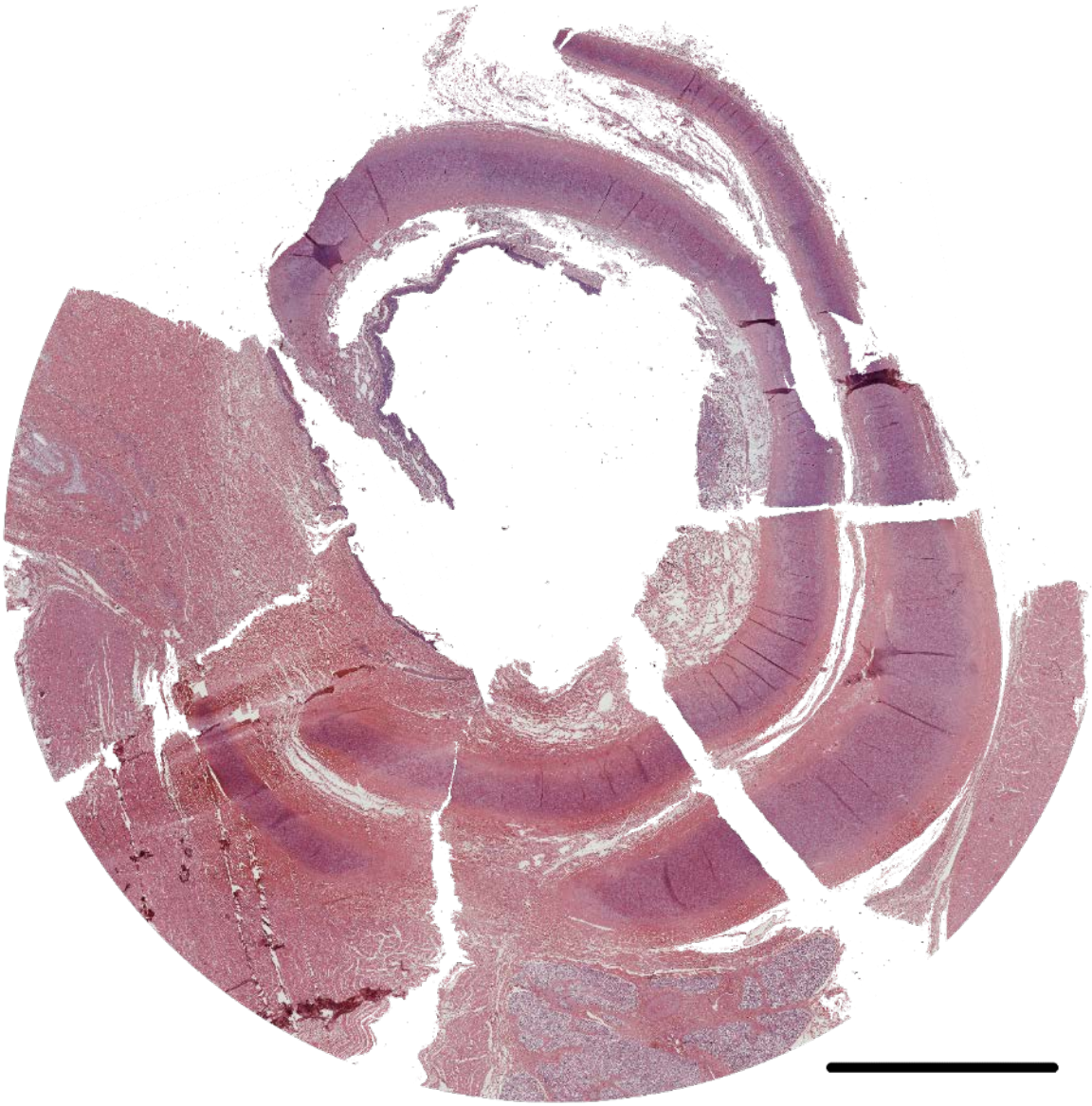

Figure 801. Reconstruction of a transverse section through the ear canal of a giraffe about 4 cm medial to the external ear opening. (Left is the rostral side). Surrounding the canal, there are two separate incomplete cartilage rings with their opening towards caudal/caudoventral. Scale: 1cm

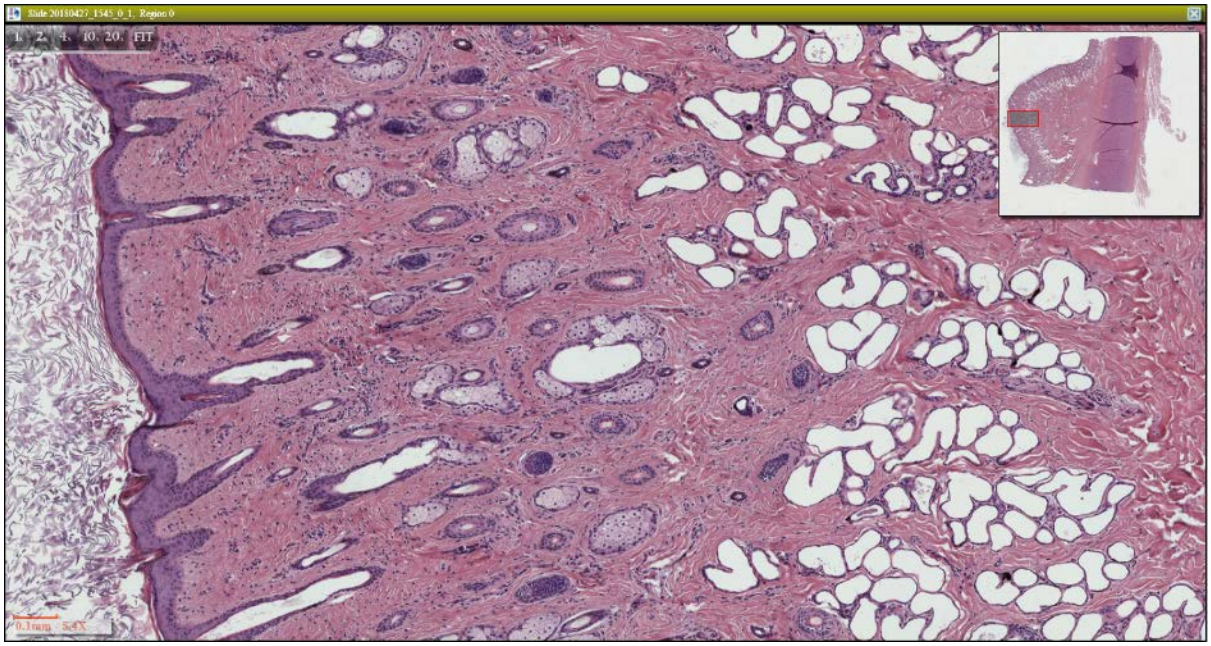

Figure 802. Histological image (HE staining) of the ear canal epithelium and glandular structures in a northern giraffe.

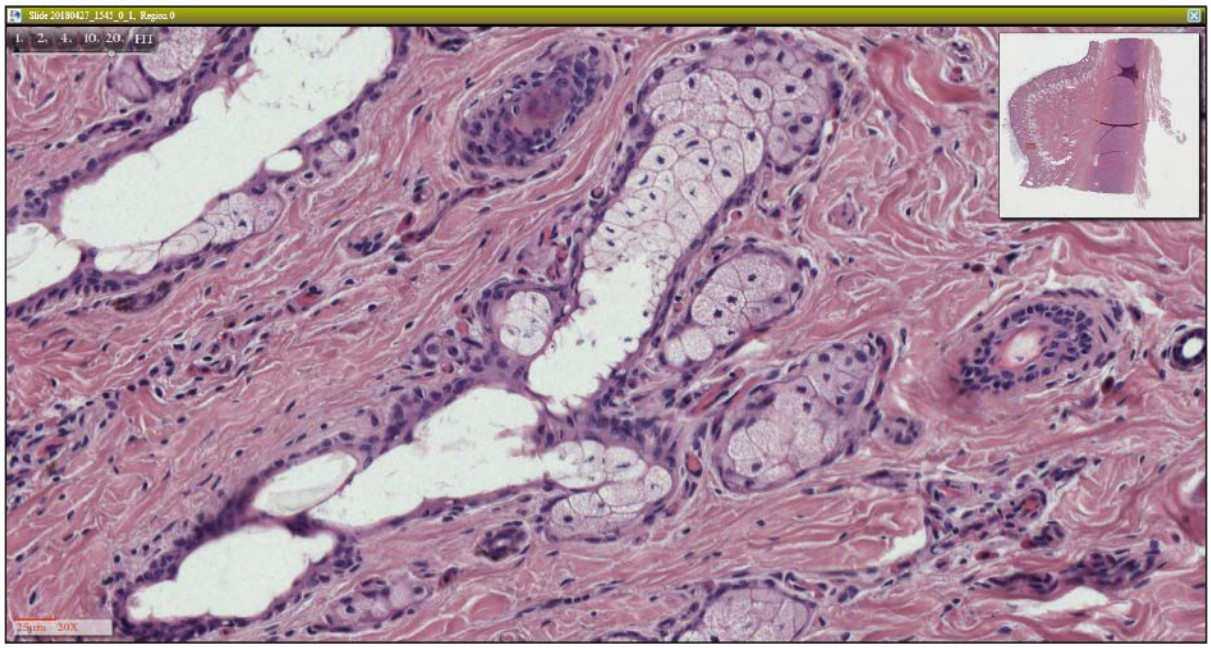

Figure 803. Histological image (HE staining) of a multilobular acinar gland in the ear canal of a northern giraffe.

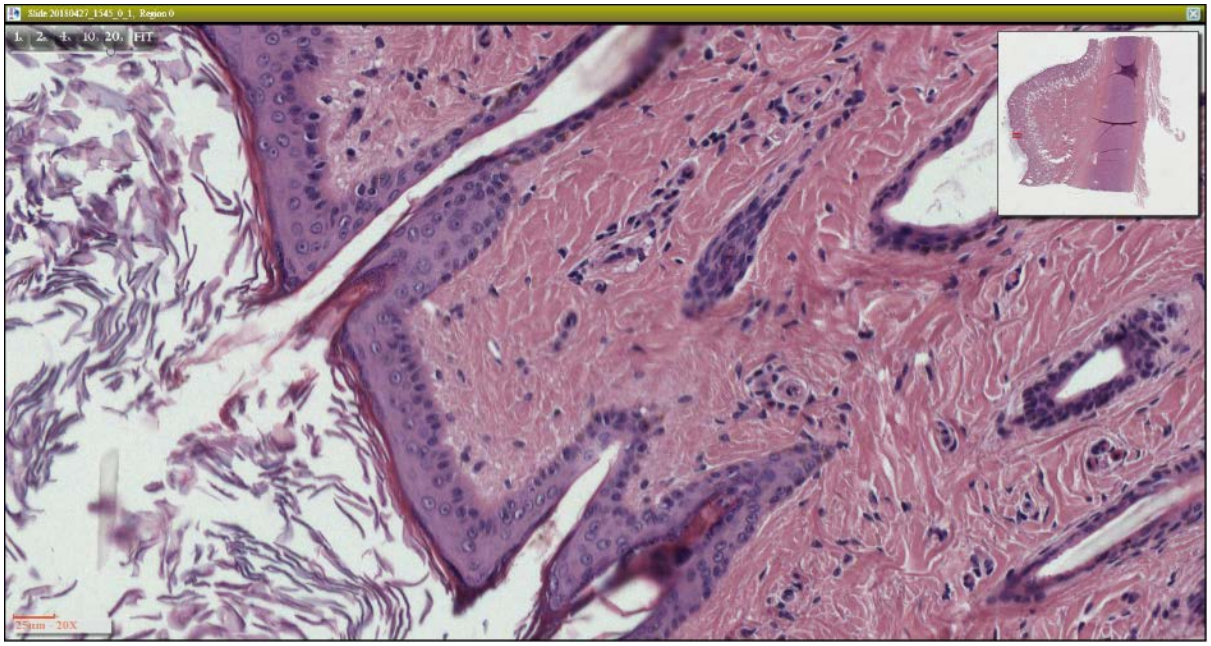

Figure 804. Histological image (HE staining) of the epithelium and glandular excretory ducts.

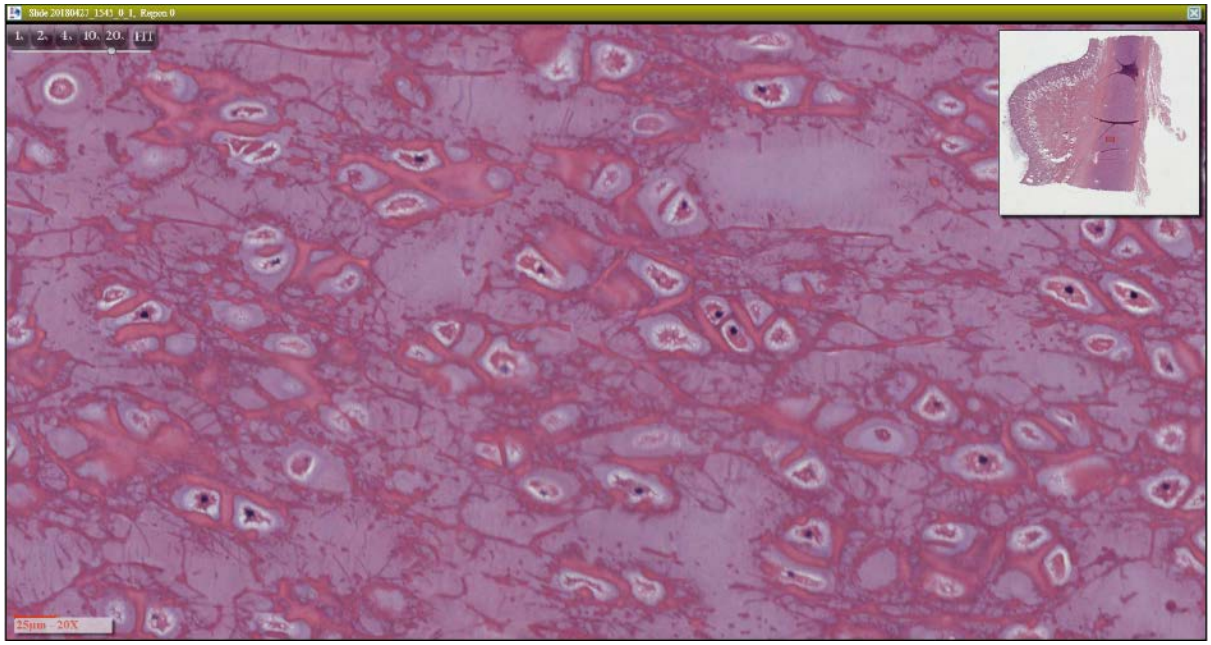

Figure 805. Histological image of the aurcilar cartilage of a northern giraffe.

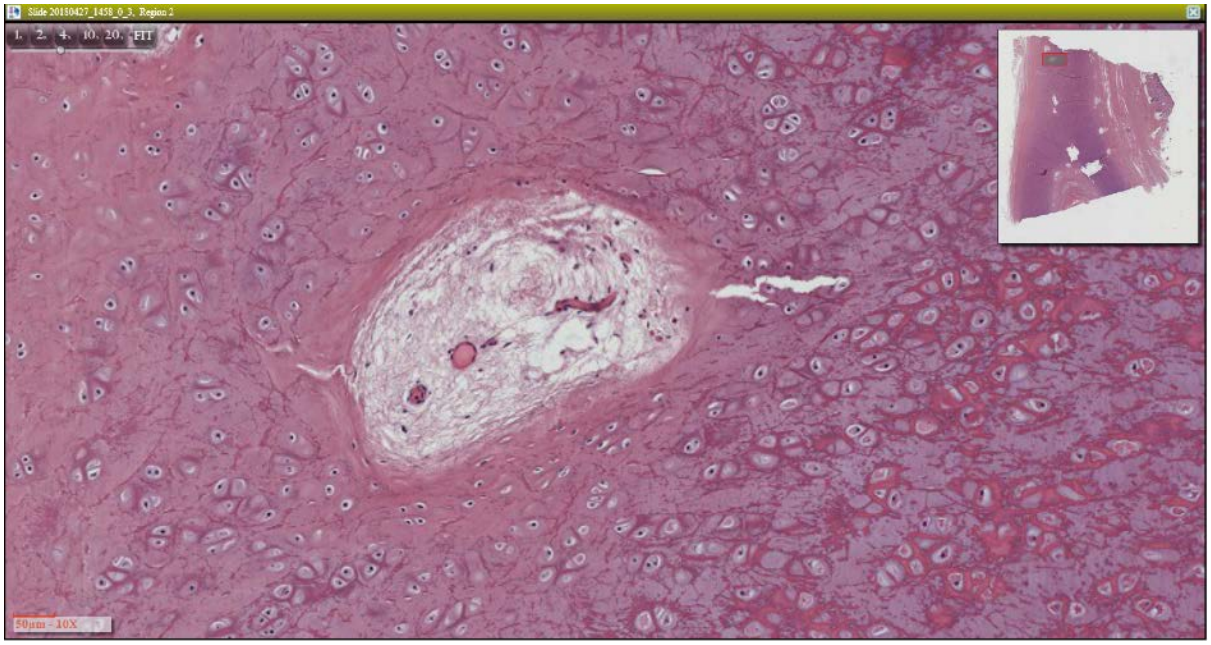

Figure 806. Histological detail image (HE staining) of the intracartilaginous vascularization

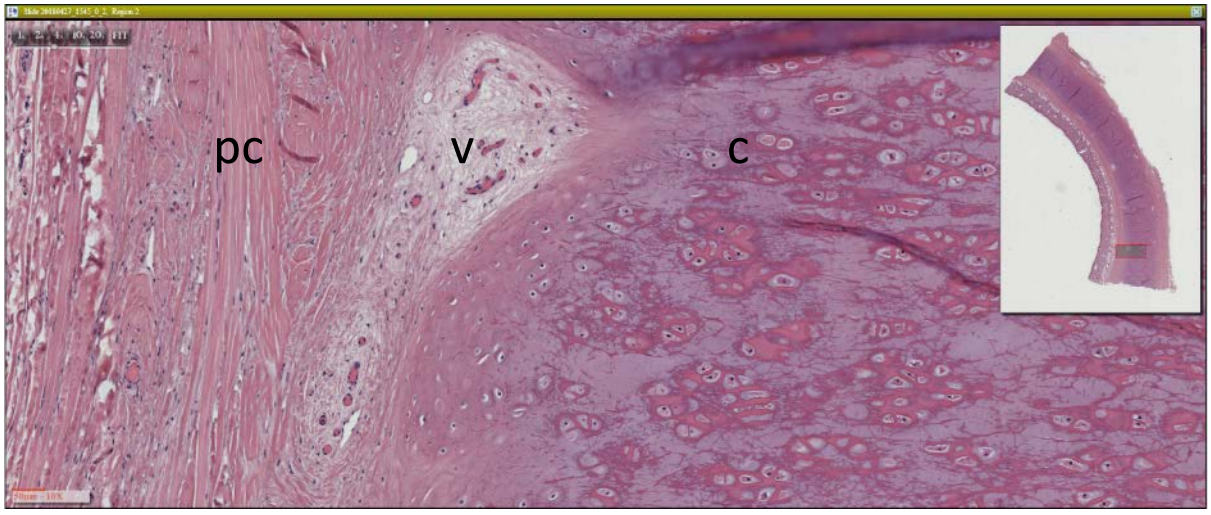

Figure 807. Histological image (HE staining) of vascular structures (v) on the border between cartilage (c) and perichondrium (pc).

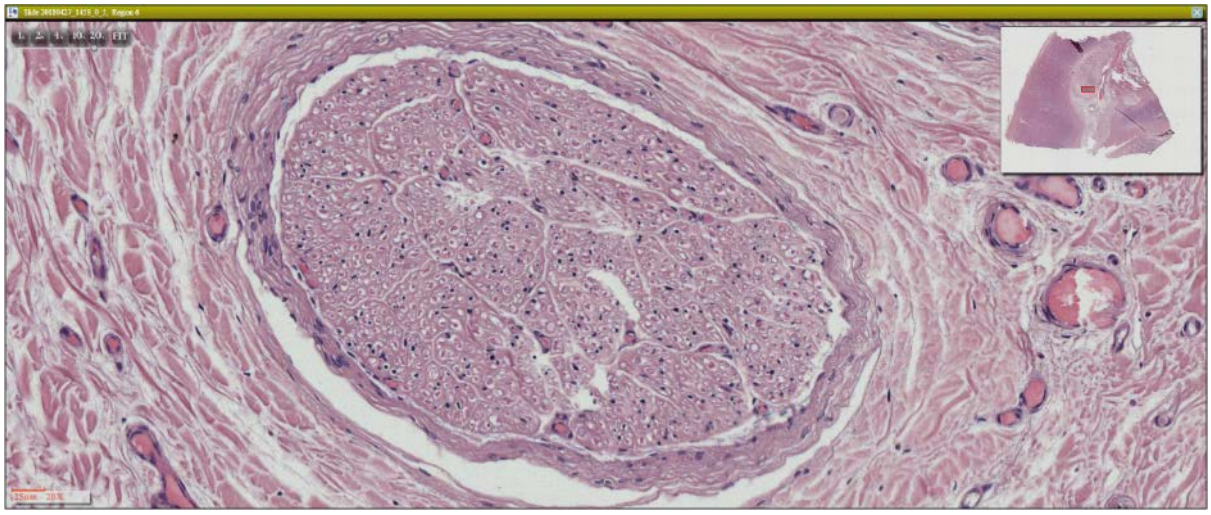

Figure 808. Histological image (HE staining) of a nerve fascicle in the dermis of the ear canal in a norterhn giraffe.

3.3.5 Western blot

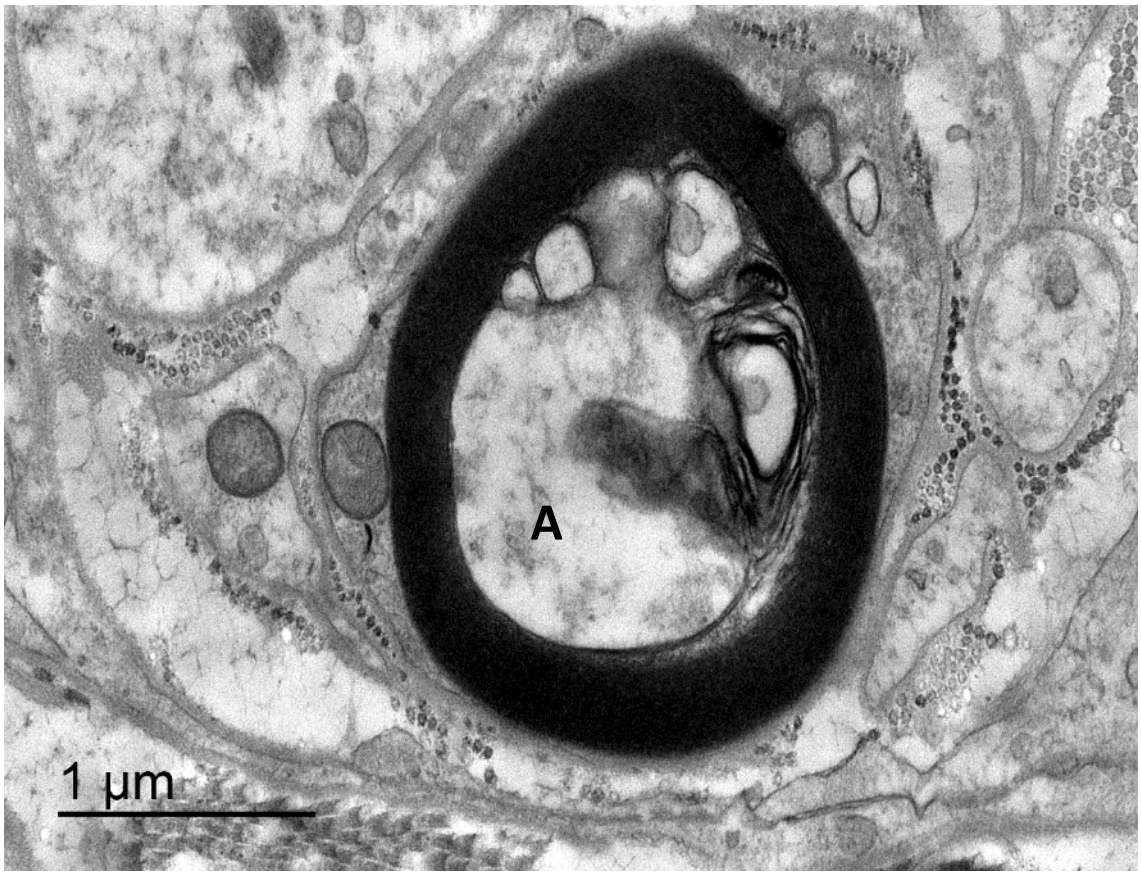

Figure 809. TEM image. Myelinated axon with myelin infolding. A: Axon; My: myelin sheath; OU: outer compartment of the Schwann cell cytoplasm; Mi: mitochondrion;

3.4 Tissue of secondary interest

3.4.1 Mandibular fat bodies

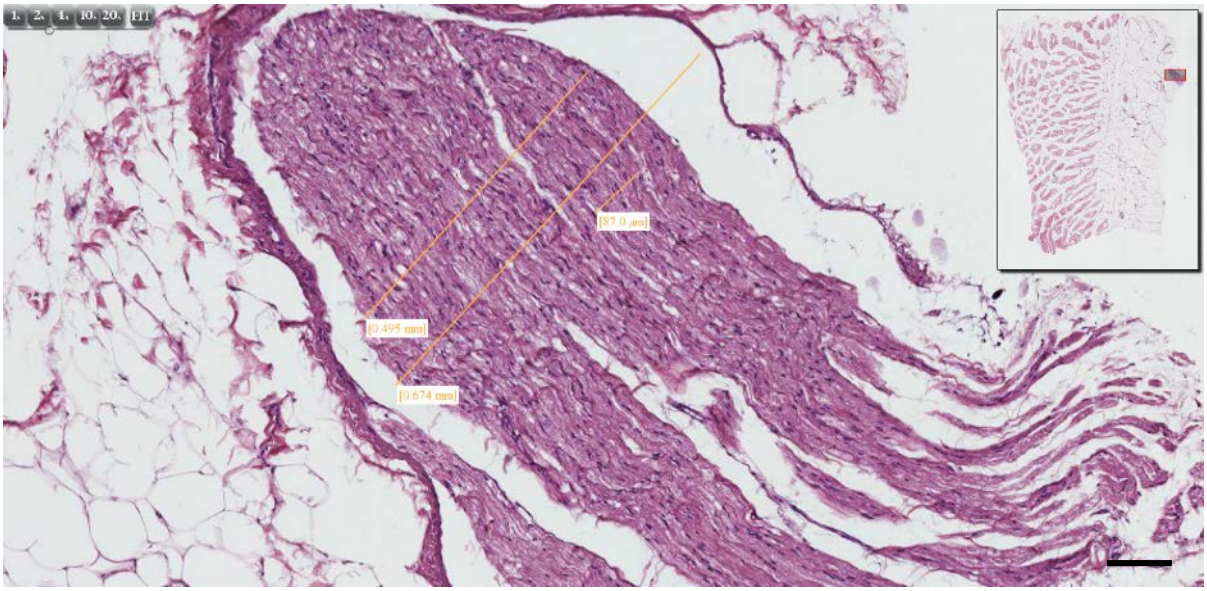

Figure 810. Histological image (HE staining) of a large nerve in the internal mandibular fat body of a striped dolphin. Scale bar 100 micron

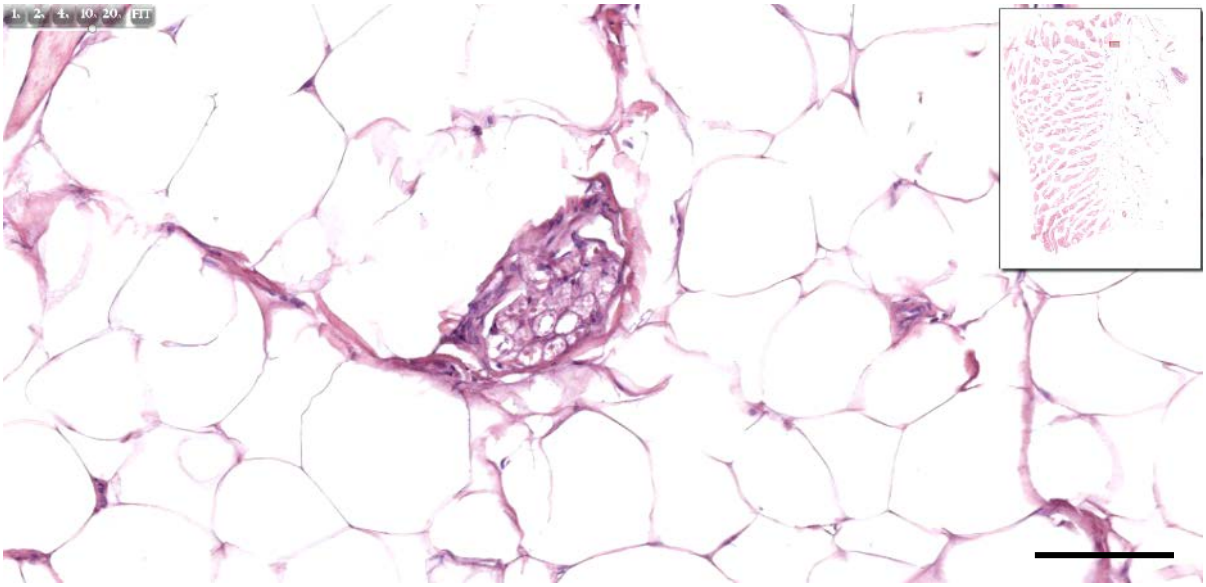

Figure 811. Histological image (HE staining) of a small nerve among the adipose tissue of the internal mandibular fat body in striped dolphin. Note the overview image on the top right with the internal mandibular fat body on the right half of the sample and the medial pterygoid muscle on the left. Scale bar 50 micron

3.5 Pathology

3.5.1 Haemorrhage

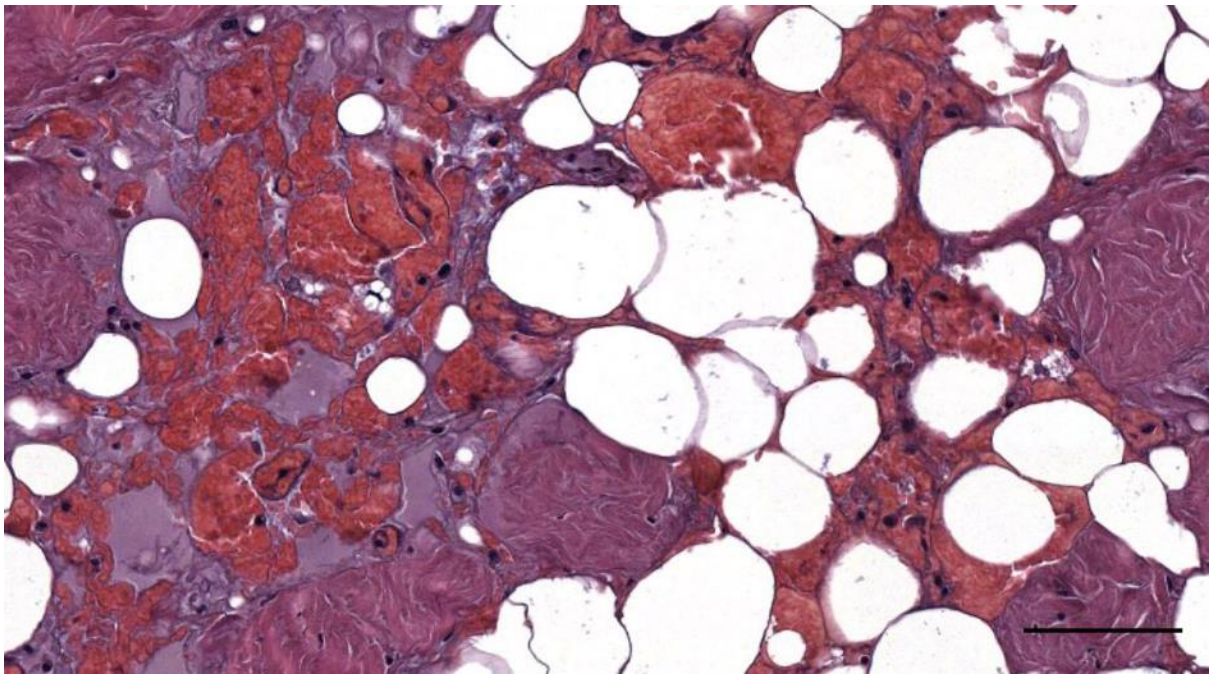

Figure 812. HE-stained histological image of the haemorrhage in the adipoconnective tissue. Scale bar 100 µm

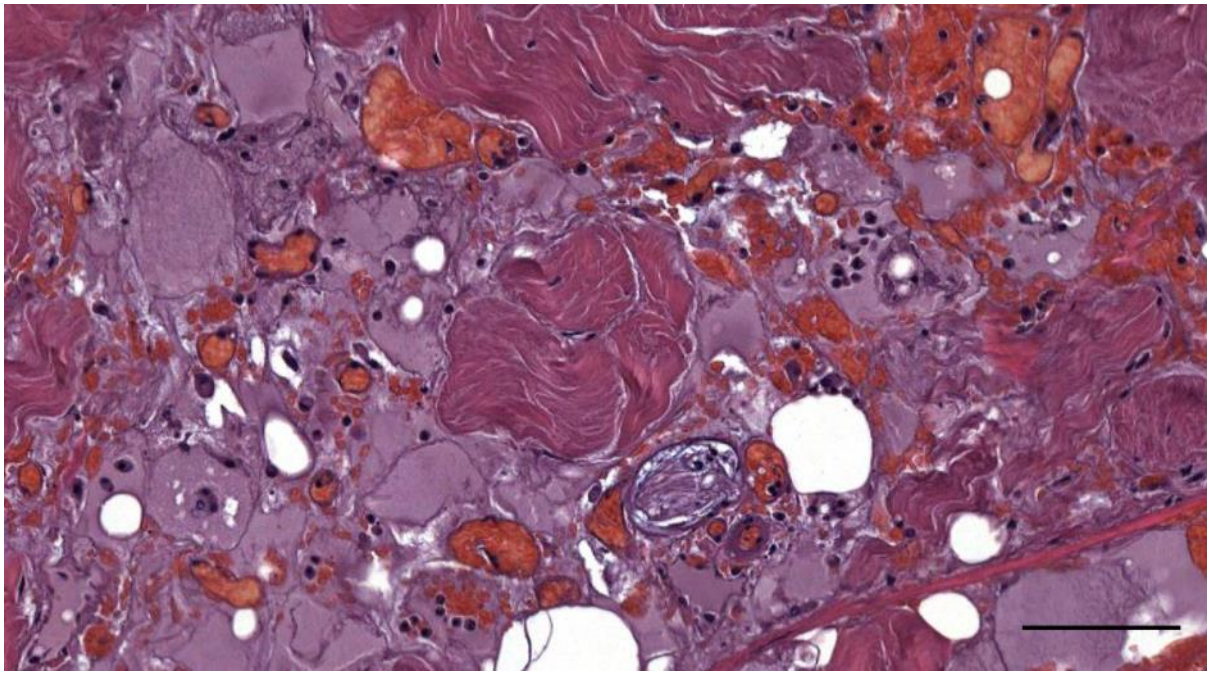

Figure 813. HE-stained histological image of the inflammatory cells and haemorrhage in the adipoconnective tissue. Scale bar 100 µm

4 Bibliography of Annexes

Aswani, Y., Varma, R., and Achuthan, G. (2016). Spontaneous external auditory canal cholesteatoma in a young male: Imaging findings and differential diagnoses. Indian J Radiol Imaging *26*, 237–240.

Banco, B., Grieco, V., Di Giancamillo, M., Greci, V., Travetti, O., Martino, P., Mortellaro, C.M., and Giudice, C. (2014). Canine aural cholesteatoma: A histological and immunohistochemical study. The Veterinary Journal *200*, 440–445.

Biswas, A. (2015). Characterization and Modeling of Vibrotactile Sensitivity Threshold of Human Finger Pad and the Pacinian Corpuscle. PhD Dissertation. Indian Institute of Technology.

Biswas, A., Manivannan, M., and Srinivasan, M.A. (2013). A biomechanical model of Pacinian Corpuscle & Skin. In 2013 Biomedical Sciences and Engineering Conference (BSEC), pp. 1–4.

Biswas, A., Muniyandi, M., and Srinivasan, M.A. (2014). Nonlinear Two Stage Mechanotransduction Model and Neural Response of Pacinian Corpuscle. (ORNL, Bionedical Science and Enginerring Center), p.

Biswas, A., Manivannan, M., and Srinivasan, M.A. (2015). Multiscale Layered Biomechanical Model of the Pacinian Corpuscle. IEEE Transactions on Haptics *8*, 31–42.

Bock, E. (1978). Nervous System Specific Proteins. Journal of Neurochemistry *30*, 7–14.

Braumann, U.-, Kuska, J.-, Einenkel, J., Horn, L.-, Loffler, M., and Hockel, M. (2005). Three-dimensional reconstruction and quantification of cervical carcinoma invasion fronts from histological serial sections. IEEE Transactions on Medical Imaging *24*, 1286–1307.

Broekaert, D., and Boedts, D. (2009). The Proliferative Capacity of the Keratinizing Annular Epithelium. Acta Oto-Laryngologica.

Bryden, M.M., and Molyneux, G.S. (1986). Ultrastructure of encapsulated mechanoreceptor organs in the region of the nares. In Research on Dolphins, M.M. Bryden, and R. Harrison, eds. (Oxford: Clarendon Press), pp. 99–107.

Cherepnov, V.L., and Chadaeva, N.I. (1981). Some characteristics of soluble proteins of Pacinian corpuscles. Bull Exp Biol Med *91*, 346–348.

Chung, J., Lee, D.H., and Choi, K.H. (2017). Ceruminous Pleomorphic Adenoma of the External Auditory Canal: Two Case Reports and Review of the Literature. Korean Journal of Otorhinolaryngology-Head and Neck Surgery *60*, 191–195.

Clendenon, J.L., Byars, J.M., and Hyink, D.P. (2006). Image Processing Software for 3D Light Microscopy. Nephron Exp Nephrol *103*, e50–e54.

Cocchia, D., Michetti, F., and Donato, R. (1981). Immunochemical and immunocytochemical localization of S-100 antigen in normal human skin. Nature *294*, 85–87.

Cranford, T.W., Krysl, P., and Hildebrand, J.A. (2008). Acoustic pathways revealed: simulated sound transmission and reception in Cuvier's beaked whale (*Ziphius cavirostris*). Bioinspiration & Biomimetics *3*, 016001.

Day, I.N.M., and Thompson, R.J. (2010). UCHL1 (PGP 9.5): Neuronal biomarker and ubiquitin system protein. Progress in Neurobiology *90*, 327–362.

De Vreese, S., André, M., Cozzi, B., Centelleghe, C., van der Schaar, M., and Mazzariol, S. (2020). Morphological Evidence for the Sensitivity of the Ear Canal of Odontocetes as shown by Immunohistochemistry and Transmission Electron Microscopy. Sci Rep *10*, 1–17.

Del Valle, M.E., Harwin, S.F., Maestro, A., Murcia, A., and Vega, J.A. (1998). Immunohistochemical analysis of mechanoreceptors in the human posterior cruciate ligament: a demonstration of its proprioceptive role and clinical relevance. The Journal of Arthroplasty *13*, 916–922.

Delyamure, S.L. (1969). Helminthofauna of Marine Mammals: Ecology and Phylogeny (I.P.S.T.).

El-Oteify, M., El-Dien, H.M.S., and Mubarak, W. (2011). Sensory nerve endings in the human female umbilical skin: light and electron microscopic study. Egyptian Journal of Histology *34*, 57–68.

García de los Ríos y Loshuertos, Á., Arencibia Espinosa, A., Soler Laguía, M., Gil Cano, F., Martínez Gomariz, F., López Fernández, A., and Ramírez Zarzosa, G. (2019). A Study of the Head during Prenatal and Perinatal Development of Two Fetuses and One Newborn Striped Dolphin (Stenella coeruleoalba, Meyen 1833) Using Dissections, Sectional Anatomy, CT, and MRI: Anatomical and Functional Implications in Cetaceans and Terrestrial Mammals. Animals *9*, 1139.

Gopinath, D. (2018). Splendore–Hoeppli phenomenon. J Oral Maxillofac Pathol *22*, 161–162.

Guinard, D., Usson, Y., Guillermet, C., and Saxod, R. (2000). PS-100 and NF 70-200 Double Immunolabeling for Human Digital Skin Meissner Corpuscle 3D Imaging. Journal of Histochemistry & Cytochemistry *48*, 295–302.

Guo, X., Xia, B., Lu, X.-B., Zhang, Z.-J., Li, Z., Li, W.-L., Xiong, A.-B., Deng, L., Tan, M.-Y., and Huang, Y.-C. (2016). Grafting of mesenchymal stem cell-seeded small intestinal submucosa to repair the deep partial-thickness burns. Connective Tissue Research *57*, 388–397.

Haro, J.J., Vega, J.A., del Valle, M.E., Calzada, B., Zaccheo, D., and Malinovsky, L. (1991). Immunohistochemical study of sensory nerve formations in human glabrous skin. Eur J Morphol *29*, 271–284.

Heilbrun, M.E., Salzman, K.L., Glastonbury, C.M., Harnsberger, H.R., Kennedy, R.J., and Shelton, C. (2003). External Auditory Canal Cholesteatoma: Clinical and Imaging Spectrum. Am J Neuroradiol *24*, 751–756.

Holt, J.J. (1992). Ear canal cholesteatoma. The Laryngoscope *102*, 608–613.

Ichihara, T. (1959). Formation mechanism of ear plug in baleen whales in relation to glove-finger. Scientific Reports of the Whales Research Institute *14*, 107–135.

Ichihara, T. (1964). Prenatal development of the ear plug in baleen whales. Scientific Reports of the Whales Research Institute *18*, 29–48.

Ismail, Mohammad.T., Al-Kafri, A., and Ismail, M. (2017). Otomycosis in Damascus, Syria: Etiology and clinical features. Curr Med Mycol *3*, 27–30.

Iwanaga, T., Fujita, T., Takahashi, Y., and Nakajima, T. (1982). Meissner's and Pacinian corpuscles as studied by immunohistochemistry for S-100 protein, neuron-specific enolase and neurofilament protein. Neuroscience Letters *31*, 117–121.

Ji, P., Chen, L., Gong, J., Yuan, Y., Li, M., Zhao, Y., and Zhang, H. (2018). Co-expression of vasoactive intestinal peptide and protein gene product 9.5 surrounding the lumen of human Schlemm's canal. Experimental Eye Research *170*, 1–7.

Kakoi, H., Anniko, M., Kinnefors, A., and Rask-Andersen, H. (1997). Auditory Epidermal Cell Migration. VII. Antigen Expression of Proliferating Cell Nuclear Antigens, PCNA and Ki-67 in Human Tympanic Membrane and External Auditory Canal. Acta Oto-Laryngologica *117*, 100–108.

Kelly, E.J., Terenghi, G., Hazari, A., and Wiberg, M. (2005). Nerve fibre and sensory end organ density in the epidermis and papillary dermis of the human hand. British Journal of Plastic Surgery *58*, 774–779.

Ketten, D.R., and Wartzok, D. (1990). Three-dimensional reconstructions of the dolphin ear. In Sensory Abilities of Cetaceans: Laboratory and Field Evidence, J.A. Thomas, and R.A. Kastelein, eds. (Boston, MA: Springer US), pp. 81–105.

Kim, J.H., Park, C., Yang, X., Murakami, G., Abe, H., and Shibata, S. (2018). Pacinian Corpuscles in the Human Fetal Finger and Thumb: A Study Using 3D Reconstruction and Immunohistochemistry. Anat. Rec. *301*, 154–165.

Kimaro, W.H., and Madekurozwa, M.-C. (2006). Immunoreactivities to protein gene product 9.5, neurofilament protein and neuron specific enolase in the ovary of the sexually immature ostrich (Struthio camelus). Experimental Brain Research *173*, 291–297.

Kokubo, M., Toshiro, H., Kudoh, K.-I., Fukuda, Y., Ohtomo, A., Nanto, H., and Ishida, H. (2002). Development of The Automatic Thin Sectioning Microtome System for Light Microscopy. The Machine to Mount Sections on The Object Glass Automatically by Using Static Electricity. Journal of the Japan Society for Precision Engineering *68*, 1605–1610.

Lepercquel, S., Broekaert, D., and Van Cauwenberge, P. (1993). Cytokeratin expression patterns in the human tympanic membrane and external ear canal. Eur Arch Otorhinolaryngol *250*, 78–81.

Linder, J.E. (1978). A simple and reliable method for the silver impregnation of nerves in paraffin sections of soft and mineralized tissues. Journal of Anatomy *127*, 543–551.

Luna, L.B. (1968). Pinkus' Acid-Orcein-Giemsa Method. Manual of Histologic Stain Methods of the Armed Foces Institute of Pathology. Third Edition, New York, pp. 77-78.

Mountcastle, V.B., LaMotte, R.H., and Carli, G. (1972). Detection thresholds for stimuli in humans and monkeys: comparison with threshold events in mechanoreceptive afferent nerve fibers innervating the monkey hand. Journal of Neurophysiology *35*, 122–136.

Mu, L., and Sanders, I. (2009). Sihler's whole mount nerve staining technique: a review. Biotechnic & Histochemistry 1–24.

Munger, B.L. (1971). Patterns of Organization of Peripheral Sensory Receptors. In Principles of Receptor Physiology, W.R. Loewenstein, ed. (Berlin, Heidelberg: Springer Berlin Heidelberg), pp. 523–556.

Nafstad, P.H.J., and Andersen, A.E. (1970). Ultrastructural investigation on the innervation of the Herbst corpuscle. Z. Zellforsch. *103*, 109–114.

Nussenbaum, B. (2020). Malignant Otitis Externa: Practice Essentials, Pathophysiology, Epidemiology.

Ortonne, J.-P., Verrando, P., Pautrat, G., and Darmon, M. (1987). Lamellar cells of sensory receptors and perineural cells of nerve endings of pig skin contain cytokeratins. Vichows Archiv A Pathol Anat *410*, 547–552.

Owen, H.H., Rosborg, J., and Gaihede, M. (2006). Cholesteatoma of the external ear canal: etiological factors, symptoms and clinical findings in a series of 48 cases. BMC Ear Nose Throat Disord *6*, 16.

Palmgren, A. (1960). Specific Silver Staining of Nerve Fibres. Acta Zoologica *41*, 239–265.

Pernick, N. (2020). Cholesteatoma.

Piepergerdes, J.C., Kramer, B.M., and Behnke, E.E. (1980). Keratosis obturans and external auditory canal cholesteatoma. The Laryngoscope *90*, 383–391.

Poláček, P., and Halata, Z. (1970). Development of simple encapsulated corpuscles in the nasolabial region of the cat. Ultrastructural study. Folia Morphol (Praha) *18*, 359–368.

Quindlen, J.C., Lai, V.K., and Barocas, V.H. (2015). Multiscale Mechanical Model of the Pacinian Corpuscle Shows Depth and Anisotropy Contribute to the Receptor's Characteristic Response to Indentation. PLOS Computational Biology *11*, e1004370.

Ramos-Vara, J.A., Kiupel, M., Baszler, T., Bliven, L., Brodersen, B., Chelack, B., West, K., Czub, S., Del Piero, F., Dial, S., et al. (2008). Suggested Guidelines for Immunohistochemical Techniques in Veterinary Diagnostic Laboratories. Journal of Veterinary Diagnostic Investigation *20*, 393–413.

Reysenbach De Haan, F.W. (1957). Hearing in whales. Acta Otolaryngol Suppl *134*, 1–114.

Roberts, N., Magee, D., Song, Y., Brabazon, K., Shires, M., Crellin, D., Orsi, N.M., Quirke, R., Quirke, P., and Treanor, D. (2012). Toward Routine Use of 3D Histopathology as a Research Tool. The American Journal of Pathology *180*, 1835–1842.

Rodig, S.J., and Dorfman, D.M. Splendore-Hoeppli Phenomenon. 2.

Saffari, T.M., Schüttenhelm, B.N., van Neck, J.W., and Holstege, J.C. (2018). Nerve reinnervation and itch behaviour in a rat burn wound model. Wound Repair and Regeneration *[Epub ahead of print]*.

Sanjuan, M., Sabatier, F., Andrac-Meyer, L., Lavieille, J.-P., and Magnan, J. (2007). Ear Canal Keratinocyte Culture: Clinical Perspective. Otology & Neurotology *28*, 504–509.

Schmechel, D., Marangos, P.J., and Brightman, M. (1978). Neurone-specific enolase is a molecular marker for peripheral and central neuroendocrine cells. Nature *276*, 834.

Sibarita, J.-B. (2005). Deconvolution Microscopy. In Microscopy Techniques, J. Rietdorf, ed. (Berlin, Heidelberg: Springer), pp. 201–243.

Sierra, E., Espinosa de los Monteros, A., Fernández, A., Díaz-Delgado, J., Suárez-Santana, C., Arbelo, M., Sierra, M.A., and Herráez, P. (2017). Muscle Pathology in Free-Ranging Stranded Cetaceans. Veterinary Pathology *54*, 298–311.

Soda, Y., and Yamamoto, Y. (2012). Morphology and chemical characteristics of subepithelial laminar nerve endings in the rat epiglottic mucosa. Histochemistry and Cell Biology *138*, 25–39.

Soto, S., Fondevila, D., González, B., Gómez-Campos, E., and Domingo, M. (2010). Multifocal Granulomatous Panniculitis with Ceroid Pigment in Two Mediterranean Striped Dolphins (Stenella coeruleoalba). Journal of Wildlife Diseases *46*, 320–325.

Spencer, P.S., and Schaumburg, H.H. (1973). An ultrastructural study of the inner core of the Pacinian corpuscle. J Neurocytol *2*, 217–235.

Stefansson, K., Wollmann, R.L., and Moore, B.W. (1982). Distribution of S-100 protein outside the central nervous system. Brain Research *234*, 309–317.

Suarez-Mier, G.B., and Buckwalter, M.S. (2015). Glial Fibrillary Acidic Protein-Expressing Glia in the Mouse Lung. ASN Neuro *7*, 175909141560163.

Takahashi, S., and Nakano, Y. (1989). Imunohistochemical demonstration of langerhans' cell in cholesteatoma using an antiserum against S-100 protein. Arch Otorhinolaryngol *246*, 48–52.

Thompson, R.J., Doran, J.F., Jackson, P., Dhillon, A.P., and Rode, J. (1983). PGP 9.5—a new marker for vertebrate neurons and neuroendocrine cells. Brain Research *278*, 224–228.

Vega, J.A., Llamosas, M.M., Huerta, J.J., and García-Fernández, J.M. (1996a). Study of human cutaneous sensory corpuscles using double immunolabelling and confocal laser scanning microscopy. The Anatomical Record *246*, 557–560.

Vega, J.A., Haro, J.J., and Del Valle, M.E. (1996b). Immunohistochemistry of human cutaneous Meissner and pacinian corpuscles. Microsc. Res. Tech. *34*, 351–361.

Vennix, P.P.C.A., Kuijpers, W., Peters, T.A., Tonnaer, E.L.G.M., and Ramaekers, F.C.S. (1996). Epidermal Differentiation in the Human External Auditory Meatus. The Laryngoscope *106*, 470–475.

Veres, T.Z., Rochlitzer, S., Shevchenko, M., Fuchs, B., Prenzler, F., Nassenstein, C., Fischer, A., Welker, L., Holz, O., Müller, M., et al. (2007). Spatial interactions between dendritic cells and sensory nerves in allergic airway inflammation. Am J Respir Cell Mol Biol *37*, 553–561.

Wang, L., Hilliges, M., Jernberg, T., Wiegleb-Edström, D., and Johansson, O. (1990). Protein gene product 9.5-immunoreactive nerve fibres and cells in human skin. Cell and Tissue Research *261*, 25–33.

Wang, Y., Xu, R., Luo, G., and Wu, J. (2015). Three-dimensional reconstruction of light microscopy image sections: present and future. Front Med *9*, 30–45.

Williams, A.L., Gerling, G.J., Wellnitz, S.A., Bourdon, S.M., and Lumpkin, E.A. (2010). Skin relaxation predicts neural firing rate adaptation in SAI touch receptors. In 2010 Annual International Conference of the IEEE Engineering in Medicine and Biology, (Buenos Aires: IEEE), pp. 6678–6681.

Wilson, P.O., Barber, P.C., Hamid, Q.A., Power, B.F., Dhillon, A.P., Rode, J., Day, I.N., Thompson, R.J., and Polak, J.M. (1988). The immunolocalization of protein gene product 9.5 using rabbit polyclonal and mouse monoclonal antibodies. Br J Exp Pathol *69, 69*, 91, 91–104.

Woodward, J.D., and Maina, J.N. (2005). A 3D digital reconstruction of the components of the gas exchange tissue of the lung of the muscovy duck, Cairina moschata. Journal of Anatomy *206*, 477–492.

Zachar, P.C., and Jonz, M.G. (2012). Confocal imaging of Merkel-like basal cells in the taste buds of zebrafish. Acta Histochemica *114*, 101–115.

Zylber, M.I., Failla, G., and Bas, A.L. (2002). Stenurus globicephalae Baylis et Daubney, 1925 (Nematoda: Pseudaliidae) from a False Killer Whale, Pseudorca crassidens (Cetacea: Delphinidae), Stranded on the Coast of Uruguay. Memórias Do Instituto Oswaldo Cruz *97*, 221–225.